CELL CYCLE REGULATION OF THE CENTROSOMAL KINASE NEK2 AND ITS SUBSTRATE C-NAP1

Thesis submitted for the degree of
Doctor of Philosophy
at the
University of Leicester

by

Rebecca Hames BSc (Hons) (Leeds)
Department of Biochemistry
University of Leicester

October 2002

ProQuest LLC
789 East Eisenhower Parkway
P.O. Box 1346
Ann Arbor, MI 48106-1346

DECLARATION

Unless otherwise acknowledged, the experimental work in this thesis has been carried out by the author in the Department of Biochemistry at the University of Leicester between October 1999 and October 2002. The work has not been submitted, and is not presently being submitted for any other degree at this or any other university.

Signed: Date:

Department of Biochemistry
University of Leicester
University Road
Leicester
LE1 7RH

CELL CYCLE REGULATION OF THE CENTROSOMAL KINASE NEK2 AND ITS SUBSTRATE C-NAP1

REBECCA HAMES

SUMMARY

The centrosome is the major microtubule organising centre in animal cells. In mitosis, it forms the two poles of the mitotic spindle upon which chromosomes are segregated. During cell cycle progression the centrosome undergoes a series of major structural and functional transitions that are regulated in part by phosphorylation. The aims of this thesis have been to investigate the regulation and function of the centrosomal kinase Nek2, which has previously been implicated in regulating centrosome cohesion at G2/M. Nek2 kinase activity is regulated by a number of mechanisms, including autophosphorylation and interaction with protein phosphatase 1. Here, we have identified two further mechanisms of regulation: (i) the expression of human Nek2 as two alternative splice variants, Nek2A and Nek2B; (ii) the specific destruction of Nek2A by the proteasome in early mitosis. This destruction follows ubiquitylation by the APC/C-Cdc20 complex and depends on a novel destruction motif which is highly related to the extended D box present in cyclin A. Previous work has indicated that Nek2 may regulate centrosome cohesion through phosphorylation of the core centrosomal protein C-Nap1. Here we show that C-Nap1 interacts with and is phosphorylated by both Nek2A and Nek2B at two distinct domains. Furthermore, both Nek2 and C-Nap1 associate with microtubules, suggesting that they may move along microtubules in a dynein dependent manner. Finally, using C-Nap1 as a bait in a yeast two hybrid interaction screen, the novel centrosomal protein BPC-1 was isolated. BPC-1 also interacted with Nek2 and may inhibit the centrosome cohesion function of Nek2. This work substantially advances our understanding of Nek2 regulation and brings us closer to understanding how centrosome cohesion is regulated through specific phosphorylation of components such as C-Nap1.

ACKNOWLEDGEMENTS

Throughout my PhD there have been many people that have helped me. The following are some but by no means all of those people. Firstly thank you to Dr Andrew Fry and all members of lab 201 for all their help and enthusiasm. Thanks also to my parents who have been supportive of my continued education through both the bad and the good times.

I would like to dedicate this work to my husband Richard who has always been there for me.

CONTENTS

ABBREVIATIONS

A_{260}	Absorbance at 260 nanometers
AD	Activation domain
APC	Adenomatous polyposis coli
APC/C	Anaphase promoting complex/cyclosome
APS	Ammonium persulphate
3-AT	3-aminotriazole
ATP	Adenosine triphosphate
BCA	Bicinchoninic acid
BCIP	5-bromo-4-chloro-3-indolyl phosphate
bp	Base pair
BPC-1	Binding partner C-Nap1-1
BSA	Bovine serum albumin
C-	Carboxy-
CaMKII	Calcium/Calmodulin kinase II
Cdc	Cell division cycle
Cdk	Cyclin dependent kinase
cDNA	Complementary deoxyribonucleic acid
CG-NAP	Centrosome and Golgi localised PKN-associated protein
Ci	Curie
cm	Centimeter
C-Nap1	Centrosomal Nek2 associated protein 1
CPE	Cytoplasmic polyadenylation element
CSF	Cytostatic factor
CTD	C-terminal domain
dATP	Deoxyadenosine triphosphate
DBD	DNA binding domain
dCTP	Deoxycytidine triphosphate
D box	Destruction box
dGTP	Deoxyguanosine triphosphate
DMEM	Dulbecco's modified eagle's medium
DMSO	Dimethylsulphoxide
DNA	Deoxyribonucleic acid
DNase	Deoxyribonuclease
dNTP	Deoxynucleotide triphosphates
dsRNAi	Double stranded RNA interference
DTT	Dithiothreitol
dTTP	Deoxythymidine triphosphate
EDTA	Ethylene diamine tetra acetic acid
EGFP	Enhanced green fluorescent protein
EGTA	Ethylene glycol-bis (β- aminoethylether) N,N,N',N'-tetraacetic acid
EST	Expressed sequence tag
FCS	Fetal calf serum
g	Gram
GST	Glutathione S transferase
GTP	Guanosine triphosphate
γ-TURC	γ-Tubulin ring complex
γ-TUSC	γ-Tubulin small complex
HEC	Highly expressed in cancer
HEPES	N-2-hydroxyethylpiperazine-N'-2-ethanesulphonic acid

IgG	Immunoglobulin G
IPTG	β-D-isopropyl-thiogalactopyranoside
IVT	*In vitro* translation
Kb	Kilobase
Kda	Kilodalton
LB	Luria-bertani
LMB	Leptomycin B
M	Molar
mA	Milliamp
MAP	Microtubule associated protein
MEN	Mitotic exit network
mg	Milligram
ml	Millilitre
mm	Millimeter
mM	Millimolar
mRNA	Messenger ribonucleic acid
Msps	Mini-spindles
MTOC	Microtubule organising centre
N-	Amino-
NBT	Nitroblue tetrazolium
NEB	Nek2 extraction buffer
Nek2	NIMA-related kinase 2
ng	Nanogram
NIMA	Never in mitosis A
NLS	Nuclear localisation signal
nm	Nanometer
nt	Nucleotide
NTD	N-terminal domain
OD	Optical density
O/N	Overnight
ONPG	O-nitrophenyl-β-galactopyranoside
ORF	Open reading frame
p160ROCK	Rho-associated coiled coil containing kinase
PAGE	Polyacrylamide gel electrophoresis
PBS	Phosphate buffered saline
PBST	Phosphate buffered saline + 0.1% (v/v) Tween-20
PCM	Pericentriolar matrix
PCR	Polymerase chain reaction
pI	Isoelectric point
Plk	Polo like kinase
PMSF	Phenylmethylsulphonyl fluoride
PP1	Protein phosphatase 1
RNA	Ribonucleic acid
RNAse	Ribonuclease
rpm	Revolutions per minute
RT	Room temperature
SCF	Skp1-cullin-F-box protein complex
SDS	Sodium dodecyl sulphate
SPB	Spindle pole body
TACC	Transforming acidic coiled coil
TCA	Trichloroacetic acid

TEMED	N,N,N',N'-tetramethylethylenediamine
Tris	Tris (hydroxymethyl) aminomethane
Tm	Melting temperature
U	Units of enzyme activity
UTR	Untranslated region
UV	Ultraviolet
µg	Microgram
µl	Microlitre
V	Volts
(v/v)	Volume per volume ratio
(w/v)	Weight per volume ratio

TABLE OF FIGURES

CHAPTER 1

INTRODUCTION

1.1 Cell division

Cell division requires that chromosomes are first duplicated and then equally segregated between two daughter cells. Failure to execute these procedures correctly can lead to cells with an abnormal content of chromosomes resulting in an excess or absence of multiple gene products. Such errors during meiosis can lead directly to birth defects, whereas during mitosis in somatic cells, errors contribute to the development and progression of cancer (Nicklas, 1997). The highly complex process of chromosome segregation occurs during mitosis on a bipolar, microtubule based scaffold called the mitotic spindle. The formation of the bipolar mitotic spindle is central to the process of cell division, hence the importance of the microtubule organising centres (MTOC), a set of organelles that co-ordinate the nucleation and arrangement of microtubules to form this dynamic structure (Brinkley, 1985).

A complete cell cycle in most somatic cells takes approximately 24 hours with mitosis constituting only 1 hour of this (Figure 1.1A). The time interval between mitotic divisions, known as interphase, is divided into three phases: G1, S and G2. It is during S phase that the DNA is replicated, the cell then prepares for mitosis during G2. 60% of cells however are in G1, a period of growth, with 30% in G2 and mitosis and 10% in S phase (Figure 1.1B). Under certain conditions cells can enter a state of quiescence termed G0. The process of mitosis or nuclear division begins when the condensing chromosomes first become visible within the prophase nucleus (Pines and Rieder, 2001) (Figure 1.1C). The subsequent breakdown of the nuclear envelope terminates prophase and initiates prometaphase, during which the chromosomes become attached to and positioned on the mitotic spindle as it forms (Figure 1.2A). Once all chromosomes are aligned near the spindle equator as pairs of sister chromatids linked together at the centromere the cell is considered to be in metaphase. Spindle microtubules attach to the chromosomes at the kinetochores, paired structures associated with the centromeres. Kinetochores regulate the attachment of microtubules from both poles of the spindle facilitating equal segregation of genetic material (Figure 1.2B). Unattached kinetochores generate signals that inhibit mitotic progression, through activation of spindle checkpoint associated proteins (Amon, 1999). Once bipolar attachment is achieved, anaphase commences, the chromatids separate along their lengths and as the spindle elongates they move apart to converge at opposite poles of the cell. During anaphase A, the chromatids split and move to opposite poles.

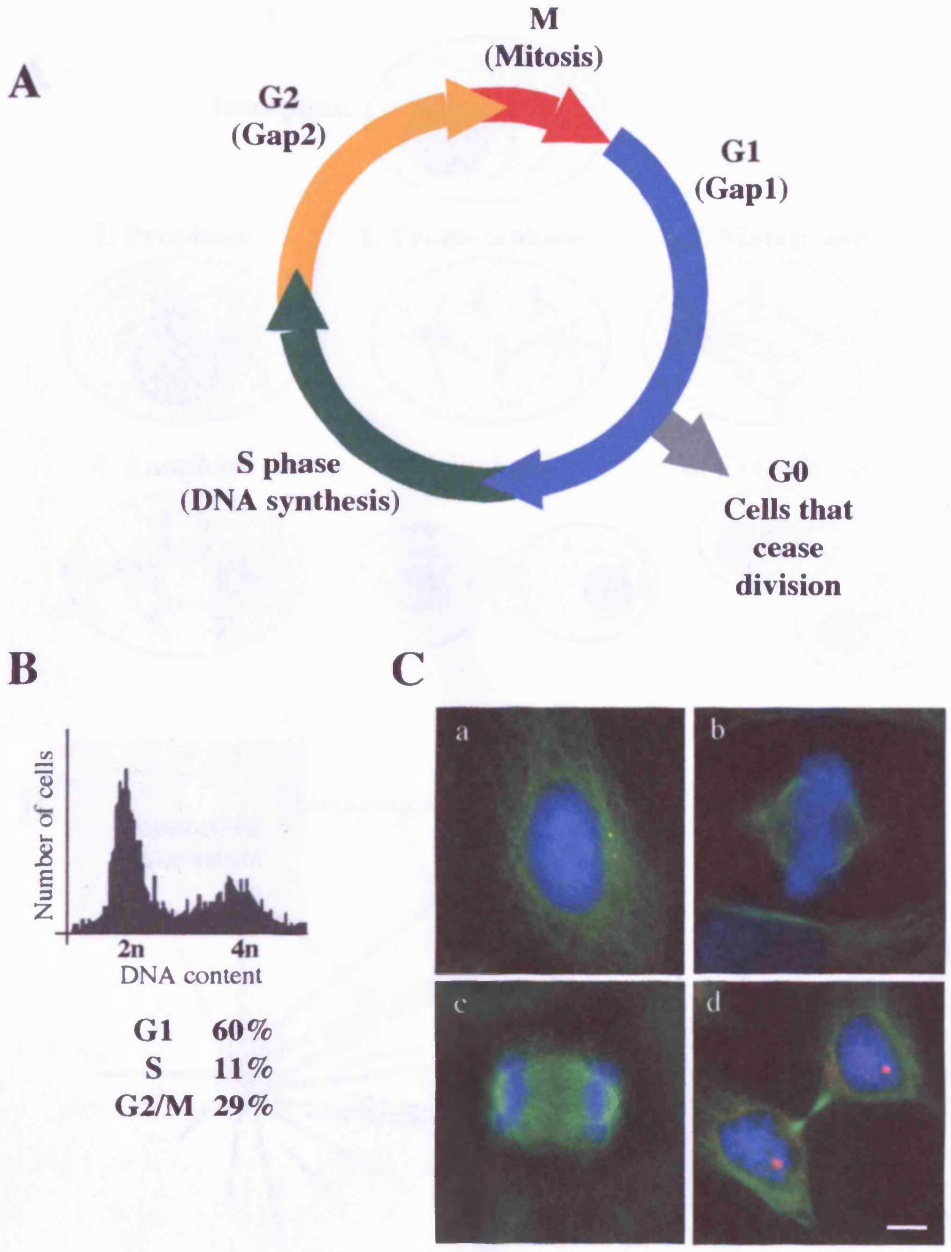

Figure 1.1 The cell cycle

(**A**) The cell cycle consists of 4 main stages G1, S, and G2 constitute interphase during which DNA is replicated, mitosis represents the stage when the cell divides into two identical daughter cells. (**B**) An asynchronous population of HeLa cells subjected to flow cytometry indicates the relative numbers of cells in each cell cycle phase. (**C**) Immunofluorescence images of HeLa cells where microtubules are labelled in green, the DNA in blue and centrosomes in red. In interphase, there is an extensive microtubule network emanating from the centrosome (**a**). As the cell enters mitosis, the duplicated centrosomes separate, the chromosomes condense and the bipolar spindle is formed (**b**). The chromosomes are pulled apart along the spindle towards each pole during anaphase (**c**). Cytokinesis then takes place to produce two identical daughter cells. Scale bar, 10 μm.

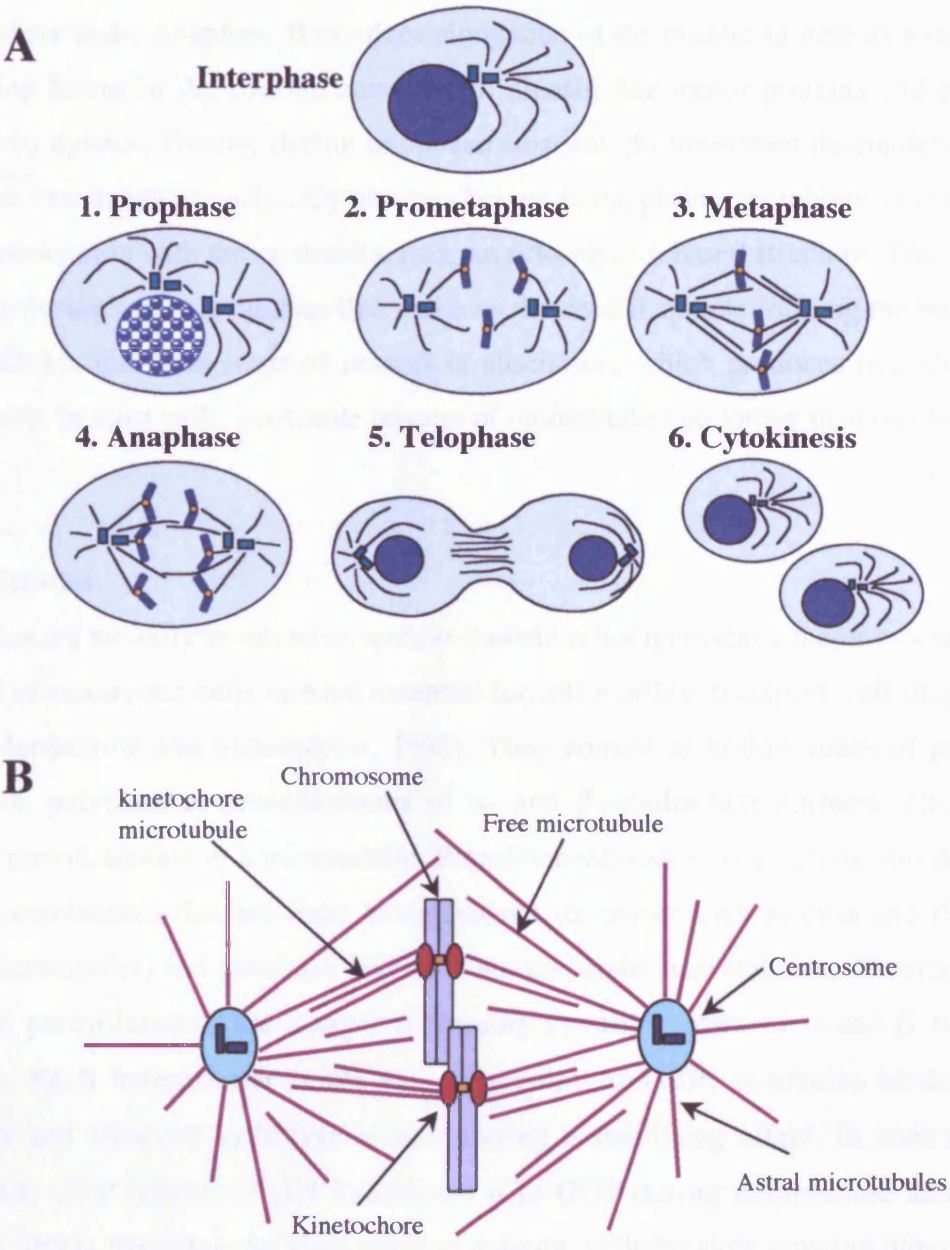

Figure 1.2 The stages of mitosis

(A) The process of mitosis can be separated into 6 distinct stages. In prophase the chromosomes condense and the spindle begins to form (1). The spindle microtubules attach to chromosomes in prometaphase (2), reaching metaphase when they line up along the cell equator (3). The chromosomes are segregated to opposite poles of the cell in anaphase (4), followed by the positioning of the contractile ring (5) in telophase. Finally cytokinesis occurs creating two daughter cells (6). **(B)** In mammalian cells, chromosome segregation takes place on a bipolar spindle consisting of microtubules nucleated mainly by the centrosome, some microtubule are released and anchored near to the centrosome. Additional microtubules are nucleated from the chromosomes. Spindle microtubules attach to the chromosomes at the kinetochores.

Forces for this chromosome movement are provided both by dynein, a minus end motor, which is present at the kinetochores and by depolymerisation of kinetochore microtubules at their positive ends. Anaphase B involves elongation of the mitotic spindle as a result of both pushing forces in the overlap zone due to kinesin-like motor proteins and pulling forces due to dynein. Finally, during telophase adjacent chromosomes de-condense and fuse to form two daughter nuclei. Cytokinesis begins as the plasma membrane invaginates due to its association with the contractile ring, an acto-myosin based structure. The furrow compresses the microtubule bundles that make up the central spindle forming the midbody (Glotzer, 2001). The final stage of mitosis is abscission, which produces two identical daughter cells. In most cells, the whole process of mitosis takes no longer than one hour.

1.2 Microtubules

Microtubules are not only involved in spindle formation but represent a major cytoskeletal component of eukaryotic cells that are essential for cell motility, transport, cell shape and polarity (Mandelkow and Mandelkow, 1995). They consist of hollow tubes of protein, formed from polymers or protofilaments of α- and β-tubulin heterodimers. There are usually 13 protofilaments in a microtubule. Protofilaments can also associate into doublet or triplet microtubules that are used in specialised structures such as cilia and flagella (doublet microtubules) and centrioles and basal bodies (triplet microtubules). Heterodimers in adjacent protofilaments are staggered forming spiralling rows of α and β tubulin monomers. Each heterodimer binds two molecules of GTP; α-tubulin binds GTP irreversibly and does not hydrolyse it, thus having a stabilising effect. In contrast, β-tubulin binds GTP reversibly and hydrolyses it to GDP during microtubule assembly (Mitchison, 1993). Microtubules have uniform polarity, with the slow growing minus ends at or near the microtubule organising centres (MTOCs) and the fast growing plus ends extending towards the cortex or chromosomes (McIntosh and Euteneuer, 1984).

Microtubule associated proteins (MAPs) interact with microtubules, to bind, stabilise and promote the assembly of microtubules (Mandelkow and Mandelkow, 1995). Tau is an example of a MAP that promotes microtubule nucleation and elongation whilst also protecting against disassembly. Interestingly in Alzheimer's disease, phosphorylated tau is unable to bind microtubules, resulting in the formation of neurofibrillary tangles in the brain that are composed of destabilised microtubules and tau aggregates (Mandelkow and

Mandelkow, 1993). The highly conserved family of MAPs, XMAP215/chTOG/Msps, bind directly to a subset of microtubules and stabilises them through an interaction with the TACC (transforming acidic coiled coil containing) proteins (Lee *et al.*, 2001). Although most MAPs bind along microtubules, a subset localise specifically to the plus ends of growing microtubules. EB1 interacts with the adenomatous polyposis coli (APC) tumour suppressor protein and binds to the plus ends of microtubules (Su *et al.*, 1995). It is thought to modulate microtubule dynamics and link microtubules to the cell cortex (Lee *et al.*, 2000; Tirnaur and Biere, 2000). Recent work suggests an additional role for EB1 in mitosis where it may promote growth and interactions of microtubules within the central spindle (Rogers *et al.*, 2002).

Motor proteins represent another class of proteins that interact with microtubules. They cause bi-directional sliding along microtubules using energy acquired from ATP hydrolysis and play an important role in mitotic spindle function (Heald, 2000). There are two major groups of motor proteins: the kinesin superfamily that are generally plus end directed motors and cytoplasmic dynein, a minus end directed motor. Dynein is a large multi-subunit enzyme that works in conjunction with dynactin to drive vesicle movement along microtubules. Pertubation of either dynein or dynactin results in either loss of spindle pole integrity by preventing microtubules from focusing at the centrosome or defective spindle pole separation (Quintyne *et al.*, 1999). One of the roles of microtubule motors is to transport components to the MTOC in a cell cycle regulated manner. Dynein has been shown to mediate centrosome assembly, an idea supported by its interaction with several centrosomal proteins (Zimmerman and Doxsey, 2000). Indeed, γ-tubulin and pericentrin have been shown to move along microtubules in a dynein dependent manner towards centrosomes (Kubo *et al.*, 1999; Merdes *et al.*, 2000; Young *et al.*, 2000). LIS1, a protein implicated in brain development, together with CLIP-170 a plus-end tracking protein regulates dynein/dynactin binding to microtubules. It is thought that LIS1 is a regulated adapter between CLIP-170 and cytoplasmic dynein at sites involved in cargo-microtubule loading, and/or in the control of microtubule dynamics (Coquelle *et al.*, 2002; Faulkner *et al.*, 2000).

The kinesin superfamily includes both plus and minus end directed motors. The BimC family of plus end directed kinesins have the capacity to slide anti-parallel microtubules in order to form the mitotic spindle. These motors are particularly important for the self-

organisation of microtubules that randomly grow around chromatin in the absence of MTOCs (Kashina *et al.*, 1997). The plus end directed motor Eg5 is also implicated in centrosome function based on the observation that loss of Eg5 activity results in failure of centrosome separation and monopolar spindles (Mountain *et al.*, 1999). Monastrol, a small molecule inhibitor of Eg5, causes cells to arrest in mitosis with monopolar spindles (Kapoor *et al.*, 2000).

1.3 The mitotic spindle

In all eukaryotes, a microtubule based structure known as the mitotic spindle is responsible for accurate chromosome segregation during mitosis. Spindle assembly and function require localised regulation of microtubule dynamics and the activity of a variety of microtubule based motor proteins (Gaglio *et al.*, 1997; Heald and Nogales, 2002; Wittmann *et al.*, 2001). The primary structure of the spindle is an antiparallel array of microtubules with their minus ends focused and anchored at the spindle poles and their plus ends projecting towards the chromosomes. Chromosomes form the secondary structural element of the spindle. The kinetochore forms a site on the centromere with a high affinity for microtubule attachment during mitosis. It is thought that the small GTPase Ran, which is essential for nuclear import during interphase, can promote microtubule polymerisation in its active GTP form (Ohba *et al.*, 1999). Chromatin bound RCC1, a Ran guanine nucleotide exchange factor, induces high levels of Ran-GTP around mitotic chromosomes and locally promotes microtubule assembly (Carazo-Salas *et al.*, 2001). Interpolar microtubules represent filaments that originate from opposite poles and interact in an anti-parallel fashion to stabilise the bipolarity of the spindle. In addition, astral microtubules extend from the poles towards the cell cortex to orientate the spindle within the cell. Within the spindle, microtubule dynamics are regulated mainly by MAPs that stimulate polymerisation and protect microtubule ends from catastrophe-promoting factors. A protein named TPX2 is thought to regulate the density of spindle microtubules and is essential for the formation of a robust bipolar spindle (Wittmann *et al.*, 2000). Furthermore, TPX2 has been implicated in targeting the kinesin-related motor Xklp2 to the spindle (Wittmann *et al.*, 1998). Most recently, TPX2 was identified as a critical component involved in promoting the Ran-GTP regulated nucleation of microtubules in the vicinity of chromosomes (Gruss *et al.*, 2001).

1.4 Microtubule organising centres

The MTOC is the term given to the organelle that forms the central region from which microtubules extend and are stabilised during mitotic spindle formation and interphase. Pickett-Heaps first proposed the notion that sites must exist where microtubule nucleation is initiated and where the free ends of microtubules can be captured (Pickett-Heaps *et al.*, 1982). MTOCs form a group of morphologically diverse but functionally related organelles that contain homologous proteins, suggesting evolution from a single ancestor. They have many different forms within cells but always lie where a large number of microtubules converge into an area occupied by an amorphous mass of electron dense material (Brinkley, 1985).

The centrosome found in eukaryotic cells is the best documented MTOC, with most animal cells containing one or more centrosomes. The spindle pole body of both budding and fission yeast is another well researched MTOC and both of these organelles will be discussed in more detail in the next sections. *Drosophila melanogaster* (*Drosophila*: fruit fly) and *Caenorhabditis elegans* (*C. elegans*: nematode worm) represent two very useful systems for advancing our understanding of centrosomal regulation as they are relatively straight forward multicellular systems that are amenable to genetic analysis. By identifying mutations that produce mitotic or centrosome abnormalities, it is possible to identify proteins that are directly involved in centrosome and mitotic regulation. Many proteins found are highly conserved in other species including vertebrates hence these studies can provide important information that is relevant to these organisms. Recently the *Dictyostelium discoideum* (*Dictyostelium*: slime mould) amoeba has become a good model system for the comparative analysis of centrosomes, with many of the structural components characterised. However, the *Dictyostelium* centrosome represents an acentriolar centrosome with a unique mode of duplication which takes place in M phase and is not synchronised with DNA synthesis as in animals and yeast, implying that many components may not be conserved between these species (Ueda *et al.*, 1999).

1.4.1 Spindle pole bodies

In the budding yeast *Saccharomyces cerevisiae* (*S. cerevisiae*) microtubules are organised by a structure called the spindle pole body (SPB). Many of the components of the SPB have been identified genetically and biochemically (Knop *et al.*, 1999). The SPB is structurally different but functionally similar to the vertebrate centrosome. The functional

similarity means that advances in SPB biology may be applicable to the vertebrate centrosome. These similarities include the observation that the mechanism of microtubule nucleation is generally conserved between the SPB and the centrosome. Additionally, regulation of SPB and centrosome duplication share some common components. Important differences though are likely to include the proteins involved in assembling the SPB and the centriole (Adams and Kilmartin, 1999).

The *S. cerevisiae* SPB is a multi-layered cylindrical structure that is embedded in the nuclear membrane throughout the cell cycle and contains no centrioles (Adams and Kilmartin, 1999). In contrast, the spindle pole body of *Schizosaccharomyces pombe* (*S. pombe)* is different in that it spends most of interphase in the cytoplasm, immediately next to the nuclear envelope (Ding *et al.*, 1997). The SPB consists of three main electron dense layers: the inner, outer and central plaques. In addition, a modified region of the nuclear membrane forming a structure known as the half bridge is attached to one side. Microtubules are nucleated from the inner and outer plaques (Figure 1.3A). As with all MTOCs, the SPB is duplicated once during each cell cycle by a conservative mechanism. The first visible marker for duplication is seen in early G1, when a small satellite containing core cytoplasmic SPB components appears on the cytoplasmic side of the half bridge. It does not contain nuclear components, thus does not nucleate microtubules. In S phase this satellite enlarges to form the duplication plaque, the half bridge elongates and bends at the proximal end of the duplication plaque. The duplication plaque then inserts into the nuclear membrane, allowing the nuclear SPB components to assemble. Finally the Tub4p complex assembles and nucleates microtubules to complete the new SPB. Prior to mitosis the SPBs separate each retaining half of the bridge that connected them in the G2 and S phase, hence the name half bridge. The two SPBs are functionally distinct and it is the old SPB that migrates into the bud. SPB inheritance is regulated by the differential interaction of cytoplasmic microtubules with the mother and bud cortex (Pereira *et al.*, 2001). As the mitotic spindle disassembles, cytokinesis occurs and the two cells separate (Adams and Kilmartin, 2000). Defective SPB duplication will result in a mitotic arrest after the DNA has duplicated and a bud has formed in a mechanism similar to the spindle checkpoint in animal cells. If defects in SPB duplication or function do occur in the absence of a functional checkpoint mechanism, genetic instability can occur in yeast, due to chromosome mis-segregation (Chial and Winey, 1999). Chromosomal instability or aneuploidy represents a major phenotype of transformed cells.

In addition to their role in mitotic spindle formation, SPBs are also thought to play a role in late mitotic events (Hoyt, 2000). A signal transduction cascade involving cell cycle regulators known as the mitotic exit network (MEN) represents a spindle position checkpoint that ensures mitotic exit and cytokinesis only occur after migration of the nucleus into the bud. Tem1p binds to the spindle pole that migrates into the bud via the Bfa1p-Bub2p GAP complex and is kept inactive until late anaphase. At this point Lte1p, a putative GEF, is released from the cortex of the bud and activates Tem1p triggering the release of Cdc14p from the nucleolus and mitotic exit (Figure 1.3B). Defects in cytoplasmic microtubule interactions with the cell cortex and misalignment of the spindle delays Tem1p activation and mitotic exit, thus co-ordinating cell cycle progression with spindle positioning (Pereira *et al.*, 2000). In animal cells misaligned spindles also delay mitotic progression, raising the possibility that there is conservation of these processes between SPBs and centrosomes (O'Connell and Wang, 2000).

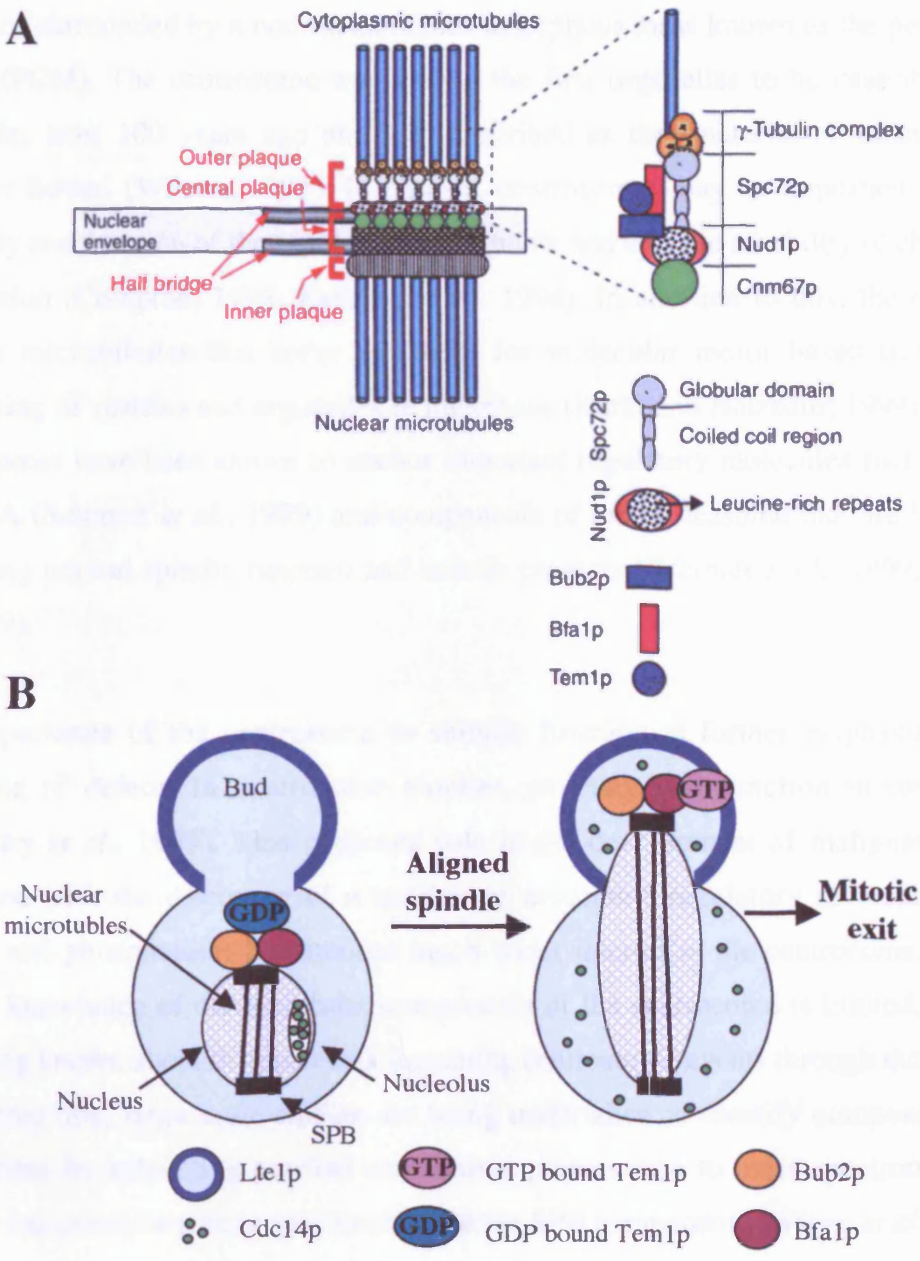

Figure 1.3 The yeast spindle pole body

(A) Illustration of the SPB substructures indicating the localisation of various components to the inner, central and outer plaques. **(B)** The spindle position checkpoint (SPC). The SPC ensures that mitotic exit and cytokinesis only occur after migration of the nucleus into the bud. This is achieved by making Tem1p activation dependent on nuclear migration. During interphase and most of mitosis Tem1p binds to the SPB that migrates into the bud via the Bfa1p-Bub2p GAP complex. Tem1p is probably kept in the inactive GDP-bound form through the Bfa1p-Bub2p GAP. With the migration of the SPB into the bud, Tem1p is exposed to the putative GEF Lte1p, which associates with the cortex of the bud until late anaphase and is then released into the cytoplasm. Lte1p activates Tem1p thereby triggering the release of Cdc14p from the nucleolus and mitotic exit (both taken from Pereira and Schiebel, 2001).

1.5 The Centrosome

The centrosome is the major MTOC in animal cells. It consists of two cylindrical centrioles surrounded by a non-membranous amorphous mass known as the pericentriolar matrix (PCM). The centrosome was among the first organelles to be described by cell biologists over 100 years ago and was described as the 'material of inheritance' by Theodor Boveri (Wilson, 1925). In mitosis, centrosomes play an important role in the assembly and function of the bipolar mitotic spindle and thus the reliability of chromosome segregation (Compton, 1998; Kellogg *et al.*, 1994). In addition to this, the centrosome anchors microtubules that serve as tracks for molecular motor based transport and positioning of vesicles and organelles in interphase (Karki and Holzbaur, 1999). Moreover centrosomes have been shown to anchor important regulatory molecules such as protein kinase A (Schmidt *et al.*, 1999) and components of the proteasome that are involved in regulating normal spindle function and mitotic progress (Schmidt *et al.*, 1999; Wigley *et al.*, 1999).

The importance of the centrosome in cellular function is further emphasized by the existence of defects in centrosome number, structure and function in tumour cells (Salisbury *et al.*, 1999). This proposed role in the development of malignant tumours combined with the discovery of a number of associated regulatory molecules such as kinases and phosphatases has aroused much wider interest in the centrosome. However, present knowledge of the molecular components of the centrosome is limited, with even less being known about the processes regulating centrosomal events through the cell cycle. To combat this, large scale studies are being undertaken to identify components of the centrosome by subjecting purified centrosome preparations to mass spectrometry. This method has previously been used to characterise SPB components (Wigge *et al.*, 1998). In addition to these proteomic approaches, genomic approaches using dsRNAi technology are being carried out in *C. elegans, Dictyostelium* and *Drosophila* to identify genes involved in mitotic progression including those that regulate centrosome and spindle function.

1.5.1 Centrosome structure and organisation

The centrosome is about 1 μm in diameter and occupies a central position in interphase cells near to the nucleus, hence the name centro-some or central body. In most animal cells it consists of two cylindrical centrioles, orientated perpendicular to each other, surrounded by a fibrous meshwork called the pericentriolar matrix (PCM) (Figure 1.4A). Centrioles

only exist in species that have at least some cells with cilia or flagella, where the centriole functions as a basal body. Centrosomes can elongate distal centriolar microtubules to produce a single non-motile primary cilium (Wheatley *et al.*, 1996). This structure has been implicated in essential cellular functions such as metering solution flow in the collecting ducts of the kidney (Pazour *et al.*, 2000). The centrioles are structurally similar to basal bodies, being constructed of nine triplets of short microtubules forming a cylinder. At the proximal end, there is a central rod with attached spokes, known as the cartwheel (Paintrand *et al.*, 1992). Centriole microtubules are polyglutamylated, a process that confers long term stability to centrioles and may control the association of microtubule associated proteins to centriole walls (Bobinnec *et al.*, 1998).

The two centrioles in a centrosome are structurally different, the mature 'mother' centriole has spoke like appendages and satellites at the end distal to its partner and is capable of nucleating a primary cilium (Figure 1.4B), (Sorokin, 1968). The immature 'daughter' centriole lacks the appendages and satellites. Markers to distinguish the two centrioles include cenexin/ODF2, ninein, and ε-tubulin that localise specifically to the mature centriole (Chang and Stearns, 2000; Lange and Gull, 1995; Mogensen *et al.*, 2000; Nakagawa *et al.*, 2001). During early S/G2 ε-tubulin is present in the older of the two centrosomes, but as the cell cycle progresses, there is eventually binding to the newer centrosome. This provides evidence that ε-tubulin is indicative of a maturation event in the centrosome, in the same way that cenexin/ODF2 is considered a marker of centriole maturation. Cenexin/ODF2 is a 96 kDa protein that is associated with the mature centriole and is acquired by the immature centriole at the G2/M phase transition (Lange and Gull, 1996). The two centrioles are linked at their proximal ends by a fibrous connection (see later section), although the molecular nature of this connection remains a mystery.

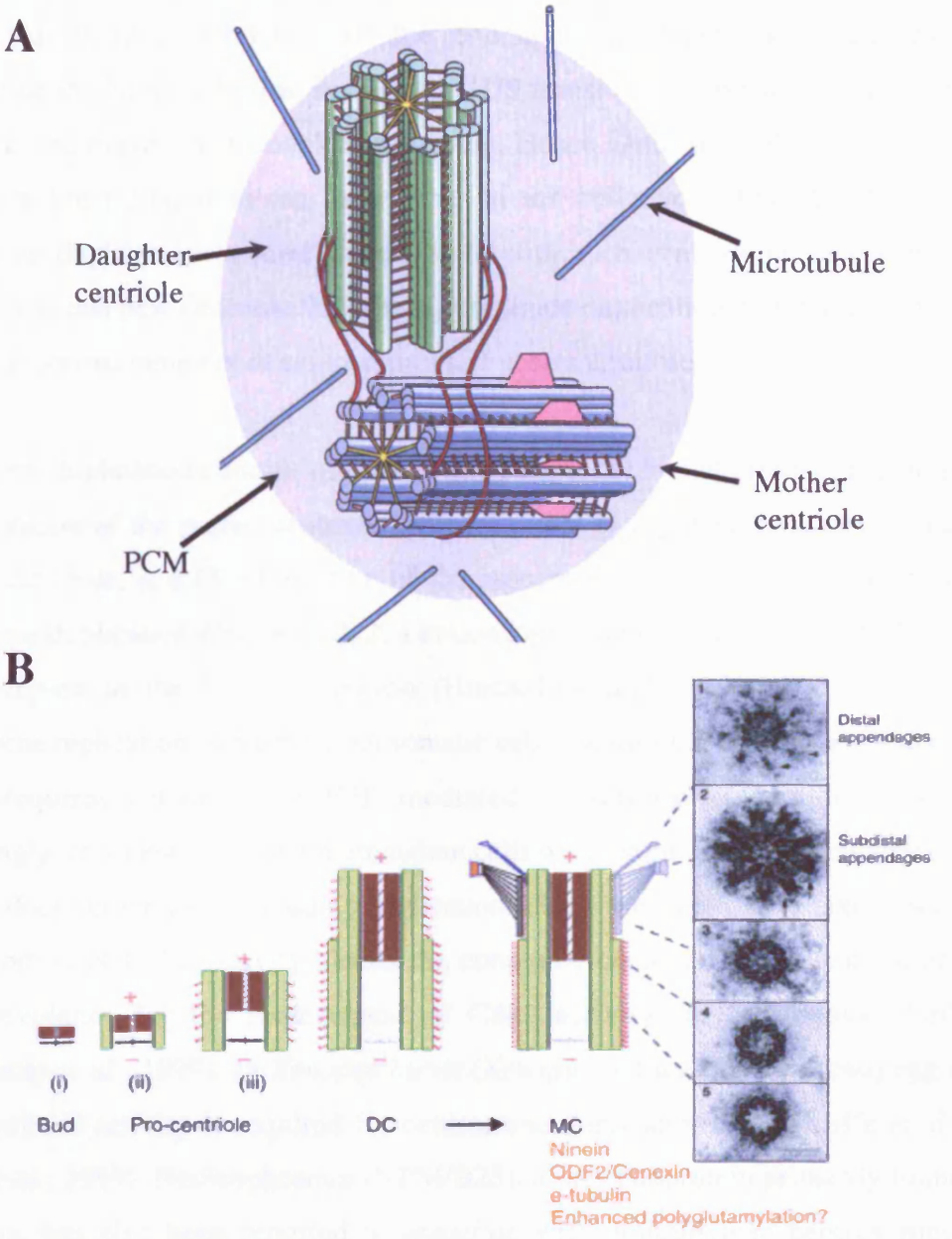

Figure 1.4 Centrosome structure

(A) A pair of centrioles is shown, each with nine triplets of microtubules. The centrioles are surrounded by the pericentriolar material (PCM) that nucleates microtubules. The maternal centriole has additional distal appendages. The proximal ends of the two centrioles are linked by a set of interconnecting fibres (red), taken from Urbani and Stearns, 1999. **(B)** Centriole-based assembly of the vertebrate centrosome. Each pro-centriole assembles from a centrin-containing bud (i) during S and G2 phase by growing singlet (ii), doublet (iii) and triplet microtubules (green) which are progressively polyglutamylated (red lines). It transforms into a fully differentiated daughter centriole (DC) in telophase. It further transforms during the next cell cycle, into a differentiated mother centriole (MC) bearing appendages, enriched in several distinct proteins. It is assumed that tubulin polyglutamylation is enhanced with time. The proximo-distal differentiation of the MC is demonstrated by serial sections on the right, taken from Bornens, 2002.

1.5.2 Centrosome duplication

Centrosomes duplicate once per cell cycle. This duplication and subsequent segregation in mitosis results in maintenance of the one centrosome/cell ratio (Stearns, 2001). Centrosome duplication begins during the G1/S transition in somatic cells and must be coupled to the events of the nuclear cell cycle. Hence centrosome duplication and DNA replication are initiated at the same time in the cell cycle. Like DNA replication, centrosome duplication is semi-conservative with each centrosome receiving one old centriole and one new centriole. Failure to coordinate duplication with the cell cycle could result in abnormal numbers of centrosomes and aberrant mitoses.

Centrosome duplication consists of three distinct steps: (1) loss of orthogonal configuration and separation of the paired centrioles, (2) synthesis of a procentriole next to each pre-existing centriole; and (3) elongation of the procentrioles (Figure 1.5). The initiation of centrosome duplication requires Cdk2, a kinase known to be activated as a Cdk2-cyclin A or E complex at the G1/S transition (Hinchcliffe and Sluder, 2001; Nigg, 1995). Centrosome replication in mammalian somatic cells requires Cdk2 complexed to cyclin A. It also requires activation of E2F mediated transcription (Meraldi *et al.*, 1999). Interestingly treatment of certain mammalian cells with hydroxyurea, which arrests cells in S phase, does not inhibit centrosome duplication. These same cells have high Cdk2 activity and inhibition of Cdk2 activity blocks the continued centrosome duplication, providing further evidence for the requirement of Cdk2 activity for centrosome duplication (Matsumoto *et al.*, 1999). In *Xenopus laevis* (*Xenopus*: African clawed toad) egg extracts Cdk2-cyclin E activity is required for centrosome duplication (Hinchcliffe *et al.*, 1999; Lacey *et al.*, 1999). Nucleophosmin (NPM/B23), a phosphoprotein primarily found in the nucleolus, has also been reported to associate with unduplicated centrosomes. Upon phosphorylation by Cdk2-cyclin E, NPM/B23 dissociates from centrosomes in what may be a prerequisite step for centrosomes to initiate duplication (Okuda *et al.*, 2000; Tokuyama *et al.*, 2001). The involvement of Cdk2 in both DNA replication and centrosome duplication demonstrates an underlying mechanism for the coordination of centrosome duplication with the cell cycle.

In addition to Cdk2, the SCF (Skp1-cullin-F box) complex, that targets proteins for destruction by the proteasome, is also thought to participate in the initiation of centrosome duplication. This is based firstly on the fact that the centrosomally localised SCF complex

is active at the G1/S transition and that inhibition of the proteasome blocks centrosome splitting (Freed *et al.*, 1999). Secondly, *Drosophila* SCF mutants result in aberrant centrosome duplication (Wojcik *et al.*, 2000). Furthermore, the calcium/calmodulin dependent protein kinase (CaMKII) is also required for the initiation of centrosome duplication in *Xenopus* egg extracts (Matsumoto and Maller, 2002). Specific inactivation of CaMKII initially blocks centrosome duplication, which can be restored by addition of CaMKII, indicating that calcium, calmodulin, and CaMKII are required for an essential step in initiation of centrosome duplication.

Following disorientation, the new pro-centriole starts to emerge from the side of the existing parental centriole. Localisation and functional studies elegantly reveal a role for ZYG-1, a *C. elegans* protein kinase, in centrosome duplication. ZYG1 is only present on centrosomes during centrosome duplication. Moreover, *zyg-1* mutants form monopolar spindles that contain only a single centriole implying that duplication did not take place (O'Connell *et al.*, 2001). Another family of proteins implicated in centrosome duplication are the Mps1 kinases and it is possible that ZYG-1 represents the *C. elegans* orthologue of Mps1 (O'Connell, 2002). Mouse Mps1 is thought to regulate centrosome duplication based on the observation that overexpression causes reduplication of centrosomes during S phase arrest. Control of centrosome duplication by mMps1 requires Cdk2. Inhibition of Cdk2 prevents centrosome reduplication and destabilises mMps1, causing its subsequent loss from centrosomes, suggesting that Cdk2 promotes the centrosome duplication function of mMps1 by regulating its stability during S phase (Fisk and Winey, 2001). Human Mps1, is a cell cycle-regulated kinase with maximal activity during M phase. It localises to kinetochores and its activity and phosphorylation state increase upon activation of the mitotic checkpoint. hMps1 is required for human cells to undergo checkpoint arrest in response to microtubule depolymerisation and is thus required for the spindle assembly checkpoint (Stucke *et al.*, 2002). Surprisingly, this study also concluded that hMps1 does not play a role in centrosome duplication in contrast to the study on mouse Mps1.

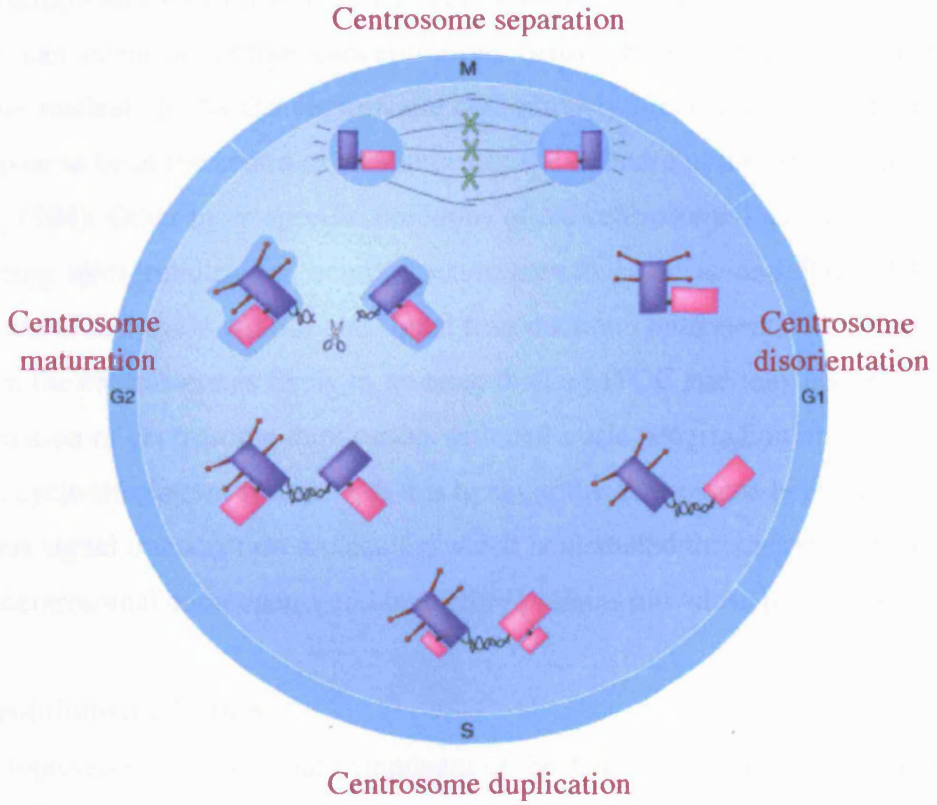

Figure 1.5 The centrosome cycle
Schematic illustration of a simplified view of the centrosome cycle in animal cells, The centriole/centrosome undergoes several transitions throughout the cell cycle. In G1, the centriolar pair consists of one mature (blue) and one immature (pink) centriole arranged in an orthogonal configuration that is relaxed (disorientation) towards the end of G1. The centrioles are likely to be connected via a proteinacous link (black). In S phase procentrioles are generated at a right angle to the mother centrioles and keep elongating until they achieve their full length in G2. Centriolar linkage disruption between the two parental centrioles occurs in late G2, as does centrosome maturation, involving the acquisition of additional pericentriolar material and of molecular markers for the centrosomal maturation of the younger parental centriole (adapted from Lange, 2002).

1.5.3 Centrosome function

The centrosome and its associated microtubules are viewed as the major organisers of the cytoskeleton, giving shape, polarity and internal order to animal cells. The main function of the centrosome is the nucleation of microtubules through the polymerisation of α and β tubulin heterodimers into polymers. The centrosome provides the conditions whereby nucleation can occur at tubulin concentrations below those required for spontaneous microtubule nucleation. As the centrosome continuously nucleates microtubules, it will always appear to be at the centre of an apparently stable microtubule array (Mitchison and Kirschner, 1984). Other more specific functions of the centrosome include the production of supporting microtubules for neurone axon growth (Ahmad and Baas, 1995). The identification of cell cycle control and signal transduction components on the centrosome implies that the centrosome is likely to be more than a MTOC and may also play a role in the coordination of centrosome duplication with cell cycle progression, in stress response and in cell cycle checkpoint control. For this to occur the centrosome is thought to interact with various signal transduction molecules, which is mediated through anchoring proteins that bring centrosomal components and regulatory proteins into close proximity.

1.5.4 Microtubule nucleation

The PCM represents the functional component of the centrosome, containing the γ-tubulin ring complexes (γ-TuRC) that nucleate and stabilise the minus ends of microtubules. γ-tubulin, a 55 kDa member of the tubulin superfamily, forms complexes with at least seven other proteins in the 25S γ-TuRC (Zheng *et al.*, 1991). Pure γ-tubulin is not capable of nucleating microtubules; for this two other proteins are needed, hGCP2 (equivalent to Spc97p) and hGCP3 (equivalent to yeast Spc98p). These three proteins form the minimal unit required for microtubule nucleation and have been termed the γ-TuSC (γ-tubulin small complex) (Oegema *et al.*, 1999). Two models have been proposed to explain how γ-tubulin nucleates microtubules. Firstly, the template model suggests that the γ-TuRC forms a template at the minus end of the microtubule, initiating growth of each of the 13 protofilaments through longitudinal contacts with γ-tubulin subunits within the γ-TuRC (Zheng *et al.*, 1995). The second idea is that γ-tubulin provides a short segment of preformed protofilament, nucleating a second filament by lateral contacts to α and β tubulin (Erickson and Stoffler, 1996). In the template model, γ-tubulin forms a single helix of subunits at the minus end, in contrast, in the protofilament model, the γ-TuRC is fully unwound, thus γ-tubulin extends into the microtubule. This observation is the basis of

work that is attempting to identify the correct method of nucleation by measuring how far γ-tubulin extends into the microtubule. To date, evidence suggests that γ-tubulin localises primarily to the ends of microtubules and does not extend very far into the microtubule implying that the template model is more likely to be correct (Moritz *et al.*, 2000; Wiese and Zheng, 2000).

γ-TuRCs are associated with the PCM through an interaction with a salt soluble centromatrix (Schnackenberg *et al.*, 1998). Salt extracted centrosomes, which lack γ-tubulin complexes, are unable to nucleate microtubules. The subsequent recruitment of γ-tubulin complexes from cytosolic extracts restores their nucleation capacity (Moritz *et al.*, 1998; Schnackenberg *et al.*, 1998). Pericentrin is thought to be important in anchoring γ-TuRCs in the centromatrix (Dictenberg *et al.*, 1998). Pericentrin is a highly conserved coiled coil protein, involved in the initial establishment of organised microtubule arrays. Anti-pericentrin antibodies are able to disrupt mitotic and meiotic divisions *in vivo* and block microtubule aster formation in *Xenopus* egg extracts (Doxsey *et al.*, 1994). A larger isoform of pericentrin, called pericentrin B or kendrin, exists in a complex with CG-NAP (centrosome and Golgi localised PKN-associated protein), which indirectly associates with γ-tubulin through binding the γ-TuRC proteins GCP2 and GCP3. Furthermore, pericentrin-B coimmunoprecipitates with PCM-1, a component of centriolar satellites (Li *et al.*, 2001). It is now thought that CG-NAP and pericentrin B/kendrin provide sites for microtubule nucleation in the mammalian centrosome by anchoring γ-TuRCs (Takahashi *et al.*, 2002). γ-tubulin complexes are also present in the cytoplasm where they have been suggested to act as a store for centrosomal recruitment (Moudjou *et al.*, 1996; Stearns and Kirschner, 1994). The extent of microtubule nucleation from the centrosome is regulated through the cell cycle. A steady increase in the amounts of both pericentrin and γ-tubulin is seen as cells progress through G2 into mitosis (Khodjakov and Rieder, 1999). As cells exit mitosis and enter G1, there is an abrupt decrease in the concentration of these components (Dictenberg *et al.*, 1998). Thus stimulation of γ-tubulin complexes to assemble at the centrosome directly affects the extent of microtubule nucleation.

Phosphorylation dependent mechanisms are thought to regulate microtubule nucleation, based on the observation that treatment of mitotic centrosomes with the phosphoepitope specific antibody MPM-2 or phosphatases, blocks microtubule nucleation (Centonze and Borisy, 1990). Cdk1-cyclin B is thought to be involved in the modification of microtubule

dynamics, perhaps by phosphorylating regulators of microtubule nucleation (Blangy *et al.*, 1995; Buendia *et al.*, 1992; Verde *et al.*, 1992). LK6, a *Drosophila* centrosomal kinase, has also been implicated in the regulation of microtubule nucleation as overexpression of active LK6 can cause defects in microtubule organisation in eggs and early embryos (Kidd and Raff, 1997). Although protein phosphorylation is a likely mode of regulation, few centrosomal substrates that directly regulate microtubule nucleation have been identified. γ-tubulin is not phosphorylated, however yeast Spc98p (GCP3), a conserved member of the γ-TuRC, is phosphorylated in a cell cycle dependent manner (Pereira *et al.*, 1998).

1.5.5 Microtubule release and anchoring

Following nucleation at the centrosome many microtubules are released and some may be captured and anchored at apical sites. This is the case in polarised epithelial cells such as cochlear cells, which display a non-radial, apico-basal microtubule array (Mogensen *et al.*, 1997). The mechanism for microtubule release is not fully understood but it is thought that severing proteins such as katanin may be involved (McNally and Thomas, 1998). Katanin, a heterodimeric microtubule-severing ATPase, is localised at mitotic spindle poles. The p60 katanin and C-terminal domain of p80 katanin both bind microtubules *in vitro*. Association of these two proteins results in an increased microtubule affinity and increased microtubule-severing activity *in vitro*. The N-terminal WD40 domain of p80 katanin acts as a negative regulator of microtubule disassembly activity and is also required for spindle pole localisation, possibly through interactions with other spindle pole proteins (McNally *et al.*, 2000). The deflagellation system of *Chlamydomonas* has provided a genetic approach to the problem of microtubule severing. The *FA* genes are essential for the regulated severing of axonemal microtubules during deflagellation, but whether these genes define new severing proteins or whether they are related to katanin activity remains to be determined (Quarmby and Lohret, 1999). Following severing, some microtubules are translocated to distant sites, dynein and dynactin have been shown to be responsible for microtubule translocation from the cell body into the axon in neurons (Ahmad and Baas, 1995).

Once severed, microtubules need to be anchored either in close proximity to the centrosome or at the apical sites to which they have been translocated. Various proteins are known to be involved in microtubule capping or anchoring including ninein, NuMA and the TACC family of proteins in combination with XMAP215/chTOG/Msps. Ninein

localises to the centrosome throughout the cell cycle and is also present at apical sites in cochlear cells where the minus ends of microtubules accumulate (Bouckson-Castaing *et al.*, 1996). Evidence suggests that ninein is released from the centrosome, translocated with the microtubules, and is responsible for the anchorage of microtubule minus ends to the apical sites. Thus ninein is a non-nucleating microtubule minus end associated protein which may have a dual role as a minus-end capping and anchoring protein (Mogensen *et al.*, 2000). Ninein, together with CEP110, has also been implicated in the maturation of a daughter centrosome into a mother centrosome as they both appear on the daughter centrosome during the telophase-G1 transition, concomitant with the maturation of the daughter centrosome into a mother centrosome (Ou *et al.*, 2002). The protein PCM-1 localises to centriolar satellites, cytoplasmic granules enriched at the centrosome, which are thought to be involved in microtubule anchoring (Kubo *et al.*, 1999). PCM-1 is a 228 kDa protein that associates with the PCM throughout the cell cycle but does appear to decrease at the onset of mitosis. It contains an ATP/GTP binding motif and is very acidic. The function of PCM-1 was originally suggested to involve inhibition of microtubule nucleation or regulation of centriole duplication (Balczon *et al.*, 1995). However, inhibition or depletion of PCM-1 leads to the formation of aggregates containing pericentrin, centrin and ninein, whose appearance correlates with inhibition of radial microtubules consistent with a role in the assembly of microtubule anchoring complexes (A. Merdes, personal communication).

The TACC family of proteins is a relatively new family of centrosomal associated proteins. D-TACC was identified following microtubule spin down experiments from *Drosophila* embryos, where it associated weakly with microtubules and strongly with centrosomes. It interacts with microtubules through its interaction with Msps. This interaction influences the number and length of centrosomal microtubules, i.e. an increase in D-TACC and Msps correlates with an increase in the number and length of microtubules (Gergely *et al.*, 2000b).

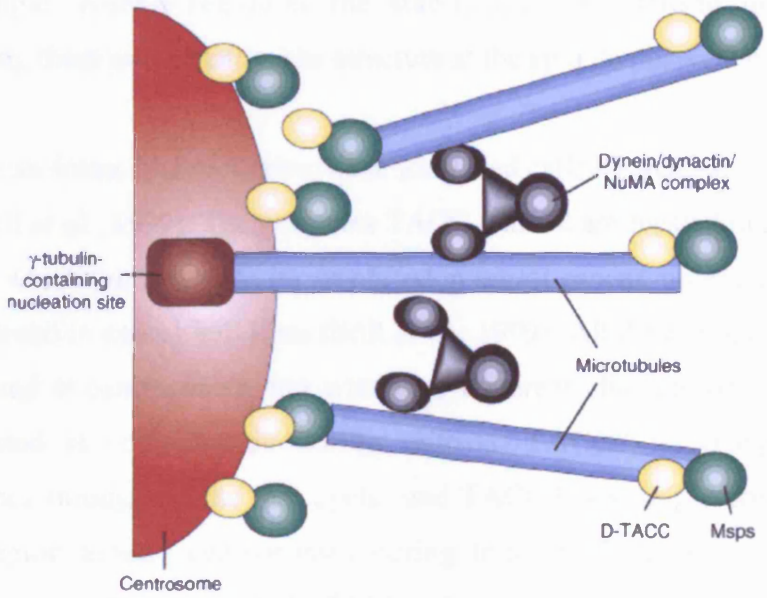

Figure 1.6 The role of D-TACC and Msps in microtubule stabilization
D-TACC (yellow) and Msps (green) co-localize at the periphery of the centrosome (red). These proteins cooperate to stabilize centrosomal microtubules (blue) in two ways. First, they bind to and stabilize the minus ends of microtubules that have been released from their -tubulin-containing nucleation sites (brown). Second, the concentration of D-TACC and Msps at the centrosome ensures that they bind to the plus ends of the centrosomal microtubules as they grow out from the centrosome. In this way, centrosomal microtubules are stabilized by D-TACC and Msps. The centrosomal microtubules also interact with motor-protein complexes, such as dynein/dynactin/NuMA (black), which function to keep the released microtubules focused at the poles. Taken from Lee *et al*, 2001.

Msps is recruited to the centrosome by D-TACC and it is thought that D-TACC and Msps cooperate to stabilise microtubules (Figure 1.6), firstly by binding and stabilising the released minus ends of microtubules. Secondly, D-TACC and Msps bind to the plus ends of microtubules as they grow out of the centrosome, thus stabilising them. Following the release of centrosomal microtubules from their nucleating sites, many are captured by complexes of microtubule-based motor proteins containing NuMA, dynein and dynactin, which tether microtubules to the poles (Merdes and Cleveland, 1997; Merdes *et al.*, 1996). For example, NuMA regulates the stabilisation of focused microtubule ends by crosslinking them into a matrix like structure at the spindle poles (Dionne *et al.*, 1999).

Three human forms of TACC have been identified called TACC-1, 2 and 3 (Gergely *et al.*, 2000a; Still *et al.*, 1999). The genes for TACC 1 and 2 are located in areas of chromosome 8 and 10, which are known to be amplified in breast cancer, upregulated TACC3 has also been observed in cancer cell lines (Still *et al.*, 1999). All three human TACC proteins are concentrated at centrosomes, but with very different characteristics: TACC1 is weakly concentrated at centrosomes during mitosis; TACC2 is strongly concentrated at centrosomes throughout the cell cycle; and TACC3 is strongly concentrated in a more diffuse region around centrosomes during mitosis (Gergely *et al.*, 2000a). TACC3 functions in a similar manner to D-TACC, where overexpression leads to an increase in the number and length of centrosomal microtubules (Gergely *et al.*, 2000a). In addition TACC3 is shown to recruit chTOG, the human homologue of Msps, to the centrosome (Lee *et al.*, 2001).

1.5.6 Bipolar spindle formation

When present centrosomes play a dominant role in bipolar spindle formation during mitosis in most animal cells. However, oocytes from mice, *Drosophila* and *Xenopus* do not contain centrosomes but are still capable of forming bipolar spindles during meiosis (Gard, 1992). In such systems, microtubules are nucleated from multiple sites near the chromatin and are organised into a bipolar spindle through the action of minus end directed motor proteins such as dynein (Heald *et al.*, 1996; Merdes and Cleveland, 1997). Ncd, a kinesin like protein with minus end directed motor activity has a major role in focusing acentrosomal poles (Matthies *et al.*, 1996). Msps also localises to the poles of acentrosomal spindles and plays a crucial role in ensuring spindle bipolarity, mediated by both Ncd and D-TACC (Cullen and Ohkura, 2001). Functional mitotic spindles have also

been shown to form in the absence of centrosomes in *Sciara* embryos. The microtubules were apparently nucleated at or near the chromosomes and the cells successfully underwent mitosis but with a greatly reduced distance between the daughter nuclei (de Saint Phalle and Sullivan, 1998). Furthermore, centrosome free spindles can be assembled *in vitro* around DNA coated beads in *Xenopus* egg extracts (Heald *et al.*, 1996). If centrosomes are microsurgically removed from BSC-1 cells before the completion of S phase, karyoplasts (acentrosomal cells) enter and complete mitosis but postmitotic karyoplasts arrest before S phase. These postmitotic karyoplasts assemble a MTOC that contains γ-tubulin and pericentrin, but not centrioles (Hinchcliffe *et al.*, 2001). In contrast to these observations, if centrosomes are completely destroyed by laser microsurgery new centrosomes do form by *de novo* assembly. Initially, clouds of PCM containing γ-tubulin and pericentrin appear, followed by formation of centrioles (Khodjakov *et al.*, 2002).

Plant cells do not contain centrosomes, microtubules are instead thought to be nucleated by the nucleus, even though a γ-tubulin homologue exists (Joshi and Palevitz, 1996; Shibaoka and Nagai, 1994). Plant cells have to breakdown their cell wall and re-construct it in order to produce daughter cells; this difference in cell morphology suggests a different regulatory pathway for cell growth compared to vertebrate cells and could explain why they divide in the absence of centrosomes. Meiosis is a specialised cell division that differs from mitosis, most strikingly due to the absence of centrosomes at the poles of female meiotic spindles (Waters and Salmon, 1997). This argues for the existence of another mechanism to control spindle assembly and establishment of bipolarity. It is clear that cell division can occur in the absence of centrosomes, but in the presence of dominant centrosomes, bipolar spindle formation is more efficient (Heald *et al.*, 1997). Thus highlighting the importance of maintaining functional centrosomes.

1.5.7 Cytokinesis and G1/S progression

The first and most striking evidence for the involvement of centrosomes in cytokinesis comes from Sluder and Reider's experiments using lasers or microsurgery to remove centrosomes resulting in an inability to pass though cytokinesis (Hinchcliffe *et al.*, 2001; Khodjakov and Rieder, 2001). Further evidence comes from the observation that before cytokinesis there is a dramatic splitting of the centrioles, where the mother centriole moves into the midbody. This also demonstrates that when, the centrioles appear to split, there is still something connecting them (Piel *et al.*, 2000). Furthermore transient, postanaphase

repositioning of the centrosome controls the release of central microtubules from the midbody and the completion of cell division, so that in the absence of centrosomes defective cytokinesis ensues (Piel *et al.*, 2001). The p160ROCK (Rho-associated coiled-coil-containing) protein kinase is a centrosomal component that is bound to the mother centriole and intercentriolar linker. Inhibition of p160ROCK in G1 induces centrosome splitting and inhibition after anaphase triggers migration of the mother centriole to the midbody, inducing mitotic exit. Thus, p160ROCK is required for centrosome positioning and centrosome-dependent exit from mitosis (Chevrier *et al.*, 2002). SPBs are also thought to play a role in late mitotic events coordinating the MEN signal transduction cascade, see section 1.4.1 (Hoyt, 2000; Pereira *et al.*, 2000).

In the absence of centrosomes, somatic cells arrest in G1, and do not initiate DNA replication (Hinchcliffe *et al.*, 2001; Khodjakov and Rieder, 2001). It is possible that the cells do not completely divide and remain attached by thin intercellular bridges, this might activate a checkpoint that monitors aberrant centrosome numbers or perhaps the presence of excess DNA (Andreassen *et al.*, 2001). Alternatively, centrosomes might be required to activate DNA replication perhaps through the recruitment or concentration of molecules that are essential for the initiation of DNA synthesis (Hinchcliffe *et al.*, 1999; Lacey *et al.*, 1999). Therefore it appears that a centrosome dependent pathway integrates spatial controls with the decision of completing cell division and this may require the repositioning of the centrosome organelle. Moreover, a consequence of having a centrosome requirement for cell-cycle progression is to ensure that dividing animal cells receive the appropriate number of functional centrosomes.

1.6 Centrosome regulation by phosphorylation

The regulation of cell cycle changes in centrosome structure and function are controlled largely by protein phosphorylation (Figure 1.7) (Fry *et al.*, 2000a). This idea is strengthened by the localisation of several distinct protein kinases at the centrosome and an increase of phosphorylated epitopes at the centrosome during mitosis (Vandre *et al.*, 1984). Cyclin dependent kinases (Cdks) represent a group of important regulators of the cell cycle that also play key roles in centrosome regulation. Other highly conserved mitotic protein kinases are the Polo and Aurora families in which mutations block mitotic progression. These kinases have been implicated in a number of mitotic events including APC

activation, spindle formation, sister chromatid separation, mitotic progression and cytokinesis (Cullen *et al.*, 2000; Glover *et al.*, 1998). In addition to kinases, phosphatases are also thought to regulate centrosome function. Protein phosphatase 1α and protein phosphatase 4 associate with centrosomes, acting in competition with centrosomal kinases (Andreassen *et al.*, 1998; Brewis *et al.*, 1993). PP4 is required for nucleation, growth and stabilisation of microtubules at centrosomes based on the finding that reduced expression of PP4 causes a reduction of γ-tubulin and consequently the number of microtubules nucleated at the centrosome (Helps *et al.*, 1998; Sumiyoshi *et al.*, 2002). PP1 forms a complex with the NIMA-related kinase Nek2, to coordinate the timing of centrosome separation with cell cycle progression, a phenomenon discussed in later sections (Helps *et al.*, 2000). Table 1.1 details protein kinases that have been associated with the centrosome and indicates their putative centrosomal functions.

Table 1.1 Centrosome associated kinases and phosphatases.

The table indicates those protein kinases and phosphatases that have been directly localised to the centrosome. Adapted from Fry et al., 2000a.

Centrosome process	Kinase/Phosphatase	Substrate
Microtubule nucleation	Cdk1 PKA LK6 PP4	CP60 AKAP450
Centrosome duplication	Mps1p DdNek2 ZYG-1	
Centrosome maturation	Cdk1 NIMA Plk Aurora-A	Eg5 Cdk1-cyclin B Cdc25, Asp D-TACC
Centrosome separation	Plk Aurora-A Nek2 PP1	Pavarotti Eg5 C-Nap1 Nek2/C-Nap1
Centrosome assembly	X-Nek2B	
Cytokinesis	Aurora-C? Plk	

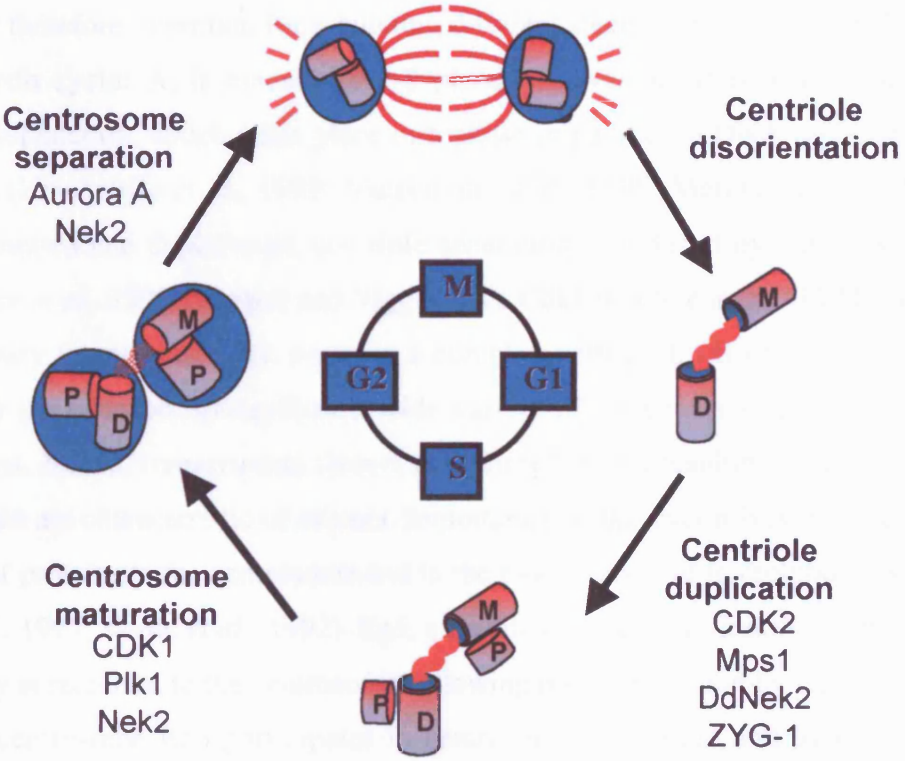

Figure 1.6 Control of the centrosome cycle by protein kinases.
The major morphological changes in structure and organisation of the centrosome are shown with respect to cell cycle position. Kinases thought to control each stage are indicated above the relevant point (adapted from Fry *et al.*, 2000).

1.6.1 Cyclin dependent kinases

Cdks play key roles in cell cycle regulation during initiation of both DNA replication and mitosis in all eukaryotic organisms (Norbury and Nurse, 1992; Nurse, 1990). They consist of a small catalytic subunit that only becomes active in the presence of a cyclin regulatory subunit. There are several different Cdks that become active at different stages of the cell cycle and are therefore important for regulating different stages of the cell cycle. Cdk2, in a complex with cyclin A, is essential for S phase progression. It is also required for centrosome duplication, which takes place in S phase in parallel to DNA replication, see section 1.5.2 (Hinchcliffe *et al.*, 1999; Matsumoto *et al.*, 1999; Meraldi *et al.*, 1999). In addition to centrosome duplication, centriole separation is induced by Cdk2-cyclinA/E activity (Lacey *et al.*, 1999; Meraldi and Nigg, 2001). Cdk1 is active at the G2/M transition and is necessary for mitotic entry, when in a complex with cyclin B (Nigg, 1995). This active kinase complex phosphorylates a wide variety of substrates including histones, nuclear lamins, MAPs, transcription factors and phosphatases, resulting in dramatic cell changes, which are characteristic of mitosis. Importantly, Cdk1-cyclin B is involved in the recruitment of proteins to the centrosome and in the modification of microtubule dynamics (Blangy *et al.*, 1995; Verde *et al.*, 1992). Eg5, a member of the bimC kinesin related motor protein family is recruited to the centrosome following phosphorylation by Cdk1-cyclin B. Once at the centrosome Eg5 participates in centrosome separation and bipolar spindle assembly (Blangy *et al.*, 1995; Sawin and Mitchison, 1995). Increased nucleation of microtubules from isolated centrosomes can be stimulated in *Xenopus* egg extracts by the addition of Cdk1-cyclin B complexes (Buendia *et al.*, 1992; Ohta *et al.*, 1993). This, in addition to its clear association with the centrosome from the onset of mitosis (Bailly *et al.*, 1989), implies that Cdk1-cyclin B activity is important for the upregulation of the microtubule nucleating capacity of centrosomes in mitosis.

1.6.2 Polo-like kinases

The polo-like kinases (Plks) are a family of cell cycle regulated serine/threonine kinases that have multiple roles during mitosis (Glover *et al.*, 1998; Nigg, 1998). The original polo gene was identified through a recessive lethal mutation in *Drosophila*. Conserved polo like homologues have now been identified in *S. cerevisiae* (Cdc5p), *S. pombe* (Plo1p), *Xenopus* (Plx) and mammals (Plk1, 2 and 3) (Golsteyn *et al.*, 1994; Sunkel and Glover, 1988). At the onset of mitosis, when their protein levels and kinase activity peaks, Plks function in centrosome maturation and establishment of the bipolar mitotic spindle. Evidence for this

comes from antibody microinjection experiments in human cells and *Drosophila* mutants that demonstrate the frequent appearance of monopolar spindles and immature centrosomes (Lane and Nigg, 1996; Sunkel and Glover, 1988). These phenotypes are likely to be due to the role of Plk in γ-tubulin recruitment through activation of Asp. Asp is a microtubule associated protein that accumulates at and focuses the minus ends of microtubules to maintain their close proximity to the centrosome. Asp phosphorylation by polo promotes the microtubule nucleating and organising capacity of the centrosome possibly through the recruitment γ-tubulin (do Carmo Avides *et al.*, 2001).

In addition to their roles in centrosome maturation, Plks are responsible in part for the transition through mitosis; however, lack of Plk does not prevent the initiation of mitosis but instead leads to an abnormal mitosis (Sunkel and Glover, 1988). Plk contributes directly to the activation and subsequent inactivation of Cdk1-cyclin B, a process required for mitotic exit. Initially, Plx1 is able to bind, phosphorylate and activate Cdc25c, the phosphatase responsible for dephosphorylating and activating Cdk1-cyclin B (Kumagai and Dunphy, 1996). Plks are also important upstream regulators of the anaphase-promoting complex/cyclosome (APC/C), a key component of the ubiquitin dependent proteolytic degradation pathway that targets mitotic cyclins for destruction based on the observation that in the absence of Plk activity, mitotic cyclins fail to be destroyed (Descombes and Nigg, 1998). Plk is thought to directly regulate the APC/C by phosphorylating and activating the APC/C components Cdc16 and Cdc27 (Kotani *et al.*, 1998). This study also demonstrated that PKA is capable of phosphorylating subunits of the APC/C and it was suggested that the activity of the APC/C is determined by the balance of Plk1 and PKA activities.

Finally, Plks are also implicated in the temporal and spatial coordination of cytokinesis as overexpression of Plk1 in mammalian cells results in an increased frequency of multinucleated cells (Mundt *et al.*, 1997). Further support for this comes from the predominance of cytokinesis defects at various stages of spermatogenesis in *Drosophila* polo mutants (Carmena *et al.*, 1998). In addition, loss of fission yeast plo1 function impairs the formation of a division septum as plo1 is required for recruiting medial ring components to the cell (Bahler *et al.*, 1998; Ohkura *et al.*, 1995). Moreover polo co-localises with Pavarotti, a kinesin related motor protein that is required for the formation of the contractile ring that is essential for cytokinesis (Adams *et al.*, 1998).

1.6.3 Aurora kinases

The Aurora kinases are another family of mitotic serine/threonine kinases that perform multiple functions during mitotic progression. Aurora kinases have been identified in many organisms resulting in a large number of different names. To simplify this confusing nomenclature, it was recently proposed that the three major types of Aurora kinase be called Aurora-A, -B and -C (Nigg, 2001). Aurora-A is required for spindle formation while Aurora-B is required for chromosome condensation and cytokinesis, less is known about the function of Aurora-C. Mammals express all three Aurora kinases, whereas *C. elegans* and *Drosophila* only express two, A and B. Both *S. pombe* and *S. cerevisiae* contain only a single Aurora kinase, Ark1 and Ipl1, respectively and it is thought that this single kinase executes functions that are separately implemented by distinct Aurora-A and Aurora-B kinases in higher systems (Chan and Botstein, 1993; Petersen *et al.*, 2001).

Aurora-B is a chromosome passenger that is involved in cytokinesis and chromosome architecture (Adams *et al.*, 2001). Cells depleted of the Aurora-B kinase show only partial chromosome condensation at mitosis associated with reduced histone H3 phosphorylation. Aurora-B is localised to the central spindle by an interaction with other chromosome passenger proteins including INCENP and survivin (Kaitna *et al.*, 2000; Speliotes *et al.*, 2000; Wheatley *et al.*, 2001). Cells lacking Aurora-B also fail to undergo cytokinesis, showing a reduced density of microtubules in the central spindle, accompanied by a failure to correctly localise the Pavarotti kinesin-like protein (Giet and Glover, 2001). Aurora-C is localised to the centrosome during mitosis from anaphase to cytokinesis, suggesting that this may also have a role in late mitosis (Kimura *et al.*, 1999). However, contrasting data suggests that Aurora-C expression is restricted to spermatogenesis only at the time when cells assemble meiotic spindles (Hu *et al.*, 2000; Tseng *et al.*, 1998).

Aurora-A, is a centrosomal kinase that has multiple functions in cell cycle progression (Dutertre *et al.*, 2002). It is present in the PCM from the beginning of S phase until early G1, when it is targeted for proteasomal destruction by the ubiquitin dependent pathway (Castro *et al.*, 2002; Giet and Prigent, 2001; Roghi *et al.*, 1998). Perhaps one of the major roles of Aurora-A is in centrosome maturation, as various proteins are recruited to the centrosome following Aurora-A dependent phosphorylation. For example, D-TACC, a regulatory protein that is essential for normal spindle function in the early embryo that interacts with Msps to organise and stabilise spindle microtubules (Gergely *et al.*, 2000b)

is phosphorylated by Aurora-A. Both proteins are reduced at the mitotic spindle poles of *Drosophila aurora-A* mutants (Giet *et al.*, 2002). Furthermore, mutations that cause mislocalisation of Aurora-A result in loss of γ-tubulin and centrosomin from the centrosome implying that Aurora-A is also required for the recruitment of these proteins to the centrosome (Berdnik and Knoblich, 2002; Hannak *et al.*, 2001). Aurora-A is involved in centrosome separation and spindle assembly (Giet *et al.*, 1999b). Evidence for this comes from the observation that a monopolar spindle is often formed in *Drosophila aurora-A* mutants (Glover *et al.*, 1995). However, this defect in separation may purely be a consequence of a defect in centrosome maturation. A bipolar spindle can form in these mutants, but one of the poles has no centrosome whilst the other contains multiple centrosomes (Giet *et al.*, 2002). Furthermore, the kinesin related protein Eg5, which is implicated in centrosome separation, is phosphorylated by Aurora-A (Giet *et al.*, 1999a).

Aurora-A is considered as a candidate oncogene as it is overexpressed in many tumours and maps to chromosome 20q13, a region frequently amplified in cancers (Bischoff *et al.*, 1998). Moreover, overexpression of Aurora-A results in transformation of NIH3T3 cells as well as centrosome amplification and aneuploidy, a phenotype that occurs at premalignant stages in transformed cells (Goepfert *et al.*, 2002; Zhou *et al.*, 1998). It has recently been shown that Aurora-A gives rise to these extra centrosomes through defects in cell division rather than through defects in centrosome duplication (Meraldi *et al.*, 2002). Cumulatively, these results suggest that Aurora-A overexpression and centrosome amplification are linked to tumour development and progression and may serve as early markers in tumourigenesis.

1.7 NIMA

The most well characterised and conserved centrosomal kinases are the Cdks, Plks and Aurora kinases. Their central role in the regulation of the eukaryotic cell cycle, and the centrosome is clear. However, in addition to these, the family of NIMA-related kinases is now emerging as another major conserved regulator of centrosome function. NIMA (Never in mitosis A) is the founding member of this family of protein kinases. It was identified through analysis of temperature sensitive mutant strains of the filamentous fungus *Aspergillus nidulans (A. nidulans)*. Early studies demonstrated that NIMA function is required specifically at the G2/M transition as a shift to the restrictive temperature causes a

G2 arrest in *nimA* mutants. Upon return to the permissive temperature, mitosis is rapidly initiated, characterised by formation of the mitotic spindle and chromosome condensation (Bergen *et al.*, 1984; Oakley and Morris, 1983; Osmani *et al.*, 1987).

The product of *nimA* (designated NIMA) has serine/threonine kinase activity and is capable of phosphorylating β-casein and histone H3 *in vitro.* (De Souza *et al.*, 2000; Lu *et al.*, 1993; Osmani *et al.*, 1991b). NIMA is cell cycle regulated with its protein levels and kinase activity low in G1, reaching maximal levels in early mitosis followed by a rapid decrease upon chromosome segregation (Osmani *et al.*, 1991b; Ye *et al.*, 1995). These changes are due to protein turnover in combination with NIMA phosphorylation. The catalytic domain of NIMA is in the N-terminus. Mutation of the putative autophosphorylation site in the N-terminus of NIMA (FXXT) inhibits NIMA kinase activity, suggesting that autophosphorylation plays a part in its activation in G2 (Pu *et al.*, 1995). In addition to autophosphorylation, a NIMA-activating kinase may be responsible for NIMA activation. The C-terminus contains multiple PEST sequences and numerous CDK1 phosphorylation sites, both of which may be involved in targeting NIMA for destruction. However, NIMA does not contain typical destruction boxes which are involved in targeting proteins for ubiquitin dependent proteolysis in mitosis. Deletion of the C-terminus does not completely inactivate NIMA but does prevent functional complementation of a temperature sensitive mutation of *nimA*, showing it to be essential for function. Partial C-terminal deletion of NIMA generates a highly toxic kinase that is not degraded during mitosis, leading to disrupted mitotic progression indicating that mitotic proteolysis of NIMA is required for mitotic exit (Pu and Osmani, 1995).

NIMA cooperates with Cdk1 to promote mitotic entry, with the activation of both kinases required for mitotic entry. In fact, Cdk1-cyclin B plays a role in the mitosis specific activation of NIMA (Osmani *et al.*, 1991a; Osmani and Ye, 1996). At mitosis, NIMA becomes enriched on chromatin and subsequently localises to the mitotic spindle and spindle pole bodies. NIMA can phosphorylate histone H3, possibly explaining its ability to promote chromosome condensation (De Souza *et al.*, 2000). Moreover the involvement of NIMA in the nuclear and SPB localisation of cyclin B provides further evidence for the role of NIMA in mitotic entry (Wu *et al.*, 1998). Overexpression of NIMA drives cells into premature mitosis from any stage in the cell cycle, characterised by premature nuclear envelope breakdown, chromatin condensation and mitotic spindle formation (Ye *et al.*,

1995). Mitotic entry can occur in the absence of activated NIMA if the bimE gene, coding for a subunit of the APC/C, is mutated. However, entry into mitosis in the absence of NIMA activation results in major mitotic defects that affect both the organisation of the nuclear envelope and mitotic spindle (Osmani *et al.*, 1991a). Interestingly, expression of NIMA in *S. pombe*, *Xenopus* oocytes or human cells also promotes mitotic events. Moreover, dominant-negative versions of NIMA can adversely affect the progression of human cells into mitosis, as they do in *A. nidulans*, suggesting that NIMA specific substrates that mediate mitotic events are conserved between species (Lu and Hunter, 1995; O'Connell *et al.*, 1994).

1.7.1 NIMA-related kinases

Many important cell cycle regulators exhibit evolutionary conservation and much work has been carried out to identify whether NIMA-related kinases (Neks) are conserved in higher eukaryotes and whether they too regulate the cell cycle (Osmani and Ye, 1996). The search for NIMA homologues has led to the description of Neks in several species ranging from fungi to humans. Despite all showing sequence similarity, the only *bona fide* functional NIMA homologue that has been identified is the *nim-1* gene of *Neurospora crassa* (Pu *et al.*, 1995). The degree of similarity between NIMA and its homologues in other species may reflect the degree of similarity between MTOCs in those respective organisms.

Structural relatives of NIMA have been identified in *S. cerevisiae* and *S. pombe,* termed Kin3 and Fin1, respectively (Jones and Rosamond, 1990; Krien *et al.*, 1998). Fin1 is a non-essential, cell cycle regulated protein whose expression is controlled both by transcriptional and translational mechanisms. Its abundance and kinase activity peak in mitosis and overexpression promotes premature chromosome condensation. However, it is not clear whether this represents normal chromosome condensation as it is not associated with histone H3 phosphorylation or condensin recruitment (Krien *et al.*, 2002). In addition, Fin1 has been implicated in spindle formation and nuclear envelope integrity (Krien *et al.*, 2002; Krien *et al.*, 1998). Furthermore, an alternative role for Fin1 in Plo1 recruitment to the SPB during mitotic commitment has been suggested (Grallert and Hagan, 2002). Less is known about the function of Kin3, the budding yeast homologue of NIMA, except that it is not essential for growth, conjugation or sporulation (Barton *et al.*, 1992; Jones and Rosamond, 1990; Schweitzer and Philippsen, 1992). Fa2p, a NIMA homologue in

Chlamydomonas reinhardtii is again non-essential for survival. Mutations in Fa2p result in a delay in the onset of mitosis combined with axonemal severing, both of which could result from disrupted centrosome assembly, alternatively, they might represent two separate mechanisms regulated by the same kinase (Mahjoub *et al.*, 2002; Marshall, 2002). Pfnek1, a NIMA related kinase found in the human malaria parasite *Plasmodium falciparum,* contains a region that is similar to an activation site conserved among MEKs (MAPK/ERK kinases) that is not present in other Neks (Dorin *et al.*, 2001). TpNrk represents a further Nek found in *Tetrahymena thermophilia*; this has a similar structure to NIMA and appears to play a role in the *Tetrahymena* cell cycle, but no specific function has yet been identified (Wang *et al.*, 1998).

Several vertebrate Neks have been identified mainly by degenerate PCR termed Nek1-Nek11, however the sequence similarity to NIMA is restricted to the catalytic domain. Nek1 was identified in human and mouse by degenerate PCR and in a phosphotyrosine expression library screen, respectively and encodes a dual specificity kinase having the capacity to phosphorylate serine, threonine and tyrosine residues (Letwin *et al.*, 1992; Schultz and Nigg, 1993). Mouse Nek1 is specifically expressed in the nervous system indicating that some vertebrate Neks may have functions unrelated to cell cycle control (Arama *et al.*, 1998). However, high expression in the gonads and differential expression in developing germ cells also suggests a role for Nek1 in meiosis (Arama *et al.*, 1998; Letwin *et al.*, 1992; Rhee and Wolgemuth, 1997; Tanaka *et al.*, 1997). Interestingly, Nek1 is mutated in a laboratory strain of mouse that suffers from severe developmental defects (Upadhya *et al.*, 2000). Mouse Nek3 and Nek4 cloned from mouse cDNA libraries represent orthologues of human Nek3 (88% identical) and STK2 (82% identical) (Chen *et al.*, 1999). The function of Nek3 is unknown as it is not cell cycle regulated and does not disrupt cell cycle progression upon overexpression (Tanaka and Nigg, 1999).

The kinase domains of murine Nek6 and Nek7 are highly similar to each other and to the F19H6.1 protein kinase of *C. elegans* and phylogenetic analysis suggests that these three proteins constitute a novel subfamily within the NIMA family of serine/threonine kinases. In contrast to the other documented NIMA-related kinases, Nek6, Nek7 and F19H6.1 harbor their catalytic domain in the C-terminus of the protein (Kandli *et al.*, 2000). Both Nek6 and Nek7 were purified as upstream kinases of the p70 ribosomal S6 kinase (Belham *et al.*, 2001), however, it has been demonstrated that Nek6 is not responsible for the

phosphorylation of S6 kinase *in vivo* (Lizcano *et al.*, 2002). Nercc1 was identified as a Nek6 binding protein and represents another member of the NIMA family of protein kinases. This has also been identified as Nek8 in a separate study (Holland *et al.*, 2002). Interestingly Nercc1 shares several features with NIMA including an N-terminal catalytic domain, Cdk1 phosphorylation sites involved in its mitotic regulation and several PEST regions that regulate protein stability (Roig *et al.*, 2002). Nercc1/Nek8 is activated in mitosis by phosphorylation to play a central role in mitotic progression by regulating spindle function and chromosome regulation (Roig *et al.*, 2002). Nercc1/Nek8 also contains a central domain with homology to RCC1, a guanine nucleotide exchange factor for the GTPase Ran, implying that regulation of Neks by GTPases may represent important pathways in the control of mitotic entry (Roig *et al.*, 2002). Phosphorylation of Bicd2, the human homolog of the *Drosophila* protein Bicaudal D, is correlated with disruption of the microtubule dependent localisation of Bicd2, implying a role for Nek8 in cell cycle independent microtubule dynamics (Holland *et al.*, 2002).

The most recently identified Nek is Nek11 (long and short isoforms), whose expression and subcellular localisation are cell cycle regulated with increased levels through S to G2/M phase. It is thought that Nek11 proteins represent novel DNA replication/damage responsive kinases suggesting that Nek11 has a role in the S phase checkpoint (Noguchi *et al.*, 2002). In general, the structural similarities between mammalian Neks and NIMA may not be indicative of common functions. Full understanding of the regulation and function of all known NIMA-related kinases would greatly facilitate our knowledge of the importance of this diverse family of kinases in cell cycle control.

1.8 Nek2 kinase

Nek2 represents the closest structural relative of NIMA in the human genome, being 44% identical in their catalytic domains, and for this reason Nek2 has become the most extensively studied of the vertebrate Neks (Fry, 2002). Vertebrate Nek2 homologues have been identified in mouse, pig, human and *Xenopus* (Figure 1.8A). The first non-vertebrate homologue of Nek2 was identified in *Dictyostelium discoideum* (Graf, 2002). As for NIMA, the most closely related proteins to Nek2 in budding and fission yeast are KIN3 and Fin1p respectively. Mammalian Nek2 is a 46 kDa serine/threonine protein kinase that was identified by degenerate PCR, using primers specific to NIMA catalytic domain

(Schultz *et al.*, 1994). Loci for the Nek2 gene were localised to both chromosome 1 and chromosome 14, suggesting that one may represent a pseudogene. Interestingly both chromosome loci have previously been genetically linked to two different forms of Usher syndrome, although as yet no evidence for the involvement of Nek2 in this disorder has been published.

Nek2 comprises an N-terminal catalytic domain and a C-terminal non regulatory domain containing two regions of coiled coils (Figure 1.8B). The catalytic domain contains motifs typical of serine/threonine protein kinases and Nek2 has been shown to phosphorylate substrates on serine and threonine residues (Fry *et al.*, 1995; Hanks and Hunter, 1995). The C-terminal coiled coil immediately downstream of the kinase domain bears a striking resemblance to a leucine zipper motif having six heptad-spaced leucine residues. It is thought that the leucine zipper promotes homodimerisation which in turn leads to trans-autophosphorylation within the C-terminal region (Fry *et al.*, 1999). All Nek2 related kinases contain a coiled coil in their C-terminal region directly following the kinase domain, indicating that despite lack of sequence homology in the C-terminal domain, homodimerisation and autophosphorylation are likely to be common properties to all these kinases. For example, Nercc1 kinase activity is regulated through a C-terminal coiled coil domain, which is necessary for its homodimerisation and subsequent autophosphorylation (Roig *et al.*, 2002). *Dictyostelium* Nek2 is also predicted to contain a similar leucine zipper motif in its C-terminus (Graf, 2002).

The *Xenopus* homologue of Nek2 exists as two variants termed X-Nek2A and X-Nek2B, which differ only in their C-terminal region. In adults, X-Nek2B shows highest expression in the ovary while it is also the major form in oocytes, eggs and early stages of embryogenesis. X-Nek2A appears after the gastrula-neurula transition in embryos and is expressed at the highest level in adults in the testis (Uto *et al.*, 1999). Mouse Nek2 is also expressed at high levels in the testis and moderate levels in the ovary (Arama *et al.*, 1998). In the testis, Nek2 is expressed primarily in pachytene and diplotene spermatocytes where the protein is localised to meiotic chromosomes within the nucleus (Rhee and Wolgemuth, 1997). In the ovary, the highest expression is again seen in meiotically active oocytes and actively dividing follicle cells (Tanaka *et al.*, 1997). In addition to germ cells, mouse Nek2 is expressed in the intestine, thymus and skin, all of which represent highly mitotic organs. In the mouse embryo, Nek2 is expressed mainly in the brain, a tissue that is still

proliferating (Tanaka *et al.*, 1997). Porcine Nek2 mRNA is expressed throughout oocyte maturation, whereas the protein is only detected on chromosomes in metaphase II (Fujioka *et al.*, 2000). The expression studies carried out in mouse and pig did not distinguish between possible Nek2A and Nek2B isoforms.

1.8.1 Nek2 cell cycle regulation

Unlike NIMA expression, which peaks in mitosis and remains high in a prometaphase mitotic arrest, Nek2 expression is high in S and G2 but low during mitotic arrest (Figure 1.8C). This continues to remain low throughout G1 (Fry *et al.*, 1995). Nek2 kinase activity reflects its expression being low in G1, increasing in S and G2 and decreasing in mitosis. The kinase activity of Nek2 is subject to several levels of regulation that ensure it is activated at the correct time during the transition from interphase to mitosis and is then irreversibly inactivated in mitosis to guarantee that mitotic entry and exit can progress normally.

Various modes of Nek2 regulation come into play throughout the cell cycle such as regulation of protein abundance at the level of transcription/translation and regulation of protein turnover. Gene expression studies have shown that Nek2 mRNA levels are highest in S and G2 (M. Pillai and A.M. Fry, unpublished results; Iyer *et al.*, 1999; Ren *et al.*, 2002). The binding of E2F4 to the Nek2 promoter in quiescent WI-38 cells, provides evidence that Nek2 is directly repressed in G1 (Ren *et al.*, 2002). E2F4 is a member of the E2F transcription factor family that represses genes in G0 and G1. This operates through recruitment of the Rb family members p130 and p107, which inhibit formation of active transcription complexes by recruiting histone deacetylases to suppress chromatin remodelling. Interestingly, $p130^{-/-}/p107^{-/-}$ mouse embryo fibroblasts demonstrate an increase in the level of Nek2 mRNA even in the absence of serum suggesting that tumours lacking p130 and p107 are likely to have substantially elevated levels of the Nek2 kinase (Ren *et al.*, 2002). Elevated levels of Nek2 have been identified in Ewing tumour derived cell lines following microarray analysis (Wai *et al.*, 2002). Furthermore, gene expression studies of breast tumour samples indicates that Nek2 is elevated in more advanced tumours, as shown by lymph node involvement (W. Lingle, personal communication). This provides some evidence that Nek2 may be involved in tumour progression but more work needs to be carried out to define a clear role for Nek2 in tumourigenesis.

Protein destruction represents a second mode of Nek2 regulation, in common with NIMA which is destroyed by the proteasome during mitosis via an APC/C mediated pathway (Ye *et al.*, 1998). Some proteins are targeted for destruction by the ATPase-dependent 26S proteasome folowing ubiquitylation of lysine residues. Ubiquitylation is carried out by a series of enzymes involving an E1 ubiquitin activating enzyme, an E2 ubiquitin conjugating enzyme and an E3 ubiquitin ligase. One example of an E3 ubiquitin ligase is the APC/C. This is a multi-subunit enzyme that requires the binding of additional adapter proteins, either Cdc20 or Cdh1, to promote ubiquitylation of target proteins (Morgan, 1999). The mechanism of action of these adapter proteins is not fully understood, but it is thought that binding to the APC/C may induce a conformational change in the complex that activates the catalytic site. Cell cycle dependent increases in APC/C activity are correlated with increased binding of Cdc20 or Cdh1. All known APC/C-Cdc20 substrates contain a destruction box (D box) composed of the approximate sequence RXXLXXXXN (Glotzer *et al.*, 1991). APC/C-Cdh1 is also able to recognise this D box motif; however, proteins targeted for destruction specifically by APC/C-Cdh1 generally contain a KEN box motif. Deletion of one or both of these motifs from target proteins results in complete stabilisation of the target protein. Nek2 contains a putative D box and KEN box in its C-terminus that may direct ubiquitylation by the APC/C-Cdh1 or APC-Cdc20. Indeed degradation of Nek2 via the APC/C-Cdh1 pathway has been suggested using experiments in *Xenopus* egg extracts (Pfleger and Kirschner, 2000), However, APC/C-Cdh1 is only activated late in mitosis, whereas the abundance and kinase activity of Nek2 decreases at the G2/M transition.

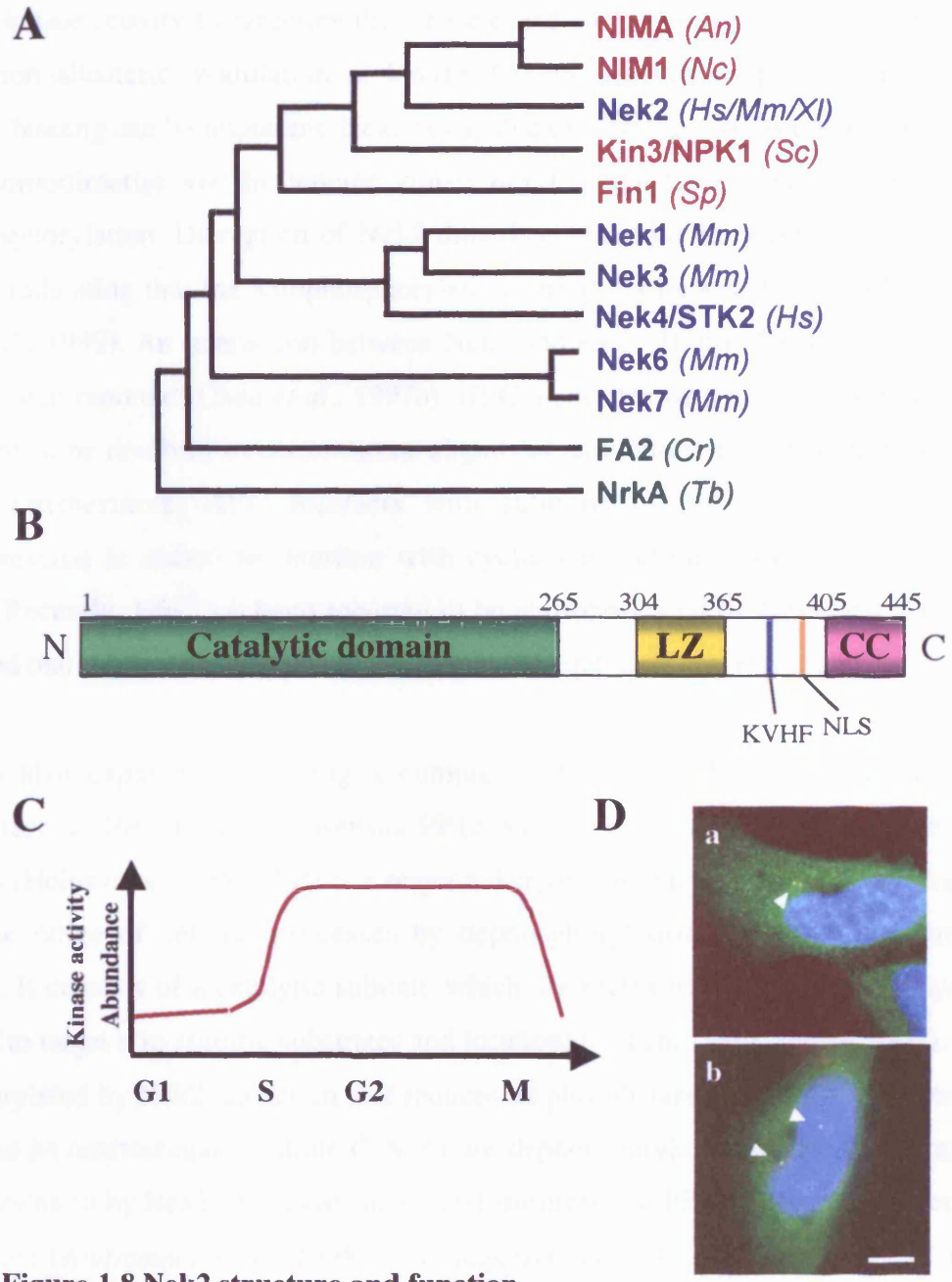

Figure 1.8 Nek2 structure and function

(A) Phylogenetic tree of the NIMA-related kinase (Nek) family. Adapted from Kandli *et al.* 2000. **(B)** Schematic diagram of the human Nek2 indicating the catalytic domain (CAT), leucine zipper (LZ), coiled coil domain (CC), putative nuclear localisation signal (NLS) and PP1c binding site (KVHF). The numbers represent the amino acid position at which domains start and end. **(C)** Schematic graph indicating the cell cycle regulation of Nek2 abundance and kinase activity, showing peak levels in S/G2 and a low level in mitosis. **(D)** HeLa cells were transiently transfected with GFP (a) or GFP-Nek2 (b), fixed after 24 hours and analysed by indirect immunofluorescence microscopy using anti-γ-tubulin antibodies to reveal centrosomes. Note the split centrosomes following overexpression of Nek2. Scale bar, 10 μm.

Another likely method of Nek2 regulation is through the formation of protein-protein complexes. Complex formation can either activate or inhibit kinases. For a start, it can regulate kinase activity by targeting the kinase to the correct cellular location or substrate. In addition allosteric modulation of kinase domain structure or prevention of kinase inhibitor binding can be important. Nek2 is capable of forming various complexes. Firstly, it can homodimerise via the leucine zipper motif in the C-terminus, allowing trans-autophosphorylation. Disruption of Nek2 dimerisation results in decreased Nek2 kinase activity, indicating that the autophosphorylation activity is important in Nek2 regulation (Fry *et al.*, 1999). An interaction between Nek2 and HEC (Highly Expressed in Cancer) has also been reported (Chen *et al.*, 1997b). HEC associates with mitotic centromeres and is thought to be involved in chromosome alignment and mitotic progression (Chen *et al.*, 1997a). Furthermore, HEC interacts with subunits of the 26S proteasome and overexpression is shown to interfere with cyclin destruction in mitosis (Chen *et al.*, 1997b). Recently, HEC has been reported to be phosphorylated by Nek2 and it has been suggested that this is necessary for chromosome segregation (Chen *et al.*, 2002).

Nek2 is also capable of forming a complex with the catalytic subunit of protein phosphatase 1 (PP1c) via a consensus PP1c binding motif (KVHF) present in its C-terminus (Helps *et al.*, 2000). PP1 is a major eukaryotic protein phosphatase that regulates a diverse range of cellular processes by dephosphorylation of serine and threonine residues. It consists of a catalytic subunit, which associates with a number of regulatory subunits to target it to specific substrates and locations (Cohen, 1990; Cohen, 2002). PP1 is phosphorylated by Nek2, an action that reduces its phosphatase activity. In addition, both Nek2 and its centrosomal substrate C-Nap1 are dephosphorylated by PP1 following their phosphorylation by Nek2. PP1 exists as several isoforms, the PP1α isoform localises to the centrosome (Andreassen *et al.*, 1998). This suggests that PP1α, Nek2 and C-Nap1 form a ternary complex at the centrosome, which is thought to regulate centriole cohesion, an idea discussed in detail in the next section.

1.8.2 Nek2 function

Although Nek2 shows highest similarity to NIMA in sequence and *in vitro* substrate specificity, there are still several important differences between them such as the lack of Cdk1 phosphorylation sites in the C-terminus of Nek2. Nek2 has been implicated in both meiosis and mitosis of male and female germ cells as well as mitosis in adult tissues. Nek2

expression is shown to peak during the meiotic stages of spermatogenesis and is also present in meiotically active oocytes (Arama *et al.*, 1998; Rhee and Wolgemuth, 1997; Tanaka *et al.*, 1997; Uto *et al.*, 1999). Nek2 is also found in mitotically dividing cells, such as embryos and cultured cells, suggesting that it has functions both in meiotic and mitotic cell cycles. Indeed, evidence suggests that porcine Nek2 may control the entry or progression of metaphase II perhaps playing a role in chromosome condensation due to its chromosomal localisation in metaphase II (Fujioka *et al.*, 2000). Unlike NIMA, overexpression of active Nek2 does not induce chromosome condensation but instead induces premature centrosome separation (Figure 1.8D) suggesting a role for Nek2 in centrosome cohesion (Fry *et al.*, 1998a). In addition to its role in centrosome cohesion, Nek2 has also been implicated in centrosome assembly and maintenance (Fry *et al.*, 2000b; Fry *et al.*, 1998a; Uto and Sagata, 2000) as well as in chromosome condensation due to its apparent association with mitotic chromosomes (Ha Kim *et al.*, 2002). More recently, the *S. pombe* NIMA homologue, Fin1 has also been implicated in mitotic commitment (Grallert and Hagan, 2002), reinforcing the idea of Nek2 being a mitotic regulator and having a role in diverse cell cycle events.

1.8.4 Centrosome separation

The observation that overexpression of Nek2 induces centrosome splitting at any stage of the cell cycle led to the idea that under normal cellular conditions Nek2 dependent phosphorylation stimulates the loss of cohesion between duplicated centrosomes in late G2. Transfection of active, but not inactive, Nek2 leads to the rapid appearance of split centrosomes in 50% of transfected cells (Fry *et al.*, 1998a). Only two dots are observed suggesting that the mother and daughter centrioles are separating rather than separation of procentioles from parental centrioles. Premature separation induced by Nek2 overexpression is not accompanied by other signs of mitotic onset such as spindle formation or chromosome condensation. In addition to Nek2, Cdk2, in association with either cyclin A or E, is also effective at inducing centrosome splitting (Meraldi and Nigg, 2001). Furthermore, microtubule depolymerisation induces centrosome splitting. However, this drug-induced splitting also requires kinase activity and can be specifically suppressed by the kinase dead mutant of Nek2 but not Cdk2. Other centrosomal kinases including Aurora-A and Plk1 do not cause centrosome splitting, implying that splitting is specific and not due to non-specific kinase activity. In a further study, activation of PKA in cells with a cell permeable cAMP analogue was also reported to cause centrosome splitting

perhaps via phosphorylation of the centriolar protein centrin (Lutz *et al.*, 2001). However, in these experiments calyculin A, a PP1 inhibitor was used, hence splitting could be due to PP1 inhibition rather than PKA activation.

How does Nek2 induce centrosome separation? The observation of electron dense material connecting centrioles of isolated centrosomes as well as the recovery of isolated centrosomes in pairs provides evidence for the existence of a dynamic intercentriolar linkage (Bornens *et al.*, 1987; Paintrand *et al.*, 1992). However, the molecular components of this stucture have yet to be identified. The Nek2 substrate C-Nap1 was identified following a yeast two-hybrid interaction screen using Nek2 as the bait (Fry *et al.*, 1998b). It was also independently identified as Cep250 using antibodies from autoimmune patients that are reactive to the centrosome (Mack *et al.*, 1998). C-Nap1 is a 281 kDa protein, consisting of two large coiled coil regions separated by a short non-coiled coil region with non-coiled coil N- and C- termini (Figure 1.9A). Unlike Nek2, which is most abundant in testis tissue, C-Nap1 is expressed at comparable levels in all tissues. Immunoelectron microscopy with domain specific antibodies has been used to demonstrate that both terminal domains and the hinge region of C-Nap1 all localise to the proximal end of centrioles (Figure 1.9B), however no evidence to suggest that C-Nap1 molecules span the entire distance between the two parental centrioles has been obtained, indicating that a putative linker structure must contain additional proteins (Mayor *et al.*, 2000). Due to this localisation, it is possible that C-Nap1 is involved in centriole cohesion perhaps by anchoring or regulating essential components of an intercentriolar linkage. Antibody-mediated interference of C-Nap1 function provides further evidence for the involvement of C-Nap1 in centriole cohesion as it too promotes splitting of parental centrioles, independently of microtubules or microfilaments (Mayor *et al.*, 2000). In addition, centrosome splitting is also induced by overexpression of truncated but not full length C-Nap1.

C-Nap1 is cell cycle regulated with its centrosomal protein levels diminishing in early mitosis and re-accumulating in late telophase/early G1 when daughter cells are still connected by post-mitotic bridges (Figure 1.9C and D) (Mayor *et al.*, 2000). The decrease from the centrosome in mitosis is thought to be due to C-Nap1 dissociation mediated by phosphorylation rather than being due to ubiquitin dependent proteolysis (Mayor *et al.*, 2002).

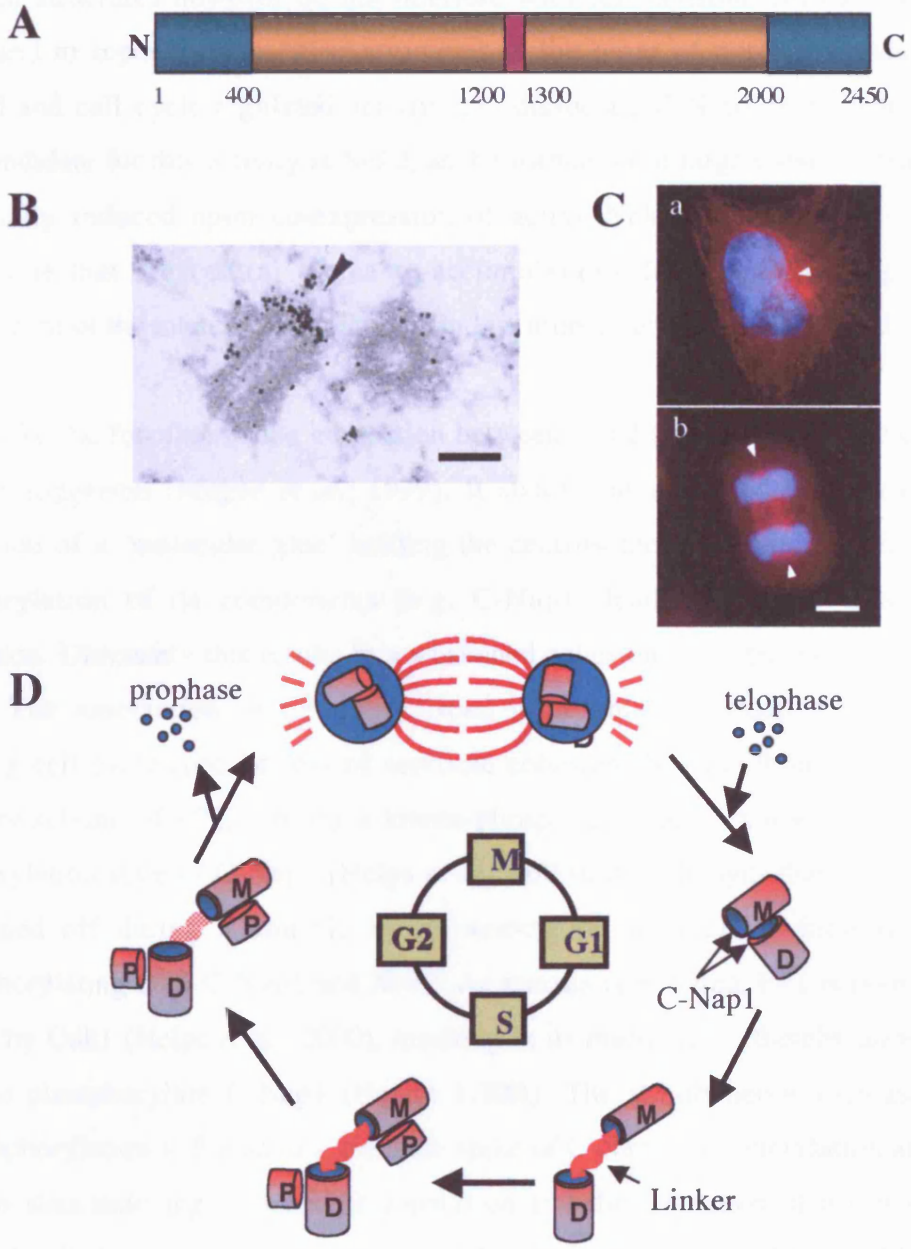

Figure 1.9 Cell cycle regulation of C-Nap1

(A) Schematic diagram of C-Nap1, orange boxes represent the two large coiled coil regions with the hinge region (pink box) connecting them and globular terminal domains (green boxes). Numbers represent amino acids positions. **(B)** Negative staining immunoelectron microscopy using anti-C-Nap1 antibodies on isolated centrosomes. Staining at the proximal end of the centriole is indicated (arrowhead). Scale bar 0.2 μm. **(C)** In interphase there is an extensive microtubule network emanating from the centrosome that contains C-Nap1 (a). Once the bipolar spindle is formed, C-Nap1 disappears from the centrosome (b). Arrowheads indicate the position of the centrosomes. Scale bar, 10 μm. **(D)** This schematic model summarises current information about the function and subcellular localisation of C-Nap1during the cell cycle (adapted from Mayor *et al.*, 2000).

Overexpression of full-length C-Nap1 causes the formation of large structures that embed the centrosome and impair its microtubule nucleation activity. These centrosome associated structures however do not interfere with cell division. Instead, centrosomes were found to separate from these structures at the onset of mitosis, indicating that a localised and cell cycle regulated activity can dissociate C-Nap1 from centrosomes. A prime candidate for this activity is Nek2, as the formation of large C-Nap1 structures was substantially reduced upon co-expression of active Nek2 (Mayor *et al.*, 2002). The mechanisms that are central to the re-accumulation of C-Nap1, leading to the re-establishment of the intercentriolar linkage in late mitosis, are not yet fully understood.

A model for the function of the interaction between Nek2 and C-Nap1 at the centrosome has been suggested (Mayor *et al.*, 1999). It states that increased Nek2 results in the degradation of a 'molecular glue' holding the centrosomes together. This is due to the phosphorylation of its components (e.g. C-Nap1) leading to their dissociation or degradation. Ultimately this results in a weakened cohesion between centrosomes (Figure 1.10A). The association of PP1 with Nek2 represents an effective mechanism for regulating cell cycle specific loss of centriole cohesion. Nek2 is thought to represent a regulatory subunit of PP1, forming a kinase-phosphatase complex that can influence the phosphorylation state of C-Nap1 (Helps *et al.*, 2000). It is thought that Nek2 activity is kept turned off during S and G2 by its association with PP1, which is constantly dephosphorylating both C-Nap1 and Nek2. As mitosis is initiated, PP1 is phosphorylated possibly by Cdk1 (Helps *et al.*, 2000), resulting in its inactivation, thereby allowing Nek2 kinase to phosphorylate C-Nap1 (Figure 1.10B). The simultaneous increase in Nek2 autophosphorylation will lead to a dramatic spike of C-Nap1 phosphorylation at the G2/M transition thus inducing centrosome separation and the formation of a bipolar mitotic spindle. Further evidence for this is the observation that inhibition of PP1 induces centrosome splitting to the same extent as Nek2 (Meraldi and Nigg, 2001). More recently, it has been shown that PP1c also binds inhibitor 2 at the same time as Nek2. This regulatory molecule is capable of increasing Nek2 kinase activity by inhibiting PP1c. Evidence for this comes from the observation that overexpression of inhibitor 2 induces centrosome splitting to the same extent as Nek2 overexpression (Eto *et al.*, 2002).

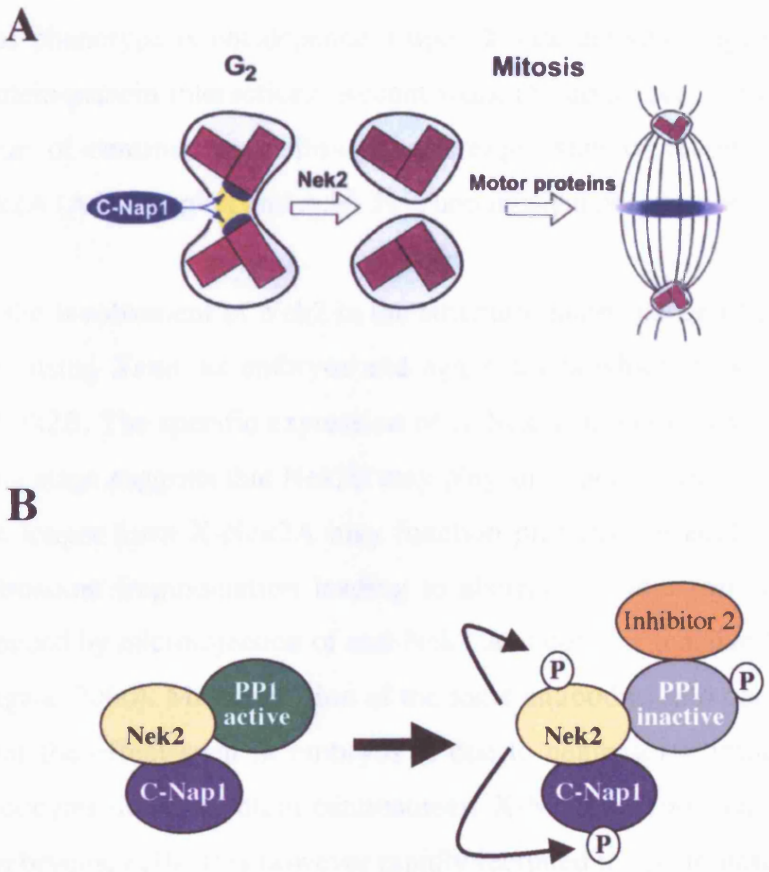

Figure 1.7 Existing model for the role of PP1, C-Nap1 and Nek2 in centrosome cohesion

(A) It is proposed that Nek2 by phosphorylating C-Nap1, causes the removal of a bridge structure between the two pairs of centrioles during the G2/M transition. Separation of the centrioles leads to formation of the bipolar mitotic spindle (Mayor *et al.,* 1999). **(B)** Nek2, C-Nap1 and PP1 form a ternary complex at the centrosome. PP1 keeps Nek2 kinase activity turned off until PP1 is inactivated at mitosis either by phosphorylation or inhibiton by inhibitor 2, allowing C-Nap1 phosphorylation to occur.

1.8.5 Structural integrity of centrosomes

In addition to centrosome cohesion, Nek2 is involved in the structural maintenance of centrosomes. This is based on the observation that long term overexpression of Nek2 in adult human cells leads to centrosome disintegration (Fry *et al.*, 1998b). Unlike centriole splitting, this phenotype is not dependent upon kinase activity, suggesting that it is the result of protein-protein interactions. Recent work in human cell lines also demonstrates fragmentation of centrosomes following overexpression of recombinant catalytically inactive Nek2A (A.J. Faragher and A.M. Fry, unpublished observations).

Support for the involvement of Nek2 in the structural maintenance of centrosomes comes from studies using *Xenopus* embryos and egg extracts which only contain the shorter isoform X-Nek2B. The specific expression of X-Nek2B in oocytes and early embryos up to the neurula stage suggests that Nek2B may play an important role in early development and that the longer form X-Nek2A may function primarily in adult tissues (Uto *et al.*, 1999). Centrosome fragmentation leading to aberrant spindle formation and cleavage failure is induced by microinjection of anti-Nek2 antibodies or inactive Nek2 into embryos (Uto and Sagata, 2000). Microinjection of the same antibodies into oocytes had no effect, implying that the effect seen in embryos is due to centrosome impairment as meiotic spindles in oocytes do not contain centrosomes. X-Nek2B is not required for entry into mitosis in embryonic cells. It is however rapidly recruited to sperm basal bodies following their incubation in egg extract, a process accompanied by Nek2B phosphorylation (Fry *et al.*, 2000b). If depleted from egg extracts, a decrease in the assembly of microtubule asters and recruitment of γ-tubulin is observed, thus demonstrating the requirement of X-Nek2B for efficient assembly of a functional centrosome.

1.8.6 Chromatin condensation

There is some controversy over whether Nek2 associates with chromosomes. An association with condensing chromosomes is observed in meiotic cells of mouse and pig (Fujioka *et al.*, 2000; Rhee and Wolgemuth, 1997). However, other studies have not observed localisation of Nek2 to chromosomes in human or *Xenopus* cells (Fry *et al.*, 1998a; Uto and Sagata, 2000). Furthermore, Nek2 can be activated *in vivo* by okadaic acid induced G2/M progression which is accompanied by induction of chromosome condensation (Ghosh *et al.*, 1998; Rhee and Wolgemuth, 1997). Interestingly, okadaic acid induced activation of Nek2 is dependent on Erk and p90Rsk2, both downstream effectors

of the MAPK pathway. Moreover p90Rsk2 phosphorylates Nek2 *in vitro* (Di Agostino *et al.*, 2002). These observations suggest that activation of Nek2 by the MAPK pathway at the G2/M may play a role in chromosome condensation. Recent work has also demonstrated that Nek2 localises to condensed chromosomes in mouse cells during prophase and metaphase, an association that disappears in anaphase. In telophase, Nek2 reappears at the midbody within the cytokinetic bridge of two daughter cells (Ha Kim *et al.*, 2002). Such multiple localisations is characteristic of proteins that influence multiple events during mitosis such as Plks and chromosome passengers (Adams *et al.*, 2001; Glover *et al.*, 1998). Functional assays in *Xenopus* egg extracts do not suggest that Nek2B interacts with chromatin as it is not recruited to condensed sperm chromatin in mitotic extracts and immunodepletion of Nek2B does not interfere with chromatin condensation or decondensation (Fry *et al.*, 2000b). Thus, there may well be a role for Nek2 in chromatin condensation in meiotic cell division but there is not enough evidence as to whether a conserved role in chromatin condensation exists for Nek2 homologues in different species at all stages of development.

1.9 Centrosomes and cancer

Cell division requires that chromosomes are first duplicated and then equally segregated between two daughter cells. Normal segregation of chromosomes is essential for maintaining genetic stability and failure of this can lead to cells with an abnormal content of chromosomes, known as aneuploidy. Aneuploidy explains the fundamental cause of some major birth defects such as Down's syndrome but is also a well known hallmark of human malignant tumours. The centrosome's role in the production of the mitotic spindle raises the suggestion that it may play an important part in the development of aneuploidy. Theodor Boveri was the first to propose this, suggesting that the characteristic loss of cell polarity and chromosome segregation abnormalities seen in cancer may arise through defects in centrosome function (Wilson, 1925). It is well documented that centrosomal defects alter the assembly and function of the mitotic spindle inducing mis-segregation of chromosomes leading to genetic instability in the absence of a functional checkpoint. This condition combined with the growth selection pressure that tumours experience provides a mechanism whereby cells can accumulate activated oncogenes and lose copies of tumour suppresser genes through gross alterations of chromosome content. Cells with these defects

will be predisposed to additional genetic lesions that could lead to the malignant neoplastic phenotype (Brinkley and Goepfert, 1998; Salisbury *et al.*, 1999).

Many studies have shown that centrosomes in malignant cells are atypical in shape, size, composition and number, and many aneuploid carcinomas demonstrate chromosomal imbalances combined with amplification and instability of centrosomes (Ghadimi *et al.*, 2000; Lingle *et al.*, 1998). A higher frequency of centrosome abnormalities is observed in advanced stage malignancies when compared to early stage and it is proposed that the centrosome defects may relate to the transition from early to late stage malignancy (Kuo *et al.*, 2000). For example, overexpression of pericentrin in prostate epithelial cell lines reproduces many of the phenotypic characteristics of high grade prostate carcinoma, such as severe centrosome and spindle defects, cellular disorganisation, and genomic instability (Pihan *et al.*, 2001). In contrast, there is also evidence to support the role of abnormal centrosomes in early tumour development rather than merely being a consequence of cancer progression (Roshani *et al.*, 2002). For example, centrosome amplification is detected in early stage *in situ* ductal breast carcinomas (Lingle *et al.*, 2002). If centrosome defects are an early event in tumourigenesis, it is possible that some are the result of deregulated centrosome duplication. For instance, centrosome amplification has been linked to defects in tumour suppressor genes due to their possible role in the regulation of centrosome duplication. BRCA1 and BRCA2 are examples of where mutations in such genes are thought to increase centrosome amplification (Tutt *et al.*, 1999; Weaver *et al.*, 2002). p53 has also been implicated in the control of centrosome duplication with centrosome amplification correlated with mutational inactivation of p53 or Mdm2 overexpression (Carroll *et al.*, 1999). In human cancers, specific residues of p53 are mutated at a high frequency, if p53 phosphorylation sites are mutated, binding to centrosomal components may no longer be possible, rendering it unable to activate or inactivate them (Tarapore *et al.*, 2001). Furthermore, deregulation of downstream targets of p53 such as p21 and GADD45A may also effect centrosome duplication. GADD45A is proposed to play a role in the prevention of genomic instability by maintaining normal centrosome numbers, with the appearance of tetraploidy and supernumary centrosomes in null cells (Hollander *et al.*, 1999). p21 inhibits premature Cdk2-cyclin E activity, which is necessary for centrosome duplication in S phase by mediating phosphorylation of nucleophosmin and its subsequent dissociation from the centrosome (Okuda *et al.*, 2000). Therefore in the absence of p21, elevated Cdk2-cyclin E levels could lead to amplification

of centrosomes through continuous phosphorylation of nucleophosmin (Spruck *et al.*, 1999).

As an alternative to the idea of deregulated centrosome duplication, it is suggested that supernumary centrosomes are merely the result of errors during cell division, combined with the inability to detect the resulting hyperploidy. Mutations in p53 are often preceded by aneuploidy (Bardi *et al.*, 1997), therefore p53 defects alone are unlikely to be a primary causative factor. It has recently been shown that suppression of p53 or Rb proteins does not directly alter centrosome numbers in mammalian primary cell lines. Instead, failure to arrest at a G1 tetraploidy checkpoint following segregation failure in mitosis results in the clustering of centrosomes at a single spindle pole in subsequent mitosis, a phenotype triggered by mitotic or cleavage failure (Borel *et al.*, 2002). Evidence for this comes from the overexpression of Aurora-A which gives rise to extra centrosomes not through the deregulation of centrosome duplication but through defects in cell division and consequent tetraploidization. Absence of a p53 checkpoint exacerbates this phenotype, providing a plausible explanation for the centrosome amplification typical of $p53^{-/-}$ cells (Meraldi *et al.*, 2002). Furthermore, centrosome amplification and chromosomal instability can occur independently of p53 mutation in some breast tumours (Lingle *et al.*, 2002).

An increase in the understanding of the causes and consequences of genomic instability would have many benefits in the prevention and treatment of cancer. At present conventional histopathological evaluation of malignant tumours (grade and stage) cannot predict accurately the behaviour of most tumours. The development of reliable prognostic markers for malignant tumours that would accurately predict not only the course but also the response of the tumour to therapy would be very beneficial. For example, antibodies raised to centrin, pericentrin and γ-tubulin have been used as markers to observe centrosome defects in a range of solid malignant tumours and in tumour derived cell lines (Kuo *et al.*, 2000; Lingle *et al.*, 1998; Pihan and Doxsey, 1999). Such markers could potentially be used to assess the usefulness of aggressive treatment. More importantly, regulators of the centrosome duplication cycle including protein kinases like Nek2, might in the future act as novel targets during the treatment of cancer.

1.10 Aims and Objectives

The aim of my proposed research is to investigate how the centrosome, the primary MTOC of animal cells, is regulated through the cell cycle. The localisation of an increasing number of protein kinases to the centrosome has revealed the importance of protein phosphorylation in controlling the structural and functional transitions that the centrosome undergoes during the cell cycle. In this project I focus on the protein kinase Nek2 and its substrate C-Nap1 and their importance in the separation of centrosomes prior to mitosis.

The aims are as follows:

1. To investigate the nature of the Nek2 regulation throughout the cell cycle in human cells.

2. To investigate the interactions between Nek2 and C-Nap1 to provide a greater insight into the structure and function of the Nek2/C-Nap1/PP1 complex present at the proximal ends of centrioles.

3. To identify candidate proteins that interact with C-Nap1 in the centrosome, with the aim of characterising the intercentriolar linkage.

CHAPTER 2

MATERIALS AND METHODS

2.1 MATERIALS

2.1.1 Suppliers

All chemicals of analytical or molecular biology grade were supplied by Sigma (Poole, UK), Fisher Scientific (Loughborough, UK) or BDH Laboratory supplies (Poole, UK) unless otherwise stated below.

Supplier	Reagent
Amersham Pharmacia Biotech (Bucks, UK)	dATP, dCTP, dTTP, dGTP Glutathione Sepharose 4B
Bio101 Inc (Carlsbad, Canada)	CSM-Amino acid mix, Yeast nitrogen base
BOC (Surrey, UK)	CO_2, dry ice
Fuji Photo Film Ltd. (Dusseldorf, Germany)	Super RX X-ray film
Gibco BRL Life Technologies Ltd. (Renfrewshire, Scotland)	Dulbeccos MEM, Penicillin/Streptomycin, Fetal Calf Serum
Invitrogen (Paisley, UK)	Lipofectamine 2000 transfection reagent, Platinum Pfx
MBI fermentas (Sunderland, UK)	Restriction enzymes, DNA size markers
Melford Laboratories Ltd (Chelsworth, UK)	IPTG, Xgal, ONPG
National Diagnostics (Hull, UK)	'Protogel' 30% (w/v) acrylamide,
New England Biolabs (Hearts, UK)	Restriction enzymes
Oxoid (Basingstoke, UK)	Bacto-agar, bacto-tryptone, yeast extract
Pierce (Rockford, USA)	BCA protein assay reagent A
Premiere Beverages (Stafford, UK)	Dried milk powder (Marvel)
Promega UK (Southampton, UK)	*In vitro* translation kit
Qiagen (Hilden, Germany)	Qiaprep miniprep reagents
Roche (Mannheim, Germany)	Restriction enzymes, calf intestinal alkaline phosphatase, Taq DNA polymerase, DNA polymerase I large (Klenow) fragment, T4 DNA ligase, T4 DNA polymerase
Schleicher and Schuell (Dassel, Germany)	Protran, nitrocellulose membrane
Whatman International (Maidstone Kent)	3MM chromatography paper

2.1.2 Antibodies

Antibody	Working conc.	Supplier
Anti-Centrin, polyclonal	1/200	Gift from E. Nigg
Anti-Cyclin A, monoclonal	1/1000 (1 μg/ml)	Upstate Biotechnology
Anti-Cyclin B, monoclonal	1/1000 (1 μg/ml)	Upstate Biotechnology
Anti-Nek2 (R31), polyclonal	1/500 (1 μg/ml)	(Schultz *et al.*, 1994)
Anti-Nek2 (R40), polyclonal	1/200 (1 μg/ml)	(Fry *et al.*, 1998a)
Anti-C-Nap1, polyclonal	1/750 (1 μg/ml)	(Fry *et al.*, 1998b)
Anti-C-Nap1 (R82), polyclonal	1/600 (1 μg/ml)	(Mayor *et al.*, 2000)
Anti-dynein (70.1), monoclonal	1/500 (1.4 μg/ml)	Sigma
Anti-α-tubulin, monoclonal	1/2000 (0.3 μg/ml)	Amersham Pharmacia
Anti-γ-tubulin, polyclonal	1/5000 (2.6 μg/ml)	Sigma
Anti-γ-tubulin, monoclonal	1/500 (0.05 mg/ml)	Sigma
Anti-GST, polyclonal	1/1000 (2 μg/ml)	Molecular Probes
Anti-Ubiquitin monoclonal	1/1000 (1 μg/ml)	Santa Cruz
Anti-myc (9E10, undiluted tissue culture supernatant), monoclonal	Undiluted	Gift from E.Nigg
Anti-Mouse monoclonal AP conjugate	1/7500 (0.1 μg/ml)	Promega
Anti Rabbit polyclonal AP conjugate	1/7500 (0.1 μg/ml)	Promega
Biotinylated donkey anti rabbit	1/100	Amersham
Biotinylated goat anti mouse	1/100	Amersham
Streptavidin Texas Red	1/200	Amersham
Hoeschst 33258	1/8000 (0.1 μg/ml)	Calbiochem
Alexa fluor 488 anti mouse	1/500 (4 μg/ml)	Molecular Probes
Alexa fluor 488 anti rabbit	1/500 (4 μg/ml)	Molecular Probes

2.1.3 Common buffers and solutions

All solutions were prepared with deionised, distilled purified water (Elgastat optima 2 water purifier) and filtered where necessary (0.22 μm filter). Wherever sterilisation was

appropriate, solutions and glassware were autoclaved at 15 pounds per square inch for 20 minutes. All pH adjustments were performed at 25°C.

Buffer	Composition
3 X SDS-PAGE loading buffer	62.5 mM Tris-HCl pH 6.8, 2% (w/v) SDS, 5% (v/v) β-mercaptoethanol, 10% (v/v) glycerol, 0.01% (v/v) bromophenol blue
Phosphate buffered saline (PBS)	137 mM NaCl, 2.7 mM Na_2HPO_4, 1.4 mM KH2PO_4
TBE	89 mM Tris-HCl, 89 mM boric acid, 1 mM ethylenediaminetetra-acetic acid (EDTA) pH 8.0
TE	10 mM Tris-HCl pH 8.0, 1 mM EDTA

2.1.4 Vectors

Plasmid vectors used for cloning were obtained as follows:

Plasmid	Source
pACT II	Clontech
pAS2	Clontech
pRcCMV	Invitrogen
pEGFP (T7)	Gift from K. Tanaka
pGAD	(James *et al.*, 1996)
pGBDU	(James *et al.*, 1996)
pGEM T-Easy	Promega
pGEX 4T	Pharmacia

2.1.5 Bacterial strains

E. coli strain	Genotype
DH5α	Φ80d*lac*ZΔM15, *rec*A1, *end*A1, *gyr*A96, *thi*-1, *hsd*R17(rK-,mK$^+$) *supE*44, *rel*A1, *deo*R, Δ[*lac*ZYA-*argF*]U169
BL21(DE3)	F$^-$, *ompT, hsdSB,*(rB$^-$ mB$^-$), *dcm, gal,* λ(DE3)

2.1.6 Yeast strains

S. Cerevisae	Genotype
PJ69-4A	MATa, trp1-901, leu2-3,112, ura3-52, his3-200, GAL4Δ gal80Δ, LYS2::GAL1-HIS3, GAL2-ADE2met2::GAL7-lacZ.

2.1.7 Radioactivity

Radioisotopes were purchased from NEN Life Science Products and had the following specific activities.

Isotope	Specific Activity
[γ-^{32}P] ATP	4500 Ci/mmol
[^{35}S] methionine (Expre^{35}S^{35}S)	1175 Ci/mmol

2.2 BACTERIAL MANIPULATIONS

2.2.1 Growth and maintenance of bacterial cultures

Liquid media was prepared, luria Bertani (LB) media (10 g/l tryptone, 5 g/l yeast extract, 5 g/l NaCl, 10 mM Tris-HCl pH 7.5. The media was sterilised by autoclaving. For plates, 2% (w/v) of agar was added prior to autoclaving. If appropriate, 100 μg/ml of ampicillin, 50 μg/ml of kanamycin or 34 μg/ml of chloramphenicol was also added. Glycerol stocks of overnight (O/N) cultures were made by adding 0.2 ml of sterile glycerol to 0.8 ml of bacterial culture and vortexing. Glycerols were stored at -80°C.

2.2.2 Preparation of competent bacteria

E. coli DH5α was streaked on LB plates and incubated O/N at 37°C. One representative colony was picked and grown for 9 hours in 2 ml LB. This starter culture was used to inoculate 500 ml LB + 10 mM $MgCl_2$. This large culture was allowed to grow slowly at room temperature (RT) for approximately 46 hours or until the OD_{600} had reached 0.5 (units/cm) and was then rapidly cooled in an ice slurry. The cells were spun down at 0°C (3000 rpm) and resuspended in 1/3 volume ice cold transformation buffer (15 mM $CaCl_2$, 250 mM KCl, 10mM Pipes, 55 mM $MnCl_2$ pH 6.7). Again the cells were pelleted and

resuspended in 1/12.5 volume buffer. 5 ml DMSO was added by gentle swirling and the cell suspension aliquoted into tubes and immediately stored at -80°C.

2.2.3 Bacterial transformation

Competent bacteria (stored at -80°C) were allowed to defrost slowly on ice. Plasmid DNA (100 ng) was added, mixed gently by pipetting and incubated on ice for 30 minutes. Cells were heat shocked for 1 minute at 42°C and returned to the ice for a further 5 minutes. Warm LB was added and the sample incubated at 37°C for 30 minutes (400 rpm). Finally the bacteria were pelleted and resuspended in 50 µl LB before being plated on selective LB agar plates and grown O/N at 37°C.

2.3 DNA MANIPULATIONS

2.3.1 Restriction enzyme digestion

Restriction digests were carried out in the appropriate buffer supplied by the manufacturer at the recommended temperature. Typically 5 µg plasmid was incubated at 37°C for 2 hours with 10 units (U) restriction enzyme. Digestion of DNA with multiple enzymes was performed in the buffer that gave optimum activity of all enzymes. Blunt end formation from 5' protruding ends was carried out using 5U Klenow in the appropriate buffer, supplemented with 5 mM dNTP for 30 minutes at RT. Removal of 3' overhangs was carried out using T4 DNA polymerase in the appropriate buffer, supplemented with 5 mM dNTP for 15 minutes at 12°C. Both blunting techniques were followed by gel extraction of the plasmid DNA.

2.3.2 Agarose gel electrophoresis

DNA in loading buffer (50% (v/v) glycerol, 100 mM EDTA, 0.3% (w/v) bromophenol blue) was observed on an agarose gel of the appropriate percentage containing 1 µg/ml ethidium bromide in 1 X TBE. 0.5 µg of DNA ladder (1 Kb or 100 bp) was used to observe size separation. Electrophoresis was conducted at 80 V until the required degree of separation was achieved. DNA bands were visualised using an UV transilluminator and photographed using a gel documentation system.

2.3.3 Dephosphorylation of DNA

Dephosphorylation of the cut vector with 5'-overhangs was achieved by the addition of 1 U CIAP (Calf Intestinal Alkaline Phosphatase) in the appropriate 10 X buffer and incubation at 37°C for 30 minutes. For dephosphorylation of blunt ends, 1U CIAP was added in the appropriate 10 X buffer and incubated at 37°C for 15 minutes, followed by addition of a further 1U CIAP and incubation at 55°C for 45 minutes. In both cases, the dephosphorylated vector was then gel extracted to remove the CIP.

2.3.4 Purification of DNA from agarose gels

DNA fragments generated either from plasmids cut with appropriate restriction enzymes or from PCR were electrophoresed through agarose gels until clearly resolved and cut out in as small a volume of agarose as possible using disposable razor blades and put into sterile eppendorf tubes. Probe fragments were then purified using a Qiagen gel extraction kit as per the manufacturer's instructions.

2.3.5 Ligation of DNA fragments to plasmid vectors

In the standard reaction 5 μg of vector was digested with the appropriate restriction endonucleases and then treated with CIAP to prevent religation of the vector. This was combined with insert DNA at an approximate molar ratio of 1:3. To this 1 μl of ligase buffer was added along with 1 μl of T4 DNA ligase with a final volume of 10 μl. The reaction was mixed and incubated either O/N at 4°C or for 4 hours at RT, followed by transformation into bacteria and plating on antibiotic selective LB agar plates.

2.3.6 Polymerase Chain Reaction

Primers were designed so as to have a GC content as close to 50% as possible, a melting temperature (Tm) of 55 to 65°C and a size of 18-29 nucleotides. In addition the primer pairs were designed to have a GC content and melting temperature as close as possible to each other. Primers were synthesised by the Protein and Nucleic Acid Chemistry Laboratory (University of Leicester, Leicester, UK). Primers were made up in H_2O at 100 ng/μl stock solutions and 100 ng of each primer added per reaction. A nucleotide mix was made up at 10 mM from individual dNTPS and used at a final concentration of 0.2 mM. 10 X reaction buffer containing 50 mM $MgCl_2$, and 1.5 U Taq DNA polymerase were added per reaction. The annealing temperature (stage 2, step 2) was altered as required to optimise the PCR for individual primer pairs. The time of the extension step (stage 2, step

3) was altered according to the length of PCR product required (1 Kb/min). All reactions were carried out in a final volume of 20 µl. A typical cycle of reactions were as follows:

Stage 1: 1 cycle	Stage 2: 30 cycles	Stage 3: 1 cycle
step1 94°C: 5mins	step1 94°C: 30 secs	step1 72°C: 10 mins.
	step2 55°C: 30 secs	
	step3 72°C: 1 min	

2.3.7 Plasmid preparations

Plasmid minipreps and maxipreps were carried out using a commercially available kit from Qiagen. The procedure was carried out as per the manufacturer's instructions. For minipreps, DNA was isolated from 5 ml of bacterial culture grown overnight at 37°C and eluted into 50 µl H_2O. For Qiafilter plasmid maxipreps DNA was isolated from 200 ml of bacterial culture grown overnight at 37°C and eluted into H_2O. The DNA concentration was determined by measuring the OD at 260 nm and the stock diluted to 1 µg/µl with H_2O.

2.3.8 Sequencing

Automatic sequencing was carried out in the Protein and Nucleic Acid Chemistry Laboratory (University of Leicester, Leicester, UK) on an ABI 377 Automated sequencer (PerkinElmer) using Big Dye technology.

2.3.9 Computer analysis of sequences

The software, Gene Jockey, was used for restriction site mapping, analysis of reading frames and alignment of sequences. The following web based resources were used for database searching and protein identification:

Website	URL
Entrez	www.ncbi.nlm.nih/entrez
ExPASy (TRANSLATE)	http:// us.expasy.org/tools/dna
NCBI BLAST	www.ncbi.nlm.nih.gov/blast
PredictProtein	www2.ebi.ac.ukt.rostlpredictproteinl
PSORT	www.psort.nibb.ac.jp
The Sanger Center Pfam.	www.sanger.ac.uklSoftwarefPfani/

2.4 PROTEIN MANIPULATIONS

2.4.1 SDS-PAGE

Protein samples were separated on SDS-PAGE gels (see table below). The gels were prepared using the Biorad Mini Protean gel system.

Gel Constituents	Stacking Gel	Resolving Gel		
% Acrylamide	4%	7.5%	10%	12%
'Protogel' (30% acrylamide)	0.65 ml	3 ml	4 ml	4.8 ml
Lower Tris (1.5 M Tris-HCl pH 8.8, 0.4% (w/v) SDS)	-	3 ml	3 ml	3 ml
Upper Tris (0.5 M Tris-HCl pH 6.8, 0.4% (w/v) SDS)	1.25 ml	-	-	-
H_2O	3 ml	6 ml	5 ml	4.2 ml
10% APS	75 µl	150 µl	150 µl	150 µl
Temed	5 µl	10 µl	10 µl	10 µl
Total	5 ml	12 ml	12 ml	12 ml

Electrophoresis was performed with 1 X running buffer (3.03 g/l of Tris base, 14.4 g/l glycine and 0.01% (w/v) SDS, pH 8.3). Equal volumes of samples were mixed with 3 X loading buffer (62.5 mM Tris-HCl pH 6.8, 2% (w/v) SDS, 10% (v/v) glycerol, 5% (v/v) 2-mercaptoethanol, 0.01% (w/v) bromophenol blue) and boiled for 5 minutes. 25 µl of all protein samples were loaded. The gels were run at 180 V for 60 minutes or until the loading dye had migrated off the bottom of the gel. Some gels were then stained with Coomassie Blue (40% (v/v) IMS, 10% (v/v) acetic acid, 0.25% (w/v) Coomassie Brilliant blue) for 30 minutes. They were then destained (25% (v/v) IMS, 7.5% (v/v) acetic acid solution) for 1-2 hours (or as required) with constant agitation. If autoradiography was required, gels were dried at 80°C for 1 hour and placed in an autoradiography cassette with X-ray film. Following the required time, film was developed using a Cronex CX-130 X-ray film processor.

2.4.2 Western blotting

Proteins were resolved on SDS-PAGE gels and transferred to nitrocellulose by semi-dry blotting using a Hoefer Semiphor apparatus (Amersham). Briefly, the gel was washed in

Western transfer buffer (192 mM glycine, 25 mM Tris base, 0-10% (v/v) Methanol), before being laid on nitrocellulose membrane, sandwiched between 3MM chromatography paper soaked in transfer buffer. Transfer was carried out for 1 hour at 1 mA/cm^2. Following transfer, the membrane was stained in ponceau red for 1 minute and washed in H_2O before being blocked in PBST (1 X PBS, 1% (v/v) Tween 20) containing 5% milk at RT for 20 minutes. The membrane was then incubated with the primary antibody in PBST with 5% (w/v) milk for 1 hour at RT. Three washes were then carried out at RT in PBST before addition of an alkaline phosphatase conjugated secondary antibody in PBST + 5% (w/v) milk and incubated for 1 hour at RT. The membrane was then washed 3 times for 10 minutes in PBST followed by a 2 minute wash in alkaline phosphatase buffer (100 mM NaCl, 5 mM $MgCl_2$, 100 mM Tris-HCl pH 9.5). The blot was then developed by the addition of the alkaline phosphatase reagents (BCIP 16.5 mg/ml, NBT 0.33 mg/ml). Once colour had developed sufficiently the blot was washed in PBST for 30 minutes.

2.4.3 Silver staining

SDS-PAGE gels were fixed in 50% (v/v) methanol/10% (v/v) acetic acid for a minimum of 15 minutes. This was followed by 15 minutes in 25% (v/v) methanol/10% (v/v) acetic acid and 15 minutes in 5 µg DTT/ml H_2O. The gel was then placed in 0.1% (w/v) $AgNO_3$ for 15 minutes, rinsed briefly in H_2O, followed by the addition of developer (3% (w/v) Na_2CO_3, 460 µl/l formaldehyde). When the appropriate colour had been achieved, the reaction was stopped with 1% (v/v) acetic acid for 5 minutes and the gel washed 5 times with H_2O.

2.4.4 BCA protein assay

The total protein content of solutions was determined using the bicinchoninic acid (BCA) assay system (Pierce, USA). 5 µl of the solution in question was diluted 1/10 in H_2O. To this 1 ml of fresh working reagent (BCA reagent A + 1/50 $CuSO_4.5H_2O$) was added, mixed and incubated at 37°C for 30 minutes. Samples were then left to cool at RT for 15 minutes before the absorbance was measured at 562 nm. Protein concentration was determined by comparison to a standard curve of absorbances using a range of BSA concentrations.

2.4.5 *In vitro* translation

In vitro translation of constructs containing T7, T3 or SP6 promoters was carried out using the TnT-coupled transcription/translation kit in the absence or presence of [^{35}S] methionine according to manufacturer's instructions (Promega Corp.). For co-precipitation

experiments, reticulocyte lysates were first incubated separately at 30°C for 90 min and then together for 20 min with 250 mg/ml cycloheximide to allow interactions without further translation. Protein A beads used in the co-immunoprecipitation were pre-incubated in reticulocyte lysate for 30 minutes prior to incubation with IVT protein mixes.

2.4.6 Immunoprecipitation

Whole cell extracts were equalised for protein content using a BCA assay (see above) and diluted 1/5 in Nek2 extraction buffer (NEB: 50 mM HEPES-KOH, pH 7.4, 5 mM $MnCl_2$, 10 mM $MgCl_2$, 5 mM EGTA, 2 mM EDTA, 100 mM NaCl, 5 mM KCL, 0.1% (v/v) Nonident P-40, 30 μg/ml RNase A, 30 μg/ml DNase I, 1 mM phenylmethylsulfonyl fluoride (PMSF), 10 μg/ml leupeptin, 1 μg/ml pepstatin A, 1% aprotinin (v/v), 20 mM β-glycerophosphate, 20 mM sodium fluoride), (Fry and Nigg, 1997). They were precleared with protein A-sepharose beads for 30 minutes at 4°C. Extracts were then incubated for 60 minutes on ice with an appropriate antibody, followed by addition of protein A-sepharose (polyclonal antibodies) or protein G-sepharose (monoclonal antibodies) for a further 45 minutes. Immune complexes were collected by centrifugation and washed at least 5 times with NEB buffer and once with 1 M NaCl, before being mixed with an equal volume of 3 X protein sample buffer and heated to 95°C for 3 minutes.

2.4.7 *In vitro* kinase assays

Immunoprecipitated protein was washed three times in NEB, followed by 50 mM HEPES-KOH, pH 7.4, 5 mM $MnCl_2$. 50 μl of kinase buffer (50 mM HEPES-KOH, pH 7.4, 5 mM $MnCl_2$, 5 mM β-glycerophosphate, 5 mM sodium fluoride, 1 mM dithiothreitol (DTT), 4 μM ATP, 10 μCi [γ-^{32}P] ATP, 0.5 mg/ml dephosphorylated casein) was added to the immune complexes, which were then incubated at 30°C for 30 minutes. Reactions were stopped by the addition of an equal volume of 3 X protein sample buffer and heated to 95°C. Reaction products were visualised by SDS-PAGE followed by autoradiography.

2.5 MAMMALIAN CELL CULTURE

2.5.1 Maintenance

HeLa epithelial, U2OS osteosarcoma, HEK293 epithelial and KE37 T-lymphoblastoid cells were grown at 37°C in a 5% CO_2 atmosphere in Dulbecco's modified Eagle's

medium (DMEM) supplemented with 10% (v/v) heat-inactivated fetal calf serum (FCS) and penicillin-streptomycin (100 IU/ml and 100 mg/ml, respectively). Human T-lymphocytes were obtained from peripheral blood donated by healthy volunteers as previously described (Churcher and Moss, 1993).

2.5.2 Storage

Cells were detached from flasks by incubating in PBS containing 0.5 mM EDTA before transferring into fresh media. The media was centrifuged at 1200 rpm for 5 minutes. The pellet was resuspended in DMEM (FCS and penicillin-streptomycin) containing 10% dimethylsulphoxide (DMSO) and an additional 10% (v/v) FCS. Aliquots were left on ice for 30 minutes, followed by slow freezing at -80°C O/N before being transferred to liquid nitrogen.

2.5.3 Preparation of whole cell extracts

To prepare cell lysates for Western blotting, cells were harvested and washed once in ice cold PBS containing 1 mM PMSF before being resuspended in NEB. Extracts were left on ice for 30 minutes, passed through a 27G needle 10 times and centrifuged at 14,000 rpm for 15 minutes at 4°C. One volume of 3 X protein sample buffer was added to the supernatant and the sample heated to 95°C for 3 minutes before analysis by SDS-PAGE (Fry and Nigg, 1997).

2.5.4 Cell cycle synchronisation

Cells were synchronised with drugs using either a double block-release method or a single incubation for 16 hours. The single arrest utilised 1 mM hydroxyurea for G1/S arrest and 1 μg/ml nocodazole for mitotic arrest. A double block was used to obtain U2OS and HeLa cells arrested at the following more specific stages of the cell cycle. G1/S: cells were presynchronised in S phase by the addition of 2 mM thymidine for 12 hours, released by transferring to fresh media for 8 hours and then resynchronised at the G1/S transition by incubation for 16 hours with 1 mM hydroxyurea. S phase: cells were incubated with 1 mM hydroxyurea for 16 hours. A time course of hydroxyurea releases was undertaken, in parallel with flow cytometric analysis to ensure that the release time was adequate for the cells to reach the desired cell cycle phase. For synchronisation in G2, cells treated with hydroxyurea were released and incubated in fresh media for 9 hours. Mitosis: cells were treated with 500 ng/ml nocodazole for 16 hours before collecting the mitotic population by

gentle pipetting. For synchronisation in G1, the nocodazole treated cells were released by three washes in PBS and replated in fresh media, they were then incubated for 6 hours before being harvested. Release of cells from drug-induced cell cycle blocks was performed by three washes in 1 X PBS and replacement into fresh media. Cell cycle distributions were confirmed by flow cytometry.

2.5.5 Flow cytometry analysis

The cell cycle distribution of the various cell populations was monitored by flow cytometric analysis. For this purpose, $1x10^6$ cells were washed in ice-cold PBS and slowly resuspended in 1 ml of 70% ethanol (-20°C) while vortexing. At this stage cells were stored for at least 24 hours at -20 °C. Immediately prior to analysis, fixed cells were gently washed in ice-cold PBS and resuspended in 1 ml of stain solution (0.02 mg/ml propidium iodide, 0.2 mg/ml RNase A in PBS). Samples were incubated at RT for 30 minutes before the DNA content was measured using a FACSCAN II (Becton Dickinson) instrument and analysed using CellQuest.

2.5.6 Protein stability

To measure protein stability in cells, cycloheximide was added to the culture medium to 50 mg/ml and cells harvested at given time intervals after cycloheximide addition. To test the role of different proteases in Nek2 degradation, cells were first pre-incubated for 1 hour with DMSO, 12.5 mM *clasto*-Lactacystin, 20 mM MG132, 100 mM ALLM (all from Calbiochem) or 200 mg/ml leupeptin (Sigma) before addition of cycloheximide. Other drugs used were nocodazole (1 μg/ml), Taxol (1 mM), staurosporine (1 μM), cisplatin (500 μM) and Leptomycin B (10 μM). Cells were pre-incubated for 1 hour with these drugs before addition of cycloheximide for the given time.

2.5.7 Transfection

For transient transfection studies, U20S or HeLa cells were seeded onto HCL-treated glass coverslips at a density of $1x10^5$/ml cells in either 35 mm dish or 60 mm dishes. After 24 hours growth they were transfected with 5 μg or 10 μg of plasmid DNA, respectively, using Lipofectamine 2000 reagent according to manufacturer's instruction. Transfection mix was left on cells for 24 hours prior to preparation of cell extracts or processing for immunofluorescence microscopy. Cells for immunofluorescence microscopy were fixed in cold methanol (-20°C) for at least 10 minutes.

2.5.8 Immunofluorescence microscopy

For antibody staining of whole cells, fixed coverslips were rehydrated in PBS for 15 minutes, blocked with 1% (w/v) BSA in PBS for 10 minutes and washed 3 times with PBS. All subsequent antibody incubations were carried out in PBS containing 3% BSA. Primary antibody incubations were carried out for 1 hour using the appropriate antibody, followed by 3 washes in PBS. Detection of primary antibodies was carried out using the following secondary reagents: biotinylated mouse anti-rabbit (1/100) followed by Texas red conjugated streptavidin (1/200) or FITC conjugated rabbit anti-mouse antibodies (1/500). Finally coverslips were incubated with Hoechst (0.1 μg/ml) for 10 seconds, then washed 3 times with PBS and briefly rinsed in H_2O. Coverslips were mounted on glass slides in 80% (v/v) glycerol, 3% (w/v) n-propylgallate mounting medium. Fluorescence microscopy was performed using a Nikon TE300 microscope and 100 X oil immersion objectives. Fluorescence images were captured using an Orca ER camera (Photometrics, Inc.) using Openlab software (Improvision) and processed using Adobe Photoshop (San Jose, CA).

2.5.9 Centrosome purification

Isolation of human centrosomes from KE37 cells was carried out as described previously (Moudjou and Bornens, 1994). The concentration of centrosomes in each fraction was determined by indirect immunofluorescence microscopy. To prepare centrosomes for microscopy the centrosome preparation was gently mixed with 5 ml 10 mM K.Pipes pH 7.2. This was then transferred into glass tubes containing HCl-washed coverslips on a coverslip support (Blomberg-Wirschell and Doxsey, 1998), before centrifugation at 25,000 g for 20 minutes at 4°C in a swinging bucket rotor. Coverslips were fixed in -20°C methanol and processed for immunofluorescence microscopy as above.

2.5.10 Hybridoma supernatant preparation

9E10 anti-myc hybridoma cells were cultured in RPMI 1640 supplemented with 10% (v/v) heat-inactivated FCS and penicillin-streptomycin (100 IU/ml and 100 mg/ml). Cells were grown to a high density, washed in PBS and resuspended in 20 ml serum free PFHM-II medium with glutamax-I and left for 4 days until the cells began to die. Cells were removed by mechanically shaking them and pelleted at 2000 rpm for 10 minutes at 4°C. The supernatant was decanted and re-centrifuged at 10,000 rpm for 10 minutes at 4°C. Following this, 1/20 1 M Tris-HCl pH 8.0 was added and the supernatant stored at -20 °C.

2.6 YEAST MANIPULATION

2.6.1 Growth and Maintenance of yeast cultures

Liquid YPD full media was prepared (20 g/l peptone, 10 g/l yeast nitrogen base, 20 g/l glucose) for growth of yeast without addition of plasmids. Following transformation, yeast were grown in selective media lacking essential amino acids (6.7 g/l yeast nitrogen base, 20 g/l glucose, 0.6-0.8 g/l CSM amino acid mix, 1.5 M NaOH). 3-Aminotriazole (3-AT) was added to 0-30 mM depending on the fusion protein expressed in the yeast. The media was sterilised by autoclaving. For plates, 2.4% (w/v) of agar was added prior to autoclaving. Glycerol stocks of O/N cultures were made by addition of 0.2 ml sterile glycerol to 0.8 ml of yeast culture and vortexing. Glycerols were stored at -80°C.

2.6.2 Yeast transformation

Yeast transformation was carried out essentially as previously described (Vojtek *et al.*, 1993). 10 ml of YPD was inoculated with one large yeast colony and incubated O/N by shaking at 30°C. The following day, this was diluted in 50 ml YPD to give an OD_{600} of 0.5 and incubated at 30°C. After 4 hours the culture was pelleted at 2500 rpm for 10 minutes at RT, washed in TE before being resuspended in 2 ml 0.1 M lithium acetate and left at RT for 10 minutes. 1 µg plasmid DNA was mixed in a tube with 100 µg ssDNA and 100 µl of yeast suspension added. To this 700 µl 0.1 M lithium acetate/40% (w/v) PEG3350/TE was added and the mix vortexed vigorously. Following a 30 minute incubation at 30°C, 80 µl DMSO was added and the mixture heat shocked at 42°C for 7 minutes before a brief spin to remove the supernatant. The pellet was washed in TE before being plated on selective medium and grown for 3 days.

2.6.3 Yeast DNA preparation

1.5 ml of a fresh yeast culture grown under selective conditions was pelleted and resuspended in STET buffer (8% (w/v) sucrose, 50 mM EDTA, 5% (v/v) Triton X-100, 50 mM Tris-HCl pH 8.0). The same amount of glass beads (0.45 mm) were added and vortexed for 5 minutes. The sample was cooled briefly on ice before centrifuging for 10 minutes at full speed. The supernatant was removed to a tube containing 7.5 M ammonium acetate, incubated for 30 minutes at -20°C and then spun for 10 minutes at full speed. The supernatant was then added to cold ethanol and the spin repeated. The pellet was washed with 70% (v/v) ethanol and then resuspended in water followed by transformation into

bacteria using the previously described method.

2.6.4 Yeast cell lysates

2 ml of a fresh yeast culture grown under selective conditions was pelleted at 2500 rpm for 10 minutes at RT and resuspended in buffer (0.25 M NaOH, 1% (v/v) β-mercaptoethanol). This was incubated on ice for 10 minutes, followed by addition of 50% (v/v) trichloroacetic acid (TCA) and another 10 minute incubation on ice. The precipitated protein was removed by centrifugation at full speed for 10 minutes. The resultant pellet was resuspended in cold acetone, vortexed vigorously and repelleted. The washed pellet was air dried and finally resuspended in protein sample buffer.

2.6.5 ONPG (*O*-nitrophenyl β galactopyranoside) assay

2 ml of a fresh yeast culture with an OD_{600} of 1 was pelleted and resuspended in Z buffer (60 mM Na_2HPO_4, 40 mM NaH_2PO_4, 1 mM KCL, 1 mM $MgSO_4$, 40 mM β-mercaptoethanol, pH 7). Chloroform and 0.1% (w/v) SDS were added and the mix incubated at 30°C for 2 minutes. 0.8 μg/ml ONPG was added and the colour allowed to develop for 20 minutes. Reactions were stopped by addition of 1 M Na_2CO_3. The cell debris was removed by centrifugation and the absorption at 420 nm measured versus a blank. Units of activity were made relative to Nek2A-Nek2A interaction, which was given an arbitrary value of 1.

2.6.6 Yeast two hybrid library screen

A yeast two hybrid screen was performed essentially as described previously (Dufee *et al.*, 1993). 5 ml of media lacking uracil was inoculated with a large yeast colony expressing a GAL4 DBD-fusion protein and incubated O/N at 30°C. The following day this was used to inoculate 100 ml of media and grown until theOD_{600} was 1. This was then diluted to an OD_{600} of 0.4 in 1 litre YPD and grown for an additional 2-4 hours at 30°C until OD_{600} equalled 0.6. The cells were pelleted at 2500 rpm at RT, washed in 500 ml TE, repelleted and resuspended in 20 ml of 100 mM lithium acetate/TE. The cells were incubated at RT for 10 minutes. 50 μg of a human testis cDNA library constructed in plasmid pACT II (Clontech) which had first been amplified by processing 4 x 10^6 colonies through Qiagen maxiprep kits as described previously was added to 100 μg denatured, sheared salmon DNA. This mix was added to the yeast suspension from the previous step and 140 ml buffer (100 mM LiAc/40% (w/v) PEG-3350/TE) was added, vortexed and incubated at

30°C for 30 minutes. 17.6 ml DMSO was added, mixed well and heat shocked at 42°C for 6 minutes with swirling, followed by rapid cooling to RT in a water bath. The yeast suspension was then pelleted at 2500 rpm, the supernatant removed and the pellet washed in 500 ml of TE, before being resuspended in 1 litre of YPD and grown at 30°C for 1 hour with shaking. Again the yeast was pelleted and washed in 500 ml TE before being resuspended in selective media lacking uracil and leucine and grown for 16 hours at 30°C. A sample was taken at this stage and grown on media lacking uracil and leucine to determine the transformation efficiency of the screen. Following this, the yeast were pelleted, washed twice in 500 ml TE and resuspended in 6 ml TE. 300 µl was plated on 20 150mm selective media plates lacking uracil/leucine/histidine/adenine and grown at 30°C for 7 days. Colonies that grew were re-streaked on fresh plates and glycerol stocks made.

2.7 Glutathione-S-transferase (GST) tagged protein purification

2.7.1 Protein Induction

The *E.coli* strain BL21 was transformed with the GST fusion proteins and grown at 37°C until an OD_{600} of 0.5 was reached. Expression was induced with 0.1 mM isopropyl-β-thiogalactopyranoside (IPTG) for 4 hours at 30°C. 1ml of cells was centrifuged at 13,000 rpm for 10 seconds and resuspended in 250 µl 3 X protein sample buffer, this was heated to 95°C for 10 minutes before the protein was resolved on 10% SDS-PAGE gels. For large scale induction 1 litre of bacteria was induced. If the protein was insoluble following lysis and sonication, growth and induction was carried out at RT O/N.

2.7.2 Bacterial cell lysis

The induced whole cell sample was pelleted by centrifugation (Sorvall RC-5B plus, SLA 1500 rotor, 8000 rpm, 4°C) for 10 minutes. Pellets were resuspended in one tenth of their original volume in buffer X (50 mM Tris-HCl, pH 8, 10 mM EDTA, 100 mM NaCl, 0.5% (v/v) Triton-X-100, 1 mM PMSF, 10 µg/ml leupeptin, 10 µg/ml pepstatin A, 10 µg/ml bestatin, 1 mM DTT). The cell suspension was sonicated in aliquots of 25 ml (MSE Soni-Prep 150, 19 mm probe, amplitude 8 µm) for 30 seconds, followed by a 1 minute gap, for a total of 4 cycles. The samples were kept on ice at all times.

2.7.3 Large scale GST protein purification

Protein purification was carried out using 1 litre of induced bacteria. The cells were harvested by centrifugation at 4°C, resuspended in ice cold buffer X and frozen at -80 °C O/N. Once defrosted, the sample was incubated on ice for 30 minutes with 0.2 mg/ml lysozyme, following this it was sonicated and the lysate centrifuged at 12,000 rpm for 20 minutes at 4°C. The supernatant was added to 2 ml of prewashed Glutathione-Sepharose beads, after incubation with mixing at 4°C for 1 hour the beads were washed three times in buffer X and then placed in a column. After further washing with PBS, the bound GST-fused proteins were eluted from the column with elution buffer (100 mM HEPES-NaOH, pH 8, 50 mM reduced glutathione). The peak fraction was dialysed against PBS and stored at -80 °C. The purity was assessed by SDS-PAGE as previously described.

2.7.4 GST pull downs

Glutathione-Sepharose beads pre-bound to GST linked proteins or GST alone were incubated O/N with 2 µl of *in vitro* translated [^{35}S] methionine/cysteine protein made using the TnT-coupled transcription /translation kit at 4°C in NETN buffer (20 mM Tris-HCl pH 8, 200 mM NaCl, 1 mM EDTA, 0.5% NP-40, 1mM DTT, 1mM PMSF, 10 µg/ml leupeptin, 10 µg/ml pepstatin A, 10 µg/ml bestatin). The samples were washed 3 times in cold NETN and resuspended in protein sample buffer. This was heated to 95°C for 5 minutes before the protein was resolved on 12% SDS-PAGE gels.

2.8 MISCELLANEOUS TECHNIQUES

2.8.1 *In vitro* degradation assays

CSF (Cytostatic factor, metaphase II-arrested) extracts were prepared as described previously (Desai *et al.*, 1999). To generate anaphase extracts, calcium chloride was added to 0.5 mM. Egg extracts (10 µl) were supplemented with 0.1 µg of GST proteins before incubation at 22°C. For proteasome inhibition, extracts were pre-incubated with 50 µM MG132 for 15 minutes at 22°C. Aliquots (2.5 µl) were taken at times indicated, mixed with protein sample buffer and separated on 12% SDS-PAGE gels. Gels were stained with Coomassie Blue, followed by autoradiography.

2.8.2 Microtubule pull down

Purified mouse brain tubulin (gift from B. Edde, Paris) was diluted to 0.4 μg/μl in microtubule stabilising buffer (80 mM K.pipes pH 6.8, 1 mM $MgCl_2$, 1 mM EGTA, 25 mM NaCl, 20 μM taxol, 100 mM GTP, 50 mM AMP-PNP). To this, either 100 μg of purified GST protein, 1 μl [^{35}S]-labelled IVT protein or 30 μl of HeLa whole cell extract was added and the mixture incubated for 30 minutes at 30°C. It was then centrifuged at 35,000 rpm for 30 minutes at RT. The supernatant was removed and an equal amount of protein sample buffer added. The pellet was resuspended in protein sample buffer. Both samples were heated to 95°C for 5 minutes before equivalent proportions of the protein mix were resolved on 12% SDS-PAGE gels and either stained with Coomassie Blue, followed by autoradiography or processed for Western blotting.

CHAPTER 3

IDENTIFICATION OF ALTERNATIVE SPLICE VARIANTS OF HUMAN NEK2

3.1 INTRODUCTION

This chapter describes the identification of alternative splice variants of the centrosomal kinase Nek2. These splice variants, termed Nek2A and Nek2B, exhibit distinct patterns of expression in mitosis, which implicates them in different functions during the cell cycle.

3.1.1 Centrosome regulation

The structure and function of the centrosome depends largely on its stage in the cell cycle. Prior to mitosis, the centrosome duplicates and as each new centrosome matures, it acquires an increased ability to nucleate microtubules by the recruitment of extra microtubule nucleating proteins (Khodjakov and Rieder, 1999). As the cell enters mitosis, the duplicated centrosomes separate and move to opposite ends of the cell and forces generated by microtubules and chromosome associated motor proteins lead to the establishment of the bipolar mitotic spindle (Heald, 2000; Wittmann *et al.*, 2001). The microtubules are arranged into spindle arrays with centrosomes forming the poles of this mitotic spindle upon which chromosomes are separated into the daughter cells at mitosis. Many of the processes which occur during the cell cycle are likely to result from protein phosphorylation and dephosphorylation (Fry *et al.*, 2000a; Nigg, 2001) due to the localisation of various kinase and phosphatases at the centrosome. The molecular processes by which the centrosome is modified by kinases and phosphatases is poorly understood. Suggestions include the idea that phosphorylation may regulate the association of proteins with the centrosome; alternatively it may target proteins for degradation via the proteasome through ubiquitination (Freed *et al.*, 1999; Tugendreich *et al.*, 1995; Wigley *et al.*, 1999).

3.1.2. Nek2 centrosomal kinase

Nek2 is a cell cycle regulated protein kinase that localises to the centrosome. Its expression and kinase activity exhibit peak levels in S and G2 phases (Fry *et al.*, 1995; Schultz *et al.*, 1994). It is thought that Nek2 may contribute to the disappearance of the intercentriolar linkage at the onset of mitosis allowing the centrosomes to separate (Mayor *et al.*, 1999). This is based on the observation that Nek2 overexpression causes premature centrosome splitting in interphase (Fry *et al.*, 1998a). Furthermore, C-Nap1, a Nek2 substrate localises to the proximal ends of the centrioles during interphase but is absent from the spindle poles in mitosis (Fry *et al.*, 1998b). Antibody-mediated interference of C-Nap1 function

promotes splitting of parental centrioles, implying a role in centrosome cohesion (Mayor *et al.*, 2000).

Nek2 is the most closely related vertebrate kinase to the mitotic regulator of the filamentous fungus *A. nidulans* NIMA, sharing 47% homology in its catalytic domain (Schultz *et al.*, 1994). It has been speculated that Nek2 may carry out similar functions to NIMA, which include chromosome condensation and mitotic spindle formation (Osmani *et al.*, 1988). However, little evidence for Nek2 having a role in chromosome condensation exists, except recent work that has shown Nek2 to be associated with mitotic chromosomes (Ha Kim *et al.*, 2002). Recent studies in *Xenopus* have demonstrated that Nek2 has additional functions in assembly and/or maintenance of centrosome structure. Depletion of Nek2 from egg extracts interferes with centrosome assembly and microtubule aster formation (Fry *et al.*, 2000b). Injection of kinase dead forms of Nek2 or neutralising antibodies into embryos causes fragmentation of spindle poles, aberrant spindle formation and abortive cleavage (Uto and Sagata, 2000). In addition, long term overexpression in adult human cells leads to centrosome disintegration suggesting that these alternative functions are not restricted to early embryos but may be involved in the regulation of the adult cell cycle (Fry *et al.*, 1998b).

It is clear that Nek2 may perform multiple functions throughout both the embryonic and adult cell cycle. The kinase activity of Nek2 is therefore subject to several levels of regulation that ensure it is activated at the correct time during the transition from interphase to mitosis and is then irreversibly inactivated in mitosis to guarantee that mitotic entry and exit can progress normally. Various modes of Nek2 regulation come into play throughout the cell cycle such as regulation of protein abundance at the level of transcription/translation and regulation of protein turnover. Another likely method of Nek2 regulation is through the formation of protein-protein complexes. Nek2 interacts with the catalytic subunit of protein phosphatase 1 (PP1c), which is capable of dephosphorylating Nek2 substrates such as C-Nap1 (Helps *et al.*, 2000). The existence of this complex limits the kinase activity of Nek2 to a small window at the G2/M phase transition, when PP1 is inactivated, hence the timing of centrosome separation being kept consistently at mitotic onset unless Nek2 levels are artificially increased. In addition, to PP1, Nek2 can also form dimers via the leucine zipper motif in its C-terminus (Fry *et al.*, 1999). This property

allows autophosphorylation, which is thought to regulate the activity of Nek2. Furthermore the dimerised molecules are also limited by PP1c, thus controlling the activation of Nek2.

Two alternative cDNAs have been identified for *Xenopus* Nek2, which encode products with distinct C-termini, which may arise through alternative splicing (Uto *et al.*, 1999). They may also be the result of gene divergence within the tetraploid *Xenopus* genome (Graf and Kobel, 1991). Importantly, the two isoforms display distinct patterns of expression during development. The shorter form, X-Nek2B shows highest expression in oocytes, eggs and early embryos with the longer form X-Nek2A, present in embryos after the gastrula-neurula transition and adult testis (Uto and Sagata, 2000). Murine Nek2 is also highly expressed in adult testis, although the existence of multiple Nek2 isoforms in mammals has not been addressed (Arama *et al.*, 1998; Rhee and Wolgemuth, 1997; Tanaka *et al.*, 1997). The presence of two immunoreactive bands on Western blots probed with anti-Nek2 antibodies prompted us to investigate the possibility of whether alternative splicing represents a common mechanism for regulating Nek2 kinase in vertebrates, more specifically in human cells. The following work provides evidence to support this, describing the identification and subsequent characterisation of alternatively spliced variants of human Nek2 kinase.

3.2. RESULTS

3.2.1 Structure of human Nek2 gene

In the original characterisation of the human Nek2 cDNA, chromosomal mapping identified two independent loci on chromosomes 1 and 14 (Schultz *et al.*, 1994). It has since been shown by PCR on somatic cell hybrid panels that highly related copies of the Nek2 cDNA exist on chromosomes 1, 2, 14 and 22. Sequencing of the PCR products revealed that only the sequence on chromosome 1 bears complete identity to the published Nek2 cDNA sequence. The other copies contain multiple single-nucleotide substitutions in residues that are critical for protein kinase activity and more importantly contain a termination codon within the catalytic domain. Moreover, the other genes lack introns, which emphasizes their existence as non-functional pseudogenes (Hames and Fry, 2002).

Two alternative cDNAs have been isolated for the *Xenopus laevis* homologue of human Nek2 that could have arisen from duplicate copies of the Nek2 gene in this tetraploid organism or, as the cDNAs diverge at a putative splice junction, they may have been generated through alternative splicing. To test whether human Nek2 is alternatively spliced, a cosmid encompassing the full length Nek2 gene from chromosome 1 was first isolated to determine its gene structure. Sequencing of the cosmid identified that Nek2 mRNA is encoded on eight exons with the initiation codon in the first exon and the UAG stop codon in exon 8. Exon 7 terminates at a position that is equivalent to the point of divergence of the two *Xenopus* Nek2 cDNAs. Sequencing of the seventh intron revealed the presence of a termination codon starting 43 nucleotides after the splice site and an alternative polyadenylation signal after a further 625 nucleotides. Based on the position of the termination codon in the seventh intron, use of this alternative polyadenylation signal would generate a human Nek2B protein of 384 amino acids with a calculated molecular weight of 44 kDa and pI of 8.64 (Figure 3.1A and B). The predicted Nek2A and Nek2B proteins would diverge in sequence after amino acid 370 causing Nek2B to lack a number of important regulatory motifs that are present in the extreme C-terminus of Nek2A (Figure 3.1C). RT-PCR performed on RNA isolated from transformed human cell lines provided strong support for the hypothesis that alternative splice forms of Nek2 do exist in humans (work carried out by A.M. Fry).

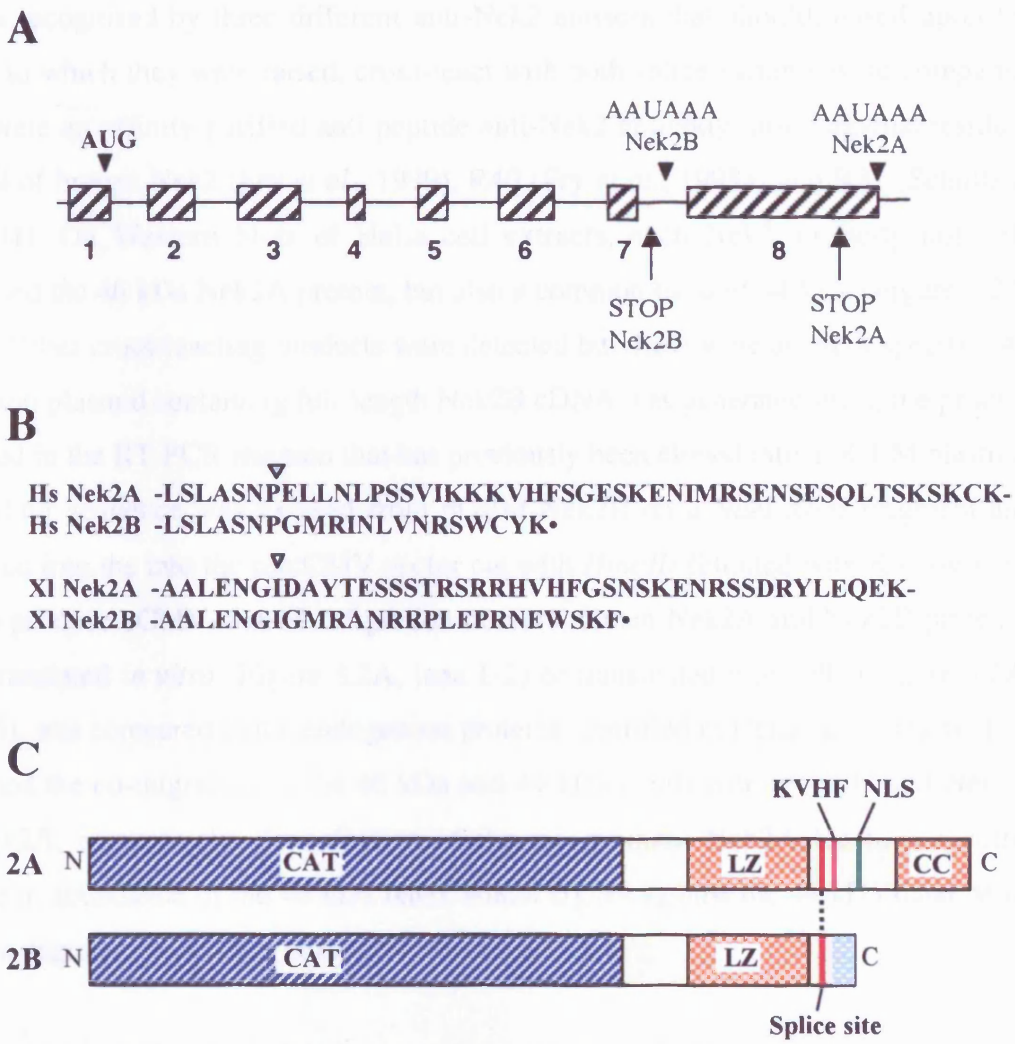

Figure 3.1 Structure of the human Nek2 splice variants
(A) Intron-exon structure of the human Nek2 gene on chromosome 1. Exons (hatched boxes) are drawn to scale, introns are not as they have not been fully sequenced. The positions of the single AUG codon, the two alternative stop sites and polyadenylation signals (AAUAAA) are indicated. **(B)** Partial protein sequences of human (Hs; from amino acid 364) and *Xenopus* (XI; from amino acid 365) Nek2A and Nek2B are shown with the position of the splice site indicated (arrowhead). The stop codons are indicated (•). **(C)** Schematic diagram of the human Nek2 splice variants indicating the catalytic domain (CAT), leucine zipper (LZ), coiled coil domain (CC), splice site, nuclear localisation signal (NLS) and PP1c binding site (KVHF).

3.2.2 Expression of human Nek2A and Nek2B

To determine whether Nek2A and Nek2B are expressed as proteins in cultured cells, the proteins recognised by three different anti-Nek2 antisera that should, based upon the regions to which they were raised, cross-react with both splice variants were compared. These were an affinity purified anti-peptide anti-Nek2 antibody raised against residues 278-299 of human Nek2 (Fry *et al.*, 1999), R40 (Fry *et al.*, 1998a) and R31 (Schultz *et al.*, 1994). On Western blots of HeLa cell extracts, each Nek2 antibody not only recognised the 46 kDa Nek2A protein, but also a common band of 44 kDa (Figure 3.2A, lane 3). Other cross-reacting products were detected but these were antisera specific. An expression plasmid containing full-length Nek2B cDNA was generated using the product amplified in the RT-PCR reaction that has previously been cloned into a pGEM plasmid. The coding sequence was excised from pGEM-Nek2B on a *NaeI-XbaI* fragment and subcloned into the into the pRcCMV vector cut with *HindIII* (blunted with Klenow) and *XbaI* to produce pCMV-Nek2B. Migration of recombinant Nek2A and Nek2B proteins, either translated *in vitro* (Figure 3.2A, lane 1-2) or transfected into cells (Figure 3.2A, lane 4-5), was compared to the endogenous proteins identified in HeLa cell extracts. This confirmed the co-migration of the 46 kDa and 44 kDa bands with recombinant Nek2A and Nek2B, respectively. Transfection of the recombinant Nek2A led to a specific increase in abundance of the 46 kDa band, which argues against the 44 kDa band being merely a degradation product of Nek2A (Figure 3.2A).

To determine whether both Nek2 isoforms are expressed ubiquitously, extracts were prepared from a variety of transformed cell lines as well as from freshly collected peripheral T lymphocytes. Western blotting revealed the presence of Nek2A and Nek2B in all transformed cell lines tested and peripheral T lymphocytes emphasizing that Nek2B expression is not confined to either transformed cells or early stages of development (Figure 3.2B). A slower migrating form of Nek2A was also detected in peripheral T lymphocytes, which was not so obvious in transformed cell lines, implying that a substantial fraction of Nek2A might exist in a post-translationally modified state (possibly phosphorylation) in primary cells (Figure 3.2B, lane 7). Unfortunately, attempts to generate Nek2A and Nek2B specific antisera using peptides based on the predicted C-termini have so far proved unsuccessful. To confirm that the two bands detected by Nek2 antibodies at 46 and 44 kDa represent Nek2 proteins rather than unrelated cross-reacting antigens an antisense oligonucleotide approach was used.

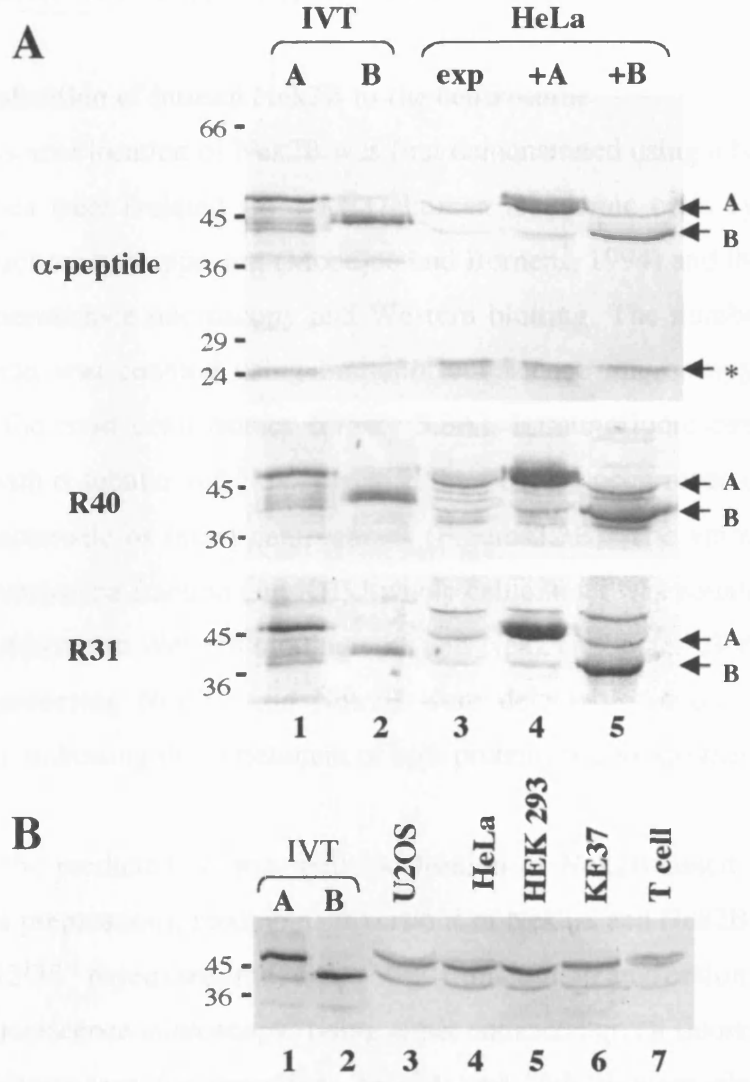

Figure 3.2 Expression of human Nek2A and Nek2B

(**A**) The migration of *in vitro* translated (IVT) Nek2A (lane 1) and Nek2B (lane 2) was compared on Western blots with proteins recognised in extracts of untransfected HeLa cells (lane 3) and HeLa cells transfected with untagged Nek2A (lane 4) and Nek2B (lane 5). The three Nek2 antibodies used (anti-peptide, R31 and R40) all recognised proteins at 46 and 44 kDa that co-migrate with recombinant Nek2A and Nek2B, respectively. A third band recognised by the anti-peptide anti-Nek2 antibody that was not recognised by the other antibodies used is indicated (*). (**B**) Western blotting with the anti-peptide anti-Nek2 antibody indicates that Nek2A and Nek2B are present in extracts of transformed cell lines (lanes 3-6) and primary cell lines (lane 7). Molecular weights (kDa) are indicated on the left of each panel.

An antisense Nek2 sequence was identified that, when introduced into human cells by liposome-mediated transfection, caused specific down-regulation of both the 46 and 44 kDa proteins, but not α-tubulin or a lower molecular weight protein recognised by the Nek2 antisera (work carried out by A.M. Fry).

3.2.3 Localisation of human Nek2B to the centrosome

The centrosomal location of Nek2B was first demonstrated using a biochemical approach. Centrosomes were isolated from KE37 human leukaemic cells by a standard sucrose gradient fractionation approach (Moudjou and Bornens, 1994) and then examined by both immunofluorescence microscopy and Western blotting. The number of centrosomes in each fraction was counted using immunofluorescence microscopy. Fractions 7 and 8 contained the most centrosomes (Figure 3.3A). Immunofluorescence staining of these fractions with α-tubulin and Nek2 revealed the frequent occurrence of two closely spaced dots, characteristic of intact centrosomes (Figure 3.3B). The amount of protein in the purified centrosome fraction and KE37 whole cell extract was equalized on silver stained gels and subjected to Western blotting with anti-Nek2 antibodies. Both 46 kDa and 44 kDa bands representing Nek2A and Nek2B were detectable in the purified centrosome preparation, indicating the enrichment of both proteins in centrosomes (Figure 3.3C).

To verify the predicted centrosomal localisation of Nek2B based on its enrichment in centrosome preparations, recombinant versions of Nek2A and Nek2B were introduced into human U2OS osteosarcoma cells by transient transfection and analysed by immunofluorescence microscopy. Using either enhanced green fluorescent protein (EGFP) or myc-epitope tags for detection, Nek2A and Nek2B were clearly detected at the centrosome as indicated by co-localisation with antibodies against C-Nap1 (Figure 3.4A) and γ-tubulin (Figure 3.4B). Interestingly, apart from at the centrosome, recombinant Nek2A and Nek2B were not present in the same subcellular compartment. Nek2A appeared to be frequently nuclear, whereas Nek2B was predominantly cytoplasmic (Figure 3.4C). The selective uptake of Nek2A into the nucleus may be through the use of a putative bipartite nuclear localisation sequence in the C-terminus of Nek2A (amino acids 361-383), that is not present in Nek2B. This remains to be tested, however one could speculate that the functions of Nek2A and Nek2B are regulated by their compartmentalism within the cell.

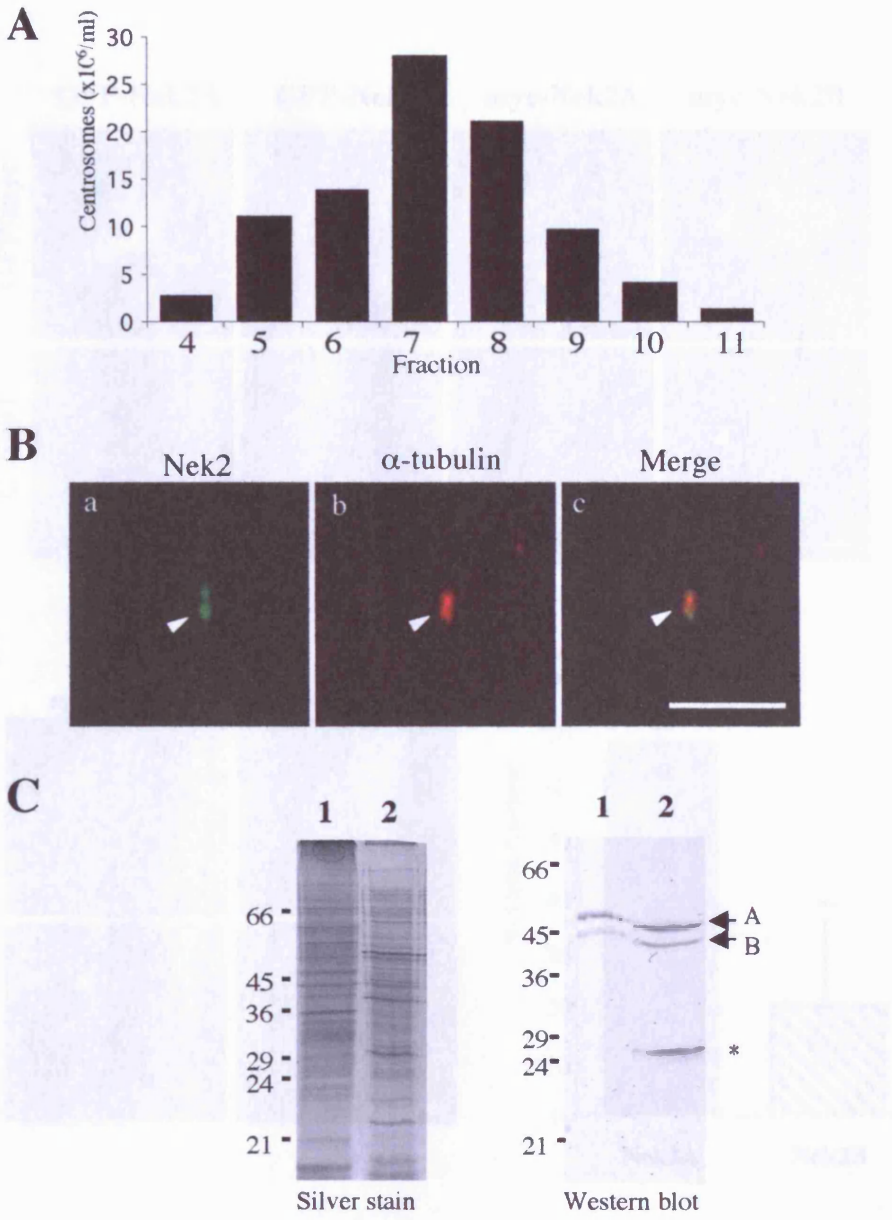

Figure 3.3 Enrichment of human Nek2A and Nek2B in purified centrosome preparations

(A) Centrosomes were isolated from KE37 human leukemia cells as described in materials and methods. The fractions eluting from the bottom of the sucrose gradient were analysed for number of centrosomes by immunofluorescence observation. **(B)** Purified centrosomes were spun onto coverslips, fixed and analysed by indirect immunofluorescence microscopy. The co-localisation of Nek2 with centrosomes as revealed by antibodies against the centriolar constituent α-tubulin is indicated (arrowhead). Scale bar, 10 μm. (C) Centrosomes purified from KE37 cells, (lane 1) and a KE37 whole cell extract (lane 2) were separated by SDS-PAGE and silver stained. The same samples were compared on a Western blot using the anti-peptide anti-Nek2 antibody. Nek2A and Nek2B were present in the centrosome preparation as indicated by the arrows. Whereas a cross reacting band was not (*). Molecular weights (kDa) are indicated on the left of each panel.

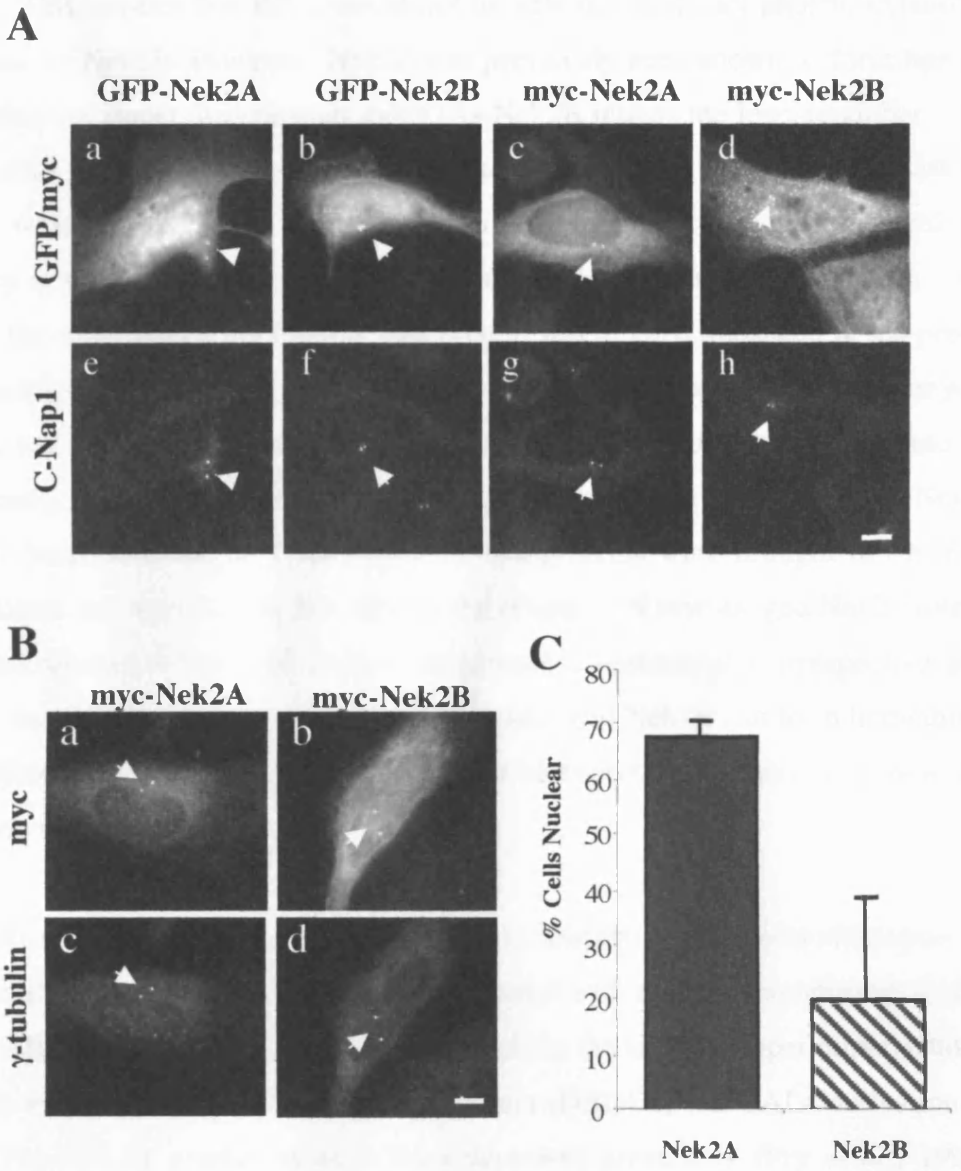

Figure 3.4 Recombinant Nek2A and Nek2B localise to the centrosome
(**A**) U2OS osteosarcoma cells were transiently transfected with GFP-Nek2A (a,e), GFP-Nek2B (b, f), myc-Nek2A (c, g) or myc-2B (d, h). Cells were fixed 24h after transfection and analysed by indirect immunofluorescence microscopy. Arrowheads indicate the co-localisation of GFP or myc signals with centrosomes as revealed by antibodies against the centrosomal protein C-Nap1. Scale bars, 10 μm. (**B**) HeLa cells were transiently transfected with myc-Nek2A (a, c) or myc-Nek2B (b, d), fixed after 24 h and analysed by indirect immunofluorescence microscopy using anti-myc antibodies to detect transfected protein and anti-γ-tubulin antibodies to reveal centrosomes. Scale bars, 10 μm. (**C**) The percentage of cells in which the transfected protein was nuclear was calculated for HeLa cells transfected with myc-tagged Nek2A and Nek2B proteins.

3.2.4 Dimerisation of Nek2 proteins

Due to its alternative C-terminus, Nek2B lacks the PP1c binding site that is present in Nek2A. This implies that PP1c would not be able to counteract phosphorylation events catalyzed by Nek2B. However, Nek2A has previously been shown to form homodimers via its leucine zipper dimerisation motif. As Nek2B retains the leucine zipper, it may be possible for PP1c to regulate Nek2B if the latter were able to heterodimerise with Nek2A. To test whether Nek2A and Nek2B can form heterodimers, recombinant Nek2 proteins made by *in vitro* translation were mixed *in vitro* and immunoprecipitated with antibodies against the myc-epitope tag (9E10). One protein was *in vitro* translated in the presence of [^{35}S]-methionine, whilst the other had a N-terminal myc tag (Figure 3.5). myc-tagged Nek2A was capable of precipitating an untagged version of both Nek2A and Nek2B. Conversely, myc-tagged Nek2B could also precipitate untagged versions of Nek2A and Nek2B. Small amounts of [^{35}S] labelled Nek2 proteins were brought down in control experiments but significantly less than in the presence of myc-tagged Nek2 proteins. We note that similar amounts of each isoform were co-precipitated irrespective of which protein was used as the bait indicating that Nek2A and Nek2B can form homodimers and heterodimers with similar efficiency as would be expected if dimerisation was regulated solely via the leucine zipper.

To confirm this result, a yeast two hybrid direct interaction assay was employed. For this purpose, the yeast strain PJ69-4A was transformed with different combinations of Nek2A and Nek2B and Nek2ΔLZ (deletion mutant lacking the leucine zipper dimerisation motif) fused to either the GAL4 DNA binding domain (DBD) or the GAL4 activation domain (AD). The Nek2A constructs have been described previously (Fry *et al.*, 1999). The Nek2B constructs were made by excising the coding sequence from pGEM-Nek2B on a *NaeI-SalI* fragment and inserting it into the yeast expression plasmids pACTII and pAS2 cut with *SmaI* and *XbaI* or *SalI*, respectively. This produced pACTII-Nek2B and pAS2-Nek2B, which contain Nek2B in frame with the GAL4 AD or GAL4 DBD respectively.

The expression of these constructs was confirmed by Western blot of whole yeast cell lysates with the anti-peptide Nek2 antibody (Figure 3.6A). A positive interaction indicating that dimerisation was taking place was indicated by growth on histidine selective media (Figure 3.6B). This indicates again that Nek2 can form homo and heterodimers. The relative strength of these interactions was determined quantitatively by measuring the

activity of the β-galactosidase reporter gene using the substrate ONPG (*O*-nitrophenyl β galactopyranoside). Nek2A homodimerisation was given an arbitrary value of 1 and all other interactions were compared to this (Figure 3.6C). Nek2A and Nek2B did not activate the reporter genes when present as DBD or AD fusions alone. The interaction between SNF1 and SNF4 was used to indicate the level of activity of β-galactosidase that is present if a positive interaction is occurring. All combinations of proteins that gave a positive result on selective media, reached a level of β-galactosidase activity higher than SNF1/SNF4. Together, growth selection and β-galactosidase activity indicate that Nek2B is capable of forming dimers with itself and with Nek2A. No interaction occurred between the leucine zipper mutant and wild type Nek2 as expected. Thus, Nek2A and Nek2B can form both homodimers and heterodimers most likely as a result of interaction through their conserved leucine zipper dimerisation motifs.

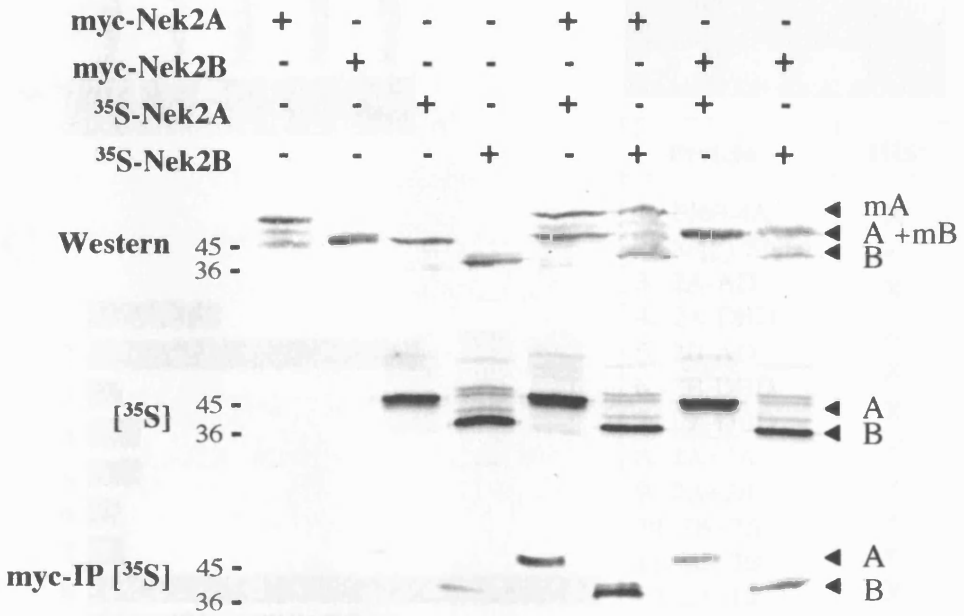

Figure 3.5 *In vitro* interaction between Nek2A and Nek2B
In vitro translated Nek2A and Nek2B were prepared in either the absence (myc-Nek2A and myc-Nek2B) or presence (^{35}S-Nek2A and ^{35}S-Nek2B) of [^{35}S] methionine. Samples were mixed as shown in the presence of cyclohexamide to prevent further translation and an aliquot taken for direct analysis by SDS-PAGE followed by either Western blotting with anti-Nek2 antibodies (top panel) or by autoradiography (middle panel). The remainder was immunoprecipitated with anti-myc antibodies, processed by SDS-PAGE and exposed for autoradiography (bottom panel). The positions of myc-Nek2A (mA), myc-Nek2B (mB), ^{35}S-Nek2A (A) and ^{35}S-Nek2B (B) are indicated on the right. Molecular weights (kDa) are indicated on the left of each panel.

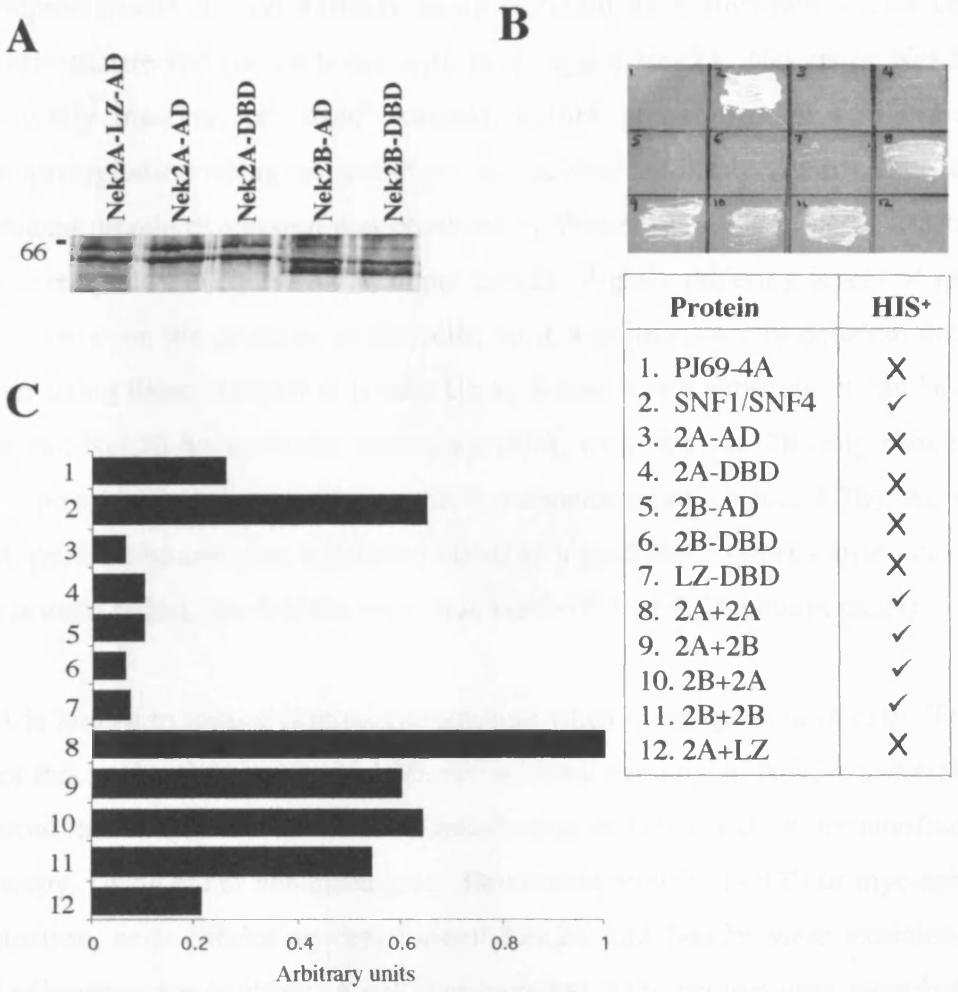

Figure 3.6 *In vitro* interaction between Nek2A and Nek2B
(A) Nek2A and Nek2B were introduced into yeast as either GAL4 DBD or AD fusion proteins and analysed by SDS-PAGE followed by Western blotting with anti-Nek2 antibodies. **(B)** Yeast PJ69-4A double transformants were tested for a positive interaction between the GAL4 BD fusion protein and GAL4 AD fusion protein by growth on media lacking histidine. **(C)** Positive interactions were confirmed using a quantitative assay for β-galactosidase activity with the substrate *ONPG*. Units of activity are relative to the Nek2A-Nek2A interaction, given an arbitrary value of 1.0. Results are the mean of three independent experiments.

3.2.5 Function of human Nek2B

To look at the relative activities of Nek2A and Nek2B, a kinase assay was carried out on immunoprecipitates of cell extracts using β-casein as a substrate. HeLa cells were transiently transfected for 24 hours with myc tagged Nek2A, Nek2B or Nek2A-K37R (catalytically inactive, or 'dead' kinase), before preparation of cell extracts and immunoprecipitation using an anti-myc monoclonal antibody (9E10). The extent of recombinant protein expression was observed by Western blotting of cell extracts prior to immunoprecipitation (Figure 3.7A, upper panel). Slightly differing levels of expression occurred between the proteins in the cells, so it was necessary to equalise their kinase activities using these expression levels. Using β-casein as a substrate, it can be seen that Nek2A and Nek2B have similar kinase activities, with Nek2-K37R only showing slight activity, possibly due to impurities in the immunoprecipitate (Figure 3.7B). As a positive control, purified baculovirus expressed histidine tagged Nek2 (work carried out by A.M. Fry) was used, to indicate that the assay was viable (Figure 3.7A bottom panel).

Nek2A is known to induce centrosome splitting when overexpressed in cells. To identify whether this is also the case for Nek2B, recombinant versions of Nek2A and Nek2B were introduced into HeLa cells by transient transfection and analysed by immunofluorescence microscopy. Using either enhanced green fluorescent protein (EGFP) or myc-epitope tags for detection, cells exhibiting centrosomal Nek2A and Nek2B were examined for the extent of centrosome splitting. A cell was included if the centrosomes were both visible and was counted as split if they were separated by approximately more than 2 μm. 100 cells were counted for each transfection. Overexpression of active Nek2A kinase induces centrosome splitting in a high frequency of cells 24 hours following transfection whereas Nek2B does not (Figure 3.8A, filled bars). However if left for 40 hours, the number of split centrosomes induced by overexpression of Nek2B is comparable to that induced by Nek2A (Figure 3.8A hatched bars). This suggests that Nek2B is less efficient at inducing split centrosomes in cells. This may reflect a difference in the affinity of Nek2B for certain centrosomal substrates as the level of kinase activity in both isoforms is comparable. This has important implications when discussing the relative roles of the Nek2 isoforms in the cell cycle, more specifically at the onset of mitosis, when the centrosomes separate.

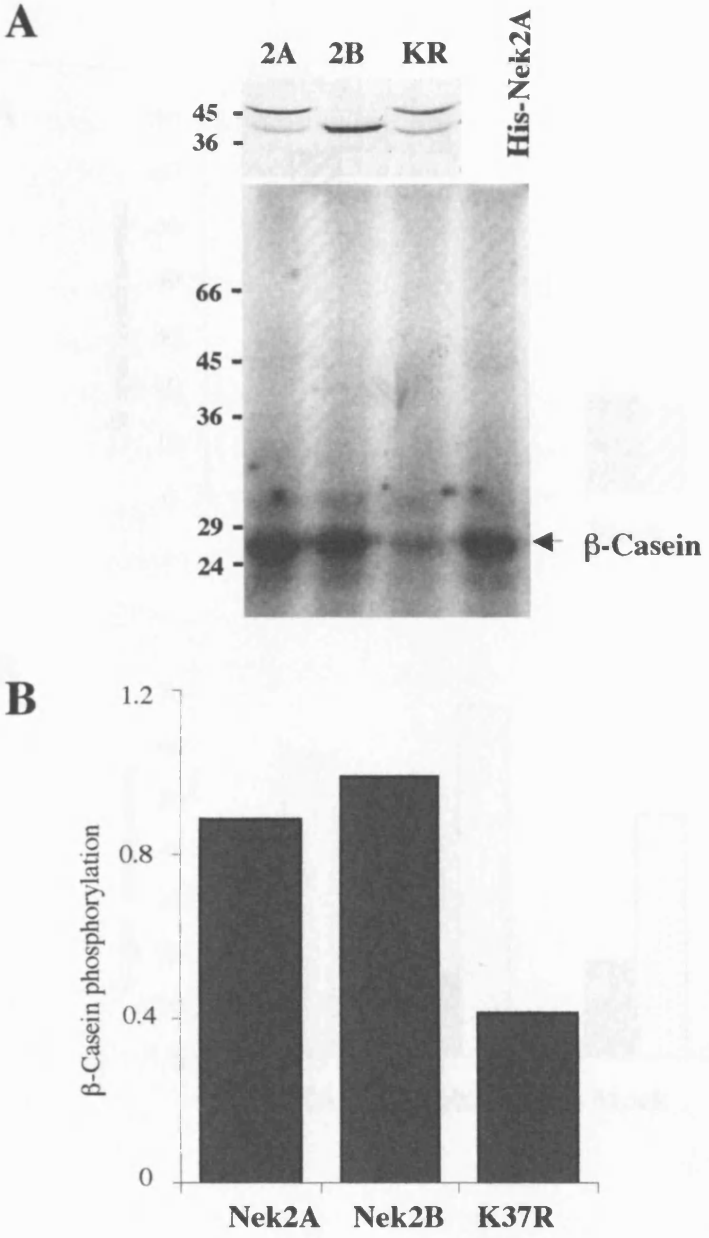

Figure 3.7 Nek2A and Nek2B exhibit similar kinase activities
(**A**) HeLa cells were transfected with myc-Nek2A (2A), myc-Nek2B (2B and myc-Nek2A-K37R (KR). An aliquot of extracts made from these cells was processed by SDS-PAGE and Western blotted with antibodies against Nek2 (top panel). The immunoprecipitates were incubated in Nek2 kinase buffer containing [^{32}P] ATP for 30 min at 30°C. Samples were subjected to SDS-PAGE and exposed to X-ray film (bottom panel). (**B**) The Western blot and autoradiograph were quantified by densitometric scanning (arbitrary units) and a comparison of kinase activity is shown.

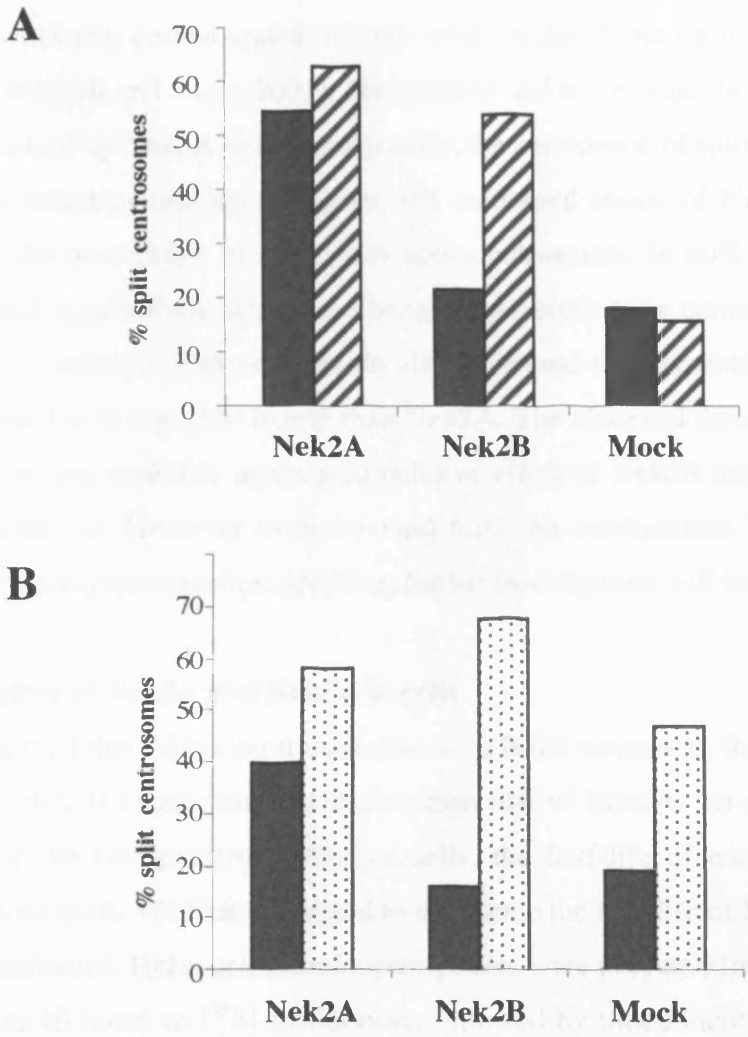

Figure 3.8 Nek2A is more efficient at causing split centrosomes
(A) HeLa cells were transfected with myc-tagged Nek2A and Nek2B proteins and left for 24 hours (filled bars) and 40 hours (hatched bars) before fixation. Cells were analysed by indirect immunofluorescence microscopy using anti-myc antibodies to detect transfected protein and anti-γ-tubulin antibodies to reveal centrosomes. The percentage of cells in which the two centrosomes were separated by more than 2 μm was calculated for and compared with mock-transfected cells. **(B)** Transfected cells were treated for 1 hour prior to fixation with either nocodazole (5μg/ml) (speckled bars) or DMSO (filled bars) and then analysed for centrosome splitting.

To determine whether an intact microtubule cytoskeleton was required for Nek2-induced centrosome splitting, a 1 hour treatment with nocodazole 24 hours following transfection of HeLa cells with Nek2A and Nek2B was employed (Figure 3.8B). Following treatment of mock transfected cells, centrosomes were split in about 50% of cells confirming previous work that demonstrated that microtubule depolymerisation induced centrosome splitting (Meraldi and Nigg, 2001). Nocodazole did not reduce the extent of centrosome splitting caused by Nek2A demonstrating that the persistence of split centrosomes does not require an intact cytoskeleton. In fact, the combined action of Nek2A and nocodazole increased the percentage of cells with split centrosomes to 60% indicating that Nek2 activity and microtubule depolymerising drugs produce a cumulative effect. Nek2B expression combined with nocodazole also increased the percentage of cells with split centrosomes but to a greater extent than Nek2A. The observed three fold increase in split centrosomes was probably again a cumulative effect of Nek2B activity and microtubule depolymerisation. However to understand fully the mechanisms by which Nek2A and Nek2B bring about centrosome splitting, further investigation will be required.

3.2.6 Stability of Nek2A and Nek2B in cells

It was observed that following transfection with Nek2 constructs, the number of cells with detectable Nek2B expression was higher than that of Nek2A. To determine whether the stability of the two proteins differ in cells, the half-life of each was determined in asynchronous cells. We first attempted to determine the half-life of Nek2 proteins by pulse chase experiments. HeLa cell immunoprecipitates were prepared from cells that were pre-labelled for 16 hours in [^{35}S] methionine, followed by timed incubations in fresh media. Cell were extracted, subjected to SDS-PAGE followed by autoradiography. However, due to the low abundance of endogenous Nek2 proteins, the immunoprecipitations were inefficient, even following optimisation. The immunoprecipitated material contained numerous proteins of a similar size to Nek2A and Nek2B making the data impossible to quantitate (data not shown). Therefore we used an alternative approach using a series of cell extracts prepared from asynchronously growing U2OS cells treated for different lengths of time with the protein synthesis inhibitor, cycloheximide was employed. The samples were separated by SDS-PAGE, Western blotted and probed with an anti-α-tubulin antibody to confirm equal loading. They were also probed with anti-Nek2 antibodies, which indicated that the levels of Nek2 decrease quite rapidly over the 4 hour period (Figure 3.9A). A half-life was calculated by plotting the relative amount of Nek2A and

Nek2B at each given time. In these cells the half-life of Nek2A was low at approximately 45 minutes. Nek2B was slightly more stable with a half-life of approximately 75 minutes (Figure 3.9B).

3.2.7 Cell cycle dependent expression of Nek2A and Nek2B

Human Nek2 was previously reported to be cell cycle regulated with peak levels in S and G2, and low levels in M and G1. These studies focused on the abundance of the 46 kDa Nek2A protein. During the first zygotic cell cycle of *Xenopus*, the abundance of X-Nek2B remains constant. It was therefore important to re-examine the relative expression of human Nek2A and Nek2B at different stages of the adult cell cycle. To optimise cell synchronisation protocols for U2OS cells, a standard growth curve was first determined (Figure 3.10A). With this in mind, a 16 hour incubation in hydroxyurea was employed to give a G1/S phase population of cells. To obtain S phase and G2 phase populations, the cells were released from the hydroxyurea block and samples taken at the given time intervals over a period of 15 hours (Figure 3.10B). The samples were separated by SDS-PAGE, Western blotted and probed with an anti-α-tubulin antibody to confirm equal loading. They were also probed with anti-Nek2 antibodies, which showed that the abundance of Nek2A increases over the initial 12 hour period before a sudden decrease at 15 hours. In contrast the abundance of Nek2B increases consistently throughout the 15 hours. In parallel, the DNA content of each sample was analysed by flow cytometry to confirm the cell cycle phase of each population. This indicated that most cells were in S phase by 3 hours and entered G2 between 9 and 12 hours. During the time between 12 and 15 hours, most cells went through mitosis and re-entered G1.

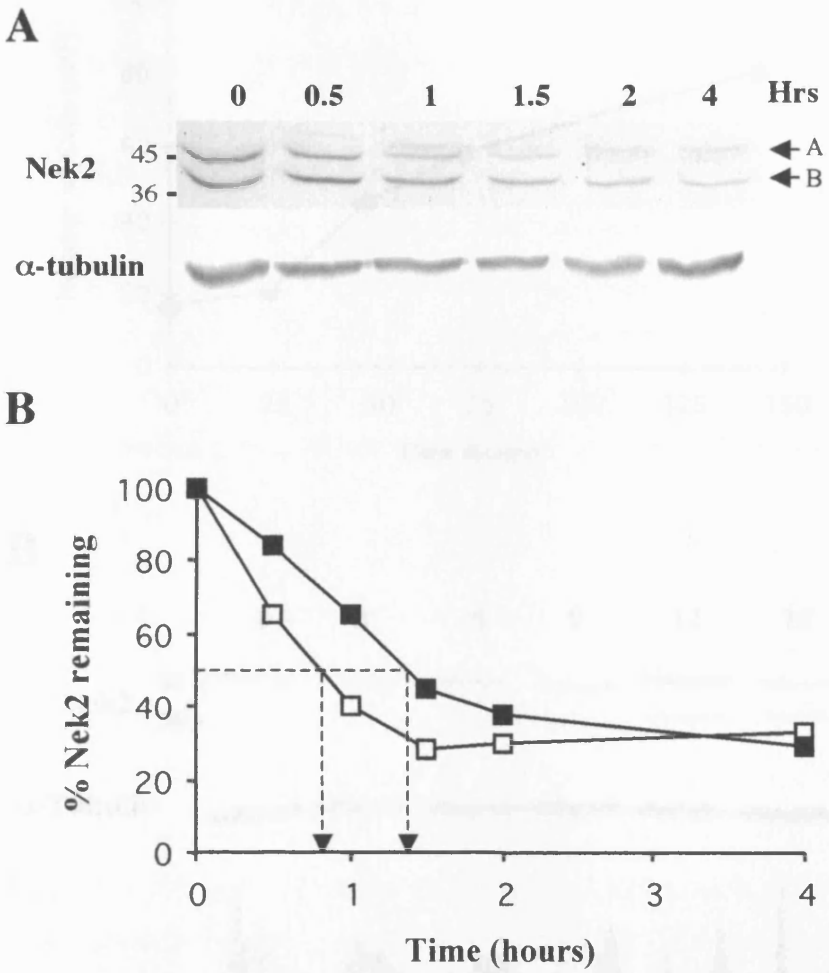

Figure 3.9 Nek2A and Nek2B are short-lived proteins
(**A**) Protein stability of Nek2A (A) and Nek2B (B) was measured on Western blots of cell extracts prepared at the times indicated (hours) after addition of cycloheximide. (**B**) The amount of Nek2 remaining at each time point is plotted with respect to the amount present at time zero (Nek2A, open squares; Nek2B, closed squares).

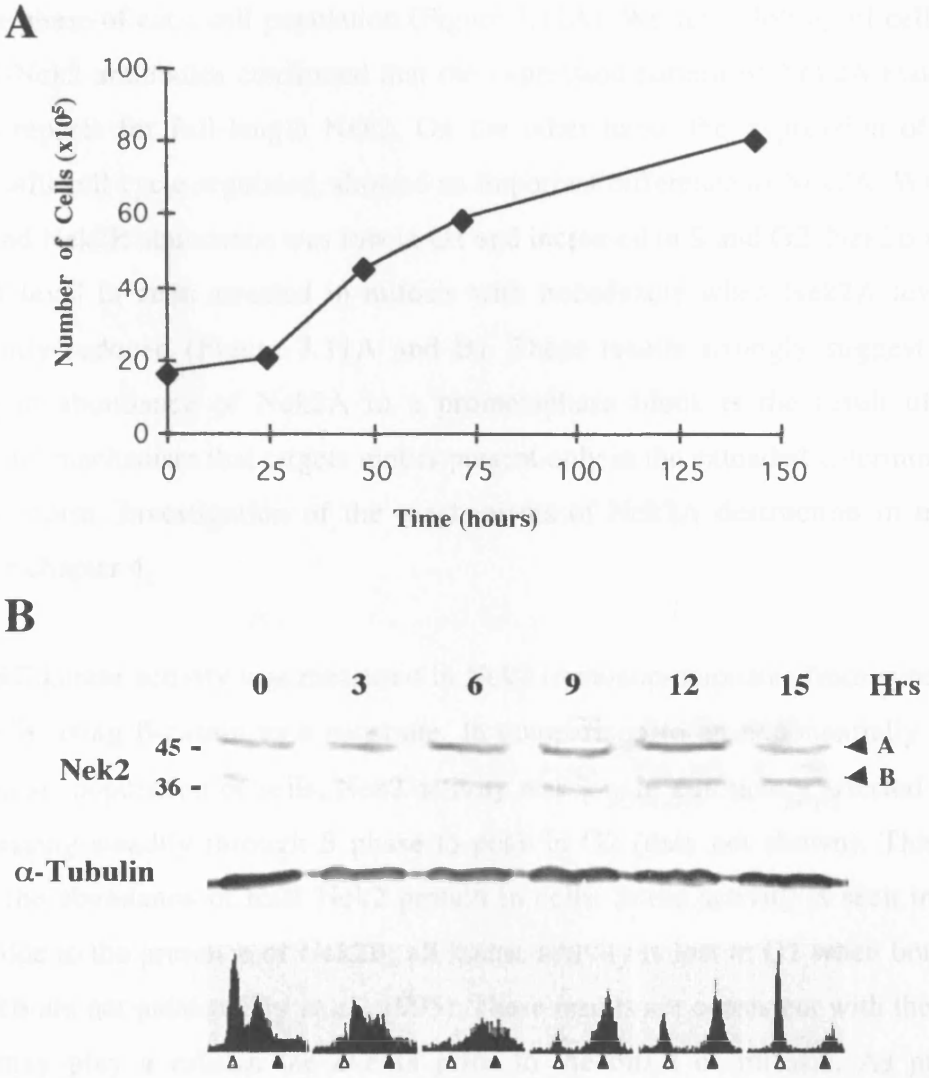

Figure 3.10 U20S cell growth and synchronisation

(**A**) To determine the growth rate of a population of U20Scells, the number of cells (x10^5) was plotted against times over a 6 day period. (**B**) U20S cell lysates were prepared following a release from a hydroxyurea block. Samples were processed by SDS-PAGE and Western blotted with antibodies against Nek2 and α-tubulin. Flow cytometry was carried out on each cell population and cell cycle profiles are shown below each lane where the open and closed arrowheads indicate 2n and 4n DNA, respectively.

Following the use of a single block, a double block-release experiment was undertaken to produce a more tightly synchronised cell population as detailed in the methods section. In parallel, the DNA content of each sample was analysed by flow cytometry to confirm the cell cycle phase of each cell population (Figure 3.11A). Western blotting of cell extracts with anti-Nek2 antibodies confirmed that the expression pattern of Nek2A matched the previous reports for full-length Nek2. On the other hand, the expression of Nek2B, although still cell cycle-regulated, showed an important difference to Nek2A. Whilst both Nek2A and Nek2B abundance was low in G1 and increased in S and G2, Nek2B remained at a high level in cells arrested in mitosis with nocodazole when Nek2A levels were significantly reduced (Figure 3.11A and B). These results strongly suggest that the decrease in abundance of Nek2A in a prometaphase block is the result of a post-translational mechanism that targets motifs present only in the extended C-terminus of the Nek2A isoform. Investigation of the mechanisms of Nek2A destruction in mitosis is detailed in chapter 4.

Total Nek2 kinase activity was measured in Nek2 immunoprecipitates from synchronised U2OS cells using β-casein as a substrate. In comparison to an exponentially growing, asynchronous population of cells, Nek2 activity was low in mitotically arrested cells and G1, increasing steadily through S phase to peak in G2 (data not shown). This activity parallels the abundance of total Nek2 protein in cells. Some activity is seen in mitosis, possibly due to the presence of Nek2B, all kinase activity is lost in G1 when both Nek2A and Nek2B are not present (Fry *et al.*, 1995). These results are consistent with the idea that Nek2A may play a role in the events prior to the onset of mitosis. As previously mentioned, the Nek2 antibody used throughout this investigation was raised against residues 278-299 of Nek2A, which are also present in Nek2B. Thus the kinase activities obtained represent both the activity of Nek2A and Nek2B, as both are immunoprecipitated by this antibody. Interestingly, the kinase activity of the combined immunoprecipitated Nek2 proteins is low when Nek2B is still present. It is possible that Nek2B is kept switched off by an unknown mechanism during mitosis. This is yet to be addressed but will form an interesting addition to our understanding of the varying functions of Nek2 isoforms in human cells.

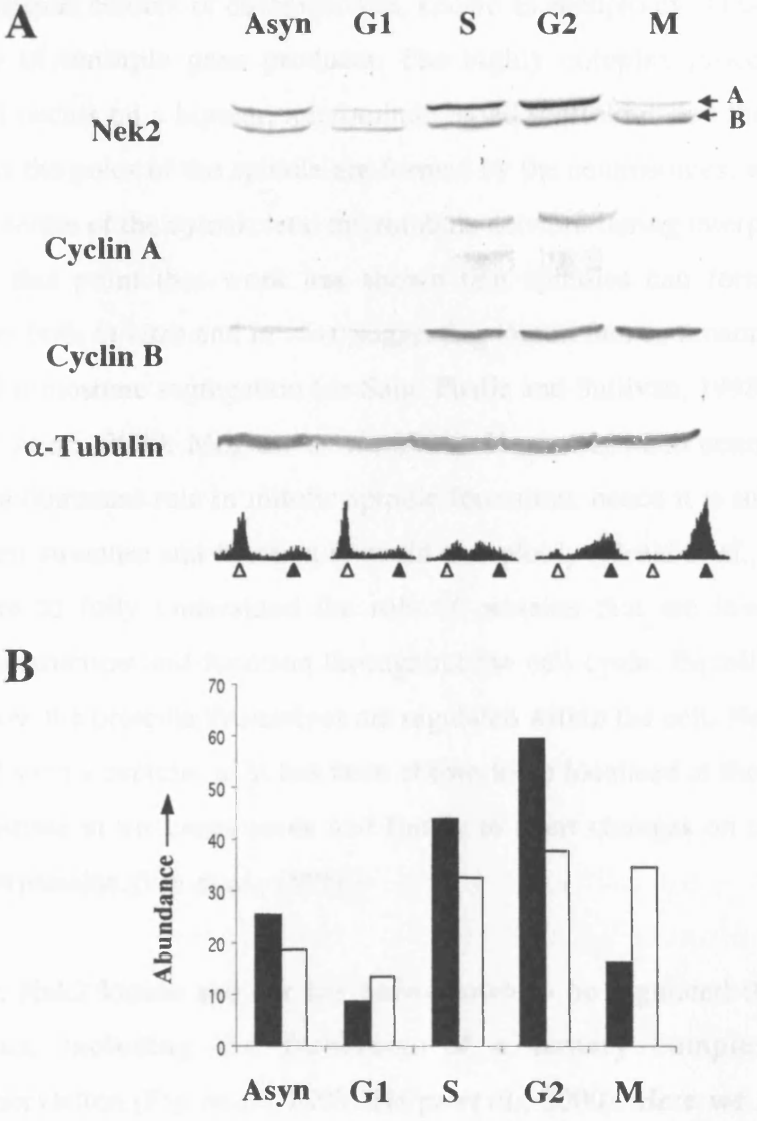

Figure 3.11 Cell cycle dependent expression of Nek2A and Nek2B
(**A**) Extracts were prepared from asynchronous (Asyn) growing U2OS cells or cells synchronised at different stages of the cell cycle. Samples were processed by SDS-PAGE and Western blotted with antibodies against Nek2, cyclin A, cyclin B or α-tubulin as indicated. Flow cytometry was carried out on each cell population and cell cycle profiles are shown below each lane where the open and closed arrows indicate 2n and 4n DNA, respectively. (**B**) The Western blots shown in (A) were quantified by densitometric scanning (arbitrary units) and a comparison of Nek2A (black bars) and Nek2B (white bars) abundance at different cell cycle stages is shown.

3.3. DISCUSSION

Cell division requires that chromosomes are first duplicated and then equally segregated between two daughter cells. Failure to execute these procedures correctly can lead to cells with an abnormal content of chromosomes, known as aneuploidy. This results in an excess or absence of multiple gene products. The highly complex process of chromosome segregation occurs on a bipolar, microtubule based scaffold called the mitotic spindle. In animal cells the poles of the spindle are formed by the centrosomes, which also act as the organising centre of the cytoskeletal microtubule network during interphase. It is important to note at this point that work has shown that spindles can form independently of centrosomes both *in vitro* and *in vivo*, suggesting that in fact centrosomes are not essential for equal chromosome segregation (de Saint Phalle and Sullivan, 1998; Heald *et al.*, 1996; Khodjakov *et al.*, 2000; Megraw *et al.*, 2001). However, when centrosomes are present they exert a dominant role in mitotic spindle formation, hence it is important to correctly regulate their structure and function to avoid anueploidy (Heald *et al.*, 1997). Therefore, it is important to fully understand the role of proteins that are involved in regulating centrosome structure and function throughout the cell cycle. Equally, it is important to elucidate how the proteins themselves are regulated within the cell. Nek2 kinase is a prime example of such a protein, as it has been shown to be localised at the centrosome, have a known substrate at the centrosome and finally to exert changes on centrosome structure upon overexpression (Fry *et al.*, 1998a).

Previously, Nek2 kinase activity has been shown to be regulated through a number of mechanisms, including the formation of a ternary complex with PP1c and autophosphorylation (Fry *et al.*, 1999; Helps *et al.*, 2000). Here we suggest that another mechanism of regulation is the expression of two alternative splice variants. There are various lines of evidence to support this. Firstly, the intron-exon structure of the human Nek2 gene located on chromosome 1 indicates that there is an intron-exon boundary at a position that is equivalent to the point of divergence of the two *Xenopus* Nek2 cDNAs. Sequencing from the point of divergence from the end of exon 7 into the seventh intron revealed the presence of a termination codon after the splice site, followed by an alternative polyadenylation signal. This implies that the splice variants may be formed through the recognition of different polyadenylation signals. Interestingly, the 3'-UTR of the predicted Nek2B cDNA sequence also contains a cytoplasmic polyadenylation element

(CPE), UUUUUAU. This CPE is known to bind factors that regulate mRNA translation in oocytes via a complex cytoplasmic polyadenylation mechanism (Richter, 1999). *Xenopus* Nek2B protein was reported to increase in abundance during oocyte maturation (Uto *et al.*, 1999); data from our laboratory confirms this (M. Pillai and A.M. Fry, unpublished observations). Hence, it is possible that vertebrate Nek2 is a general target for this highly specific form of developmentally regulated translational control.

The second line of evidence for the existence of alternative splice variants is the expression of two mRNAs and proteins of the predicted size in human cell lines. Three different Nek2 antisera were used to demonstrate that both the 46 kDa band of Nek2A and the smaller 44 kDa band of Nek2B were present. In combination with this, *in vitro* translated and overexpressed versions of recombinant Nek2A and Nek2B co-migrated precisely with the endogenous proteins. Finally, antisense oligonucleotides, complementary to a region of the Nek2 cDNA common to both isoforms, inhibited expression of the 46 kDa and 44 kDa products, but not other control proteins. Taken together, the RT-PCR, Western blot and antisense data presented here provide compelling evidence that human Nek2 is expressed as two distinct isoforms from a single gene on chromosome 1. The presence of alternative splice variants of Nek2 in *Xenopus* and now in humans strongly suggests that this form of regulation is conserved amongst vertebrate Nek2 kinases.

With the above evidence indicating that alternative splice forms do exist in human cells, the question of why they exist becomes apparent. In *Xenopus*, the generation of splice variants appears to be due to the need for different levels of centrosome regulation at different stages of development. In fertilised eggs and early embryos, Nek2B is the only isoform detected, with a switch to Nek2A occurring at the time of the gastrula-neurula transition (Uto *et al.*, 1999). In human cells, although Nek2B was detected in primary and transformed adult cells, Nek2A was always more abundant. It is possible that in earlier stages of development human Nek2B is more abundant and plays a role in the initial assembly of the zygotic centrosome as has been shown for X-Nek2B (Fry *et al.*, 2000b). If this is the case, it raises the question of why Nek2B is still present in adult cells if it carries no additional function. It is possible that it is merely a remnant of embryonic development. However this seems unlikely due to the observation that Nek2B exhibits a similar level of kinase activity as Nek2A due to the presence of the catalytic domain in the N-terminus. In addition, both proteins localise to the centrosome, which would mean that both are capable

of fulfilling the role of Nek2 at the centrosome. However, the fact that Nek2B is still present in mitosis when Nek2A has been degraded (Hames *et al.*, 2001), suggests that Nek2B is regulated in a way that does not interfere with Nek2A function.

The difference in the stability of the two isoforms may provide an effective mechanism for regulating their respective functions. The importance of Nek2A degradation in mitosis due to motifs present in distinct C-terminus is discussed in more detail in chapter 4 (Hames *et al.*, 2001). In brief, its degradation may allow C-Nap1 to re-accumulate at the proximal ends of the centrioles in telophase (Mayor *et al.*, 2000), allowing the intercentriolar linkage to be re-established and cytokinesis to occur (Piel *et al.*, 2001). Nek2B's apparent stability in mitosis, may again point to a function in early development. It has been observed that exogenous Nek2A is unstable during mitosis of early embryos, whereas Nek2B is not (Uto *et al.*, 1999). Maintaining a stable version of the Nek2 protein may therefore facilitate the rapid cell cycles that take place during early embryogenesis.

Subcellular location of the two splice variants may be a mechanism by which their activity is regulated. As stated previously, both localise to the centrosome, suggesting that the motif responsible for this is not contained in the C-terminus of the proteins. However, the centrosomal pool of endogenous Nek2 only accounts for about 10% of the total protein within the cell. The distribution of the remaining 90% is unclear due to its low abundance. Recombinant Nek2A is frequently seen in the nucleus, but recombinant Nek2B is predominantly cytoplasmic. The selective uptake of Nek2A into the nucleus may be due to a putative bipartite nuclear localisation sequence in the C-terminus of Nek2A that is not present in Nek2B. Perhaps Nek2A function is therefore restricted to the nucleus in certain phases of the cell cycle, which would allow a selective function for Nek2A. It has been suggested that Nek2A may be associated with chromosomes in mitosis and like NIMA may have some role in chromosome condensation (Ha Kim *et al.*, 2002; Rhee and Wolgemuth, 1997).

The predicted function for Nek2 at the centrosome is the initiation of loss of centrosome cohesion in prophase, preceeding nuclear envelope breakdown and spindle formation. A model for Nek2 function proposes that phosphorylation in late G2 of substrates such as C-Nap1 leads directly to the dissolution of the intercentriolar linkage that holds centrosomes together during interphase (Mayor *et al.*, 1999). In adult cells both Nek2A and Nek2B

exhibit cell cycle expression in line with a role late in the cell cycle. The interaction of Nek2A with active PP1c in S and G2 phases and inactive PP1c in prophase could explain how targets of Nek2 only become phosphorylated at the onset of mitosis. Nek2B lacks the PP1c binding motif that is present in the C-terminus of Nek2A. However, heterodimerisation with Nek2A via the leucine zipper motif present in both isoforms, may also allow PP1c to exert its dephosphorylating effect on Nek2B substrates, until it is inactivated at the G2/M transition. The fact that Nek2A disappears, whilst Nek2B persists beyond prometaphase, may provide an alternative mechanism to ensure that Nek2 function is completed in early mitosis. However, Nek2B is not capable of stimulating centrosome splitting to the same extent as Nek2A. Microtubule depolymerisation alone induces centrosome splitting, however in combination with Nek2A overexpression the extent of splitting increased suggesting a role for the microtubule cytoskeleton in centrosome cohesion (Jean *et al.*, 1999) and it has been suggested that microtubule depolymerisation causes an imbalance in the activities of centrosome-associated kinases and phosphatases (Meraldi and Nigg, 2001). Intriguingly the cumulative effect of Nek2B and depolymerisation of microtubules induced split centrosomes to the same extent as Nek2A and microtubule depolymerisation. The underlying mechanisms controlling Nek2A and Nek2B functions are not known but the difference in splitting induced by each could be attributed to their affinity for different substrates or inhibitors. Microtubule depolymerisation, may reduce the inhibition of Nek2B function that is in play in mitosis by reducing the influx of particular proteins to the centrosome. Thus allowing Nek2B kinase activity to be upregulated, inducing loss of centrosome cohesion. This is pure speculation and further work will need to be carried out to substantiate it.

Data presented in this chapter provides compelling evidence that human Nek2 is expressed as two distinct isoforms through alternative splicing from a single gene on chromosome 1. These isoforms designated Nek2A and Nek2B are found in both primary and transformed cell lines and can exist as homo and heterodimers. Both variants localise to the centrosome with the non-centrosomal function of Nek2B being predominantly cytoplasmic and Nek2A more frequently in the nucleus. Overexpression of Nek2A is more efficient at inducing centrosome splitting. This, combined with the observation that Nek2B, the more stable isoform remains constant in mitosis when the less stable Nek2A disappears suggest that Nek2B may perform a different function to Nek2A in the cell. This has important implications in our understanding of Nek2 regulation and control of centrosome structure

during mitosis. The elucidation of Nek2A and Nek2B functions will require new approaches. More specifically, selective inhibition of each of the proteins, possibly by microinjection of isoform specific antibodies would help us to understand their dual roles and regulation. A dsRNAi approach would also greatly aid our understanding of Nek2 function throughout the cell cycle as RNAi oligos specific to Nek2A or Nek2B can be designed.

CHAPTER 4

APC/C MEDIATED DESTRUCTION OF NEK2A OCCURS IN EARLY MITOSIS AND DEPENDS ON A CYCLIN A TYPE D BOX

4.1. INTRODUCTION

This chapter describes the identification of a degradation motif in the extreme C-terminus of Nek2A, which bears a striking resemblance to the extended destruction box of cyclin A. The APC/C mediated destruction of Nek2A in early mitosis depends upon this motif, with deletion resulting in stabilisation of Nek2A in prometaphase arrested cells (Hames *et al.*, 2001).

4.1.1 Importance of protein degradation in mitotic progression

Cell cycle progression is controlled by a number of different mechanisms including transcriptional regulation (e.g. cyclins), post-translational modifications (e.g. Cdks) and destruction of proteins (e.g. securin). Of these regulatory mechanisms, destruction by the proteasome represents the most effective method for the complete inactivation of modified proteins. Proteasomal destruction requires the prior modification of proteins by covalent attachment of ubiquitin catalysed by ubiquitin ligase enzymes. Key cell cycle regulated ubiquitin ligases include the multi-subunit complexes SCF (Skp1-cullin-F-box protein complex) or the APC/C (anaphase promoting complex/cyclosome) (Peters, 1998). A functional cell cycle requires the ordered accumulation and destruction of specific cyclin proteins, which in turn control the activity of their associated cyclin dependent kinases. Ubiquitin mediated protein destruction in mitosis, plays a critical role in the regulation of these cyclins. For example cyclin A accumulates in S phase and is specifically destroyed in prometaphase (den Elzen and Pines, 2001; Geley *et al.*, 2001). Cyclin B accumulates throughout G2, followed by destruction in metaphase (Clute and Pines, 1999; Wakefield *et al.*, 2000). This degradation, in combination with transcriptional and translational controls in the S and G2 phases of the cell cycle enables uninhibited cell cycle progression to occur.

4.1.2 The APC/C

The APC/C functions as a cell cycle regulated ubiquitin ligase that mediates the destruction of cell cycle regulatory factors by the proteasome during mitosis. It is activated at the metaphase-anaphase transition and remains active until late G1 (Morgan, 1999; Page and Hieter, 1999; Zechariae and Nasmyth, 1999). The 20S multi-subunit complex requires the addition of WD containing adapter proteins, either Cdc20 or Cdh1, to promote ubiquitylation of target proteins (Morgan, 1999). The mechanism of action of these proteins is not fully understood, but it is thought that their binding to the APC/C may

induce a conformational change in the complex that activates the catalytic site. Cell cycle dependent increases in APC/C activity are correlated to increased binding of Cdc20 or Cdh1. In metaphase, the APC/C is phosphorylated either by Cdk1, PKA or Plk1, which initiates binding of Cdc20 (Kramer *et al.*, 2000). At the same time, Cdh1 is phosphorylated by Cdk1 preventing it from binding the APC/C. This complex is then responsible for the degradation of targeted substrates during metaphase. For example, securin is destroyed in metaphase, resulting in sister chromatid separation, thus enabling chromosome segregation (Zur and Brandeis, 2001). Cyclin B is also destroyed by the APC/C-Cdc20, to allow cytokinesis and mitotic exit (Clute and Pines, 1999). Cdk1 is inactivated in anaphase, leading to Cdh1 dephosphorylation, in this form Cdh1 is then capable of binding to the APC/C. This second form of active APC/C then targets Cdc20 for destruction (Pfleger and Kirschner, 2000). The APC/C-Cdh1 remains active throughout G1 until it is inactivated by an E2F inducible factor, possibly Emi1, at the onset of S phase (Hsu *et al.*, 2002). A number of proteins including MAD2, MAD2B and Emi1 negatively regulate APC/C function. These proteins inhibit the APC/C via the WD adapter proteins (Chen and Fang, 2001; Pfleger *et al.*, 2001; Reimann *et al.*, 2001). MAD2 is involved in the spindle assembly checkpoint, which prevents APC/C-Cdc20 from destroying cyclin B and securins in the presence of unattached kinetochores (Shah and Cleveland, 2000). Emi1 also inhibits the APC/C-Cdc20 in late G2 to promote mitotic entry and is itself destroyed in early mitosis. It then re-accumulates at the G1/S transition to inhibit APC/C-Cdh1, allowing S phase entry (Hsu *et al.*, 2002; Reimann *et al.*, 2001). MAD2B can also inhibit both the APC/C-Cdc20 and APC/C-Cdh1. It is possible that the different actions of these inhibitors contribute to the timing of destruction of different APC/C substrates.

All known APC/C-Cdc20 substrates contain a destruction box (D box) that essentially conforms to the consensus sequence RXXLXXXXN (Glotzer *et al.*, 1991). APC/C-Cdh1 is also able to recognise this D box motif. However, proteins targeted for destruction specifically by APC/C-Cdh1 often contain a KEN box motif. The existence of this second destruction box allows specificity in the timing of protein degradation during mitosis due to differences in the timing of Cdh1 and Cdc20 activation. Deletion of one or both of these motifs from target proteins often results in complete stabilisation. For example, securin contains both a D box and a KEN box with complete stabilisation only occurring when both sequences are mutated (Zur and Brandeis, 2001).

4.1.3 Regulation of Nek2 kinase

NIMA is a cell cycle regulated kinase that has been implicated in the control of mitotic entry (Osmani and Ye, 1996). The APC/C is responsible for its degradation in late mitosis, with C-terminally truncated forms of NIMA no longer regulated in this way existing as stable, but toxic forms within the cell, that prevent normal mitotic progression (Pu and Osmani, 1995). The activity and abundance of Nek2, the most closely related vertebrate kinase to NIMA, is cell cycle regulated, peaking in S and G2 before diminishing in mitosis, much like NIMA (Schultz *et al.*, 1994). The existence of a complex containing Nek2 and PP1 limits Nek2 kinase activity to a small window at the G2/M phase transition, when PP1 is inactivated (Helps *et al.*, 2000). Nek2 is thought to be involved in regulating centrosome separation prior to mitosis, based on the observation that overexpression causes premature centrosome splitting in interphase (Fry *et al.*, 1998b). Other work suggests additional functions in assembly and/or maintenance of centrosome structure and more recently Nek2 has been proposed to play a role in chromosome condensation and mitotic spindle formation based on its localisation to mitotic chromosomes (Ha Kim *et al.*, 2002; Fry *et al.*, 2000b).

Two alternative splice variants of Nek2 with distinct C-termini are expressed in human and *Xenopus* cells, termed Nek2A and Nek2B. These two isoforms display distinct patterns of expression during development. X-Nek2A is most highly expressed in testis, whereas X-Nek2B shows highest expression in the ovary (Uto *et al.*, 1999). In contrast, in embryonic cell cycles X-Nek2B levels do not vary, however if ectopic X-Nek2A is added, the protein is rapidly degraded (Uto and Sagata, 2000). In human cells, these two isoforms also differ in their cell cycle regulation, with Nek2B expression remaining high in mitosis, when Nek2A has diminished. This implies that they may carry out different functions in the cell, but more importantly, suggests that there is a difference in the control of their degradation (Hames and Fry, 2002). These observations, combined with the presence of various putative degradation motifs in the extreme C-terminus of Nek2A which are missing in Nek2B, promoted the following work that provides evidence to support the model that APC/C mediated destruction of Nek2A is responsible for the diminished levels seen in early mitosis.

4.2. RESULTS

4.2.1 Destruction of Nek2A in early mitosis

In human somatic cells, both Nek2A and Nek2B are expressed at low levels in G1 and high levels in S and G2. However, in prometaphase arrested cells, Nek2A expression decreases whereas that of Nek2B remains high. To determine the precise timing of Nek2A disappearance, extracts were prepared from U2OS cells released from an S phase arrest in the presence of 500 ng/ml nocodazole. Nek2A expression decreased abruptly between 10 and 12 hours after release from the block (Figure 4.1A). This was coincident with both the time of mitotic entry as judged by microscopic examination of cells and with the disappearance of cyclin A, a protein known to be targeted for destruction in prometaphase (den Elzen and Pines, 2001; Geley *et al.*, 2001). The drop in expression of Nek2A was accompanied by the appearance of a weak, higher molecular weight smear suggestive of phosphorylation. However, even taking this into account, the overall level of Nek2A consistently decreased at least two to three fold with respect to S and G2 phase cells (Figure 4.1B). In contrast, the abundance of Nek2B remained elevated in these cells as they entered mitosis. In fact Nek2B levels consistently increased throughout G2, peaking in mitosis. To determine, the timing of Nek2B disappearance, cells were released from a prometaphase block and allowed to enter G1 (Figure 4.1C). Nek2B protein decreased between 4 and 8 hours after release. In contrast, cyclin B1 levels dropped rapidly as the cells entered G1 being completely ablated 2 hours after release. Nek2B protein therefore persists until early G1 and disappears slowly throughout G1. In this experiment, Nek2A levels decreased further upon entry into G1 and remained low until entry into the subsequent S phase when there was a sudden three to four fold increase in its abundance (Figure 4.1D).

4.2.2 Increased stability of Nek2A in S phase

To determine whether loss of Nek2 proteins was due to activation of their destruction, rather than a decrease in their translation, the half-life of both Nek2A and Nek2B was measured in cells that had been treated with cycloheximide, a compound that interacts with the translocase enzyme and blocks protein synthesis in eukaryotic cells. Cells were collected over a 4 hour period following addition of cycloheximide (Figure 4.2A).

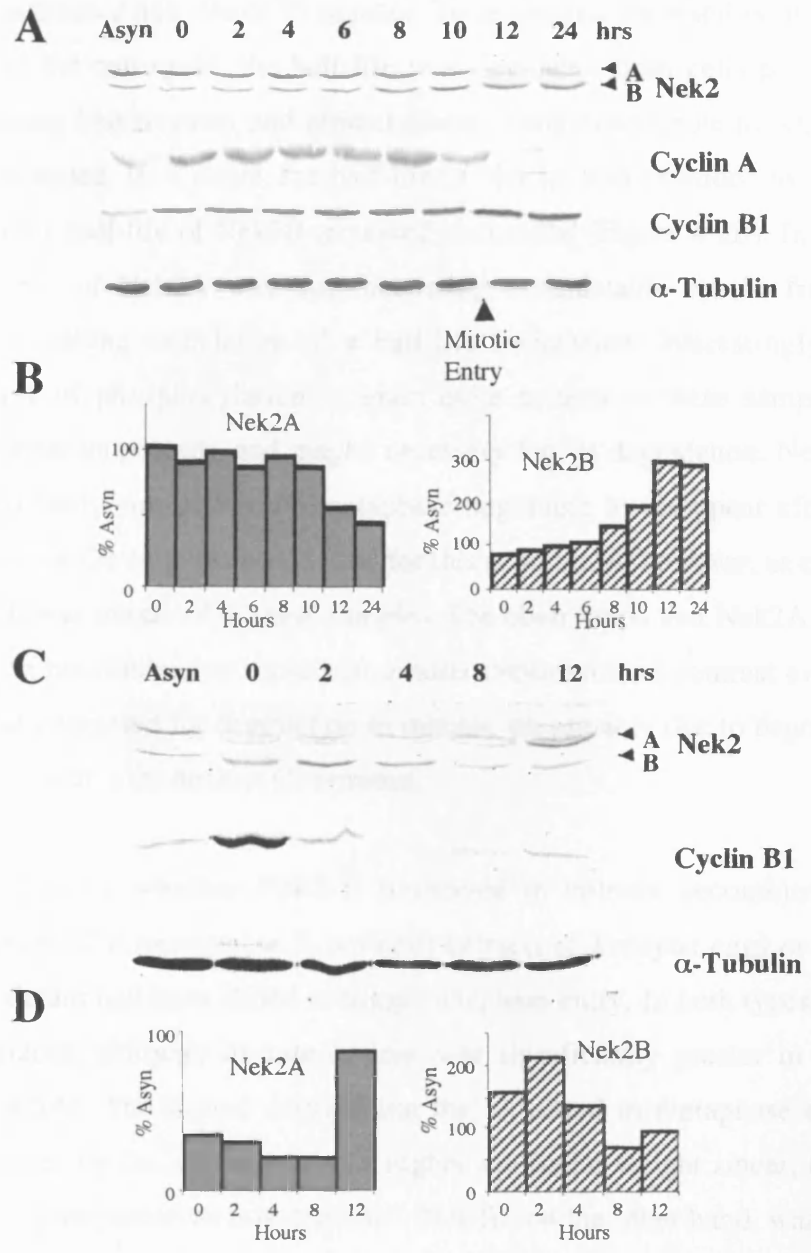

Figure 4.1 Cell cycle dependent expression of Nek2A and Nek2B
(**A**) Extracts prepared from asynchronous U2OS cells (Asyn) or cells released from an initial hydroxyurea block into medium containing nocodazole for the indicated times (hours) were Western blotted and probed with antibodies against Nek2, cyclin A, cyclin B1 and α-tubulin. Mitotic entry was observed by phase microscopy to occur between 10 and 12 hours after release. Positions of Nek2 splice variants (A and B) are indicated. (**B**) The abundance of Nek2A and Nek2B remaining was quantified by densitometry and plotted on histograms with respect to percentage of protein in asynchronous cells (**C**) Western blots of extracts prepared from cells released from a nocodazole block for the times indicated (hours) were probed with the same antibodies. (**D**) The abundance of Nek2A and Nek2B remaining was quantified by densitometry and plotted on histograms with respect to the percentage of protein in asynchronous cells.

In asynchronous cells, Nek2A decreased rapidly, representing a good example of a short lived protein, with an estimated half-life of 45 minutes. Nek2B was slightly more stable, with an estimated half-life of 75 minutes. To investigate the stability of Nek2A at different phases of the cell cycle, the half-life was calculated from cells pre-synchronised in S phase, using hydroxyurea and prometaphase, using nocodazole to which cycloheximide had been added. In S phase, the half-life of Nek2A was extended to more than 4 hours, whereas the half-life of Nek2B remained unchanged (Figure 4.2B). In prometaphase, the initial level of Nek2A was low, becoming undetectable by the first time-point (30 minutes) making calculation of a half-life impossible. Interestingly, an upper band, suggestive of phosphorylation is again quite evident in these samples, implying that phosphorylation preceds, and maybe necessary for, its degradation. Nek2B protein levels remained fairly constant in prometaphase beginning to disappear after a few hours. A population of G1 cells were also used for this experiment, however, as expected no Nek2A or Nek2B was observed in these samples. The observation that Nek2A is relatively stable in S phase but diminishes rapidly in mitosis implies that in contrast to Nek2B, Nek2A is specifically targeted for destruction in mitosis, presumably due to degradation motifs that may be present in its distinct C-terminus.

To test directly whether Nek2 is destroyed in mitosis, recombinant proteins were incubated in CSF (metaphase II-arrested) extracts of *Xenopus* eggs or in CSF extracts to which calcium had been added to trigger anaphase entry. In both types of extract, Nek2A was unstable, although its rate of loss was significantly greater in anaphase extracts (Figure 4.3A). The slower degradation that occurred in metaphase extracts was again accompanied by the appearance of a higher molecular weight smear, indicating possible Nek2 phosphorylation as it is degraded. Nek2B, on the other hand, was completely stable in CSF extracts both before and after addition of calcium. There was no appearance of an upper band for Nek2B for the duration of the experiment. For comparison, the stability of cyclins A and B1 were measured in these extracts (Figure 4.3A and B). As previously reported, cyclin B1 was only degraded after calcium addition, i.e. degradation occurs only in anaphase, whereas cyclin A was degraded both before and after calcium addition, although, like Nek2A, degradation was more rapid in anaphase extracts (Geley *et al.*, 2001; Glotzer *et al.*, 1991). Taken together, the results shown in Figures 4.1, 4.2 and 4.3 demonstrate that Nek2A is destroyed in early mitosis with very similar timing to cyclin A destruction, whereas Nek2B is stable until early G1.

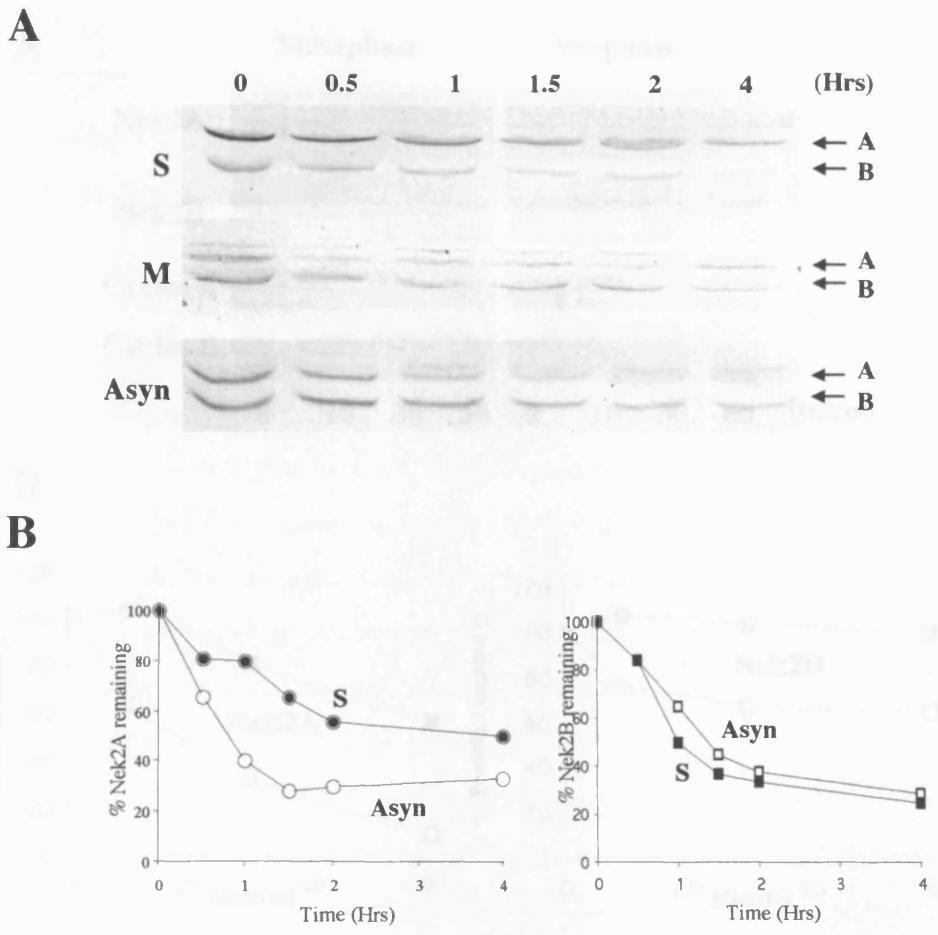

Figure 4.2 *In vivo* stability of Nek2A is decreased in mitosis
(**A**) Protein stability of Nek2 was measured on Western blots of extracts of cells presynchronised in S phase (S) and prometaphase (M) then prepared at the times indicated (hours) after addition of cycloheximide. Nek2 stability in S and M phases was compared to the stability in asynchronous cells (Asyn). (**B**) The amount of Nek2A (left graph) and Nek2B (right graph) remaining at each time point is plotted with respect to the amount present at time zero (100 %) (Asyn, open circles/squares; S, closed circles/squares).

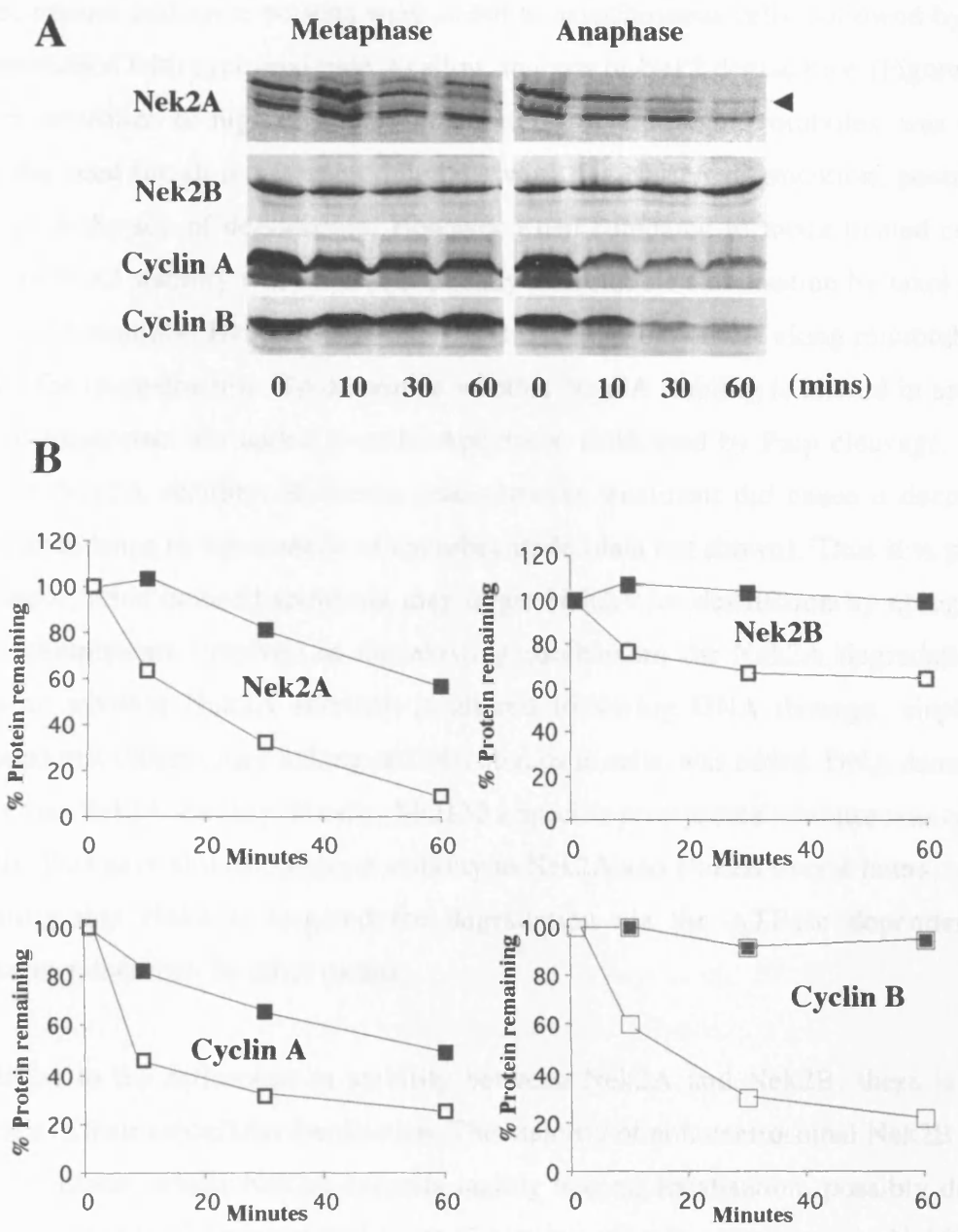

Figure 4.3 *In vitro* stability of Nek2A is decreased in mitosis
(A) *In vitro* degradation assays were performed by addition of [^{35}S]-labelled Nek2A, Nek2B, cyclin A or cyclin B1 to CSF extracts with (anaphase) or without (metaphase) addition of calcium. Samples were collected at the times indicated (min), separated by SDS-PAGE and exposed to autoradiography. **(B)** The amount of protein remaining at each time is plotted with respect to the amount at time zero in metaphase (closed squares) and anaphase (open squares) extracts for Nek2A, Nek2B, cyclin A or cyclin B1.

4.2.3 Increased Nek2 stability following inhibition of the proteasome

To investigate the mechanisms underlying the difference in stability between Nek2A and Nek2B, various cell cycle poisons were added to asynchronous cells, followed by a four hour incubation with cycloheximide, to allow analysis of Nek2 degradation (Figure 4.4A). A short incubation of high dose nocodazole to depolymerise microtubules, was used to assess the need for an intact microtubule network for Nek2A degradation, possibly for transport to the site of degradation. However when compared to mock treated cells, no change in Nek2 stability was observed. Equally microtubule stabilisation by taxol did not alter Nek2A stability. Hence it is unlikely that transport of Nek2A along microtubules is required for its destruction. To determine whether Nek2A stability is altered in apoptotic cells, staurosporine was added to cells. Apoptosis, confirmed by Parp cleavage, had no effect on Nek2A stability. However, staurosporine treatment did cause a decrease in Nek2A abundance in the absence of cycloheximide (data not shown). Thus it is possible that staurosporine induced apoptosis may target Nek2A for destruction by upregulating certain components involved in the existing mechanism for Nek2A degradation. To determine whether Nek2A stability is altered following DNA damage, cisplatin, a compound that causes cross-linking of DNA strands in cells, was added. DNA damage had no effect on Nek2A stability. Finally, MG132 a specific proteasome inhibitor was added to the cells. This gave almost complete stability to Nek2A and Nek2B over 4 hours, strongly suggesting that Nek2 is targeted for degradation via the ATPase dependent 26S proteasome rather than by other means.

In addition to the difference in stability between Nek2A and Nek2B, there is also a difference in their subcellular localisation. The majority of non-centrosomal Nek2B resides in the cytoplasm, whilst Nek2A exhibits mainly nuclear localisation, possibly due to a putative nuclear localisation signal in its C-terminus that is not present in Nek2B. The specificity of degradation may be affected by compartmentalisation of Nek2 into the nucleus or the cytoplasm. This mechanism is evident in the control of MyoD destruction. This skeletal muscle transcription factor, present in the nucleus is specifically degraded by the ubiquitin-proteasome system that is present in the nucleoplasm (Floyd *et al.*, 2001). To see if this mechanism may regulate Nek2, Leptomycin B (LMB), a compound capable of inhibiting nuclear export, was added to HeLa and U20S cells for 4 hours (Figure 4.4C). If the nuclear localisation of Nek2A is important in the control of its destruction an increase (nuclear mediated destruction) or decrease (centrosomal mediated destruction) in Nek2A

stability would be evident. In addition if cytoplasmic Nek2B regulation required dimerisation with Nek2A, then Nek2B would be stabilised if Nek2A was confined to the nucleus. No difference in the stability of Nek2A or Nek2B was seen in cells treated with LMB, compared to mock (methanol) treated cells. These results suggest that nuclear specific localisation of Nek2A does not appear to contribute to its instability in cells. However, more detailed work need to be undertaken to fully understand whether the localisation of Nek2 proteins may play a role in their cell cycle regulation.

4.2.4 Proteasome dependent Nek2A destruction

Given the result from Figure 4.4 suggesting that Nek2A is destroyed by the proteasome, more extensive analysis was required to determine whether this was indeed the case. For this, the stability of Nek2A was measured in cells pre-incubated with various protease inhibitors, followed by incubation with cycloheximide (Lee and Goldberg, 1998) (Figure 4.5Aand B). DMSO, used as a mock treatment, demonstrated that normal degradation of Nek2A and Nek2B occurred under these conditions. In the presence of either MG132, a potent proteasome inhibitor, or lactacystin, a specific inhibitor of the 20S proteasome (Fenteany *et al.*, 1995), the half-life of Nek2A and Nek2B was extended to more than 4 hours. In contrast, incubation with ALLM, a calpain inhibitor, did not alter the half-life of Nek2A. Treatment with leupeptin, an inhibitor of trypsin and cysteine proteases, caused a moderate increase in Nek2A half-life consistent with the inhibition of one of the major peptidase activities (trypsin-like) of the proteasome (Coux *et al.*, 1996). For comparison, the stability of cyclin B1 was also measured in these extracts. As previously reported, cyclin B1 was stable in the presence of strong inhibitors of the proteasome, MG132 and lactacystin, but not leupeptin or ALLM (Figure 4.5C). These results confirm that cyclin B1 and Nek2A are both targeted for destruction by the 26S proteasome.

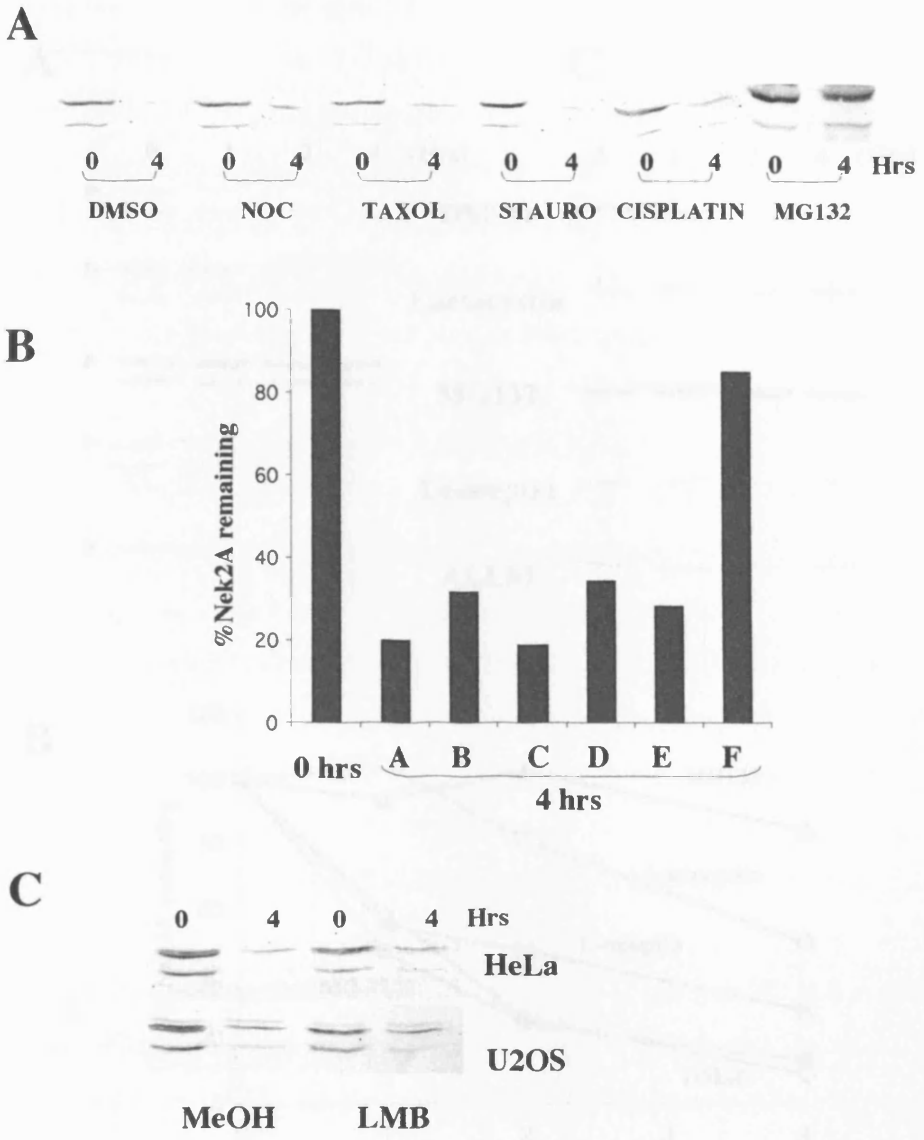

Figure 4.4 Identification of the processes involved in Nek2 instability
(**A**) Hela cells were pretreated with 1 μl/ml DMSO, 1 μg/ml nocodazole, 1 μM taxol, 1 μM staurosporine, 500 μM cisplatin or 20 μM MG132 for 1 hour before addition of 50 μg/ml cycloheximide for 4 hours. Cells were then extracted, Western blotted and probed with anti-Nek2 antibodies. (**B**) The fraction of Nek2A remaining at 4 hours in the presence of the above drugs is shown with respect to the amount at 0 hours. (**C**) HeLa and U2OS cells were pre-treated with 70% methanol (MeOH) or 10 mM leptomycin B (LMB) before addition of cycloheximide for either 0 or 4 hours as indicated. Cells were then extracted, Western blotted and probed with anti-Nek2 antibodies.

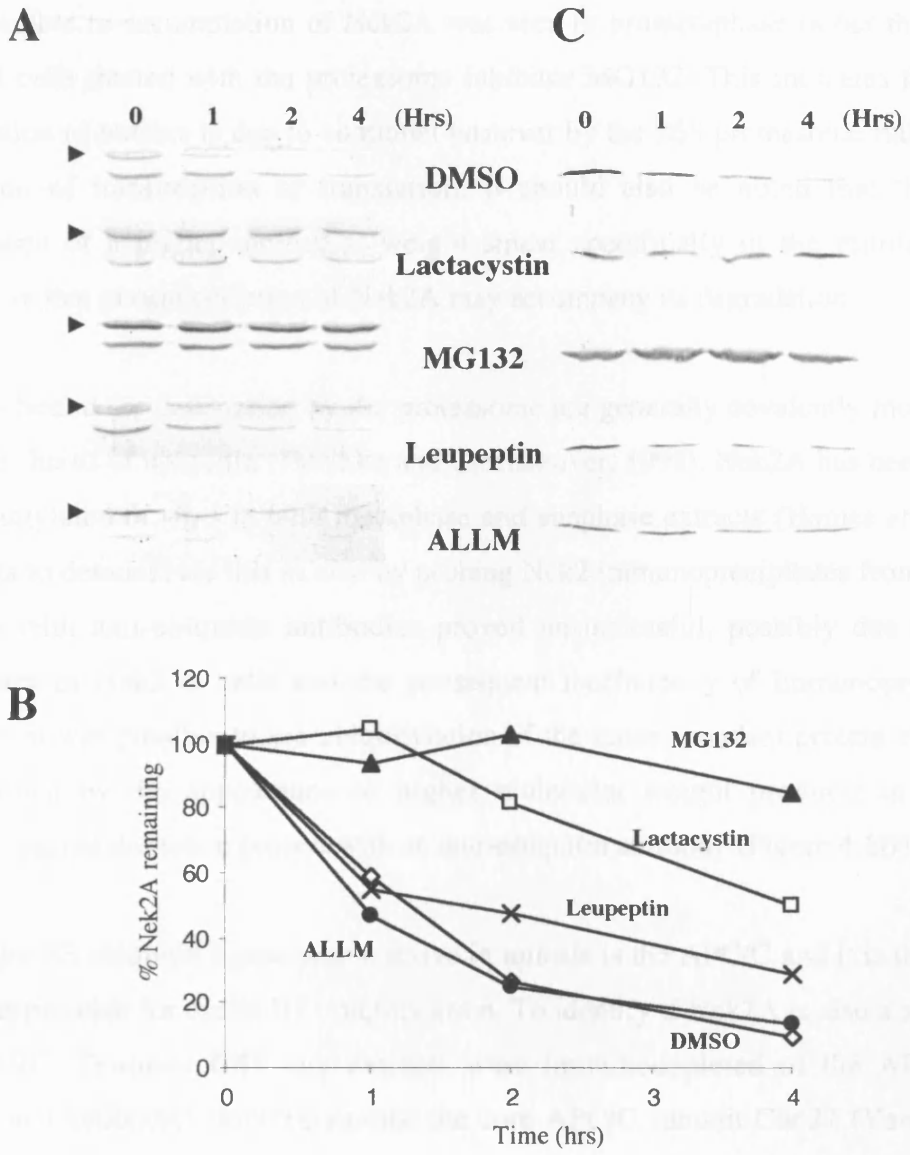

Figure 4.5 The mitotic destruction of Nek2 is proteasome dependent
(A) Protein stability of Nek2A and Nek2B in asynchronous HeLa cells was measured by Western blotting of cell extracts prepared at the times indicated after addition of cycloheximide, following a 1 hour pre-incubation with 1 μl/ml DMSO, 12.5 μM lactacystin, 20 μM MG132, 100 μM ALLM or 200 μg/ml leupeptin. The position of Nek2A is indicated (arrowhead). **(B)** The amount of Nek2A shown in (A) was determined by quantitative densitometry and shown with respect to the amount of protein at time zero (100%); DMSO (open diamonds), lactacystin (open squares), MG132 (filled triangles), ALLM (filled circles), leupeptin (crosses). **(C)** Cyclin B1 protein stability was determined as in (A).

4.2.5 Specific destruction of Nek2A in mitosis

To determine whether specific destruction of Nek2A in mitosis is due to the proteasome, MG132 was added to cells pre-arrested in either S phase or prometaphase (Figure 4.6A). The selective re-accumulation of Nek2A was seen in prometaphase rather than S phase arrested cells treated with the proteasome inhibitor MG132. This indicates that Nek2A degradation in mitosis is due to continual turnover by the 26S proteasome rather than by inhibition of transcription or translation. It should also be noted that there is the appearance of a higher molecular weight smear specifically in the mitotic extracts, suggestive that phosphorylation of Nek2A may accompany its degradation.

Proteins bound for destruction by the proteasome are generally covalently modified with multiple chains of ubiquitin (Hershko and Ciechanover, 1998). Nek2A has been shown to be ubiquitylated *in vitro* in both metaphase and anaphase extracts (Hames *et al.*, 2001). Attempts to demonstrate this *in vivo* by probing Nek2 immunoprecipitates from HeLa cell extracts with anti-ubiquitin antibodies proved unsuccessful, possibly due to the low abundance of Nek2 in cells and the consequent inefficiency of immunoprecipitation. However it was possible to see ubiquitylation of the more abundant protein cyclin B1 *in vivo* shown by the appearance of higher molecular weight products in cyclin B1 immunoprecipitates when probed with an anti-ubiquitin antibody (Figure 4.6B).

The major E3 ubiquitin ligase that is active in mitosis is the APC/C and it is this complex that is responsible for cyclin B1 ubiquitylation. To identify if Nek2A is also a substrate for the APC/C, *Xenopus* CSF egg extracts were immunodepleted of the APC/C using monoclonal antibodies directed against the core APC/C subunit Cdc27 (Yamano *et al.*, 1998). In these extracts the destruction of cyclin A and cyclin B1 was significantly delayed as compared with mock depleted extracts confirming the successful depletion of the APC/C (Figure 4.6C). Nek2A destruction was also delayed, indicating that the APC/C is responsible for its ubiquitylation and targeting to the proteasome for destruction (work carried out by S. Wattam). Addition of neutralising antibodies against the APC/C adapter protein Cdc20 is known to block APC/C-Cdc20 mediated degradation of cyclin B (Lorca *et al.*, 1998). The degradation of Nek2A in both metaphase and anaphase extracts was also blocked by the addition of these antibodies providing additional strong evidence for the role of APC/C-Cdc20 in the mitotic destruction of Nek2A (Hames *et al.*, 2001).

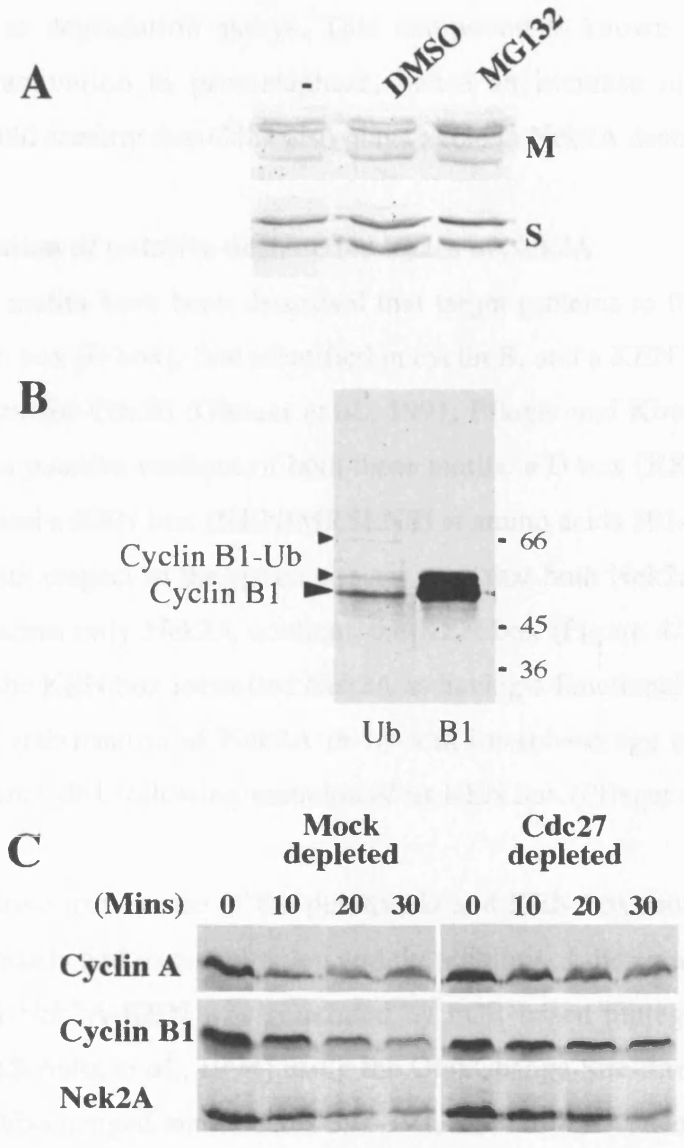

Figure 4.6 Specific APC/C mediated destruction of Nek2A in mitosis
(A) Cells arrested in either S phase (S) or prometaphase (M) were treated for 4 hours with 1 μl/ml DMSO, 20 μm MG132 or left untreated (-). Cells were extracted, Western blotted and probed with anti-Nek2 antibodies. **(B)** HeLa cells treated with 20 μM MG132 for 4 hours were extracted, followed by immunoprecipitation of cyclin B1. Samples were Western blotted and probed with an anti-Ubiquitin antibody (Ub) and anti-cyclin B1 antibody (B1). Un-modifed protein or protein with a single ubiquitin is indicated (large arrowhead). Higher molecular weight ubiquitylated products are indicated (small arrowheads). **(C)** Degradation assays were performed on cyclin A, cyclin B1 and Nek2 in anaphase extracts that had been either mock depleted (left panels) or Cdc27-depleted (right panels). Samples were collected at the times indicated (min), separated by SDS-PAGE and exposed to autoradiography (work carried out by S.Wattam).

Nek2A can also be destroyed by APC/C-Cdh1 (Pfleger and Kirschner, 2000; S. Wattam and A.M. Fry, unpublished results). To confirm this roscovitin, a specific Cdk2 inhibitor can be added to degradation assays. This compound is known to induce premature APC/C-Cdh1 activation in prometaphase, hence an increase in the rate of Nek2A destruction would confirm that Cdh1 also plays a role in Nek2A destruction.

4.2.6 Examination of putative destruction boxes in Nek2A

Two sequence motifs have been described that target proteins to the APC/C: a 9 amino acid destruction box (D box), first identified in cyclin B, and a KEN box, initially found in the APC/C regulator Cdc20 (Glotzer *et al.*, 1991; Pfleger and Kirschner, 2000). Human Nek2A contains putative versions of both these motifs: a D box (**RKFLSLASN**) at amino acids 361-369 and a KEN box (**KEN**IMRSENS) at amino acids 391-400. The positions of these motifs with respect to the splice site are such that both Nek2A and Nek2B contain the D box, whereas only Nek2A contains the KEN box (Figure 4.7A). The initial work that described the KEN box identified Nek2A as having a functional KEN box motif. This was shown by stabilisation of Nek2A *in vitro* in interphase egg extracts supplemented with recombinant Cdh1 following mutation of its KEN box (Pfleger and Kirschner, 2000).

To test the relative importance of the putative D and KEN box motifs in cells they were mutated individually and in combination and the stability of the resulting constructs tested *in vivo*. pGEM-Nek2A-KEN was generated by PCR-based mutagenesis of the pGEM-Nek2 plasmid (Schultz *et al.*, 1994) using the QuikChange Site-directed Mutagenesis Kit (Stratagene). This changed amino acids 391-393, KEN to AAA, and 399, N to A. pGEM-Nek2A-R361L was made by mutagenising the pGEM-Nek2 plasmid using the Transformer Site-directed Mutagenesis Kit (Clontech), changing amino acid 361 from an R to an L (work carried out by A.M. Fry). To test the stability of mutated proteins, HeLa cells were transfected with myc tagged versions of the mutated Nek2A constructs, as well as with wild type Nek2A and Nek2B. The abundance of the expressed myc-tagged protein was analysed after 4 hours in the presence of cycloheximide. The transfected cells were also pre-incubated with the proteasome inhibitor MG132 to confirm that the reduction seen in expression of the recombinant proteins was due to proteasomal degradation (Figure 4.7B). All of the mutated proteins were degraded to a similar extent over the 4 hour period. In addition, all of the proteins were stabilised in the presence of MG132. The degradation of transfected proteins was also comparable to the destruction of endogenous

Nek2A and Nek2B. The abundance of protein remaining after 4 hours cycloheximide treatment was quantified and again showed that the mutated proteins were all destroyed at approximately the same rate (Figure 4.7C). Although, partial stabilisation of the KEN box mutated protein was seen, repeat experiments showed this to be very minor. The stability of the mutated proteins was also analysed *in vitro,* using CSF extracts. These experiments (carried out by S. Wattam), confirmed that mutation of the KEN box slowed Nek2A degradation in metaphase but not anaphase, whilst the mutation of D box had no effect at all (data not shown).

The stability of Nek2A with D and KEN box mutations was investigated specifically in mitosis. HeLa cells expressing the myc tagged mutated proteins were synchronised in either S phase using hydroxyurea or prometaphase using nocodazole (Figure 4.8A). The amount of protein that remained in prometaphase as a percentage of S phase protein was quantified (Figure 4.8B). All ectopically expressed proteins detected in S phase arrested cells were significantly reduced in prometaphase arrested cells to a similar extent as endogenous wild type Nek2A. Therefore, the D and KEN box either alone or in combination cannot account for the destruction of Nek2A that occurs in prometaphase. Together, these results suggest that the putative D box does not appear to be functional under these conditions. The KEN box, however does appear to have some importance but not in early mitosis. Thus another factor must be involved in the targeting of Nek2A for APC/C mediated destruction in early mitosis.

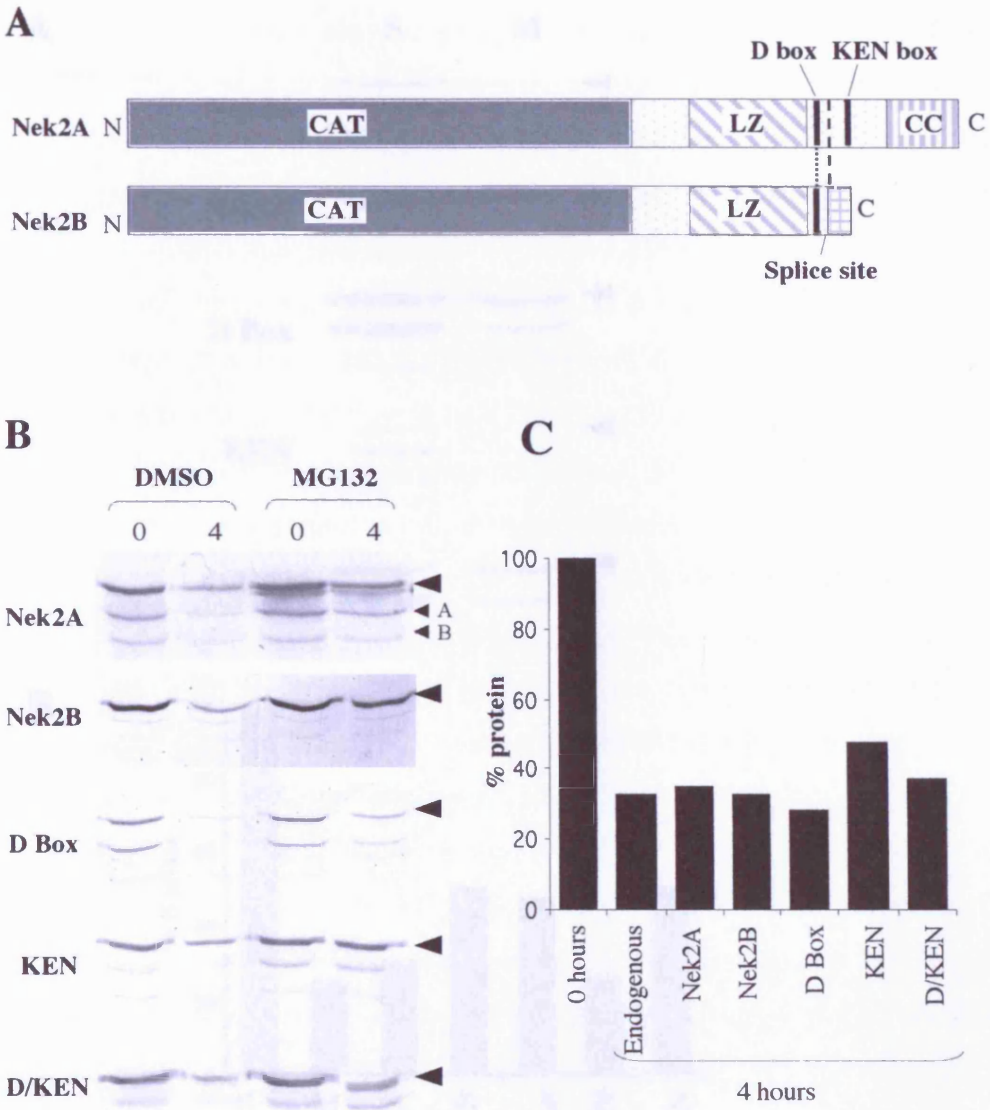

Figure 4.7 Examination of putative destruction boxes in Nek2A
(A) Schematic diagram of the human Nek2 splice variants indicating the catalytic domain (CAT), leucine zipper (LZ), coiled coil domain (CC), splice site, D box and KEN box. **(B)** Extracts of HeLa cells transfected with myc-Nek2A, myc-Nek2B, myc-R361L (D box), myc-KEN or myc-D/KEN were pre-treated with 1 µl/ml DMSO or 20 µM MG132 before addition of cycloheximide for either 0 or 4 hours as indicated. Transfected protein is indicated by black arrowheads, endogenous Nek2A and Nek2B are indicated (A and B). **(C)** The fraction of each protein remaining at 4 hours after cycloheximide treatment, as a percentage of the amount at 0 hours is shown.

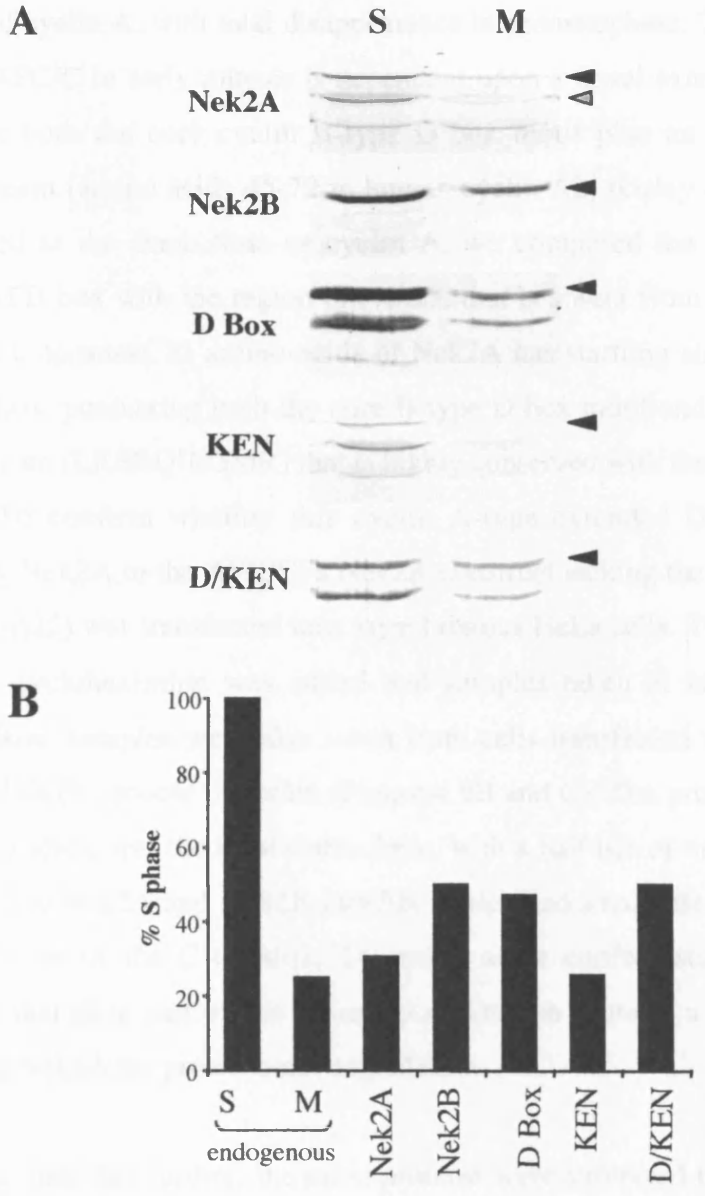

Figure 4.8 Examination of the role of putative destruction boxes in cell cycle stability of Nek2A

(**A**) Extracts of HeLa cells transfected with myc-Nek2A, myc-Nek2B, myc-R361L (D box), myc-KEN or myc-D/KEN were arrested in S phase (S) or prometaphase (M). Extracts were Western blotted and probed with anti-Nek2 antibodies and the position of transfected (black arrows) and endogenous Nek2 proteins (grey arrow) are indicated. (**B**) The mitotic degradation of each myc tagged Nek2 protein is represented by the fraction remaining in M phase arrested cells, where the amount in S phase arrested cells is considered 100%.

4.2.7 Identification of a cyclin A-type D box

Previous results have indicated that the timing of destruction of Nek2A is almost identical to that of cyclin A, with total disappearance in prometaphase. The destruction of cyclin A by the APC/C in early mitosis is dependent upon a novel extended form of a D box that contains both the core cyclin B-type D box motif plus an additional short sequence downstream (amino acids 45-72 in human cyclin A2; (Geley *et al.*, 2001). As Nek2A is destroyed at the same time as cyclin A, we compared the sequence of the cyclin A extended D box with the region of Nek2A that is absent from Nek2B. We found that the extreme C-terminal 23 amino-acids of Nek2A has startling similarity with the cyclin A-type D box, possessing both the core B-type D box motif and a 10 amino acid sequence downstream (LKSRQILGMR) that is highly conserved with the cyclin A extension (Figure 4.9A). To confirm whether this cyclin A-type extended D box was responsible for targeting Nek2A to the APC/C, a Nek2A construct lacking the C-terminal 25 amino acids (Nek2A-Δ25) was transfected into asynchronous HeLa cells. To assess the stability of this protein, cycloheximide was added and samples taken at intervals over 2 hours. For comparison, samples were also taken from cells transfected with wild type Nek2A and Nek2A-D/KEN double mutation (Figure 4.9B and C). The protein lacking the C-terminal 25 amino acids, was the most stable form, with a half-life of more than 2 hours, compared to wild type Nek2A and Nek2A-D/KEN, which had a half-life of 30-45 minutes. The fact that deletion of the C-terminal 25 amino acids confers stability on Nek2A strongly suggests that all or part of this 25 amino acid region contains a motif that is responsible for targeting Nek2A for proteasomal degradation.

To investigate this further, the same proteins were subjected to additional testing of their stability, using the same procedures as before (Figures 4.8. and 4.9). In addition, another construct with both the KEN box mutation and the C-terminal 25 amino acids missing was made to see whether loss of both motifs created a completely stable protein throughout the cell cycle. pCMVmyc-Nek2A-KENΔ25 was made by excising an *NheI* C-terminal fragment containing the KEN box motif from pCMVmyc-Nek2A-Δ25 and replacing it with the corresponding fragment containing the KEN box mutation from pGEM-Nek2A-KEN. Treatment with cycloheximide for 4 hours confirmed that Nek2A-Δ25 had a half-life of significantly more than 2 hours in asynchronous cells (Figure 4.10A and B). In these cells, endogenous Nek2A was degraded at the previously observed rate.

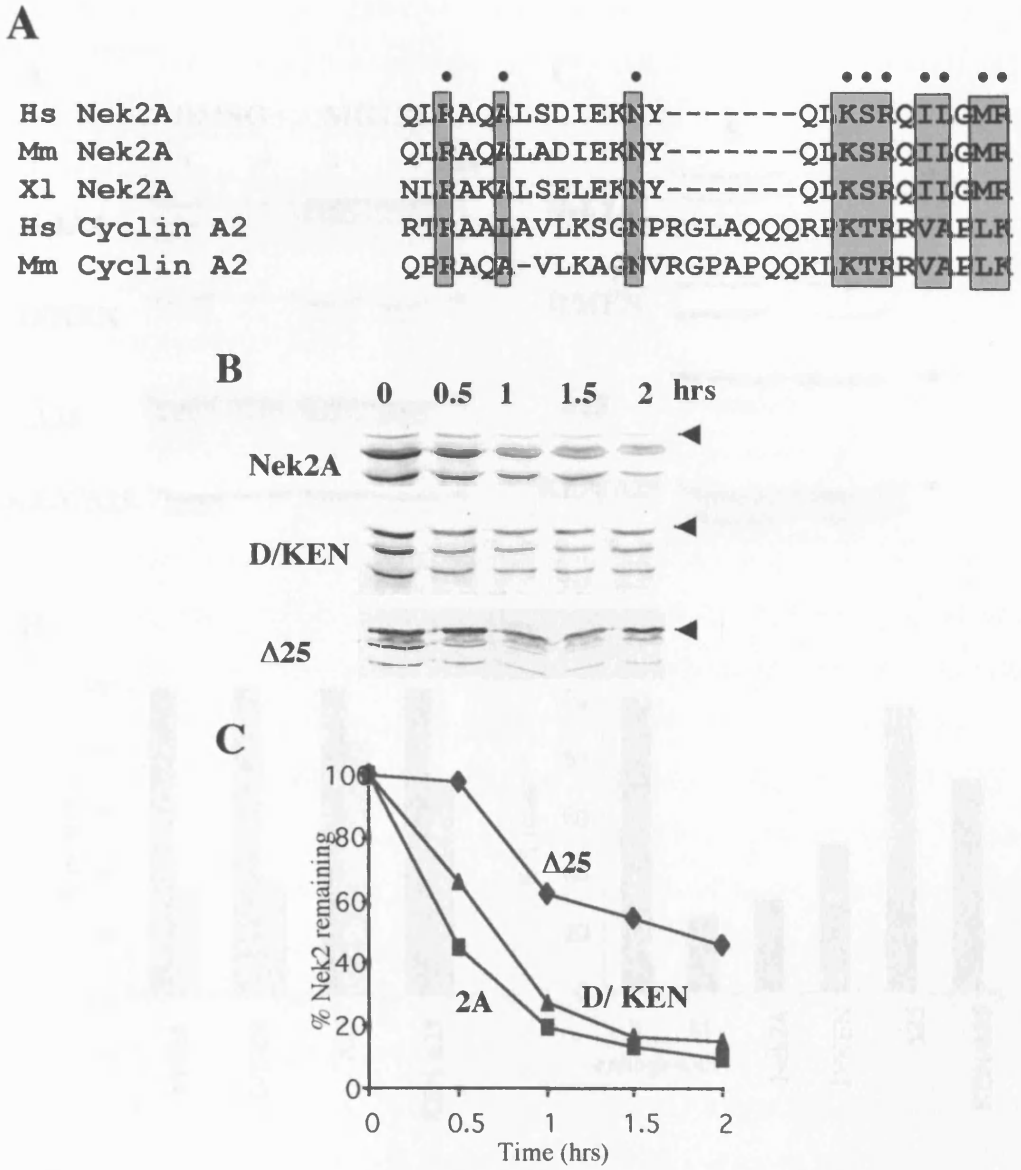

Figure 4.9 Identification of a cyclin A-type D box in the C terminus of Nek2A

(**A**) Comparison of the C-terminal 25 amino acids of human (Hs), mouse (Mm) and frog (Xl) Nek2A with the extended D-box of human and mouse cyclin A2. The three key residues of the classical D-box are shaded together with the residues downstream that are either identical or have only conservative changes. (**B**) The stability of myc-Nek2A, myc-Nek2A-D/KEN and myc-Nek2A-Δ25 was measured in cells that were prepared at the times indicated (hours) after addition of cycloheximide. Arrowheads indicate recombinant protein (**C**) The amount of Nek2 remaining at each time point is plotted with respect to the amount present at time zero (100 %) (squares, myc-Nek2A; diamonds, myc-Nek2A-Δ25; triangles, myc-Nek2A-D/KEN).

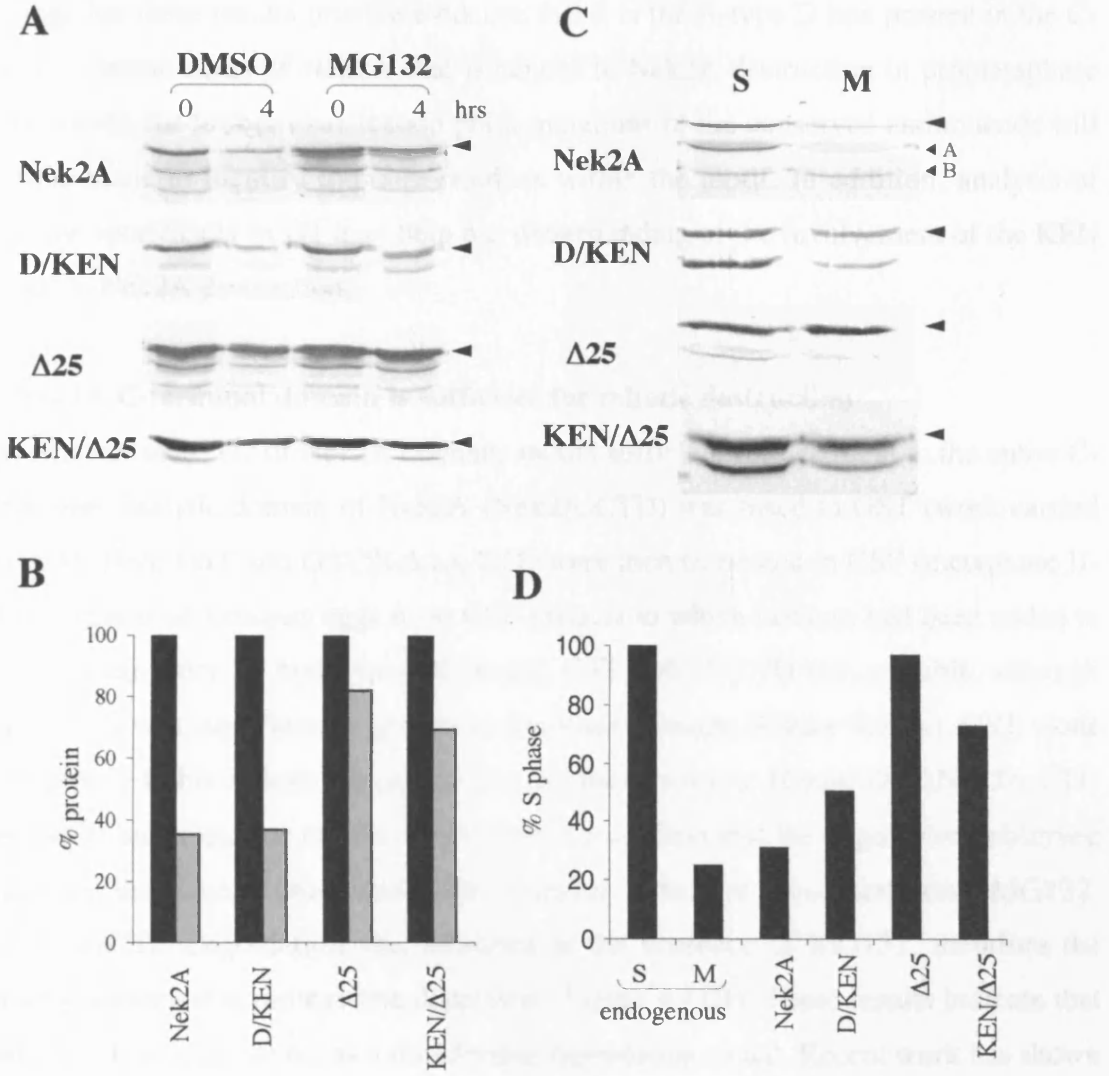

Figure 4.10 Examination of the extended cyclin-A type D box in the C-terminus of Nek2A

(**A**) Extracts were prepared from HeLa cells transfected with myc-Nek2A, myc-Nek2A-R361L/KEN, myc-Nek2A-Δ25 and myc-Nek2A-KEN/Δ25 were pre-treated with DMSO or MG132 before addition of cycloheximide for either 0 or 4 hours as indicated. Transfected proteins are indicated (arrowheads). (**B**) The fraction of each protein remaining at 4 hours (grey bars) in the absence of MG132 is shown as a percentage of the amount at 0 hours (black bars). (**C**) Extracts where prepared from of HeLa cells transfected with myc-Nek2A, myc-Nek2B, myc-R361L, myc-KEN or myc-R361l/KEN were arrested in S-phase (S) or prometaphase (M). All extracts were Western blotted and probed with anti-Nek2 antibodies. The position of transfected (black arrows) and endogenous (A and B) Nek2 proteins are indicated. (**D**) The mitotic degradation of each myc tagged Nek2 construct is represented by the fraction remaining in prometaphase arrested cells, where the amount in S phase arrested cells is considered as 100 %.

In contrast, Nek2A-Δ25 was not degraded in prometaphase arrested cells, with 97% of protein present at S phase remaining in prometaphase (Figure 4.10C and D). Nek2A-KENΔ25 also had a half-life of over 4 hours and was mostly stable in prometaphase. Taken together these results provide evidence that it is the A-type D box present in the C-terminal 25 amino acids of Nek2A that is central to Nek2A destruction in prometaphase cells. However, for further clarification point mutations of the conserved amino acids will need to be made to identify the core residues within the motif. In addition, analysis of degradation specifically in G1 may help our understanding of the involvement of the KEN box motif in Nek2A destruction.

4.2.8 Nek2A C-terminal domain is sufficient for mitotic destruction

To test whether the CTD of Nek2A contains motifs sufficient for destruction, the entire C-terminal non-catalytic domain of Nek2A (Nek2A-CTD) was fused to GST (work carried out by A.M. Fry). GST and GST:Nek2A-CTD were then incubated in CSF (metaphase II-arrested) extracts of *Xenopus* eggs or in CSF extracts to which calcium had been added to trigger anaphase entry. In both types of extract, GST:Nek2A-CTD was unstable, although its rate of loss was significantly greater in anaphase extracts (Figure 4.11A). GST alone was completely stable in both metaphase and anaphase extracts. Hence, GST:Nek2A-CTD carries motifs sufficient for mitotic destruction. To confirm that the degradation observed was due to the proteasome, anaphase extracts were pre-incubated with MG132. GST:Nek2A-CTD degradation was inhibited in the presence of MG132, therefore the degradation observed is proteasome dependent (Figure 4.11B). These results indicate that the Nek2A C-terminus can act as a transferable degradation signal. Recent work has shown that GST fused to the C-terminal 25 amino acids of Nek2 alone is also degraded in both metaphase II and anaphase extracts (M. Hayes and A.M. Fry, unpublished observations). The destruction of cyclin B1 is strongly inhibited by addition of a protein fragment containing the *S. pombe* cyclin B D box (Yamano *et al.*, 1998). However, this fragment had only a mild inhibitory effect on the destruction of cyclin A or Nek2A (Hames *et al.*, 2001). In contrast, the destruction of both cyclins was significantly delayed by the addition of GST:Nek2A-CTD fusion protein containing the degradation motifs of Nek2A (Figure 4.11C, work carried out by S. Wattam). These competition experiments could indicate that, as a result of the extended nature of the cyclin A-type D box, the presence of the smaller B-type D box could not entirely prevent the APC/C from recognising cyclin A or Nek2A (Hames *et al.*, 2001).

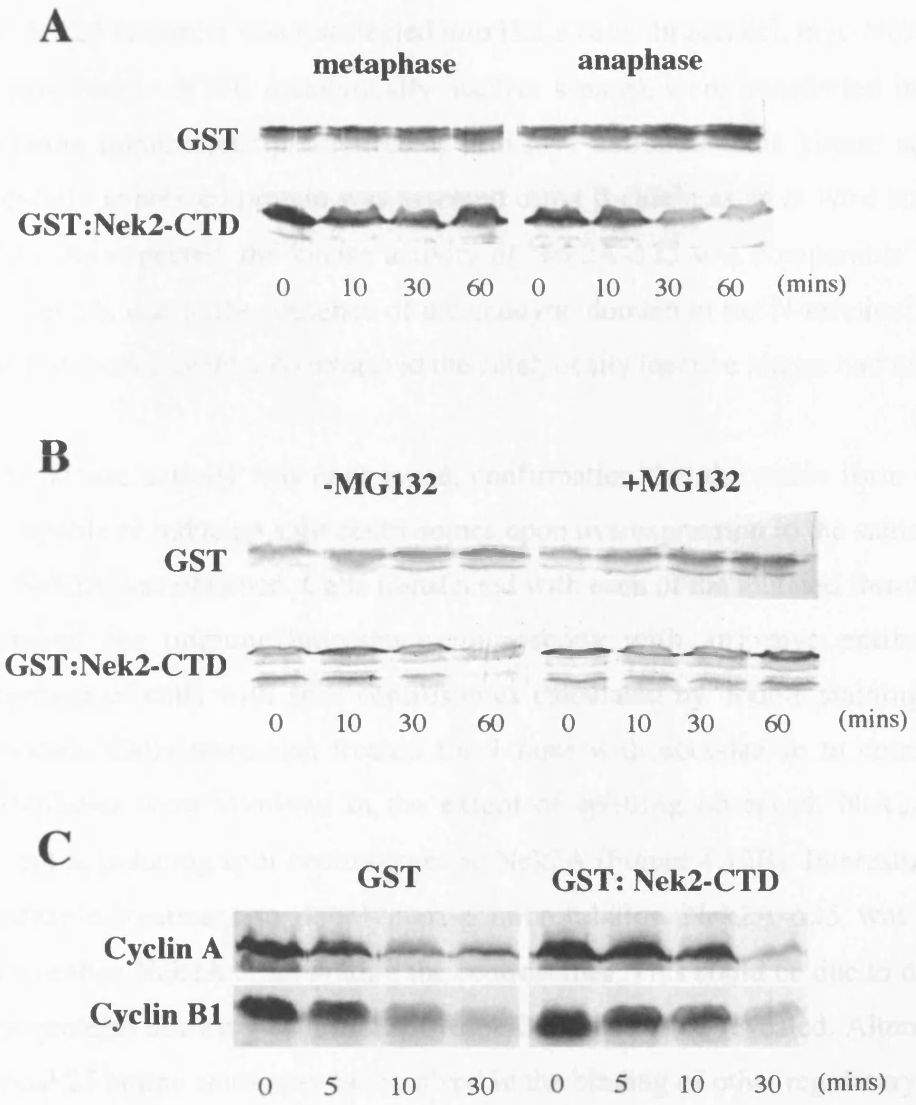

Figure 4.11 The Nek2A C terminal domain is sufficient for mitotic destruction

(**A**) *In vitro* degradation assays were performed with 200 ng of GST or GST:Nek2-CTD in 10 µl CSF extracts with (anaphase) or without (metaphase) addition of calcium and samples taken at the times indicated (mins) analysed by Western blot probed with anti-GST antibodies. (**B**) Degradation assays were performed in anaphase extracts containing DMSO or 50 mM MG132 and samples taken at the times indicated (mins) and analysed by Western blot probed with anti-GST antibodies. (**C**) Degradation assays were performed with cyclin A and cyclin B1 in anaphase extracts in the presence of 1 µg GST (left panels) or GST:Nek2-CTD (right panels). Samples were collected at the times indicated (min), separated by SDS-PAGE and exposed to autoradiography (work carried out by S.Wattam).

4.2.9 Phenotypic changes attributed to Nek2A stability

To determine whether non-degradable Nek2A was in anyway toxic to cells the myc-Nek2A-Δ25 construct was transfected into HeLa cells. In parallel, myc-Nek2A (wild type) and myc-Nek2A-K37R (catalytically inactive kinase), were transfected into HeLa cells. Following immunoprecipitation using anti-myc antibodies, the kinase activity of each ectopically expressed protein was assessed using β-casein as an *in vitro* substrate (Figure 4.12A). As expected, the kinase activity of Nek2A-Δ25 was comparable to that of wild type Nek2A, due to the presence of the catalytic domain in the N-terminal domain, being present in both proteins. As expected the catalytically inactive kinase had no activity.

As the kinase activity was unchanged, confirmation that the stable form of Nek2A was also capable of inducing split centrosomes upon overexpression to the same extent as wild type Nek2A was obtained. Cells transfected with each of the mutated forms of Nek2 were processed for immunofluoresence microscopy with anti-myc antibodies and the percentage of cells with split centrosomes calculated by double staining with C-Nap1 antibodies. Cells were also treated for 1 hour with nocodazole to determine whether microtubules were involved in the extent of splitting observed. Nek2A-Δ25 was as efficient at inducing split centrosomes as Nek2A (Figure 4.12B). Interestingly, following nocodazole treatment to depolymerise microtubules, Nek2A-Δ25 was slightly more effective than Nek2A at separating the centrosomes. This could be due to different folding of the proteins allowing different active/binding sites to be revealed. Alternatively, the C-terminal 25 amino acids may be involved in the binding of other regulatory molecules that alter Nek2 function and that are possibly linked to microtubules. A more likely explanation for this difference is that Nek2A-Δ25, due to its increased stability in cells, was expressed at higher levels than wild type Nek2A. The relative ability of all the mutated proteins used previously to induce split centrosomes was also analysed (Figure 4.12C). This indicated that none were as effective as wild type Nek2A at inducing split centrosomes, however, they were not as inefficient as Nek2B. Thus, although Nek2A-Δ25 is as stable as Nek2B in mitosis, it is still more efficient at inducing split centrosomes, implying that Nek2B may target different substrates to Nek2A when inducing centrosome separation.

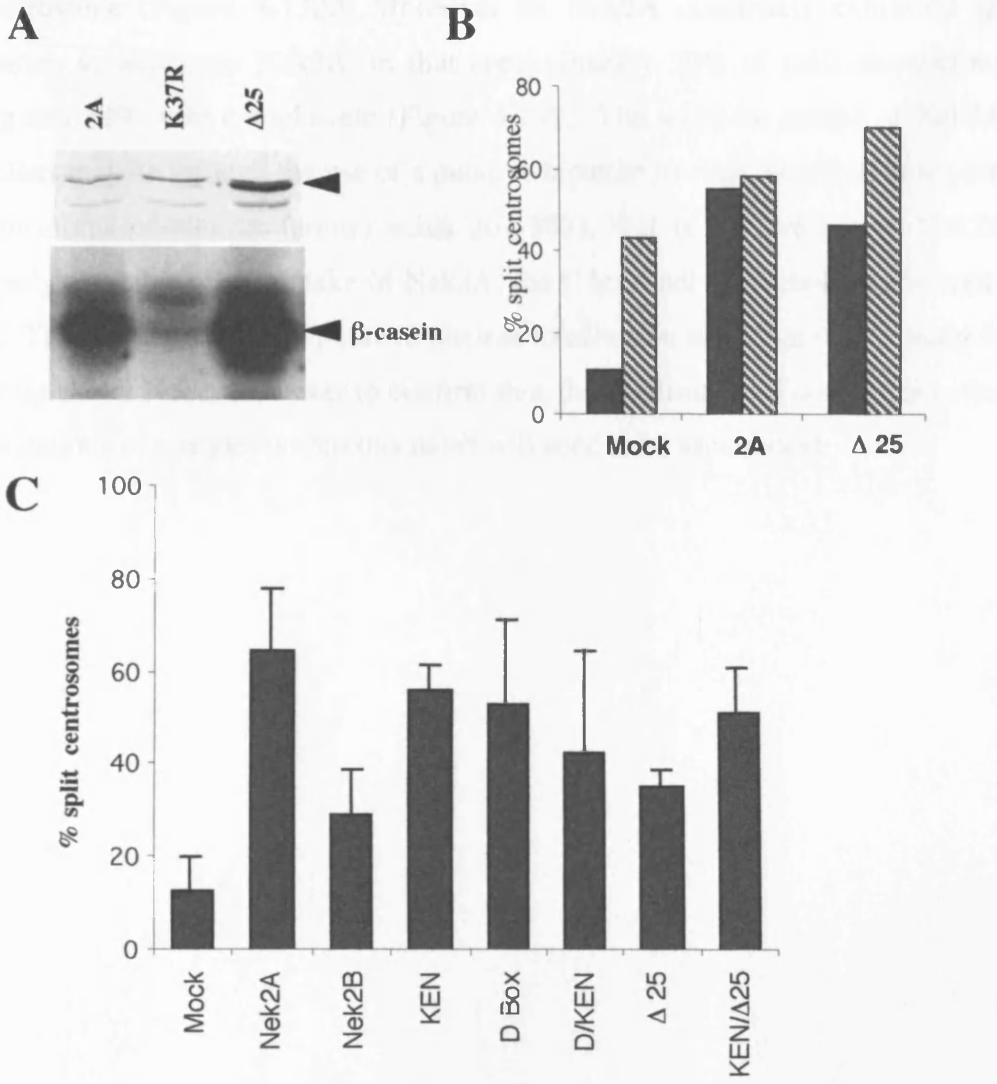

Figure 4.12 The effect of mutations of the putative destruction boxes on Nek2 function

(**A**) HeLa cells were transfected with myc-Nek2A (2A), myc-Nek2A-K37R (K37R) and myc-Nek2-Δ25 (Δ25). An aliquot of extracts made from these cells was processed by SDS-PAGE, Western blotted and probed with anti-Nek2 antibodies (top panel). The remainder was immunoprecipitated and incubated in Nek2 kinase buffer containing [^{32}P] γ-ATP for 30 min at 30°C. Samples were separated by SDS-PAGE and exposed to autoradiography (bottom panel). (**B**) Cells transfected with myc-Nek2A (2A) and myc-Nek2-Δ25 (Δ25) were treated for 1 hour prior to fixation with 5μg/ml nocodazole (hatched bars) or 1μl/ml DMSO (filled bars). Cells were analysed by indirect immunofluorescence microscopy. The percentage of cells in which the two centrosomes were separated by more than 2 μm was calculated and compared with mock-transfected cells (mock). (**C**) HeLa cells were transfected with myc-Nek2A, myc-Nek2B, myc-R361L(D box), myc-KEN, myc-D/KEN, myc-Nek2A-Δ25 and myc-Nek2A-KEN/Δ25 and left for 24 hours before fixation and analysed for centrosome separation as above.

The subcellular localisation of each of the mutated proteins was also analysed to identify any relationship between stability and localisation. All recombinant proteins localised to the centrosome (Figure 4.13A). Moreover all Nek2A constructs exhibited similar localisation to wild type Nek2A, in that approximately 50% of cells showed nuclear staining and 50% were cytoplasmic (Figure 4.13B). The selective uptake of Nek2A into the nucleus may be through the use of a putative bipartite nuclear localisation sequence in the C-terminus of Nek2A (amino acids 361-383), that is not present in Nek2B. To completely abolish nuclear uptake of Nek2A, the C-terminal 126 amino acids need to be deleted. This suggests that the putative nuclear localisation sequence is necessary for the nuclear uptake of Nek2. However to confirm this, the localisation of constructs containing point mutations of residues within this motif will need to be ascertained.

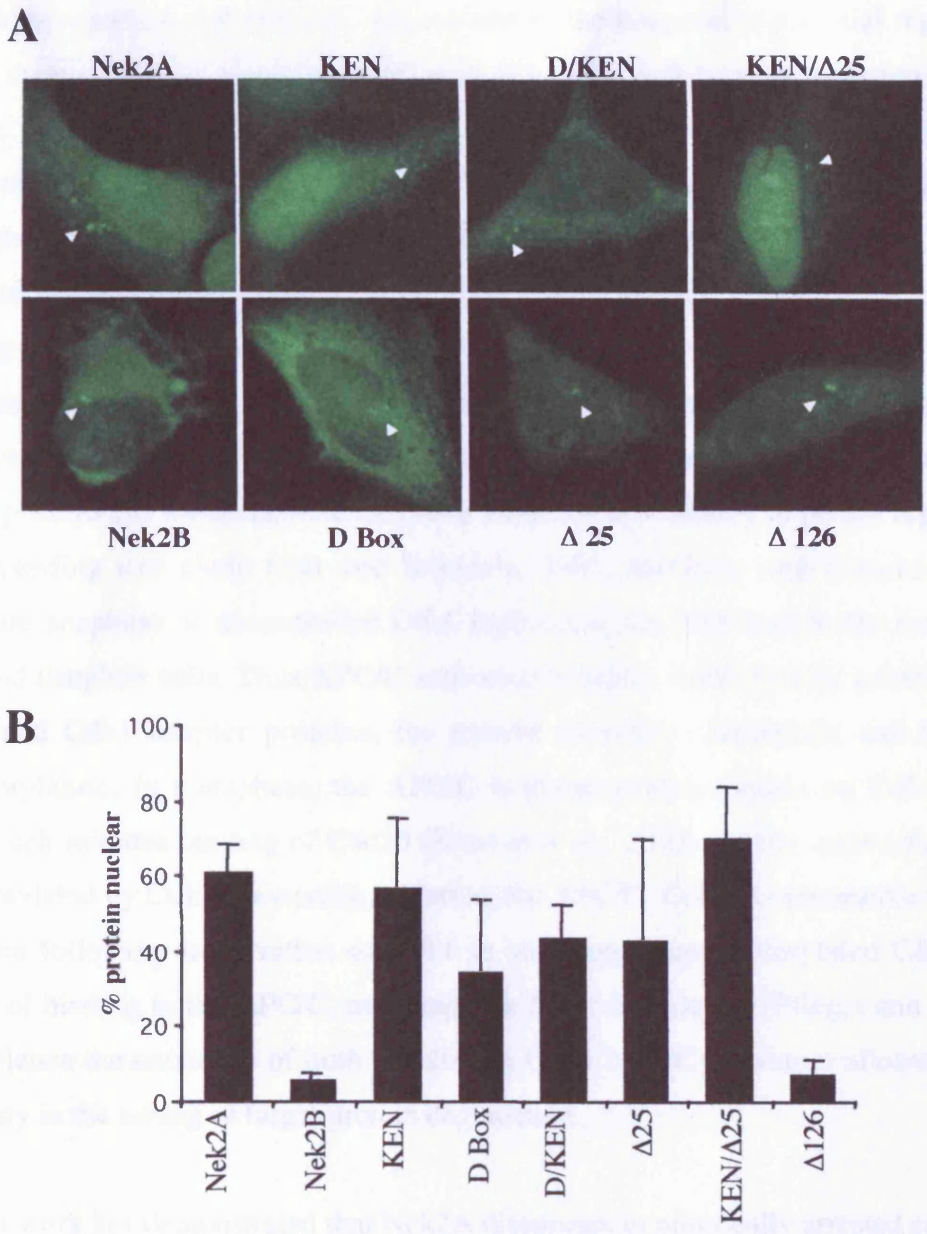

Figure 4.13 The effect of mutations of the putative destruction boxes on Nek2 subcellular localisation

(A) HeLa cells were transiently transfected with myc-Nek2A, myc-Nek2B, myc-R361L (D box), myc-KEN, myc-D/KEN, myc-Nek2A-Δ25, myc-Nek2A-KEN/Δ25 and myc-Nek2A-Δ126. Cells were fixed 24 hours after transfection and analysed by indirect immunofluorescence microscopy. Recombinant proteins were visualised by staining with anti-myc antibodies. **(B)** The percentage of cells in which the transfected protein was nuclear was calculated for HeLa cells transfected with the above myc-tagged Nek2 proteins. Results are the mean of three independent experiments.

4.3. DISCUSSION

The ubiquitin proteasome pathway is important in the temporal and spatial regulation of the cell cycle through elimination of proteins regulating cell cycle progression in either a positive or negative manner (Hershko and Ciechanover, 1998). This is particularly important for normal mitotic progression, which requires the ordered accumulation and destruction of specific cyclin proteins, which in turn control the activity of their associated cyclin dependent kinases. The ubiquitin ligase responsible for ubiquitylating cyclins and targeting them to the proteasome is the APC/C (King *et al.*, 1995; Sudakin *et al.*, 1995). The separation of sister chromatids at the metaphase-anaphase transition depends on APC/C mediated destruction of securins, while the destruction of geminin, an inhibitor of DNA replication, at the metaphase-anaphase transition is necessary to permit replication in the succeeding cell cycle (Zur and Brandeis, 2001; McGarry and Kirschner, 1998). Premature anaphase or uncontrolled DNA replication can both lead to the formation of aneuploid daughter cells. Thus APC/C activation is tightly controlled by association with Cdc20 and Cdh1 adapter proteins, the spindle assembly checkpoint and by APC/C phosphorylation. In metaphase, the APC/C is phosphorylated either by Cdk1, PKA or Plk1, which initiates binding of Cdc20 (Kramer *et al.*, 2000). At the same time, Cdh1 is phosphorylated by Cdk1 preventing it binding the APC/C. Cdh1 is responsible for APC/C activation following inactivation of Cdk1 in anaphase, dephosphorylated Cdh1 is then capable of binding to the APC/C, targeting Cdc20 for destruction (Pfleger and Kirschner, 2000). Hence the existence of both Cdc20 and Cdh1 APC/C activators allows cell cycle specificity in the timing of target protein degradation.

Previous work has demonstrated that Nek2A disappears in mitotically arrested cells (Fry *et al.*, 1995; Hames and Fry, 2002; Schultz *et al.*, 1994), is unstable in interphase egg extracts supplemented with Cdh1 (Pfleger and Kirschner, 2000) and is degraded when injected into dividing embryos (Uto and Sagata, 2000). This prompted us to investigate if, when and how human Nek2 proteins are destroyed during mitosis. The results presented here show that Nek2A is destroyed by the proteasome following ubiquitylation by the E3 ubiquitin ligase APC/C-Cdc20. Furthermore, degradation of Nek2A occurs in early mitosis, coincident with cyclin A destruction, and depends upon a motif in its extreme C-terminus that is almost identical to the extended D box present in cyclin A (Geley *et al.*, 2001).

In synchronised cells, Nek2A is destroyed early in mitosis coincident, within the limits of the experiment, with the destruction of cyclin A. Moreover, Nek2A is absent in cells arrested in prometaphase with the microtubule poison nocodazole. Hence, the destruction of Nek2A, like that of cyclin A but not cyclin B, is independent of the spindle assembly checkpoint. Nek2B does not disappear until G1, in contrast to cyclin B, which is rapidly destroyed by the proteasome in late mitosis. The destruction of Nek2A did not appear to be related to its location within the cell, as confinement to the nucleus by LMB, an inhibitor of nuclear export did not enhance its degradation. Nek2A degradation did not appear to be related to the binding of microtubules, since disruption of microtubules by nocodazole and taxol did not enhance or restrict Nek2A degradation. Induction of apoptosis and DNA damage did not affect Nek2 degradation, the only compound tested that did exert stability on Nek2 was the proteasome inhibitor MG132.

Confirmation of the involvement of the 26S proteasome was shown by prolongation of Nek2A half-life *in vivo* after treatment with proteasome inhibitors. Lactacystin, a specific 20S proteasome inhibitor stabilised Nek2A. MG132, a less specific potent proteasome inhibitor with additional inhibitory activities against cysteine proteases and calpain, also stabilised Nek2A. However, ALLM, a specific calpain II inhibitor had no effect. Stabilisation of Nek2 *in vivo* by proteasome inhibitors supports the conclusion that the 26S proteasome is involved in Nek2 degradation. Furthermore, the addition of proteasome inhibitors to cells arrested in prometaphase allowed the re-accumulation of Nek2A indicating that its loss specifically in prometaphase is due to continual turnover by the 26S proteasome rather than to inhibition of transcription or translation.

In common with cyclin A, Nek2A is unstable in egg extracts arrested in metaphase II of meiosis but is destroyed more rapidly in CSF extracts triggered to enter anaphase. In these extracts the APC/C ubiquitin ligase is strongly activated. Nek2A can also be destroyed in interphase extracts which contain APC/C proteins by the addition of the APC/C activator Cdh1 (Pfleger and Kirschner, 2000). The identification of destruction motifs that are known to be recognised by the APC/C in the non-catalytic C-terminus of Nek2A provides further evidence that Nek2A is an APC/C substrate. This is in common with NIMA, whose destruction is also targeted for ubiquitylation by the APC/C via motifs present in its non-catalytic C-terminus. The demonstration that Nek2A is ubiquitylated *in vitro* supports the idea that polyubiquitylation is a signal for Nek2A degradation. Finally, depletion of the

APC/C via anti-cdc27 antibodies significantly reduced the rate of Nek2A destruction. Taken together, these results demonstrate that the APC/C can target Nek2A for destruction by the proteasome.

The APC/C requires adapter proteins to recognise its substrates. So which adapter proteins are required to recognise Nek2A? Early embryos of frogs and flies were thought until recently to only possess one APC/C adapter protein, Cdc20, with Cdh1 being expressed later in development when cell cycles introduce the first G1 phase (Lorca *et al.*, 1998; Sigrist and Lehner, 1997). However, Cdh1 mRNA has recently been shown to be expressed in *Xenopus* embryos of all developmental stages. Cdh1 protein expression was not found, possibly due to its low abundance in embryos. Interestingly, loss of Cdh1 in embryonic cell cycles induces a prolonged mitotic arrest, suggesting that it does in fact play a role in cell cycle regulation of these early stages (Zhou *et al.*, 2002). It is likely that Nek2A is targeted for destruction in meiotic egg extracts, by the APC/C-Cdc20 complex, however, Nek2A can also be destroyed by APC/C-Cdh1 (Pfleger and Kirschner, 2000). Thus Nek2A, like other APC/C substrates (e.g. securin and cyclin B) can be recognised by the APC/C in complex with either Cdc20 or Cdh1. The observation that Nek2A levels remain low throughout G1 combined with its degradation in meiotic extracts, suggests that Nek2A destruction in early mitosis by APC/C-Cdc20 is maintained in G1 by APC/C-Cdh1. Nek2B is not degraded in prometaphase cells or metaphase II extracts, in line with results showing that *Xenopus* Nek2B is stable throughout the first embryonic cell cycle (Fry *et al.*, 2000b). It is unclear whether the decrease in Nek2B upon entry into G1 is due to degradation or some other mechanism such as reduced transcription.

Nek2A and cyclin A are both destroyed via the APC/C early in mitosis when the APC/C is unable to target other substrates such as cyclin B or securin for destruction. Inhibition towards these latter substrates is regulated by the spindle checkpoint protein Mad2, which in the presence of unattached kinetochores binds directly to Cdc20 and inhibits the APC/C (Fang *et al.*, 1998b). The mechanism by which the APC/C is prevented from destroying cyclin B in metaphase II arrested eggs is not fully understood, because at this cell cycle stage, not only are all kinetochores attached but the spindle assembly checkpoint is also not functional (Minshull *et al.*, 1994). Emi1, an early mitotic inhibitor of the APC/C has recently been shown to be necessary and sufficient to inhibit the APC/C and to prevent mitotic exit in CSF arrested eggs. Emi1 may therefore be the unknown mediator of CSF

activity, which contributes to cyclin B stability in these extracts until they are triggered to enter anaphase by the addition of calcium (Reimann and Jackson, 2002). Emi1 is able to inhibit the APC/C in combination with both Cdc20 and Cdh1, similar to Mad2B, but not to Mad2 which is only capable of inhibiting Cdc20. Emi1 promotes S phase entry by inhibiting APC/C-Cdh1 mediated degradation of cyclin A (Hsu *et al.*, 2002). It may also play a role in the regulation of Nek2 destruction via APC/C-Cdh1 allowing accumulation of Nek2 at the onset of S phase.

The finding that Nek2A and cyclin A share a similar extended destruction box suggests that this may be key to recognition of early mitotic substrates by the APC/C. Deletion of this motif stabilised Nek2A in both cells and extracts. Moreover this motif is highly conserved among vertebrate Nek2 kinases, unlike the other potential D box (amino acids 361-369) that is present in human Nek2A and Nek2B, but not in the Nek2 sequences of other vertebrates. Indeed, mutation of this latter D box had no stabilising effect whatsoever, suggesting that it has no function in regulating Nek2A destruction. The KEN box, on the other hand, is conserved in mammalian and frog Nek2A and its mutation partially stabilised Nek2A in extracts but not in mitotic cells. Possibly the extended D box is targeted by the APC/C-Cdc20 in early mitosis, whereas the KEN box is targeted by APC/C-Cdh1, in late mitosis and G1. This is supported by the observation that Cdh1 recognises D boxes preferentially but can also recognise KEN boxes, whereas Cdc20 is more selective for the D box (Pfleger and Kirschner, 2000). Recently, Aurora A, a mitotic spindle pole associated protein has been shown to contain a D box which is preferentially recognised by APC/C-Cdh1 (Castro *et al.*, 2002). This could be the case for Nek2A, if the extended D box is recognised both by Cdc20 and Cdh1. However, as yet it is still unknown whether the KEN box or the extended D box is central to Nek2A degradation in G1. Four different Cdh1 homologues have been identified in chick, which are also thought to exist in humans and flies. These homologues show differential expression patterns and substrate specificities, with Cdh1-B and Cdh1-C targeting Nek2A (Wan and Kirschner, 2001). It is possible that Nek2A destruction is regulated by different Cdh1 homologues at different times in the cell cycle. This combined with the possibility for differential inhibition by Emi1, Mad2 or Mad2B, would provide a mechanism to explain the differences seen between timing and localisation of destruction of APC/C targets. Additional regulation may be brought about by the existence of multiple APC/C complexes in cells that have different localisation, timing and substrate specificities.

Cyclin B destruction is spatially regulated, with spindle associated protein preferentially degraded in mitosis. Two core APC/C subunits, Cdc16 and Cdc27 only weakly associate with mitotic spindles during mitosis, implying that a spatial restriction of the APC/C cannot explain the spatially regulated destruction of cyclin B. Instead, different subpopulations of the APC/C may be activated at different times to degrade cyclin B (Huang and Raff, 2002).

The destruction of both Nek2A and cyclin A was significantly delayed by the addition of a GST fusion protein containing the degradation motifs of Nek2A. This fusion could itself be destroyed, indicating that the Nek2A C-terminus can act as a transferable degradation signal. If Mad2 acts by competing only for the same site as the B type D box, this could explain why the spindle assembly checkpoint does not prevent destruction of proteins with the extended A type D box. The exact residues that are critical within the A type D box will require further investigation but one possibility is that a phosphorylation site is involved in substrate recognition in a manner similar to substrate recognition by the SCF ubiquitin ligase (Jackson *et al.*, 2000). Nek2A is transiently phosphorylated before its destruction and it appears that this is not autophosphorylation (Hames *et al.*, 2001). Hence, it is possible that there is a Nek2 kinase kinase that is somehow involved in targeting Nek2A and perhaps cyclin A to the APC/C.

The proposed role of Nek2 in the loss of centriolar cohesion at the G2/M transition, allowing formation of a bipolar mitotic spindle, is supported by its centrosomal localisation combined with its ability to stimulate split centrosomes upon overexpression. Furthermore its interaction with and phosphorylation of C-Nap1, a protein implicated in centriole cohesion suggests that Nek2A plays a critical role in centrosome disjunction (Fry *et al.*, 1998b; Fry *et al.*, 1998a; Mayor *et al.*, 2000). It has been proposed that Nek2A stimulates loss of cohesion between centrosomes by triggering disassembly of an intercentriolar linkage (Mayor *et al.*, 1999). The destruction of Nek2A in early mitosis may in some way be necessary for the re-establishment of the intercentriolar linkage in late mitosis (Figure 4.14). C-Nap1, which disappears from centrosomes in late G2, reappears around telophase (Mayor *et al.*, 2000) at the same time as a flexible linker is re-established between centriole pairs of the future daughter cells (Piel *et al.*, 2000). The persistence of Nek2B at this time may seem to pose a problem for this hypothesis. However, Nek2B does not bind PP1, nor does it stimulate centrosome splitting with the same efficiency as Nek2A (Hames *et al.*,

2001). Hence, Nek2B may not have an equivalent function in regulating the intercentriolar linkage. Instead, Nek2B may rather contribute to the stability of mitotic spindle poles as inhibition of Nek2B leads to centrosome fragmentation in early *Xenopus* embryos (Uto and Sagata, 2000). Cells expressing stable Nek2A did not cause an increase in the extent of centrosome splitting as compared to wild type Nek2A as might have been expected. This implies that Nek2A and Nek2B are likely to bring about centrosome separation through different mechanisms perhaps involving different substrates.

Another important question is whether Nek2A destruction is necessary for mitotic exit. Overexpression of stable NIMA mutants does cause a mitotic arrest in *Aspergillus* cells without preventing destruction of cyclin B (Pu and Osmani, 1995). No evidence for mitotic delay was seen in cells expressing stable Nek2A constructs. However, transient overexpression is a very difficult system to detect subtle changes in mitosis. Preliminary work using stable cell lines expressing GFP-Nek2A has indicated that exit from mitosis is slowed down in these cells (A. Faragher and A.M. Fry, unpublished observations). Cyclin A overexpression also delays mitotic progression, however this could be due to either competition for the APC/C or abnormal maintenance of Cdk1 activity (den Elzen and Pines, 2001; Geley *et al.*, 2001). The use of stable cell lines expressing stable Nek2 lacking both the functional KEN box and extended D box will hopefully provide an insight into the need for Nek2A destruction for mitotic exit and in cell cycle progression. It is possible that a checkpoint mechanism similar to the spindle checkpoint is responsible for making sure that mitotic entry does not occur until centrosomes are fully separated for formation of a bipolar mitotic spindle. Alternatively, a checkpoint may exist that ensures that the intercentriolar linkage is re-established prior to cytokinesis. If this is the case, APC/C mediated destruction may play an integral role in maintaining these checkpoints.

The centrosome has been implicated in protein degradation, being identified as a site for concentration of active proteasomal complexes and associated regulatory proteins (Fabunmi *et al.*, 2000; Wigley *et al.*, 1999). It is not clear whether destruction of Nek2A occurs uniformly throughout the cell or whether its degradation starts preferentially at the centrosome as shown for cyclin B1 (Clute and Pines, 1999; Huang and Raff, 2002). Thus, the centrosomal pool of Nek2A could be destroyed in prometaphase via APC/C-Cdc20 present at centrosomes. Following this, further non-centrosomal destruction of Nek2A in G1 is mediated by APC/C-Cdh1. Ultimately, the mechanism by which Nek2A is degraded

may involve a number of different stages each controlled by different complexes of proteins and inhibitors with specific localisations and activities within the cell. Moreover, the idea that de-ubiquitylation is as important as ubiquitylation has not been investigated. It has been suggested that a subunit of the proteasome, Rpn11, is responsible for removing ubiquitin chains, allowing targeted proteins to enter the 'cylinder' of the proteasome, thus regulation of this activity may affect the rate that proteins are destroyed (R. Deshaies, unpublished observations).

Data presented in this chapter provides convincing evidence that the destruction of Nek2A in early mitosis is mediated by the proteasome and is dependent upon the APC/C-Cdc20 ubiquitin ligase. Importantly, this destruction is regulated by a motif in the extreme C-terminus of Nek2A, which is similar to the extended destruction box of cyclin A. However, the role of Nek2A destruction in centrosome dynamics and mitotic progression in cells still remains to be fully understood. Defects in the ubiquitin-proteasome pathway have been linked to different cancers and genetic diseases (Ciechanover, 1998). Dysfunction of the ubiquitin-proteasome pathway might contribute to the up-regulation of Nek2 in cancer cells.

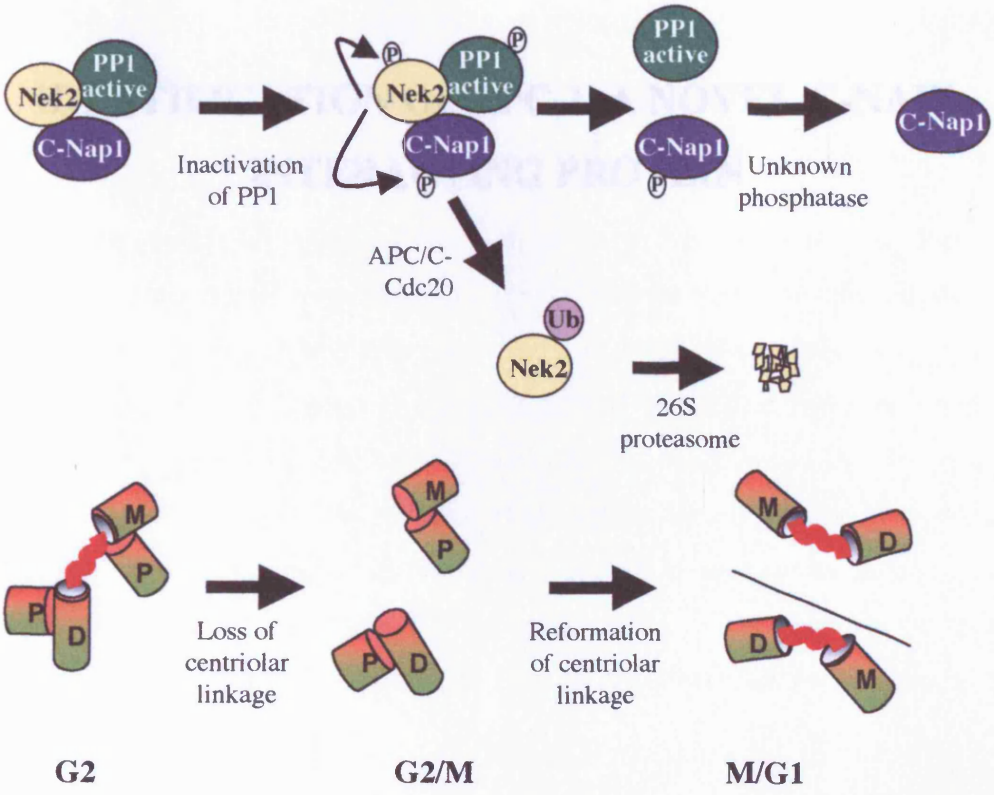

Figure 4.14 A hypothetical model for the role of Nek2A destruction in mitosis

A complex consisting of Nek2A, C-Nap1 and PP1 exists in G2 at the proximal ends of centrioles and may form an anchoring structure for the intercentriolar linkage. Nek2A expression is high in G2, but its association with active PP1 keeps it and C-Nap1 in a dephosphorylated state. Upon phosphorylation and inactivation of PP1 at the G2/M transition, Nek2A and C-Nap1 become hyperphosphorylated, leading to displacement of C-Nap1 and disjunction of centrosomes. Centrosomes can then separate to opposite ends of the cell as a bipolar spindle is formed. Upon progress into mitosis, the APC/C becomes active towards Nek2A, causing its ubiquitylation and destruction. With Nek2A no longer present, C-Nap1 can be dephosphorylated at some point later in mitosis, allowing it to re-associate with disorientated centrioles and establish a new intercentriolar linkage.

CHAPTER 5

IDENTIFICATION OF BPC-1, A NOVEL C-NAP1 INTERACTING PROTEIN

5.1. INTRODUCTION

This chapter describes the identification of a novel centrosomal protein named BPC-1. This protein was identified using the C-terminal domain (CTD) of C-Nap1 as a bait in a yeast two hybrid interaction screen of a human testis cDNA library. BPC-1 was also found to interact with Nek2 and overexpression interfered with the premature centrosome separation induced by Nek2A overexpression.

5.1.1 Centrosome cohesion

The centrosome undergoes specific changes in structure throughout the cell cycle. These changes are thought to be regulated in part by protein phosphorylation due to the abundance of kinases and phosphatases at the centrosome. Upon mitotic entry, duplicated centrosomes separate and migrate to opposite ends of the cell to form the poles of the bipolar mitotic spindle. As a cell exits mitosis, the two daughter cells each inherit one centrosome comprising two centrioles. In telophase the centrioles lose their orthogonal orientation and move apart, this event known as centriole disorientation, is thought to be a pre-requisite for centriole duplication (Lacey *et al.*, 1999). More recently the separation and subsequent movement of centrioles has been implicated in the completion of mitosis and cytokinesis (Piel *et al.*, 2000).

The difference in mobility of the mother and daughter centriole highlights the dynamic structure of the centrosome, with the distance between the centrioles fluctuating at different stages of the cell cycle. Despite this apparent dynamic structure, the centrosome still appears as a pair of centrioles in most fixed cells. In addition, biochemical isolation of centrosomes permits the recovery of a pair of centrioles. Taken together, these observations suggest that centrioles are linked by a cell cycle regulated cohesive structure. The observation of electron dense material connecting the centrioles in electron microscopy of isolated centrosomes provides further evidence for the existence of a dynamic intercentriolar linkage (Fuller *et al.*, 1995; Paintrand *et al.*, 1992). The observation of the structure readily in isolated centrosomes but with more difficulty in intact cells has led to doubts concerning the existence of such a structure. It has therefore also been proposed that centrioles are held together purely by the microtubule cytoskeleton (Jean *et al.*, 1999). In support of this, drugs that affect the dynamics of the microtubule network or the actin microfilament system, modulate centrosome cohesion (Buendia *et al.*, 1990; Euteneuer and Schliwa, 1985). More recent work shows that microtubule

depolymerisation can cause centrosome splitting, however this drug induced splitting also requires kinase activity and is specifically suppressed by a dominant negative mutant of Nek2A (Meraldi and Nigg, 2001). Centrosome separation at the onset of mitosis correlates with a peak in Nek2 activity, raising the possibility that Nek2A regulates centrosome cohesion (Fry *et al.*, 1998a). Interestingly, phosphorylation of centrin also correlates with loss of centrosome cohesion, suggesting that centrosome separation is a complex process involving many different proteins (Lutz *et al.*, 2001). A specific model for centrosome separation has been proposed that involves Nek2 kinase and its centrosomal substrate C-Nap1 (Mayor *et al.*, 1999).

5.1.2 C-Nap1, a centrosomal substrate of Nek2

C-Nap1 is a 281 kDa protein consisting of two large coiled coil regions separated by a putative hinge region and with non-coiled coil N- and C-terminal domains. It was identified as a substrate for Nek2 following a yeast two hybrid interaction screen using Nek2 as the bait (Fry *et al.*, 1998b). C-Nap1 is specifically associated with the proximal ends of centrioles, independently of microtubules and is able to interact with centrosomes via both its C-terminal and N-terminal domains (Mayor *et al.*, 2002; Mayor *et al.*, 2000). The existing model for the function of Nek2 and C-Nap1 at the centrosome states that increased expression or activity of Nek2 at the G2/M transition results in loss of centriole cohesion due to phosphorylation of linkage components (e.g. C-Nap1) leading to their dissociation or degradation (Mayor *et al.*, 1999). In confirmation of this model, antibody mediated interference of C-Nap1 function causes centrosome splitting in a similar manner to overexpression of Nek2A. In addition, the same phenotype could be induced by inhibition of protein phosphatase 1α (Meraldi and Nigg, 2001). PP1α inhibits Nek2 kinase activity throughout S and G2, thus inhibition would upregulate Nek2 kinase activity. More recently, it has been shown that PP1 also binds inhibitor 2 at the same time as Nek2. This regulatory molecule is capable of increasing Nek2 kinase activity by inhibiting PP1. Evidence for this comes from the observation that overexpression of inhibitor 2 induces centrosome splitting to the same extent as Nek2 overexpression (Eto *et al.*, 2002).

5.1.3 Components of the intercentriolar linkage

Molecular characterisation of the intercentriolar linkage has hardly begun, with few components having been identified. The identification of proteins that localise to the linkage would greatly help the general understanding of centrosome cohesion and its

regulation. C-Nap1 does not span the gap between centrioles, instead, localising to the proximal end of centrioles, suggesting that it is not the only component of the linkage but may contribute to its structure by acting as an anchor for other integral proteins that localise more specifically to the intercentriolar region. δ-tubulin is one of a few proteins that is thought to localise to the intercentriolar region (Chang and Stearns, 2000). δ-tubulin may exist as a dynamic polymer, like α/β tubulin polymers or in complex with other proteins. δ-tubulin has also been shown to be enriched at the spindle poles only during mitosis, an observation which does not support the role of δ-tubulin in centrosome cohesion as no intercentriolar linkage is present during mitosis (Smrzka *et al.*, 2000). More recently p160ROCK, has been shown to localise to the region between centrioles and may emerge as a marker of the linker in cells (Chevrier *et al.*, 2002).

The lack of knowledge of intercentriolar linkage components, combined with C-Nap1 localisation to the proximal ends of the centrioles, prompted us to use a yeast two hybrid screen to identify novel proteins that interact with C-Nap1 at the centrosome and may contribute to centrosome cohesion.

5.2. RESULTS

5.2.1 The yeast two hybrid system

To screen for cDNAs encoding proteins able to interact with the C-terminal domain (CTD) of C-Nap1, the general scheme outlined in Figure 5.1A was employed. The yeast two hybrid system uses two plasmid borne gene fusions that are co-transformed into a host yeast strain containing inducible reporter genes. The protein of interest is encoded as a gene fusion to the GAL4 DNA binding domain (DBD). A second protein, or a library of proteins, is encoded as a gene fusion to the GAL4 transcription activation domain (AD). Interaction between the two proteins results in bringing the AD close to the DBD, inducing the activation of adjacent reporter genes, which ultimately generates a phenotypic signal (Fields and Song, 1989). The *S. cerevisiae* strain PJ69-4A containing three reporter genes, each under the control of a different inducible GAL4 promoter was used to express the various GAL4 fusion proteins in this chapter (Figure 5.1B). This triple system, with the LacZ, histidine and adenine auxotrophic markers displays excellent sensitivity and low background, allowing more selective screening of cDNA libraries with reduced incidence of false positives (James *et al.*, 1996).

For the purposes of this investigation, two C-Nap1 DBD fusion proteins were constructed. The C-Nap1-CTD (amino acids 1962-2403) was isolated as a *SmaI-BglII* fragment from pBS-C-Nap1 and subcloned into pGBDU-C2 cut with *BamHI* (blunted) and *BglII*. The N-terminal domain (NTD; amino acids 1-488) was isolated as a *ClaI-HaeII* (blunted) fragment from pBS-C-Nap1 and subcloned into pGBDU-C3 cut with *ClaI-BglII* (blunted). The two terminal globular domains of C-Nap1 were used so as to avoid the extensive coiled coil regions that span the majority of C-Nap1 (Figure 5.2A). Both domains were fused to GAL4 DBD and will now be referred to as CTD-DBD and NTD-DBD. In addition to the above C-Nap1 DBD fusions, a construct containing Nek2A fused to GAL4-AD (pACTII-Nek2A) was also used (Fry *et al.*, 1999). PJ69-4A was transformed with these constructs and with plasmids containing the DBD or AD alone. Yeast were grown on selective media lacking uracil in the case of DBD fusions or leucine for AD fusions. The expression of CTD-DBD, NTD-DBD and Nek2-AD was confirmed by Western blot of yeast cell extracts using specific C-Nap1 and Nek2 antibodies. Proteins of the correct size were resolved for each, 74 kDa, 71 kDa and 57 kDa respectively (Figure 5.2B). No protein was detected in yeast containing empty vectors.

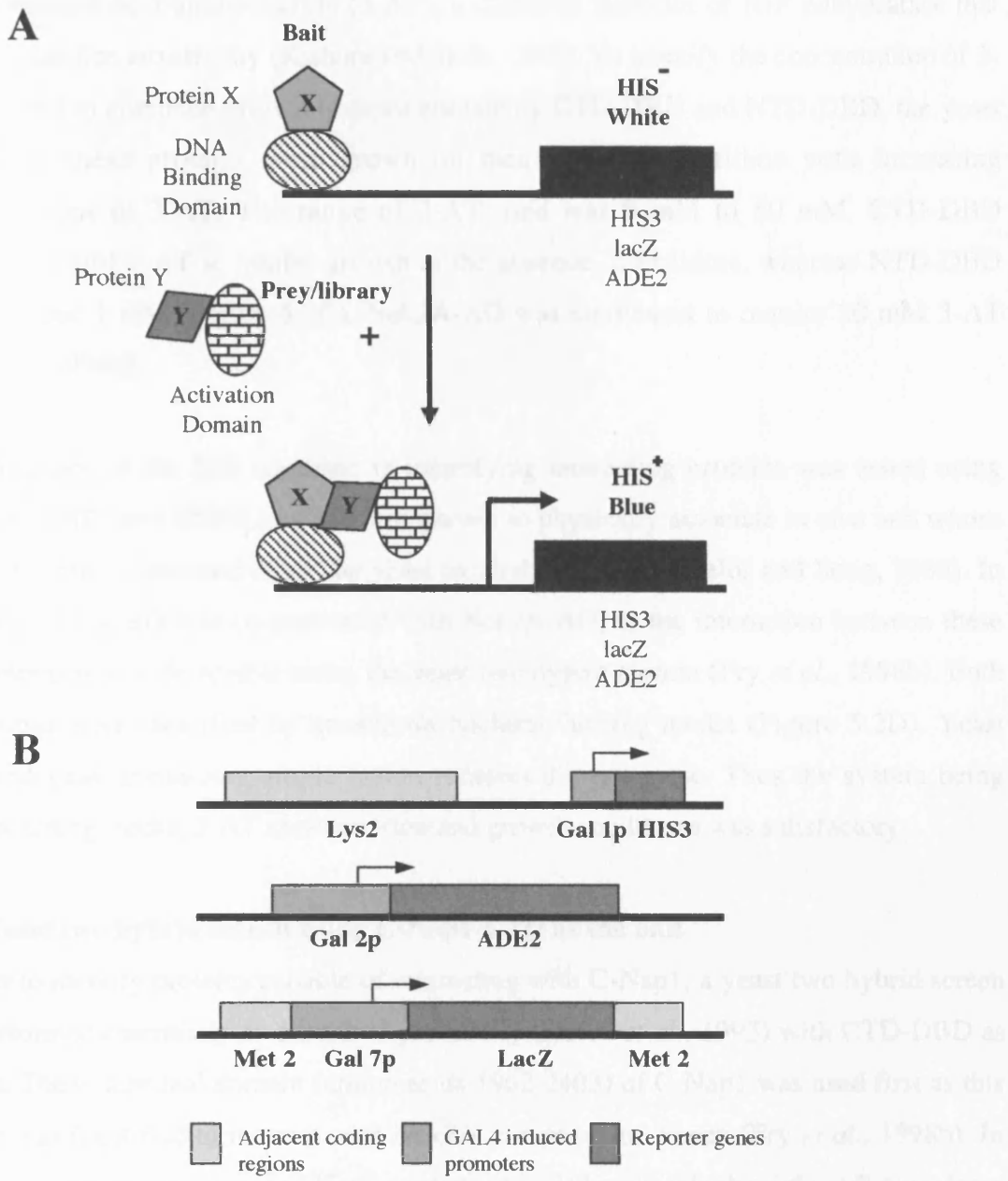

Figure 5.1 Schematic representation of yeast two hybrid technology
(**A**) The GAL4 DNA binding domain fused to protein X represents the bait fusion. The GAL4 activation domain fused to protein Y represents the prey fusion or library. These fusion proteins are incapable of inducing transcription alone. When both fusion proteins are expressed together in yeast, a positive interaction brings the GAL4 domains into close proximity, resulting in transcriptional activation of reporter genes (HIS3, LacZ and ADE2), allowing selection of positive interactions. (**B**) In the case of the yeast strain PJ69-4A, selection is based on three reporter genes HIS3, lacZ and ADE2, each under the control of different GAL4 inducible promoters.

The GAL1-HIS3 fusion has residual HIS3 expression sufficient to allow growth without exogenous histidine even in the absence of GAL4. This can be overcome by growing cells in the presence of 3-aminotriazole (3-AT), a chemical inhibitor of IGP dehydratase that restores histidine auxotrophy (Kishore and Shah, 1988). To identify the concentration of 3-AT required to eliminate growth of yeast containing CTD-DBD and NTD-DBD, the yeast expressing these proteins were grown on media lacking histidine with increasing concentrations of 3-AT. The range of 3-AT used was 0 mM to 50 mM. CTD-DBD required 15 mM 3-AT to inhibit growth in the absence of histidine, whereas NTD-DBD only required 1 mM (Figure 5.2C). Nek2A-AD was confirmed to require 30 mM 3-AT (Fry *et al.*, 1998b).

The efficiency of the HIS selection in identifying interacting proteins was tested using fusions to SNF1 and SNF4, two proteins known to physically associate *in vivo* and whose interaction can be detected using the yeast two hybrid system (Fields and Song, 1989). In addition, CTD-DBD was co-expressed with Nek2A-AD, as the interaction between these two proteins is also detectable using the yeast two hybrid system (Fry *et al.*, 1998b). Both interactions were identified by growth on histidine lacking media (Figure 5.2D). Yeast alone and yeast containing single fusion proteins did not grow. Thus the system being used, including media, 3-AT concentration and growth conditions was satisfactory.

5.2.2 Yeast two hybrid screen using C-Nap1-CTD as the bait

In order to identify proteins capable of interacting with C-Nap1, a yeast two hybrid screen was performed essentially as described previously (Dufee *et al.*, 1993) with CTD-DBD as the bait. The C-terminal domain (amino acids 1962-2403) of C-Nap1 was used first as this domain was identified to interact with Nek2A in a previous screen (Fry *et al.*, 1998b). In addition, a large proportion of C-Nap1 consists of coiled coils, which might pull out a large number of false positives if used in a library screen due to the conservation of sequence in many coiled coil containing proteins. The library screen was carried out using a human testis cDNA library containing 3.2 x 10^6 independent clones constructed in pACTII (gift from I. Eperon). The library was first amplified in *E.coli*, with 4 x 10^6 colonies processed through Qiagen maxiprep kits to provide sufficient library DNA for the screen. Yeast expressing CTD-DBD were transformed with 50 μg of the human testis cDNA library. Transformants were plated on selective medium (lacking uracil, leucine and histidine) supplemented with 15 mM 3-AT.

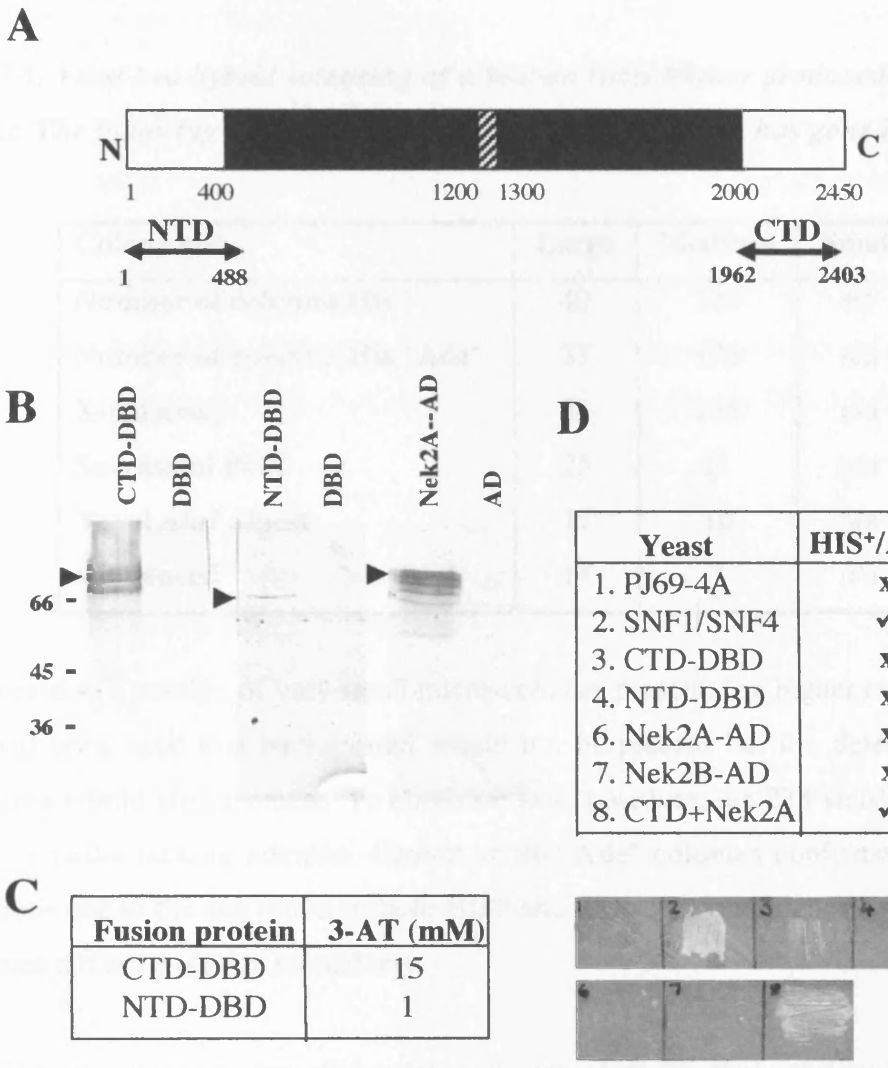

Yeast	HIS+/ADE+
1. PJ69-4A	x
2. SNF1/SNF4	✓
3. CTD-DBD	x
4. NTD-DBD	x
6. Nek2A-AD	x
7. Nek2B-AD	x
8. CTD+Nek2A	✓

Figure 5.2 Analysis of GAL4 fusion protein expression
(**A**) Schematic diagram of C-Nap1, showing the two large coiled coil regions (black boxes) with the hinge region (hatched box) connecting them and globular terminal domains (white boxes). Numbers represent amino acids positions. Arrows indicate the regions of C-Nap1 fused to the DBD for use in yeast two hybrid analysis of Nek2 and C-Nap1 interactions. (**B**) Yeast lysates were prepared from yeast containing CTD-DBD, NTD-DBD, Nek2-AD, DBD and AD followed by SDS-PAGE and Western blotting using specific anti-C-Nap1-C term, anti-C-Nap1-N term and anti-Nek2 antibodies, respectively. Proteins of the correct size were resolved in each case (arrowheads). Molecular weights (kDa) are indicated on the left of the panel. (**C**) The concentration of 3-AT needed to eliminate growth on histidine lacking media is shown. (**D**) PJ69-4A single or double transformants were tested for a positive interaction between the GAL4 DBD fusion protein and GAL4 AD fusion protein by growth on media lacking histidine and adenine. SNF1/SNF4 represents a known positive interaction.

Following two weeks incubation at 30°C, 233 colonies had grown. Of these, 40 were classed as big colonies, 129 as medium and 64 as small colonies (Table 5.1).

Table 5.1. ***Yeast two hybrid screening of a human testis library produced 233 potential positives. The following table indicates how far the investigation has gone in each case.***

Colony size	Large	Medium	Small
Number of colonies His $^+$	40	129	64
Number of colonies His $^+$ Ade$^+$	37	125	n/a
X-gal assay	35	125	n/a
Successful PCR	25	21	n/a
Novel *AluI* digest	17	10	n/a
Sequenced	14	2	n/a

There was also a number of very small micro-colonies present. If a higher concentration of 3-AT had been used this background would not be present but the detection of weak interactions would also decrease. To eliminate false positives, the 233 yeast colonies were grown on media lacking adenine. Growth of His$^+$Ade$^+$ colonies confirmed the positive interactions due to the activation of both HIS3 and ADE2 reporter genes. A small number of colonies did not pass this second test.

After primary selection, transformants were screened for their ability to produce β-galactosidase by growth of blue colonies on plates containing X-gal (data not shown). Again, a small number of colonies were eliminated at this stage. At this point, the emphasis turned to the largest colonies, with the smaller colonies being stored as glycerol stocks for screening at a later date. Total DNA was prepared from the selected positive colonies and the library insert amplified by PCR using pACTII specific primers (AATACCACTACAATGGATGATG and GCTCTAGAGTTGAAGTGAACTTGCGGG). The low efficiency of plasmid DNA purification from yeast and contamination from genomic DNA meant that not all of the positive inserts could be amplified. However, if the PCR was successful, the amplified products were digested with *AluI*. This frequently cutting restriction endonuclease produced a set of fragments of the positive clone that enabled quick identification of duplicate inserts, reducing the number of colonies being screened. As novel inserts were identified, the PCR product was sequenced using the

forward pACTII specific primer. Proteins coded by the library insert cDNA that were not in frame with the GAL4 AD were discarded. In total, 17 different inserts were identified from 42 colonies of which 14 have been sequenced, all were shown to be in frame with the GAL4 activation domain. Database comparisons revealed the encoded proteins, which are given in table 5.2. However so far, only the most frequently appearing protein, C11orf1, has been studied in more detail. Of the other proteins identified, of particular interest are the unknown proteins HUM ZD77604, HSD 3.1 and MGC13016 as nothing is known of their function or localisation. Interestingly, Rab11B localises to the centrosome (G. Gould personal communication), indicating the possibility of centrosomal interaction. However, further biochemical analysis of the interaction between C-Nap1-CTD and Rab11B proved negative.

Table 5.2. ***In frame, sequenced inserts pulled out as positives in a yeast two hybrid screen of a human testis library using C-Nap1-CTD as the bait.***

	Number of hits	Accession number
C11orf1	8	AJ250229
HUM ZD77604	3	AF086415
SCAND1	2	AF207829
HSD 3.1	2	XM029409
Partial C11orf1	1	AJ250229
LENG4	1	NM024298
MGC13016	1	XM051263
SNX1	1	BC008444
Nuf2R	1	NM031423
SCP3	1	NM013041
Rab11B	1	NM004218
Complement subunit C1	1	XM032536
NADH dehydrogenase	1	NC001807
Glycogenin	1	U31525

5.2.3 Identification of C11orf1 as a C-Nap1 interacting protein

Of the 42 large colonies, 8 appeared to contain a library insert of 1250 bp, which gave rise to the same digestion pattern after *AluI* treatment. Following sequencing, the insert fused to the GAL4 AD was identified as region of the novel protein C11orf1. C11orf1 is encoded by a novel human gene found on human chromosome 11q13–q22. It was discovered using the method of EST based *in silico* gene cloning. This is where the clustering of ESTs together to form continuous sequences allows the open reading frame of a gene to be predicted. Nothing is known about C11orf1, except that it contains a region that suggests nuclear localisation (O'Brian *et al.*, 2000). Analysis of the sequence on chromosome 11 provided by the human genome sequencing project, allowed the intron-exon structure of C11orf1 to be predicted by following the [gt-ag] consensus rule. The published sequence is likely to span 4 exons, however, the insert pulled out in the screen (clone 12) does not encompass the proposed C11orf1 start site but has an alternative start site situated in the middle of the predicted intron 1 (Figure 5.3A). Interestingly, the sequence identified in the screen contains a region of DNA not present in the published C11orf1 sequence. This additional region may represent an alternative exon (exon 1a), possibly created by alternative splicing.

cDNA isolated by PCR from clone 12, was subcloned into pGEM using the pGEM-T Easy vector system. From this construct, clone 12 was isolated as an *EcoRI-SalI* fragment and subcloned into pACTII cut with *EcoRI* and *XhoI* in frame with the AD. This was then transformed into yeast expressing CTD-DBD and grown on media lacking histidine and adenine, to reconfirm the interaction. In parallel, it was co-expressed in yeast with the GAL4-DBD alone to eliminate the possibility that the interaction was directly with the DBD rather than C-Nap1-CTD. In addition transformation into yeast expressing the GAL4 DBD fused to the nuclear protein Lamin A, was used to confirm that the interaction wasn't occurring directly with the DBD when it was fused to an arbitrary protein. Both of these interactions proved negative, thus confirming that clone 12 cDNA, which is highly related to C11orf1, encodes a protein that interacts in the yeast two hybrid system with C-Nap1-CTD (Figure 5.3B). Finally, a quantitative assay for β-galactosidase activity with the substrate *O*-nitrophenyl-β-galactopyranoside (ONPG) was performed to give a measure of the strength of interaction (Figure 5.3C). Results confirm that clone 12 interacts specifically with CTD-DBD and induces a β-galactosidase activity similar to the SNF1/SNF4 interaction.

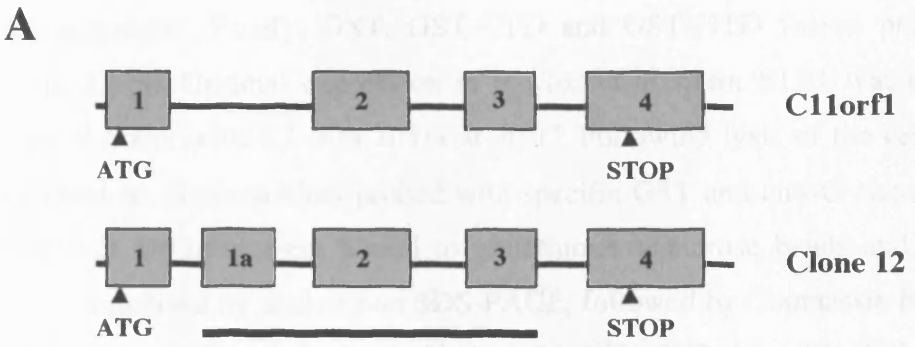

B

Yeast	HIS+/ADE+
1. PJ69-4A	x
2. SNF1/SNF4	✓
3. CTD-DBD	x
4. Clone 12-AD	x
5. CTD+clone 12	✓
6. CTD+LaminA	x

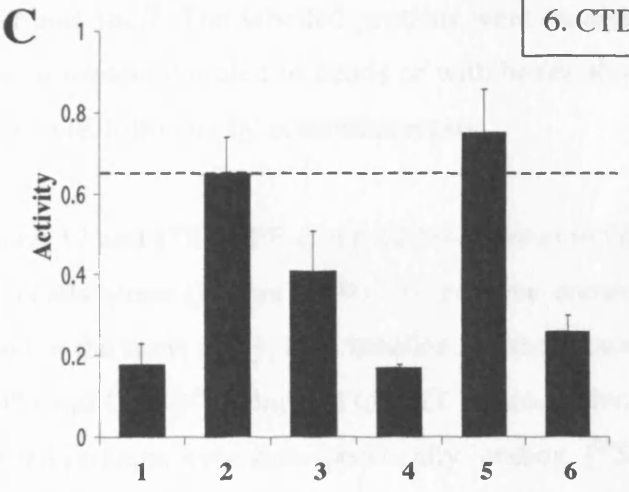

Figure 5.3 Identification of C-Nap1 CTD interaction with clone 12
(**A**) Schematic diagram of C11Orf1 and clone 12 from a yeast 2 hybrid screen using C-Nap1 C terminal domain (CTD) as the bait. The intron-exon structure is shown (not to scale) as taken from chromosome 11q13-q22 sequence, indicating the start (ATG) and stop sites of each protein. The sequence of the clone identified in the screen is shown (black bar). (**B**) Yeast PJ69-4A single or double transformants were tested for a positive interaction between the GAL4 DBD fusion protein and GAL4 AD fusion protein by growth on media lacking histidine. (**D**) The same yeast were tested using a quantitative assay for β-galactosidase activity with the substrate *O*-nitrophenyl-β-galactopyranoside (*ONPG*). Units of activity are relative to the Nek2A-Nek2A interaction, given an arbitrary value of 1.0. Results are the mean of three independent experiments. SNF1/SNF4 represents a known positive interaction, a positive result is shown where activity is equal to or greater than SNF1/SNF4 (dotted line).

5.2.4 Interaction of clone 12 with C-Nap1-CTD *in vitro*

The interaction between C-Nap1 and clone 12 was confirmed biochemically using a GST pull down technique. Firstly, GST, GST-CTD and GST-NTD fusion proteins were expressed in *E.coli*. Optimal expression in the bacterial strain BL21 was obtained by inducing for 4 hours with 0.1 mM IPTG at 30°C. Following lysis of the cells, proteins were confirmed on Western blots probed with specific GST and anti-C-Nap1 antibodies (see Figure 6.2). Proteins were bound to glutathione sepharose beads and the protein concentration equalised by analysis on SDS-PAGE, followed by Coomassie Blue staining and Western blotting (Figure 5.4A). [^{35}S]-clone 12, [^{35}S]-GFP-clone 12, [^{35}S]-Nek2A and [^{35}S]-Nek2B labelled proteins were *in vitro* translated using pGEM-clone 12, pEGFP-clone 12, pGEM-Nek2A and pGEM-Nek2B, respectively. pEGFP-clone12 was prepared using clone 12 specific primers (GCGCCCTGCAGATACCACTACAATG and GCGCCCGC GGTTTCAGTATTACGA), to amplify clone 12 cDNA from pGEM-clone 12. The fragment was cut with *PstI* and *SacII* and subcloned into pEGFP (C1), a mammalian expression vector containing an enhanced green fluorescent protein that had also been cut with *PstI* and *SacII*. The labelled proteins were incubated with an equal amount of each GST fusion protein coupled to beads or with beads alone and the bound portion analysed by SDS-PAGE followed by autoradiography.

[^{35}S]-Clone 12 and [^{35}S]-GFP-clone 12 both bound to GST-CTD and GST-NTD but not to GST or beads alone (Figure 5.4B). As positive controls, [^{35}S]-Nek2A and [^{35}S]-Nek2B were used in the same assay, both labelled proteins bound specifically to beads coated with GST-CTD and GST-NTD but not to GST or beads alone. To eliminate the possibility that the labelled proteins were non-specifically binding, [^{35}S]-Lamin A was used as a negative control, Lamin A did not bind to any of the coupled proteins or the beads alone. These experiments provide evidence that clone 12 interacts with C-Nap1 at both the C- and N-terminal domains. Further work was carried out to look at the strength of the interaction between C-Nap1 and clone 12 by increasing the NaCl concentration of the wash buffer from 100 mM to 750 mM. The interaction between GST-CTD and [^{35}S]-clone 12 was lost at a NaCl concentration of 750 mM but was still detectable at 500 mM emphasising that this is a strong interaction (data not shown). In fact, the GST-CTD protein bound to the beads also diminished at these high salt concentrations, thus it is possible that the interaction between clone 12 and the C-Nap1-CTD can survive stronger salt concentrations than GST with glutathione.

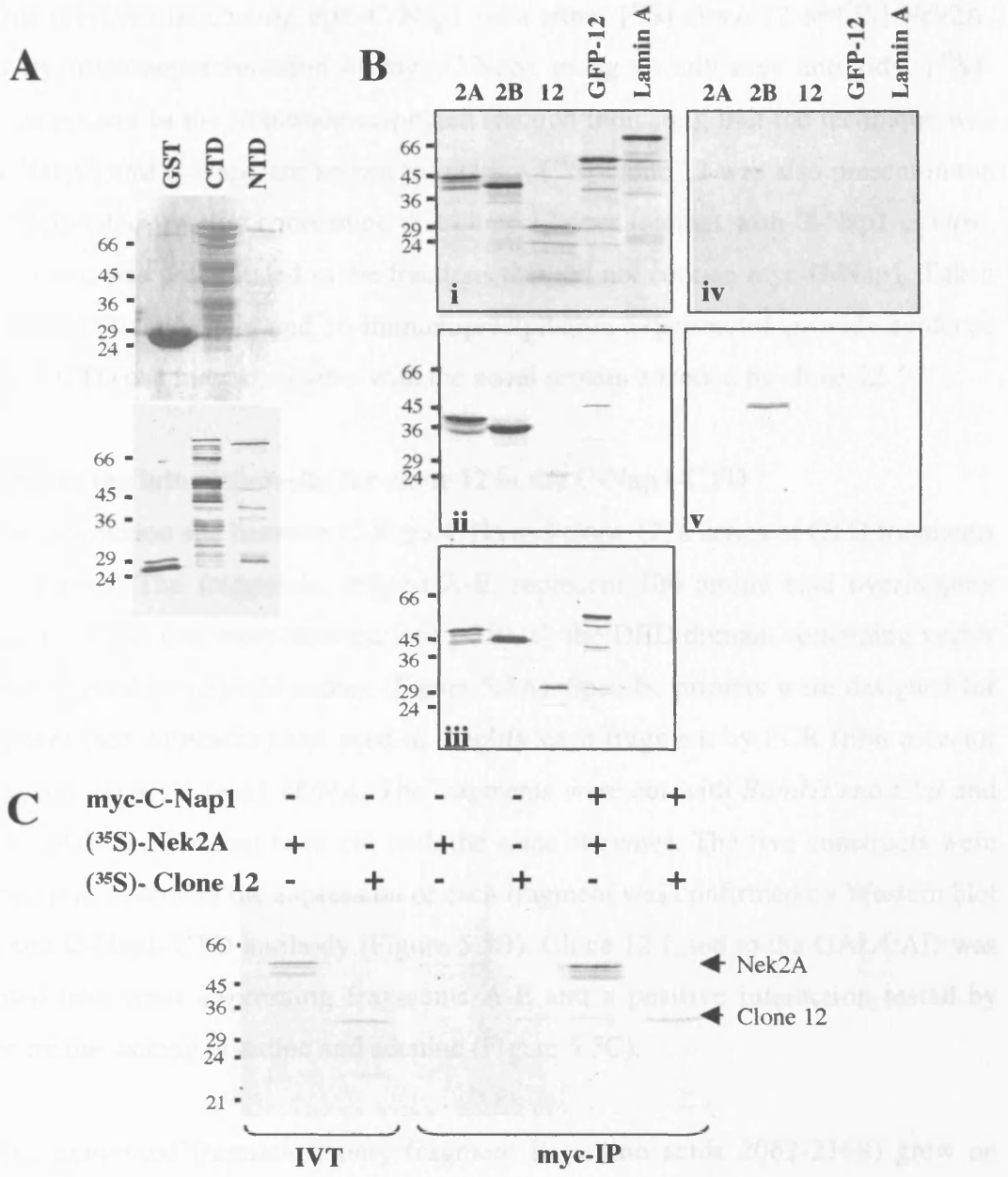

Figure 5.4 Interaction of C-Nap1-CTD with clone 12 *in vitro*

(A) Glutathione sepharose beads were mixed with bacterial cell lysates containing GST, GST-CTD and GST-NTD. An aliquot was taken for direct analysis by SDS-PAGE with Coomasie Blue staining (upper panel) and Western blotting using an anti-GST antibody (lower panel). **(B)** *In vitro* translated (IVT) Nek2A (2A), Nek2B (2B), clone 12 (12), GFP-clone 12 (GFP-12) and lamin A were prepared in the presence of [^{35}S] methionine. An aliquot was taken for direct analysis by SDS-PAGE followed by autoradiography (i). The GST fusion proteins coupled to sepharose beads were incubated with the IVT proteins O/N at 4 °C, washed and analysed by SDS-PAGE followed by autoradiography (ii:GST-CTD, iii: GST-NTD, iv: beads, v: GST). Nek2B showed a weak interaction with GST alone. **(C)** IVT Nek2A and clone12 were prepared in the presence of [^{35}S] methionine and myc-C-Nap1 was prepared in its absence. Samples were mixed as shown in the presence of cycloheximide to prevent further translation and then immunoprecipitated with anti-myc antibodies, processed by SDS-PAGE and exposed for autoradiography. Molecular weights (kDa) are indicated on the left of each panel.

In parallel, co-immunoprecipitation of *in vitro* translated proteins was carried out (Figure 5.4C). This involved incubating myc-C-Nap1 with either [^{35}S]-clone 12 or [^{35}S]-Nek2A, followed by immunoprecipitation of myc-C-Nap1 using an anti-myc antibody. [^{35}S]-Nek2A was present in the immunoprecipitated fraction indicating that the technique was viable as Nek2A and C-Nap1 are known to interact. [^{35}S]-clone 12 was also present in the immunoprecipitated fraction confirming that clone 12 does interact with C-Nap1 *in vitro*. No [^{35}S] protein was precipitated in the fractions that did not contain myc-C-Nap1. Taken together, the GST pull down and co-immunoprecipitation experiments provide evidence that C-Nap1-CTD can interact *in vitro* with the novel protein encoded by clone 12.

5.2.5 Mapping the interaction site for clone 12 in the C-Nap1-CTD

To map the interaction site between C-Nap1-CTD and clone 12, a series of CTD fragments were constructed. The fragments, termed A-E, represent 100 amino acid overlapping sections of the CTD that were inserted into pGBDU, the DBD domain containing vector used in the original two hybrid screen (Figure 5.5A). Specific primers were designed for each fragment (see Appendix) and used to amplify each fragment by PCR from a vector containing full length C-Nap1 cDNA. The fragments were cut with *BamHI* and *ClaI* and ligated into pGBDU that had been cut with the same enzymes. The five constructs were transformed into yeast and the expression of each fragment was confirmed by Western blot using an anti-C-Nap1-CTD antibody (Figure 5.5B). Clone 12 fused to the GAL4 AD was transformed into yeast expressing fragments A-E and a positive interaction tested by growth on media lacking histidine and adenine (Figure 5.5C).

Of the five expressed fragments, only fragment B (amino acids 2062-2168) grew on selective media, indicating that the binding region for clone 12 lies within this section of C-Nap1. To confirm this, a quantitative assay for β-galactosidase activity with the substrate ONPG was performed. (Figure 5.5D). The interaction between SNF1 and SNF4 used to indicate the level of activity of β-galactosidase that is present if a positive interaction is occurring. Fragment B was the only DBD fusion protein that interacted with clone 12-AD and induced a higher level of β-galactosidase activity than SNF1/SNF4. This confirms the region of C-Nap1-CTD involved in the interaction with clone 12 to lie between amino acids 2062-2168. Co-immunoprecipitation procedures will be needed to confirm this interaction *in vitro*.

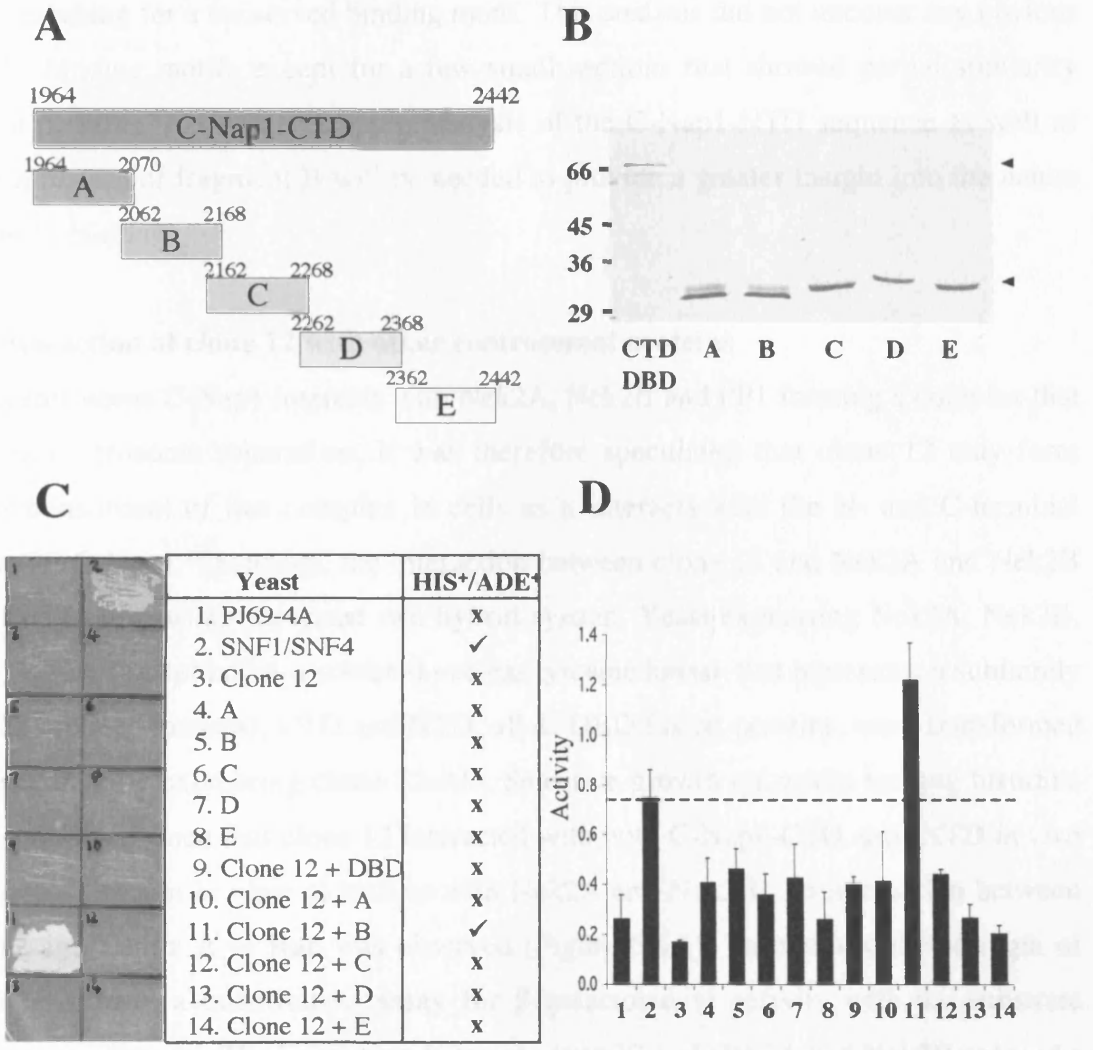

Figure 5.5 Clone 12 interacts with C-Nap1-CTD between amino acids 2062-2168

(A) Schematic diagram of fragments of C-Nap1-CTD, termed A-E, fused to GAL4 DBD. **(B)** Lysates were prepared from yeast expressing fragments A-E and CTD-DBD, followed by SDS-PAGE and Western blot using anti-C-Nap1-CTD antibodies. Proteins of the correct size were resolved in each case, indicated by arrowheads. Molecular weights (kDa) are indicated on the left. **(C)** Yeast PJ69-4A single and double transformants were tested for a positive interaction between the GAL4 DBD fusion protein and GAL4 AD fusion protein by growth on media lacking histidine and adenine. **(D)** The same yeast were tested using a quantitative assay for β-galactosidase activity with the substrate *ONPG*. Units of activity are relative to the Nek2A-Nek2A interaction, given an arbitrary value of 1.0. Results are the mean of three independent experiments. SNF1/SNF4 represents a known positive interaction, a positive result is shown where activity is equal to or greater than SNF1/SNF4 (dotted line).

The observation that clone 12 interacts *in vitro* with both C-Nap1-CTD and -NTD prompted a comparison of the sequence of fragment B with that of C-Nap1-NTD with the aim of searching for a conserved binding motif. This analysis did not uncover any obvious clone 12 binding motifs except for a few small sections that showed partial similarity between proteins. A similar mapping analysis of the C-Nap1-NTD sequence as well as further mutation of fragment B will be needed to provide a greater insight into the nature of clone 12 binding.

5.2.6 Interaction of clone 12 with other centrosomal proteins

At the centrosome C-Nap1 interacts with Nek2A, Nek2B and PP1 forming a complex that regulates centrosome separation. It was therefore speculated that clone 12 may form another constituent of this complex in cells as it interacts with the N- and C-terminal domains of C-Nap1. Therefore, the interaction between clone 12 and Nek2A and Nek2B was tested *in vivo* using the yeast two hybrid system. Yeast expressing Nek2A, Nek2B, Lamin A, Rak (an epithelial-associated nuclear tyrosine kinase that represents a subfamily of the Src-related kinases), CTD and NTD, all as DBD fusion proteins, were transformed into yeast already expressing clone 12-AD. Selective growth on media lacking histidine and adenine confirmed that clone 12 interacted with both C-Nap1-CTD and -NTD *in vivo* as previously shown *in vitro* as well as with Nek2A and Nek2B. No interaction between clone 12 and Lamin A or Rak was observed (Figure 5.6A). To measure the strength of these interactions, a quantitative assay for β-galactosidase activity with the substrate ONPG was performed. The interaction between clone 12 and Nek2A and Nek2B induced a higher level of β-galactosidase activity than SNF1/SNF4, implying that there is a strong interaction between these proteins (Figure 5.6B). Together growth selection and β-galactosidase activity, confirm the interaction between clone 12 and Nek2A and Nek2B.

A

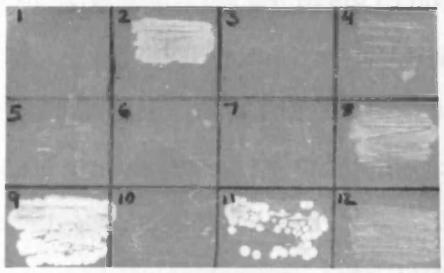

Yeast	HIS⁺/ADE⁺
1. PJ69-4A	x
2. SNF1/SNF4	✓
3. Clone 12	x
4. CTD	x
5. NTD	x
6. Nek2A	x
7. Nek2B	x
8. Clone 12 + CTD	✓
9. Clone 12 + NTD	✓
10. Clone 12 + LaminA	x
11. Clone 12 + Nek2A	✓
12. Clone 12 + Nek2B	✓
13. Clone 12 + Rak	x

B

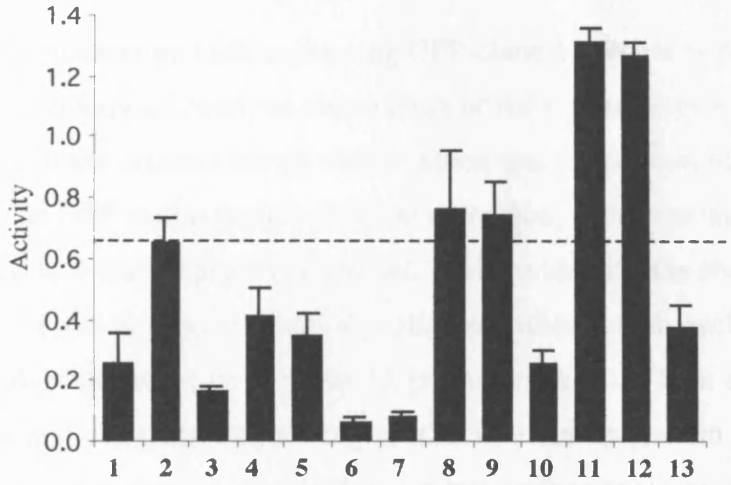

Figure 5.6 Clone 12 also interacts with Nek2A and Nek2B
(**A**) PJ69-4A double transformants expressing clone 12 in combination with Nek2, C-Nap1, Rak or Lamin A were tested for a positive interaction by growth on media lacking histidine and adenine. (**B**) The same yeast were tested using a quantitative assay for β-galactosidase activity with the substrate *ONPG*. Units of activity are relative to the Nek2A-Nek2A interaction, given an arbitrary value of 1.0. Results are the mean of three independent experiments. SNF1/SNF4 represents a known positive interaction, thus, a positive results was taken where the activity is equal to or greater than SNF1/SNF4 (dotted line).

5.2.7 Subcellular localisation of clone 12

Having demonstrated an interaction between C-Nap1 and Nek2 with clone 12 both *in vivo* and *in vitro*, the next step was to identify the subcellular localisation of clone12 to see whether these interactions are likely to take place at the centrosome. Localisation of clone 12 was observed by fusing it to GFP (see section 4.2.4). This vector was transiently transfected into HeLa cells and analysed by indirect immunofluorescence microscopy. The centrosome was revealed by antibodies against C-Nap1 (Figure 5.7A-D). 55% of cells exhibited co-localisation of GFP-clone 12 with at least one of the two dots that represent the centrioles of the centrosome seen. Interestingly, other structures within the cell showed concentrated GFP signals (Figure 5.7A), although it is unknown at this time what these structures represent. GFP alone was also transfected into HeLa cells (Figure 5.7E). The GFP protein alone was shown to localise non-specifically throughout the cell, with no concentration at the centrosome. Thus the centrosomal localisation of GFP-clone 12 is due to clone 12 targeting and not to GFP.

Extracts were made from cells expressing GFP-clone 12. Western blotting using a specific anti-HA tag antibody allowed the observation of the expressed protein due to the presence of an HA tag in the original library vector which was included in the PCR product created for cloning the GFP fusion protein. Prior to extraction, cells expressing GFP-clone12 were synchronised in S and M phases of the cell cycle to identify the abundance of clone 12 at different cell cycle phases. In addition, cells were treated with cycloheximide for 0 and 4 hours to look at the stability of clone 12 protein in cells. In both cases, clone 12 protein levels remained constant, suggesting that it is a stable protein that is not cell cycle regulated (data not shown). Antibodies against endogenous protein will be required to confirm these results.

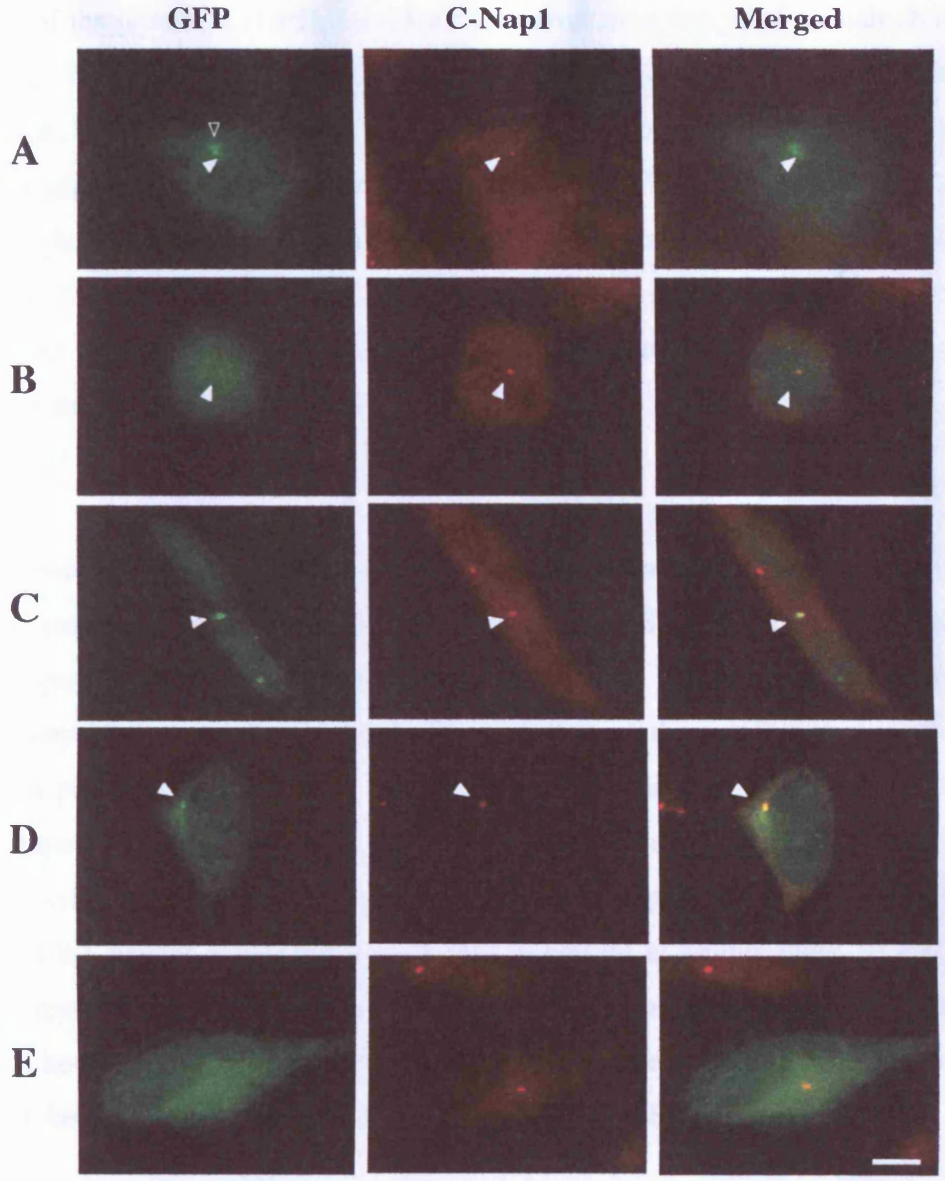

Figure 5.7 Clone 12 associates with the centrosome
HeLa cells were transiently transfected with GFP-clone 12 (A-D) or GFP alone (E), fixed with cold methanol after 24 hr and analysed by indirect immunofluorescence microscopy. Arrowheads indicate the co-localisation of GFP signals with centrosomes as revealed by antibodies against the centrosomal protein C-Nap1. The open arrowhead (A) indicates other unknown cellular structures that show GFP localisation. Scale bar, 10 μm.

5.2.8 Identification and cloning of full length BPC-1

The protein isolated in the yeast two hybrid screen referred to as clone 12 represents a fragment of the protein C11orf1, encoded by a novel gene found on human chromosome 11q13-q22. With confirmation of the interaction with C-Nap1-CTD and localisation to the centrosome, the next step was to obtain the full length protein. Four image clone ESTs were identified that contained full length C11orf1 (2270610, 3703519, 4441403 and 4656696). As previously mentioned, the region of cDNA isolated in the screen included an extra exon that was not present in the original C11orf1 sequence. Interestingly all four ESTs did not contain this extra sequence. EST 2270610 was selected for further study and from now on the protein encoded by this EST will be referred to as BPC-1 (Binding Partner of C-Nap1-1).

BPC-1 is encoded by 150 amino acids with a calculated molecular mass of 17.7 kDa and a predicted isoelectric point of 8.7 (Figure 5.8A). The EST is thought to encompass the complete protein due to the putative initiator methionine being preceded upstream by an in-frame termination codon. Also at the 3' end following the putative stop codon the EST includes a polyadenylation signal and polyA tail. Examination of the predicted BPC-1 protein sequence indicates that it is unlikely to form coiled coils and does not contain any known motifs that may be involved in degradation or protein-protein interactions (e.g PEST motifs), except a possible D box that is present at amino acids 16-25. Database searches revealed that ESTs are available that encode proteins with high homology to BPC-1 in both mouse and cow (Figure 5.8B). Unfortunately, no such protein homologues have been be identified in yeast, *Drosophila* or *Xenopus* EST databases as yet.

5.2.9 Subcellular localisation of BPC-1

With clone 12 found to localise to the centrosome, it was necessary to confirm that BPC-1 also associates with the centrosome. To do this, BPC-1 was fused to EGFP. The complete sequence was amplified by PCR using specific primers (GCGCAGATCTATGGATGCCTCCCAGTGT and GCGCGAATTCTTAAGGCTTTGA ATAGCT) from image clone 2270610. The product was digested with *EcoRI* and *BglII* and inserted into the pEGFP C1 mammalian expression vector in frame with EGFP. GFP-BPC-1 was transiently transfected into HeLa cells and analysed by indirect immunofluorescence microscopy. The centrosome was revealed by antibodies against C-Nap1. 65% of cells exhibited co-localisation of GFP-BPC-1 with at least one of the two

dots that represent the centrioles of the centrosome (Figure 5.9Aa-h). GFP alone transfected into HeLa cells did not co-localise to the centrosome (Figure 5.9Ai-l). Interestingly, the GFP-BPC-1 signal was not observed between the centrioles as would be expected for a protein that forms part of the intercentriolar linkage, suggesting that it localises more directly to the centrioles or PCM. Non-centrosomal BPC-1 appeared to be predominantly cytoplasmic, with only 10% of cells expressing BPC-1 displaying nuclear localisation.

As BPC-1 was centrosomal, the dependence of this localisation on the microtubule or actin filament networks was investigated. Cells transfected with GFP-BPC-1 were treated with various cell poisons. Cells were either incubated on ice for 30 minutes or treated for 4 hours with nocodazole (6μg/ml) to depolymerise microtubules. Treatment with taxol (5 μM) for 4 hours stabilised microtubules and a 1 hour incubation with cytochalasin D (10 μg/ml) disrupted the actin network. The effect of each treatment was confirmed by staining of microtubules or actin with anti-α-tubulin and anti-actin antibodies respectively (data not shown). Following depolymerisation or stabilisation of microtubules, there was no observable decrease in the amount of BPC-1 at the centrosome (Figure 5.9B). Indicating that BPC-1 localises to the centrosome independently of microtubules. Cytochalasin D, a drug that disrupts the actin cytoskeleton, also had no implications for BPC-1 localisation to the centrosome. Taken together, these results provide persuasive evidence that BPC-1 can be considered as a core component of the centrosome.

To provide final proof that BPC-1 is a centrosomal protein it will be necessary to produce a specific BPC-1 antibody. To achieve this, a substantial amount of purified protein needs to be obtained. Due to the relative insolubility of BPC-1 when fused to GST and expressed in *E.coli* (see below) and the failure of techniques designed specifically to purify insoluble protein from inclusion bodies, a new strategy will be employed. BPC-1 will be expressed as a fusion to a His tag, to enable purification under denaturing conditions. Alternatively, an MBP fusion will be used, as this method of purification is known to improve the solubility of proteins. Once antibodies have been obtained, they can also be used to study the ultrastructural localisation of BPC-1 by immunoelectron microscopy of whole cells and isolated centrosomes.

A

```
cggcacgaggaacctttttcacctcgtctgaaatggctgcctcccagtgtctctgctgc
                                  M  A  A  S  Q  C  L  C  C
tcaaaatttctcttccagagacagaacctcgcctgtttcctcacaaacccacactgtggc
 S  K  F  L  F  Q  R* Q  N  L* A  C  F  L  T  N* P  H  C  G
agccttgttaatgcagatggccatggtgaagcgtggacagattggaataatatgtccaag
 S  L  V  N  A  D  G  H  G  E  A  W  T  D  W  N  N  M  S  K
tttttccagtatggatggcgatgcaccactaatgagaatacctattcaaaccgtaccctg
 F  F  Q  Y  G  W  R  C  T  T  N  E  N  T  Y  S  N  R  T  L
atgggcaactggaaccaggaaagatatgacctgaggaatatcgtgcagcccaaacccttg
 M  G  N  W  N  Q  E  R  Y  D  L  R  N  I  V  Q  P  K  P  L
ccttcccagtttggacactactttgaaacaacatatgatacaagctacaacaacaaaatg
 P  S  Q  F  G  H  Y  F  E  T  T  Y  D  T  S  Y  N  N  K  M
ccactttcaacacatagatttaagcgagagcctcactggttcccaggacatcaacctgaa
 P  L  S  T  H  R  F  K  R  E  P  H  W  F  P  G  H  Q  P  E
ctggatcctccccgatacaaatgcacagaaaagtcaacttacatgaatagctattcaaag
 L  D  P  P  R  Y  K  C  T  E  K  S  T  Y  M  N  S  Y  S  K
cctaaaattgggcatcactcaggatgtgtataagatcttaatattgactagtttcacatc
 P  -
caggtttctaagaaatgataagatacttcacttttccagagtgaaatgtaggagggagca
cattctaagtacagctaaaaatttagctcactgtaacacagtttcactctctgaataaat
aaagcaaaaaacacagtaaaaaaaaa
```

B

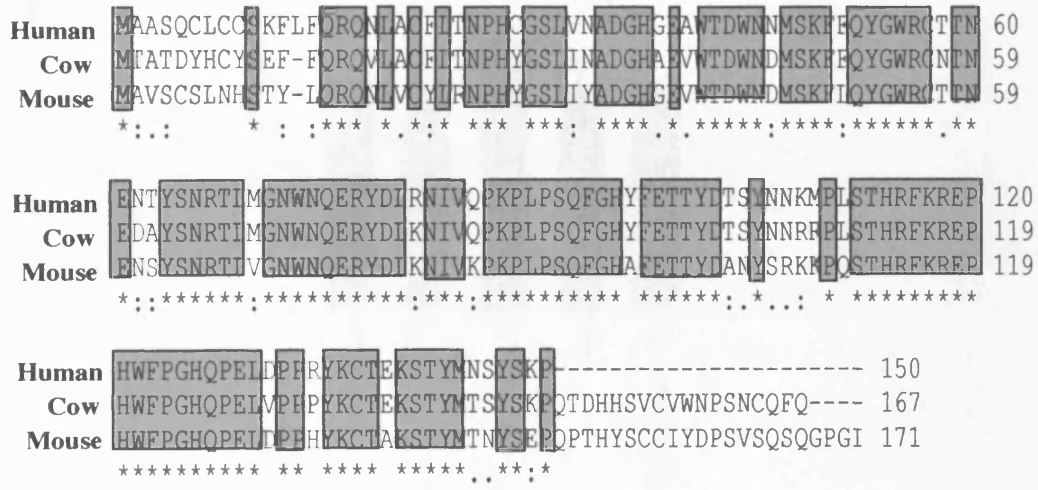

Figure 5.8 Nucleotide and deduced amino acid sequence of BPC-1
(**A**) Amino acids are given in single letter code, The translation stop and start codon are underlined. The polyadenylation signal at the 3' end of the BPC-1 cDNA is also underlined. A putative D box is indicated by asterisks. (**B**) Alignment of the amino acids of BPC-1 with putative homologues in cow and mouse sequence data from EST databases. Grey boxes represent conserved residues.

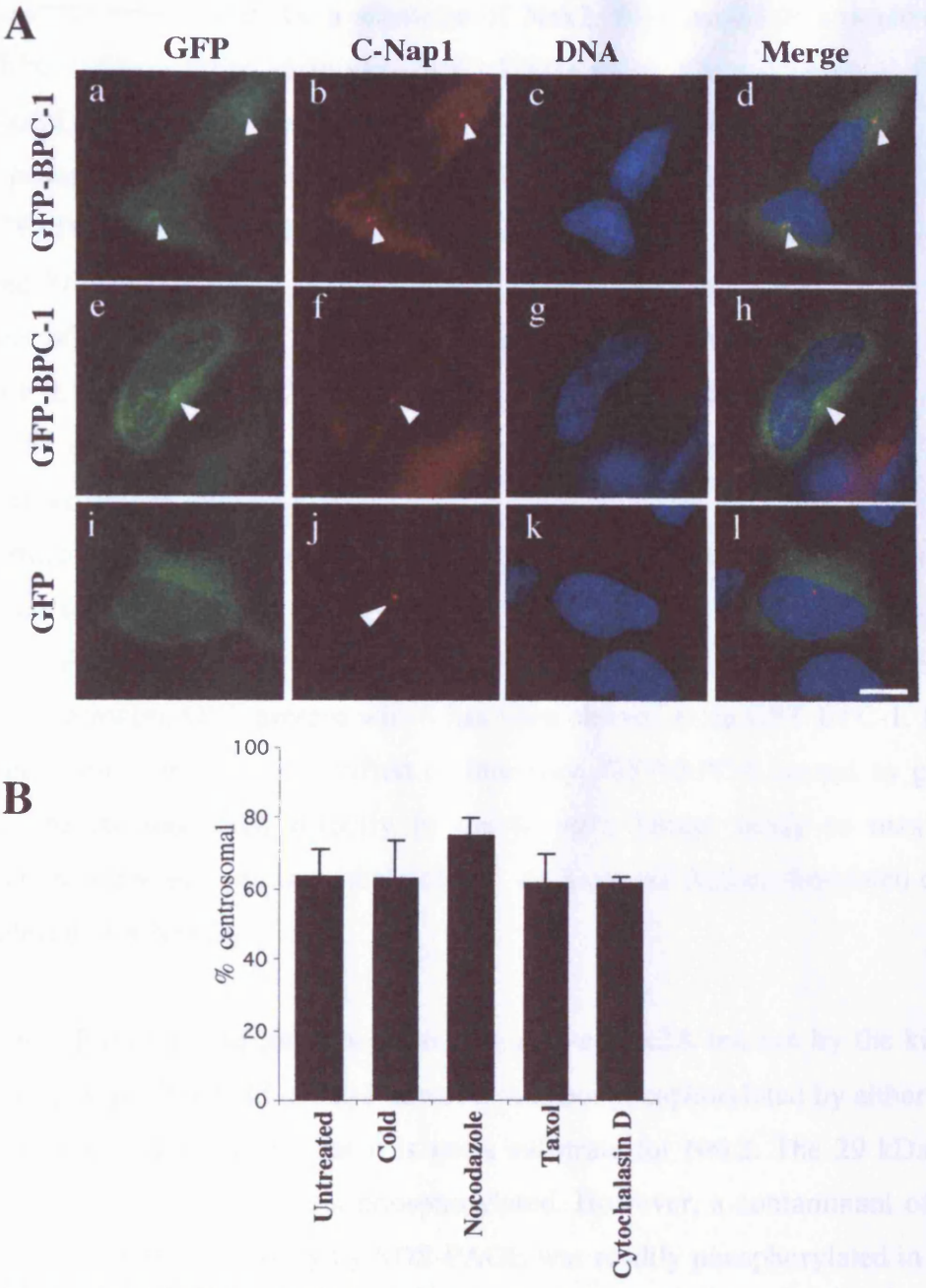

Figure 5.9 BPC-1 associates with the centrosome independently of microtubules and actin

(**A**) Asynchronous HeLa cells were transiently transfected with GFP-BPC-1 (a-h) and GFP (i-l), Cells were fixed 20hr after transfection and analysed by indirect immunofluorescence microscopy. Arrowheads indicate the co-localisation of GFP signals with centrosomes as revealed by antibodies against the centrosomal protein C-Nap1. Scale bar, 10 μm. (**B**) HeLa cells were transiently transfected with GFP and GFP-BPC-1, following a 20 hour incubation at 37°C, cells were either incubated on ice for 30 minutes, treated for 4 hours with nocodazole (6 μg/ml), or taxol (5 μM) or 1 hour with cytochalasin D (10 μg/ml). Cells were then fixed and analysed by indirect immunofluorescence. The number of transfected cells that showed co-localisation of C-Nap1 and GFP-BPC-1 was quantified for both untreated and treated cells under each of the above conditions.

5.2.10 BPC-1 is not a good substrate of Nek2A

The observed interaction of clone 12, the shortened form of BPC-1, with Nek2 raised the possibility that BPC-1 may be a substrate of Nek2. To examine this possibility, GST tagged BPC-1 was used in an *in vitro* Nek2 kinase assay. For this purpose, BPC-1 was fused to GST and expressed in *E.coli* (Figure 5.10A). BPC-1 was amplified by PCR using specific primers (GCGCGAATTCATGGCTGACTCCCAGTGT and GCGCCTCGAGTT AAGGCTTTGAAT AGCT) from image clone 2270610. The product was digested with *EcoRI* and *XhoI* and inserted into pGEX-4T1 digested with the same enzymes. Optimal expression of GST-BPC-1 in the bacterial strain BL21 was obtained by inducing for 16 hours with 0.1 mM IPTG at RT. Following lysis of the cells, only about 2% of the protein was soluble (Figure 5.10B). The expressed protein was confirmed as GST-BPC-1 on Western blots probed with anti-GST antibodies indicating that the expression of a protein of the correct size was fused to GST (Figure 5.10B). The soluble GST-BPC-1 was fused to glutathione sepharose beads and purified protein eluted in five fractions by reduced glutathione (Figure 5.10C). A lower band of about 29 kDa was purified with GST-BPC-1, possibly representing GST protein which has been cleaved from GST-BPC-1. Due to the low concentration of protein purified in this way, GST-BPC-1 bound to glutathione sepharose beads was used directly in the *in vitro* kinase assay to maximize the concentration of protein with minimal volume. As a control dephosphorylated casein was used a substrate for Nek2A.

As expected, β-casein was phosphorylated by active Nek2A but not by the kinase dead version (Nek2A-K37R). GST-BPC-1 however was not phosphorylated by either the active or the dead kinase suggesting that it is not a substrate for Nek2. The 29 kDa band co-purified with BPC-1 was also not phosphorylated. However, a contaminant of about 32 kDa that is not observed directly by SDS-PAGE was readily phosphorylated in the assay. This phosphorylation is not due to Nek2A kinase activity as the same level of phosphorylation was seen with both active and dead Nek2A, thus it must be due to contaminant kinases in the purified BPC-1 preparation.

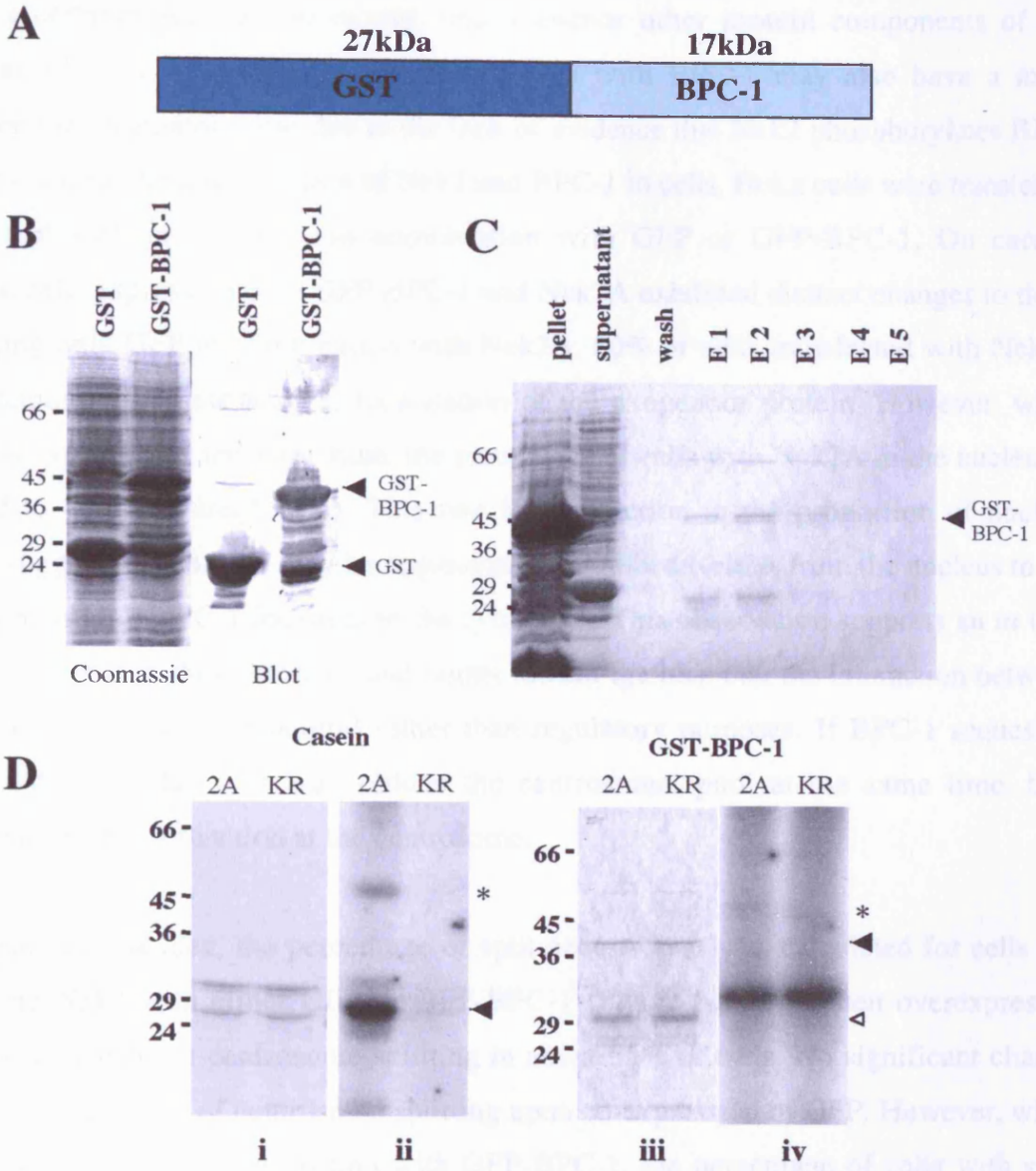

Figure 5.10 GST-BPC-1 is not phosphorylated by Nek2
(**A**) Schematic diagram representing BPC-1 fused to GST. (**B**) GST-BPC-1 and GST were expressed in BL21 *E. coli* and cell lysates analysed by SDS-PAGE with Coomassie Blue staining (left panel) and Western blotting with anti-GST antibodies (right panel). Arrowheads indicate recombinant protein expression. (**C**) Bacterial lysate was passed over glutathione sepharose linked beads. Protein was eluted off the beads using reduced glutathione into five fractions (E1-E5). The pellet, supernatant, wash fraction and elutions were analysed by SDS-PAGE. (**C**) Purified Nek2A-His (2A) and Nek2A-K37R-His (KR) were incubated in Nek2 kinase buffer containing [^{32}P] γ-ATP for 30 min at 30°C, with either casein or GST-BPC-1. Samples were subjected to SDS-PAGE and Coomassie Blue staining (i and iii) and exposed to X-ray film (ii and vi). The black arrowhead in (i) indicates β-casein and in (iii) GST-BPC-1. The white arrowhead in (iii) shows an unknown contaminant in BPC-1 purification. The asterisk indicates Nek2A autophosphorylation.

5.2.11 Effects of co-expression of Nek2 and BPC-1

It is possible that BPC-1 binds to C-Nap1 and Nek2 at the proximal end of centrioles and that this complex may act to recruit and/or anchor other protein components of the intercentriolar linkage. The interaction of Nek2 with BPC-1 may also have a more structural than regulatory role due to the lack of evidence that Nek2 phosphorylates BPC-1. To investigate the dual function of Nek2 and BPC-1 in cells, HeLa cells were transiently transfected with myc-Nek2A in combination with GFP or GFP-BPC-1. On careful analysis, cells expressing both GFP-BPC-1 and Nek2A exhibited distinct changes to those expressing only GFP in combination with Nek2A. 80% of cells transfected with Nek2A alone demonstrate some nuclear localisation of the exogenous protein. However, when BPC-1 is expressed at the same time, the percentage of cells with Nek2A in the nucleus is reduced to 40% (Figure 5.11A). This two fold reduction in the proportion of nuclear Nek2A suggests that BPC-1 may be sequestering expressed Nek2A from the nucleus to the cytoplasm as 90% BPC-1 localises to the cytoplasm. This observation supports an *in vivo* interaction between these proteins and points toward the idea that the interaction between BPC-1 and Nek2 is for structural rather than regulatory purposes. If BPC-1 sequesters Nek2 in the cytoplasm, it may reduce the centrosomal pool at the same time, thus compromising Nek2 function at the centrosome.

To investigate this idea, the percentage of split centrosomes was calculated for cells co-expressing Nek2 with either GFP or GFP-BPC-1 (Figure 5.11B). When overexpressed alone, Nek2A induces centrosome splitting in about 55% of cells. No significant change was seen in the extent of centrosome splitting upon co-expression of GFP. However, when Nek2A is expressed in conjunction with GFP-BPC-1, the percentage of cells with split centrosomes drops from 55% to 22%. This significant decrease may be due to Nek2A protein binding to the overexpressed BPC-1 rather than to other proteins involved in centrosome separation such as C-Nap1, thus rendering Nek2A unable to cause premature separation of the centrosome. Interestingly, when overexpressed in cells alone, BPC-1 does not produce any observable phenotype in fixed cells. If BPC-1 was acting to inhibit centrosome separation through the binding of essential proteins (e.g. C-Nap1 and Nek2), you might expect to see either a block at the G2/M transition or an increased frequency of monopolar spindles. This was not evident in the transient transfections carried out. However, no mitotic cells expressing GFP-BPC-1 could be found at all, suggesting that the transfected cells may be undergoing cell death upon entry into mitosis. Further studies of

the consequences of overexpressing BPC-1 would benefit from observing individual cells microinjected with a GFP-BPC-1 construct or by generating an inducible GFP-BPC-1 cell line.

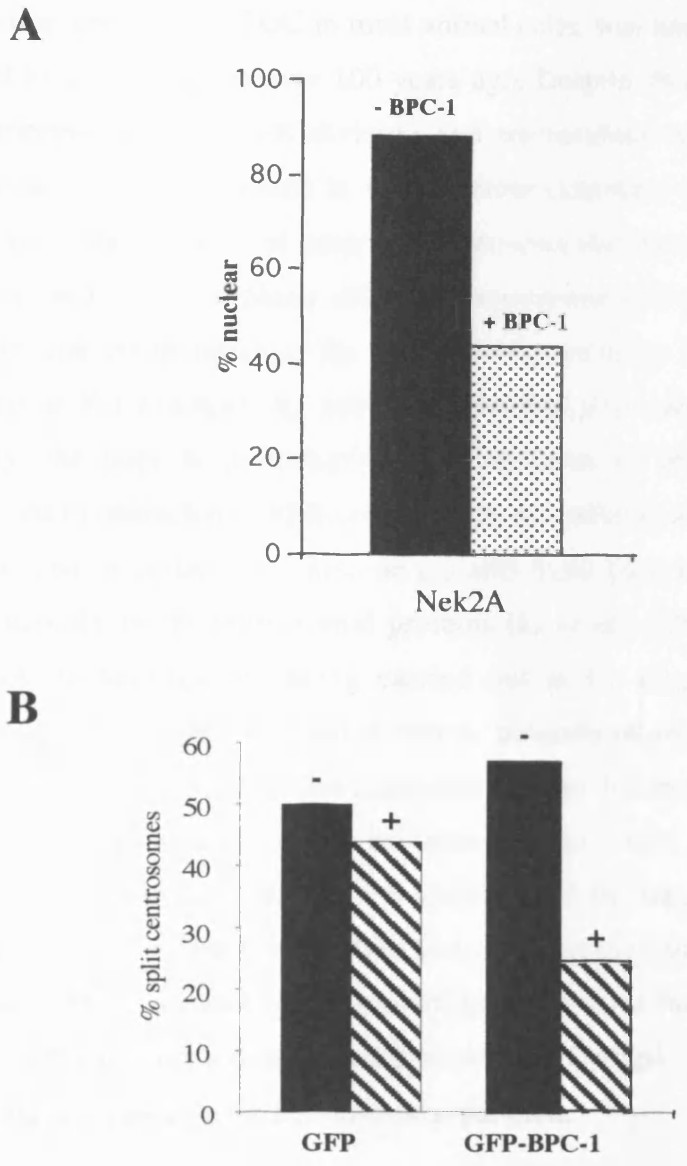

Figure 5.11 BPC-1 binds Nek2 in the cytoplasm and decreases Nek2 induced centrosome separation

Asynchronous HeLa cells were transiently transfected with both myc-Nek2 and GFP-BPC-1, following a 20 hr incubation cells were fixed and analysed by indirect immunofluorescence. (**A**) The percentage of cells in which the transfected protein was nuclear was calculated for HeLa cells with (black bars) and without (dotted bars) GFP-BPC-1 co-expression. (**B**) The percentage of cells in which the two centrosomes were separated by more than 2 μm was calculated with (hatched bars) and without (black bars) GFP-BPC-1 or GFP co-expression.

5.3. DISCUSSION

The centrosome, the major MTOC in most animal cells, was among the first organelles to be described by cell biologists over 100 years ago. Despite its major role in a number of essential processes such as cell division and microtubule nucleation, the molecular characterisation of the centrosome is still far from complete (Andersen, 1999; Doxsey, 2001). Moreover, the majority of centrosome proteins that have been identified have not been characterised in detail. Many different experimental strategies have been used to identify molecular components of the centrosome, including large scale proteomic and genomic screens For example, by subjecting purified centrosome preparations to mass spectrometry, the hope is to identify all components of the centrosome, a method previously used to characterise SPB components. In addition, anti-centrosome antibodies that are produced in certain autoimmune patients have been used to screen expression libraries to identify novel centrosomal proteins (Li *et al.*, 2001). Genomic approaches using dsRNAi technology are being carried out in *C. elegans, Dicytostelium* and *Drosophila* to identify genes involved in mitotic progression including those that regulate centrosome and spindle function. One additional strategy for identifying novel centrosome components involves searching for proteins that are able to interact with known centrosomal proteins. In this chapter, we have applied this approach using C-Nap1, the centrosomal substrate of Nek2, as the bait in a yeast two hybrid screen. By doing this we have identified BPC-1, a novel component of the centrosome that not only localises to the centrosome, but also interacts with Nek2 as well as C-Nap1. BPC-1 thus represents, a possible regulatory molecule for centrosome separation.

The screen of a human testis cDNA library using C-Nap1-CTD as the bait was initially undertaken with the aim of identifying novel centrosomal proteins that may be involved in the intercentriolar linkage that exists during interphase. The screen yielded a large number of possible cDNAs that may encode centrosomal proteins, however, only the 42 most viable clones, based on the size of the yeast colony after two weeks were selected for further analysis. Of these, some were eliminated in subsequent screening processes. Of those sequenced, a few more were eliminated due to their unlikely involvement at the centrosome including human mitochondrial NADH dehydrogenase and glycogenin, a skeletal muscle component. The unknown genes MGC1306, HSD 3.1 and clone HUM ZD77604 were found to represent novel proteins that interacted with C-Nap1-CTD in the

yeast two hybrid system, however, *in vitro* confirmation of these interactions has not yet been carried out. Rab11B, a small G protein related to the RAS oncogene family, was also identified, but did not co-immunoprecipitate with C-Nap1 *in vitro*. A large fragment of a C11orf1, coded for on chromosome 11 (clone 12), represented the most interesting protein identified in so much as it was identified multiple times in the screen. The interaction between this protein and C-Nap1-CTD was confirmed both *in vivo* using direct yeast two hybrid interactions and *in vitro* by GST pull down and co-immunoprecipitation approaches. In addition, GFP fusions of both clone 12 and the full length C11orf1 protein localised to the centrosome. Hence for simplicity, we now refer to this protein as BPC-1, for binding partner of C-Nap1-1. Further analysis of the site of interaction revealed a 100 amino acid (2062-2168) region of C-Nap1 that specifically interacts with BPC-1. Furthermore the interaction of the protein with C-Nap1-NTD and Nek2 raised the possibility that a conserved motif for binding could be identified. However, no such motif has yet been identified. Further mutational analysis of C-Nap1-CTD may help to reveal the existence of such a motif.

An EST was identified that encoded the full length protein represented by BPC-1 with a predicted molecular mass of 17.7 kDa. Analysis of the sequence did not reveal the existence of any specific domains such as coiled coils. In addition no degradation motifs could be identified, except for a putative D box (RXXLXXXXXN) in the N terminus. Preliminary investigation looking at the stability of BPC-1 in *Xenopus* egg extracts has indicated that this it is a relatively stable protein, suggesting that the destruction box is not functional. The lack of homology to any other centrosomal proteins makes speculation of a cellular function difficult. However, the existence of potential homologues in mouse and cow is suggestive that BPC-1 is a functionally conserved protein at least throughout vertebrates. BPC-1 was found to localise to the centrosome independently of microtubule and actin microfilaments. It was also shown to be predominantly cytoplasmic, which doesn't agree with the prediction of a nuclear protein based on Reinhardt's method for nuclear/cytoplasmic localisation.

The function of BPC-1 has not been identified in this work as no distinct phenotype was observed upon overexpression. It is unlikely that it is a major component of the structure that links centrioles as no protein was present between the centrioles. However, due to the ability of BPC-1 to bind both C-Nap1-NTD and -CTD as well as Nek2A and Nek2B, it is

tempting to speculate that it plays a role in the maintenance of centrosome cohesion. An existing model for Nek2 function proposes that phosphorylation in late G2 of substrates such as C-Nap1 leads directly to the dissolution of the intercentriolar linkage that holds centrosomes together during interphase (Mayor *et al.*, 1999). BPC-1 may contribute to this model by anchoring or recruiting proteins such as C-Nap1 and Nek2 to the proximal end of the centrioles. The lack of phosphorylation of BPC-1 by Nek2 suggests that it is not regulated in a cell cycle manner by changes in Nek2 activity, but may have a more structural role. In addition, preliminary evidence suggests that BPC-1 is stable throughout the cell cycle. The fact that no mitotic cells overexpressing BPC-1 were observed after transient transfection could imply that overexpression of BPC-1 causes a block in mitotic progression, possibly inducing cell death. The mechanism for this could involve a block in the dissolution of the intercentriolar linkage or an increase in the recruitment of its components, leading to an increase in the strength centriole cohesion. This may activate a checkpoint mechanism to ensure that a bipolar, rather than a monopolar spindle is formed (Figure 5.13).

Expression of BPC-1 in cells that are also overexpressing Nek2A, results in two interesting observations. Firstly, selective uptake of Nek2A into the nucleus through the use of a putative bipartite nuclear localisation sequence in its C-terminus is disrupted. Instead, Nek2A localises to the cytoplasm with BPC-1. This may compromise regulatory mechanisms for Nek2 that involve partitioning it to the nucleus as opposed to the cytoplasm. In addition, it has been suggested that Nek2A may be associated with chromosomes in mitosis reinforcing the idea of Nek2A also being a mitotic regulator similar to NIMA (Ha Kim *et al.*, 2002; Rhee and Wolgemuth, 1997). If BPC-1 expression causes sequestering of Nek2A away from the nucleus, any such functions would be compromised.

Perhaps a more interesting observation is the decrease in the appearance of prematurely separated centrosomes that are normally induced by Nek2A overexpression when BPC-1 is also overexpressed. The proposed function of Nek2 in centrosome separation at the G2/M transition is based on the fact that its overexpression causes split centrosomes (Fry *et al.*, 1998a). When BPC-1 is also overexpressed in the same cells, as already mentioned, Nek2 appears to move from the nucleus to the cytoplasm. It is possible that it also moves away from the centrosome to form a complex with BPC-1 in the cytoplasm, thus decreasing the

amount of Nek2 at the centrosome that is able to phosphorylate components of the intercentriolar linkage to induce centrosome splitting (Figure 5.12). This mechanism could be confirmed by quantifying the amount of Nek2A associated fluorescence at the centrosome when expressed alone or in combination with BPC-1. Another consequence of Nek2-BPC-1 complexes could be a decrease in Nek2 kinase activity, perhaps by blocking its ability to form dimers, reducing the extent of autophosphorylation. Alternatively, BPC-1 may block the site of interaction with substrates such as C-Nap1, reducing the efficiency of their phosphorylation (Figure 5.13A). This could be tested by measuring the relative kinase activity of Nek2 in cells also overexpressing BPC-1 or by measuring the extent of C-Nap1 phosphorylation, however, it would be difficult to use transient transfections in these experiments due to low transfection efficiency.

To understand fully the mechanism by which Nek2, C-Nap1 and BPC-1 function at the centrosome would be the next aim of this work. A speculative model for the combined role of these proteins is shown in Figure 5.13B. In late G2, the intercentriolar linkage is held in place by C-Nap1 and BPC-1. Nek2 activity is kept switched off by the dephosphorylating activity of PP1. BPC-1 acts to stabilise and recruit the proteins of this complex at the proximal end of centrioles. As the cell begins the G2/M transition, Nek2 becomes active, leading to phosphorylation of C-Nap1 producing a conformational change in C-Nap1 structure causing the release of components of the linkage. Nek2 may also phosphorylate other components of the intercentriolar linkage activating their dissociation or degradation. BPC-1 is not affected by Nek2 activation directly, but maybe cannot bind phosphorylated components of the linkage. At the onset of mitosis, Nek2 is degraded by the 26S proteasome and centriole cohesion is completely lost, allowing the formation of the mitotic bipolar spindle. This model will need extensive testing to confirm the relative roles of the three proteins involved. In addition, identification of further components of the linkage would greatly help our understanding of the processes involved in centriole cohesion.

Data presented in this chapter provide compelling evidence that BPC-1 is a novel component of the centrosome. By using the yeast two hybrid system, BPC-1 was shown to interact with C-Nap1 and Nek2. BPC-1 localises to the centrosome independently of microtubules and co-expression with Nek2A in cells appears to interfere with the centrosome splitting phenotype induced by overexpression of Nek2A alone. This has important implications in our understanding of Nek2 regulation and control of centrosome

structure during mitosis. The determination of BPC-1 function will require new approaches. More specifically, selective inhibition by microinjection of inhibitory antibodies or through a dsRNAi approach would increase our understanding of its role at the centrosome.

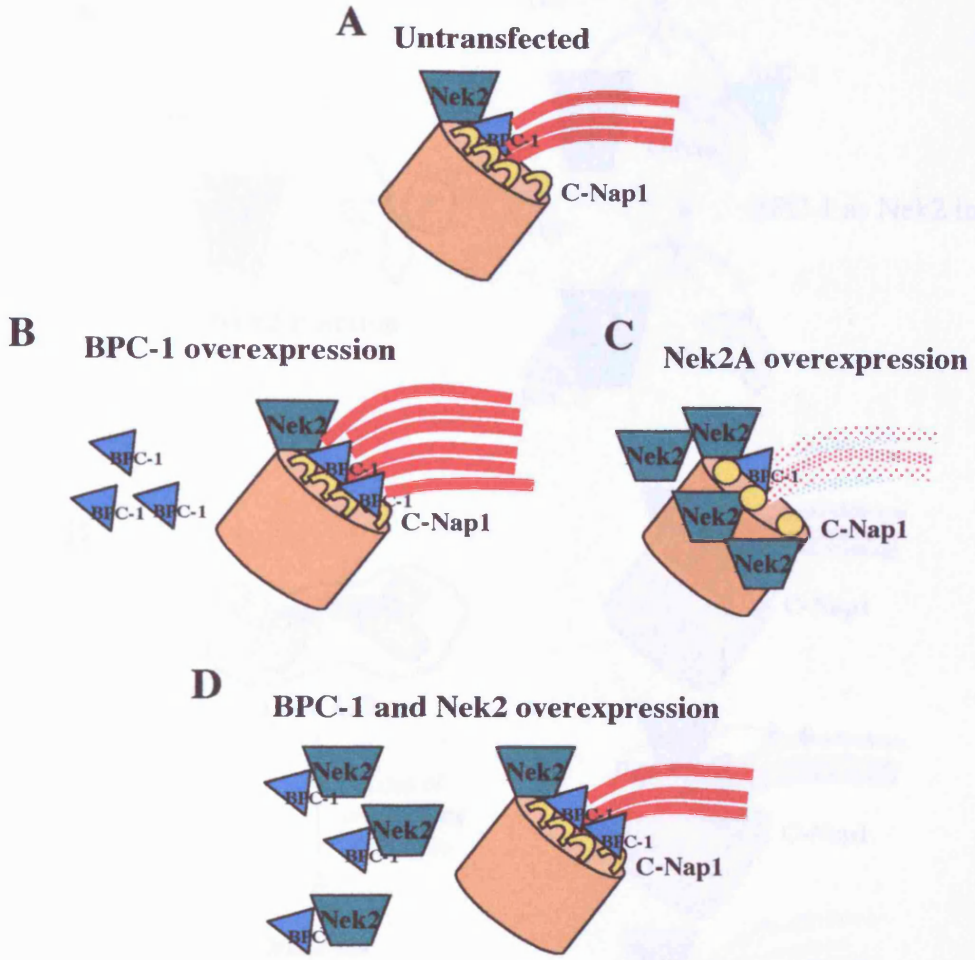

Figure 5.12 Proposed mechanism of action of BPC-1 overexpression
(**A**) In interphase cells, C-Nap1, Nek2 and BPC-1 exist in a complex at the proximal end of centrioles anchoring components of the intercentriolar linkage. (**B**) overexpression of BPC-1 in cells causes the recruitment of additional components of the intercentriolar linkage. (**C**) Overexpression of Nek2A in cells induces loss of centriole cohesion. (**D**) If both Nek2 and BPC-1 are overexpressed at the same time, BPC-1 sequesters Nek2 from the centrosome and nucleus to the cytoplasm, compromising its function in centriole cohesion.

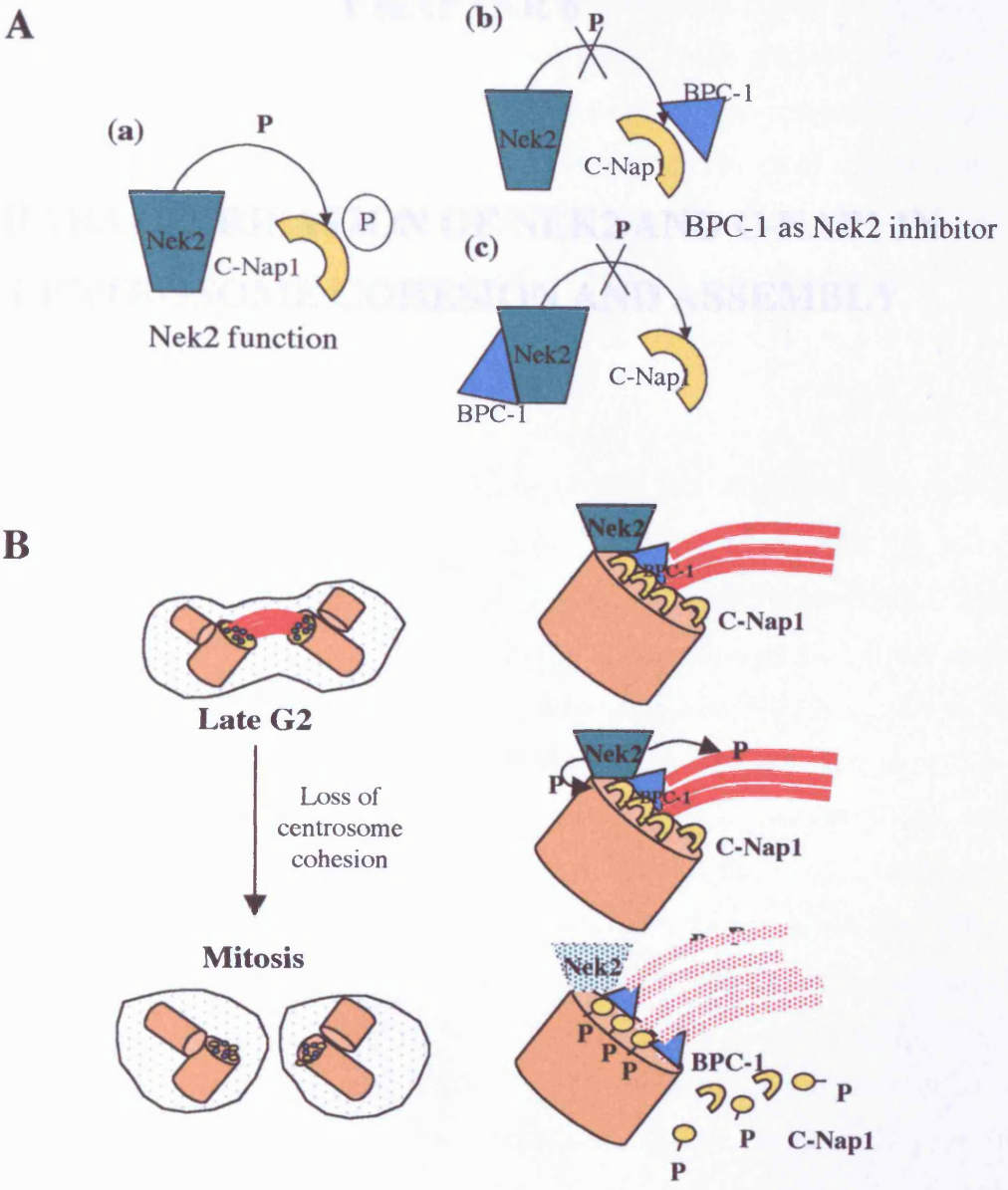

Figure 5.13 Proposed role for BPC-1, Nek2 and C-Nap1 in centriole cohesion

(**A**) Nek2 phosphorylates C-Nap1 in late G2 (a), BPC-1 may inhibit C-Nap1 phosphorylation through a direct interaction with either C-Nap1 (b) or Nek2 (c). (**B**) In late G2, the intercentriolar linkage is held in place by C-Nap1 and BPC-1. BPC-1 acts to stabilise the proteins of this complex at the proximal end of centrioles. As the cell begins the G2/M transition, Nek2 becomes active, leading to phosphorylation of C-Nap1 producing a confirmational change in C-Nap1 structure causing the release of components of the linkage. Nek2 may also phosphorylate components of the intercentriolar linkage activating their dissociation or degradation. BPC-1 is not affected by Nek2 activation directly, but cannot bind phosphorylated components of the linkage. At the onset of mitosis, Nek2 is degraded by the 26S proteosome and centriole cohesion is completely lost, allowing the formation of a bipolar spindle.

CHAPTER 6

CHARACTERISATION OF NEK2 AND C-NAP1 IN CENTROSOME COHESION AND ASSEMBLY

6.1. INTRODUCTION

This chapter describes work that maps the domains of interaction between Nek2 and C-Nap1 by employing yeast two hybrid, co-immunoprecipitation and *in vitro* phosphorylation techniques. Ultimately, the aim was to increase the present knowledge on how these two proteins interact to control centriole cohesion and assembly. In addition, the involvement of microtubules and the minus end directed motor dynein in mediating the delivery of both Nek2 and C-Nap1 to the centrosomes in a cell cycle regulated manner was investigated.

6.1.1 Nek2 function at the centrosome

Nek2 expression and kinase activity exhibit peak levels in S and G2 phases. This combined with the observation that overexpression causes premature centrosome splitting in interphase, led to the idea that Nek2 is involved in regulating centrosome separation prior to mitosis (Fry *et al.*, 1998a; Fry *et al.*, 1995). C-Nap1, identified by its interaction with Nek2, localises to the proximal ends of the centrioles during interphase but is absent from the spindle poles in mitosis (Fry *et al.*, 1998a). Antibody mediated interference of C-Nap1 function and overexpression of truncated mutants also causes premature centrosome splitting (Mayor *et al.*, 2000). Thus a model for Nek2 function proposes that phosphorylation in late G2 of substrates such as C-Nap1 leads directly to the dissolution of the intercentriolar linkage that holds centrosomes together during interphase (Mayor *et al.*, 1999). The C-terminal domain (CTD) of C-Nap1 was identified in the original yeast two hybrid screen that used Nek2 as the bait. The same work demonstrated that this domain of C-Nap1 was phosphorylated by Nek2 *in vitro* (Fry *et al.*, 1998a). No other data has been produced to look more precisely at the site of interaction between Nek2A and C-Nap1 and/or putative phosphorylation sites. Thus the work in this chapter investigates whether further binding sites or phosphorylation sites for Nek2 exist in C-Nap1.

The localisation of Nek2 and C-Nap1 in a complex with PP1 at the proximal end of the centrioles is known to be important in the control of centrosome cohesion, however the mechanism that keeps them there is unknown. It is possible that they are required to interact with core components of the centriole such as centrin. Moreover they may be required for recruiting centrin to the centrosome in early development. Nek2 has already been implicated in centrosome assembly and maintenance. Evidence for this includes the

observation that X-Nek2B recruitment to the sperm basal body immediately following incubation in egg cytoplasm is required for efficient recruitment of γ-tubulin (Fry *et al.*, 1998a). Furthermore specific inhibition of X-Nek2B function causes fragmentation or dispersal of centrosomes in early embryos (Uto and Sagata, 2000). Long term overexpression of both dead and live Nek2A in adult human cells also leads to centrosome disintegration suggesting that these alternative functions are not restricted to early embryos but may be involved in the regulation of the adult cell cycle (A.J. Faragher and A.M. Fry, unpublished observations; Fry *et al.*, 1998b). This involvement of Nek2 and C-Nap1 in the recruitment of additional proteins to the centrosome was investigated by looking at any interaction of Nek2 and C-Nap1 with both γ-tubulin, which is known to be recruited to the centrosome during centrosome maturation in G2 and centrin.

6.1.2 Centrosome assembly

The assembly of the zygotic centrosome occurs following fertilisation, when sperm basal bodies that have entered egg cytoplasm are converted into active centrosomes capable of nucleating microtubule asters. Conversion takes 7-10 minutes, during this time components of the PCM necessary for microtubule nucleation (e.g. γ-tubulin) are recruited and assembled around the centrioles (Felix *et al.*, 1994; Stearns and Kirschner, 1994). Many centrosomal proteins also undergo cell cycle regulated assembly onto centrosomes from cytoplasmic pools throughout the adult cell cycle. The minus end directed motor dynein has been shown to mediate centrosome assembly, an idea supported by its interaction with some centrosomal proteins (Zimmerman and Doxsey, 2000). Pericentrin a component of the PCM has been implicated in the recruitment of γ-tubulin to centrosomes (Dictenberg *et al.*, 1998). However both γ-tubulin and pericentrin have been shown to move along microtubules in a dynein dependent manner towards centrosomes (Kubo *et al.*, 1999; Merdes *et al.*, 2000; Young *et al.*, 2000). This demonstrates that microtubule and dynein dependent pathways for assembly of centrosomal proteins represent important mechanisms for cell cycle regulated control of centrosomes. The existence of abnormal centrosomes, possibly due to misregulation of centrosome assembly or maintenance may induce the formation of dysfunctional spindles resulting in mis-segregation of chromosomes, a phenomenon known to contribute to genomic instability and tumour development (Salisbury *et al.*, 1999; Pihan and Doxsey, 1999; Doxsey, 1998; Lingle *et al.*, 1998). C-Nap1 is cell cycle regulated with its centrosomal protein levels diminishing in early mitosis and re-accumulating in G1 (Fry *et al.*, 1998b).

C-Nap1 is thought to dissociate from the centrosome in miotisis, a process mediated by phosphorylation rather than ubiquitin dependent proteolysis (Mayor *et al.*, 2002). The mechanisms that are central to the re-accumulation of C-Nap1 leading to the re-establishment of the intercentriolar linkage in late mitosis are not understood and it is possible that dynein mediated transport along microtubules may be an important factor. Nek2 is also a cell cycle regulated protein and previous work has demonstrated that the disappearance from the centrosome in mitosis is due to ubiquitin mediated degradation by the proteasome. However, the method of reassembly onto the centrosome during S and G2 is not understood, thus, as for C-Nap1, microtubule based transport may play a role in this. In addition to microtubule dependent transport other unknown mechanisms of recruitment such as diffusion or random binding to other centrosomal proteins may also play a role in the centrosomal assembly of C-Nap1 and Nek2. Work carried out in this chapter begins to look at microtubule dependent transport as a method for the cell cycle regulated delivery of Nek2 and C-Nap1 to the centrosome and addresses the question of whether microtubule associated motors such as dynein may play a role.

6.2. RESULTS

6.2.1 Interaction of C-Nap1 with other centrosomal proteins

At the centrosome C-Nap1-CTD interacts with Nek2A and PP1 forming a large complex that regulates centrosome separation. Previous work has shown that it is the CTD of C-Nap1 that interacts with Nek2A. To investigate whether the N-terminal domain (NTD) of C-Nap1 also interacts with Nek2A and Nek2B, the yeast two hybrid technique was employed. Yeast expressing Nek2A and Nek2B AD fusion proteins, were transformed with C-Nap1-CTD (amino acids 1962-2403) and -NTD (amino acids 1-488) fused to the DBD domain or the DBD alone. The two domains were inserted into the pGBDU vector in frame with the GAL4 DBD (see 5.2.1 for details). In addition to the interaction between C-Nap1-CTD and -NTD with Nek2, their interaction with other core centrosomal components was tested. γ-tubulin, a component of γ-TuRCs present in the PCM, was fused to the AD. This construct was made by excising an *XhoI-NotI* (blunted) fragment from pBS-γ-tubulin and inserting it into pGAD-C3 cut with *SalI* and *BglII* (blunted). Centrin, a 20 kDa protein component of centrioles was also fused to the AD. Centrin was isolated as a *ClaI* (blunted)-*SacI* fragment from pBS-centrin and inserted into pACTII cut with *SmaI* and *SacI*. Yeast expressing γ-tubulin and centrin AD fusion proteins, were also transformed with CTD-DBD, NTD-DBD or DBD alone.

No growth on media lacking histidine and adenine indicated that no interaction between C-Nap1-NTD or -CTD and γ-tubulin was occurring; equally, no interaction with centrin was observed (Figure 6.1). As expected, C-Nap1-CTD did interact with Nek2A but it also interacted with Nek2B suggesting that the site of interaction does not lie in their distinct C-terminal domains (Figure 6.1B). Interestingly, C-Nap1-NTD also interacted with both Nek2A and Nek2B (Figure 6.1C). No interaction was seen between DBD alone with Nek2A or Nek2B (Figure 6.6A). To confirm these interactions, a quantitative ONPG assay was performed. The previously described interaction between SNF1 and SNF4 was used to indicate the level of β-galactosidase activity that represents a positive interaction (Fields and Song, 1989). In agreement with the growth selection, the level of β-galactosidase activity achieved when γ-tubulin or centrin were expressed in combination with either C-Nap1-CTD or C-Nap1-NTD was no higher than that achieved with the AD alone. The β-galactosidase activity induced by the interaction between the CTD or NTD with Nek2A or

Nek2B was 2-3 fold greater than the SNF1/SNF4 induced activity, confirming that, at least in yeast, C-Nap1 interacts with Nek2A and Nek2B via both its CTD and NTD.

6.2.2 Purification of C-Nap1-CTD and -NTD

In order to test these interactions *in vitro*, C-Nap1-CTD (amino acids 1962-2403) and C-Nap1-NTD (amino acids 1-488) were purified as GST fusion proteins. Full length C-Nap1 was not used due to its large size and extensive coiled coil domains that may have increased its insolubility making purification from bacterial lysates difficult. The two domains were inserted into the pGEX vector, in frame with an N-terminal GST tag (Figure 6.2A). C-Nap1-CTD was excised from pBS-C-Nap1 as a *SmaI-NotI* fragment and inserted into pGEX-4T3 using the same sites. C-Nap1-NTD was excised from pBS-C-Nap1 as a *SalI-HaeII* fragment and inserted into pGEX-4T2 using the *SalI* and *NotI* sites. GST-CTD and GST-NTD constructs were transformed into the *E.coli* bacterial strain BL21. Various different growth temperatures, IPTG concentrations, induction times and lysis methods were undertaken with the aim of increasing the solubility of induced protein. Optimal expression of soluble GST-CTD and GST-NTD was obtained by inducing for 4 hours with 0.1 mM IPTG at 30°C. However, following lysis, about 90% of the protein still remained insoluble. The soluble fractions of GST-CTD and GST-NTD were fused to glutathione sepharose beads and the purified protein eluted by reduced glutathione into five fractions (Figure 6.2B). Following purification, a relatively pure, but small fraction of GST-NTD and a more concentrated fraction of GST-CTD was produced. Both were confirmed to be GST fusions of the correct size by Coomassie Blue staining of SDS-PAGE and on Western blots probed with anti-GST antibodies (Figure 6.2C). The purified fraction of GST-CTD appeared to contain a number of additional lower molecular weight proteins, which were assumed to be degradation products as they were also recognised by the GST antibodies. The addition of a number of protease inhibitors to the purification procedures did not eliminate this problem.

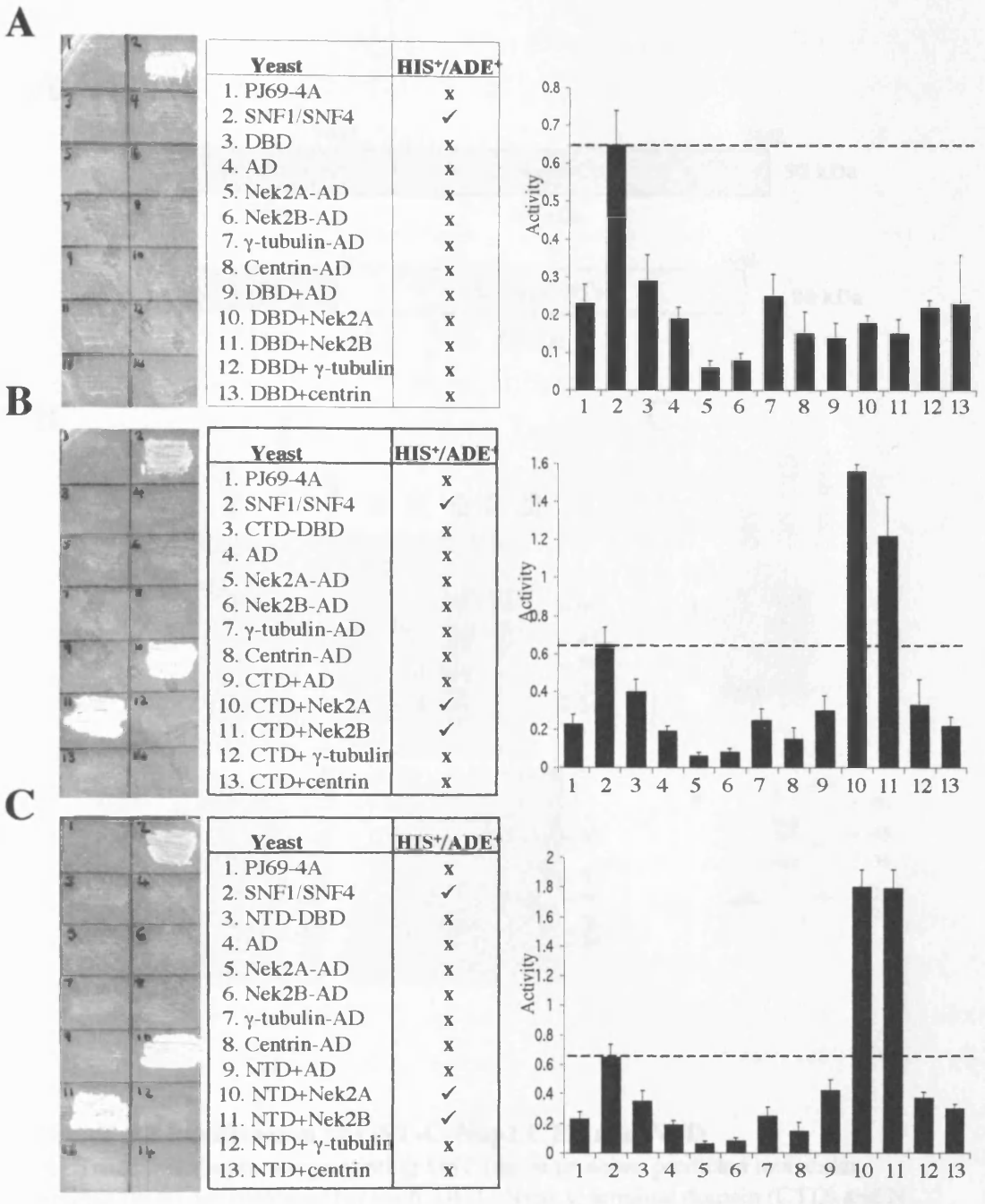

Figure 6.1 Nek2A and Nek2B interact with both the N- and C-terminal domains of C-Nap1

Yeast PJ69-4A single or double transformants were tested for a positive interaction between the GAL4 DBD fusion protein and GAL4 AD fusion protein by growth on media lacking histidine and adenine (left panels). The same yeast were tested using a quantitative assay for β-galactosidase activity with the substrate *ONPG* (right panel). Units of activity are relative to the Nek2A-Nek2A interaction, given an arbitrary value of 1.0. Results are the mean of three independent experiments. SNF1/SNF4 represents a known positive interaction; a positive result is shown where activity is equal to or greater than SNF1/SNF4 (dotted line). Interaction with Nek2A, Nek2B, γ-tubulin and centrin was tested for (**A**) the DBD proteins alone, (**B**) the C-Nap1-CTD and (**C**) the C-Nap1-NTD.

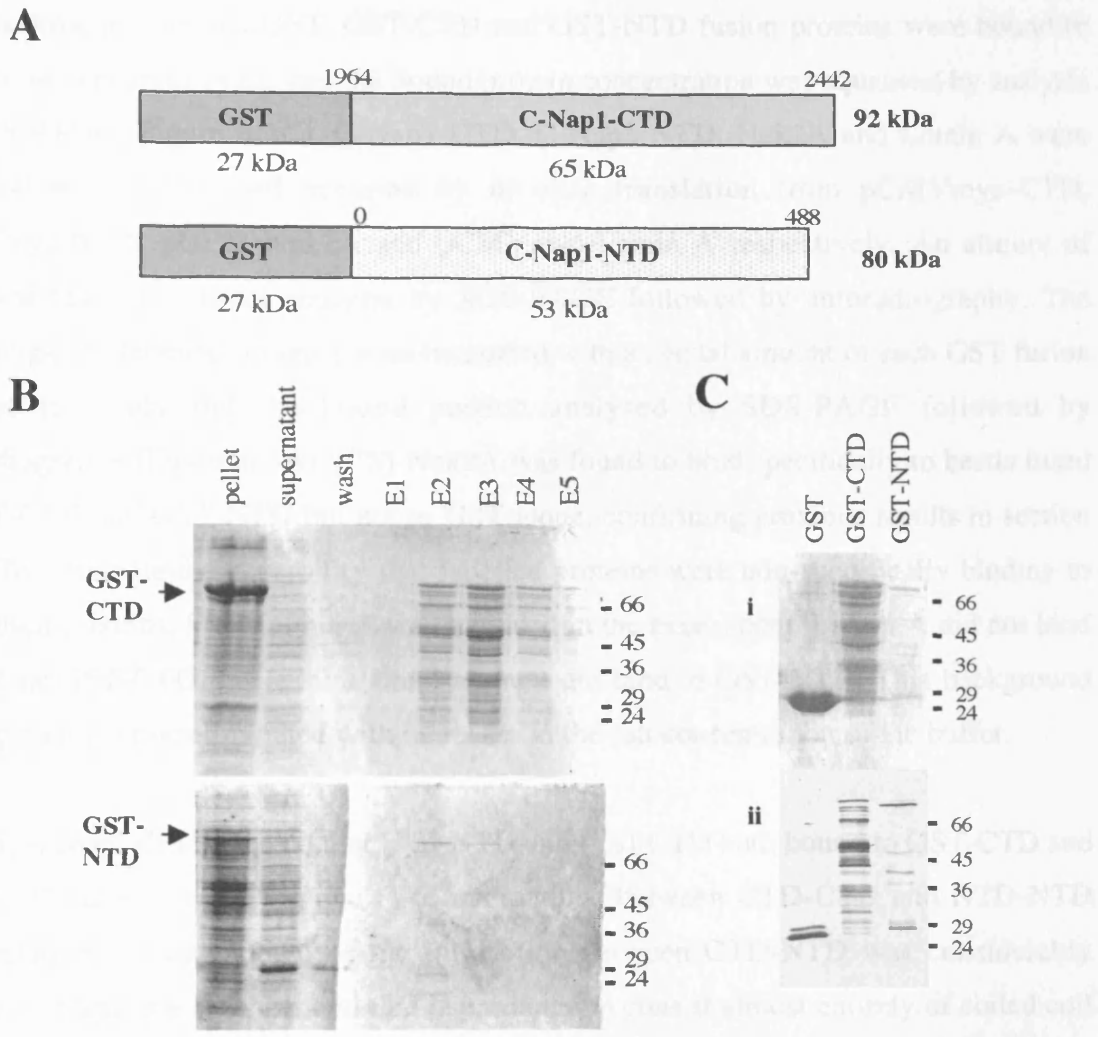

Figure 6.2 Purification of GST-C-Nap1 CTD and NTD

(**A**) Schematic diagram representing GST fusion proteins, predicted molecular weights (kDa) are indicated for each. (**B**) C-Nap1 C terminal domain (CTD) and N terminal domain (NTD) were expressed as GST coupled proteins in bacteria. Bacterial lysate was passed over glutathione sepharose linked beads. Protein was eluted off the beads using reduced glutathione into five fractions (E1-E5). The pellet, supernatant, wash fraction and elutions were analysed by SDS-PAGE with Coomassie Blue staining. Purified GST-CTD and GST-NTD are indicated (arrows). (**C**) Eluted proteins were analysed by Coomassie Blue staining (i) and Western blotting with anti-GST antibodies (ii). Purified GST protein was included. Molecular weights (kDa) are indicated on the right of each panel.

6.2.3 Intramolecular interactions of C-Nap1

The interaction between C-Nap1 and Nek2 was confirmed biochemically using a GST pull down technique. Purified GST, GST-CTD and GST-NTD fusion proteins were bound to glutathione sepharose beads and the bound protein concentration was equalised by analysis on SDS-PAGE (Figure 6.2C). C-Nap1-CTD, C-Nap1-NTD, Nek2A and Lamin A were prepared as [^{35}S]-labelled proteins by *in vitro* translation from pCMVmyc-CTD, pCMVmyc-NTD, pGEM-Nek2A and pCMVmyc-Lamin A respectively. An aliquot of each was taken for direct analysis by SDS-PAGE followed by autoradiography. The remaining [^{35}S]-labelled proteins were incubated with an equal amount of each GST fusion coupled to beads and the bound portion analysed by SDS-PAGE followed by autoradiography (Figure 6.3A). [^{35}S]-Nek2A was found to bind specifically to beads fused to GST-CTD and GST-NTD but not to GST alone, confirming previous results in section 6.2.1. To eliminate the possibility that labelled proteins were non-specifically binding to GST fused proteins, [^{35}S]-Lamin A was included in the experiment. Lamin A did not bind to GST or GST-CTD, however a small amount did bind to GST-NTD. This background binding could not be eliminated with increases in the salt concentration of the buffer.

This experiment also indicated that [^{35}S]-NTD and [^{35}S]-CTD both bound to GST-CTD and GST-NTD but not to GST alone. The interactions between CTD-CTD and NTD-NTD were relatively strong, however the interaction between CTD-NTD was considerably weaker. C-Nap1 is a large protein that is predicted to consist almost entirely of coiled coil domains except for regions located at the extreme N- and C-terminus and a short central section that contains multiple proline resdues. It has been postulated that the centre non-coiled coil region might act like a hinge allowing C-Nap1 to fold back upon itself (Fry *et al.*, 1998b). The structure of C-Nap1 may play an integral part in the regulation of centrosome cohesion, possibly involving alterations in the angle of the hinge that may affect the proximity of the different domains. In addition, C-Nap1 may exist in large complexes of molecules or as dimers, which again may serve to regulate its function in a cell cycle regulated manner. The results of the binding assay detailed above imply that the terminal domains of C-Nap1 are capable of binding each other, therefore as a step toward understanding the structure of C-Nap1 and consequently its function at the centrosome, interaction studies using the CTD and NTD were also carried out using the yeast two hybrid technique.

The CTD and NTD were fused to the DBD domain (see section 6.2.1). In addition C-Nap1-NTD was fused to the GAL4 activation domain (AD), by isolating a *ClaI-HaeII* (blunted) fragment from pBS-C-Nap1 and subcloning it into pGAD-C3 cut with *ClaI* and *BglII* (blunted). The yeast strain PJ69-4A was transformed with these constructs and with plasmids containing the AD alone. The expression of CTD-DBD and NTD-DBD had previously been confirmed by Western blot using specific C-Nap1 antibodies showing that proteins of the correct size were resolved for each, 74 kDa and 71 kDa respectively (see Figure 5.2B). Different combinations of DBD and AD proteins were transformed into yeast, where a positive interaction was indicated by growth on histidine and adenine selective media (Figure 6.3B). Selective growth suggested that C-Nap1-NTD was able to interact with both itself and with C-Nap1-CTD. The relative strength of these interactions was determined quantitatively by measuring the activity of the β-galactosidase reporter gene using the substrate ONPG (Figure 6.3C). The interaction between SNF1 and SNF4 was used to indicate the level of activity of β-galactosidase that is present if a positive interaction is occurring. CTD and NTD did not activate the reporter genes when present as DBD fusions alone. Nor did they activate reporter genes when present with the AD or DBD alone. However, when in combination, the interaction between CTD and NTD induced a similar level of activity as SNF1/SNF4. This was also true for the interaction between NTD and NTD. Taken together, growth selection and β-galactosidase activity indicate that C-Nap1-CTD is capable of interacting with C-Nap1-NTD and that C-Nap1-NTD can interact with itself. Unfortunately, it has so far proved impossible to clone the CTD into the AD vector and thus it remains unknown whether an interaction is occurring between C-Nap1-CTD and itself.

These experiments suggest that C-Nap1-CTD and -NTD interact both *in vivo* (yeast two hybrid technique) and *in vitro* (GST pull down). In addition, they both interact with themselves, thus providing compelling evidence that C-Nap1-CTD and -NTD form hetero and homodimers. The implications of these interactions at the centrosome are as yet not known but further work looking at C-Nap1 structure at an ultrastructural level may help our understanding of how C-Nap1 structural changes may contribute to centrosome cohesion.

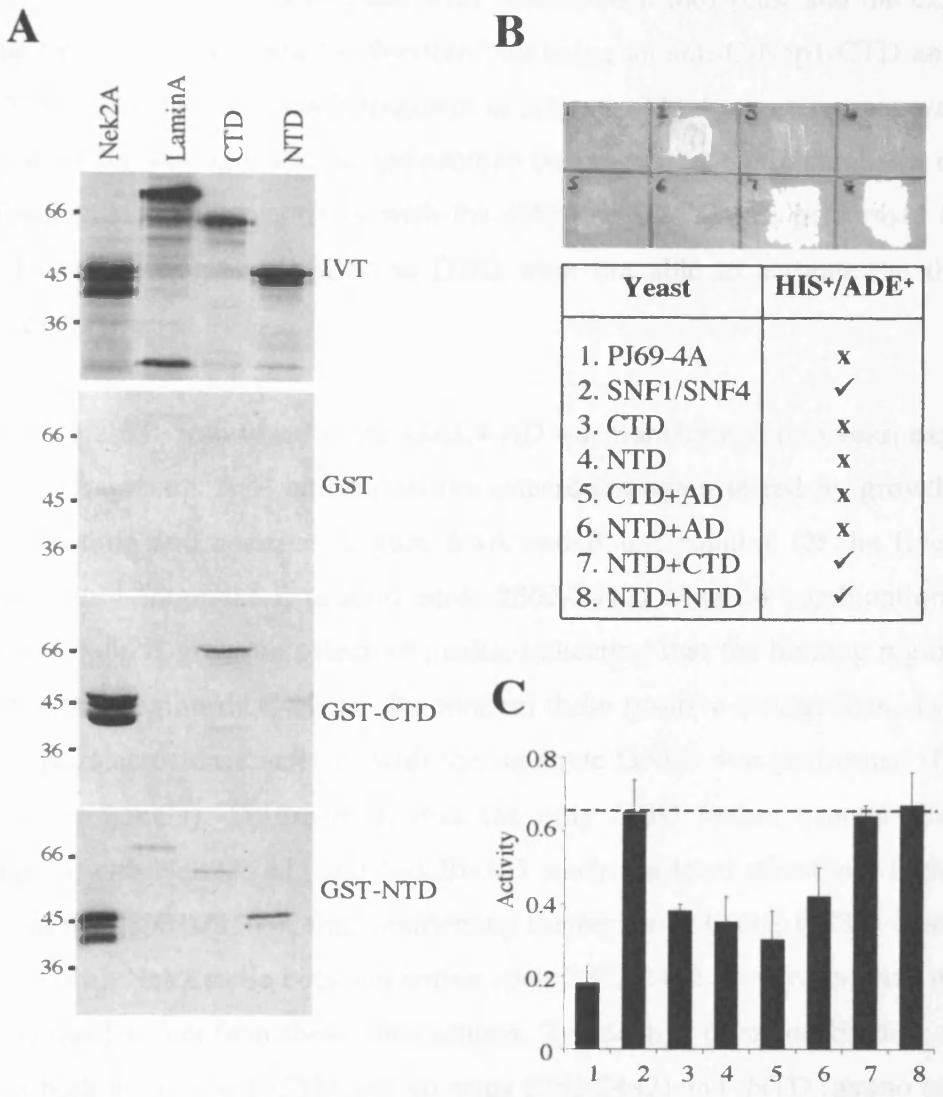

Figure 6.3 Intramolecular interactions of C-Nap1

(A) *In vitro* translated (IVT) Nek2A, C-Nap1-CTD, C-Nap1-NTD and lamin A were prepared in the presence of [^{35}S] methionine. An aliquot was taken for direct analysis by SDS-PAGE followed by autoradiography (IVT). GST fusion proteins as indicated were coupled to sepharose beads and incubated with the IVT proteins overnight at 4°C, washed and analysed by SDS-PAGE followed by autoradiography. Molecular weights (kDa) are indicated on the left of each panel. **(B)** Yeast PJ69-4A single or double transformants were tested for a positive interaction between the GAL4 DBD fusion protein and GAL4 AD fusion protein by growth on media lacking histidine and adenine. **(C)** The same yeast were tested using a quantitative assay for β-galactosidase activity with the substrate *ONPG*. Units of activity are relative to the Nek2A-Nek2A interaction, given an arbitrary value of 1.0. Results are the mean of three independent experiments. SNF1/SNF4 represents a known positive interaction, a positive result is shown where activity is equal to or greater than SNF1/SNF4 (dotted line).

6.2.4 Mapping the region of interaction between C-Nap1-CTD and Nek2

To better define the interaction for Nek2 on C-Nap1-CTD, a series of 100 amino acid CTD fragments termed A-E fused to DBD were transformed into yeast and the expression of each fragment was confirmed by Western blot using an anti-C-Nap1-CTD antibody (see Figure 5.5B). The ability of each fragment to activate GAL4 reporter genes was tested by growth on media lacking histidine and adenine (see Figure 5.5C). In parallel, a quantitative assay for β-galactosidase activity with the substrate ONPG was performed (see Figure 5.5D). The CTD fragments fused to DBD were not able to activate the three GAL4 reporter genes present.

Nek2A and Nek2B both fused to the GAL4 AD was transformed into yeast expressing C-Nap1-CTD fragments A-E and a positive interaction again tested by growth on media lacking histidine and adenine (Figure 6.4A and B left panels). Of the five expressed fragments, only fragment E (amino acids 2362-2442) when in combination with both Nek2A and Nek2B grew on selective media, indicating that the binding region for Nek2 lies within this region of C-Nap1. To confirm these positive interactions, a quantitative assay for β-galactosidase activity with the substrate ONPG was performed (Figure 6.4A and B, right panels). Fragment E was the only DBD fusion protein that when in combination with Nek2A-AD and Nek2B-AD reached a level of activity higher than the postive control, SNF1/SNF4, thus confirming the region of C-Nap1-CTD involved in the interaction with Nek2 to lie between amino acids 2362-2442. *In vitro* binding experiments will be needed to confirm these interactions. To identify common binding motifs that appear in both the C-Nap1-CTD (amino acids 2362-2442) and -NTD (amino acids 1-488), the two sequences were analysed. The motif RLXXSL appeared in both domains, which may represent a common Nek2 binding motif. Mutation of these residues followed by the use of the mutated proteins in both the yeast two hybrid system and pull down assays will help to confirm or eliminate the involvement of this common motif in Nek2 binding or even phosphorylation of C-Nap1.

6.2.5 Mapping the region of interaction between C-Nap1-CTD and -NTD

To map the region of C-Nap1-CTD to which the NTD interacts, the same series of CTD fragments fused to the GAL4 DBD were employed. Yeast containing each CTD fragment were transformed with C-Nap1-NTD fused to the AD. A positive interaction was indicated by growth on histidine and adenine selective media (Figure 6.5A). The results suggested

that C-Nap1-NTD was able to interact with both fragments A and C. The relative strength of these interactions was determined quantitatively by measuring the activity of the β-galactosidase reporter gene using the substrate ONPG (Figure 6.5B). As before, fragments A and C gave a positive result, inducing a similar level of β-galactosidase activity as SNF1/SNF4. Intriguingly fragment B gave an intermediate result, inducing a β-galactosidase activity that was higher than basal levels but not as high as SNF1/SNF4. As the fragments either side of this region do appear to interact with NTD, it seems likely that NTD is capable of interacting with C-Nap1-CTD between amino acids 1964-2268. Furthermore, the fact that both A and C can interact suggests that there is more than one site of interaction and a specific motif will not be identifiable. Interestingly, the novel centrosomal protein BPC-1, interacts with C-Nap1-CTD within this region, implying that it may disturb the interaction between C-Nap1-CTD and NTD. C-Nap1-NTD also does not bind to the CTD in the same region that Nek2 binds to it, implying that C-Nap1-CTD is capable of binding both Nek2 and C-Nap1-NTD at the same time. To rule out non-specific binding of the NTD to any DBD fused protein, Lamin A-DBD was transformed into yeast already expressing NTD-AD, this combination did not activate reporter genes implying that the activation of reporter genes is due to the interaction between the NTD and CTD fragment. To confirm these results, an *in vitro* method will need to be applied such as co-immunoprecipitation or GST pull down. In addition, further truncations of the fragment identified may provide greater insight into the specific sequences required for CTD-NTD binding.

A

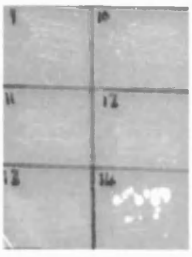

Yeast	HIS+/ADE+
9. Nek2A + DBD	x
10. Nek2A + A	x
11. Nek2A + B	x
12. Nek2A + C	x
13. Nek2A + D	x
14. Nek2A + E	✓

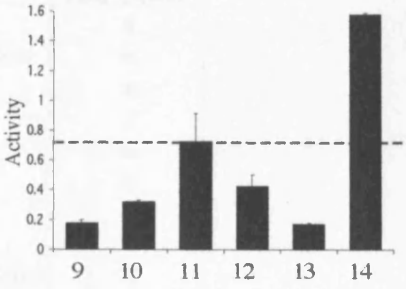

B

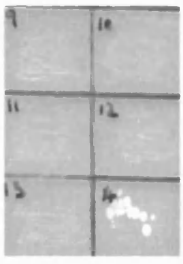

Yeast	HIS+/ADE+
9. Nek2B + DBD	x
10. Nek2B + A	x
11. Nek2B + B	x
12. Nek2B + C	x
13. Nek2B + D	x
14. Nek2B + E	✓

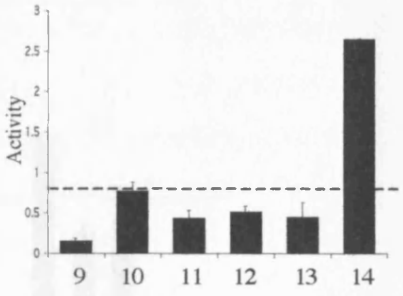

C

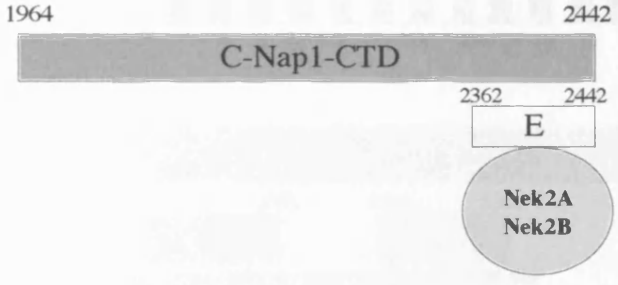

Figure 6.4 Nek2A and Nek2B interact with C-Nap1-CTD between amino acids 2362-2442

(**A**) PJ69-4A double transformants containing Nek2A and CTD fragments A-E were tested for a positive interaction between the GAL4 DBD and GAL4 AD fusion proteins by growth on media lacking histidine and adenine (left panels). The same yeast were tested using a quantitative assay for β-galactosidase activity with the substrate ONPG (right panels). Units of activity are relative to the Nek2A-Nek2A interaction, given an arbitrary value of 1.0. Results are the mean of three independent experiments. SNF1/SNF4 represents a known positive interaction, a positive result is shown where activity is equal to or greater than SNF1/SNF4 (dotted line). (**B**) The same procedures were carried out using yeast containing Nek2B and the CTD fragments A-E. (**C**) Schematic diagram showing the fragment of C-Nap1-CTD with which Nek2A and Nek2B interacts. Numbers represent positions of amino acids.

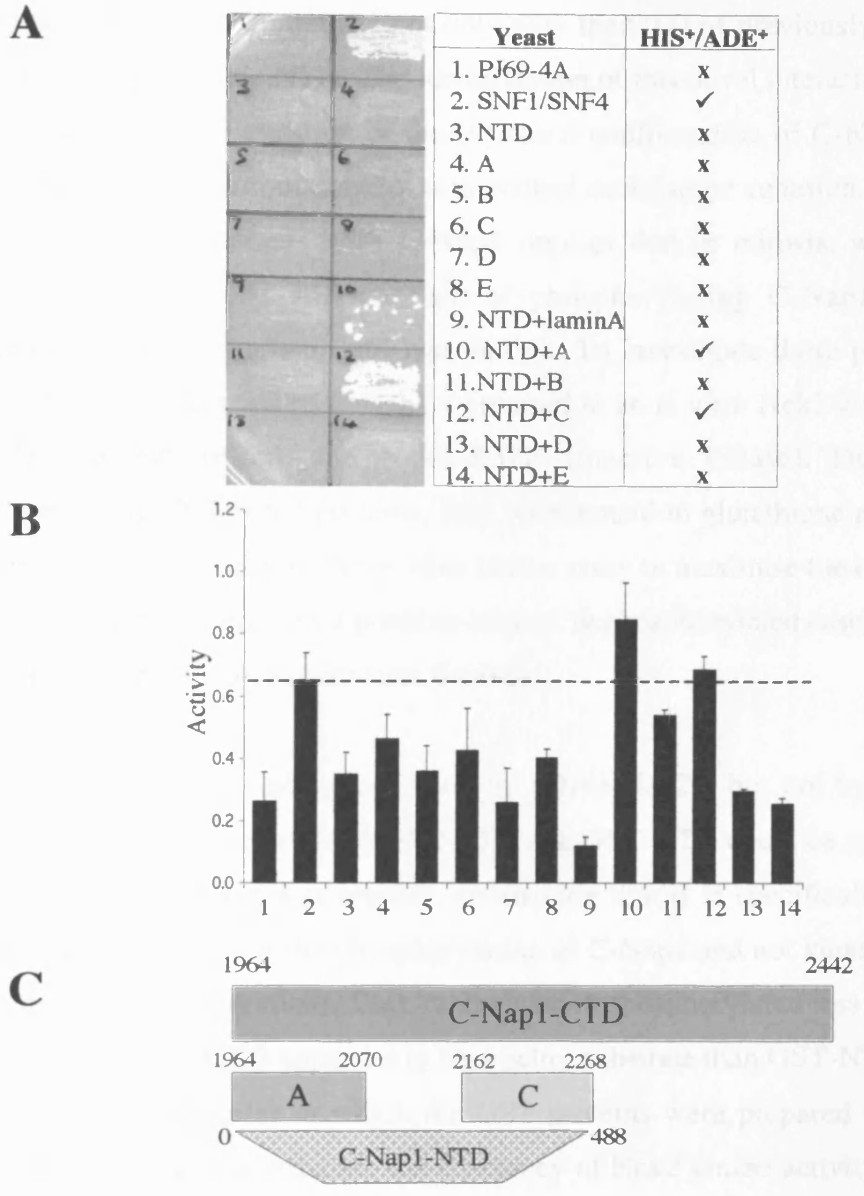

Figure 6.5 C-Nap1-NTD interacts with C-Nap1-CTD between amino acids 1964-2268

(**A**) Yeast PJ69-4A single or double transformants were tested for a positive interaction between the GAL4 DBD fusion protein and GAL4 AD fusion protein by growth on media lacking histidine and adenine. (**B**) The same yeast were tested using a quantitative assay for β-galactosidase activity with the substrate *ONPG*. Units of activity are relative to the Nek2A-Nek2A interaction, given an arbitrary value of 1.0. Results are the mean of three independent experiments. SNF1/SNF4 represents a known positive interaction, a positive result is shown where activity is equal to or greater than SNF1/SNF4 (dotted line). (**C**) Schematic diagram showing the fragments of C-Nap1-CTD with which C-Nap1-NTD interacts.

6.2.6 *In vitro* phosphorylation of C-Nap1

Analysis of the interaction between Nek2 and C-Nap1 using the yeast two hybrid system has demonstrated that Nek2 interacts not only with the CTD as previously shown (Fry *et al.*, 1998b), but also with the NTD. The identification of this novel interaction between the NTD and Nek2 raises the question of the structural conformation of C-Nap1 and how it interacts at the proximal end of centrioles to control centrosome cohesion. In addition the fact that Nek2B also interacts with C-Nap1 implies that in mitosis, when Nek2A is destroyed, Nek2B may be still capable of phosphorylating C-Nap1, keeping the intercentriolar linkage disrupted until late mitosis. To investigate these possibilities, the purified GST-tagged domains of C-Nap1 were used in an *in vitro* Nek2 kinase assay with purified His-tagged Nek2A and Nek2-K37R (inactive kinase). Due to the low concentration of the GST fused proteins, they were bound to glutathione sepharose beads which were then used directly in the *in vitro* kinase assay to maximise the concentration of protein with minimal volume. As a positive control, dephosphorylated casein was added to the assay as Nek2 readily phosphorylates β-casein.

As expected, β-casein was phosphorylated by active Nek2A but not by Nek2A-K37R (Figure 6.6). Phosphorylation of both GST-CTD and GST-NTD could be seen when active Nek2A but not dead kinase was present, confirming that it is specifically Nek2 kinase activity that is responsible for the phosphorylation of C-Nap1 and not kinase contaminants present in the protein preparations. Both proteins were phosphorylated less efficiently than β-casein, however GST-CTD appeared to be a better substrate than GST-NTD. To rule out the possibility that the buffer in which the GST proteins were prepared or the beads to which they were bound was reducing the efficiency of Nek2 kinase activity, an assay was done in parallel that contained both GST-NTD and β-casein (data not shown). The extent of β-casein phosphorylation was comparable to the control assay with no GST-NTD, confirming that the conditions used were not affecting Nek2 kinase activity. GST alone was not phosphorylated in the presence of either dead or active Nek2 confirming that it was specifically the C-Nap1 domains that were phosphorylated and not the GST tag. Interestingly, in the assay containing active Nek2A, Nek2 autophosphorylation is evident as a smear at 46 kDa. Analysis of C-Nap1 domain phosphorylation during the cell cycle and the mapping of Nek2A and Nek2B dependent phosphorylation sites will be required to fully understand the significance of C-Nap1-Nek2 interactions in centrosome cohesion.

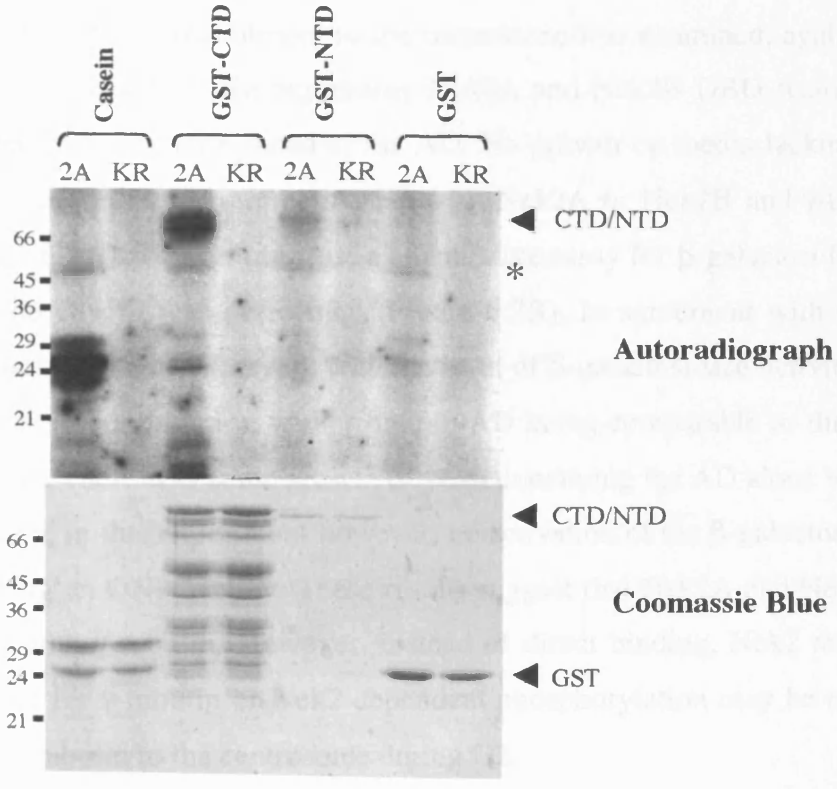

Figure 6.6 GST-CTD and GST-NTD are both phosphorylated by Nek2A

Purified His-Nek2A (2A) and His-Nek2A-K37R (KR) were incubated in Nek2 kinase buffer containing [^{32}P] γ-ATP for 30 min at 30°C with dephosphorylated casein, GST-CTD, GST-NTD or GST alone. Samples were subjected to SDS-PAGE before Coomassie Blue staining (bottom panel) followed by autoradiography (top panel). Arrowheads indicate substrates and * indicates Nek2A autophosphorylation. Molecular weights (kDa) are indicated on the left of each panel.

6.2.7 Nek2A and Nek2B do not interact with other known centrosomal proteins

X-Nek2B has previously been shown to be involved in the recruitment of γ-tubulin to the centrosome in *Xenopus* egg extracts. Therefore, to investigate whether human Nek2 may be involved in a similar mechanism in human cells, the association of Nek2 with γ-tubulin, possibly enabling its direct recruitment to the centrosome was examined, again using the yeast two hybrid approach. Yeast expressing Nek2A and Nek2B DBD fusion proteins, were transformed with γ-tubulin fused to the AD. No growth on media lacking histidine and adenine indicated that no interaction between Nek2A or Nek2B and γ-tubulin was occurring (Figure 6.7A). To confirm this, a quantitative assay for β-galactosidase activity with the substrate ONPG was performed (Figure 6.7B). In agreement with the growth selection, no interaction was observed, with the level of β-galactosidase activity achieved when Nek2A was in combination with γ-tubulin-AD being comparable to that achieved with the AD alone. There was some growth of yeast containing the AD alone with Nek2B on selective media, in this experiment however, no activation of the β-galactosidase gene was seen following an ONPG assay. These results suggest that Nek2A and Nek2B do not directly interact with γ-tubulin. However, instead of direct binding, Nek2 may act as a recruitment signal for γ-tubulin or Nek2 dependent phosphorylation may be required for the assembly of γ-tubulin to the centrosome during G2.

Centrin is a 20 kDa protein component of centrioles that has been implicated in centrosome duplication and separation. Mutations in the yeast homologue, cdc31, result in monopolar spindle formation and cell cycle arrest (Stearns and Winey, 1997; Salisbury, 1995; Schiebel and Bornens, 1995). Recently aberrant centrin phosphorylation has been demonstrated in human breast tumours that have supernumerary centrioles (Lingle *et al.*, 1998). Centrin is phosphorylated at the G2/M transition by a serine/threonine kinase causing the release of calcium that is thought to aid centrosome separation (Lutz *et al.*, 2001). PKA is thought to be responsible for centrin phosphorylation in interphase, however, PKA is not active at the G2/M transition when centrin is again phosphorylated, implying that another kinase is responsible. Nek2 kinase activity is high at the G2/M transition and it is possible that Nek2 may be responsible for centrin phosphorylation at this stage in the cell cycle.

To test this hypothesis, the existence of a direct interaction between Nek2 and centrin was first examined using the yeast two hybrid approach. Centrin fused to the GAL4 AD was

introduced into yeast expressing Nek2A and Nek2B DBD fusions. A small amount of growth of yeast containing Nek2A and centrin was seen on histidine/adenine selective plates. No growth of yeast containing Nek2B and centrin was observed (Figure 6.7A). A quantitative ONPG assay was performed to identify whether centrin was in fact interacting with Nek2A. This again proved inconclusive as an intermediate β-galactosidase activity was seen when compared to SNF1/SNF4 suggesting a possible interaction with centrin. In an attempt to prove or disprove the interaction between Nek2A and centrin, an *in vitro* co-immunoprecipitation experiment was performed. This involved incubating myc-Nek2A or myc-Nek2A-K37R (kinase dead) with [^{35}S]-centrin or [^{35}S]-Nek2A, followed by immunoprecipitation using an anti-myc antibody. The presence of [^{35}S]-Nek2A in the immunoprecipitate confirms that Nek2A dimerises with itself and demonstrates that the procedure was effective. [^{35}S]-centrin was not present in the immunoprecipitated fraction suggesting that centrin does not interact with Nek2A *in vitro*. [^{35}S]-C-Nap1-CTD was included in the experiment as a positive control, this was pulled down by myc-Nek2A demonstrating that the technique used was capable of identifying viable interactions.

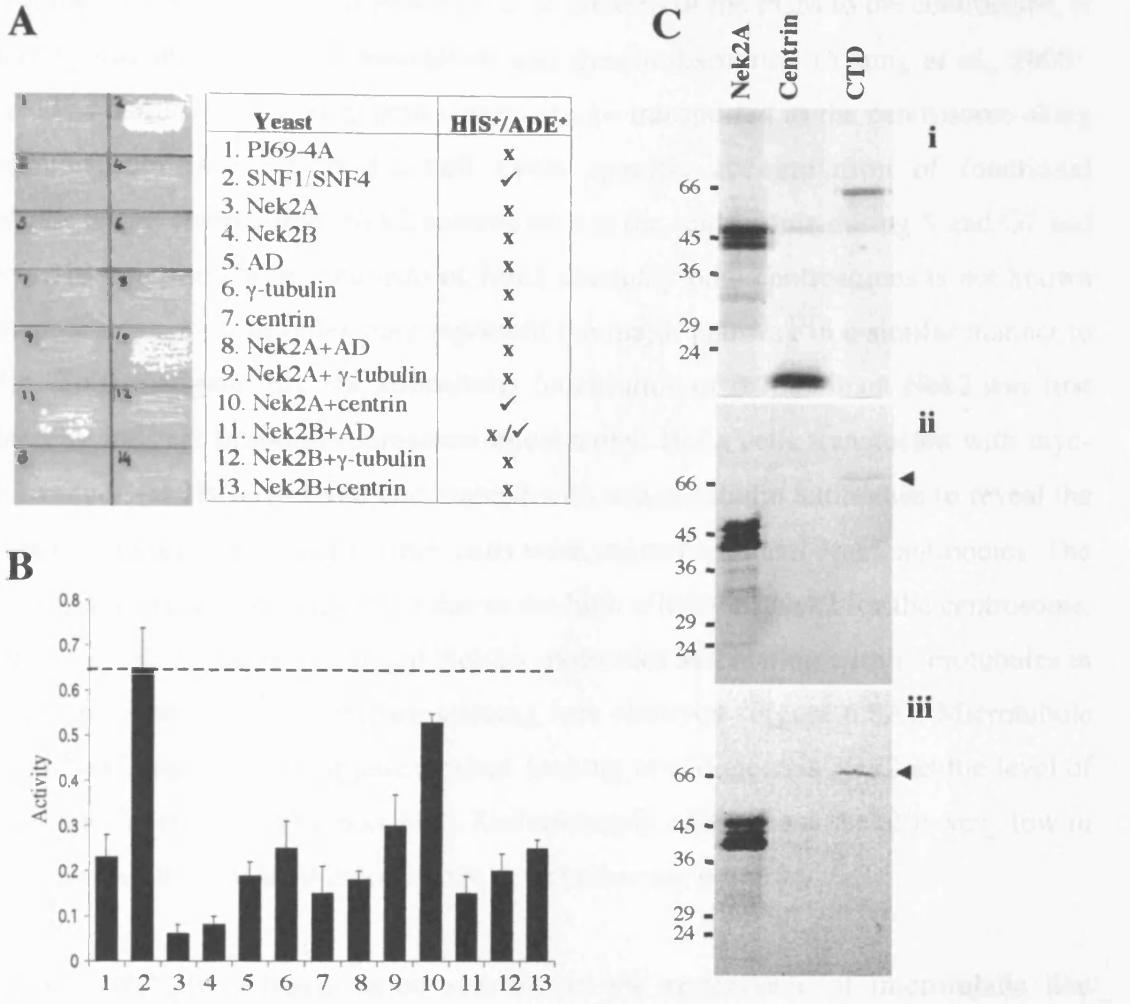

Figure 6.7 Nek2 exhibits a weak interaction with centrin

(A) Yeast PJ69-4A single or double transformants were tested for a positive interaction between the GAL4 DBD fusion protein and GAL4 AD fusion protein by growth on media lacking histidine and adenine. **(B)** The same yeast were tested using a quantitative assay for β-galactosidase activity with the substrate *ONPG*. Units of activity are relative to the Nek2A-Nek2A interaction, given an arbitrary value of 1.0. Results are the mean of three independent experiments. SNF1/SNF4 represents a known positive interaction; a positive result is shown where activity is equal to or greater than SNF1/SNF4 (dotted line). **(C)** *In vitro* translated Nek2A, centrin and C-Nap1-CTD were prepared in presence of [^{35}S] methionine. An aliquot of each was taken for direct analysis by SDS-PAGE followed by autoradiography (i). In addition myc-Nek2A and myc-Nek2A-K37R were prepared in the absence of [^{35}S] methionine. [^{35}S] labelled proteins were incubated with unlabelled myc-Nek2A (ii) or myc-Nek2A-KR (iii) in the presence of cycloheximide to prevent further translation. Mixes were immunoprecipitated with anti-myc antibodies, processed by SDS-PAGE followed by autoradiography. Arrows indicate co-precipitated CTD but not centrin. Molecular weights (kDa) are indicated on the left of each panel.

6.2.8 Nek2 association with microtubules

Centrosome assembly is important for mitotic spindle formation and it has been shown that the recruitment of pericentrin and γ-tubulin, core proteins of the PCM to the centrosome, is inhibited by microtubule depolymerisation and dynein disruption (Young *et al.*, 2000). These studies demonstrate that dynein cargos can be transported to the centrosome along microtubules, contributing to the cell cycle specific accumulation of functional components of the centrosome. Nek2 accumulates at the centrosome during S and G2 and disappears in mitosis. The mechanism of Nek2 assembly onto centrosomes is not known but transport along microtubules may represent the major pathway in a similar manner to γ-tubulin. To investigate this, the subcellular localisation of recombinant Nek2 was first visualised by indirect immunofluoresence microscopy. HeLa cells transfected with myc-Nek2A or myc-Nek2B were fixed and stained with anti-α-tubulin antibodies to reveal the microtubule network. At the same time, cells were stained with anti-Nek2 antibodies. The centrosome was visualised in the cells due to the high affinity of Nek2 for the centrosome. It was not possible to see recombinant Nek2A molecules associating with microtubules in the cytoplasm, instead a more diffuse staining was observed (Figure 6.8A). Microtubule associated Nek2 may only be apparent when looking at endogenous Nek2 as the level of protein in the transfected cells was high. Unfortunately endogenous Nek2 is very low in abundance and visualisation of cytoplasmic protein was not possible.

Interestingly, Nek2B overexpression resulted in the appearance of microtubule like filaments but co-staining with α-tubulin antibodies did not imply co-localisation. In an attempt to identify what these filaments represented, cells transfected with Nek2B were also co-stained with anti-actin antibodies to reveal the actin filament network (Figure 6.8B). Some co-localisation was seen between Nek2B and actin, but the majority of the filamentous network of Nek2B did not co-localise with actin suggesting that over-expression of Nek2B results in the formation of filaments independently of microtubules or actin.

To identify whether endogenous Nek2 associates with microtubules *in vivo*, HeLa cell extracts were prepared under conditions to promote or inhibit microtubule depolymerisation. Nocodazole was added to cells and the extract prepared entirely on ice to promote depolymerisation. In contrast, taxol was used to stabilise microtubules and extracts prepared at RT. GTP and AMP-PNP were added to the RT extract to further

stabilise microtubule assembly and motor binding. The assembled microtubules were pelleted at 35,000 rpm in a fixed angle rotor and subjected to Western blot analysis (Figure 6.8C and D). 80% of α-tubulin remained polymerised in the RT sample, with 55% polymerised in the cold sample indicating that, although inefficient, the procedure employed did reduce the extent of microtubule polymerisation. It is possible that if a more robust lysis buffer was used, depolymerised tubulin may be released more effectively from cells and remain in the supernatant rather than being pelleted following the high speed spin. As expected γ-tubulin co-pelleted with microtubules (Young *et al.*, 2000), the proportion of associated protein was reduced in extracts that contained less polymerised microtubules indicating that the γ-tubulin present in the pellet was associating with microtubules. Nek2A also co-pelleted with microtubules under both conditions, with the overall percentage of Nek2A in the pellet being reduced from 85% to 65% following depolymerisation of microtubules, implying that Nek2 is binding microtubules *in vivo*. The abundance of Nek2B in these samples was too low to assess the extent of microtubule binding.

To confirm the interaction between Nek2 and microtubules, an *in vitro* binding assay was undertaken. Initially, purified GST:Nek2-CTD and GST were incubated with purified microtubules, subjected to high speed centrifugation to pellet the microtubules and the pellet probed for the presence of the GST proteins. GST proteins co-pelleted with microtubules but unfortunately they also appeared in the pellet fraction following centrifugation in the absence of microtubules (data not shown). This meant that it was not viable to use the purified GST proteins under these conditions to identify microtubule association, as they were themselves pelleted. Therefore *in vitro* translated proteins were substituted into the assay.

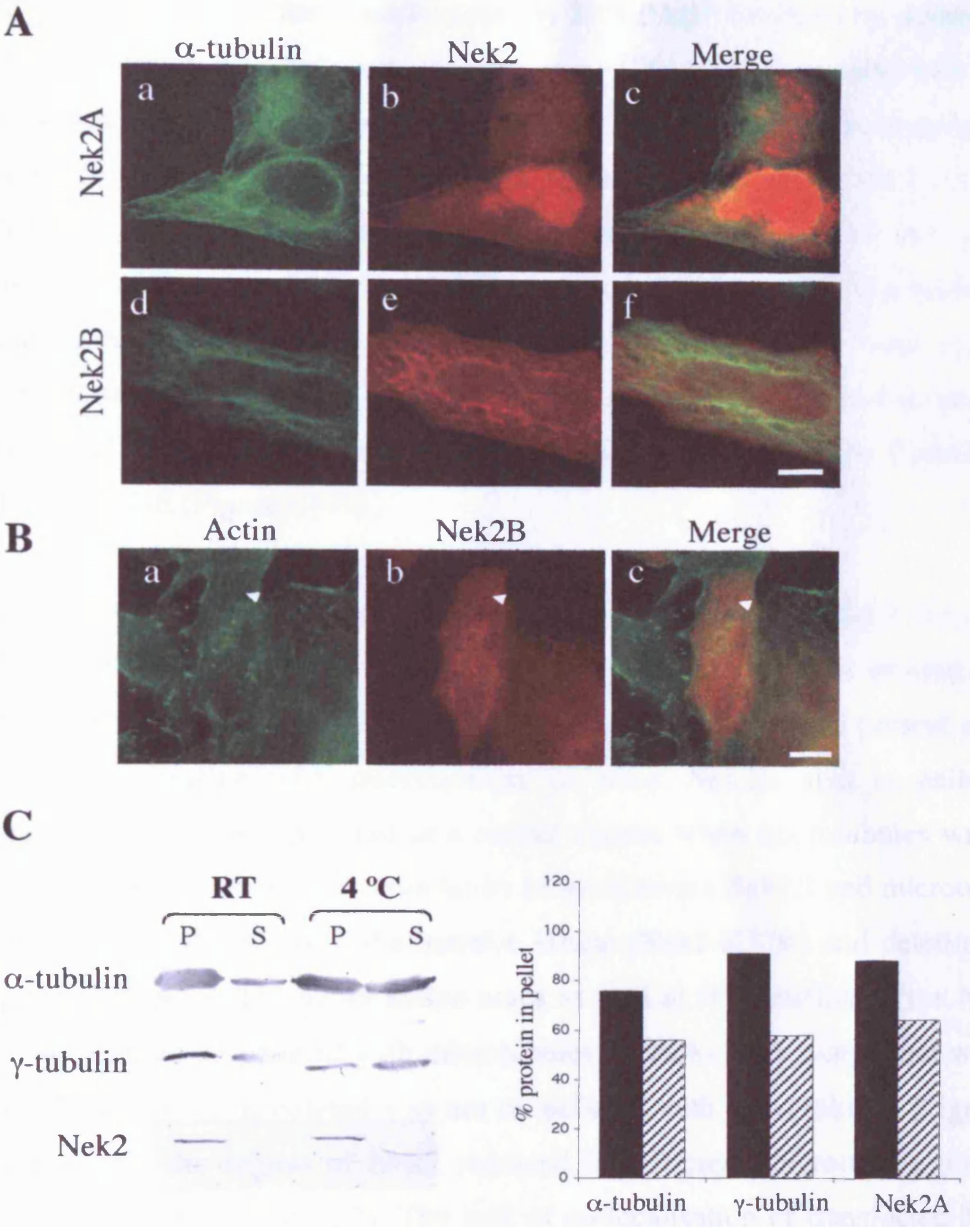

Figure 6.8 Nek2 associates with microtubules *in vivo*

(A) Asynchronous HeLa cells were transiently transfected with myc-Nek2A or myc-Nek2B and following a 24 hr incubation, cells were fixed and analysed by indirect immunofluorescence microscopy. Microtubules were revealed by anti-α-tubulin antibodies and recombinant Nek2 by anti-Nek2 antibodies. **(B)** Asynchronous HeLa cells were transiently transfected with myc-Nek2B, cells were fixed and actin filaments were revealed by anti-actin antibodies and recombinant Nek2B by anti-myc antibodies. Arrowheads indicate co-localisation. Scale bar, 10 μm. **(C)** HeLa cell extracts were prepared at RT or 4°C to retain or disassemble microtubules respectively. Extracts were centrifuged at 35,000 rpm for 30 minutes at RT or 4°C. Pellet (P) and supernatant (S) fractions were analysed by Western blot using specific antibodies against Nek2, α-tubulin and γ-tubulin. The percentage of total protein in the pellet at RT (black bars) and 4°C (hatched bars) was calculated for Nek2, α-tubulin and γ-tubulin.

[^{35}S]-Nek2A, [^{35}S]-Nek2A-K37R, [^{35}S]-Nek2B and a range of [^{35}S]-Nek2A deletion mutants were prepared by *in vitro* translation (Figure 6.9A). An aliquot of each [^{35}S]-labelled protein was taken for direct analysis by SDS-PAGE followed by autoradiography to confirm similar expression levels. The remaining [^{35}S]-labelled proteins were incubated with microtubules that had been purified from adult mice brains using a simple taxol based method (kind gift from Dr. B. Edde, Paris, France) and subjected to high speed centrifugation to pellet the microtubules. Equal amounts of the pellet and supernatant fractions were analysed by SDS-PAGE followed by autoradiography. The nuclear protein [^{35}S]-Lamin A was also prepared as it is unlikely to associate with cytoplasmic microtubules and would thus act as a negative control. As shown previously, microtubules were effectively pelleted by high speed centrifugation as shown by the Coomassie Blue stained SDS-PAGE (Figure 6.9B).

The majority of Lamin A remained in the supernatant, with a small amount contaminating the pellet fraction. Additional wash steps did not reduce the amount of contamination. Nek2A was more concentrated in the pellet when microtubules were present suggesting that it was associating with microtubules *in vitro*. Nek2B also co-pelleted with microtubules but was also pelleted to a certain degree when microtubules were absent suggesting that perhaps a weaker association exists between Nek2B and microtubules. Of the other Nek2 constructs used, the inactive kinase (Nek2-K37R) and deletion mutants missing the C-terminal 25 and 49 amino acids as well as the deletion of the N-terminal catalytic domain, all co-pelleted with microtubules. Nek2A-Δ126 a construct with the C-terminal 126 amino acids deleted was not co-pelleted with microtubules (Figure 6.9C). This implies that the region of Nek2 required for efficient microtubule binding lies between amino acids 319 and 370. The lack of co-localisation of transfected Nek2 with microtubules by immunofluorescence microscopy implies that Nek2 may not associate with cytoplasmic microtubules but may associate more with centriolar microtubules. It could be that this association anchors Nek2 containing complexes to the centrosome during interphase to ensure that centrosome cohesion remains intact. Alternatively, further analysis of the localisation of endogenous Nek2 using high resolution deconvolution microscopy may reveal microtubule association.

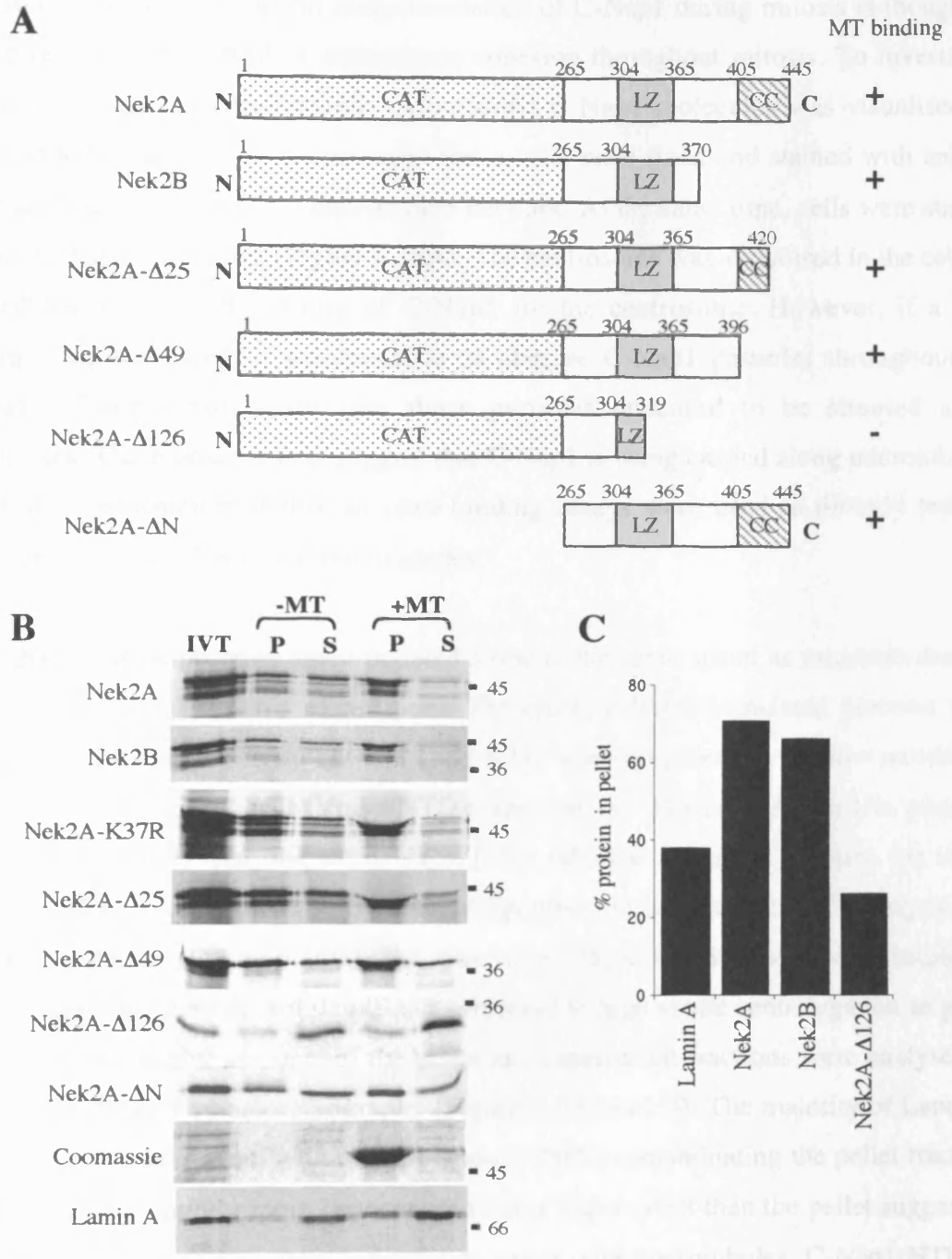

Figure 6.9 Nek2 binds to microtubules between amino acids 319 and 370
(A) Schematic diagram of the human Nek2 splice variants and deletion mutants that were *in vitro* translated in the presence of [^{35}S], indicating the catalytic domain (CAT), leucine zipper (LZ) and coiled coil domain (CC): numbers represent amino acids. **(B)** An aliquot of each [^{35}S] -labelled protein was taken for direct analysis by SDS-PAGE and autoradiography (IVT), the remainder was centrifuged at 35,000 rpm for 30 minutes at RT in the presence (+MT) or absence (-MT) of purified microtubules. Samples of the pellet (P) and supernatant (S) were taken for direct analysis by SDS-PAGE followed by autoradiography. Molecular weights (kDa) are indicated on the right of panels. **(C)** The percentage of protein in the pellet of samples incubated with microtubules is shown for Lamin A, Nek2A, Nek2B and Nek2A-Δ126.

6.2.9 Specific association of C-Nap1-NTD with microtubules

The dissociation and subsequent re-accumulation of C-Nap1 during mitosis is thought to be necessary for the control of centrosome cohesion throughout mitosis. To investigate this, the localisation of endogenous cytoplasmic C-Nap1 molecules was visualised by indirect immunofluoresence microscopy. HeLa cells were fixed and stained with anti-α-tubulin antibodies to reveal the microtubule network. At the same time, cells were stained with anti-C-Nap1 antibodies (Figure 6.10A). The centrosome was visualised in the cells as expected due to the high affinity of C-Nap1 for the centrosome. However, if a high exposure time was used, it was possible to observe C-Nap1 particles throughout the cytoplasm. Upon closer inspection these particles appeared to be situated along microtubules. These observations suggest that C-Nap1 is being carried along microtubules. For further confirmation of this, *in vitro* binding assays were used to directly test the interaction between C-Nap1 and microtubules.

GST-C-Nap1 fusion proteins again pelleted alone at the same speed as microtubules and were thus not useful for this experiment. Therefore, *in vitro* translated proteins were employed in the assay. [^{35}S]-CTD and [^{35}S]-NTD were prepared by *in vitro* translation from pCMVmyc-CTD and pCMVmyc-NTD respectively. [^{35}S]-Lamin A was also prepared as a negative control. An aliquot of each [^{35}S]- labelled protein was taken for direct analysis by SDS-PAGE followed by autoradiography to confirm that similar expression levels were obtained (Figure 6.10B). The remaining [^{35}S]-labelled proteins were incubated with or without purified microtubules and subjected to high speed centrifugation to pellet the microtubules. Equal amounts of the pellet and supernatant fractions were analysed by SDS-PAGE followed by autoradiography (Figure 6.10C and D). The majority of Lamin A remained in the supernatant, with a small amount (20%) contaminating the pellet fraction. C-Nap1-CTD was slightly more concentrated in the supernatant than the pellet suggesting that no association or a very weak association exists with microtubules. C-Nap1-NTD on the other hand became more obviously concentrated in the pellet fraction following incubation with microtubules suggesting that C-Nap1-NTD does interact with microtubules. It has not been possible so far to confirm an association between endogenous microtubules and C-Nap1 from HeLa cell extracts due to the low abundance and difficulty in western blotting endogenous full length C-Nap1.

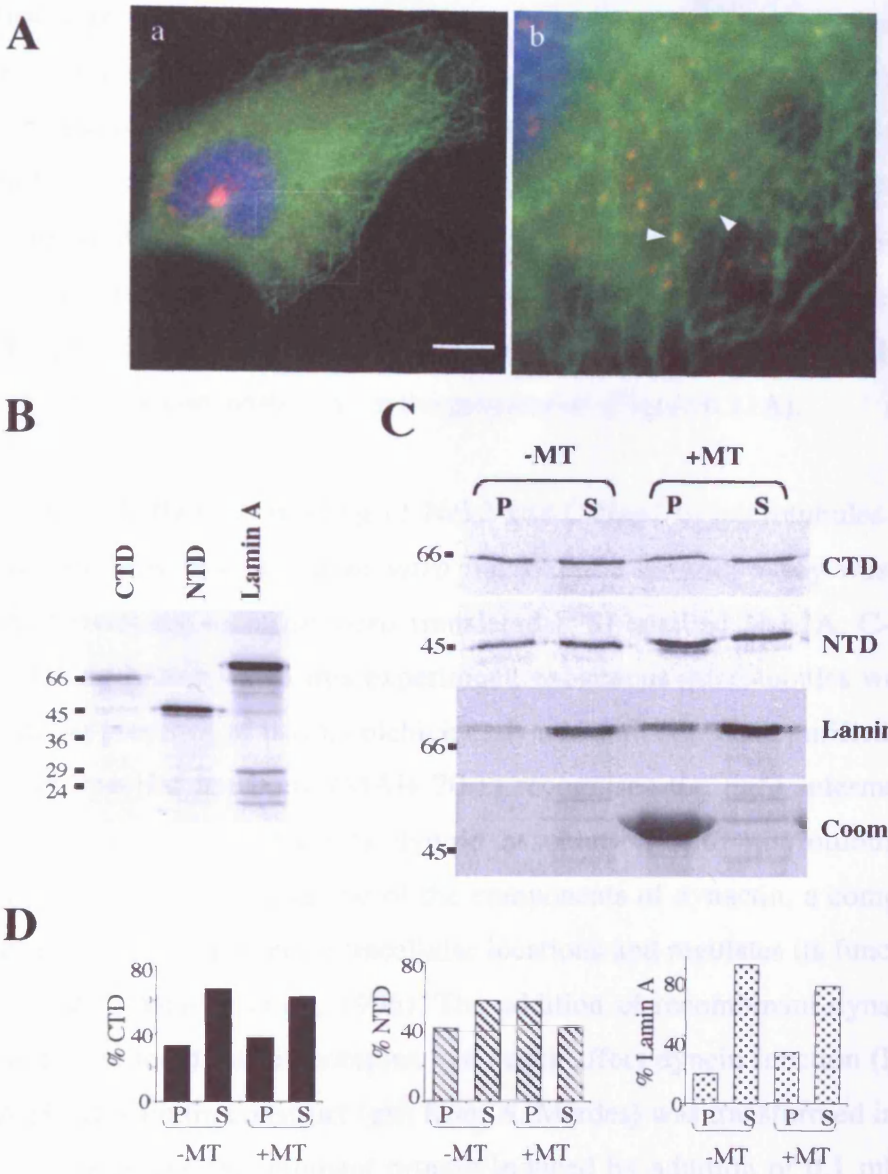

Figure 6.10 C-Nap1-NTD associates with microtubules
(**A**) HeLa cells were fixed and analysed by indirect immunofluorescence microscopy. Arrowheads indicate the co-localisation of C-Nap1 along microtubules, revealed by anti-α-tubulin (green) and anti-C-Nap1 (red) antibodies. Scale bar, 10 μm. The inset box in (a) represents the region that is enlarged in (b). (**B**) *In vitro* translated CTD, NTD and lamin were prepared in presence of [^{35}S] methionine, an aliquot was taken for direct analysis by SDS-PAGE followed by autoradiography. (**C**) *In vitro* translated products from (B) were centrifuged at 35,000 rpm for 30 minutes at RT in the presence (+MT) or absence (-MT) of purified microtubules. Samples of the pellet (P) and supernatant (S) fractions were taken for direct analysis by SDS-PAGE followed by autoradiography. Molecular weights (kDa) are indicated on the left of each panel. (**D**) The percentage of protein in the pellet and supernatant was plotted with respect to total protein for each of the samples from (C).

6.2.10 Dynein dependent association of C-Nap1 with microtubules

The association of Nek2 and C-Nap1 with microtubules seen *in vitro* may be due to an interaction with other proteins present in the preparations. To identify whether additional proteins were present in the tubulin preparations a sample of polymerised microtubules was subjected to SDS-PAGE and Coomassie Blue staining to reveal the protein content. The major protein present in the preparations was tubulin (55 kDa) as expected but a few weak bands could also be detected possibly representing microtubule associated proteins or molecular motors. Western blotting confirmed that the major band contained α-tubulin and additional probing demonstrated that the light intermediate chain of dynein was also present at very low concentrations in the preparation (Figure 6.11A).

To determine whether the binding of Nek2 and C-Nap1 to microtubules required motor complexes such as dynein, an *in vitro* microtubule binding assay was carried out as described previously using *in vitro* translated [^{35}S]-labelled Nek2A, C-Nap1-CTD, C-Nap1-NTD and Lamin A. In this experiment, exogenous microtubules were added to all samples in the presence of taxol, colchicine, dynein antibodies and purified His-dynamitin. The dynein specific antibody (MAB 70.1) recognises the light intermediate chain of cytoplasmic dynein and disrupts dynein association with microtubules (Karki and Holzbaur, 1999). Dynamitin is one of the components of dynactin, a complex of proteins that targets dynein to different intracellular locations and regulates its function (Karki and Holzbaur, 1995; Merdes *et al.*, 1996). The addition of recombinant dynamitin has been shown to disrupt the dynactin complex and hence affect dynein function (Echeverri *et al.*, 1996). A His-dynamitin construct (gift from A. Merdes) was transformed into BL21 *E.coli* and expression of the recombinant protein induced by addition of 0.1 mM IPTG for 16 hours at RT. The small amount of soluble His-dynamitin present in bacterial cell lysates was purified using nickel agarose beads and the fraction containing the protein dialysed into PBS (Figure 6.11B).

Following taxol stabilisation, Nek2A and C-Nap1-NTD co-pelleted with microtubules and C-Nap1-CTD and lamin A did not (Figure 6.11C). Colchicine induced destabilisation of microtubules caused a decrease in the amount of microtubules pelleted and consequently a decrease in the amount of associated Nek2A and C-Nap1-NTD. The addition of the dynein antibody caused a significant shift of C-Nap1-NTD from the pellet to the supernatant, strongly suggesting that this domain is associating with microtubules via dynein (Figure

6.11B). No change was seen for Nek2A implying that dynein is not involved in any microtubule mediated transport of Nek2A that may be occurring. The addition of dynamitin to the assay produced a similar affect as the dynein antibody, in that it caused a shift of C-Nap1-NTD from the microtubule containing pellet to the supernatant, reinforcing the idea that C-Nap1-NTD associates with microtubules via dynein *in vitro*. Further confirmation of this will need to be undertaken including the use of relevant controls to ensure that the methods used to induce dynein dissociation from microtubules are adequate. In addition further *in vivo* studies using live cell imaging to observe the rate of C-Nap1 movement along microtubules and quantitative immunofluoresence microscopy will increase our understanding of the role of dynein mediated cell cycle regulated centrosome assembly of C-Nap1.

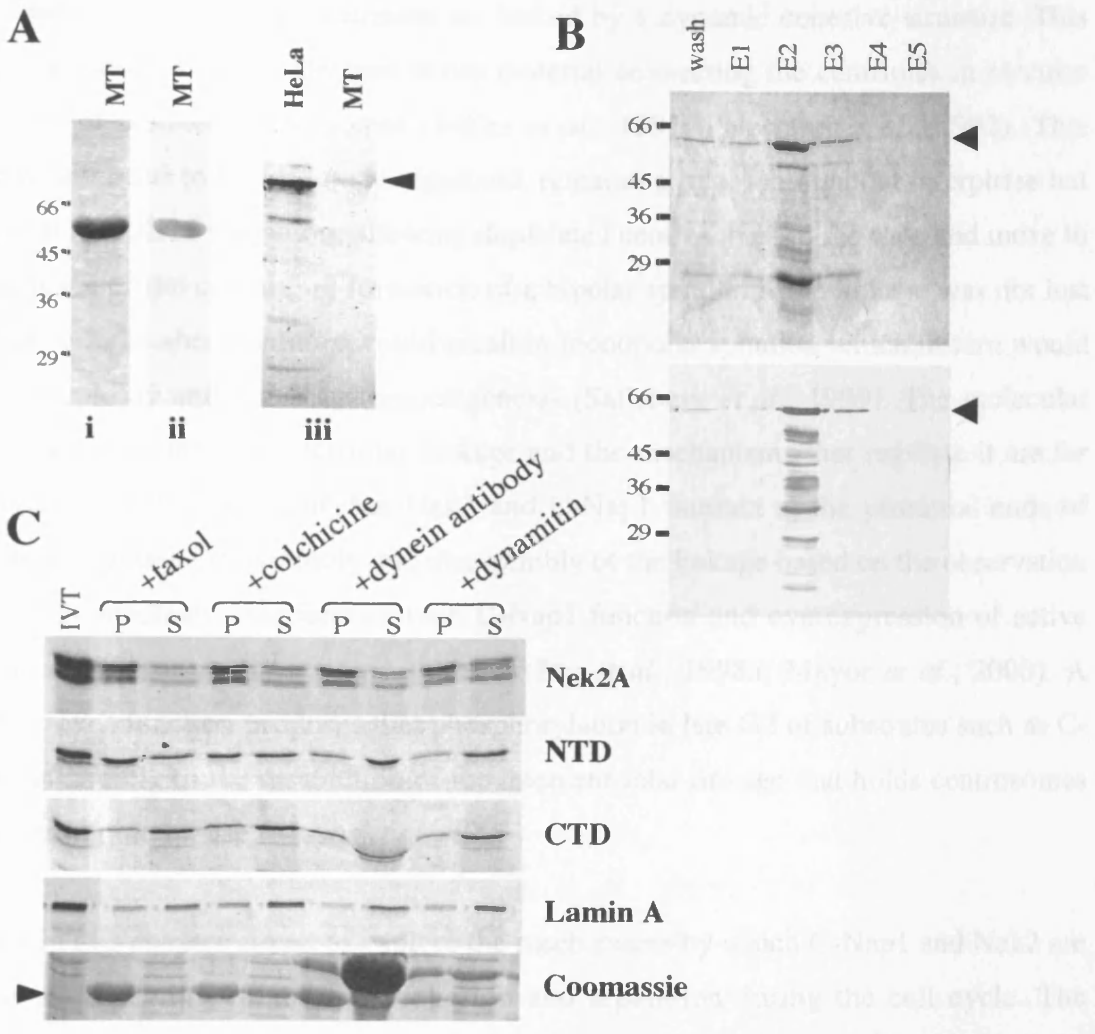

Figure 6.11 Dynein dependent association of C-Nap1 NTD with microtubules

(A) 2 μg purified microtubules (MT) were analysed directly by SDS-PAGE and Coomassie Blue staining (i), and Western blotting using anti-α-tubulin (ii) and anti-dynein (iii) antibodies. Comparison with HeLa cell extract (HeLa) indicates the expected molecular weight of the light intermediate chain of dynein (arrowhead). **(B)** His-dynamitin was expressed in bacteria and bacterial lysate was passed over nickel agarose beads. Protein was eluted off the beads using imidazole into five fractions (E1-E5). The wash fraction and elutions were analysed by SDS-PAGE followed by Coomassie Blue staining (upper panel) or Western blotting with anti-His antibodies (lower panel). Purified His-dynamitin is indicated (arrows). Molecular weights (kDa) are indicated on the left of each panel. **(C)** *In vitro* translated Nek2A, C-Nap1-NTD, C-Nap1-CTD and lamin A were prepared in presence of [^{35}S] methionine. Labelled proteins were incubated with purified microtubules in the presence of taxol (10 μM), colchicine (20 μM), dynein antibodies (0.1 mg/ml) or His-dynamitin (5 μg/ml), samples were centrifuged at 35,000 rpm for 30 minutes at RT, samples of the pellet (P) and supernatant (S) fractions were taken for direct analysis by SDS-PAGE followed by autoradiography. The bottom panel shows Coomassie Blue staining of the SDS-PAGE to demonstrate the presence of purified tubulin in each fraction (arrowhead).

6.3. DISCUSSION

There is some evidence that centrioles are linked by a dynamic cohesive structure. This includes the observation of electron dense material connecting the centrioles in electron microscopy of isolated centrosomes (Fuller *et al.*, 1995; Paintrand *et al.*, 1992). This linkage would need to be cell cycle regulated, remaining intact throughout interphase but disrupted at the G2/M transition, allowing duplicated centrosomes to separate and move to opposite poles of the cell aiding formation of a bipolar spindle. If the linkage was not lost in mitosis, spindle abnormalities would result in monopolar spindles, which in turn would lead to aneuploidy and possibly tumourigenesis (Salisbury *et al.*, 1999). The molecular characterisation of the intercentriolar linkage and the mechanisms that regulate it are far from understood. It is thought that Nek2 and C-Nap1 interact at the proximal ends of centrioles to regulate the assembly and disassembly of the linkage based on the observation that antibody mediated interference with C-Nap1 function and overexpression of active Nek2 causes premature centrosome splitting (Fry *et al.*, 1998a; Mayor *et al.*, 2000). A model for Nek2 function proposes that phosphorylation in late G2 of substrates such as C-Nap1 leads directly to the dissolution of the intercentriolar linkage that holds centrosomes together during interphase (Mayor *et al.*, 1999).

The work in this chapter aimed to explore the mechanisms by which C-Nap1 and Nek2 are involved in regulating centrosome cohesion and separation during the cell cycle. The results indicate that C-Nap1 interacts with Nek2A via both its CTD and NTD. In addition, not only does C-Nap1 interact with Nek2A it also interacts with the shorter isoform Nek2B through both the CTD and NTD. Further analysis of C-Nap1-CTD revealed that the site of Nek2 interaction lies between amino acids 2362 and 2442. It is likely that a common Nek2 binding motif exists in the NTD and CTD and analysis of the sequence indicated that the only common motif was RLXXSL. This may represent a Nek2 binding motif, however, it is not present in the sequence of BPC-1, another centrosomal Nek2 binding protein. Mutation of these residues followed by the use of the mutated proteins in both the yeast two hybrid system and *in vitro* Nek2 kinase assays will help to confirm or eliminate the involvement of this common motif in Nek2 binding of C-Nap1.

In vitro kinase assays demonstrate that C-Nap1-CTD and -NTD are both phosphorylated by Nek2A. C-Nap1 phosphorylation is thought to be the trigger for C-Nap1 dissociation

from the centrosome in mitosis and Nek2 is likely to be responsible for C-Nap1 phosphorylation in G2. Phosphorylation may cause the dissociation of C-Nap1 molecules by inducing a structural change perhaps involving the flexible hinge. The observation that cells expressing C-Nap1 in combination with inactive Nek2A contain vary large aggregates of C-Nap1 compared to the smaller patches present in cells expressing active Nek2A reinforces the idea that Nek2 can regulate oligomerisation of C-Nap1 (Mayor *et al.*, 2002). The relative contribution of Nek2A and Nek2B dependent phosphorylation may be important as Nek2B remains present in mitosis whilst Nek2A is destroyed by the proteasome. C-Nap1 may be kept phosphorylated by Nek2B throughout mitosis, keeping it dissociated from the centrosome until Nek2B levels decrease in G1. The specific effects of Nek2B dependent phosphorylation of C-Nap1 in mitosis will need to be addressed, perhaps by the use of purified Nek2B protein in kinase assays. Moreover, cell cycle specificity for C-Nap1-CTD or -NTD phosphorylation by Nek2A or Nek2B may further explain the centrosomal dissociation and re-association of C-Nap1. The work presented here does not exclude the possibility that other centrosomal kinases such as Aurora-A and Plk may be involved in regulating C-Nap1 phosphorylation.

In addition to its role in centrosome cohesion, Nek2 has also been implicated in centrosome assembly and maintenance (Fry *et al.*, 1998a; Uto and Sagata, 2000). Depletion of X-Nek2B from egg cytoplasm delays the appearance of microtubule asters in combination with a delay in γ-tubulin recruitment, implying that X-Nek2B plays a role in centrosome assembly, more specifically in γ-tubulin recruitment. There are various mechanisms that have been suggested to explain how X-Nek2B could act to recruit proteins to the centrosome. Firstly it may act in a structural fashion as an early building block of the centrosome onto which other proteins dock. Secondly, X-Nek2B kinase activity may be required for catalysing the assembly of the centrosome through phosphorylation of centrosomal proteins or assembly factors. Finally, X-Nek2B may act as a direct assembly factor for the γ-TuRC itself (Uto and Sagata, 2000). It is likely that human Nek2 may also be important for centrosome assembly and maintenance based on the observation that long term overexpression in adult human cells leads to centrosome disintegration (Fry *et al.*, 1998b). Preliminary work looking at the association of Nek2 with γ-tubulin indicated that Nek2A and Nek2B do not directly interact with γ-tubulin, thus ruling out direct binding as the mechanism for recruitment. Instead, as mentioned above Nek2 may act as a recruitment signal for γ-tubulin perhaps via phosphorylation of other

centrosomal proteins leading to the assembly of γ-tubulin onto the centrosome during G2. Further work will need to be carried out to investigate these possibilities including the use of γ-tubulin in cell cycle specific Nek2 kinase assays. More importantly, disruption of Nek2 expression through the use of dsRNAi or microinjection of Nek2 specific antibodies followed by the observation of the relative levels of core centrosomal proteins such as γ-tubulin will increase our knowledge of Nek2 function in centrosome assembly.

Continuing in the same vein, the direct interaction of Nek2 with another core component of the centrosome was investigated. Centrin, a component of centrioles, bound weakly to Nek2A *in vivo* but did not bind *in vitro* suggesting that Nek2 is not involved in the anchoring of centrin at centrioles. Interestingly, centrin is phosphorylated at the G2/M transition by a serine/threonine kinase causing the release of calcium, which is thought to aid centrosome separation (Lutz *et al.*, 2001). Nek2 kinase activity is high at the G2/M transition suggesting that Nek2 may be responsible for centrin phosphorylation at this stage in the cell cycle. Following purification of GST-centrin from bacterial cell lysates and inclusion in an *in vitro* Nek2 kinase assay, no phosphorylation of centrin was evident (data not shown). This would imply that Nek2 is not involved in centrin regulation at the G2/M transition and is most likely not involved in its assembly onto the centrosome. However, further work will be required to rule out any possible contribution of Nek2 activity to centrin regulation

Data presented here indicates that C-Nap1-CTD interacts with both itself and C-Nap1-NTD. Further analysis revealed that the site of NTD interaction lies between amino acids 1964 and 2268. C-Nap1-NTD does not bind to the CTD in the same region that Nek2 binds to it, implying that the CTD is capable of binding both Nek2 and the NTD at the same time, to form a complex of regulatory proteins at the proximal ends of centrioles. Interestingly, BPC-1 a novel centrosomal C-Nap1 interacting protein, does interact with C-Nap1-CTD within the same region as C-Nap1-NTD. This implies that BPC-1 could inhibit either homo or heterodimerisation of C-Nap1, possibly having an adverse affect on the regulation of centriole cohesion. BPC-1 has previously been shown to inhibit the premature centrosome splitting induced by Nek2A overexpression. The inhibition of C-Nap1 oligomerisation may represent the mechanism of action of BPC-1 (see Chapter 5). The most distinctive structural feature of C-Nap1 is the presence of five domains: N-terminus, long coiled coil, hinge, long coiled coil and C-terminus. The identification of C-

Nap1 homologues in other species and the extent of conservation between the domains will greatly facilitate our understanding of the importance of each domain. To date, a small region of mouse C-Nap1 has been identified called INMP (Menz *et al.*, 1996) and a large fragment of *Xenopus* C-Nap1 is in the process of being cloned (J. Rapley and A.M. Fry, unpublished results).

The structure of the SMC (structural maintenance of chromosomes) protein is very similar to C-Nap1 in that it also has the five domains, including two large coiled coils and a middle hinge region. It has been found that the terminal domains of SMC are brought together by the anti-parallel arrangement of the coiled coils folded at a flexible hinge (Melby *et al.*, 1998). It is possible that the domains of C-Nap1 are arranged in a similar manner. The globular N- and C-domains of two C-Nap1 molecules may bind at the proximal end of centrioles, with the coiled coils in a parallel or antiparallel arrangement. The flexible hinge region may bring the arms and terminal domains together or open up to separate them, alternatively a single molecule may fold up or open out (Figure 6.12A). It is possible that the movement of the hinge is central to the ability of C-Nap1 to control centrosome cohesion. This movement may be regulated by Nek2 phosphorylation or by the interaction with other centrosomal components. Interestingly, no interaction was found between C-Nap1 and centrin or γ-tubulin, implying that these core centrosomal proteins do not play a part in the regulation of C-Nap1 function and most likely are not involved in centrosome cohesion.

If C-Nap1 was able to dimerise it may also exist in large complexes in cells. The appearance of aggregates following overexpression of C-Nap1 emphasizes the ability of C-Nap1 to oligomerise. Further evidence for the predicted structural appearance of C-Nap1 comes from the observation that recombinant C-Nap1-CTD and -NTD both localise to the centrosome, whilst the middle region does not (Mayor *et al.*, 2000). This suggests that the terminal domains anchor C-Nap1 at the centriole with the coiled coils and hinge region projecting out into the intercentriolar space, where it perhaps binds components of the intercentriolar linkage. However, immunoelectron microscopy has shown that the N-terminus appears to be slightly further away from the proximal end than the hinge region but there is no evidence to suggest that C-Nap1 molecules span the entire distance between the two parental centrioles (Mayor *et al.*, 2000). The fact that the noncentrosomal middle region and the N-terminus are able to induce split centrosomes upon overexpression to

almost the same extent as Nek2, suggests that components of the intercentriolar linkage bind to both the middle region and the N-terminus of C-Nap1. The accumulation of recombinant N-terminus and hinge region in the cytoplasm may cause centrosome splitting by sequestering essential components of the linkage thus preventing them from forming the structure that links the centrosomes. The C-terminus is perhaps more important for the anchoring of C-Nap1 to the proximal end of the centriole as it localises to the centrosome in 100% of cells and is less effective at causing centrosome splitting (Mayor *et al.*, 2000). The molecular components that make up the intercentriolar linkage are as yet unknown but work is planned to address this by carrying out a yeast two hybrid screen using the middle hinge region of C-Nap1 as the bait to identify novel proteins that may be involved in C-Nap1 regulation or form part of the intercentriolar linkage.

Microtubule dynamics, particularly minus end directed motility, are likely to be important for determining local concentrations of both structural and regulatory proteins at the centrosome including components of the intercentriolar linkage. The linkage is thought to have a dynamic structure therefore any change in the local concentrations of either linker components or regulators of linker assembly would be expected to have a profound effect on centrosome integrity. As previously mentioned, Nek2 is involved in the regulation of centriole cohesion and is a cell cycle regulated protein. Therefore the role of microtubules in Nek2 assembly and function at the centrosome was examined. Nek2A and Nek2B were both found to bind to microtubules via a motif present in the sequence between amino acids 319 and 370, which has yet to be identified. The observed association was dependent on the microtubules being polymerised and stable. The association of Nek2 with the centrosome is independent of microtubules (Fry *et al.*, 1998a), implying that although Nek2 associates with microtubules, they are not necessary for Nek2 to be maintained at the centrosome. The lack of co-localisation of recombinant Nek2 with cytoplasmic microtubules in fixed HeLa cells may simply reflect the excess of protein present in transiently transfected cells. Further experiments indicated that the association of Nek2 with microtubules was independent of dynein, implying minus end directed transport along microtubules is not necessary for Nek2 assembly onto the centrosome. The direct microtubule binding combined with the fact that Nek2 is located at the proximal ends of centrioles (Fry *et al.*, 1998b) suggests that Nek2 may associate directly with centriolar microtubules. At the centrosome, Nek2A and Nek2B exist in a large complex with C-Nap1 and PP1. This complex is present at the proximal ends of centrioles and is thought to

regulate centriole cohesion through the combination of kinase and phosphatase activities. Based on the findings in this chapter, Nek2 association with centriolar microtubules may play a role in anchoring the complex to the proximal ends of centrioles.

In addition to Nek2, C-Nap1 is also an important molecule in the control of centrosome cohesion, with its disassembly following its phosphorylation necessary for loss of centriole cohesion. The mechanisms of C-Nap1 reassembly following mitosis are not understood. To investigate the role of microtubules and dynein mediated transport in C-Nap1 reassembly, the direct association of C-Nap1 with microtubules was examined. C-Nap1-NTD alone was found to bind to microtubules *in vitro*, dependent on the microtubules being polymerised and stable. The association of C-Nap1 with the centrosome is independent of microtubules (Fry *et al.*, 1998b), implying that although C-Nap1 associates with microtubules, they are not necessary for C-Nap1 to be maintained at the centrosome. Further work indicated that the association of C-Nap1-NTD with microtubules was dependent on dynein, implying that minus end directed transport along microtubules could play a role in C-Nap1 assembly onto the centrosome, perhaps at specific stages of the cell cycle. To reinforce the idea that C-Nap1 is transported along microtubules, C-Nap1 molecules could be seen on cytoplasmic microtubules in fixed HeLa cells. To characterise the involvement of dynein in C-Nap1 assembly, quantitative immunofluorescence can be carried out to look at the increase in abundance of centrosomal C-Nap1 following treatment with various inhibitors of microtubule or dynein function. Furthermore, measurement of the rate of movement of C-Nap1 antibody molecules along microtubules using time lapse microscopy will enable us to predict whether a dynein-mediated mechanism of movement is likely.

Overexpression of C-Nap1 causes the appearance of aggregates or patches within cells (Mayor *et al.*, 2002). These patches contain Nek2 but not γ-tubulin and are consequently not able to nucleate microtubules. This is consistent with our results that C-Nap1 cannot bind γ-tubulin directly. The NTD is necessary for the formation of these patches suggesting that it is central to patch assembly, possibly by recruiting other proteins such as Nek2 to these aggregates via dynein dependent transport. Thus the NTD may act as a general transporter or assembly factor for components of the intercentriolar linkage. Furthermore, C-Nap1-NTD may play a role in the localisation of Nek2, PP1 and C-Nap1 to the proximal ends of the centrioles, to form the complex that regulates centrosome cohesion. In addition

C-Nap1-NTD may be connected to the minus ends of centriolar microtubules through its interaction with dynein, an interaction which may anchor the larger complex in which C-Nap1 is found at the proximal ends of centrioles.

The data presented in this chapter provides evidence that C-Nap1 interacts with and is phosphorylated by Nek2A and Nek2B not only at the CTD as previously shown, but also at the NTD. Our data also implies that C-Nap1 can interact with itself, a result that is supported by the appearance of large aggregates upon overexpression (Mayor *et al.*, 2002). Purification of full length C-Nap1 and rotary shadowing electron microscopy of individual molecules may help us to understand how C-Nap1 structural conformation and phosphorylation state helps to regulate centrosome cohesion. Both Nek2 and C-Nap1 associate with microtubules, a property that may contribute to the localisation of these proteins to the proximal end of parental centrioles. C-Nap1-NTD associates with microtubules in a dynein dependent manner suggesting a role for C-Nap1 in the assembly of the intercentriolar linkage, perhaps acting as a transporter of cargos along microtubules in a cell cycle specific manner (Figure 6.12B). Together these observations bring us closer to understanding how centrosome cohesion is regulated through specific phosphorylation of components such as C-Nap1 and the recruitment and anchorage of core components in a microtubule dependent manner. However we are still some way from having a full molecular understanding of the intercentriolar linkage.

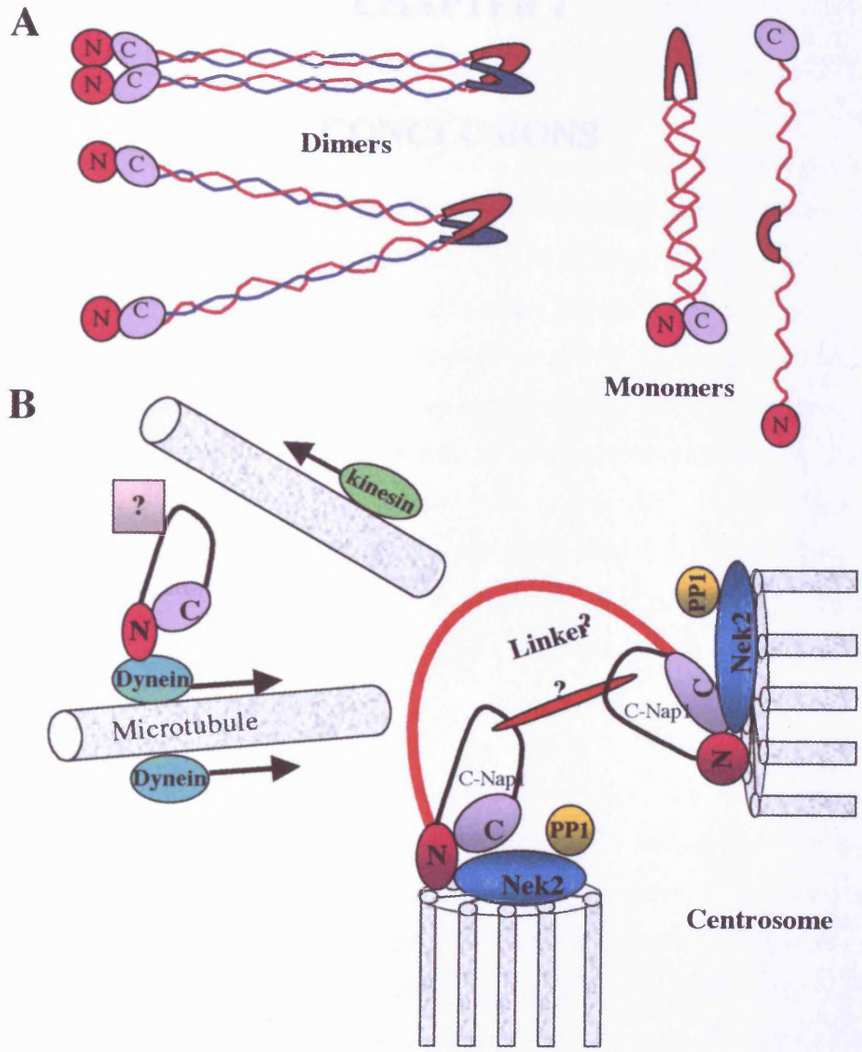

Figure 6.12 C-Nap1 structure and function in centriole cohesion
(A) A schematic model of the proposed structure of C-Nap1 either as a dimer or a monomer. The CTD and NTD globular domains interact, as might the rigid coiled coils. The hinge region is flexible permitting a scissoring movement and the folded rod conformation may be altered depending on the phosphorylation status of C-Nap1 or the association of other regulatory molecules. **(B)** Nek2, C-Nap1 and PP1 exist in a complex at the proximal end of the centrioles and act together to control centriole cohesion throughout the cell cycle. Nek2 and C-Nap1-NTD associate with centriolar microtubules to anchor the complex and intercentriolar linkage in place. C-Nap1 terminal domains can associate, perhaps due to the flexible properties of the coiled coil domains and middle hinge region. This forms a structural anchor for proteins involved in centriole cohesion. C-Nap1 is a dynein cargo, that can be transported to centrosomes on microtubules, possibly bringing additional centrosomal proteins with it, that are involved in centriole cohesion. This transport may be cell cycle dependent and play an important role in the disruption and re-assembly of the intercentriolar linkage in mitosis.

CHAPTER 7

CONCLUSIONS

7.0 CONCLUSIONS

7.1 Why study centrosomal proteins?

In animal cells, the centrosome is the major MTOC, influencing all microtubule dependent processes, including bipolar spindle formation, organelle transport, cell shape, polarity and motility (Doxsey, 2001; Kellogg *et al.*, 1994). It is well established that bipolar spindles can assemble in the absence of centrosomes; however, when present these organelles exert a dominant influence on the number of spindle poles (Raff, 2001; Rieder *et al.*, 2001). Non-centrosomal mechanisms for spindle formation exist in plants and certain specialised animal cells. However, this should not distract from the fact that most animal cell divisions do occur in the presence of centrosomes and this probably enhances both the speed and precision of spindle assembly and the fidelity of chromosome segregation. Moreover the centrosome is structurally conserved among all higher animals and many *bona fide* centrosomal components, such as γ-tubulin, pericentrin and centrin, are highly conserved. Given its complexity and conservation, it is likely that the centrosome performs essential functions as otherwise it would have been eliminated during evolution by random mutations.

As centrosomes act dominantly when present in somatic cells, their deregulation is thought to contribute to the spindle abnormalities, chromosome missegregation and genetic instability that is typically seen in many cancer cells. These defects are likely to occur in combination with alterations in other cellular pathways such as apoptosis, cell cycle progression, cell cycle checkpoints and cell growth regulation (Brinkley and Goepfert, 1998; Salisbury *et al.*, 1999). Increased centrosome numbers and centrosome defects have been observed in both aggressive tumours and in some low grade tumours and pre-cancerous lesions (Lingle *et al.*, 2002; Pihan *et al.*, 2001). It is not clear whether these centrosome abnormalities are generated by misregulation of centrosome duplication, or as a consequence of mitotic misregulation resulting in tetraploidy (Carroll *et al.*, 1999; Meraldi *et al.*, 2002). Thus, as yet a direct link between centrosome defects and cancer has not been established.

It is likely that the centrosome is more than just an MTOC and perhaps the MTOC functions of this organelle are not essential for the survival of individual cells. For instance, with the exception of cilia and flagella formation, functional microtubule arrays can be organised during interphase and mitosis in the absence of centrosomes (Wheatley *et*

al., 1996). Furthermore, recent studies suggest a role for centrosomes in cytokinesis and G1/S progression (Hinchcliffe *et al.*, 2001; Piel *et al.*, 2001). In particular, when centrosomes were removed from somatic vertebrate cells by either microsurgery or laser ablation, a significant proportion of cells completed cell division but then failed to undergo the next round of DNA synthesis (Hinchcliffe *et al.*, 2001; Khodjakov and Rieder, 2001). The mechanisms behind these observations have not yet been elucidated. Our understanding of centrosome composition is still limited and a full appreciation of how centrosomes contribute to cellular function will require isolation and characterisation of the estimated hundreds of centrosome-associated molecules. The use of mass spectrometry will facilitate analysis of centrosome fractions and provide a framework for piecing together the centrosome structure, in much the same way that this technology has facilitated the functional characterisation and molecular organisation of the yeast SPB (Wigge *et al.*, 1998).

As a cell progresses through the cell cycle, the centrosome undergoes a series of major structural and functional transitions that are essential for both centrosome function and mitotic spindle formation. It is important to fully understand the role of proteins that are involved in regulating centrosome structure and function throughout the cell cycle as aberrations in centrosome control can interfere with bipolar spindle formation and chromosome segregation. A number of kinases and phosphatases have been localised at the centrosome suggesting that phosphorylation plays a major role in centrosome regulation (Fry *et al.*, 2000a). The Cdk, Polo and Aurora families of kinases have been implicated in a number of cell cycle events including centrosome duplication, APC/C activation, spindle formation, sister chromatid separation, mitotic progression and cytokinesis (Cullen *et al.*, 2000; Glover *et al.*, 1998; Nigg, 1995; Nigg, 2001). Furthermore, the family of NIMA-related kinases is now emerging as another major conserved regulator of centrosome function (Fry, 2002). In addition to kinases, phosphatases are also thought to regulate centrosome function. Protein phosphatase 1α and protein phosphatase 4 associate with centrosomes and presumably act in competition with centrosomal kinases (Andreassen *et al.*, 1998; Brewis *et al.*, 1993). An example of where this occurs is the interaction of PP1 with the NIMA related kinase Nek2, this kinase-phosphatase complex coordinates the timing of centrosome separation with cell cycle progression (Helps *et al.*, 2000). The work presented in this thesis addresses the regulation and function of the centrosomal kinase Nek2 and its substrate C-Nap1. However, many questions still remain to be answered as discussed below.

7.2 What is the role of Nek2B in cells?

Nek2 is a cell cycle regulated protein kinase that localises to the centrosome and is thought to be involved in regulating centrosome separation prior to mitosis (Fry *et al.*, 1998a). Previously, Nek2 kinase activity has been shown to be regulated through a number of mechanisms, including the formation of a ternary complex with PP1c and C-Nap1, as well as by autophosphorylation (Fry *et al.*, 1999; Helps *et al.*, 2000). Here, we demonstrate that another mechanism of regulation is the expression of two alternative splice variants, Nek2A and Nek2B (Hames and Fry, 2002). These splice variants differ in their mitotic stability, with Nek2B remaining present throughout mitosis. Nek2A is degraded in mitosis possibly to allow the re-establishment of the intercentriolar linkage as cells exit mitosis. The fact that Nek2B remains may seem to conflict with this idea. However as Nek2B cannot stimulate centrosome splitting with the same efficiency as Nek2A, this hypothesis remains valid.

The difference in the efficiency of splitting induced by Nek2A versus Nek2B could be attributed to their affinity for different substrates or inhibitors. Nek2B does lack the PP1c binding motif that is present in the C-terminus of Nek2A. However, heterodimerisation with Nek2A via the leucine zipper motif present in both isoforms, may allow PP1c to inhibit Nek2B dependent phosphorylation until it is inactivated at the G2/M transition. If Nek2B does have an affinity for certain substrates that are not phosphorylated by Nek2A, it would be interesting to identify such proteins, however the use of a yeast two hybrid interaction screen would prove impossible as the only difference between Nek2A and Nek2B is the C-terminal 12 amino acids. Instead, specific depletion of Nek2B in cells could be used to understand the role of Nek2B perhaps through the use of Nek2B antibodies in micro-injection experiments or dsRNAi technology. If no specific function can be attributed to Nek2B it would seem surprising that Nek2B is still present in adult cells. It is possible that it is merely a remnant of embryonic development where it has been shown to be required for centrosome assembly and maintenance (Uto and Sagata, 2000). The existence of a non-degradable version of Nek2 may be more efficient for the rapid cell cycles that are characteristic during embryogenesis.

7.3 What is the purpose of Nek2A destruction?

Previous work has demonstrated that Nek2A disappears in mitotically arrested cells (Fry *et al.*, 1995; Schultz *et al.*, 1994), is unstable in interphase egg extracts supplemented with Cdh1 (Pfleger and Kirschner, 2000) and is degraded when injected into dividing embryos (Uto and Sagata, 2000). This prompted us to investigate if, when and how human Nek2 proteins are destroyed during mitosis. The results presented here show that Nek2A is destroyed by the proteasome following ubiquitylation by the E3 ubiquitin ligase APC/C-Cdc20 (Hames *et al.*, 2001). Furthermore, degradation of Nek2A occurs in early mitosis, coincident with cyclin A destruction, and depends upon a motif in its extreme C-terminus that is almost identical to the extended D box present in cyclin A (Geley *et al.*, 2001).

The destruction of Nek2A in early mitosis may in some way be necessary for the re-establishment of the intercentriolar linkage in late mitosis, perhaps by ensuring that C-Nap1 can reaccumulate on the centrosome at the same time as a flexible linker is re-established between centriole pairs of the future daughter cells. Alternatively, Nek2A destruction may be necessary for mitotic exit. Overexpression of stable NIMA mutants does cause a mitotic arrest in *Aspergillus* cells without preventing destruction of cyclin B (Pu and Osmani, 1995). Preliminary work using stable cell lines expressing GFP-Nek2A has indicated that exit from mitosis is slowed down in these cells (A.J Faragher and A.M. Fry, unpublished observations). The use of stable cell lines expressing stable Nek2 lacking both the functional KEN box and extended D box will hopefully provide an insight into the need for Nek2A destruction for mitotic exit and in cell cycle progression.

APC/C mediated destruction is known to play an integral role in the control of the cell cycle and it is possible that in addition to specific regulation of cyclins, Nek2 regulation may also be important. If this is the case then a checkpoint mechanism similar to the spindle checkpoint may be responsible for making sure that mitotic entry does not occur until centrosomes are fully separated for formation of a bipolar mitotic spindle. If so, Nek2 degradation may be inhibited by Emi1 until centrosome disjunction has occurred. Emi1 is a protein known to inhibit the APC/C-Cdc20 in late G2 to promote mitotic entry by allowing cyclin B accumulation. Emi1 is itself destroyed in early mitosis, possibly following centrosome separation, thus allowing the APC/C to mediate Nek2A destruction. At the G1-S transition, Emi1 is transcriptionally induced by the E2F transcription factor. Emi1-dependent stabilisation of APC/C-Cdh1 targets, such as cyclin A and possibly Nek2

is then thought to promote S phase entry (Hsu *et al.*, 2002; Reimann *et al.*, 2001). Alternatively, a checkpoint may exist that ensures that the intercentriolar linkage is re-established prior to cytokinesis.

7.4 What is the function of BPC-1?

In an attempt to further understand the dual roles of Nek2 and C-Nap1 in centrosome cohesion, a yeast two hybrid interaction screen was carried out using the C-terminal 54 kDa of C-Nap1. This enabled the identification of a novel centrosomal protein named BPC-1. Although the original plan was to identify proteins that form part of the intercentriolar linkage, localisation of GFP-BPC-1 suggests that it is unlikely to span the intercentriolar gap. However it may constitute part of an anchoring complex that also contains Nek2 and C-Nap1, situated on the proximal end of the centrioles. This complex may be responsible for the recruitment and/or stabilisation of other potential components of the intercentriolar linkage such as p160ROCK or δ-tubulin (Chang and Stearns, 2000; Chevrier *et al.*, 2002).

On further analysis, BPC-1 was also found to interact with Nek2A and Nek2B. Functional studies have demonstrated that BPC-1 appears to counteract the centrosome splitting phenotype induced by Nek2A overexpression. This suggests that BPC-1 might inhibit the kinase activity of Nek2A perhaps by blocking its ability to form dimers or reducing the extent of autophosphorylation. Alternatively, BPC-1 may block the site of interaction with substrates such as C-Nap1, reducing the efficiency of their phosphorylation. These theories could be tested by measuring the relative kinase activity of Nek2 in cells also overexpressing BPC-1 or by measuring the extent of C-Nap1 phosphorylation. The inhibition of Nek2A activity by BPC-1 may purely be due to sequestering of active kinase away from the centrosome so that it can no longer phosphorylate C-Nap1. Quantitative immunofluorescence techniques will allow us to measure the amount of Nek2 at the centrosome in the absence or presence of BPC-1. Future work will be aimed at confirming our present knowledge of BPC-1 localisation and cell cycle regulation through the production of BPC-1 specific antibodies. More importantly perhaps will be depletion of BPC-1 in cells through the use of dsRNAi or antibody microinjection with the aim of identifying the cellular function of BPC-1.

7.5 How do C-Nap1 and Nek2 interact at the centrosome?

It is thought that Nek2 and C-Nap1 interact at the proximal ends of centrioles to regulate the assembly and disassembly of the intercentriolar linkage based on the observation that antibody mediated interference with C-Nap1 function and overexpression of Nek2 both cause centrosome splitting. An investigation into specific interactions has shown that C-Nap1 interacts with and is phosphorylated by Nek2A and Nek2B not only at the CTD as previously shown, but also at the NTD. The centrosome association of C-Nap1 may well be regulated through specific phosphorylation of either the N- or C-terminus, perhaps in a cell cycle specific manner. This may represent an important mechanism for the control of centrosome cohesion through the regulation of C-Nap1.

Data also implies that C-Nap1 can exist as multimers in cells, characterised by the appearance of large aggregates upon overexpression. C-Nap1-CTD interacts with both itself and C-Nap1-NTD but it is not clear whether these are likely to be intra- or inter-molecular interactions *in vivo*. C-Nap1-NTD does not bind to the CTD in the same region that Nek2 binds to it, implying that the CTD is capable of binding both Nek2 and the NTD at the same time, to form a complex of regulatory proteins at the proximal ends of centrioles. Interestingly, BPC-1 does interact with C-Nap1 CTD within part of the same region as C-Nap1 NTD. This implies that BPC-1 could inhibit C-Nap1 oligomerisation, possibly having an adverse affect on the regulation of centriole cohesion. It is possible that the globular N- and C-domains of two C-Nap1 molecules may bind at the proximal end of centrioles, with the coiled coils in a parallel or antiparallel arrangement. The flexible hinge region may bring the arms and terminal domains of adjacent molecules together or open them up to separate them. Alternatively, a single molecule may fold up or open out. It is possible that the movement of the hinge is central to the ability of C-Nap1 to control centrosome cohesion. This movement may be regulated by Nek2 phosphorylation or by the interaction with other centrosomal components.

7.6 Why do Nek2 and C-Nap1 associate with microtubules?

Both Nek2 and C-Nap1 appear to associate with microtubules, a property that may contribute to their localisation at the proximal end of parental centrioles. The role of Nek2 in centrosome assembly or stability was demonstrated both in the early embryo and in somatic cells (Fry *et al.*, 2000b; Fry *et al.*, 1998a; Uto and Sagata, 2000). However, it was

not shown in these experiments whether Nek2 contributed to centriole, as opposed to centrosome, stability. The localisation of the ternary complex Nek2/C-Nap1/PP1 at the proximal end of both centrioles could control docking of the intercentriolar linkage, and therefore the distance between both centrioles. Another possibility could be that C-Nap1 acts as a minus end capping protein, which requires control of its phosphorylation state by Nek2 and PP1 to protect proximal ends from disassembly. C-Nap1-NTD associates with microtubules in a dynein dependent manner suggesting a further role for C-Nap1 in the assembly of the intercentriolar linkage, perhaps acting as a transporter of cargos along microtubules in a cell cycle specific manner. Alternatively, C-Nap1 may function as a docking site for intercentriolar linkage components on the proximal end of centrioles.

7.7 Final comments

This thesis has contributed significantly to our understanding of Nek2 regulation but unraveling Nek2 function remains a difficult task and there is still a long way to go. Previously, a single step model was thought to be responsible for the loss of centrosome cohesion at the onset of mitosis. This states that Nek2 dependent phosphorylation in late G2 of substrates such as C-Nap1 leads directly to the dissolution of the intercentriolar linkage that holds centrosomes together during interphase (Mayor *et al.*, 1999). The identification of two splice variants of Nek2, one of which (Nek2B) is not degraded in mitosis raises the suggestion that the loss of cohesion is perhaps more complicated, however, no data has been obtained to support such a theory. With this in mind, I am tentatively suggesting a two stage model that could explain the dual roles of C-Nap1 and Nek2 in centrosome separation at the onset of mitosis (Figure 7.1). This is based on preliminary work suggesting that C-Nap1 may not dissociate from duplicated centrosomes when they first separate in late G2, coincident with Nek2 dependent phosphorylation, but rather remains at the centrosome until the bipolar spindle is formed in early mitosis.

The first step in the loss of centrosome cohesion may occur in late G2. At this stage, PP1 becomes inactivated, possibly by Cdk1 dependent phosphorylation or through binding of inhibitor 2. The resulting activation of Nek2A results in the phosphorylation of C-Nap1 and loss of centrosome cohesion. The phosphorylation may be specific to a single domain of C-Nap1, most likely the NTD as this domain is most effective at inducing centrosome splitting when overexpressed in cells. If this phosphorylation could stimulate a

conformational change in C-Nap1 structure, the molecule may no longer be able to bind components of the linkage, thus inducing loss of an intact intercentriolar linkage. It is possible that the NTD is able to partially anchor or recruit components of the intercentriolar linkage and that the CTD may be more important for anchoring C-Nap1 and its associated complex of Nek2 and PP1 to the proximal end of the parental centrioles. Following loss of cohesion, the centrosomes will be able to move to opposite poles of the cell through the action of microtubule dependent motors such as Eg5, a centrosome and spindle associated kinesin related motor that is regulated by both Cdk1 and Aurora-A (Blangy *et al.*, 1995; Giet *et al.*, 1999a).

In early mitosis, Nek2A is destroyed by the proteasome whilst Nek2B remains present. It is possible that Nek2B can only phosphorylate a small proportion of known Nek2A substrates, thus accounting for its diminished ability to promote splitting. Nek2B specific phosphorylation of C-Nap1-CTD may cause C-Nap1 to fully dissociate from the centrosome as the spindle is formed. Nek2B levels decrease in late mitosis/early G1 due to transcriptional repression, allowing unphosphorylated C-Nap1 to re-accumulate at the centrosome, thus re-establishing the intercentriolar linkage. Preliminary evidence has suggested that over expression of the kinase dead form of Nek2A causes an increase in the amount of C-Nap1 protein present at the interphase centrosome. This observation requires confirmation but if proven to be correct would reinforce the idea that C-Nap1 phosphorylation is necessary for dissociation of the protein from centrosomes. To confirm or eliminate this two step model, the specificity of Nek2A and Nek2B for different substrates needs to be elucidated.

Further work will need to be undertaken to fully understand the mechanism of centrosome cohesion in cells. However, the significance of the work detailed here is shown from the observation that Nek2 gene expression is elevated in advanced tumours (W. Lingle, personal communication). This provides some evidence that Nek2 may be involved in tumour progression, perhaps through de-regulation of centrosome cohesion that can lead to genetic instability as a direct consequence of mis-segregation of chromosomes. However, more thorough work needs to be carried out to define a clear role for Nek2 and C-Nap1 in tumourigenesis.

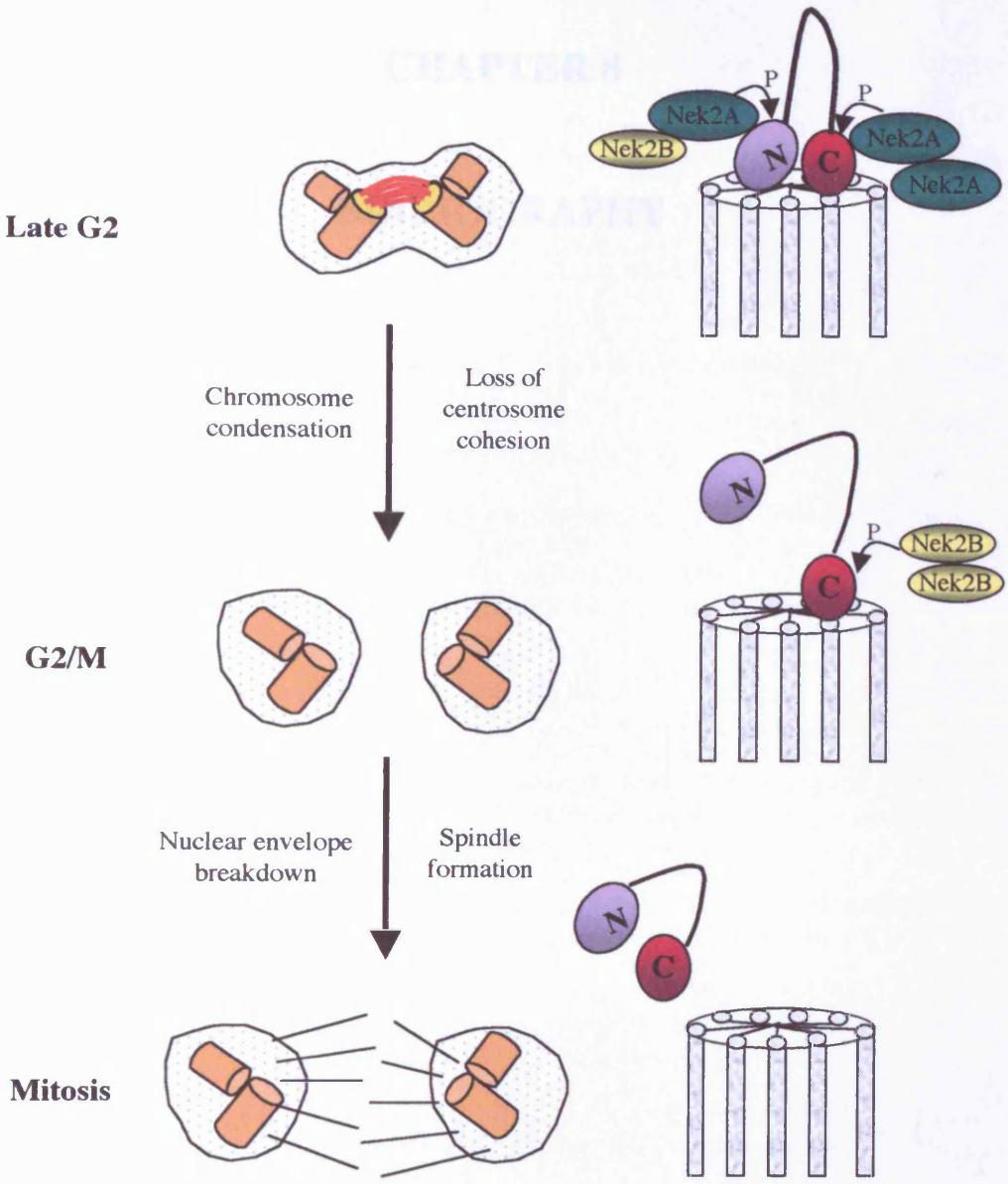

Figure 7.1 Proposed role for Nek2 and C-Nap1 in centriole cohesion
In late G2 Nek2A dimers become active and phosphorylate C-Nap1-NTD. This stimulates a conformational change in C-Nap1 structure resulting in loss of the intercentriolar linkage. The centrosomes separate to opposite poles of the cell forming the poles of the bipolar mitotic spindle upon which chromosome segregation can occur. In early mitosis Nek2A is destroyed leaving Nek2B to phosphorylate C-Nap1-CTD, this causes the dissociation of C-Nap1 from the centrosome. Nek2B levels decrease in late mitosis/early G1 possibly due to transcriptional repression, allowing C-Nap1 to re-accumulate at the centrosome, thus re-establishing the intercentriolar linkage.

CHAPTER 8

BIBLIOGRAPHY

Adams, I. R., and Kilmartin, J. V. (1999). Localisation of core spindle pole body (SPB) components during SPB duplication in *Saccharomyces cerevisiae*. J Cell Biol *145*, 809-823.

Adams, I. R., and Kilmartin, J. V. (2000). Spindle pole body duplication: a model for centrosome duplication? Trends Cell Biol *10*, 329-335.

Adams, R. R., Carmena, M., and Earnshaw, W. C. (2001). Chromosomal passengers and the (aurora) ABCs of mitosis. Trends Cell Biol *11*, 49-54.

Adams, R. R., Tavares, A. A., Salzberg, A., Bellen, H. J., and Glover, D. M. (1998). *pavarotti* encodes a kinesin-like protein required to organize the central spindle and contractile ring for cytokinesis. Genes Dev *12*, 1483-1494.

Ahmad, F. J., and Baas, P. W. (1995). Microtubules released from the neuronal centrosome are transported into the axon. J Cell Sci *108*, 2761-2769.

Amon, A. (1999). The spindle checkpoint. Curr Opin Genet Dev *9*, 69-75.

Andersen, S. S. L. (1999). Molecular characteristics of the centrosome. Int Rev Cytology *187*, 51-109.

Andreassen, P. R., Lacroix, F. B., Villa-Moruzzi, E., and Margolis, R. L. (1998). Differential subcellular localisation of protein phosphatase-1 alpha, gamma 1 and delta isoforms during both interphase and mitosis in mammalian cells. J Cell Biol *141*, 1207-1215.

Andreassen, P. R., Lohez, O. D., Lacroix, F. B., and Margolis, R. L. (2001). Tetraploid state induces p53-dependent arrest of nontransformed mammalian cells in G1. Mol Biol Cell *12*, 1315-1328.

Arama, E., Yanai, A., Kilfin, G., Bernstein, A., and Motro, B. (1998). Murine NIMA-related kinases are expressed in patterns suggesting distinct functions in gametogenesis and a role in the nervous system. Oncogene *16*, 1813-1823.

Bahler, J., Steever, A. B., Wheatley, S., Wang, Y., Pringle, J. R., Gould, K. L., and McCollum, D. (1998). Role of polo kinase and Mid1p in determining the site of cell division in fission yeast. J Cell Biol *143*, 1603-1616.

Bailly, E., Doree, M., Nurse, P., and Bornens, M. (1989). p34cdc2 is located in both nucleus and cytoplasm; part is centrosomally associated at G2/M and enters vesicles at anaphase. EMBO J *8*, 3985-3995.

Balczon, R., Bao, L., Zimmer, W. E., Brown, K., Zinkowski, R. P., and Brinkley, B. R. (1995). Dissociation of centrosome replication events from cycles of DNA synthesis and mitotic division in hydroxyurea-arrested Chinese hamster ovary cells. J Cell Biol *130*, 105-115.

Bardi, G., Parada, L. A., Bomme, L., Pandis, N., Willen, R., Johansson, B., Jeppsson, B., Beroukas, K., Heim, S., and Mitelmasn, F. (1997). Cytogenetic comparisons of synchronous carcinomas and polyps in patients with colorectal cancer. Brit J Cancer *76*, 765-769.

Barton, A. B., Davies, C. J., Hutchison, C. A. D., and Kaback, D. B. (1992). Cloning of chromosome I DNA from *Saccharomyces cerevisiae*: analysis of the FUN52 gene, whose product has homology to protein kinases. Gene *117*, 137-140.

Belham, C., Combs, M. J., and Avruch, J. (2001). Identification of the NIMA family kinases NEK6/7 as regulators of the p70 ribosomal S6 kinase. Curr Biol *11*, 1155-1167.

Berdnik, D., and Knoblich, J. A. (2002). Drosophila Aurora-A Is Required for Centrosome Maturation and Actin- Dependent Asymmetric Protein Localisation during Mitosis. Curr Biol *12*, 640-647.

Bergen, L. G., Upshall, A., and Morris, N. R. (1984). S-phase, G2 and nuclear division mutants of *Aspergillus nidulans*. J Bacteriol *159*, 114-119.

Bischoff, J. R., Anderson, L., Zhu, Y., Mossie, K., Ng, L., Souza, B., Schryver, B., Flanagan, P., Clairvoyant, F., Ginther, C., *et al.* (1998). A homologue of *Drosophila* aurora kinase is oncogenic and amplified in human colorectal cancers. Embo J *17*, 3052-3065.

Blangy, A., Lane, H. A., Dherin, P., Harper, M., Kress, M., and Nigg, E. A. (1995). Phosphorylation by P34(Cdc2) regulates spindle association of human eg5, a kinesin-related motor essential for bipolar spindle formation *in-vivo*. Cell *83*, 1159-1169.

Blomberg-Wirschell, M., and Doxsey, S. (1998). Rapid isolation of centrosomes. Methods Enzymol *298*, 228-238.

Bobinnec, Y., Khodjakov, A., Mir, L. M., Rieder, C. L., Edde, B., and Bornens, M. (1998). Centriole disassembly *in vivo* and its effect on centrosome structure and function in vertebrate cells. J Cell Biol *143*, 1575-1589.

Borel, F., Lohez, O. D., Lacroix, F. B., and Margolis, R. L. (2002). Multiple centrosomes arise from tetraploidy checkpoint failure and mitotic centrosome clusters in p53 and RB pocket protein-compromised cells. Proc Natl Acad Sci (USA) *99*, 9819-9824.

Bornens, M., Paintrand, M., Berges, J., Marty, M.-C., and Karsenti, E. (1987). Structural and chemical characterization of isolated centrosomes. Cell Motil Cytoskeleton *8*, 238-249.

Bouckson-Castaing, V., Moudjou, M., Ferguson, D. J. P., Mucklow, S., Belkaid, Y., Milon, G., and Crocker, P. R. (1996). Molecular characterization of ninein, a new coiled-coil protein of the centrosome. J Cell Sci *109*, 179-190.

Brewis, N. D., Street, A. J., Prescott, A. R., and Cohen, P. T. (1993). PPX, a novel protein serine/threonine phosphatase localised to centrosomes. Embo J *12*, 987-996.

Brinkley, B. R. (1985). Microtubule Organising Centres. Ann Rev Cell Biol *1*, 145-172.

Brinkley, B. R., and Goepfert, T. M. (1998). Supernumerary centrosomes and cancer: Boveri's hypothesis resurrected. Cell Motil cytoskeleton *41*, 281-288.

Buendia, B., Bre, M., Griffiths, G., and Karsenti, E. (1990). Cytoskeletal control of centrioles movement during the establishment of polarity in Madin-Darby canine kidney cells. J Cell Biol *110*, 1123-1135.

Buendia, B., Draetta, G., and Karsenti, E. (1992). Regulation of the microtubule nucleating activity of centrosomes in *Xenopus* egg extracts: role of cyclin-A-associated protein-kinase. J Cell Biol *116*, 1431-1442.

Carazo-Salas, R. E., Gruss, O. J., Mattaj, I. W., and Karsenti, E. (2001). Ran-GTP coordinates regulation of microtubule nucleation and dynamics during mitotic-spindle assembly. Nat Cell Biol *3*, 228-234.

Carmena, M., Riparbelli, M. G., Minestrini, G., Tavares, A. M., Adams, R., Callaini, G., and Glover, D. M. (1998). *Drosophila* polo kinase is required for cytokinesis. J Cell Biol *143*, 659-671.

Carroll, P. E., Okuda, M., Horn, H. F., Biddinger, P., Stambrook, P. J., Gleich, L. L., Li, Y. Q., Tarapore, P., and Fukasawa, K. (1999). Centrosome hyperamplification in human cancer: chromosome instability induced by p53 mutation and/or Mdm2 overexpression. Oncogene *18*, 1935-1944.

Castro, A., Arlot-Bonnemains, Y., Vigneron, S., Labbe, J. C., Prigent, C., and Lorca, T. (2002). APC/Fizzy-Related targets Aurora-A kinase for proteolysis. EMBO Rep *3*, 457-462.

Centonze, V. E., and Borisy, G. G. (1990). Nucleation of microtubules from mitotic centrosomes is modulated by a phosphorylated epitope. J Cell Sci *95*, 405-411.

Chan, C. S., and Botstein, D. (1993). Isolation and characterization of chromosome-gain and increase-in-ploidy mutants in yeast. Genetics *135*, 677-691.

Chang, P., and Stearns, T. (2000). Delta-tubulin and epsilon-tubulin: two new human centrosomal tubulins reveal new aspects of centrosome structure and function. Nat Cell Biol *2*, 30-35.

Chen, A., Yanai, E., Arama, E., Kilfin, G., and Motro, B. (1999). NIMA-related kinases: isolation and characterisation of murine *nek3 and nek4* cDNAs, and chromosomal localisation of *nek1, nek2 and nek3*. Gene *234*, 127-137.

Chen, J., and Fang, G. (2001). MAD2B is an inhibitor of the anaphase-promoting complex. Genes Dev *15*, 1765-1770.

Chen, Y., Riley, D. J., Chen, P.-L., and Lee, W.-H. (1997a). HEC, a novel nuclear protein rich in leucine heptad repeats specifically involved in mitosis. Mol Cell Biol *17*, 6049-6056.

Chen, Y., Sharp, D., and Lee, W.-H. (1997b). HEC binds to the seventh regulatory subunit of the 26S proteasome and modulates the proteolysis of mitotic cyclins. J Biol Chem *272*, 24081-24087.

Chen, Y., Riley, D. J., Zheng, L., Chen, P.-L., and Lee, W.-H. (2002). Phosphorylation of the mitotic regulator protein Hec1 by Nek2 kinase is essential for faithful chromosome segregation. J Biol Chem, In press.

Chevrier, V., Piel, M., Collomb, N., Saoudi, Y., Frank, R., Paintrand, M., Narumiya, S., Bornens, M., and Job, D. (2002). The Rho-associated protein kinase p160ROCK is required for centrosome positioning. J Cell Biol *157*, 807-817.

Chial, H. J., and Winey, M. (1999). Mechanisms of genetic instability revealed by analysis of yeast spindle pole body duplication. Biol Cell *91*, 439-450.

Churcher, Y., and Moss, S. E. (1993). Modulation of protein tyrosine phosphorylation during G1/S transition in activated human T-lymphoblasts. J Biol Chem *268*, 26144-26149.

Ciechanover, A. (1998). The ubiquitin-proteasome pathway: on protein death and cell life. EMBO J *17*, 7151-7160.

Clute, P., and Pines, J. (1999). Temporal and spatial control of cyclin B1 destruction in metaphase. Nat Cell Biol *1*, 82-87.

Cohen, P. (1990). The structure and regulation of protein phosphatases. Ann Rev Biochem *58*, 453-508.

Cohen, P. T. W. (2002). Protein phosphatase 1 - targeted in many directions. J Cell Sci *115*, 241-256.

Compton, D. A. (1998). Focusing on spindle poles. J Cell Sci *111*, 1477-1481.

Coquelle, F. M., Caspi, M., Cordelieres, F. P., Dompierre, J. P., Dujardin, D. L., Koifman, C., Martin, P., Hoogenraad, C. C., Akhmanova, A., Galjart, N., *et al.* (2002). LIS1, CLIP-170's key to the dynein/dynactin pathway. Mol Biol Cell *22*, 3089-3102.

Coux, O., Tanaka, K., and Goldberg, A. L. (1996). Structure and functions of the 20S and 26S proteosomes. Ann Rev Biochem *65*, 801-847.

Cullen, C. F., May, K. M., Hagan, I. M., Glover, D. M., and Ohkura, H. (2000). A new genetic method for isolating functionally interacting genes: high plo1(+)-dependent mutants and their suppressors define genes in mitotic and septation pathways in fission yeast. Genetics *155*, 1521-1534.

Cullen, C. F., and Ohkura, H. (2001). Msps protein is localised to acentrosomal poles to ensure bipolarity of *Drosophila* meiotic spindles. Nat Cell Biol *3*, 637-642.

de Saint Phalle, B., and Sullivan, W. (1998). Spindle assembly and mitosis without centrosomes in parthenogenetic *sciara* embryos. J Cell Biol *141*, 1383-1391.

De Souza, C. P. C., Osmani, A. H., Wu, L.-P., Spotts, J. L., and Osmani, S. A. (2000). Mitotic histone H3 phosphorylation by the NIMA kinase in *Aspergillus nidulans*. Cell *102*, 293-302.

den Elzen, N., and Pines, J. (2001). Cyclin A is destroyed in prometaphase and can delay chromosome alignment and anaphase. J Cell Biol *153*, 121-135.

Desai, A., Murray, A., Mitchison, T. J., and Walczak, C. E. (1999). The use of *Xenopus* egg extracts to study mitotic spindle assembly and function *in vitro*. In Mitosis and Meiosis, C. L. Rieder, ed. (Acad. Press), pp. 385-412.

Descombes, P., and Nigg, E. A. (1998). The polo-like kinase Plx1 is required for M phase exit and destruction of mitotic regulators in *Xenopus* egg extracts. EMBO J *17*, 1328-1335.

Di Agostino, S., Rossi, P., Geremia, R., and Sette, C. (2002). The MAPK pathway triggers activation of Nek2 during chromosome condensation in mouse spermatocytes. Development *129*, 1715-1727.

Dictenberg, J. B., Zimmerman, W., Sparks, C. A., Young, A., Vidair, C., Zheng, Y., Carrington, W., Fay, F. S., and Doxsey, S. J. (1998). Pericentrin and gamma-tubulin form a protein complex and are organized into a novel lattice at the centrosome. J Cell Biol *141*, 163-174.

Ding, R., West, R. R., Morphew, D. M., Oakley, B. R., and McIntosh, J. R. (1997). The spindle pole body of *Schizosaccharomyces pombe* enters and leaves the nuclear envelope as the cell cycle proceeds. Mol Biol Cell *8*, 1461-1479.

Dionne, M. A., Howard, L., and Compton, D. A. (1999). NuMA is a component of an insoluble matrix at mitotic spindle poles. Cell Motil Cytoskeleton *42*, 189-203.

do Carmo Avides, M., Tavares, A., and Glover, D. M. (2001). Polo kinase and Asp are needed to promote the mitotic organizing activity of centrosomes. Nat Cell Biol *3*, 421-424.

Dorin, D., Le Roch, K., Sallicandro, P., Alano, P., Parzy, D., Poullet, P., Meijer, L., and Doerig, C. (2001). Pfnek-1, a NIMA-related kinase from the human malaria parasite *Plasmodium falciparum*. Biochemical properties and possible involvement in MAPK regulation. Eur J Biochem *268*, 2600-2608.

Doxsey, S. (1998). The centrosome - a tiny organelle with big potential. Nat Genet *20*, 104-106.

Doxsey, S. (2001). Re-evaluating centrosome function. Nat Revs: Mol Cell Biol *2*, 688-698.

Doxsey, S. J., Stein, P., Evans, L., Calarco, P. D., and Kirschner, M. (1994). Pericentrin, a highly conserved centrosome protein involved in microtubule organisation. Cell *76*, 639-650.

Durfee, T., Becherer, K., Chen, P.-L., Yeh, S.-H., Yang, Y., Kilburn, A. E., Lee, W.-H., and Elledge, S. J. (1993). The retinoblastoma protein associates with the protein phosphatase type 1 catalytic subunit. Genes Dev *7*, 555-569.

Dutertre, S., Descamps, S., and Prigent, C. (2002). On the role of aurora-A in centrosome function. Oncogene *21*, 6175-6183.

Echeverri, C. J., Paschal, B. M., Vaughan, K. T., and Vallee, R. B. (1996). Molecular characterisation of the 50 kDa subunit of dynactin reveals function for the complex in chromosome alignment and spindle organisation during mitosis. J Cell Biol *132*, 617-633.

Erickson, H. P., and Stoffler, D. (1996). Protofilaments and rings, two conformations of the tubulin family conserved from bacterial FtsZ to alpha/beta and gamma tubulin. J Cell Biol *135*, 5-8.

Eto, M., Elliott, E., Prickett, T. D., and Brautigan, D. L. (2002). Inhibitor-2 regulates protein phosphatase-1 complexed with NimA-related kinase to induce centrosome separation. J Biol Chem *6*, 6.

Euteneuer, U., and Schliwa, M. (1985). Evidence for an involvement of actin in the positioning and motility of centrosomes. J Cell Biol *101*, 96-103.

Fabunmi, R. P., Wigley, W. C., Thomas, P. J., and DeMartino, G. N. (2000). Activity and regulation of the centrosome-associated proteosome. J Biol Chem *275*, 409-413.

Fang, G., Yu, H., and Kirschner, M. (1998b). The checkpoint protein MAD2 and the mitotic regulator CDC20 form a ternary complex with the anaphase-promoting complex to control anaphase initiation. Genes Dev *12*, 1871-1883.

Faulkner, N. E., Dujardin, D. L., Tai, C. Y., Vaughan, K. T., O'Connell, C. B., Wan, Y., and Vallee, R. B. (2000). A role for the lisencephaly gene LIS1 in mitosis and cytoplasmic dynein function. Nat Cell Biol *2*, 784-791.

Felix, M. A., Antony, C., Wright, M., and Maro, B. (1994). Centrosome assembly *in vitro*: role of gamma-tubulin recruitment in *Xenopus* sperm aster formation. J Cell Biol *124*, 19-31.

Fenteany, G., Standaart, R. F., Lane, W. S., Choi, S., Corey, E. J., and Schrieber, S. L. (1995). Inhibition of proteosome activities and subunit-specific amino-terminal thronine modification by lactacystin. Science *268*, 726-731.

Fields, S., and Song, O. (1989). A novel genetic system to detect protein-protein interactions. Nature *340*, 245-246.

Fisk, H. A., and Winey, M. (2001). The mouse Mps1p-like kinase Regulates Centrosome Duplication. Cell *106*, 95-104.

Floyd, Z. E., Trausch-azar, J. S., Reinstein, E., Ciechanover, A., and Schwartz, A. L. (2001). The nuclear ubiquitin-proteosome system degrades MyoD. J Biol Chem *276*, 22468-22475.

Freed, E., Lacey, K. R., Huie, P., Lyapina, S. A., Deshaies, R. J., Stearns, T., and Jackson, P. K. (1999). Components of the SCF ubiquitin ligase localise to the centrosome and regulate the centrosome duplication cycle. Genes Dev *13*, 2242-2257.

Fry, A. M. (2002). The Nek2 protein kinase: a novel regulator of centrosome structure. Oncogene *21*, 6184-6194.

Fry, A. M., Arnaud, L., and Nigg, E. A. (1999). Activity of the human centrosomal kinase, Nek2, depends upon an unusual leucine zipper dimerisation motif. J Biol Chem *274*, 16304-16310.

Fry, A. M., Descombes, P., Twomey, C., Bacchieri, R., and Nigg, E. A. (2000b). The NIMA-related kinase X-Nek2B is required for efficient assembly of the zygotic centrosome in *Xenopus laevis*. J Cell Sci *113*, 1973-1984.

Fry, A. M., Mayor, T., Meraldi, P., Stierhof, Y.-D., Tanaka, K., and Nigg, E. A. (1998b). C-Nap1, a novel centrosomal coiled-coil protein and candidate substrate of the cell cycle-regulated protein kinase Nek2. J Cell Biol *141*, 1563-1574.

Fry, A. M., Mayor, T., and Nigg, E. A. (2000a). Regulating centrosomes by protein phosphorylation. Curr Top Dev Biol *49*, 291-312.

Fry, A. M., Meraldi, P., and Nigg, E. A. (1998a). A centrosomal function for the human Nek2 protein kinase, a member of the NIMA-family of cell cycle regulators. EMBO J *17*, 470-481.

Fry, A. M., and Nigg, E. A. (1997). Characterization of mammalian NIMA-related kinases. Methods Enzymol *283*, 270-282.

Fry, A. M., Schultz, S. J., Bartek, J., and Nigg, E. A. (1995). Substrate specificity and cell cycle regulation of the Nek2 protein kinase, a potential human homolog of the mitotic regulator NIMA of *Aspergillus nidulans*. J Biol Chem *2705*, 12899-12905.

Fujioka, T., Takebayashi, Y., Ito, M., and Uchida, T. (2000). Nek2 expression and localisation in porcine oocyte during maturation. Biochem Biophys Res Comm *279*, 799-802.

Fuller, S. D., Gowen, B. E., Reinsch, S., Sawyer, A., Buendia, B., Wepf, R., and Karsenti, E. (1995). The core of the mammalian centriole contains gamma-tubulin. Curr Biol *5*, 1384-1393.

Gaglio, T., Dionne, M. A., and Compton, D. A. (1997). Mitotic spindle poles are organised by structural and motor proteins in addition to centrosomes. J Cell Biol *138*, 1055-1066.

Gard, D. L. (1992). Microtubule organisation during maturation of *Xenopus* oocytes: assembly and rotation of the meiotic spindles. Dev Biol *151*, 516-530.

Geley, S., Kramer, E., Gieffers, C., Gannon, J., Peters, J.-M., and Hunt, T. (2001). Anaphase-promoting complex/cyclosome-dependent proteolysis of human cyclin A starts at the beginning of mitosis and is not subject to the spindle assembly checkpoint. J Cell Biol *153*, 137-147.

Gergely, F., Karlsson, C., Still, I., Cowell, J., Kilmartin, J., and Raff, J. W. (2000a). The TACC domain identifies a family of centrosomal proteins that can interact with microtubules. Proc Natl Acad Sci (USA) *97*, 14352-14357.

Gergely, F., Kidd, D., Jeffers, K., Wakefield, J. G., and Raff, J. W. (2000b). D-TACC: a novel centrosomal protein required for normal spindle function in the early *Drosophila* embryo. Embo J *19*, 241-252.

Ghadimi, B. M., Sackett, D. L., Difilippantonio, M. J., Schock, E., Neumann, T., Jauho, A., Auer, G., and Reid, T. (2000). Centrosome amplification and instability occurs exclusively in aneuploid, but not diploid colorectal cancer cell lines, and correlates with numerical chromosomal abberations. Genes, Chromosomes and Cancer *27*, 183-190.

Ghosh, S., Paweletz, N., and Schroeter, D. (1998). Cdc2-independent induction of premature mitosis by okadaic acid in HeLa cells. Exp Cell Res *242*, 1-9.

Giet, R., and Glover, D. M. (2001). *Drosophila* aurora B kinase is required for histone H3 phosphorylation and condensin recruitment during chromosome condensation and to organize the central spindle during cytokinesis. J Cell Biol *152*, 669-682.

Giet, R., McLean, D., Descamps, S., Lee, M. J., Raff, J. W., Prigent, C., and Glover, D. M. (2002). *Drosophila* Aurora A kinase is required to localise D-TACC to centrosomes and to regulate astral microtubules. J Cell Biol *156*, 437-451.

Giet, R., and Prigent, C. (2001). The non-catalytic domain of the *Xenopus laevis* Aurora A kinase localises the protein to the centrosome. J Cell Sci *114*, 2095-2104.

Giet, R., Uzbekov, R., Cubizolles, F., Le Guellec, K., and Prigent, C. (1999a). The *Xenopus laevis* aurora-related protein kinase pEg2 associates with and phosphorylates the kinesin-related protein XlEg5. J Biol Chem *274*, 15005-15013.

Giet, R., Uzbekov, R., Kireev, I., and Prigent, C. (1999b). The *Xenopus laevis* centrosome aurora/Ipl1-related kinase. Biol Cell *91*, 461-470.

Glotzer, M. (2001). Animal cell cytokinesis. Ann Rev Cell Dev Biol *17*, 351-386.

Glotzer, M., Murray, A., W., and Kirschner, M. W. (1991). Cyclin is degraded by the ubiquitin pathway. Nature *349*, 132-138.

Glover, D. M., Hagan, I. M., and Tavares, A. A. (1998). Polo-like kinases: a team that plays throughout mitosis. Genes Dev *12*, 3777-3787.

Glover, D. M., Leibowitz, M. H., McLean, D. A., and Parry, H. (1995). Mutations in aurora prevent centrosome separation leading to the formation of monopolar spindles. Cell *81*, 95-105.

Goepfert, T. M., Adigun, Y. E., Zhong, L., Gay, J., Medina, D., and Brinkley, W. R. (2002). Centrosome amplification and overexpression of aurora A are early events in rat mammary carcinogenesis. Cancer Res *62*, 4115-4122.

Golsteyn, R. M., Schultz, S. J., Bartek, J., Ziemieck, A., Ried, T., and Nigg, E. A. (1994). Cell cycle analysis and chromosomal localisation of human Plk1, a putative homologue of the mitotic kinases *Drosophila* polo and *Saccharomyces cerevisiae* Cdc5. J Cell Sci *107*, 1509-1517.

Graf, J.-D., and Kobel, H. R. (1991). Genetics of *Xenopus laevis*. Methods Cell Biol *36*, 19-34.

Graf, R. (2002). DdNek2, the first non-vertebrate homologue of human Nek2, is involved in the formation of microtubule-organizing centers. J Cell Sci *115*, 1919-1929.

Grallert, A., and Hagan, I. M. (2002). *S. pombe* NIMA related kinase, Fin1, regulates spindle formation, and an affinity of Polo for the SPB. EMBO J *21*, 3096-3107.

Gruss, O. J., Carazo-Salas, R. E., Schatz, C. A., Guarguaglini, G., Kast, J., Wilm, M., Le Bot, N., Vernos, I., Karsenti, E., and Mattaj, I. W. (2001). Ran induces spindle assembly by reversing the inhibitory effect of importin alpha on TPX2 activity. Cell *104*, 83-93.

Ha Kim, Y., Yeol Choi, J., Jeong, Y., Wolgemuth, D. J., and Rhee, K. (2002). Nek2 localises to multiple sites in mitotic cells, suggesting its involvement in multiple cellular functions during the cell cycle. Biochem Biophys Res Commun *290*, 730-736.

Hames, R. S., and Fry, A. M. (2002). Alternative splice variants of the human centrosomal kinase Nek2 exhibit distinct patterns of expression in mitosis. Biochem J *361*, 77-85.

Hames, R. S., Wattam, S. L., Yamano, H., Bacchieri, R., and Fry, A. M. (2001). APC/C-mediated destruction of the centrosomal kinase Nek2A occurs in early mitosis and depends upon a cyclin A-type D-box. EMBO J *20*, 7117-7127.

Hanks, S. K., and Hunter, T. (1995). The eukaryotic protein kinase superfamily: kinase (catalytic) domain structure and classification. FASEB J *9*, 576-596.

Hannak, E., Kirkham, M., Hyman, A. A., and Oegema, K. (2001). Aurora-A kinase is required for centrosome maturation in *Caenorhabditis elegans*. J Cell Biol *155*, 1109-1116.

Heald, R. (2000). Motor function in the mitotic spindle. Cell *102*, 399-402.

Heald, R., and Nogales, E. (2002). Microtubule dynamics. J Cell Sci *115*, 3-4.

Heald, R., Tournebize, R., Blank, T., Sandaltzopoulos, R., Becker, P., Hyman, A., and Karsenti, E. (1996). Self-organisation of microtubules into bipolar spindle around artificial chromosomes in *Xenopus* egg extracts. Nature *382*, 420-425.

Heald, R., Tournebize, R., Habermann, A., Karsenti, E., and Hyman, A. (1997). Spindle assembly in *Xenopus* egg extracts: respective roles of centrosomes and microtubule self-organisation. J Cell Biol *138*, 615-628.

Helps, N. R., Brewis, N. D., Lineruth, K., Davis, T., Kaiser, K., and Cohen, P. T. (1998). Protein phosphatase 4 is an essential enzyme required for organisation of microtubules at centrosomes in *Drosophila* embryos. J Cell Sci *111*, 1331-1340.

Helps, N. R., Luo, X., Barker, H. M., and Cohen, P. T. W. (2000). NIMA-related kinase 2 (Nek2), a cell cycle-regulated protein kinase localised to centrosomes, is complexed to protein phosphatase 1. Biochem J *349*, 509-518.

Hershko, A., and Ciechanover, A. (1998). The ubiquitin system. Ann Rev Biochem *76*, 425-479.

Hinchcliffe, E. H., Li, C., Thompson, E. A., Maller, J. L., and Sluder, G. (1999). Requirement of Cdk2-cyclin E activity for repeated centrosome reproduction in *Xenopus* egg extracts. Science *283*, 851-854.

Hinchcliffe, E. H., Miller, F. J., Cham, M., Khodjakov, A., and Sluder, G. (2001). Requirement of a centrosomal activity for cell cycle progression through G1 into S phase. Science *291*, 1547-1550.

Hinchcliffe, E. H., and Sluder, G. (2001). Centrosome duplication: three kinases come up a winner! Curr Biol *11*, R698-701.

Holland, P. M., Milne, A., Garka, K., Johnson, R. S., Willis, C., Sims, J. E., Rauch, C. T., Bird, T. A., and Duke Virca, G. (2002). Purification, cloning and characterization of Nek8, a novel NIMA-related kinase, and its candidate substrate Bicd2. J Biol Chem *277*, 16229-16240.

Hollander, M. C., Sheikh, M. S., Bulavin, D. V., Lundgren, K., Augeri-Henmueller, L., Shehee, R., Molinaro, T. A., Kim, K. E., Tolosa, E., Ashwell, J. D., *et al.* (1999). Genomic instability in Gadd45a-deficient mice. Nat Genet *23*, 176-184.

Hoyt, M. A. (2000). Exit from mitosis: spindle pole power. Cell *102*, 267-270.

Hsu, J. Y., Reimann, J. D. R., Sorensen, C. S., Lukas, J., and Jackson, P. K. (2002). E2F-dependent accumulation of hEmi1 regulates S phase entry by inhibiting APC^{Cdh1}. Nat Cell Biol *4*, 358-366.

Hu, H. M., Chuang, C. K., Lee, M. J., Tseng, T. C., and Tang, T. K. (2000). Genomic organisation, expression, and chromosome localisation of a third aurora-related kinase gene, Aie1. DNA Cell Biol *19*, 679-688.

Huang, J.-Y., and Raff, J. W. (2002). The dynamic localisation of the *Drosophila* APC/C: evidence for the existence of multiple complexes that perform distinct functions and are differentially localised. J Cell Sci *115*, 2847-2856.

Iyer, V. R., Eisen, M. B., Ross, D. T., Schuler, G., Moore, T., Lee, J. C., Trent, J. M., Staudt, L. M., Hudson, J., and Boguski, M. S. (1999). The transcriptional program in the response of human fibroblasts to serum. Science *283*, 83-87.

Jackson, P. K., Eldridge, A. G., Freed, E., Furstenthal, L., Hsu, J. Y., Kaiser, B. K., and Reimann, J. D. R. (2000). The lore of the RINGs: substrate recognition and catalysis by ubiquitin ligases. Trends Cell Biol *10*, 429-439.

James, P., Halladay, J., and Craig, E. A. (1996). Genomic libraries and a host strain designed for highly efficient two-hybrid selection in yeast. Genetics *144*, 1425-1436.

Jean, C., Tollon, Y., Raynaud-Messina, B., and Wright, M. (1999). The mammalian interphase centrosome: two independent units maintained together by the dynamics of the microtubule cytoskeleton. Eur J Cell Biol *78*, 549-560.

Jones, D. G., and Rosamond, J. (1990). Isolation of a novel protein kinase-encoding gene from yeast by oligodeoxyribonucleotide probing. Gene *90*, 87-92.

Joshi, H. C., and Palevitz, B. A. (1996). g-Tubulin and microtubule organisation in plants. Trends Cell Biol *6*, 41-44.

Kaitna, S., Mendoza, M., Jantsch-Plunger, V., and Glotzer, M. (2000). INCENP and an aurora-like kinase form a complex essential for chromosome segregation and efficient completion of cytokinesis. Curr Biol *10*, 1172-1781.

Kandli, M., Feige, E., Chen, A., Kilfin, G., and Motro, B. (2000). Isolation and characterization of two evolutionarily conserved murine kinases (Nek6 and Nek7) related to the fungal mitotic regulator, NIMA. Genomics *68*, 187-196.

Kapoor, T. M., Mayer, T. U., Coughlin, M. L., and Mitchison, T. J. (2000). Probing spindle assembly mechanisms with monastrol, a small molecule inhibitor of the mitotic kinesin, Eg5. J Cell Biol *150*, 975-988.

Karki, S., and Holzbaur, E. L. F. (1995). Affinity chromatography demonstrates a direct binding between cytoplasmic dynein and the dynactin complex. J Biol Chem *270*, 28806-28811.

Karki, S., and Holzbaur, E. L. F. (1999). Cytoplasmic dynein and dynactin in cell division and intracellular transport. Curr Opin Cell Biol *11*, 45-53.

Kashina, A. S., Rogers, G. C., and Scholey, J. M. (1997). The bimC family of kinesins: essential bipolar mitotic motors driving centrosome separation. Biochim Biophys Acta *1357*, 257-271.

Kellogg, D. S., Moritz, M., and Alberts, B. M. (1994). The centrosome and cellular organisation. Ann Rev Biochem *63*, 639-674.

Khodjakov, A., Cole, R. W., Oakley, B. R., and Rieder, C. L. (2000). Centrosome-independent mitotic spindle formation in vertebrates. Curr Biol *10*, 59-67.

Khodjakov, A., and Rieder, C. L. (1999). The sudden recruitment of g-tubulin to the centrosome at the onset of mitosis and its dynamic exchange throughout the cell cycle, do not require microtubules. J Cell Biol *146*, 585-596.

Khodjakov, A., and Rieder, C. L. (2001). Centrosomes enhance the fidelity of cytokinesis in vertebrates and are required for cell cycle progression. J Cell Biol *153*, 237-242.

Khodjakov, A., Rieder, C. L., Sluder, G., Cassels, G., Sibon, O., and Wang, C. L. (2002). *De novo* formation of centrosomes in vertebrate cells arrested during S phase. J Cell Biol *158*, 1171-1181.

Kidd, D., and Raff, J. W. (1997). LK6, a short lived protein kinase in *Drosophila* that can associate with microtubules and centrosomes. J Cell Sci *110*, 209-219.

Kimura, M., Matsuda, Y., Yoshioka, T., and Okano, Y. (1999). Cell cycle-dependent expression and centrosome localisation of a third human aurora/Ipl1-related protein kinase, AIK3. J Biol Chem *274*, 7334-7340.

King, R. W., Peters, J. M., Tugendreich, S., Rolfe, M., Hieter, P., and Kirschner, M. W. (1995). A 20S complex containing CDC27 and CDC16 catalyzes the mitosis-specific conjugation of ubiquitin to cyclin B. Cell *81*, 279-288.

Kishore, G. M., and Shah, D. M. (1988). Amino acid biosynthesis inhibitors as herbicides. Ann Rev Biochem *57*, 627-663.

Knop, M., Pereira, G., and Schiebel, E. (1999). Microtubule organisation by the budding yeast spindle pole body. Biol Cell *4-5*, 291-304.

Kotani, S., Tugendreich, S., Fujii, M., Jorgensen, P.-M., Watanabe, N., Hoog, C., Hieter, P., and Todokoro, K. (1998). PKA and MPF-activated polo-like kinase regulate anaphase promoting complex activity and mitosis progression. Mol Cell *1*, 371-380.

Kramer, E. R., Scheuringer, N., Podtelejnikov, V., Mann, M., and Peters, J.-M. (2000). Mitotic regulation of the APC activator proteins CDC20 and CDH1. Mol Biol Cell *11*, 1555-1569.

Krien, M. J., West, R. R., John, U. P., Koniaras, K., McIntosh, J. R., and O'Connell, M. J. (2002). The fission yeast NIMA kinase Fin1p is required for spindle function and nuclear envelope integrity. EMBO J *21*, 1713-1722.

Krien, M. J. E., Bugg, S. J., Palatsides, M., Asouline, G., Morimyo, M., and O'Connell, M. J. (1998). A NIMA homologue promotes chromatin condensation in fission yeast. J Cell Sci *111*, 967-976.

Kubo, A., Sasaki, H., Yuba-Kubo, A., Tsukita, S., and Shiina, N. (1999). Centriolar satellites: molecular characterization, ATP-dependent movement toward centrioles and possible involvement in ciliogenesis. J Cell Biol *147*, 969-980.

Kumagai, A., and Dunphy, W. G. (1996). Purification and molecular cloning of Plx1, a Cdc25-stimulatory kinase from *Xenopus* egg extracts. Science *273*, 1377-1380.

Kuo, K. K., Sato, N., Mizumoto, K., Maehara, N., Yonemasu, H., Ker, C. G., Sheen, P. C., and Tanaka, M. (2000). Centrosome abnormalities in human carcinomas of the gallbladder and intrahepatic and extrahepatic bile ducts. Hepatology *31*, 59-64.

Lacey, K. R., Jackson, P. K., and Stearns, T. (1999). Cyclin-dependant kinase control of centrosome duplication. Proc Natl Acad Sci (USA) *96*, 2817-2822.

Lane, H. A., and Nigg, E. A. (1996). Antibody microinjection reveals an essential role for human polo-like kinase 1 (Plk1) in the functional maturation of mitotic centrosomes. J Cell Biol *135*, 1701-1713.

Lange, B. M. H. (2002). Integration of the centrosome in cell cycle control, stress response and signal transduction pathways. Curr Opin Cell Biol *14*, 35-43.

Lange, B. M. H., and Gull, K. (1995). A molecular marker for centriole maturation in the mammalian cell cycle. J Cell Biol *130*, 919-927.

Lange, B. M. H., and Gull, K. (1996). Structure and function of the centriole in animal cells - progress and questions. Trends Cell Biol *6*, 348-352.

Lee, D. H., and Goldberg, A. L. (1998). Proteasome inhibitors: valuable new tools for cell biologists. Trends Cell Biol *8*, 397-403.

Lee, I., Tirnauer, J., Li, S. C., Schuyler, J. Y., Liu, L., and Pellman, D. (2000). Positioning of the mitotic spindle by a cortical-microtubule capture mechanism. Science *287*, 2260-2262.

Lee, M. J., Gergely, F., Jeffers, K., Peak-Chew, S. Y., and Raff, J. W. (2001). Msps/XMAP215 interacts with the centrosomal protein D-TACC to regulate microtubule behaviour. Nat Cell Biol *3*, 643-649.

Letwin, K., Mizzen, L., Motro, B., Ben-David, Y., Bernstein, A., and Pawson, T. (1992). A mammalian dual specificity protein kinase, Nek1, is related to the NIMA cell cycle regulator and highly exprssed in meiotic germ cells. EMBO J *11*, 3521-3531.

Li, Q., Hansen, D., Killilea, A., Joshi, H. C., Palazzo, R. E., and Balczon, R. (2001). Kendrin/pericentrin-B, a centrosome protein with homology to pericentrin that complexes with PCM-1. J Cell Sci *114*, 797-809.

Lingle, W. L., Barrett, S. L., Negron, V. C., D'Assoro, A. B., Boeneman, K., Liu, W., Whitehead, C. M., Reynolds, C., and Salisbury, J. L. (2002). Centrosome amplification drives chromosomal instability in breast tumour development. Proc Natl Acad Sci (USA) *99*, 1978-1983.

Lingle, W. L., Lutz, W. H., ingle, J. N., Maihle, N. J., and Salisbury, J. L. (1998). Centrosome hypertrophy in human breast tumours: implications for genomic stability and cell polarity. Proc Natl Acad Sci (USA) *95*, 2950-2955.

Lizcano, J. M., Deak, M., Morrice, N., Kieloch, A., Hastie, C. J., Dong, L., Schutkowski, M., Reimer, U., and Alessi, D. R. (2002). Molecular basis for the substrate specificity of NIMA-related kinase-6 (NEK6). Evidence that NEK6 does not phosphorylate the hydrophobic motif of ribosomal S6 protein kinase and serum- and glucocorticoid-induced protein kinase *in vivo*. J Biol Chem *277*, 27839-27849.

Lorca, T., Castro, A., Martinez, A.-M., Morin, N., Sigrist, S., Lehner, C., Doree, M., and Labbe, J.-C. (1998). Fizzy is required for activation of the APC-cyclosome in *Xenopus* egg extracts. EMBO J *17*, 3565-3575.

Lu, K. P., and Hunter, T. (1995). The NIMA kinase: a mitotic regulator in *Aspergillus nidulans* and vertebrate cells. In Progress in Cell Cycle Research, L. Meijer, S. Guidet, and H. Y. L. Tung, eds. (New York, Plenum Press), pp. 187-205.

Lu, K. P., Osmani, S. A., and Means, A. R. (1993). Properties and regulation of the cell cycle-specific NIMA protein kinase of *Aspergillus nidulans*. J Biol Chem *268*, 8769-8776.

Lutz, W., Lingle, W. L., McCormick, D., Greenwood, T. M., and Salisbury, J. L. (2001). Phosphorylation of centrin during the cell cycle and its role in centriole separation preceding centrosome duplication. J Biol Chem *276*, 20774-20780.

Mack, G. J., Rees, J., Sandblom, O., Balczon, R., Fritzler, M. J., and Rattner, J. B. (1998). Autoantibodies to a group of centrosomal proteins in human autoimmune sera reactive with the centrosome. Arthritis and Rheumatology *41*, 551-558.

Mahjoub, M. R., Montpetit, B., Zhao, L., Finst, R. J., Goh, B., Kim, A. C., and L.M., Q. (2002). The *FA2* gene of *Chlamydomonas* encodes a NIMA family kinase with roles in cell cycle progression and microtubule severing during deflagellation. J Cell Sci *115*, 1759-1768.

Mandelkow, E., and Mandelkow, E. M. (1995). Microtubules and microtubule-associated proteins. Curr Opin Cell Biol *7*, 72-81.

Mandelkow, E.-M., and Mandelkow, E. (1993). Tau as a marker for Alzheimer's disease. Trends Biochem Sci *18*, 480-483.

Marshall, W. F. (2002). Putting Nek into the cellular guillotine. Trends Cell Biol *12*, 358.

Matsumoto, Y., Hayashi, K., and Nishida, E. (1999). Cyclin-dependent kinase 2 (Cdk2) is required for centrosome duplication in mammalian cells. Curr Biol *9*, 429-432.

Matsumoto, Y., and Maller, J. L. (2002). Calcium, calmodulin, and CaMKII requirement for initiation of centrosome duplication in *Xenopus* egg extracts. Science *295*, 499-502.

Matthies, H. J., McDonald, H. B., Goldstein, L. S., and Theurkauf, W. E. (1996). Anastral meiotic spindle morphogenesis: role of the non-claret disjunctional kinesin-like protein. J Cell Biol *134*, 455-464.

Mayor, T., Hacker, U., Stierhof, Y. D., and Nigg, E. A. (2002). The mechanism regulating the dissociation of the centrosomal protein C-Nap1 from mitotic spindle poles. J Cell Sci *115*, 3275-3284.

Mayor, T., Meraldi, P., Stierhof, Y.-D., Nigg, E. A., and Fry, A. M. (1999). Protein kinases in control of the centrosome cycle. FEBS Letters *452*, 92-95.

Mayor, T., Stierhof, Y. D., Tanaka, K., Fry, A. M., and Nigg, E. A. (2000). The centrosomal protein C-Nap1 is required for cell cycle-regulated centrosome cohesion. J Cell Biol *151*, 837-846.

McGarry, T. J., and Kirschner, M. W. (1998). Geminin, an inhibitor of DNA replication, is degraded during mitosis. Cell *93*, 1043-1053.

McIntosh, J. R., and Euteneuer, U. (1984). Tubulin hooks as probes for microtubule polarity: and analysis of the method and an evaluation of data on microtubule polarity in the mitotic spindle. J Cell Biol *98*, 525-533.

McNally, F. J., and Thomas, S. (1998). Katanin is responsible for the M-phase microtubule-severing activity in *Xenopus* eggs. Mol Biol Cell *9*, 1847-1861.

McNally, K. P., Bazirgan, O. A., and McNally, F. J. (2000). Two domains of p80 katanin regulate microtubule severing and spindle pole targeting by p60 katanin. J Cell Sci *113*, 1623-1633.

Megraw, T. L., Kao, L.-R., and Kaufman, T. (2001). Zygotic development without functional mitotic centrosomes. Curr Biol *11*, 116-120.

Melby, T. E., Ciampaglio, C. N., Briscoe, G., and Erickson, H. P. (1998). The symmetrical structure of structural maintenance of chromosomes (SMC) and MukB proteins: long, antiparallel coiled coils folded at a flexible hinge. J Cell Biol *142*, 1595-1604.

Menz, K., Radomski, N., and Jost, E. (1996). INMP, a novel intranuclear matrix protein related to the family of intermediate filament like proteins: molecular cloning and sequence analysis. Biochim Biophys Acta *1309*, 14-20.

Meraldi, P., Honda, R., and Nigg, E. A. (2002). Aurora-A overexpression reveals tetraploidization as a major route to centrosome amplification in p53-/- cells. Embo J *21*, 483-492.

Meraldi, P., Lukas, C., Fry, A. M., Bartek, J., and Nigg, E. A. (1999). Centrosome duplication in mammalian somatic cells requires E2F and Cdk2-Cyclin A. Nat Cell Biol *1*, 88-93.

Meraldi, P., and Nigg, E. A. (2001). Centrosome cohesion is regulated by a balance of kinase and phosphatase activities. J Cell Sci *114*, 3749-3757.

Merdes, A., and Cleveland, D. W. (1997). Pathways of spindle pole formation: different mechanisms, conserved components. J Cell Biol *138*, 953-956.

Merdes, A., Heald, R., Samejima, K., Earnshaw, W. C., and Cleveland, D. W. (2000). Formation of spindle poles by dynein/dynactin-dependent transport of NuMA. J Cell Biol *149*, 851-862.

Merdes, A., Ramyar, K., Vechio, J. D., and Cleveland, D. W. (1996). A complex of NuMA and cytoplasmic dynein is essential for mitotic spindle assembly. Cell *87*, 447-458.

Minshull, J., Sun, H., Tonks, N. K., and Murray, A. W. (1994). A MAP kinase-dependent spindle assembly checkpoint in *Xenopus* egg extracts. Cell *79*, 475-486.

Mitchison, T., and Kirschner, M. (1984). Microtubule assembly nucleated by isolated centrosomes. Nature *312*, 232-237.

Mitchison, T. J. (1993). Localisation of an exchangeable GTP binding site at the plus end of microtubules. Science *261*, 1044-1047.

Mogensen, M. M., Mackie, J. B., Doxsey, S. J., Stearns, T., and Tucker, J. B. (1997). Centrosomal deployment of gamma-tubulin and pericentrin: evidence for a microtubule-nucleating domain and a minus-end docking domain in certain mouse epithelial cells. Cell Motil Cytoskeleton *36*, 276-290.

Mogensen, M. M., Malik, A., Piel, M., Bouckson-Castaing, V., and Bornens, M. (2000). Microtubule minus-end anchorage at centrosomal and non-centrosomal sites: the role of ninein. J Cell Sci *113*, 3013-3023.

Morgan, D. O. (1999). Regulation of the APC and the exit from mitosis. Nat Cell Biol *1*, E47-E53.

Moritz, M., Braunfeld, M. B., Guenebaut, V., Heuser, J., and Agard, D. A. (2000). Structure of the g-tubulin ring complex: a template for microtubule nucleation. Nat Cell Biol *2*, 365-370.

Moritz, M., Zheng, Y., Alberts, B. M., and Oegema, K. (1998). Recruitment of the g-tubulin ring complex to *Drosophila* salt-stripped centrosome scaffolds. J Cell Biol *142*, 775-786.

Moudjou, M., Bordes, N., Paintrand, M., and Bornens, M. (1996). Gamma-tubulin in mammalian-cells - the centrosomal and the cytosolic forms. J Cell Sci *109*, 875-887.

Moudjou, M., and Bornens, M. (1994). Isolation of centrosomes from cultured animal cells. In Cell Biology: a laboratory handbook, J. E. Celis, ed. (London, Academic Press Inc.), pp. 595-604.

Mountain, V., Simerly, C., Howard, L., Ando, A., Schatten, G., and Compton, D. A. (1999). The kinesin-related protein, HSET, opposes the activity of Eg5 and cross-links microtubules in the mammalian mitotic spindle. J Cell Biol *147*, 351-366.

Mundt, K. E., Golsteyn, R. M., Lane, H. A., and Nigg, E. A. (1997). On the regulation and function of human polo-like kinase 1 (PLK1): effects of overexpression on cell cycle progression. Biochem Biophys Res Commun *239*, 377-385.

Nakagawa, Y., Yamane, Y., Okanoue, T., Tsukita, S., and Tsukita, S. (2001). Outer dense fiber 2 is a widespread centrosome scaffold component preferentially associated with mother centrioles: its identification from isolated centrosomes. Mol Biol Cell *12*, 1687-1697.

Nicklas, R. B. (1997). How cells get the right chromosomes. Science *275*, 632-637.

Nigg, E. A. (1995). Cyclin-dependent protein kinases: key regulators of the eukaryotic cell cycle. Bioessays *17*, 471-480.

Nigg, E. A. (1998). Polo-like kinases: positive regulators of cell division from start to finish. Curr Opin Cell Biol *10*, 776-783.

Nigg, E. A. (2001). Mitotic kinases as regulators of cell division and its checkpoints. Nature Revs: Mol Cell Biol 2, 21-32.

Noguchi, K., Fukazawa, H., Murakami, Y., and Uehara, Y. (2002). Nek11, A new member of the NIMA family of kinases, involved in DNA replication and genotoxic stress responses. J Biol Chem *277*, 39656-39665.

Norbury, C., and Nurse, P. (1992). Animal cell cycles and their control. Annu Rev Biochem *61*, 441-470.

Nurse, P. (1990). Universal control mechanism regulating onset of M-phase. Nature *344*, 503-508.

O'Brian, K. P., Tapia-Paez, I., Stahle-Backdahl, M., Kedra, D., and Dumanski, J. P. (2000). Characterisation of five novel human genes in the 11q13-q22 region. Biochem Biophys Res Commun *273*, 90-94.

O'Connell, C. B., and Wang, Y. L. (2000). Mammalian spindle orientation and position respond to changes in cell shape in a dynein-dependent fashion. Mol Biol Cell *11*, 1765-1774.

O'Connell, K. F. (2002). The ZYG-1 kinase, a mitotic and meiotic regulator of centriole replication. Oncogene *21*, 6201-6208.

O'Connell, K. F., Caron, C., Kopish, K. R., Hurd, D. D., Kemphues, K. J., Li, Y., and White, J. G. (2001). The *C. elegans zyg-1* gene encodes a regulator of centrosome duplication with distinct maternal and paternal roles in the embryo. Cell *105*, 547-558.

O'Connell, M. J., Norbury, C., and Nurse, P. (1994). Premature chromatin condensation upon accumulation of NIMA. EMBO J *13*, 4926-4937.

Oakley, B. R., and Morris, N. R. (1983). A mutation in *Aspergillus nidulans* that blocks the transition from interphase to prophase. J Cell Biol *96*, 1155-1158.

Oegema, K., Wiese, C., Martin, O. C., Milligan, R. A., Iwamatsu, A., Mitchison, T. J., and Zheng, Y. (1999). Characterisation of two related *Drosophila* gamma-tubulin complexes that differ in their ability to nucleate microtubules. J Cell Biol *144*, 721-33.

Ohba, T., Nakamura, M., Nishitani, H., and Nishimoto, T. (1999). Self-organisation of microtubule asters induced in *Xenopus* egg extracts by GTP-bound Ran. Science *284*, 1356-1358.

Ohkura, H., Hagan, I. M., and Glover, D. M. (1995). The conserved *Schizosaccharomyces pombe* kinase plo1, required to form a bipolar spindle, the actin ring, and septum, can drive septum formation in G1 and G2 cells. Genes Dev *9*, 1059-1073.

Ohta, K., Shiina, N., Okumura, E., Hisanaga, S., Kishimoto, T., Endo, S., Gotoh, Y., Nishida, E., and Sakai, H. (1993). Microtubule nucleating activity of centrosomes in cell-free-extracts from *Xenopus* eggs: involvement of phosphorylation and accumulation of pericentriolar material. J Cell Sci *104*, 125-137.

Okuda, M., Horn, H. F., Tarapore, P., Tokuyama, Y., Smulian, A. G., Chan, P.-K., Knudsen, E. S., Hofmann, I. A., Snyder, J. D., Bove, K. E., and Fukasawa, K. (2000). Nucleophosmin/B23 is a target of CDK2/Cyclin E in centrosome duplication. Cell *103*, 127-140.

Osmani, A. H., McGuire, S. L., and Osmani, S. A. (1991a). Parallel activation of the NIMA and p34cdc2 cell cycle-regulated protein kinases is required to initiate mitosis in *A. nidulans*. Cell *67*, 283-291.

Osmani, A. H., O'Donnell, K., Pu, R. T., and Osmani, S. A. (1991b). Activation of the nimA protein kinase plays a unique role during mitosis that cannot be bypassed by absence of the bimE checkpoint. Embo J *10*, 2669-2679.

Osmani, S. A., May, G. S., and Morris, N. R. (1987). Regulation of the mRNA levels of *nimA*, a gene required for the G2-M transition in *Aspergillus nidulans*. J Cell Biol *104*, 1495-1504.

Osmani, S. A., Pu, R. T., and Morris, N. R. (1988). Mitotic induction and maintenance by overexpression of a G2-specific gene that encodes a potential protein kinase. Cell *53*, 237-244.

Osmani, S. A., and Ye, X. S. (1996). Cell cycle regulation in *Aspergillus* by two protein kinases. Biochem J *317*, 633-641.

Ou, Y. Y., Mack, G. J., Zhang, M., and Rattner, J. B. (2002). CEP110 and ninein are located in a specific domain of the centrosome associated with centrosome maturation. J Cell Sci *115*, 1825-1835.

Page, A. M., and Hieter, P. (1999). The anaphase-promoting complex: new subunits and regulators. Ann Rev Biochem *68*, 583-609.

Paintrand, M., Moudjou, M., Delacroix, H., and Bornens, M. (1992). Centrosome organisation and centriole architecture: their sensitivity to divalent cations. J Struct Biol *108*, 107-128.

Pazour, G. J., Dickert, B. L., Vucica, Y., Seeley, E. S., Rosenbaum, J. L., Witman, G. B., and Cole, D. G. (2000). *Chlamydomonas* IFT88 and its mouse homologue, polycystic kidney disease gene tg737, are required for assembly of cilia and flagella. J Cell Biol *151*, 709-718.

Pereira, G., Hofken, T., Grindlay, J., Manson, C., and Schiebel, E. (2000). The Bub2p spindle checkpoint links nuclear migration with mitotic exit. Mol Cell *6*, 1-10.

Pereira, G., Knop, M., and Schiebel, E. (1998). Spc98p directs the yeast gamma-tubulin complex into the nucleus and is subject to cell cycle-dependent phosphorylation on the nuclear side of the spindle pole body. Mol Biol Cell *9*, 775-793.

Pereira, G., Tanaka, T. U., Nasmyth, K., and Schiebel, E. (2001). Modes of spindle pole body inheritance and segregation of the Bfa1p-Bub2p checkpoint protein complex. EMBO J *20*, 6359-6370.

Peters, J.-M. (1998). SCF and APC: the Yin and Yang of cell cycle regulated proteolysis. Curr Opin Cell Biol *10*, 759-768.

Petersen, J., Paris, J., Willer, M., Philippe, M., and Hagan, I. M. (2001). The *S. pombe* aurora-related kinase Ark1 associates with mitotic structures in a stage dependent manner and is required for chromosome segregation. J Cell Sci *114*, 4371-4384.

Pfleger, C. M., and Kirschner, M. W. (2000). The KEN box: an APC recognition signal distinct from the D box targeted by Cdh1. Genes Dev *14*, 655-665.

Pfleger, C. M., Salic, A., Lee, E., and Kirschner, M. (2001). Inhibition of Cdh1-APC by the MAD2-related protein MAD2L2: a novel mechanism for regulating Cdh1. Genes Dev *15*, 1759-1764.

Pickett-Heaps, J. D., Tippit, D. H., and Porter, K. R. (1982). Rethinking mitosis. Cell *29*, 729-744.

Piel, M., Meyer, P., Khodjakov, A., Rieder, C. L., and Bornens, M. (2000). The respective contributions of the mother and daughter centrioles to centrosome activity and behaviour in vertebrate cells. J Cell Biol *149*, 317-329.

Piel, M., Nordberg, J., Euteneuer, U., and Bornens, M. (2001). Centrosome-dependent exit of cytokinesis in animal cells. Science *291*, 1550-1553.

Pihan, G. A., and Doxsey, S. J. (1999). The mitotic machinery as a source of genetic instability in cancer. Cancer Biol *9*, 289-302.

Pihan, G. A., Purohit, A., Wallace, J., Malhotra, R., Liotta, L., and Doxsey, S. J. (2001). Centrosome defects can account for cellular and genetic changes that characterise prostate cancer progression. Cancer Res *61*, 2212-2219.

Pines, J., and Rieder, C. L. (2001). Re-staging mitosis: a contemporary view of mitotic progression. Nat Cell Biol *3*, E3-E6.

Pu, R. T., and Osmani, S. A. (1995). Mitotic destruction of the cell cycle regulated NIMA protein kinase of *Aspergillus nidulans* is required for mitotic exit. EMBO J *14*, 995-1003.

Pu, R. T., Xu, G., Wu, L., Vierula, J., O'Donnell, K., Ye, X. S., and Osmani, S. A. (1995). Isolation of a functional homologue of the cell cycle-specific NIMA protein kinase of *Aspergillus nidulans* and functional analysis of conserved residues. J Biol Chem *270*, 18110-18116.

Quarmby, L. M., and Lohret, T. A. (1999). Microtubule severing. Cell Motil Cytoskeleton *43*, 1-9.

Quintyne, N. J., Gill, S. R., Eckley, D. M., Crego, C. L., Compton, D. A., and Schroer, T. A. (1999). Dynactin is required for microtubule anchoring at centrosomes. J Cell Biol *147*, 321-334.

Raff, J. W. (2001). Centrosomes: central no more? Curr Biol *11*, R159-R161.

Reimann, J. D. R., Freed, E., Hsu, J. Y., Kramer, E. R., Peters, J.-M., and Jackson, P. K. (2001). Emi1 is a mitotic regulator that interacts with Cdc20 and inhibits the anaphase promoting complex. Cell *105*, 645-655.

Reimann, J. D. R., and Jackson, P. K. (2002). Emi1 is required for cytostatic factor arrest in vertebrate eggs. Nature *416*, 850-854.

Ren, B., Cam, H., Takahashi, Y., Volkert, T., Terragni, J., Young, R. A., and Dynlacht, B. D. (2002). E2F integrates cell cycle progression with DNA repair, replication, and G2/M checkpoints. Genes Dev *16*, 245-256.

Rhee, K., and Wolgemuth, D. J. (1997). The NIMA-related kinase 2, Nek2, is expressed in specific stages of the meiotic cell cycle and associates with meiotic chromosomes. Development *124*, 2167-2177.

Richter, J. D. (1999). Cytoplasmic polyadenylation in development and beyond. Microbiol Mol Biol Rev *63*, 446-456.

Rieder, C. L., Faruki, S., and Khodjakov, A. (2001). The centrosome in vertebrates: more than a microtubule-organizing center. Trends Cell Biol *11*, 413-419.

Rogers, S. L., Rogers, G. C., Sharp, D. J., and Vale, R. D. (2002). *Drosophila* EB1 is important for proper assembly, dynamics and positioning of the mitotic spindle. J Cell Biol *158*, 873-884.

Roghi, C., Giet, R., Uzbekov, R., Morin, N., Chartrain, I., Le Guellec, R., Couturier, A., Doree, M., Philippe, M., and Prigent, C. (1998). The *Xenopus* protein kinase pEg2 associates with the centrosome in a cell cycle-dependent manner, binds to the spindle microtubules and is involved in bipolar mitotic spindle assembly. J Cell Sci *111*, 557-572.

Roig, J., Mikhailov, A., Belham, C., and Avruch, J. (2002). Nercc1, a mammalian NIMA-family kinase, binds the Ran GTPase and regulates mitotic progression. Genes Dev *16*, 1640-1658.

Roshani, L., Fujioka, K., Auer, G., Kjellman, M., Lagercrantz, S., and Larsson, C. (2002). Aberrations of centrosomes in adrenocortical tumours. Int J Oncol *20*, 1161-1165.

Salisbury, J. L. (1995). Centrin, centrosomes, and mitotic spindle poles. Curr Opin Cell Biol *7*, 39-45.

Salisbury, J. L., Whitehead, C. M., Lingle, W. L., and Barrett, S. L. (1999). Centrosomes and cancer. Biol Cell *91*, 451-460.

Sawin, K. E., and Mitchison, T. J. (1995). Mutations in the kinesin-like protein Eg5 disrupting localisation to the mitotic spindle. Proc Natl Acad Sci (USA) *92*, 4289-4293.

Schiebel, E., and Bornens, M. (1995). In search of a function for centrins. Trends Cell Biol *5*, 197-201.

Schmidt, P., Dransfield, D. T., Claudio, J. O., Hawley, R. G., Trotter, K. W., Migram, S. L., and Goldenring, J. R. (1999). AKAP 350, a multiply spliced proteins kinase anchoring protein associated with centrosomes. J Biol Chem *274*, 3055-3066.

Schnackenberg, B. J., Khodjakov, A., Rieder, C. L., and Palazzo, R. E. (1998). The disassembly and reassembly of functional centrosomes *in vitro*. Proc Natl Acad Sci (USA) *95*, 9295-9300.

Schultz, S. J., Fry, A. M., Sütterlin, C., Ried, T., and Nigg, E. A. (1994). Cell cycle-dependent expression of Nek2, a novel human protein kinase related to the NIMA mitotic regulator of *Aspergillus nidulans*. Cell Growth Differ *5*, 625-635.

Schultz, S. J., and Nigg, E. A. (1993). Identification of 21 novel human protein kinases, including 3 members of a family related to the cell cycle regulator *nimA* of *Aspergillus nidulans*. Cell Growth Diff *4*, 821-830.

Schweitzer, B., and Philippsen, P. (1992). NPK1, a nonessential protein kinase gene in *Saccharomyces cerevisiae* with similarity to *Aspergillus nidulans* nimA. Mol Gen Genet *234*, 164-167.

Shah, J. V., and Cleveland, D. W. (2000). Waiting for anaphase: mad2 and the spindle assembly checkpoint. Cell *103*, 997-1000.

Shibaoka, H., and Nagai, R. (1994). The plant cytoskeleton. Curr Opin Cell Biol *6*, 10-15.

Sigrist, S. J., and Lehner, C. F. (1997). *Drosophila* fizzy-related downregulates mitotic cyclins and is required for cell proliferation arrest and entry into endocycles. Cell *90*, 671-681.

Smrzka, O.W., Delgehyr, N., and Bornens, M. (2000). Tissue-specific and subcellular localisation of mammalian δ-tubulin. Curr Biol *10*, 413-416.

Sorokin (1968). Reconstruction of centriole formation and ciliogenesis in mammalian lungs. J Cell Sci *3*, 207-230.

Speliotes, E. K., Uren, A., Vaux, D., and Horvitz, H. R. (2000). The survivin-like *C. elegans* BIR-1 protein acts with the Aurora-like kinase AIR-2 to affect chromosomes and the spindle midzone. Mol Cell *6*, 211-223.

Spruck, C. H., Won, K. A., and Reed, S. I. (1999). Deregulated cyclin E induces chromosome instability. Nature *401*, 297-300.

Stearns, T. (2001). Centrosome duplication. a centriolar pas de deux. Cell *105*, 417-420.

Stearns, T., and Kirschner, M. (1994). *In vitro* reconstitution of centrosome assembly and function: the central role of gamma-tubulin. Cell *76*, 623-637.

Stearns, T., and Winey, M. (1997). The cell center at 100. Cell *91*, 303-309.

Still, I. H., Vince, P., and Cowell, J. K. (1999). The third member of the transforming acidic coiled coil-containing gene family, TACC3, maps in 4p16, close to translocation breakpoints in multiple myeloma, and is upregulated in various cancer cell lines. Genomics *58*, 165-170.

Stucke, V. M., Sillje, H. H., Arnaud, L., and Nigg, E. A. (2002). Human Mps1 kinase is required for the spindle assembly checkpoint but not for centrosome duplication. Embo J *21*, 1723-1732.

Su, L. K., Burrel, D. E., Hill, J., Gyuris, R., Brent, R., Wiltshire, J., Trent, B., Vogelstein, B., and Kinzler, K. W. (1995). APC binds to novel protein EB1. Cancer Res *55*, 2972-2977.

Sudakin, V., Ganoth, D., Dahan, A., Heller, H., Hershko, J., Luca, F. C., Ruderman, J. V., and Hershko, A. (1995). The cyclosome, a large complex containing cyclin-selective ubiquitin ligase activity, targets cyclins for destruction at the end of mitosis. Mol Cell Biol *6*, 185-197.

Sumiyoshi, E., Sugimoto, A., and Yamamoto, M. (2002). Protein phosphatase 4 is required for centrosome maturation in mitosis and sperm meiosis in *C. elegans*. J Cell Sci *115*, 1403-1410.

Sunkel, C. E., and Glover, D. M. (1988). Polo, a mitotic mutant of *Drosophila* displaying abnormal spindle poles. J Cell Sci *89*, 25-38.

Takahashi, M., Yamagiwa, A., Nishimura, T., Mukai, H., and Ono, Y. (2002). Centrosomal proteins CG-NAP and Kendrin provide microtubule nucleation sites by anchoring gamma-tubulin ring complex. Mol Biol Cell *13*, 3235-3245.

Tanaka, K., and Nigg, E. A. (1999). Cloning and characterization of the murine Nek3 protein kinase, a novel member of the NIMA family of putative cell cycle regulators. J Biol Chem *274*, 13491-13497.

Tanaka, K., Parvinen, M., and Nigg, E. A. (1997). The *in vivo* expression pattern of mouse Nek2, a NIMA-related kinase, indicates a role in both mitosis and meiosis. Exp Cell Res *237*, 264-274.

Tarapore, P., Tokuyama, Y., Horn, H. F., and Fukasawa, K. (2001). Difference in the centrosome duplication regulatory activity among p53 'hot spot' mutants: potential role of Ser 315 phosphorylation-dependent centrosome binding of p53. Oncogene *20*, 6851-6863.

Tirnaur, J. S., and Biere, B. E. (2000). EB1 proteins regulate microtubule dynamics, cell polarity and chromosomal instability. J Cell Biol *149*, 761-766.

Tokuyama, Y., Horn, H. F., Kawamura, K., Tarapore, P., and Fukasawa, K. (2001). Specific phosphorylation of nucleophosmin on Thr(199) by cyclin- dependent kinase 2-cyclin E and its role in centrosome duplication. J Biol Chem *276*, 21529-21537.

Tseng, T. C., Chen, S. H., Hsu, Y. P., and Tang, T. K. (1998). Protein kinase profile of sperm and eggs: cloning and characterization of two novel testis-specific protein kinases (AIE1, AIE2) related to yeast and fly chromosome segregation regulators. DNA Cell Biol *17*, 823-833.

Tugendreich, S., Tomkiel, J., Earnshaw, W., and Hieter, P. (1995). CDC27Hs colocalises with CDC16Hs to the centrosome amd mitotic spindle amd is essential for the metaphase to anaphase transition. Cell *81*, 261-268.

Tutt, A., Gabriel, A., Bertwistle, D., Connor, F., Paterson, H., Peacock, J., Ross, G., and Ashworth, A. (1999). Absence of BRCA2 causes genome instability by chromosome breakage and loss associated with centrosome amplification. Curr Biol *9*, 1107-11010.

Ueda, M., Schliwa, M., and Euteneuer, U. (1999). Unusual centrosome cycle in *Dictyostelium* : correlation of dynamic behavior and structural changes. Mol Biol Cell *10*, 151-160.

Upadhya, P., Birkenmeier, E. H., Birkenmeier, C. S., and Barker, J. E. (2000). Mutations in a NIMA-related kinase gene, Nek1, cause pleiotropic effects including a progressive polycystic kidney disease. Proc Natl Acad Sci (USA) *97*, 217-221.

Uto, K., Nakajo, N., and Sagata, N. (1999). Two structural variants of Nek2 kinase, termed Nek2A and Nek2B, are differentially expressed in *Xenopus* tissues and development. Dev Biol *208*, 456-464.

Uto, K., and Sagata, N. (2000). Nek2B, a novel maternal form of Nek2 kinase, is essential for the assembly or maintenance of centrosomes in early *Xenopus* embryos. EMBO J *19*, 1816-1826.

Vandre, D. D., Davis, F. M., Rao, P. N., and Borisy, G. G. (1984). Phosphoproteins are components of mitotic microtubule organizing centers. Proc Natl Acad Sci (USA) *81*, 4439-4443.

Verde, F., Dogterom, M., Stelzer, E., Karsenti, E., and Leibler, S. (1992). Control of microtubule dynamics and length by cyclin A-dependent and cyclin B-dependent kinases in *Xenopus* egg extracts. J Cell Biol *118*, 1097-1108.

Vojtek, A. B., Hollenberg, S. M., and Cooper, J. A. (1993). Mammalian Ras interacts directly with the serine/threonine kinase Raf. Cell *74*.

Wai, D. H., Schaefer, K. L., Schramm, A., Korsching, E., Van Valen, F., Ozaki, T., Boecker, W., Schweigerer, L., Dockhorn-Dworniczak, B., and Poremba, C. (2002). Expression analysis of pediatric solid tumour cell lines using oligonucleotide microarrays. Int J Oncol *20*, 441-451.

Wakefield, J. G., Huang, J.-Y., and Raff, J. W. (2000). Centrosomes have a role in regulating the destruction of cyclin B in early *Drosophila* embryos. Curr Biol *10*, 1367-1370.

Wan, Y., and Kirschner, M. (2001). Identification of multiple CDH1 homologues in vertebrates conferring different substrate specificities. Proc Natl Acad Sci (USA) *98*, 13066-13071.

Wang, S., Nakashima, S., Sakai, H., Numata, O., Fujiu, K., and Nozawa, Y. (1998). Molecular cloning and cell-cycle-dependent expression of a novel NIMA (never-in-mitosis in *Aspergillus nidulans*)-related protein kinase (TpNrk) in *Tetrahymena* cells. Biochem J *334*, 197-203.

Waters, J. C., and Salmon, E. (1997). Pathways of spindle assembly. Curr Opin Cell Biol *9*, 37-43.

Weaver, Z., Montagna, C., Xu, X., Howard, T., Gadina, M., Brodie, S. G., Deng, C. X., and Ried, T. (2002). Mammary tumours in mice conditionally mutant for *Brca1* exhibit gross genomic instability and centrosome amplification yet display a recurring distribution of genomic imbalances that is similar to human breast cancer. Oncogene *21*, 5097-5107.

Wheatley, D. N., Wang, A. M., and Strugnell, G. E. (1996). Expression of primary cilia in mammalian cells. Cell Biol Int *20*, 73-81.

Wheatley, S., Carvalho, A., Vagnarelli, P., and Earnshaw, W. (2001). INCENP is required for proper targeting of survivin to the centromeres and the anaphase spindle during mitosis. Curr Biol *11*, 886-890.

Wiese, C., and Zheng, Y. (2000). A new function for the g-tubulin ring complex as a microtubule minus-end cap. Nat Cell Biol *2*, 358-364.

Wigge, P. A., Jensen, O. N., Holmes, S., Souès, S., Mann, M., and Kilmartin, J. (1998). Analysis of the *Saccharomyces* Spindle Pole by Matrix-assisted Laser Desorption/Ionization (MALDI) Mass Spectrometry. J Cell Biol *141*, 967-977.

Wigley, W. C., Fabunmi, R. P., Lee, C. R., Marino, C. R., Muallem, S., DeMartino, G. N., and Thomas, P. J. (1999). Dynamic association of proteasomal machinery with the centrosome. J Cell Biol *145*, 481-490.

Wilson, E. B. (1925). The cell in development and heredity (New York, McMillan).

Wittmann, T., Boleti, H., Antony, C., Karsenti, E., and Vernos, I. (1998). Localisation of the kinesin-like protein Xklp2 to spindle poles requires a leucine zipper, a microtubule-associated protein, and dynein. J Cell Biol *143*, 673-685.

Wittmann, T., Hyman, A., and Desai, A. (2001). The spindle: a dynamic assembly of microtubules and motors. Nat Cell Biol *3*, E28-E34.

Wittmann, T., Wilm, M., Karsenti, E., and Vernos, I. (2000). TPX2, a novel *Xenopus* MAP involved in spindle pole organisation. J Cell Biol *149*, 1405-1418.

Wojcik, E. J., Glover, D. M., and Hays, T. S. (2000). The SCF ubiquitin ligase protein slimb regulates centrosome duplication in *Drosophila*. Curr Biol *10*, 1131-1134.

Wu, L., Osmani, S. A., and Mirabito, P. M. (1998). A role for NIMA in the nuclear localisation of cyclin B in *Aspergillus nidulans*. J Cell Biol *141*, 1575-1587.

Yamano, H., Tsurumi, C., Gannon, J., and Hunt, T. (1998). The role of the destruction box and its neighbouring lysine residues in cyclin B for anaphase ubiquitin-dependent proteolysis in fission yeast: defining the D-box receptor. EMBO J *17*, 5670-5678.

Ye, X. S., Fincher, R. R., Tang, A., Osmani, A. H., and Osmani, S. A. (1998). Regulation of the anaphase-promoting complex/cyclosome by *bimA*^{APC3} and proteolysis of NIMA. Mol Biol Cell *9*, 3019-3030.

Ye, X. S., Xu, G., Pu, R. T., Fincher, R. R., McGuire, S. L., Osmani, A. H., and Osmani, S. A. (1995). The NIMA protein kinase is hyperphosphorylated and activated downstream of p34cdc2/cyclin B: coordination of two mitosis promoting kinases. Embo J *14*, 986-994.

Young, A., Dictenberg, J. B., Purohit, A., Tuft, R., and Doxsey, S. J. (2000). Cytoplasmic dynein-mediated assembly of pericentrin and gamma tubulin onto centrosomes. Mol Biol Cell *11*, 2047-2056.

Zechariae, W., and Nasmyth, K. (1999). Whose end is destruction: cell division and the anaphase-promoting complex. Genes Dev *13*, 2039-2058.

Zheng, Y., Jung, M. K., and Oakley, B. R. (1991). Gamma-tubulin is present in *Drosophila melanogaster* and *Homo sapiens* and is associated with the centrosome. Cell *65*, 817-823.

Zheng, Y., Wong, M. L., Alberts, B., and Mitchison, T. (1995). Nucleation of microtubule assembly by a gamma-tubulin-containing ring complex. Nature *378*, 578-583.

Zhou, H., Kuang, J., Zhong, L., Kuo, W. L., Gray, J. W., Sahin, A., Brinkley, B. R., and Sen, S. (1998). Tumour amplified kinase STK15/BTAK induces centrosome amplification, aneuploidy and transformation. Nat Genet *20*, 189-193.

Zhou, Y., Ching, Y.-P., Ng, R. W. M., and Jin, D.-Y. (2002). The APC regulator Cdh1 is essential for the progression of embryonic cell cycles in *Xenopus*. Biochem Biophys Res Commun *294*, 120-126.

Zimmerman, W., and Doxsey, S. J. (2000). Construction of centrosomes and spindle poles by molecular motor-driven assembly of protein particles. Traffic *1*, 927-934.

Zur, A., and Brandeis, M. (2001). Securin degradation is mediated by fzy and fzr, and is required for complete chromatid separation but not for cytokinesis. EMBO J *20*, 792-801.

APPENDIX

Plasmid title: pGBDU-C-Nap1-CTD
Short code: CTD-DBD
Date made : November 1999
Storage: 0.6 mg/ml in H_2O (-20°C)

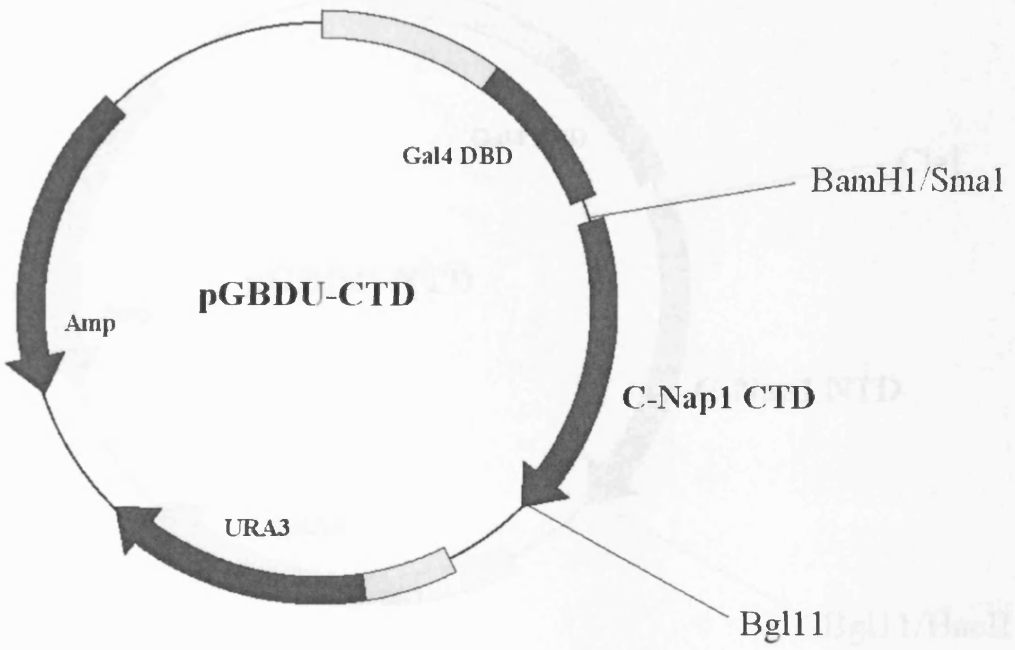

Cloning strategy:
Isolate C-Nap1-CTD (amino acids 1962-2403) from pBSmyc-C-Nap1 as a *Sma1/BglII* fragment.
Linearise pGBDU-C3 using *BamH1* (Klenow blunted) and *BglII*.
Ligate and sequence.

Sequencing primer
GBDU-RP: TCGGAAGAGAGTAGT

Plasmid title: pGBDU-C-Nap1-NTD
Short code: NTD-DBD
Date made : October 1999
Storage: 0.7 mg/ml in H_2O (-20°C)

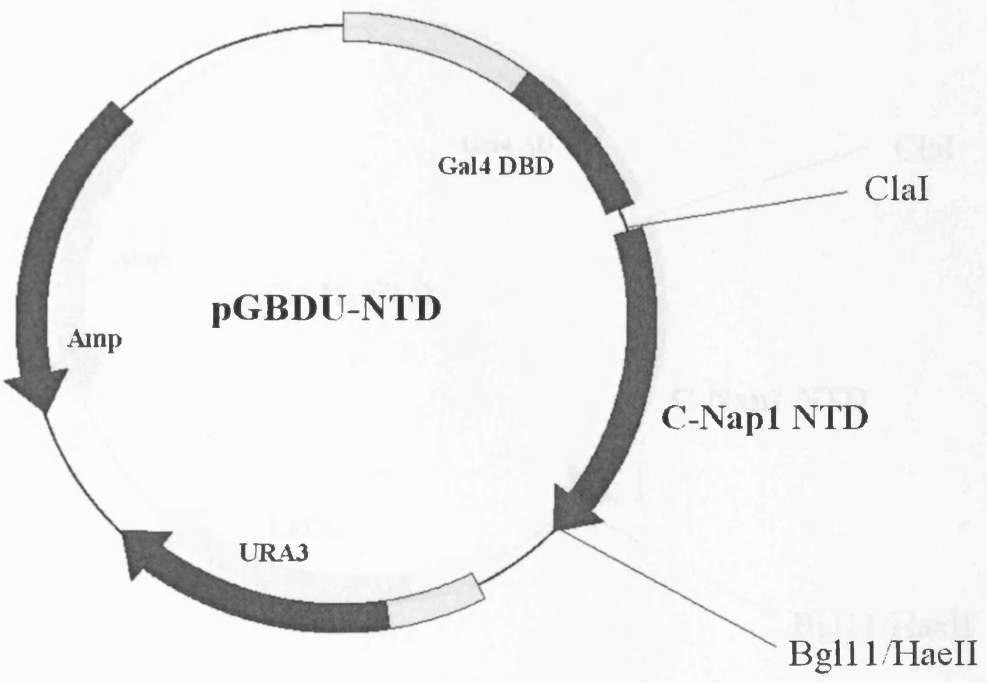

Cloning strategy:
Isolate C-Nap1 -NTD (amino acids 1-488) from pBSmyc-C-Nap1 as a *Cla1/HaeII* (T4 DNA Pol blunted) fragment.
Linearise pGBDU-C3 using *Cla1* and *BglII* (Klenow blunted).
Ligate and sequence.

Sequencing primer
GBDU-RP: TCGGAAGAGAGTAGT

Plasmid title: pGAD-C-Nap1-NTD
Short code: NTD-AD
Date made : October 2000
Storage: 1 mg/ml in H_2O (-20°C)

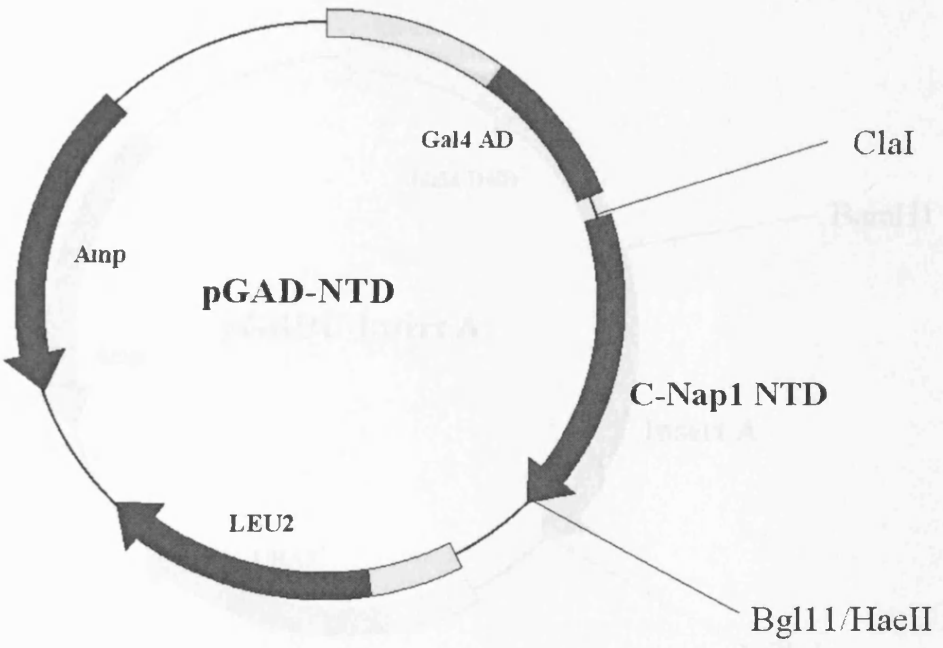

Cloning strategy:
Isolate C-Nap1-NTD (amino acids 1-488) from pBSmyc-C-Nap1 as a *ClaI/HaeII* (Klenow blunted) fragment.
Linearise pGAD-C2 using *ClaI* and *BglII* (Klenow blunted).
Ligate and sequence.

Sequencing primer
GAD-RP: TTCGATGATGAAGATACC

Plasmid title: pGBDU-C-Nap1-CTD (A)
Short code: A-DBD
Date made : April 2002
Storage: 1 mg/ml in H_2O (-20°C)

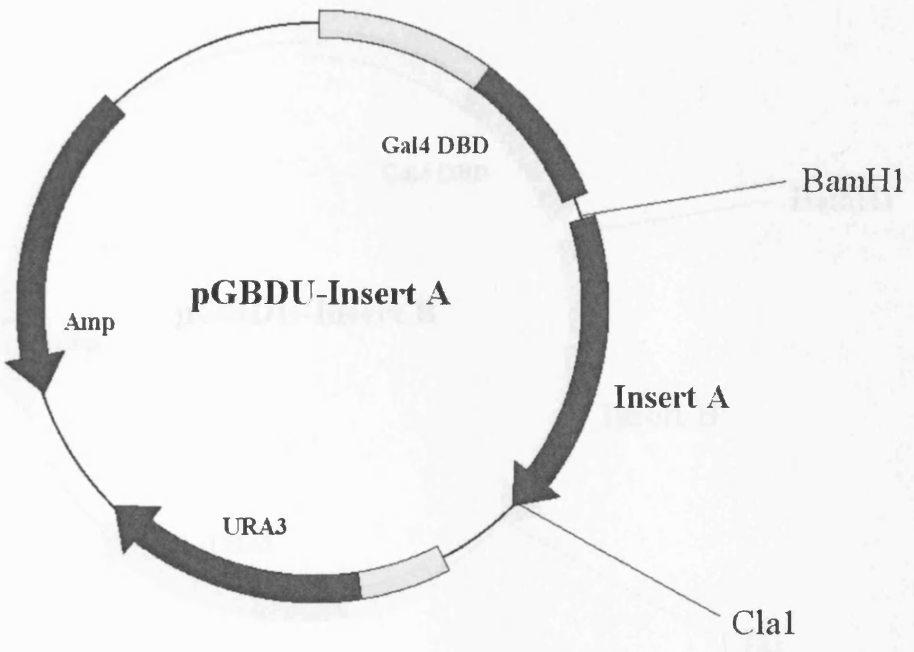

Cloning strategy:
Amplify C-Nap1-CTD (amino acids1964-2070) from pBSmyc-C-Nap1 using CNap-1 and CNap-2 (see below)
Digest PCR product and pGBDU-C2using *BamH1* and *Cla1*
Ligate and sequence

Cloning Primers
CNap-1: GCGCGGATCCGGGCTGAGGCTCTGCA
CNap-2: GCGCATCGATCTGGGCCAGAGACTTCT

Sequencing primer
GBDU-RP: TCGGAAGAGAGTAGT

Plasmid title: pGBDU-C-Nap1-CTD (B)
Short code: B-DBD
Date made : April 2002
Storage: 1 mg/ml in H_2O (-20°C)

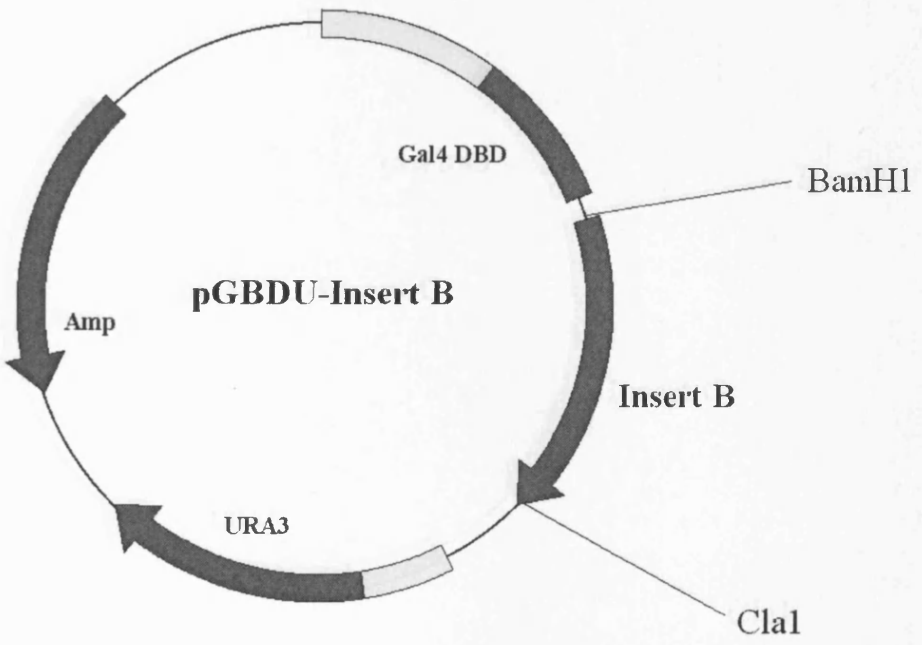

Cloning strategy:
Amplify C-Nap1-CTD (amino acids 2062-2168) from pBSmyc-C-Nap1 using CNap-4 and CNap-4 (see below)
Digest PCR product and pGBDU-C2 using *BamH1* and *Cla1*
Ligate and sequence

Cloning Primers
CNap-3: GCGCGGATCCAGAAGTCTCTGGCCCAG
CNap-4: GCGCATCGATAATCTGCCTGGCTTCTG

Sequencing primer
GBDU-RP: TCGGAAGAGAGTAGT

Plasmid title: pGBDU-C-Nap1-CTD (C)
Short code: C-DBD
Date made : April 2002
Storage: 1 mg/ml in H_2O (-20°C)

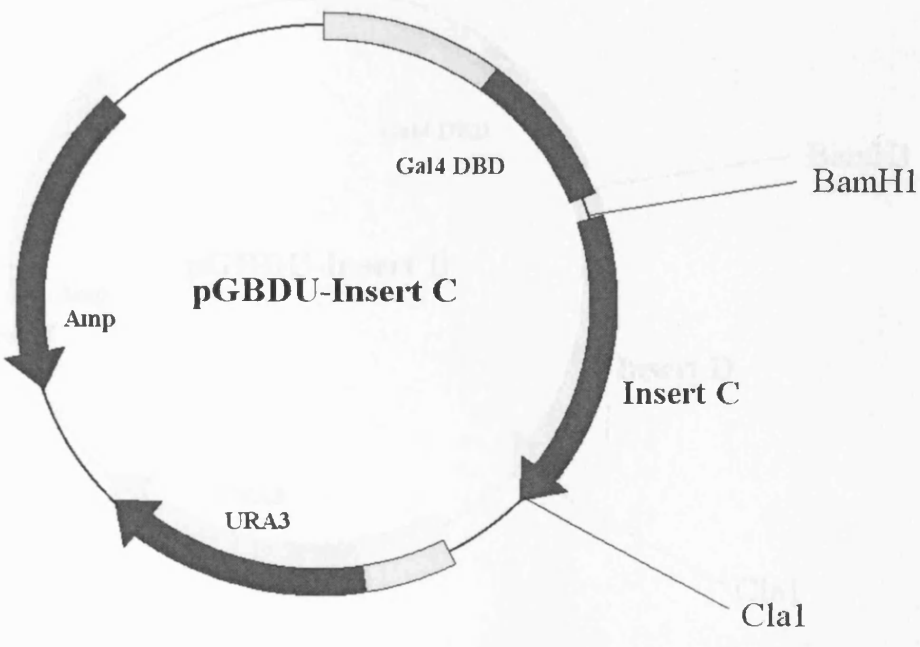

Cloning strategy:
Amplify C-Nap1- CTD (amino acids 2162-2268) from pBSmyc-C-Nap1 using CNap-5 and CNap-6 (see below)
Digest PCR product and pGBDU-C2 using *BamH1* and *Cla1*
Ligate and sequence

Cloning Primers
CNap-5: GCGCGGATCCCAGAAGCCAGGCAGATT
CNap-6: GCGCATGGATTGACTGCTTCTCCATTC

Sequencing primer
GBDU-RP: TCGGAAGAGAGTAGT

Plasmid title: pGBDU-C-Nap- CTD (D)
Short code: D-DBD
Date made : April 2002
Storage: 1 mg/ml in H_2O (-20°C)

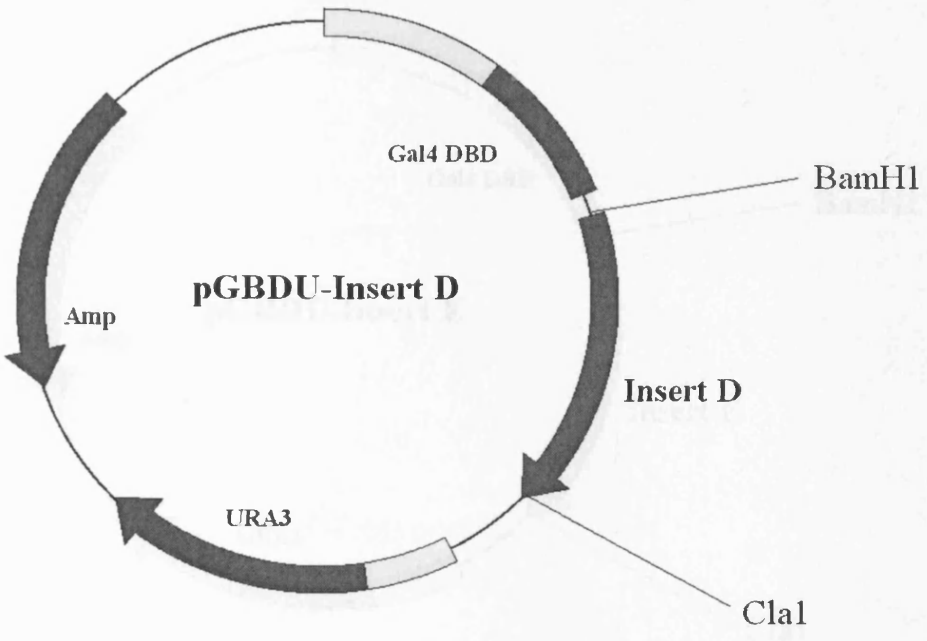

Cloning strategy:
Amplify C-Nap1-CTD (amino acids 2262-2368) from pBSmyc-C-Nap1 using CNap-7 and CNap-8 (see below)
Digest PCR product and pGBDU-C2 using *BamH1* and *Cla1*
Ligate and sequence

Cloning Primers
CNap-7: GCGCGGATCCGAATGGAGAAGCAGTCA
CNap-8: GCGCATCGATCCGCTCCAAAGTCAGCT

Sequencing primer
GBDU-RP: TCGGAAGAGAGTAGT

Plasmid title: pGBDU-C-Nap1 CTD (E)
Short code: E-DBD
Date made : April 2002
Storage: 1 mg/ml in H_2O (-20°C)

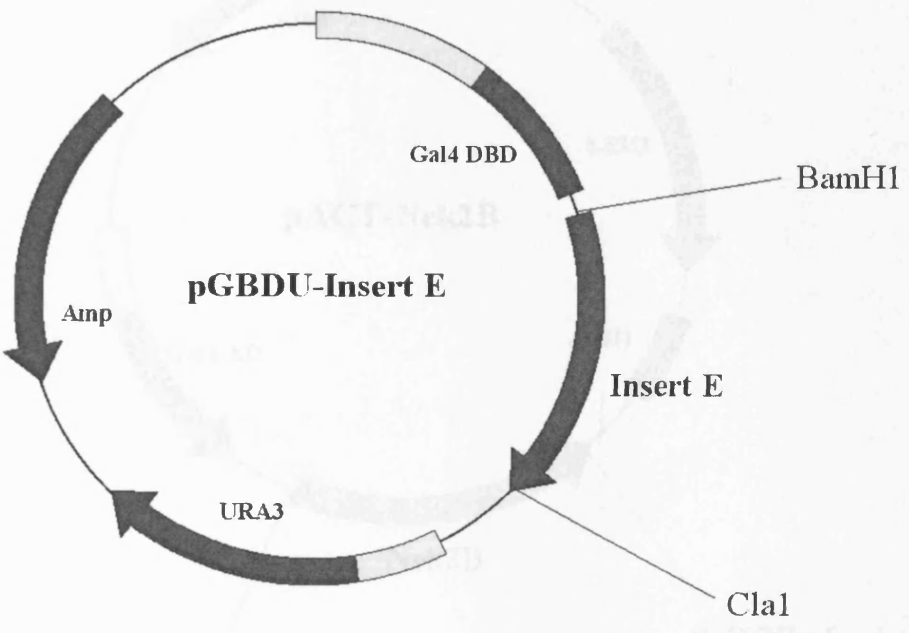

Cloning strategy:
Amplify C-Nap1-CTD (amino acids 2362-2442) from pBSmyc-C-Nap1 using CNap-9 and CNap-10 (see below)
Digest PCR product and pGBDU-C2 using *BamH1* and *Cla1*
Ligate and sequence

Cloning Primers
CNap-9: GCGCGGATCCAGCTGACTTTGGAGCGG
CNap-10: GCGCATCGATCCTGGAGGCGGCTTGGGT

Sequencing primer
GBDU-RP: TCGGAAGAGAGTAGT

Plasmid title: pACT-Nek2B
Short code: Nek2B-AD
Date made : October 2000
Storage: 1 mg/ml in H_2O (-20°C)

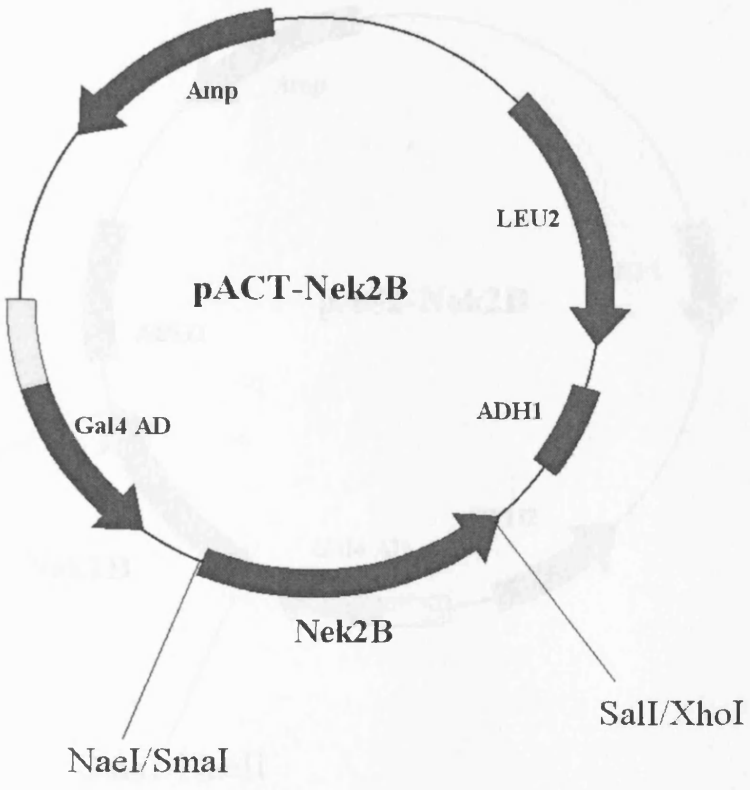

Cloning strategy:
Isolate Nek2B from pGEM-Nek2B as a *NaeI1/Sal1* fragment.
Linearise pACT using *Sma1* and *Xho1*.
Ligate and sequence.

Sequencing primer
ACT-RP: AATACCACTACAATGGATGATG
ACTR-RP: GCTCTAGAGTTGAAGTGAACTTGCGGG

Plasmid title: pAS2-Nek2B
Short code: Nek2B-DBD
Date made : October 2000
Storage: 1 mg/ml in H_2O (-20°C)

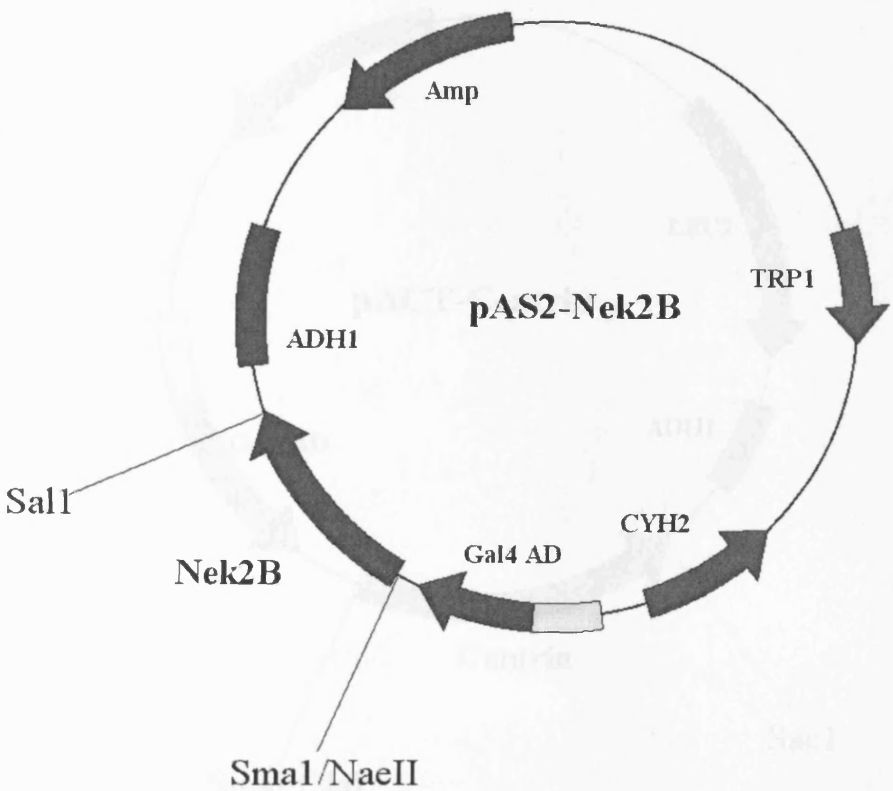

Cloning strategy:
Isolate Nek2B from pGEM-Nek2B as a *NaeI1/Sal1* fragment.
Linearise pAS2 using *Sma1* and *Xho1*.
Ligate and sequence.

Sequencing primers
AS2-RP: ACTCTCTTCCGATGATGA
AS2R-RP: AAGCAACCTGACCTACAG

Plasmid title: pACT-Centrin
Short code: Centrin-AD
Date made : July 2000
Storage: 1 mg/ml in H_2O (-20°C)

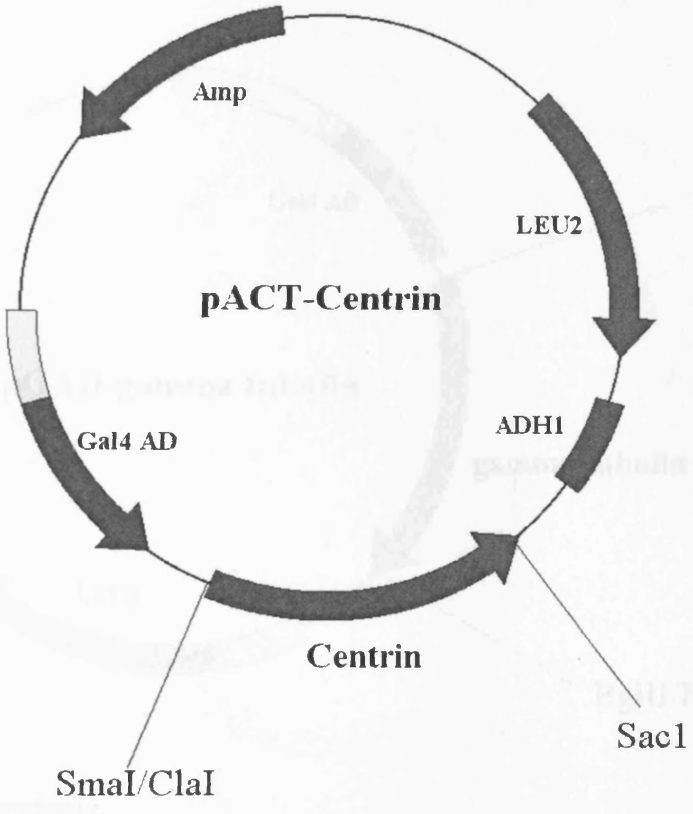

Cloning strategy:
Isolate centrin from pBS-centrin as a *ClaI1/Sac1* fragment.
Linearise pACT using *Sma1* and *Sac1*.
Ligate and sequence.

Sequencing primer
ACT-RP: AATACCACTACAATGGATGATG
ACTR-RP: GCTCTAGAGTTGAAGTGAACTTGCGGG

Plasmid title: pGAD-gamma tubulin
Short code: gamma tubulin-AD
Date made : October 2000
Storage: 1 mg/ml in H_2O (-20°C)

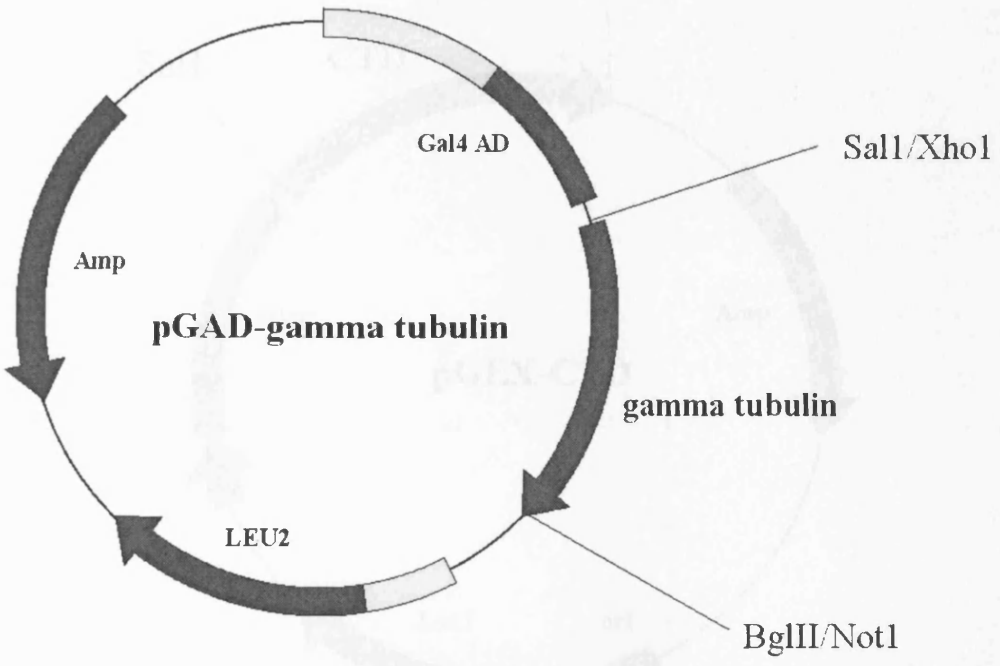

Cloning strategy:
Isolate gamma tubulin from pBS-gamma tubulin as a *Xho1/Not1* (Klenow blunted) fragment.
Linearise pGAD-C3 using *Sal1* and *BglII.*
Ligate and sequence.

Sequencing primer
GAD-RP: TTCGATGATGAAGATACC
GADR-RP: GAGATCGTGCACGATGAC (same as GBDUR-RP)

Plasmid title:pGEX-CTD
Short code: GST-CTD
Date made : June 2000
Storage: 1 mg/ml in H_2O (-20°C)

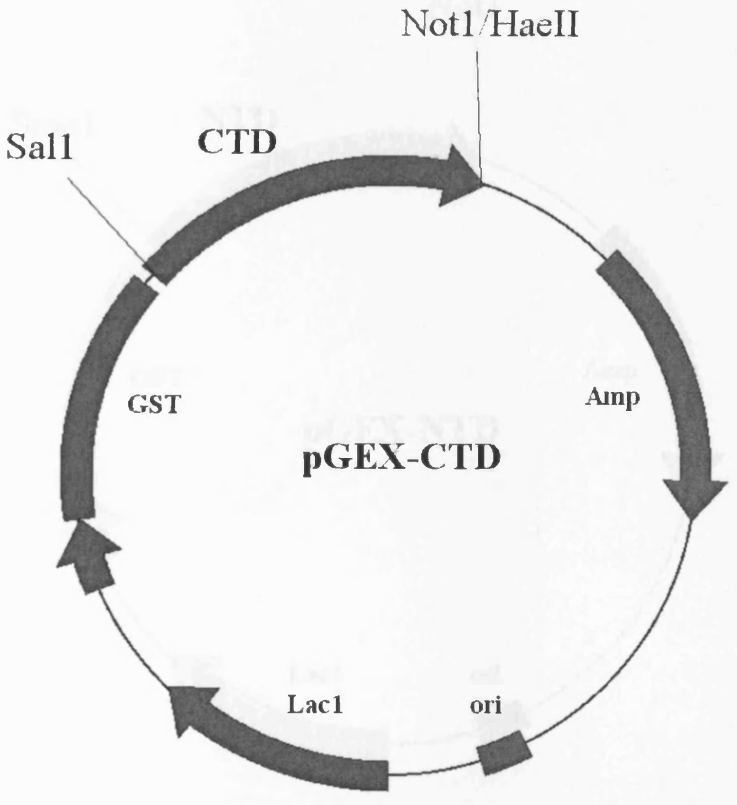

Cloning strategy:
Isolate C-Nap1-CTD from pBSmycC-Nap1 as a *Sma1/Not1* fragment.
Linearise pGEX-4T1 using *Sma1* and *Not1*.
Ligate and sequence.

Sequencing primer
GEX4-RP: TATAGCATGGCCTTTGCA
GEX4R-RP: GACAAGCTGTGACCGTCT

Plasmid title:pGEX-NTD
Short code: GST-NTD
Date made : June 2000
Storage: 1 mg/ml in H_2O (-20°C)

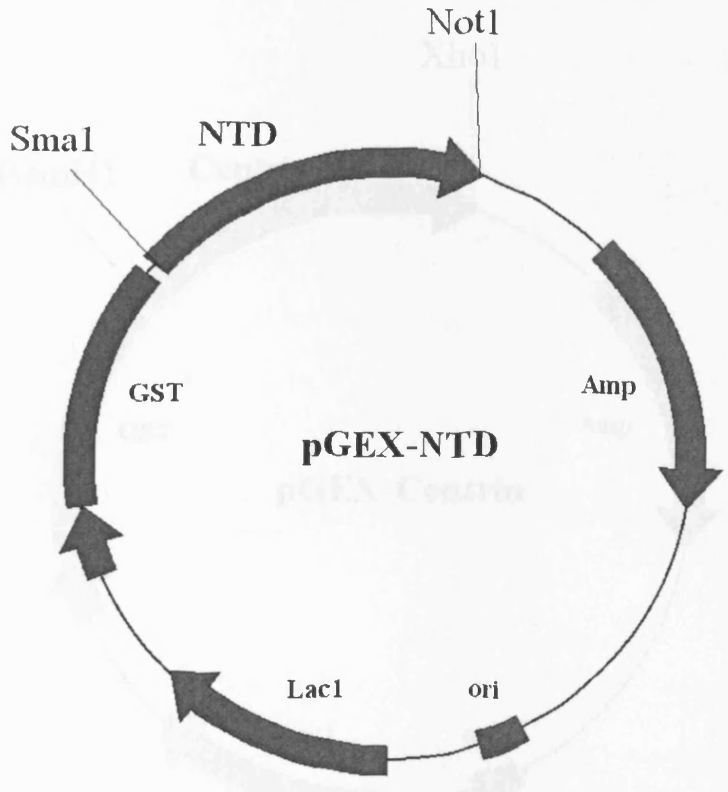

Cloning strategy:
Isolate C-Nap1-NTD from pBSmycC-Nap1 as a *Sma1/Not1* fragment.
Linearise pGEX-4T1 using *Sma1* and *Not1*.
Ligate and sequence.

Sequencing primer
GEX4-RP: TATAGCATGGCCTTTGCA
GEX4R-RP: GACAAGCTGTGACCGTCT

Plasmid title:pGEX-Centrin
Short code: GST-Centrin
Date made : April 2002
Storage: 1 mg/ml in H_2O (-20°C)

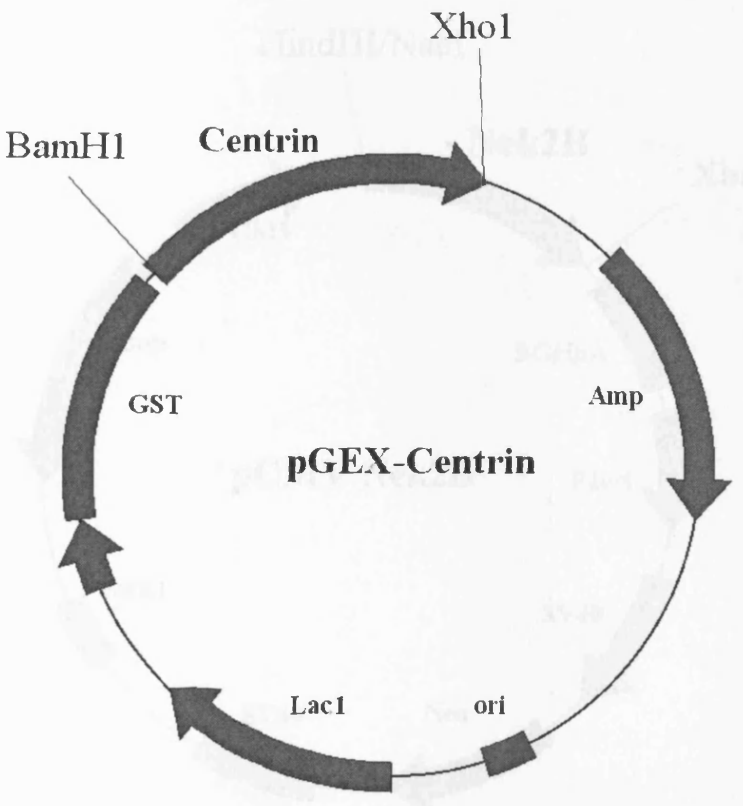

Cloning strategy:
Amplify Centrin from pBS-Centrin using CENF and CENR (see below)
Digest PCR product and pGEX-4T1 using *BamH1* and *Xho1*
Ligate and sequence

Cloning Primers
CENF: GCGCGGATCCATGGCCTCCCCATTTAAGAAG
CENR:GCGCCTCGAGTTAATAGAGGCTGGTCTT

Sequencing primers
GEX4-RP: TATAGCATGGCCTTTGCA
GEX4R-RP: GACAAGCTGTGACCGTCT

Plasmid title: pCMV-Nek2B
Short code: CMV-Nek2B
Date made : October 2000
Storage: 1 mg/ml in H_2O (-20°C)

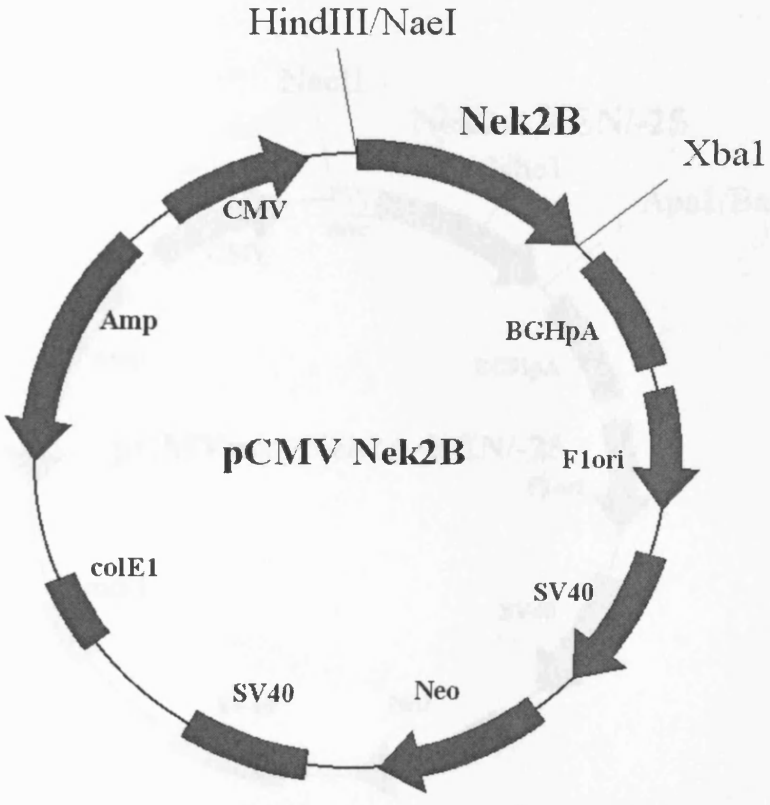

Cloning strategy:
Isolate Nek2B from pGEM-Nek2B as a *NaeI1/Xba1* fragment.
Linearise pCMV using *HindIII* (Klenow blunted) and *Xba1*.
Ligate and sequence.

Sequencing primer
T7: AATACGACTCACTATAGGG

Plasmid title: pCMVmyc-Nek2A KEN/-25
Short code: KEN25
Date made : October 2001
Storage: 1 mg/ml in H_2O (-20°C)

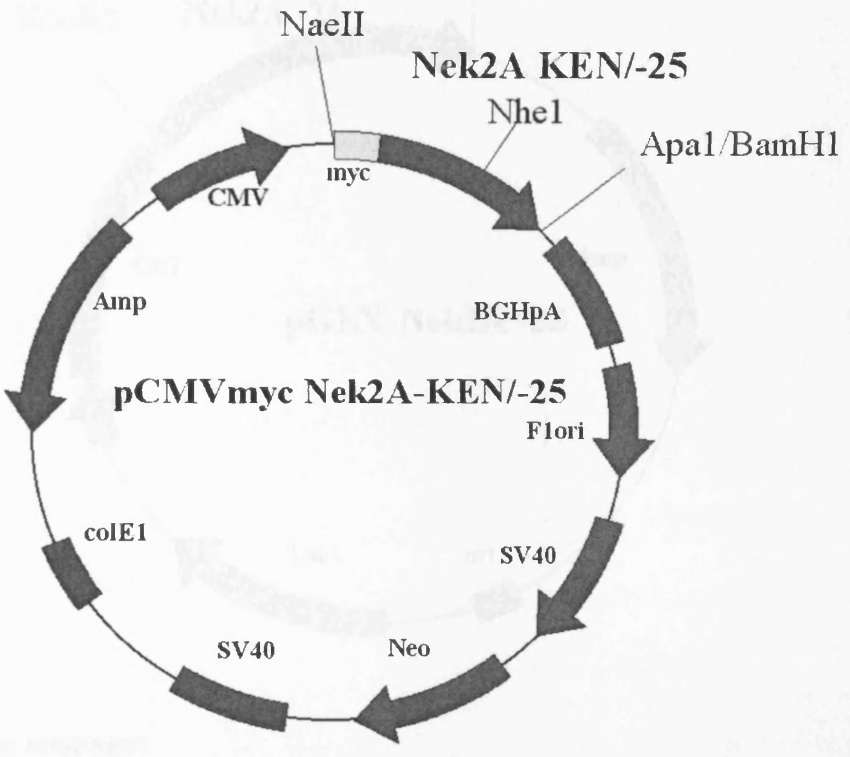

Cloning strategy:
Isolate a *Nhe1/Apa1* (T4 DNA Pol blunted) fragment from pGEM-Nek2A-KEN/-25.
Isolate a *Nhe1/BamH1* (Klenow blunted) fragment from pCMVmyc-Nek2A.
Swap fragments and sequence.

Sequencing primer
AF013: GTGAGAGACTAGCAGAGGAC

Plasmid title:pGEX-NEK2A-last 25 amino acids
Short code: GST-25
Date made : February 2002
Storage: 1 mg/ml in H_2O (-20°C)

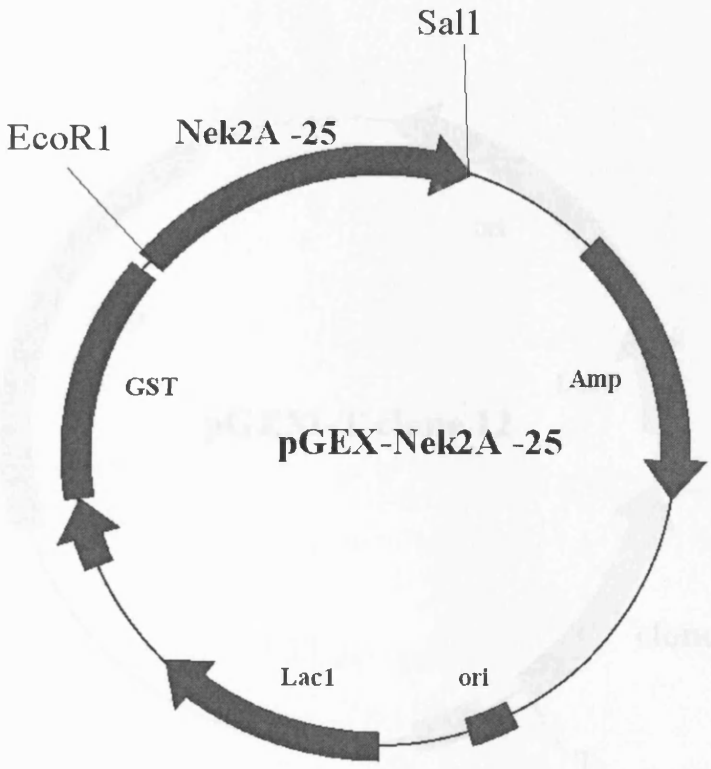

Cloning strategy:
Amplify Nek2A (amino acids 420-445) from pGEM-Nek2A using JIM2 and JIM1R (see below)
Digest PCR product and pGEX-4T1 using *EcoR1* and *Sal1*
Ligate and sequence

Cloning Primers
JIM2: GCGCGAATTCCAGCTGCGGGCTCAAG
JIM1R: GCGCGTCGACCTCTGTGTCTCTCTACCT

Sequencing primers
GEX4-RP: TATAGCATGGCCTTTGCA
GEX4R-RP: GACAAGCTGTGACCGTCT

Plasmid title:pGEM-T clone 12
Short code: GEM12
Date made : April 2001
Storage: 1 mg/ml in H_2O (-20°C)

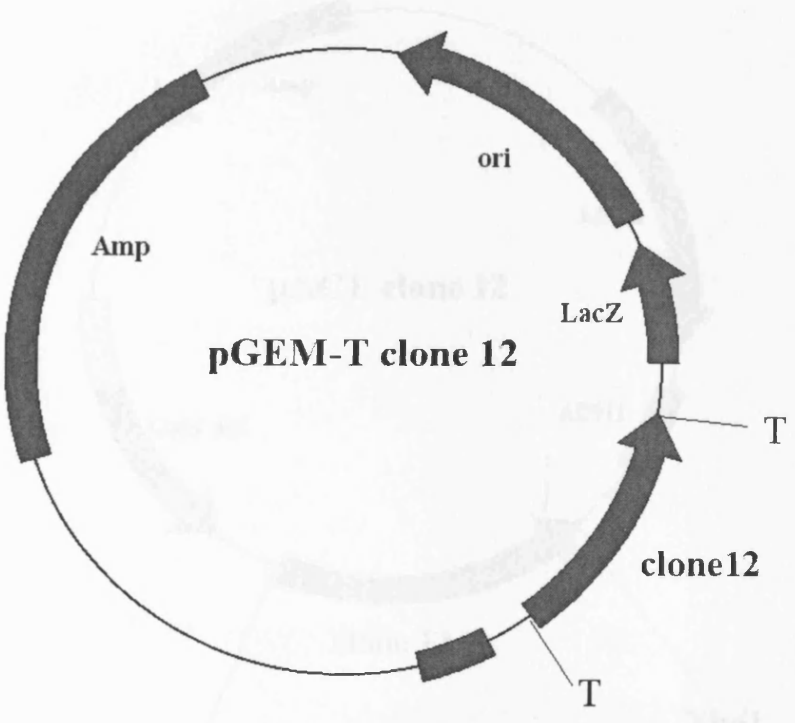

Cloning strategy:
Amplify clone 12 from pACT-clone 12 present in yeast DNA preparations using ACT-RP and ACT-RP (see below).
Insert into pGEM T easy, as per manufacturers instructions
Sequence.

Sequencing primer
ACT-RP: AATACCACTACAATGGATGATG
ACTR-RP: GCTCTAGAGTTGAAGTGAACTTGCGGG

Plasmid title: pACT-clone 12
Short code: 12-AD
Date made : October 2000
Storage: 1 mg/ml in H_2O (-20°C)

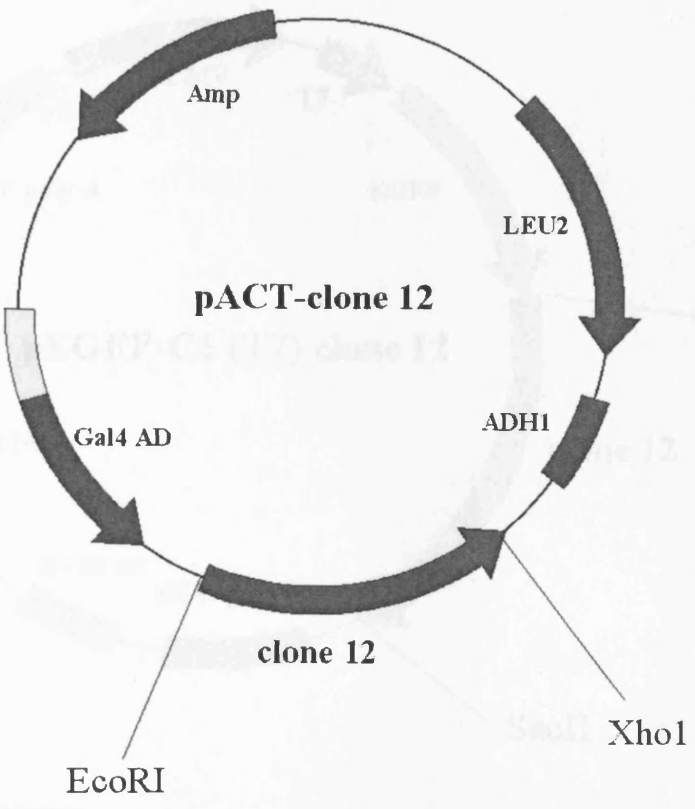

Cloning strategy:
Isolate clone 12 from pGEM clone 12 as a *EcoR1/Sal1* fragment.
Linearise pACT using *EcoR1* and *Xho1*.
Ligate and sequence.

Sequencing primer
ACT-RP: AATACCACTACAATGGATGATG
ACTR-RP: GCTCTAGAGTTGAAGTGAACTTGCGGG

Plasmid title: pEGFP-C1 (T7) clone 12
Short code: GFP-12
Date made : June 2001
Storage: 1 mg/ml in H_2O (-20°C)

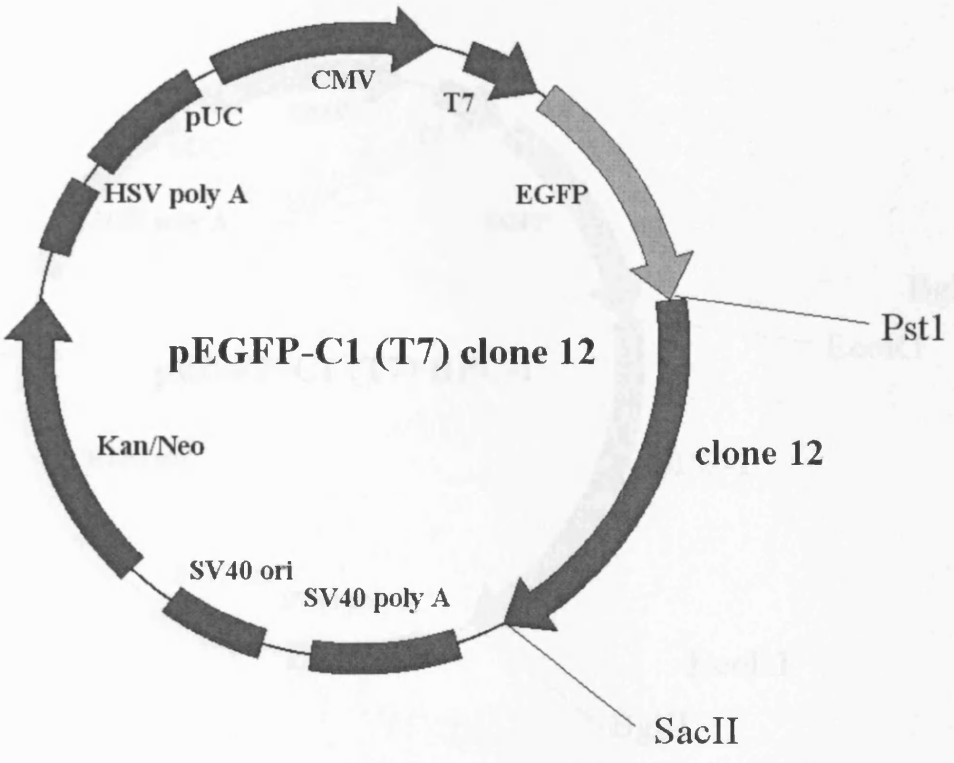

Cloning strategy:
Amplify clone 12 from pGEM-12 using RP18/06 and RP18/06R (see below)
Digest PCR product and pEGFP using *Pst1* and *SacII*
Ligate and sequence

Cloning Primers
RP18/06: GCGCCTGCAGATACCACTACAATG
RP18/06R:GCGCCCGCGGTTTCAGTATCTACGA

Sequencing primers
GFP-RP: ACTACCTGAGCACCCAGT

Plasmid title: pEGFP-C1 (T7) BPC-1
Short code: GFP-BPC-1
Date made : April 2002
Storage: 1 mg/ml in H_2O (-20°C)

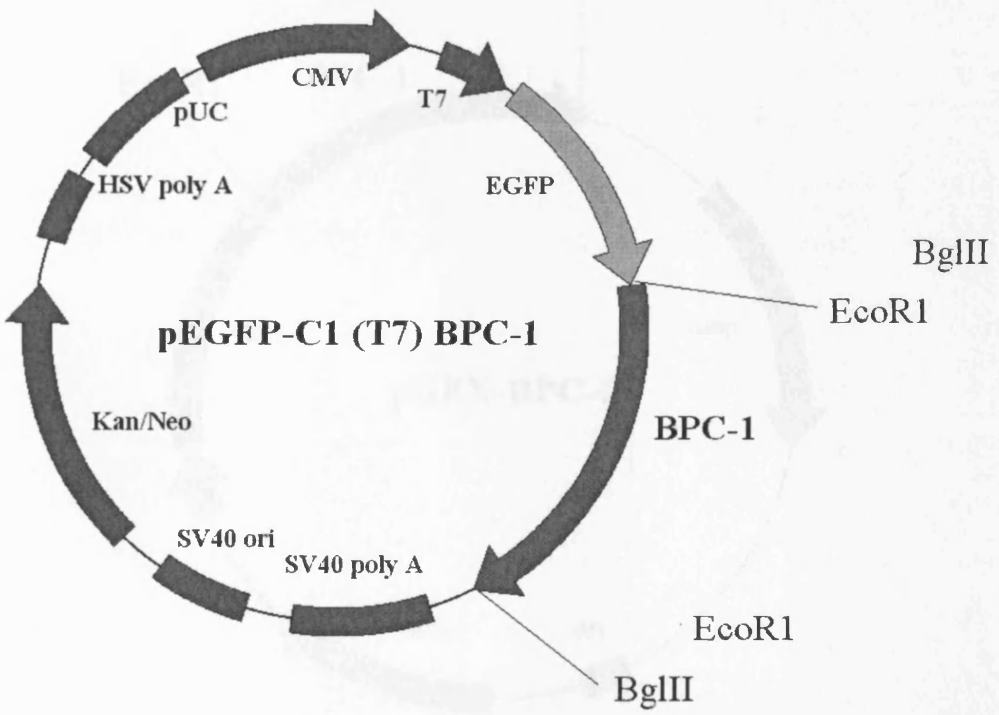

Cloning strategy:
Amplify BPC-1 from image clone 2270610 using GFP-F and GFP-R (see below)
Digest PCR product and pEGFP using *EcoR1* and *BglII*
Ligate and sequence

Cloning Primers
GFP-F: GCGCAGATCTATGGATGCCTCCCAGTGT
GFP-R: GCGCGAATTCTTAAGGCTTTGAATAGCT

Sequencing primers
GFP-RP: ACTACCTGAGCACCCAGT

Plasmid title:pGEX-BPC-1
Short code: GST-BPC-1
Date made : April 2002
Storage: 1 mg/ml in H_2O (-20°C)

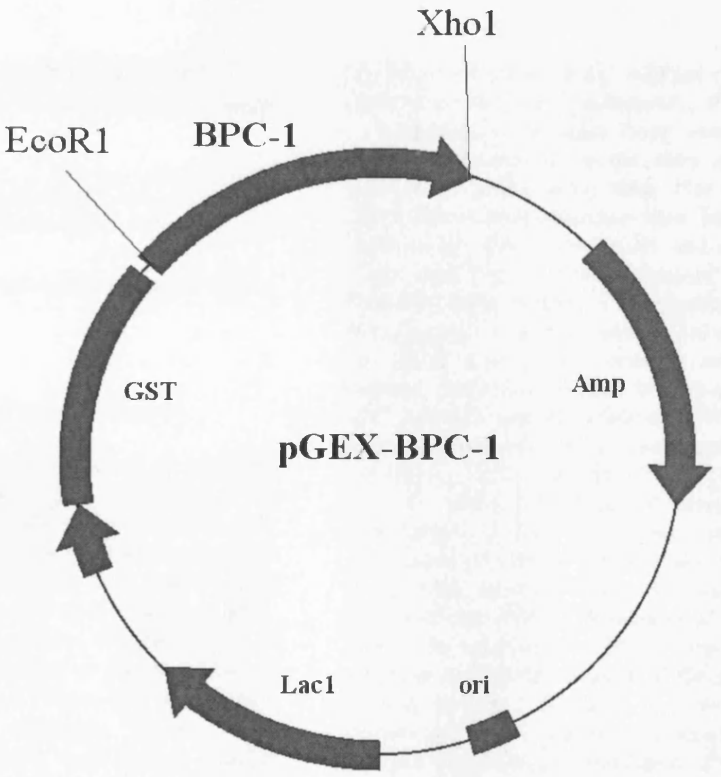

Cloning strategy:
Amplify BPC-1 from image clone image clone 2270610 using GST-F and GST-R (see below)
Digest PCR product and pGEX-4T1 using *EcoR1* and *Xho1*
Ligate and sequence

Cloning Primers
GST-F: GCGCGAATTCATGGCTGACTCCCAGTGT
GST-R: GCGCCTCGAGTTAAGGCTTTGAATAGCT

Sequencing primers
GEX4-RP: TATAGCATGGCCTTTGCA
GEX4R-RP: GACAAGCTGTGACCGTCT

The EMBO Journal Vol. 20 No. 24 pp. 7117–7127, 2001

APC/C-mediated destruction of the centrosomal kinase Nek2A occurs in early mitosis and depends upon a cyclin A-type D-box

Rebecca S.Hames[1], Samantha L.Wattam[1], Hiroyuki Yamano[2,3], Rachid Bacchieri[1,4] and Andrew M.Fry[1,5]

[1]Department of Biochemistry, University of Leicester, Leicester LE1 7RH, [2]ICRF Clare Hall Laboratories, South Mimms, Herts EN6 3LD, UK and [3]Unit Process and Combined Circuit, PRESTO, Japan Science and Technology, Japan

[4]Present address: Laboratoire Arago, CNRS, 66650 Banyuls-sur-Mer, France

[5]Corresponding author
e-mail: amf5@le.ac.uk

R.S.Hames and S.L.Wattam contributed equally to this work

Nek2 is a NIMA-related kinase implicated in regulating centrosome structure at the G_2/M transition. Two splice variants have been identified that exhibit distinct patterns of expression during cell cycle progression and development. Here we show that Nek2A, but not Nek2B, is destroyed upon entry into mitosis coincident with cyclin A destruction and in the presence of an active spindle assembly checkpoint. Destruction of Nek2A is mediated by the proteasome and is dependent upon the APC/C–Cdc20 ubiquitin ligase. Nek2 activity is not required for APC/C activation. Nek2A destruction in early mitosis is regulated by a motif in its extreme C-terminus which bears a striking resemblance to the extended destruction box (D-box) of cyclin A. Complete stabilization of Nek2A requires deletion of this motif and mutation of a KEN-box. Destruction of Nek2A is not inhibited by the cyclin B-type D-box, but the C-terminal domain of Nek2A inhibits destruction of both cyclins A and B. We propose that recognition of substrates by the APC/C–Cdc20 in early mitosis depends upon possession of an extended D-box motif.

Keywords: APC/Cdc20/centrosome/cyclin A/Nek2

Introduction

Progress through mitosis is governed by a number of regulatory mechanisms that include protein phosphorylation, subcellular distribution and protein degradation (Nigg, 2001; Pines and Rieder, 2001). Of these, protein degradation is perhaps the most effective way to ensure that individual steps cannot be reversed. One key regulator of mitotic destruction is a multisubunit E3 ubiquitin ligase known as the anaphase-promoting complex or cyclosome (APC/C) (Morgan, 1999; Page and Hieter, 1999; Zachariae and Nasmyth, 1999). The APC/C catalyzes the covalent attachment of ubiquitin molecules to a substrate, thereby targeting it for degradation by the multiple peptidase activities of the ATPase-dependent 26S proteasome (Hershko and Ciechanover, 1998).

A number of proteins have now been recognized as APC/C substrates. However, they are not all targeted for destruction at the same time. For example, cyclin A is destroyed in prometaphase (den Elzen and Pines, 2001; Geley *et al.*, 2001), cyclin B1 and securins in metaphase (Clute and Pines, 1999; Wakefield *et al.*, 2000; Zur and Brandeis, 2001) and Ase1 in anaphase (Juang *et al.*, 1997). What regulates this sequential destruction of proteins by the APC/C is not clear. Certainly, activation of the APC/C requires additional events including phosphorylation of APC subunits and association of WD-containing adaptor proteins (Morgan, 1999). Two such adaptors have been identified, Cdc20 and Cdh1. These proteins act as adaptors for the APC/C at different times in mitosis. Phosphorylation of the APC/C in early mitosis promotes association of Cdc20. At the same time, phosphorylation of the other adaptor, Cdh1, by Cdk1 prevents its association with the APC/C (Kotani *et al.*, 1999; Kramer *et al.*, 2000). Destruction of APC/C targets in metaphase and anaphase is therefore regulated through Cdc20. However, in late mitosis, G_1 and G_0, when Cdk1 has been inactivated, Cdh1 becomes associated with the APC/C and takes over the role of adaptor. This switch from Cdc20 to Cdh1 is completed by the destruction of Cdc20 itself by APC/C–Cdh1 (Pfleger and Kirschner, 2000). Current evidence, however, does not support the notion that Cdc20 and Cdh1 determine the substrate specificity of the APC/C, as most substrates studied so far, including cyclin B1, securin and Cdc6, can be targeted by both Cdc20 and Cdh1 (Petersen *et al.*, 2000; Zur and Brandeis, 2001). The use of both adaptors ensures that destruction begun in mitosis is continued into the subsequent G_1. Cdc20 itself is an exception to this rule in that it can be targeted for destruction by APC/C–Cdh1 but not by APC/C–Cdc20.

The APC/C is also negatively regulated by a number of proteins including MAD2, MAD2L2 (also called MAD2B) and Emi1, which inhibit the APC/C via the WD adaptor proteins (Chen and Fang, 2001; Pfleger *et al.*, 2001; Reimann *et al.*, 2001). MAD2 is directly involved in the spindle assembly checkpoint preventing APC/C–Cdc20 from destroying cyclin B and securins in the presence of unattached kinetochores (Shah and Cleveland, 2000). Emi1 also inhibits APC/C–Cdc20 in early mitosis and is itself destroyed later in mitosis through an APC/C-independent pathway (Reimann *et al.*, 2001). Whether Emi1 contributes to the spindle checkpoint is unclear. MAD2L2 can inhibit both Cdc20- and Cdh1-complexed APC/C and it is possible that the different actions of these APC/C inhibitors contribute to the timing of destruction of different APC/C substrates.

Another substrate of the APC/C is the NIMA kinase of *Aspergillus nidulans* (Ye *et al.*, 1998). NIMA is required

for mitotic entry in *Aspergillus* and its destruction by the APC/C is required for mitotic exit (Pu and Osmani, 1995). The most closely related vertebrate protein to NIMA by sequence is Nek2 (Nigg, 2001). However, whether Nek2 has an equivalent role in regulating mitotic entry remains unclear. Instead, Nek2 has been found to be a core component of the centrosome and, upon overexpression, it can stimulate centrosome splitting (Fry *et al.*, 1998a). Its activity is cell cycle regulated, with peak levels in S and G_2 (Fry *et al.*, 1995). However, direct interaction with the catalytic subunit of protein phosphatase 1 may limit the activity of Nek2 to a brief window at the onset of mitosis when PP1 is switched off (Puntoni and Villa-Moruzzi, 1997; Helps *et al.*, 2000). The function of Nek2 may be to facilitate centriole disjunction at G_2/M by promoting disassembly of an intercentriolar linkage (Mayor *et al.*, 1999; Fry *et al.*, 2000a; Hinchcliffe and Sluder, 2001). In support of this, a centrosomal substrate of Nek2, called C-Nap1, has properties consistent with holding centrioles together during interphase (Fry *et al.*, 1998b; Mayor *et al.*, 2000). Experiments performed with the *Xenopus laevis* homolog of Nek2 suggest additional functions for this kinase in assembly and maintenance of centrosome structure (Fry *et al.*, 2000b; Uto and Sagata, 2000).

Two splice variants of Nek2 have been identified, Nek2A and Nek2B, that encode products with distinct C-termini (Uto *et al.*, 1999; Hames and Fry, 2001). In *Xenopus*, these isoforms display distinct patterns of expression during development, with Nek2B present in oocytes, eggs and early embryos and Nek2A present in late embryos and adults (Uto *et al.*, 1999). Nek2 splice variants also vary in their expression through the cell cycle. In adult human cell cycles, Nek2A is maximal in S/G_2 and low in M/G_1, whereas Nek2B remains at its peak throughout S, G_2 and M, and is low only in G_1 (Hames and Fry, 2001). Nek2B expression is invariant during early embryonic cell cycles (Fry *et al.*, 2000b), whereas Nek2A, if added ectopically, is rapidly degraded (Uto and Sagata, 2000). These observations prompted us to consider the possibility that Nek2A is subject to degradation in mitosis as a result of sequences in its C-terminus that are missing from Nek2B. Here, we demonstrate that human Nek2A is an early mitotic target of the APC/C–Cdc20 and present evidence to support a model in which recognition of substrates by the APC/C before inactivation of the spindle assembly checkpoint relies on the presence of a cyclin A-like extended destruction box.

Results

Nek2A is destroyed in early mitosis

In human somatic cells, both Nek2 splice variants are expressed at low levels in G_1 and at high levels in S and G_2. However, in prometaphase-arrested cells, Nek2A expression is low, whereas that of Nek2B remains high. To determine exactly when Nek2 proteins disappear, extracts were prepared from U2OS cells released from an arrest at the G_1/S transition in the presence of nocodazole. Nek2A expression decreased abruptly between 10 and 12 h after release from the block (Figure 1A). This was coincident both with the time of mitotic entry as judged by microscopic examination of cells and with the disappearance of cyclin A, a protein known to be targeted for destruction in prometaphase (den Elzen and Pines, 2001; Geley *et al.*, 2001). The drop in expression of Nek2A was accompanied by the appearance of a weak, higher molecular weight smear suggestive of phosphorylation. However, even taking this into account, the overall level of Nek2A consistently decreased at least 2- to 3-fold with respect to S and G_2 phase cells. In contrast, the abundance of Nek2B remained elevated in these cells and, taking into account the appearance of a higher molecular weight smear for Nek2B as well, even increased into mitosis. To observe when Nek2B protein disappears, cells were released from a nocodazole block into G_1 (Figure 1B). Nek2B protein decreased between 4 and 8 h after release, whereas cyclin B1 levels disappeared more rapidly. Nek2B protein therefore persists until early G_1. In this experiment, Nek2A levels dropped slightly further upon entry into G_1 and remained low until the time of entry into the next S phase when there was a sudden 3- to 4-fold increase in its abundance (Figure 1B).

To determine whether loss of Nek2 proteins was due to increased degradation, their half-lives were measured following treatment with the protein synthesis inhibitor cycloheximide (Figure 1C). In asynchronous cells, the stability of Nek2A was very low, with an estimated half-life of 45 min. The half-life of Nek2B was slightly longer at ~75 min. However, in S phase-arrested cells, the half-life of Nek2A was extended to >4 h, whereas the half-life of Nek2B was unchanged. In either M or G_1 cells, the level of Nek2A was so low that it became undetectable by the first time point (30 min), making calculation of a half-life impossible (data not shown). To test directly whether Nek2 was destroyed in mitosis, recombinant proteins were incubated in cytostatic factor (CSF) (metaphase II-arrested) extracts of *Xenopus* eggs or in CSF extracts to which calcium had been added to trigger anaphase entry (Figure 1D). In both types of extract, Nek2A was unstable, although its rate of loss was significantly greater in anaphase extracts. The slower degradation that occurred in metaphase extracts was again accompanied by the appearance of a higher molecular weight smear. Nek2B, on the other hand, was completely stable in CSF extracts both before and after addition of calcium (Figure 1D). Both Nek2 isoforms were stable when incubated in interphase extracts, indicating that neither components of the reticulocyte lysate system used for generating recombinant proteins nor those of the interphase egg cytosol were sufficient for Nek2A degradation (data not shown). For comparison, the stability of cyclins A and B1 was measured in these extracts. As previously reported, cyclin B1 was only degraded after calcium addition, whereas cyclin A was degraded both before and after calcium addition although, like Nek2A, degradation was more rapid in anaphase extracts (Glotzer *et al.*, 1991; Geley *et al.*, 2001). Taken together, these results demonstrate that Nek2A is destroyed upon entry into mitosis with very similar timing to cyclin A, whereas Nek2B is stable at least until late mitosis/early G_1.

Nek2A is destroyed in mitosis by the proteasome

To determine whether Nek2A is destroyed by the 26S proteasome, its half-life was measured in cells pre-incubated with various protease inhibitors (Lee and Goldberg, 1998). In the presence of either MG132 or

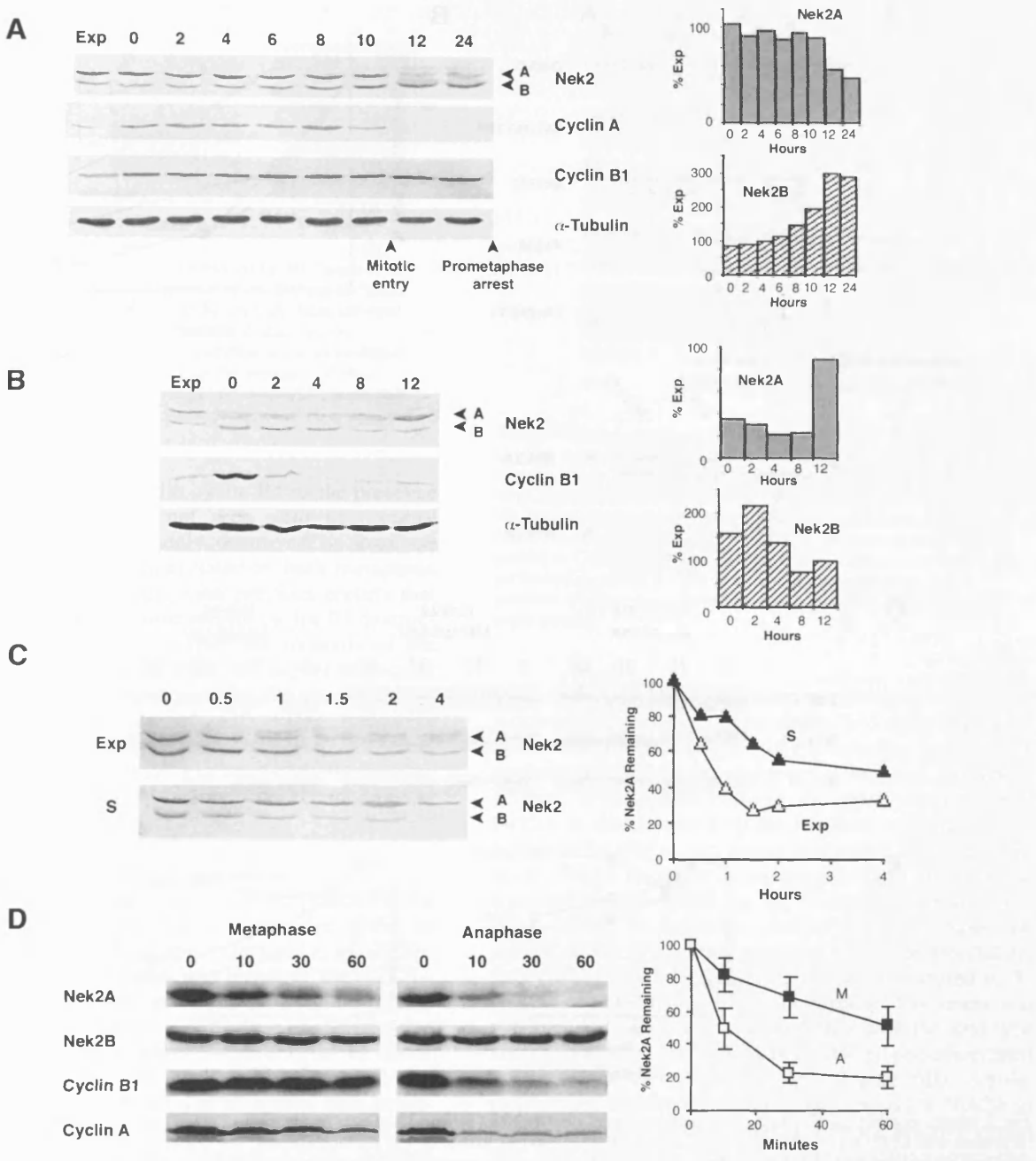

Fig. 1. Nek2A is destroyed in early mitosis. (**A**) Extracts prepared from exponentially growing U2OS cells (Exp) or cells released from a thymidine–hydroxyurea block into medium containing nocodazole for the times indicated (h) were immunoblotted with antibodies against Nek2, cyclin A, cyclin B1 and α-tubulin. Mitotic entry was observed by phase microscopy to occur between 10 and 12 h after release. The positions of Nek2 splice variants (A and B) are indicated. The abundance of Nek2A and Nek2B proteins present at each time point with respect to the amount in exponential cells was quantified by densitometry and is shown in the histograms on the right. (**B**) Immunoblots of extracts prepared following release from a nocodazole block for the times indicated (h). Again, histograms on the right show the quantified levels of Nek2A and Nek2B proteins. (**C**) Protein stability of Nek2A (A) and Nek2B (B) in exponential (Exp) and S phase-arrested (S) cells was measured on immunoblots of cell extracts prepared at the times indicated (h) after addition of cycloheximide. On the right, the amount of Nek2A protein remaining at each time point is plotted with respect to the amount present at time zero (Exp, open triangles; S, closed triangles). (**D**) *In vitro* degradation assays were performed by addition of ^{35}S-labeled Nek2A, Nek2B, cyclin B1 or cyclin A to CSF extracts with (anaphase) or without (metaphase) addition of calcium. Samples were collected at the times indicated (min), separated by SDS–PAGE and exposed to autoradiography. The amount of Nek2A protein remaining at each time is plotted with respect to the amount at time zero in metaphase (M, closed squares) and anaphase (A, open squares) extracts. Results are taken from six independent experiments and error bars represent standard deviations.

lactacystin, strong inhibitors of the proteasome, the half-life of Nek2A was extended to >4 h (Figure 2A and B). In contrast, ALLM, a calpain inhibitor, did not alter the half-life of Nek2A at all. Leupeptin, an inhibitor of trypsin and cysteine proteases, caused a moderate increase in Nek2A half-life, consistent with an inhibition of one of the major peptidase activities (trypsin-like) of the proteasome (Coux *et al.*, 1996). To determine specifically whether the

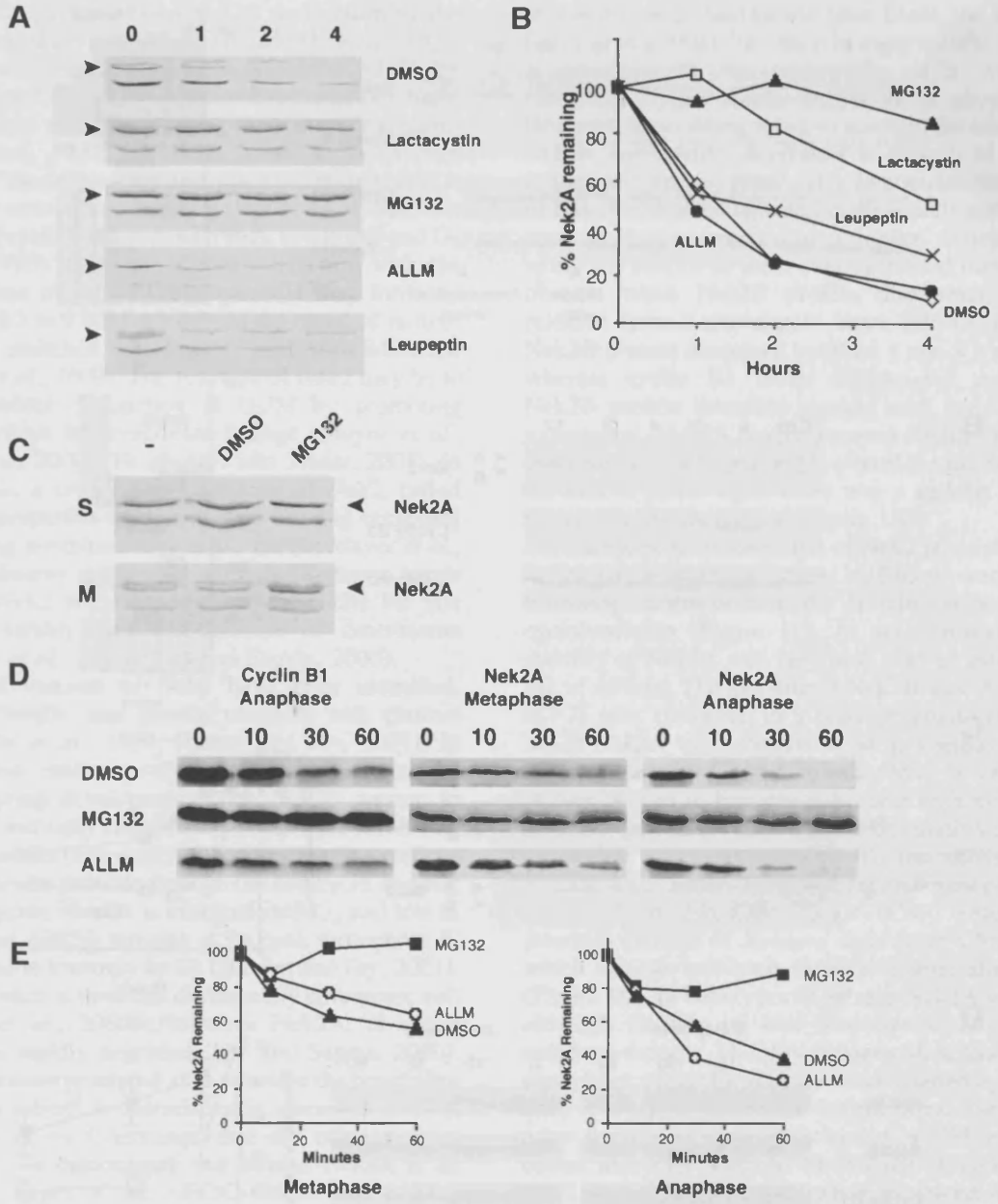

Fig. 2. Mitotic destruction of Nek2A is proteasome dependent. (**A**) Nek2 protein stability was determined as in Figure 1C except following a 1 h pre-incubation with DMSO, 12.5 μM lactacystin, 20 μM MG132, 100 μM ALLM or 200 μg/ml leupeptin. The position of Nek2A is indicated (arrows). (**B**) The amount of Nek2A in the blots shown in (A) was determined by quantitative densitometry and shown with respect to the amount of protein at time zero (100%); DMSO (open diamonds), lactacystin (open squares), MG132 (filled triangles), ALLM (filled circles), leupeptin (crosses). (**C**) Cells arrested in either S (hydroxyurea) or M (nocodazole) were treated for 4 h with nothing (–), DMSO or 20 μM MG132, before extraction and immunoblotting with Nek2 antibodies. (**D**) Degradation assays were performed with cyclin B1 or Nek2A in extracts containing DMSO, 50 μM MG132 or 50 μM ALLM. (**E**) The amount of Nek2A remaining in metaphase (left graph) and anaphase (right graph) extracts in the presence of DMSO (closed triangles), MG132 (closed squares) and ALLM (open circles) with time was quantified from the autoradiographs shown in (D).

mitotic destruction of Nek2A is due to the proteasome, MG132 was added to cells pre-arrested in either S or M phase (Figure 2C). Whereas addition of MG132 caused no detectable change in the amount of Nek2A present in S phase cells, it led to a significant increase in the level of Nek2A in prometaphase cells. Addition of MG132, but not ALLM, also prevented Nek2A destruction in both metaphase and anaphase egg extracts (Figure 2D and E). These results provide confirmation that the proteasome is responsible for removing Nek2A in mitosis.

Nek2A is ubiquitylated in mitosis

Proteins bound for destruction by the proteasome generally are covalently modified with multiple chains of ubiquitin (Hershko and Ciechanover, 1998). To determine whether Nek2A can be covalently conjugated with ubiquitin, His-tagged ubiquitin was added to mitotic extracts carrying recombinant proteins before affinity purification with nickel–agarose beads (Figure 3). Some unmodified protein was present in all the precipitates. However, long exposure revealed a ladder of increasing

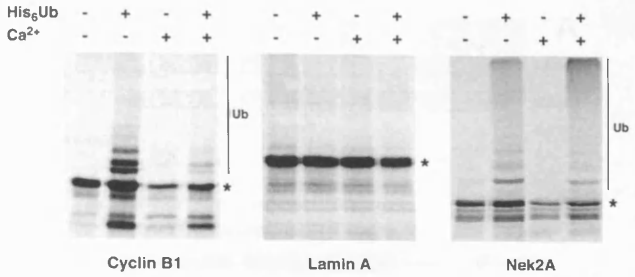

Fig. 3. Ubiquitylation of Nek2A. ^{35}S-labeled cyclin B1, lamin A or Nek2A were added to CSF extracts either with or without Ca^{2+} and His_6-ubiquitin as indicated. After 30 min incubation, samples were precipitated using Ni^{2+}-NTA–agarose beads and analyzed by SDS–PAGE and autoradiography. In all samples, some unmodified protein (*) was precipitated irrespective of the presence of His_6-ubiquitin. However, high molecular weight products (Ub) were only detected with cyclin B1 and Nek2A in the presence of His_6-ubiquitin.

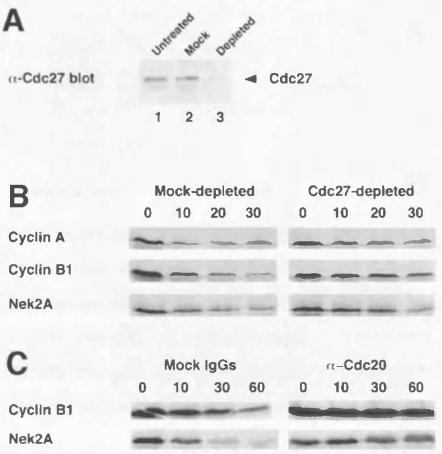

Fig. 4. Mitotic destruction of Nek2A is APC/C-Cdc20 dependent. (**A**) Egg extracts, which had been untreated (lane 1) or depleted with non-specific mouse IgGs (lane 2) or anti-Cdc27 mAb AF3 (lane 3), were immunoblotted with commercial anti-Cdc27 antibody. (**B**) Degradation assays were performed on cyclin A, cyclin B1 and Nek2A in anaphase extracts that had been either mock-depleted (left panels) or Cdc27-depleted (right panels). (**C**) Degradation assays were performed on cyclin B1 and Nek2A in anaphase extracts in the presence of either mock IgGs (left panels) or anti-Cdc20 antibodies (right panels).

molecular weight products with cyclin B1 in the presence of His_6-ubiquitin that was not seen with the control protein, lamin A. Although only destroyed in anaphase extracts, cyclin B1 was ubiquitylated in both metaphase and anaphase extracts, in line with previous reports that ubiquitylation alone is not sufficient for cyclin B1 destruction (Kramer *et al.*, 2000). Despite the intensity of the Nek2A signal being weak, at least two higher molecular weight products were detected in the presence of His_6-ubiquitin at intervals of ~10 kDa, indicative of ubiquitylation. Ubiquitylation of Nek2A occurred in both metaphase and anaphase extracts, with the weaker signal in anaphase most probably due to incomplete inhibition of the proteasome.

Nek2A destruction is APC/C dependent

The major E3 ubiquitin ligase that is active in mitosis is the APC/C. However, other ubiquitin ligases are active in mitosis including the SCF complex (Jackson *et al.*, 2000). To determine whether Nek2A is a target of the APC/C, monoclonal antibodies directed against the core APC/C subunit Cdc27 (Yamano *et al.*, 1998) were used to remove the APC/C from egg extracts (Figure 4A). In these extracts, the destruction of cyclin B1, cyclin A and Nek2A was significantly delayed as compared with mock-depleted extracts (Figure 4B). In a different approach, antibodies raised against the *Xenopus* APC/C adaptor protein Cdc20 (also called Fizzy), that block APC/C–Cdc20-dependent degradation, were added to extracts (Lorca *et al.*, 1998). These antibodies blocked the degradation not only of cyclin B1 but also of Nek2A in both metaphase and anaphase extracts, providing additional strong evidence for the role of the APC/C–Cdc20 in the mitotic destruction of Nek2A (Figure 4C).

Nek2 activity is not required for APC/C activation or Nek2A destruction

Phosphorylation of APC/C subunits is necessary for its activation (Charles *et al.*, 1998; Descombes and Nigg, 1998; Shirayama *et al.*, 1998; Kotani *et al.*, 1999). We therefore tested whether Nek2 kinase activity was required for APC/C activation by removing the predominant splice variant present in egg extracts, X-Nek2B, by immunodepletion. Despite removal of >95% of X-Nek2B (Figure 5A), depleted extracts remained as efficient as mock-treated extracts in their ability to destroy cyclin B1, cyclin A and Nek2A (Figure 5B). It therefore seems highly unlikely that Nek2 kinase activity is required for APC/C activity. In metaphase extracts, the slower destruction of Nek2A is accompanied by the transient appearance of a higher molecular weight smear suggestive of phosphorylation. Nek2A has been shown previously to dimerize and trans-autophosphorylate on its C-terminal domain (Fry *et al.*, 1999). To determine whether the higher molecular weight products are the result of autophosphorylation, catalytically inactive Nek2 (K37R) was incubated in X-Nek2B-depleted extracts. To our surprise, this smear was still apparent, albeit a little weaker than with the wild-type kinase, indicating that Nek2A must also be phosphorylated by a distinct cytoplasmic kinase (Figure 5B). Similar results were obtained using inactive *Xenopus* X-Nek2A in depleted extracts (data not shown). As the inactive kinase was still destroyed, these experiments demonstrate that Nek2 activity is not required for its own destruction.

Nek2A destruction depends upon a cyclin A-like destruction box in its extreme C-terminus

Two sequence motifs have been described that target proteins to the APC/C: a nine amino acid destruction box (D-box), first identified in cyclin B, and a KEN-box, initially found in the APC/C regulator, Cdc20 (Glotzer *et al.*, 1991; Pfleger and Kirschner, 2000). Human Nek2A contains putative versions of both these motifs: a D-box (**R**KF**L**LSLA**SN**) at amino acids 361–369 and a KEN-box (**KEN**IMRSE**NS**) at amino acids 391–400. The positions of these motifs with respect to the splice site are such that both Nek2A and Nek2B contain the D-box, whereas only Nek2A contains the KEN-box (Figure 6A). During the initial description of the KEN-box, it was shown that human Nek2A was unstable in interphase egg extracts

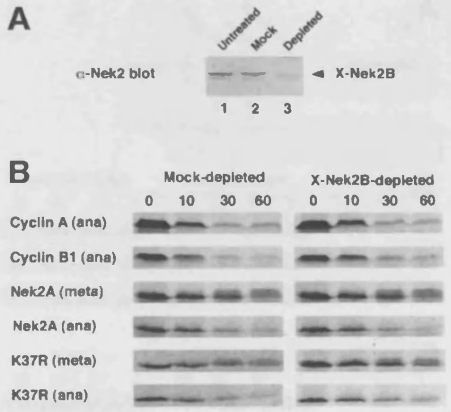

Fig. 5. Nek2 kinase activity is not required to activate the APC/C. (**A**) Egg extracts that were untreated (lane 1) or depleted with non-specific rabbit IgGs (lane 2) or anti-*Xenopus* Nek2B antibodies (lane 3) were immunoblotted with anti-*Xenopus* Nek2B antibodies. (**B**) Degradation assays were performed on cyclin A, cyclin B1, Nek2A or catalytically inactive Nek2A (K37R) in mock-depleted (left panels) or Nek2-depleted (right panels) anaphase (ana) or metaphase (meta) extracts.

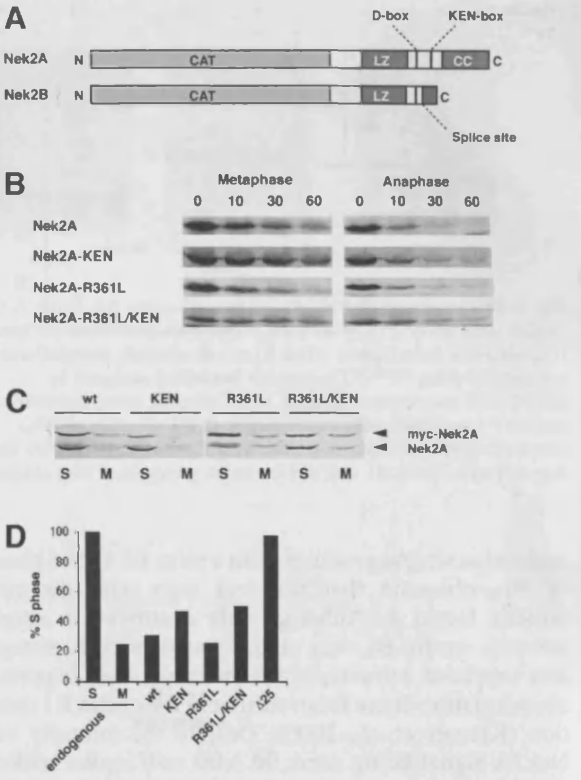

Fig. 6. Examination of putative destruction boxes in Nek2A. (**A**) Schematic diagram of the human Nek2 splice variants indicating the catalytic domain (CAT), leucine zipper (LZ), coiled-coil domain (CC), splice site, D-box and KEN-box. (**B**) *In vitro* degradation assays were performed in metaphase and anaphase extracts with Nek2A, Nek2A-KEN, Nek2A-R361L and Nek2A-R361L/KEN. (**C**) HeLa cells were transfected with myc-tagged wild-type Nek2A, Nek2A-KEN, Nek2A-R361L or Nek2A-R361L/KEN before arrest in either S phase (S) or prometaphase (M). Cell extracts were immunoblotted with Nek2 antibodies to detect transfected myc-Nek2A and endogenous Nek2A proteins as indicated. (**D**) The mitotic degradation of each myc-tagged Nek2A construct is represented by the fraction (%) remaining in M phase-arrested cells, where the amount in S phase-arrested cells is considered as 100%. For comparison, the change in endogenous Nek2A is also shown.

supplemented with recombinant Cdh1 but could be stabilized by mutation of its KEN-box (Pfleger and Kirschner, 2000). To test the importance of the D- and KEN-box motifs for Nek2A destruction, they were mutated individually or in combination and the stability of the resulting constructs assessed in egg extracts (Figure 6B). Mutation of the D-box had no effect on Nek2 destruction, while mutation of the KEN-box slowed the destruction of Nek2A in metaphase, but not anaphase, extracts. Mutation of the D- and KEN-box in the same construct provided no additional stabilization over mutation of the KEN-box alone. The stability of these proteins was also tested *in vivo* by analyzing the abundance of transfected protein (Figure 6C and D). All ectopically expressed proteins were detected in S phase but were significantly reduced in prometaphase-arrested cells. Hence, the D- and KEN-box alone or in combination cannot account for the destruction of Nek2A that occurs in early mitotic cells. In line with this, ubiquitylation was still observed with the KEN-box mutant (data not shown).

Destruction of cyclin A by the APC/C in early mitosis is dependent upon a novel extended form of D-box that contains both the core cyclin B-type D-box motif plus an additional short sequence downstream (amino acids 45–72 in human cyclin A2; Geley *et al.*, 2001). As Nek2A is destroyed at the same time as cyclin A, we compared the sequence of the cyclin A extended D-box with the region of Nek2A that is absent from Nek2B. We found that the extreme C-terminal 23 amino acids of Nek2A have startling similarity to the cyclin A D-box, possessing both the core B-type D-box motif and a 10 amino acid sequence downstream (LKSRQILGMR) that is highly conserved with the cyclin A extension (Figure 7A). Expression of a Nek2A construct lacking the C-terminal 25 amino acids (Nek2A-Δ25) produced a protein that was no longer degraded in prometaphase-arrested cells (Figure 7B and 6D) and had a half-life of significantly more than 4 h in asynchronous cells (Figure 7C and D). Hence, it is this A-type D-box that is key to Nek2A destruction in prometaphase cells. Nek2A-Δ25 was stable in metaphase extracts but still slowly degraded in anaphase extracts (Figure 7E). However, a double mutant lacking both the KEN-box and C-terminal 25 amino acids was completely stable (Figure 7E).

To test whether the Nek2A C-terminal D-box could compete with cyclin B destruction, we purified the entire C-terminal non-catalytic domain as a GST fusion protein (Figure 8A). At low concentrations, this protein was itself destroyed in egg extracts in a proteosomal-dependent manner, indicating that it carries motifs sufficient for mitotic destruction (Figure 8B). When added in excess, it delayed the destruction of both cyclin A and cyclin B1, emphasizing that Nek2A is a target of the same destruction machinery as the cyclins (Figure 8C). When an excess of an N-terminal fragment of *Schizosaccharomyes pombe* cyclin B that contains the B-type D-box (N70; Yamano *et al.*, 1998) was added, the destruction of cyclin B1 was strongly inhibited, but that of cyclin A and Nek2A was

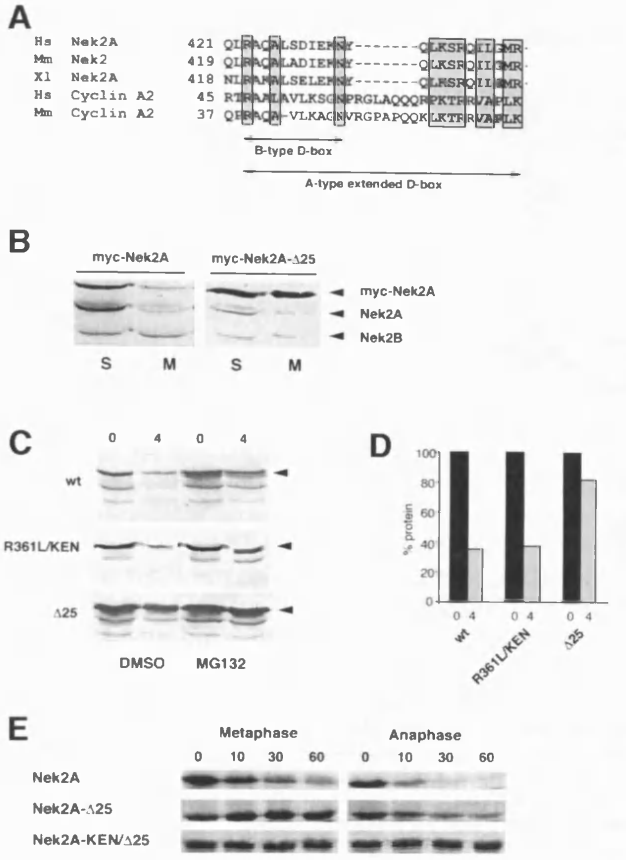

Fig. 7. Identification of a cyclin A-type D-box in the C-terminus of Nek2A. (**A**) Comparison of the C-terminal 25 amino acids of human (Hs), mouse (Mm) and frog (Xl) Nek2A with the extended D-box of human and mouse cyclin A2. The three key residues of the classical D-box are shaded, together with the residues downstream that are either identical or have only conservative changes. (**B**) Extracts of HeLa cells transfected with myc-Nek2A (left panel) or myc-Nek2A-Δ25 (right panel) and arrested in S phase (S) or prometaphase (M) were immunoblotted with Nek2 antibodies and the position of transfected and endogenous Nek2 proteins indicated. (**C**) HeLa cells transfected with myc-Nek2A (top panel), myc-Nek2A-R361L/KEN (middle panel) and myc-Nek2A-Δ25 (bottom panel) were pre-treated with DMSO or MG132 before addition of cycloheximide for either 0 or 4 h as indicated. (**D**) The fraction (%) of each expressed protein remaining at 4 h in the absence of MG132 is shown with respect to the amount at 0 h. (**E**) Destruction assays were carried out in metaphase or anaphase extracts with Nek2A, Nek2A-Δ25 and Nek2A-KEN/Δ25.

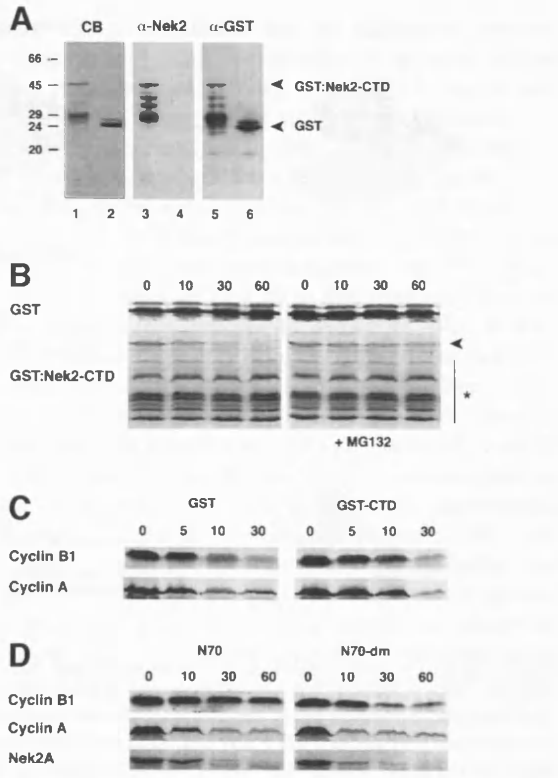

Fig. 8. The Nek2 C-terminal domain interferes with destruction of cyclins A and B. (**A**) Purified GST–Nek2-CTD (lanes 1, 3 and 5) and GST alone (lanes 2, 4 and 6) separated on 15% SDS–polyacrylamide gels and stained with Coomassie Blue (lanes 1 and 2), or immunoblotted with antibodies against Nek2 (lanes 3 and 4) or GST (lanes 5 and 6). Molecular weights (kDa) are indicated on the left. (**B**) Degradation assays were performed with 200 ng of GST or GST–Nek2-CTD in 10 μl of anaphase extracts in the absence (left panels) or presence (right panels) of 50 μM MG132. Samples taken at the times indicated (min) were analyzed by immunoblotting with anti-GST antibodies. Note that only the full-length GST–Nek2-CTD protein (arrowhead), and not the lower molecular weight truncated forms (asterisk), is degraded in the absence of MG132. (**C**) Degradation assays were performed with cyclin B1 and cyclin A in anaphase extracts in the presence of 1 μg GST (left panels) or GST–Nek2-CTD (right panels). (**D**) Degradation assays were performed in anaphase extracts with cyclin B1, cyclin A and Nek2A in the presence of 1 μg of an N-terminal 70 amino acid fragment of *S.pombe* Cdc13 (N70, left panels) or an identical fragment but with mutations in the destruction box (N70-dm right panels).

only weakly inhibited (Figure 8D). These intriguing results suggest that the cyclin A/Nek2A-type D-box contains additional sequences, presumably in the downstream extension, that allow recognition by the APC/C independently of its core B-type D-box.

Discussion

Previous work has demonstrated that Nek2A disappears in mitotically arrested cells (Schultz *et al.*, 1994; Fry *et al.*, 1995; Hames and Fry, 2001), is unstable in interphase egg extracts supplemented with recombinant Cdh1 (Pfleger and Kirschner, 2000) and is degraded when injected into dividing embryos (Uto and Sagata, 2000). This prompted us to investigate if, when and how human Nek2 proteins are destroyed during mitosis. The results presented here show that Nek2A is destroyed by the proteasome following ubiquitylation by the E3 ubiquitin ligase APC/C–Cdc20. Furthermore, degradation of Nek2A first occurs in early mitosis, coincident with cyclin A destruction, and depends upon a motif in its extreme C-terminus that is almost identical to the extended D-box present in cyclin A (Geley *et al.*, 2001).

Nek2A is an early mitotic target of the APC/C

In synchronized cells, Nek2A is destroyed early in mitosis coincident, within the limits of the experiment, with the destruction of cyclin A. Moreover, Nek2A is absent in cells arrested in prometaphase with the microtubule poison nocodazole. Hence, the destruction of Nek2A, like that of cyclin A but not cyclin B, is independent of the spindle assembly checkpoint. Proteasome inhibitors added to cells arrested in prometaphase allowed the re-accumulation of Nek2A, indicating that its loss is due to continual turnover by the 26S proteasome rather than to inhibition of

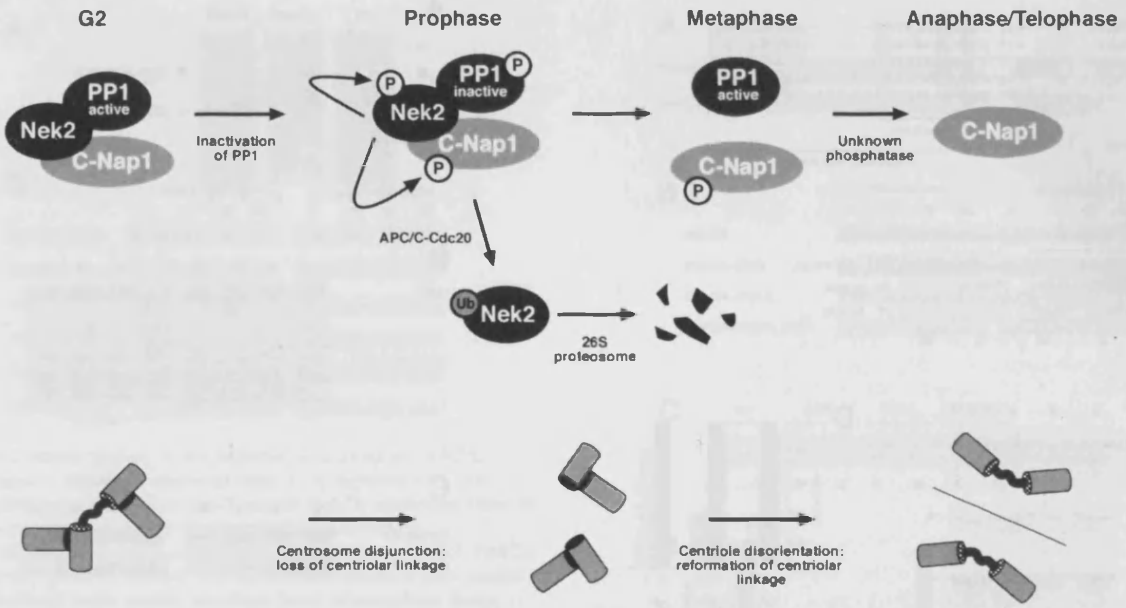

Fig. 9. The role of Nek2A destruction in mitosis. Current data, presented here and elsewhere, predict that a complex would exist in G_2 composed of Nek2A, C-Nap1 and PP1. This complex, present at the proximal ends of centrioles, may form an anchoring structure for the intercentriolar linkage. Nek2A expression is high in G_2, but its association with active PP1 keeps it and C-Nap1 in a dephosphorylated state. Upon phosphorylation and inactivation of PP1 at the G_2/M transition, Nek2 and C-Nap1 become hyperphosphorylated, leading to displacement or degradation of C-Nap1 and disjunction of centrosomes. Centrosomes can then separate to opposite ends of the cell as a bipolar spindle is formed. Upon progress into mitosis, the APC/C becomes active towards Nek2A, causing its ubiquitylation and destruction. With Nek2A no longer present, C-Nap1 can be dephosphorylated at some point later in mitosis, allowing it to reassociate with disoriented centrioles and establish a new intercentriolar linkage.

transcription or translation. Also in common with cyclin A, Nek2A is unstable in egg extracts arrested in metaphase II of meiosis but is destroyed more rapidly in CSF extracts triggered to enter anaphase. Only these latter extracts can destroy cyclin B. Hence, the destruction mechanism that is active in prometaphase of an adult cell cycle seems also to be active in metaphase-II of meiosis.

The destruction of Nek2A, again in common with cyclin A, is directed by the APC/C ubiquitin ligase. In this study, it is shown that Nek2A can be ubiquitylated during mitosis. More specifically, depletion of the APC/C via anti-Cdc27 antibodies significantly reduced the rate of Nek2A destruction, while inhibitory Cdc20 antibodies blocked it completely. Nek2A can also be destroyed in interphase extracts, which possess APC/C proteins, simply by addition of the other APC/C activator Cdh1 (Pfleger and Kirschner, 2000). The identification of its C-terminal destruction motifs provides final confirmation that Nek2A is an APC/C substrate. Hence, Nek2A shares another common property with its fungal homolog NIMA. Although their destruction motifs appear to be different, both are targeted by the APC/C through their non-catalytic C-terminal domains.

Early embryos of frogs and flies possess only one APC/C adaptor protein, Cdc20, as Cdh1 is only expressed later in development when cell cycles introduce the first G_1 phase (Sigrist and Lehner, 1997; Lorca *et al.*, 1998). Nek2A must therefore be targeted for destruction, at least in meiotic egg extracts, by the APC/C–Cdc20 complex, explaining the prevention of Nek2A destruction by inhibitory anti-Cdc20 antibodies. However, Nek2A can also be destroyed by APC/C–Cdh1 (Pfleger and Kirschner, 2000). Thus, Nek2A, like other APC/C substrates (e.g. securin, cyclin B and Cdc6), can be recognized by the APC/C in complex with either Cdc20 or Cdh1. Nek2A abundance remains at very low levels throughout G_1 and, although not formally proven here, it seems reasonable to predict that destruction begun in early mitosis by APC/C–Cdc20 is maintained into G_1 (and G_0) by APC/C–Cdh1. Nek2B, the shorter splice variant, is not destroyed in prometaphase cells or metaphase II extracts. Neither is it destroyed in anaphase or interphase extracts, in line with results showing that *Xenopus* Nek2B is stable throughout the first embryonic cell cycle (Fry *et al.*, 2000b). However, Nek2B does decrease in abundance in cells upon re-entry into G_1. The half-life of Nek2B did not change significantly between asynchronous and S phase-arrested cells, although the proteasome inhibitor MG132 did cause a moderate increase in its stability. It therefore remains unclear whether the decrease of Nek2B in G_1 is due to degradation or some other mechanism such as reduced transcription.

What regulates the timing of mitotic APC/C substrates?

Nek2A and cyclin A are both destroyed via the APC/C early in mitosis when the APC/C is unable to target other substrates, such as cyclin B or securin, for destruction. Inhibition of the APC/C towards these latter substrates is regulated by the spindle checkpoint protein Mad2 which, in the presence of unattached kinetochores, binds directly to Cdc20 (Shah and Cleveland, 2000). The mechanism by which the APC/C is prevented from destroying cyclin B in metaphase II-arrested eggs is not known, because at this cell cycle stage, not only are all kinetochores attached, but

also the spindle assembly checkpoint is not functional (Minshull *et al.*, 1994).

The finding that Nek2A and cyclin A share a similar extended destruction box suggests that this may be key to recognition of early mitotic substrates by the APC/C. Deletion of this motif stabilized Nek2A in both cells and extracts. Moreover, this motif is highly conserved among vertebrate Nek2 kinases, unlike the other potential D-box (amino acids 361–369) that is present in human Nek2A and Nek2B, but not in the Nek2 sequences of other vertebrates. Indeed, mutation of this latter D-box had no stabilizing effect whatsoever, suggesting that it has no function in regulating Nek2 destruction. The KEN-box, on the other hand, is conserved in mammalian and frog Nek2A and its mutation partially stabilized Nek2A in extracts, although not in mitotic cells. It seems plausible that the extended destruction box present in the extreme C-terminus is targeted by APC/C–Cdc20 in early mitosis, whereas the KEN-box is targeted by APC/C–Cdh1 in late mitosis and G_1. This fits with the notion that Cdc20 acts most effectively on D-box-type sequences, but can also recognize KEN-boxes, whereas Cdh1 is more selective for the KEN-box (Pfleger and Kirschner, 2000).

The destruction of cyclin B1 was strongly inhibited by addition of a protein fragment containing a B-type D-box. However, this fragment had only a mild inhibitory effect on the destruction of cyclin A or Nek2A. In contrast, the destruction of both cyclins was significantly delayed by a GST fusion protein containing the degradation motifs of Nek2A. This fusion protein could itself be destroyed, indicating that the Nek2A C-terminus could act as a transferable degradation signal. These competition experiments could reflect a quantitative difference in the extent of ubiquitylation required to destroy these proteins, with cyclin B requiring more ubiquitylation than cyclin A or Nek2A. Alternatively, they could indicate that, as a result of the extended nature of the cyclin A-type D-box, the presence of the smaller B-type D-box could not entirely prevent the APC/C from recognizing cyclin A or Nek2A. If Mad2 acts by competing for the same site as the B-type D-box, then this could equally explain why the spindle assembly checkpoint does not prevent destruction of proteins with the extended A-type D-box. Exactly which residues are critical within this A-type D-box will require further investigation, but one possibility is that a phosphorylation site is involved in a manner reminiscent of substrate recognition by the SCF ubiquitin ligase (Jackson *et al.*, 2000). Nek2A is transiently phosphorylated before its destruction and this appears not to be solely via autophosphorylation. It is attractive to speculate that there may be a Nek2 kinase kinase that is somehow involved in targeting Nek2A, and perhaps cyclin A, to the APC/C.

What is the purpose of Nek2A destruction?

The timing of Nek2 kinase activation, its interaction with PP1 and now the timing of its destruction all support a role for Nek2A immediately prior to the onset of mitosis. Taken together with its localization to the centrosome, its ability to stimulate centrosome splitting upon overexpression and its interaction with C-Nap1, a protein implicated in centrosome cohesion, it seems likely that Nek2A plays a critical role in centrosome disjunction at the G_2/M transition (Hinchcliffe and Sluder, 2001). If, as has been proposed, Nek2A stimulates loss of cohesion between centrosomes by triggering disassembly of an intercentriolar linkage (Mayor *et al.*, 1999), then Nek2A destruction may somehow be necessary to allow re-establishment of the intercentriolar linkage in late mitosis (Figure 9). C-Nap1, which disappears from centrosomes in late G_2, reappears around telophase (Mayor *et al.*, 2000), at the same time as a flexible linker is re-established between the new centriole pairs of the future daughter cells (Piel *et al.*, 2000). The persistence of Nek2B at this time may seem to pose a problem for this hypothesis. However, Nek2B does not bind PP1, nor does it stimulate centrosome splitting with the same efficiency as Nek2A (Hames and Fry, 2001). Hence, Nek2B may not have an equivalent function in regulating the intercentriolar linkage. Instead, Nek2B protein may contribute to the stability of mitotic spindle poles as inhibition of Nek2B leads to centrosome fragmentation in early *Xenopus* embryos (Uto and Sagata, 2000). Another important question is whether the destruction of Nek2A is necessary for mitotic exit. So far, we have not seen any evidence for substantial delays in mitosis upon expression of mutant Nek2A constructs (data not shown). Overexpression of a stabilized NIMA mutant did cause a mitotic arrest in *Aspergillus* cells without preventing destruction of cyclin B, suggesting that there is a genuine need to down-regulate NIMA activity (Pu and Osmani, 1995). Cyclin A overexpression also delays progression through mitosis, although this could be due to either competition for the APC/C or abnormal maintenance of Cdk1 activity (den Elzen and Pines, 2001; Geley *et al.*, 2001). The challenge now is to demonstrate the role of Nek2A destruction in both centrosome dynamics and mitotic progression in living cells.

Materials and methods

Cell culture, synchronization and transfection

HeLa and U2OS cells were grown at 37°C in a 5% CO_2 atmosphere in Dulbecco's modified Eagle's medium (DMEM) supplemented with 10% fetal calf serum and penicillin–streptomycin (100 IU/ml and 100 μg/ml, respectively). The following protocols were used to obtain U2OS cells arrested at specific stages of the cell cycle. G_1/S: cells were pre-synchronized in S phase by the addition of 2 mM thymidine for 12 h, released by transferring to fresh medium for 8 h and then re-synchronized at the G_1/S transition by incubation for 16 h with 1 mM hydroxyurea. S phase: cells were incubated with 1 mM hydroxyurea for 16 h. M phase: cells were treated with 500 ng/ml nocodazole for 16 h before collecting the mitotic population by gentle pipetting. Release of cells from drug-induced cell cycle blocks was performed by three washes in 1× phosphate-buffered saline (PBS) and replacement into fresh medium. Cell cycle distributions were confirmed by flow cytometry. To measure protein stability in cells, cycloheximide was added to 50 μg/ml and cells were harvested at given time intervals after cycloheximide addition. To test the role of different proteases, cells were first pre-incubated for 1 h with dimethylsulfoxide (DMSO), 12.5 μM *clasto*-lactacystin, 20 μM MG132, 100 μM ALLM (all from Calbiochem) or 200 μg/ml leupeptin (Sigma) before addition of cycloheximide. Transient transfections were carried out using Lipofectamine 2000 reagent (Invitrogen Life Technologies) according to the manufacturer's instructions.

Cell extraction and immunoblotting

Cell extractions and immunoblotting were performed as described previously (Fry *et al.*, 1998a). The following antibodies were used for immunoblots: anti-Nek2 (Zymed anti-peptide antibody; Fry *et al.*, 1999), 1.0 μg/ml; anti-human cyclin B1 (UBI), 0.8 μg/ml; anti-human cyclin A (UBI), 1.0 μg/ml; anti-α-tubulin (Amersham Pharmacia), 0.15 μg/ml; anti-Cdc27 (Transduction Laboratories), 1.0 μg/ml; and anti-GST (Molecular Probes), 0.3 μg/ml.

Plasmid construction and mutagenesis

pGEM:Nek2A-KEN was generated by PCR-based mutagenesis of the pGEM:Nek2 plasmid (Schultz *et al.*, 1994) using the QuikChange Site-directed Mutagenesis Kit (Stratagene). This changes amino acids 391–393, KEN to AAA, and 399, N to A. pCMVmyc:Nek2A-KEN was made by excising an *Nhe*I C-terminal fragment containing the KEN-box motif from pCMVmyc:Nek2A (Fry *et al.*, 1998a) and replacing it with the corresponding fragment containing the KEN-box mutation from pGEM:Nek2A-KEN. pGEM:Nek2A-R361L was made by mutagenizing the pGEM-Nek2 plasmid using the Transformer Site-directed Mutagenesis Kit (Clontech). To make pCMVmyc:Nek2A-R361L, the Nek2A-R361L fragment was excised from pGEM:Nek2A-R361L on a *Nae*I–*Xba*I fragment and subcloned into the *Sma*I–*Xba*I sites of a pBlueScript-myc vector (Schmidt-Zachmann and Nigg, 1993), creating pBS:myc-Nek2A-R361L. The myc-Nek2A-R361L insert was then excised from this plasmid on a *Sal*I (blunted)–*Xba*I fragment and subcloned into pRcCMV (Invitrogen) cut with *Hin*dIII (blunted)–*Xba*I. pGEM:Nek2A-R361L/KEN was generated by performing site-directed mutagenesis on the pGEM:Nek2A-R361L plasmid using the QuikChange Site-directed Mutagenesis Kit (Stratagene), and to make pCMVmyc:Nek2A-R361L/KEN site-directed mutagenesis was performed on the pCMVmyc:Nek2A-R361L plasmid. To make pGEM:-Nek2A-Δ25, a C-terminal fragment of Nek2A was amplified by PCR using a 3′ PCR primer that introduced a stop and *Bam*HI site immediately after amino acid 420. This was digested at an internal *Eco*RV site and the *Bam*HI site. An *Eco*RV–*Bam*HI fragment was then excised from pGEM:Nek2 and replaced with the corresponding amplified fragment. pCMVmyc:Nek2A-Δ25 was made by excising the N-terminal 420 amino acids of Nek2A together with an N-terminal myc tag from pBSmyc-Nek2 (Fry *et al.*, 1998a) on a *Sal*I–*Pvu*II blunted fragment and subcloning into pRcCMV (Invitrogen) cut with *Hin*dIII–*Xba*I and blunted. Finally, to make pGEM:Nek2A-KEN/Δ25, a *Dra*II fragment containing most of the Nek2A coding sequence and encompassing the KEN-box was excised from pGEM:Nek2A-KEN and used to replace the corresponding *Dra*II fragment from pGEM:Nek2A-Δ25. All constructs were confirmed by DNA sequencing on an ABI sequencer (Perkin Elmer) using BigDye technology at the University of Leicester Protein and Nucleic Acid Laboratory.

In vitro degradation assays and immunodepletions

CSF (metaphase II-arrested) or interphase extracts were prepared as described (Desai *et al.*, 1999). To generate anaphase extracts, calcium chloride was added to 0.5 mM. Substrates were prepared by coupled *in vitro* transcription–translation in reticulocyte lysates (TNT, Promega), in the presence of [^{35}S]cysteine/methionine (NEN), using the appropriate plasmids. Egg extracts (10 μl) were supplemented with 1.5 μl of *in vitro* translation mix and 0.3 μl of cycloheximide (10 mg/ml) before incubation at 22°C. Aliquots (2.5 μl) were taken at the times indicated, mixed with protein sample buffer and separated on 12% SDS–polyacrylamide gels. Gels were fixed and stained with Coomassie Blue, soaked in Amplify (Amersham), dried and exposed either to X-ray film (Fuji) or to phosphoimaging screens. Immunodepletions were carried out as described (Descombes and Nigg, 1998), with the exception of using two 30 min rounds of depletion with antibody coated to protein A–dynabeads (Dynal).

Ubiquitylation assay

Ubiquitylation assays were essentially as described in Funabiki and Murray (2000). Specifically, CSF extract (20 μl) was pre-incubated for 15 min at 22°C with MG132 (50 μM final concentration) before addition of cycloheximide (250 μg/ml final concentration) and 3 μl of *in vitro* translation mix containing ^{35}S-labeled recombinant protein. To this was added 0.2 μl of either dH_2O or $CaCl_2$ (0.5 mM final concentration) and 1.3 μl of either His_6-ubiquitin (0.5 mg/ml final concentration; Calbiochem) or His_6-ubiquitin buffer [20 mM Tris–HCl pH 8, 20 mM NaCl, 1 mM dithiothreitol (DTT)]. Samples were incubated for 30 min at 22°C before removing 2.5 μl for direct analysis by SDS–PAGE. To the remainder, 1 ml of buffer I [20 mM Tris–HCl pH 7.5, 500 mM NaCl, 10 mM *N*-ethylmaleimide, 5 mM imidazole, 1 mM phenylmethylsulfonyl fluoride (PMSF)] was added, mixed and spun at 14 K for 5 min at 4°C to remove insoluble material. Ni^{2+}-NTA–agarose beads (Qiagen) were prepared by washing three times in buffer I, incubating with rabbit reticulocyte lysate for 30 min at 4°C on a rotating wheel, and washing again three times with buffer I. The supernatant from the ubiquitylation reaction was added to 10 μl of beads and the sample rotated for 30 min at 4°C. Beads were pelleted and washed three times with 1 ml of buffer II (20 mM Tris–HCl pH 8.0, 500 mM NaCl, 25 mM imidazole, 10 mM *N*-ethylmaleimide, 1 mM PMSF, 0.5% Triton X-100, 0.5% Tween-20) and once with buffer I, before finally resuspending in 30 μl of protein sample buffer. Samples were separated on 8% SDS–polyacrylamide gels, dried and exposed to X-ray film or phosphoimager screens.

Recombinant protein expression in Escherichia coli

The C-terminal domain (CTD) of human Nek2A (amino acids 265–445) was excised from pGEM-Nek2 on an *Xmn*I fragment and inserted into the *Sma*I site of the pGEX-KG vector to generate pGEX:Nek2-CTD. This was transformed into BL21 *E.coli* and induced for 4 h with 0.4 mM isopropyl-β-D-thiogalactopyranoside before bacterial lysis and protein purification using standard procedures.

Acknowledgements

We thank Tim Hunt (South Mimms) and Jon Pines (Cambridge) for *Xenopus* cyclin B1 and human cyclin A plasmids, respectively, Sue Shackleton (Leicester) for human lamin A plasmid, Thierry Lorca (Montpellier) for anti-Cdc20 (Fizzy) antibodies, and Eilis Byrne (Leicester) for purified GST protein. We are grateful to Erich Nigg (Munich) for helpful comments on the manuscript and to all members of the laboratory for useful discussion. This work was supported by grants to A.M.F. from The Wellcome Trust and Cancer Research Campaign. A.M.F. is a Lister Institute Research Fellow. R.S.H. is supported by a studentship from the BBSRC. H.Y. is supported by a grant from PRESTO of the Japan Science and Technology Corporation.

References

Charles,J.F., Jaspersen,S.L., Tinker-Kulberg,R.L., Hwang,L., Szidon,A. and Morgan,D.O. (1998) The Polo-related kinase Cdc5 activates and is destroyed by the mitotic cyclin destruction machinery in *S.cerevisiae*. *Curr. Biol.*, **8**, 497–507.

Chen,J. and Fang,G. (2001) MAD2B is an inhibitor of the anaphase-promoting complex. *Genes Dev.*, **15**, 1765–1770.

Clute,P. and Pines,J. (1999) Temporal and spatial control of cyclin B1 destruction in metaphase. *Nature Cell Biol.*, **1**, 82–87.

Coux,O., Tanaka,K. and Goldberg,A.L. (1996) Structure and functions of the 20S and 26S proteasomes. *Annu. Rev. Biochem.*, **65**, 801–847.

den Elzen,N. and Pines,J. (2001) Cyclin A is destroyed in prometaphase and can delay chromosome alignment and anaphase. *J. Cell Biol.*, **153**, 121–135.

Desai,A., Murray,A., Mitchison,T.J. and Walczak,C.E. (1999) The use of *Xenopus* egg extracts to study mitotic spindle assembly and function *in vitro*. In Rieder,C.L. (ed.), *Mitosis and Meiosis*. Academic Press, San Diego, CA, pp. 385–412.

Descombes,P. and Nigg,E.A. (1998) The polo-like kinase Plx1 is required for M phase exit and destruction of mitotic regulators in *Xenopus* egg extracts. *EMBO J.*, **17**, 1328–1335.

Fry,A.M., Schultz,S.J., Bartek,J. and Nigg,E.A. (1995) Substrate specificity and cell cycle regulation of the Nek2 protein kinase, a potential human homolog of the mitotic regulator NIMA of *Aspergillus nidulans*. *J. Biol. Chem.*, **270**, 12899–12905.

Fry,A.M., Meraldi,P. and Nigg,E.A. (1998a) A centrosomal function for the human Nek2 protein kinase, a member of the NIMA-family of cell cycle regulators. *EMBO J.*, **17**, 470–481.

Fry,A.M., Mayor,T., Meraldi,P., Stierhof,Y.-D., Tanaka,K. and Nigg,E.A. (1998b) C-Nap1, a novel centrosomal coiled-coil protein and candidate substrate of the cell cycle-regulated protein kinase Nek2. *J. Cell Biol.*, **141**, 1563–1574.

Fry,A.M., Arnaud,L. and Nigg,E.A. (1999) Activity of the human centrosomal kinase, Nek2, depends upon an unusual leucine zipper dimerization motif. *J. Biol. Chem.*, **274**, 16304–16310.

Fry,A.M., Mayor,T. and Nigg,E.A. (2000a) Regulating centrosomes by protein phosphorylation. *Curr. Top. Dev. Biol.*, **49**, 291–312.

Fry,A.M., Descombes,P., Twomey,C., Bacchieri,R. and Nigg,E.A. (2000b) The NIMA-related kinase X-Nek2B is required for efficient assembly of the zygotic centrosome in *Xenopus laevis*. *J. Cell Sci.*, **113**, 1973–1984.

Funabiki,H. and Murray,A.W. (2000) The *Xenopus* chromokinesin Xkid is essential for metaphase chromosomes alignment and must be degraded to allow anaphase chromosomes movement. *Cell*, **102**, 411–424.

Geley,S., Kramer,E., Gieffers,C., Gannon,J., Peters,J.-M. and Hunt,T. (2001) Anaphase-promoting complex/cyclosome-dependent proteo-

lysis of human cyclin A starts at the beginning of mitosis and is not subject to the spindle assembly checkpoint. *J. Cell Biol.*, **153**, 137–147.

Glotzer,M., Murray,A.W. and Kirschner,M.W. (1991) Cyclin is degraded by the ubiquitin pathway. *Nature*, **349**, 132–138.

Hames,R.S. and Fry,A.M. (2002) Alternative splice variants of the human centrosome kinase Nek2 exhibit distinct patterns of expression in mitosis. *Biochem. J.*, **361**, in press.

Helps,N.R., Luo,X., Barker,H.M. and Cohen,P.T.W. (2000) NIMA-related kinase 2 (Nek2), a cell cycle-regulated protein kinase localized to centrosomes, is complexed to protein phosphatase 1. *Biochem. J.*, **349**, 509–518.

Hershko,A. and Ciechanover,A. (1998) The ubiquitin system. *Annu. Rev. Biochem.*, **67**, 425–479.

Hinchcliffe,E.H. and Sluder,G. (2001) 'It takes two to tango': understanding how centrosome duplication is regulated throughout the cell cycle. *Genes Dev.*, **15**, 1167–1181.

Jackson,P.K., Eldridge,A.G., Freed,E., Furstenthal,L., Hsu,J.Y., Kaiser,B.K. and Reimann,J.D.R. (2000) The lore of the RINGs: substrate recognition and catalysis by ubiquitin ligases. *Trends Cell Biol.*, **10**, 429–439.

Juang,Y.L., Huang,J.-Y., Peters,J.-M., McLaughlin,M.E., Tai,C.Y. and Pellman,D. (1997) APC-mediated proteolysis of Ase1 and the morphogenesis of the mitotic spindle. *Science*, **275**, 1311–1314.

Kotani,S., Tanaka,H., Yasuda,H. and Todokoro,K. (1999) Regulation of APC activity by phosphorylation and regulatory factors. *J. Cell Biol.*, **146**, 791–800.

Kramer,E.R., Scheuringer,N., Podtelejnikov,V., Mann,M. and Peters, J.-M. (2000) Mitotic regulation of the APC activator proteins CDC20 and CDH1. *Mol. Biol. Cell*, **11**, 1555–1569.

Lee,D.H. and Goldberg,A.L. (1998) Proteasome inhibitors: valuable new tools for cell biologists. *Trends Cell Biol.*, **8**, 397–403.

Lorca,T., Castro,A., Martinez,A.-M., Morin,N., Sigrist,S., Lehner,C., Doree,M. and Labbe,J.-C. (1998) Fizzy is required for activation of the APC-cyclosome in *Xenopus* egg extracts. *EMBO J.*, **17**, 3565–3575.

Mayor,T., Meraldi,P., Stierhof,Y.-D., Nigg,E.A. and Fry,A.M. (1999) Protein kinases in control of the centrosome cycle. *FEBS Lett.*, **452**, 92–95.

Mayor,T., Tanaka,K., Stierhof,Y.-D., Fry,A.M. and Nigg,E.A. (2000) The centrosomal protein C-Nap1 displays properties supporting a role in cell cycle-regulated centrosome cohesion. *J. Cell Biol.*, **151**, 837–846.

Minshull,J., Sun,H., Tonks,N.K. and Murray,A.W. (1994) A MAP kinase-dependent spindle assembly checkpoint in *Xenopus* egg extracts. *Cell*, **79**, 475–486.

Morgan,D.O. (1999) Regulation of the APC and the exit from mitosis. *Nature Cell Biol.*, **1**, E47–E53.

Nigg,E.A. (2001) Mitotic kinases as regulators of cell division and its checkpoints. *Nature Rev. Mol. Cell Biol.*, **2**, 21–32.

Page,A.M. and Hieter,P. (1999) The anaphase-promoting complex: new subunits and regulators. *Annu. Rev. Biochem.*, **68**, 583–609.

Petersen,B.O. *et al.* (2000) Cell cycle- and cell growth-regulated proteolysis of mammalian CDC6 is dependent on APC–CDH1. *Genes Dev.*, **14**, 2330–2343.

Pfleger,C.M. and Kirschner,M.W. (2000) The KEN box: an APC recognition signal distinct from the D box targeted by Cdh1. *Genes Dev.*, **14**, 655–665.

Pfleger,C.M., Salic,A., Lee,E. and Kirschner,M. (2001) Inhibition of Cdh1–APC by the MAD2-related protein MAD2L2: a novel mechanism for regulating Cdh1. *Genes Dev.*, **15**, 1759–1764.

Piel,M., Meyer,P., Khodjakov,A., Rieder,C.L. and Bornens,M. (2000) The respective contributions of the mother and daughter centrioles to centrosome activity and behaviour in vertebrate cells. *J. Cell Biol.*, **149**, 317–329.

Pines,J. and Rieder,C.L. (2001) Re-staging mitosis: a contemporary view of mitotic progression. *Nature Cell Biol.*, **3**, E3–E6.

Pu,R.T. and Osmani,S.A. (1995) Mitotic destruction of the cell cycle regulated NIMA protein kinase of *Aspergillus nidulans* is required for mitotic exit. *EMBO J.*, **14**, 995–1003.

Puntoni,F. and Villa-Moruzzi,E. (1997) Protein phosphatase-1α, γ1 and δ: changes in phosphorylation and activity in mitotic HeLa cells and in cells released from the mitotic block. *Arch. Biochem. Biophys.*, **340**, 177–184.

Reimann,J.D.R., Freed,E., Hsu,J.Y., Kramer,E.R., Peters,J.-M. and Jackson,P.K. (2001) Emi1 is a mitotic regulator that interacts with Cdc20 and inhibits the anaphase promoting complex. *Cell*, **105**, 645–655.

Schmidt-Zachmann,M.S. and Nigg,E.A. (1993) Protein localization to the nucleolus: a search for targeting domains in nucleolin. *J. Cell. Sci.*, **105**, 799–806.

Schultz,S.J., Fry,A.M., Sütterlin,C., Ried,T. and Nigg,E.A. (1994) Cell cycle-dependent expression of Nek2, a novel human protein kinase related to the NIMA mitotic regulator of *Aspergillus nidulans*. *Cell Growth Differ.*, **5**, 625–635.

Shah,J.V. and Cleveland,D.W. (2000) Waiting for anaphase: Mad2 and the spindle assembly checkpoint. *Cell*, **103**, 997–1000.

Shirayama,M., Zachariae,W., Ciosk,R. and Nasmyth,K. (1998) The polo-like kinase Cdc5p and the WD-repeat protein Cdc20p/fizzy are regulators and substrates of the anaphase promoting complex in *Saccharomyces cerevisiae*. *EMBO J.*, **17**, 1336–1349.

Sigrist,S.J. and Lehner,C.F. (1997) *Drosophila* fizzy-related downregulates mitotic cyclins and is required for cell proliferation arrest and entry into endocycles. *Cell*, **90**, 671–681.

Uto,K. and Sagata,N. (2000) Nek2B, a novel maternal form of Nek2 kinase, is essential for the assembly or maintenance of centrosomes in early *Xenopus* embryos. *EMBO J.*, **19**, 1816–1826.

Uto,K., Nakajo,N. and Sagata,N. (1999) Two structural variants of Nek2 kinase, termed Nek2A and Nek2B, are differentially expressed in *Xenopus* tissues and development. *Dev. Biol.*, **208**, 456–464.

Wakefield,J.G., Huang,J.-Y. and Raff,J.W. (2000) Centrosomes have a role in regulating the destruction of cyclin B in early *Drosophila* embryos. *Curr. Biol.*, **10**, 1367–1370.

Yamano,H., Tsurumi,C., Gannon,J. and Hunt,T. (1998) The role of the destruction box and its neighbouring lysine residues in cyclin B for anaphase ubiquitin-dependent proteolysis in fission yeast: defining the D-box receptor. *EMBO J.*, **17**, 5670–5678.

Ye,X.S., Fincher,R.R., Tang,A., Osmani,A.H. and Osmani,S.A. (1998) Regulation of the anaphase-promoting complex/cyclosome by *bimA*^{APC3} and proteolysis of NIMA. *Mol. Biol. Cell*, **9**, 3019–3030.

Zachariae,W. and Nasmyth,K. (1999) Whose end is destruction: cell division and the anaphase-promoting complex. *Genes Dev.*, **13**, 2039–2058.

Zur,A. and Brandeis,M. (2001) Securin degradation is mediated by fzy and fzr and is required for complete chromatid separation but not for cytokinesis. *EMBO J.*, **20**, 792–801.

Received September 4, 2001; revised October 29, 2001; accepted November 2, 2001

SPECIAL NOTE

THIS ITEM IS BOUND IN SUCH A MANNER AND WHILE EVERY EFFORT HAS BEEN MADE TO REPRODUCE THE CENTRES, FORCE WOULD RESULT IN DAMAGE

Biochem. J. (2002) **361**, 77–85 (Printed in Great Britain)

Alternative splice variants of the human centrosome kinase Nek2 exhibit distinct patterns of expression in mitosis

Rebecca S. HAMES and Andrew M. FRY[1]

Department of Biochemistry, University of Leicester, University Road, Leicester LE1 7RH, U.K.

Nek2 is a cell-cycle-regulated protein kinase that localizes to the centrosome and is likely to be involved in regulating centrosome structure at the G_2/M transition. Here, we localize the functional human *Nek2* gene to chromosome 1 and show that alternative polyadenylation signals provide a mechanism for generating two distinct isoforms. Sequencing of products generated by reverse transcriptase PCR, immunoblotting of cell extracts and transfection of antisense oligonucleotides together demonstrate that human Nek2 is expressed as two splice variants. These isoforms, designated Nek2A and Nek2B, are detected in primary blood lymphocytes as well as adult transformed cells. Nek2A and Nek2B, which can form homo- and hetero-dimers, both localize to the centrosome, although only Nek2A can induce centrosome splitting upon overexpression. Importantly, Nek2A and Nek2B exhibit distinct patterns of cell-cycle-dependent expression. Both are present in low amounts in the G_1 phase and exhibit increased abundance in the S and G_2 phases. However, Nek2A disappears in prometaphase-arrested cells, whereas Nek2B remains elevated. These results demonstrate that two alternative splice variants of the human centrosomal kinase Nek2 exist that differ in their expression patterns during mitosis. This has important implications for our understanding of both Nek2 protein kinase regulation and the control of centrosome structure during mitosis.

Key words: cell cycle, centriole, phosphorylation.

INTRODUCTION

The centrosome is the primary organizer of the microtubule (MT) network in animal cells [1–3]. It is composed of two stable cylindrical structures, called centrioles, each of which is associated with a proteinaceous mass, known as pericentriolar material (PCM). Whereas centrioles are relatively simple in composition, comprised mostly of post-translationally modified α- and β-tubulin, the PCM is more complex. Experimentally, the PCM can be separated into a salt-insoluble meshwork of fibres, termed the centromatrix, and a soluble fraction of proteins that are held in place through association with either centrioles or the centromatrix [4,5].

Progression through the cell cycle is accompanied by gross changes in structural organization as well as the MT nucleation capacity of the centrosome. Centrosomes duplicate once per cell cycle to ensure bipolarity of the mitotic spindle as well as stable inheritance of one centrosome at each division [6]. Duplication is characterized by the appearance and gradual elongation of two new centrioles that grow perpendicular to and in close association with parental centrioles. In late G_2 phase of the cell cycle, centrosomes gain an increased capacity for MT nucleation through recruitment of additional PCM [7]. As mitosis begins, duplicated centrosomes move apart towards opposite ends of the cell, and forces generated by MT- and chromosome-associated motor proteins lead to establishment of the bipolar mitotic spindle [8,9]. In telophase, the new centrioles lose their tight association with parental centrioles, but appear to remain connected through establishment of a structure that has been referred to as the intercentriolar linkage [10–12].

Many of the changes that occur during the centrosome cycle are likely to result from protein phosphorylation [13,14]. Cyclin-dependent kinases, polo kinases, aurora kinases and NIMA (never in mitosis A)-related kinases (Neks), as well as protein phosphatase (PP) 1α and PP4, all associate with the centrosome at some point in the cell cycle. At the present time, however, little is known about how phosphorylation events modify centrosome structure or MT nucleation activity. Phosphorylation may act through regulating the association of proteins with the centrosome. Equally, phosphorylation could target centrosomal proteins for degradation and, as components of ubiquitin ligase enzymes and the proteosome have been detected at the centrosome, this could take place without need for prior dissociation [15–17].

Nek2 is a serine/threonine kinase that localizes to the centrosome throughout the cell cycle [18]. Its expression and activity are regulated by the cell cycle, with peak levels in the S and G_2 phases [19,20]. However, Nek2 interacts with the catalytic subunit of PP1, which is capable of dephosphorylating both Nek2 itself and other Nek2 substrates [21]. This direct competition between kinase and phosphatase means that centrosomal targets of Nek2 may only become significantly phosphorylated when PP1 activity is reduced at the G_2/M transition [22,23]. Overexpression of wild-type, but not catalytically dead, Nek2 to a level that is likely to be in excess of endogenous PP1 induces premature centrosome splitting [18]. This raises the possibility that Nek2 normally functions to promote centrosome separation. In support of this hypothesis, a Nek2 substrate has been identified, called centrosomal Nek2-associated protein 1 (C-Nap1), which has properties consistent with it being a component of the intercentriolar linkage [24,25]. C-Nap1 localizes to proximal ends of centrioles during interphase, but is absent from mitotic spindle poles. Furthermore, interference with C-Nap1 by antibody microinjection or expression of dominant-negative constructs also

Abbreviations used: MT, microtubule; PCM, pericentriolar material; NIMA, never in mitosis A; Nek, NIMA-related kinase; PP, protein phosphatase; C-Nap1, centrosomal Nek2-associated protein 1; RT-PCR, reverse transcriptase PCR; GFP, green fluorescent protein.

[1] To whom correspondence should be addressed (e-mail amf5@le.ac.uk).

leads to premature centrosome splitting [26]. The role of Nek2 may therefore be to phosphorylate C-Nap1 and, perhaps, other structural proteins of the centrosome, triggering their dissociation or degradation and, in so doing, cause the intercentriolar linkage to be broken.

Recent studies on the *Xenopus laevis* homologue of Nek2 suggest additional functions in assembly and/or maintenance of centrosome structure. In *Xenopus* egg extracts, depletion of Nek2 interferes with centrosome assembly and MT aster formation from the sperm basal body [27]. Meanwhile, injection of neutralizing antibodies or kinase-dead Nek2 constructs into embryos causes fragmentation of spindle poles, aberrant spindle formation and abortive cleavage [28]. This function for Nek2 may not be restricted to early embryos, as long-term overexpression of wild-type or catalytically inactive Nek2 also leads to centrosome disintegration in adult human cells [18]. Two alternative cDNAs have been isolated for *Xenopus Nek2* that encode products with distinct C-termini. These products could arise through allelic differences in the duplicate copies of the *Nek2* gene in the tetraploid *X. laevis* genome [29]. Equally, they could arise through alternative splicing. The two isoforms display distinct patterns of developmentally regulated expression, with the shorter form, X-Nek2B, present in oocytes, eggs and early embryos, and the longer form, X-Nek2A, present in embryos after the gastrula/neurula transition as well as in adult testis [30]. Murine Nek2 is also highly expressed in adult testis, although the possible existence of multiple Nek2 isoforms in mammals has not been addressed [31–33]. We therefore decided to examine whether alternative splicing represents a mechanism for regulating Nek2 kinase in vertebrates and, more specifically, in human cells. Our results reveal the existence of two alternatively spliced variants of the human Nek2 kinase. Both isoforms can localize to the centrosome but, importantly, they are subject to distinct patterns of cell-cycle-regulated expression with specific differences in mitosis.

EXPERIMENTAL

Genomic sequence analysis

For somatic cell hybrid analysis, a human monochromosomal somatic cell hybrid DNA panel was obtained from the U.K. HGMP Resource Centre (Hinxton, Cambridge, U.K.) [34]. PCR reactions were performed with the Expand high-fidelity PCR system (Roche Biochemicals) on 1 μl of each chromosomal hybrid in a total reaction volume of 20 μl, using 5′ and 3′ oligonucleotide primers complementary to the original *Nek2* cDNA sequence. PCR products were either separated on 1% agarose gels or purified using a PCR purification kit (Qiagen) for sequencing. To determine the genomic structure of human *Nek2*, a human single chromosome library representing chromosome 1 (LL01NC01) produced at the Lawrence Livermore National Laboratory was obtained as a high-density gridded filter from the U.K. HGMP Resource Centre. To generate a probe, *Nek2* cDNA was excised as a *Nae*I *Xba*I fragment from pGEM-Nek2 and radiolabelled with [α^{32}P]dCTP using the Prime-It random priming kit (Stratagene). Positive clones were identified by autoradiography of the filter following overnight hybridization with the probe at 65 °C. Representative cosmids were ordered from the U.K. HGMP Resource Centre and sequenced using a range of oligonucleotide primers in the Protein and Nucleic Acid Chemistry Laboratory (University of Leicester, Leicester, U.K.) on an ABI 377 Automated Sequencer (PerkinElmer) using Big Dye technology.

Reverse transcriptase PCR (RT-PCR) and isolation of human *Nek2B* cDNA

RNA was isolated from HeLa and U2OS cells using TRI rea[gent] (Sigma) according to manufacturer's instructions. RNAs [were] treated with amplification-grade DNase I (Gibco) for 15 m[in] room temperature before stopping the reaction with a one[-]vol. of 25 mM EDTA and heating to 65 °C for 10 min. DN[ase]-treated RNAs were reverse transcribed at 42 °C for 50 min [with] oligo(dT) and Moloney-murine-leukaemia virus reverse t[ran]scriptase (Promega) according to manufacturer's instruct[ions] and PCR reactions performed for 35 cycles (94 °C for 30 s, 5[5 °C] for 30 s and 72 °C for 30 s) with oligonucleotide AF008 (5′-GGCGAATTCCATACCGTTAC-3′) as a 5′ primer and AF[017] (5′-GCCAGAGACAGGAACTTCCG-3′; specific for *Nek2*) or AF017 (5′-GCTACCTAAGCCACTTTGGGAG-3′; specific for *Nek2B*) as a 3′ primer. To generate plasmid pGEM-Nek2B, carrying the complete open reading frame of *Nek2B*, the 49[-]bp RT-PCR product from AF008/AF017 was first subcloned into the pCR2.1 TA cloning vector (Invitrogen) to create pCR2.1-Nek2B. A partial *Sac*I fragment, encompassing the C-terminus of Nek2A, was then excised from pGEM-Nek2 [19] and replaced with the equivalent *Sac*I fragment from pCR2.1-Nek2B, encoding the C-terminus of Nek2B. As these are splice variants, the sequences 5′ to the splice site are identical.

Plasmid constructs

The following constructs were generated for protein expression in eukaryotic cells: pEGFP-Nek2A, pEGFP-Nek2B and pCMV-myc:Nek2B (pCMV-myc:Nek2A has been described in [18]). To create pEGFP-Nek2A and pEGFP-Nek2B, the coding region was excised on a *Nae*I *Bam*HI fragment from pGEM-Nek2A [19] and pGEM-Nek2B, respectively, and subcloned into the *Sal*I (blunted with Klenow) *Bam*HI sites of the pEGFP(C1) vector (Invitrogen) that had been modified by the introduction of a T7 promoter upstream of the green fluorescent protein (GFP) coding region (a kind gift from Dr K. Tanaka, Paterson Institute for Cancer Research, Manchester, U.K.). For pCMV-myc:Nek2B, the coding sequence was excised from pGEM-Nek2B on a *Nae*I *Xba*I fragment and subcloned into the pBlueScript:myc vector cut with *Sma*I and *Xba*I, to create pBS-myc:Nek2B. The in-frame fusion of Nek2B with a Myc-epitope tag was then excised from pBS-myc:Nek2B on a *Sal*I (blunted with Klenow) *Xba*I fragment and subcloned into the pReCMV vector (Invitrogen) cut with *Hin*dIII (blunted with Klenow) and *Xba*I.

Cell culture and transfections

HeLa epithelial, U2OS osteosarcoma, HEK-293 epithelial and KE37 T-lymphoblastoid cells were grown at 37 °C in a 5% CO_2 atmosphere in Dulbecco's modified Eagle's medium supplemented with 10% heat-inactivated fetal calf serum and penicillin/streptomycin (100 i.u./ml and 100 μg/ml, respectively). Human T-lymphocytes were obtained from peripheral blood donated by healthy volunteers as described previously [35]. Transient transfection of expression plasmids was carried out using either Lipofectamine 2000 reagent according to manufacturer's instructions (Life Technologies), or calcium phosphate, as described elsewhere [36]. For oligonucleotide transfections, the following phosphorothioate-modified oligodeoxynucleotides were synthesized by Interactiva (Hybaid, Ulm, Germany): 5′-GAGCCTGTGCCAATGGTG-3′ (antisense) and 5′-CACCATGGCACAGGCTC-3′ (sense). These were introduced into cells using Lipofectamine 2000 at a final concentration of 200 nM in cell-culture medium. The transfection mix was left on the cells for

24 h prior to preparation of cell extracts or processing for immunofluorescence microscopy. Cell extractions were as described [37,38].

Cell synchronization and flow cytometry

To obtain cells synchronized at different stages of the cell cycle, U2OS cells were first presynchronized in the S phase by the addition of 2 mM thymidine for 12 h and released by transfer into fresh medium for 8 h. Cells were then resynchronized, either at the G_1/S boundary or in the M phase, by incubation for 16 h with 1 mM hydroxyurea or 1 μg/ml nocodazole, respectively. S- and G_2-phase populations were obtained by releasing from the block induced by hydroxyurea for 3 and 9 h, respectively. The M-phase population was obtained by gently pipetting the mitotically arrested cells from the nocodazole block, while the G_1-phase population was obtained by releasing from the nocodazole block for 6 h. Release of cells from drug-induced blocks was performed by three washes in 1 × PBS and replacement in fresh medium. Cell-cycle distributions were confirmed by flow cytometry. For this purpose, 1×10^6 cells were washed in ice-cold PBS and slowly resuspended while vortex-mixing in 1 ml of 70 % ethanol (−20 °C) before storage at −20 °C. Prior to flow-cytometric analysis, fixed cells were washed gently in ice-cold PBS, resuspended in 1 ml of DNA stain (0.02 mg/ml propidium iodide/0.2 mg/ml RNase A in PBS) and incubated at room temperature for 30 min. DNA content was measured using a FACScan II instrument (Becton Dickinson) and analysed using CellQuest.

Miscellaneous techniques

In vitro translation of Nek2 constructs was done using the TnT-coupled transcription/translation kit in the absence or presence of [^{35}S]methionine/cysteine (Expre^{35}S^{35}S; NEN Life Science Products) according to manufacturer's instructions (Promega). For co-precipitation experiments, reticulocyte lysates were first incubated separately at 30 °C for 90 min and then together for 20 min with 250 μg/ml cycloheximide to allow interactions without further translation. Immunological techniques were performed as described previously [18,36,37]. Primary antibodies used in this study were: α-Nek2 (R31, 1:500; R40, 1 μg/ml; anti-peptide antibody, 1 μg/ml [18,19,38]); α-C-Nap1 (R63, 1 μg/ml [24]); α-Myc (9E10, undiluted tissue-culture supernatant); α-cyclin A (1 μg/ml; Upstate Biotechnology); α-cyclin B1 (1 μg/ml; Upstate Biotechnology) and α-α-tubulin (0.3 μg/ml; Amersham Pharmacia Biotech). Fluorescence images were captured using a Quantix 1400 CCD camera (Photometrics) using SmartCapture software and processed using Adobe Photoshop (San Jose, CA, U.S.A.).

RESULTS

Structure of the human *Nek2* gene

In the original characterization of the human *Nek2* cDNA, two gene loci were identified by fluorescence *in situ* hybridization, at 1q32.2–1q41 and 14q12 [19]. Genomic clones containing the *Nek2* sequence have also been deposited in the GenBank nucleotide sequence database from chromosome 22-specific libraries. Meanwhile, a number of partial cDNA sequences have been identified by PCR amplification that are highly related, but non-identical, to regions within the Nek2 catalytic domain [39]. To address the possible existence of multiple human *Nek2* genes, PCR reactions were performed on a panel of somatic cell hybrids using non-degenerate oligonucleotide primers complementary to the published *Nek2* cDNA. Products were amplified from chromosomes 1, 2, 14 and 22, suggesting that highly related copies do exist on at least four different chromosomes (Figure 1A). Investigation of the human genome sequence confirmed the existence of a single *Nek2* sequence on each of these chromosomes, but no others. Sequencing of the PCR products (confirmed later by analysis of the human genome sequence) revealed that only the sequence on chromosome 1 bears complete identity with the published *Nek2* cDNA and hence must encode the *bona fide* Nek2 protein. Multiple single-nucleotide substitutions are present in the *Nek2* sequences on chromosomes 2, 14 and 22. Some of these cause amino acid substitutions in residues that are known to be critical for protein kinase activity. More importantly, a termination codon replaces glutamate-126 within the N-terminal catalytic domain of the chromosome 2, 14 and 22 sequences. Hence, any protein expression would lead to truncated polypeptides with a predicted molecular mass of 14.6 kDa. Scrutiny of the human genome database indicated that these other *Nek2* sequences lack introns, which implies strongly that they are pseudogenes that have arisen from the integration of fully processed Nek2 mRNAs (Figure 1B).

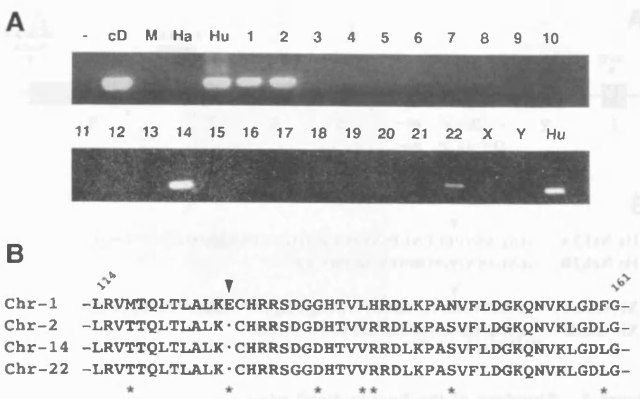

Figure 1 The functional human *Nek2* gene is located on chromosome 1

(**A**) Somatic cell hybrid analysis. Oligonucleotide primers complementary to regions within the *Nek2* 3′-untranslated region were used in PCR reactions on DNA isolated from a panel of mouse and hamster somatic cell hybrids carrying individual human chromosomes as indicated. Controls were no DNA (−), *Nek2* cDNA (cD), and total mouse (M), hamster (Ha) or human (H) DNA. Fragments of the expected size were identified in panels containing chromosomes 1, 2, 14 and 22. (**B**) Partial protein sequences (amino acids 114–161) of hypothetical products from the different *Nek2* genes based on DNA sequencing of PCR products generated from the somatic cell hybrids using primers within the catalytic domain. Note that *Nek2* genes on chromosomes 2, 14 and 22 would encode proteins with a termination codon (●) instead of Glu-126 (arrowhead) and lack the conserved DFG (amino acids 159–161) of classical serine/threonine kinases. Asterisks indicate positions where the chromosome 2, 14 and 22 sequences differ from that of chromosome 1.

Two alternative cDNAs have been isolated for the *X. laevis* homologue of human *Nek2* [27,30]. These could have arisen from duplicate copies of the *Nek2* gene in this tetraploid organism or, as the cDNAs diverge at a putative splice junction, they may have been generated through alternative splicing. To test whether human *Nek2* is alternatively spliced, a cosmid encompassing the full-length *Nek2* gene from chromosome 1 was isolated to first determine its gene structure. Sequencing of the cosmid indicated that Nek2 mRNA is encoded on eight exons, with the initiation codon in exon 1 and the UAG stop codon in exon 8 (Figure 2A and Table 1). Exon 7 terminates at a position that is equivalent to the point of divergence of the two *Xenopus Nek2* cDNAs. Sequencing of the seventh intron revealed the presence of a

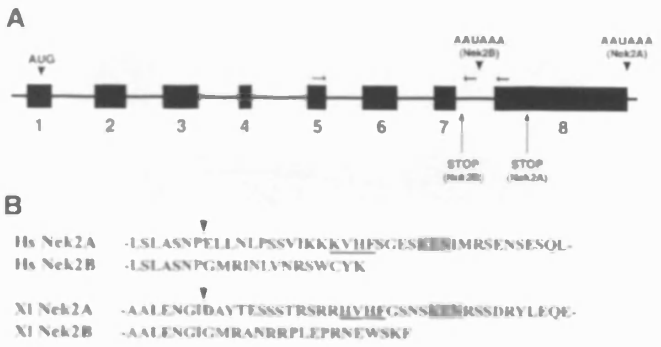

Figure 2 Structure of the human *Nek2* gene

(**A**) Intron–exon structure of the human *Nek2* gene on chromosome 1. Exons (black boxes) are drawn to scale. However, as not all introns have been fully sequenced these are not to scale. The positions of the single AUG initiation codon, the two alternative protein stop sites and polyadenylation signals (AAUAAA), and the primers used for RT-PCR reactions (horizontal arrows) are indicated. (**B**) Partial protein sequences of human (Hs; from amino acid 364) and *Xenopus* (Xl; from amino acid 365) Nek2A and Nek2B are shown with the position of the splice site indicated (arrowhead). In both species, Nek2B terminates soon after the splice site, whereas the C-termini of the Nek2As are somewhat longer. The conserved KEN box destruction motif is shaded and the PP1-binding site is underlined. Human Nek2B has the GenBank accession number AY045701.

termination codon starting 43 nucleotides after the splice site and an alternative polyadenylation signal after a further 625 nucleotides (Figure 2A). Based on the position of the termination codon in the seventh intron, use of this alternative polyadenylation signal would generate a human Nek2B protein of 384 amino acids, with a calculated molecular mass of 44.9 kDa and a pI value of 8.64. The predicted Nek2A and Nek2B proteins would diverge in sequence after amino acid 370, causing Nek2B to lack a number of important regulatory motifs that are present in the extreme C-terminus of Nek2A (Figure 2B).

Expression of Nek2A and Nek2B in primary and transformed cells

To determine whether alternative splice variants of Nek2 are expressed in human cells, RT-PCR reactions were performed on RNA isolated from cultured human cells. Forward and reverse primers were synthesized that would allow amplification of a fragment from the known Nek2A mRNA or from a product generated from the hypothetical Nek2B mRNA. RT-PCR products representing both Nek2A and Nek2B were generated readily using RNA isolated from either U2OS or HeLa cells and sequencing confirmed these to be the predicted Nek2 products (Figure 3A). Amplification was dependent upon the presence of reverse transcriptase and gave rise to products of the expected sizes, ruling out the possibility that they were generated from either genomic DNA or unspliced primary transcripts.

To determine whether Nek2A and Nek2B are expressed as proteins in cultured cells, we re-examined the proteins recognized by Nek2 antibodies on Western blots. The anti-peptide Nek2 antibody described previously [38] was capable of recognizing both splice variants, as indicated by detection of recombinant Nek2A and Nek2B proteins translated *in vitro* (Figure 3B, lanes 1 and 2). The full-length recombinant Nek2B protein was generated using the product from the RT-PCR reaction. In extracts of HeLa cells, the Nek2 antibody recognized proteins of 48 and 44 kDa, which co-migrated with the *in vitro*-translated Nek2A and Nek2B proteins respectively (Figure 3B, lane 3). Two other previously described Nek2 antisera raised against bacterially expressed Nek2 fragments (R31 and R40) also detected both the 48 and 44 kDa proteins (results not shown). Transfection of HeLa cells with recombinant Nek2A led to a specific increase in abundance of the 48 kDa product; likewise, transfection with Nek2B caused only the 44 kDa product to become more abundant (Figure 3B, lanes 4 and 5). This argues strongly against the 44 kDa band being a degradation product of Nek2A, as there is no reason to suspect that the transfected protein would be processed differently from the endogenous protein. Although one additional cross-reacting band was detected with the anti-peptide antibody, this was not recognized by the other Nek2 antisera, leading us to conclude that HeLa cells specifically express two splice variants of the Nek2 kinase.

To determine whether both Nek2 isoforms are expressed in primary as well as transformed cells, extracts were prepared from a variety of transformed cell lines and from freshly collected peripheral T-lymphocytes. Western blotting revealed the presence of Nek2A and Nek2B in all cell lines tested and peripheral T-lymphocytes, emphasizing that Nek2B expression is not confined to either transformed cells or early stages of development (Figure 3C). A slower-migrating form of Nek2 was also detected in peripheral T-lymphocytes. This was not detected in transformed cell lines, implying that a substantial fraction of Nek2 might exist in a post-translationally modified state in primary cells.

Unfortunately, attempts to generate Nek2A- and Nek2B-specific antisera using peptides based on the predicted C-termini have so far proved unsuccessful. To confirm that the two bands detected by Nek2 antibodies at 48 and 44 kDa represent Nek2 proteins rather than unrelated cross-reacting antigens, we therefore used an antisense oligonucleotide approach. An antisense *Nek2* sequence was identified that, when introduced into human cells by liposome-mediated transfection, specifically caused down-regulation of both the 48 and 44 kDa proteins, but not

Table 1 Intron–exon boundaries of the human *Nek2* gene

Nucleotide sequences before and after each splice junction in the human *Nek2* gene sequence are indicated. Exon and intron sequences around the splice sites are shown in upper and lower case, respectively, and the conserved gt–ag of splice-site donor and acceptor are in bold. Position numbers relate to those used in the original isolation of the *Nek2* cDNA [19].

Exon no.	Exon sequence	Intron sequence	Exon sequence	Exon no.
1	TGATGGCAAG^{178}	**gt**gagcctgggacctaccct...ctlggaaattctlatttc**ag**	A^{179}TATTAGTTT	2
2	CCAAGGAAAG^{396}	**gt**aagcataatcttttaaaa...tataactgctttggttttt**ag**	G^{397}CAATACTTA	3
3	CATGTCTCCT^{637}	**gt**aagtatttcagaatttag...taccctttttccctgtat**ag**	G^{638}AACAAATGA	4
4	GTGCATTAAT^{720}	**gt**aagtatgatgaagacaga...ttcttctttttaaccct**ag**	G^{721}CCTCCATTT	5
5	AAACTTAAAG^{847}	**gt**aaagatgataagatgata...actgagtatttttttcccc**ag**	G^{848}ATTACCATC	6
6	AGATTGGAGC^{1067}	**gt**aagtctgaatgggggtca...tccattctctttttaaag**ag**	A^{1068}GAAAGAACA	7
7	AGTAATCCAG^{1193}	**gt**atgagaatcaacttggtc...ttttctttttccttctaa**ag**	A^{1194}ACTTCTTAA	8

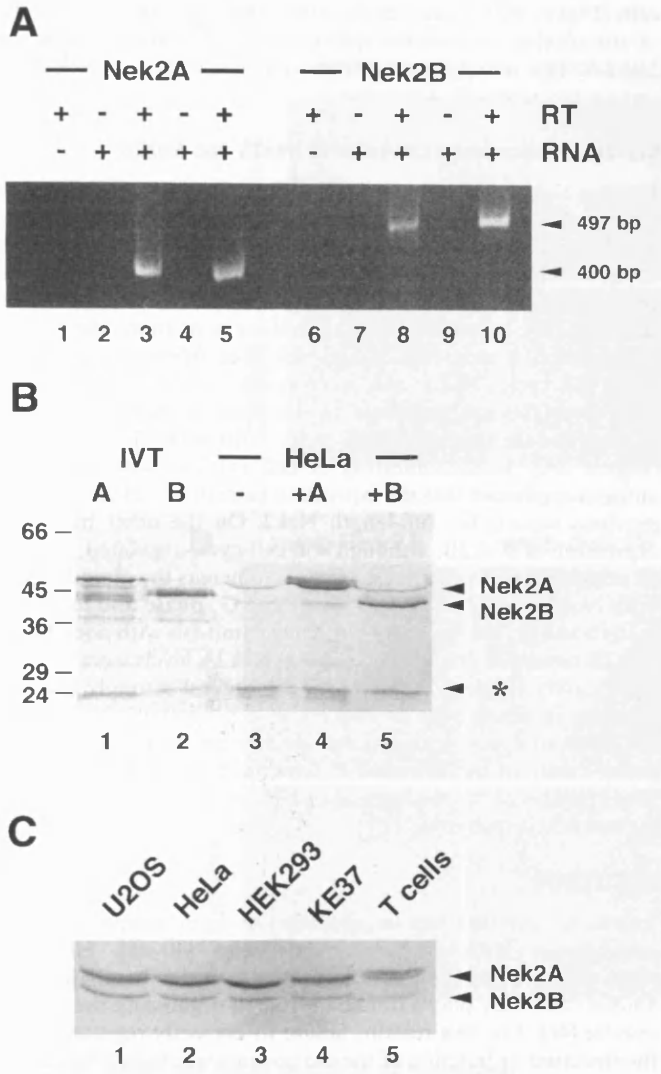

Figure 3 Expression of human Nek2A and Nek2B

(**A**) RT-PCR demonstrates the synthesis of processed mRNAs representing both human Nek2A and Nek2B. RNA isolated from HeLa (lanes 2, 3, 7 and 8) or U2OS (lanes 4, 5, 9 and 10) cells was used in RT-PCR reactions with or without the addition of reverse transcriptase (RT), as indicated. No RNA was added to the reactions shown in lanes 1 and 6. PCR primers were designed (see Figure 2A) that would specifically amplify products from mRNA encoding either Nek2A (lanes 1–5) or Nek2B (lanes 6–10). As the 5′ primer was made to sequence in exon 5, products generated from either genomic or unspliced primary transcripts would still contain intron sequence and so be much larger than those amplified. PCR fragment sizes are indicated (bp). (**B**) The migration of *in vitro*-translated (IVT) Nek2A (lane 1) and Nek2B (lane 2) was compared on Western blots with proteins recognized in extracts of untransfected HeLa cells (lane 3) and HeLa cells transfected with untagged Nek2A (lane 4) or Nek2B (lane 5). The anti-peptide anti-Nek2 antibody recognizes proteins at 48 and 44 kDa that co-migrate with recombinant Nek2A and Nek2B, respectively. A third band recognized by this antibody in HeLa cell extracts (*) was not recognized by other Nek2 antisera tested. (**C**) Western blotting with the anti-peptide Nek2 antibody indicates that Nek2A and Nek2B are present in extracts of the transformed cell lines shown in lanes 1–4 and T-lymphocytes collected from peripheral blood (lane 5).

tubulin or the lower-molecular-mass protein recognized by the Nek2 antisera (Figure 4A). The corresponding sense sequence (as well as scrambled and mismatch sequences; results not shown) did not cause suppression of either Nek2 isoform. Indirect immunofluorescence microscopy of cells stained with Nek2 antibodies revealed that Nek2 was detected at the centrosome in

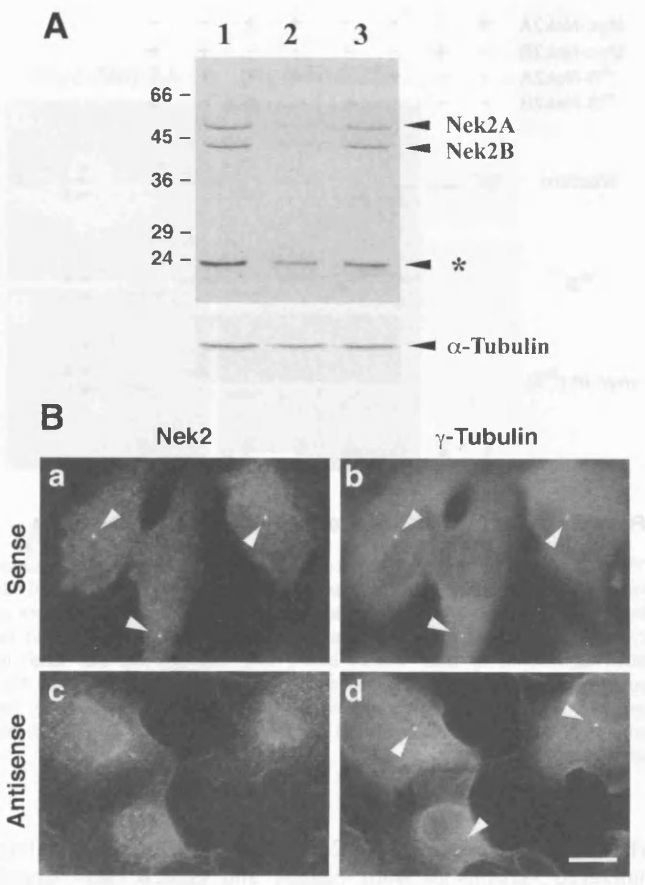

Figure 4 Antisense oligonucleotides inhibit expression of Nek2A and Nek2B

(**A**) No DNA (lane 1), or 200 nM antisense (lane 2) or sense (lane 3) *Nek2* oligonucleotides was introduced into HeLa cells by liposome-mediated transfection. After 24 h, cells were lysed and extracts processed for Western blotting with anti-peptide Nek2 (top panel) or α-tubulin (bottom panel) antibodies. The positions of Nek2A, Nek2B and α-tubulin proteins are indicated together with the low-molecular-mass protein that cross-reacts with the anti-peptide Nek2 antibody (*). Molecular masses (kDa) are indicated on the left of the Nek2 blot. (**B**) HeLa cells were treated with 250 nM sense (a, b) or antisense (c, d) *Nek2* oligonucleotides and processed for immunofluorescence microscopy using anti-peptide Nek2 (a, c) and anti-γ-tubulin (b, d) antibodies. Nek2 was detected at centrosomes in the presence of sense, but not antisense, oligonucleotides (arrowheads). Scale bar, 10 μm.

the presence of sense, but not antisense, oligonucleotides (Figure 4B). Taken together, the RT-PCR, immunoblot and antisense data provide compelling evidence that human Nek2 is expressed as two distinct isoforms from a single gene on chromosome 1.

Dimerization of Nek2 proteins

Due to its alternative C-terminus, Nek2B protein lacks the PP1-binding site that is present in Nek2A. This implies that PP1 would not be able to counteract phosphorylation events catalysed by Nek2B. However, Nek2A has been shown previously to form homodimers via its leucine zipper dimerization motif [38]. As Nek2B retains the leucine zipper, it may be possible for PP1 to regulate Nek2B if the latter is able to heterodimerize with Nek2A. To test whether Nek2A and Nek2B can form heterodimers, recombinant Nek2 proteins were mixed *in vitro* and immunoprecipitated with antibodies against an N-terminal Myc-epitope tag that was present on either one or the other protein

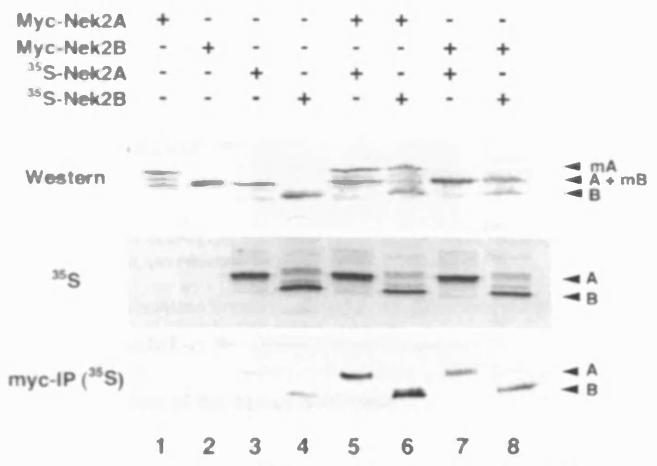

Figure 5 Nek2A and Nek2B can form homodimers and heterodimers

The Nek2 proteins indicated were prepared by coupled *in vitro* transcription/translation reactions in either the absence (Myc-Nek2A and Myc-Nek2B) or presence (^{35}S-Nek2A and ^{35}S-Nek2B) of [^{35}S]methionine/cysteine. Samples were mixed as shown in the presence of cycloheximide to prevent further translation and an aliquot taken for direct analysis by SDS/PAGE, followed by either Western blotting with Nek2 antibodies (top panel) or autoradiography (middle panel). The remainder was immunoprecipitated with anti-Myc antibodies, processed by SDS/PAGE and exposed for autoradiography (bottom panel). The positions of Myc-Nek2A (mA), Myc-Nek2B (mB), ^{35}S-Nek2A (A) and ^{35}S-Nek2B (B) are indicated on the right.

(Figure 5). Myc-tagged Nek2A was capable of precipitating untagged versions of both Nek2A and Nek2B. Myc-tagged Nek2B could also precipitate untagged versions of Nek2A and Nek2B. Small amounts of ^{35}S-labelled Nek2 proteins were brought down in control precipitations, but significantly less than in the presence of the Myc-tagged Nek2 proteins. The observation that similar amounts of each isoform were co-precipitated irrespective of which protein was used as the bait indicates that Nek2A and Nek2B can form both homodimers and heterodimers with similar efficiency.

Localization of human Nek2B to centrosomes

Indirect immunofluorescence microscopy and biochemical fractionation have been used to show that endogenous Nek2 is a core component of the human centrosome. Whereas the antibodies used would not distinguish between the two isoforms in microscopy, both the 48 and 44 kDa Nek2 products were present on Western blots of enriched centrosome preparations [18]. *Xenopus* X-Nek2B is also rapidly recruited from egg cytoplasm to the sperm basal body during centrosome assembly and localizes to centrosomes when transfected into *Xenopus* cultured cells [27,28]. Based on these data, we would expect both Nek2 isoforms to be present at the centrosome of adult human cells. To verify this prediction, recombinant versions of Nek2A and Nek2B were introduced into U2OS and HeLa cells by transient transfection and analysed by immunofluorescence microscopy. Using either enhanced GFP or Myc-epitope tags for detection, Nek2A and Nek2B were clearly detected at the centrosome, as indicated by co-localization with antibodies against C-Nap1 (Figure 6A) and γ-tubulin (Figure 6B). As reported previously, overexpression of active Nek2A kinase induced centrosome splitting in a high proportion of cells [18]. Strikingly, however, overexpression of Nek2B did not cause any significant change in the percentage of cells with split centrosomes compared with non-transfected cells (Figure 6C). These results imply that Nek2B is not capable of stimulating centrosome splitting with the same efficiency as Nek2A. This may reflect a difference in the affinity of Nek2B for certain centrosomal substrates.

Cell-cycle-dependent expression of Nek2A and Nek2B

Human Nek2 was reported previously to be cell-cycle-regulated with peak levels in the S and G_2 phases and low levels in the G_0 and G_1 phases [19,20]. These studies focused on the abundance of the 48 kDa Nek2A protein. However, during the first zygotic cell cycle of *Xenopus laevis*, the abundance of X-Nek2B remains constant [27]. It was important therefore to examine the relative expression of human Nek2A and Nek2B at different stages of the adult cell cycle. HeLa cells were synchronized carefully using drug arrest/release protocols, as described in the Experimental section, and the stage of the cell cycle confirmed by flow cytometry (Figure 7A). Immunoblotting of cell extracts with anti-Nek2 antisera confirmed that the expression pattern of Nek2A matched previous reports for full-length Nek2. On the other hand, the expression of Nek2B, although still cell-cycle-regulated, showed an important difference from Nek2A. Whereas the abundance of both Nek2A and Nek2B was low in the G_1 phase and increased in the S and G_2 phases, in cells arrested in mitosis with nocodazole Nek2B remained at a high level when Nek2A levels were reduced significantly (Figure 7). These results suggest strongly that the decrease in abundance of Nek2A in a prometaphase block is the result of a post-translational mechanism that targets motifs present only in the extended C-termini of the Nek2A isoform. Investigation of the mechanism of Nek2A destruction in mitosis is currently in progress.

DISCUSSION

It is now clear that bipolar spindles can form independently of centrosomes both *in vitro* and *in vivo* [40–45]. However, when centrosomes are present, as they are in the vast majority of animal cells, they play a dominant role in organizing the mitotic spindle [46]. For this reason, failure to correctly regulate either the structure or function of the centrosome would be expected to increase the possibility of misformed spindles and chromosome mis-segregation. Indeed, the prevalence of aneuploidy in tumour cells correlates well with the high incidence of centrosome defects, although the cause and effect of this relationship remains open to question [47,48]. Nek2 is one of only a handful of protein kinases that have so far been shown to (i) localize to the centrosome, (ii) alter centrosome structure upon overexpression or inhibition and (iii) have a *bona fide* substrate at the centrosome. Understanding its regulation is therefore of considerable importance in interpreting its contribution to centrosome regulation through the cell cycle.

Previously, it has been shown that Nek2 is regulated through a number of mechanisms that include homodimerization, trans auto-phosphorylation and association with the protein phosphatase PP1 [21,38]. Here, using several lines of evidence, we show that Nek2 is also regulated through the generation of alternative splice variants. First, two previously identified cDNAs for *Xenopus laevis* diverge at a position equivalent to an exon–intron boundary in the human *Nek2* gene located on chromosome 1. Secondly, distinct Nek2 products are amplified from human RNA by RT-PCR using primers that are specific for the two isoforms. Thirdly, several different anti-Nek2 antisera recognize common bands at the predicted molecular masses of Nek2A (48 kDa) and Nek2B (44 kDa). Fourthly, the 48 and 44 kDa proteins co-migrate precisely with *in vitro*-translated and -overexpressed versions of recombinant Nek2A and Nek2B.

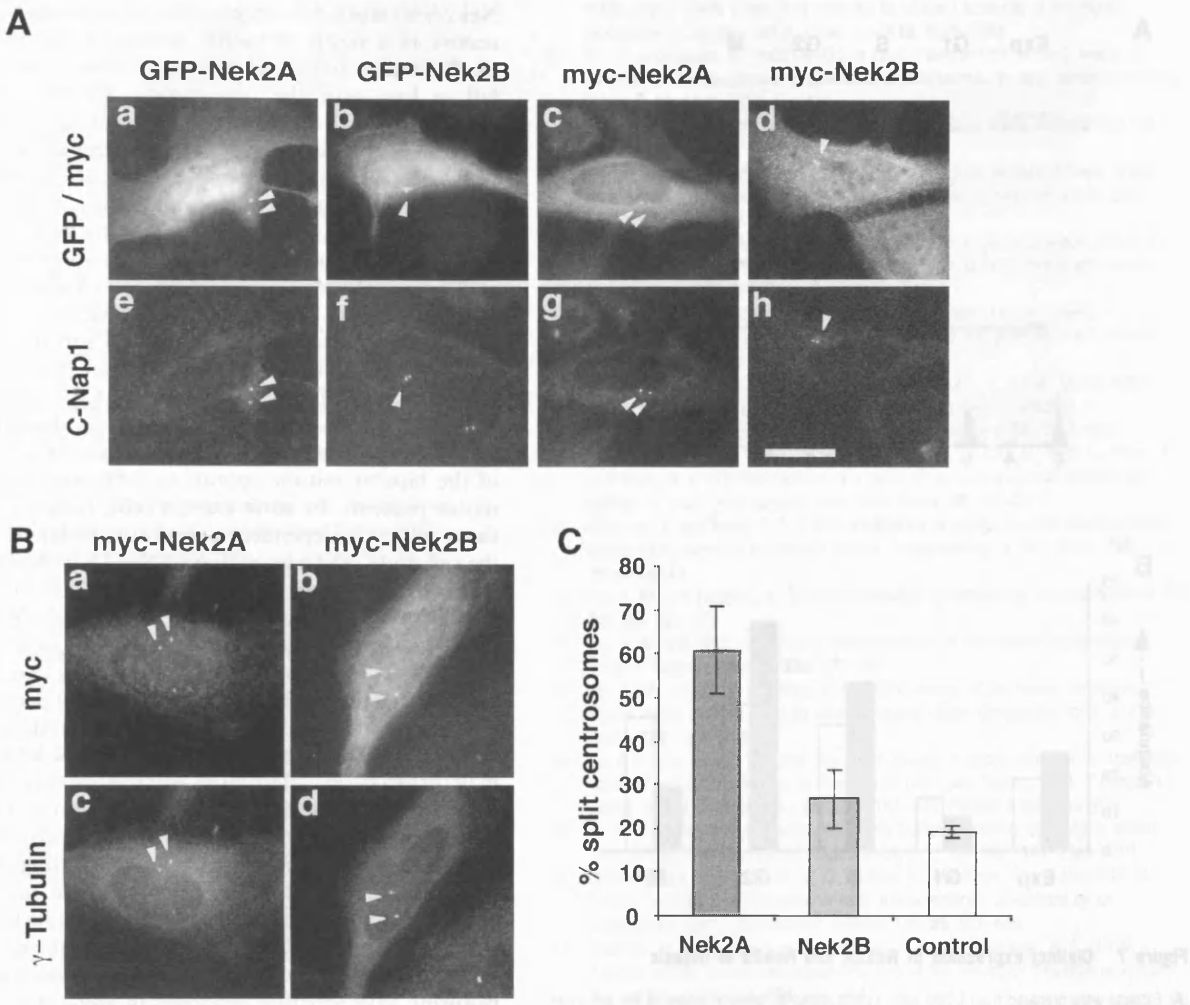

Figure 6 Nek2A and Nek2B localize to the centrosome

(**A**) U2OS osteosarcoma cells were transiently transfected with GFP-Nek2A (a, e), GFP-Nek2B (b, f), Myc-Nek2A (c, g) or Myc-Nek2B (d, h). Cells were fixed 24 h after transfection and analysed by indirect immunofluorescence microscopy. Arrowheads indicate the co-localization of GFP signal (a, b) and anti-Myc antibodies (c, d) with centrosomes, as revealed by antibodies against the centrosomal protein C-Nap1 (e–h). (**B**) HeLa cells were transiently transfected with Myc-Nek2A (a, c) or Myc-Nek2B (b, d), fixed after 24 h and analysed by indirect immunofluorescence microscopy using anti-Myc antibodies to detect transfected protein (a, b) and anti-γ-tubulin antibodies to reveal centrosomes (c, d). Scale bars, 10 μm. (**C**) The percentage of cells in which the two centrosomes were separated by more than 2 μm was calculated for HeLa cells transfected with Myc-tagged Nek2A and Nek2B proteins and compared with non-transfected cells (control).

Finally, antisense oligonucleotides, complementary to a region of the *Nek2* cDNA common to both isoforms, inhibit expression of the 48 and 44 kDa products, but not other control proteins. The presence of alternative splice products in humans, and most likely *Xenopus*, suggests strongly that this form of regulation is conserved amongst vertebrate Nek2 kinases.

So what is the purpose of generating alternative splice variants? It seems unlikely that they are required in different subcellular compartments, as evidence presented here and elsewhere indicates that both Nek2 proteins are present at the centrosome. For instance, recombinant Nek2A and Nek2B can localize to the centrosome, proteins of 48 and 44 kDa are recognized by anti-Nek2 antibodies in preparations of isolated human centrosomes, and the *Xenopus* Nek2B protein is recruited to sperm basal bodies from egg extracts *in vitro* [18,27]. The fact that Nek2A and Nek2B can form heterodimers further supports the notion that, where their expression levels are similar, they are likely to be found in the same subcellular compartment. Differences would only become apparent if one isoform was present in considerable excess, as X-Nek2B is in early *Xenopus* embryos. In this respect, it is interesting that the non-centrosomal pool of recombinant Nek2B protein was predominantly cytoplasmic, whereas that of Nek2A was frequently nuclear (R. S. Hames and A. M. Fry, unpublished work). The selective uptake of Nek2A into the nucleus may be through use of a putative bipartite nuclear localization sequence in the C-terminus of Nek2A (amino acids 361–383) that is missing from Nek2B, although this remains to be tested.

One reason for generating alternative splice variants may lie in the need for different levels of centrosome regulation at different stages of development. In fertilized eggs and early embryos of *Xenopus*, Nek2B is the only isoform detected, whereas a switch in expression to Nek2A occurs at the time of the gastrula–neurula transition [30]. Although we could detect Nek2B in both primary and transformed adult cells, Nek2A was always more abundant. The presence of an alternative polyadenylation site within intron

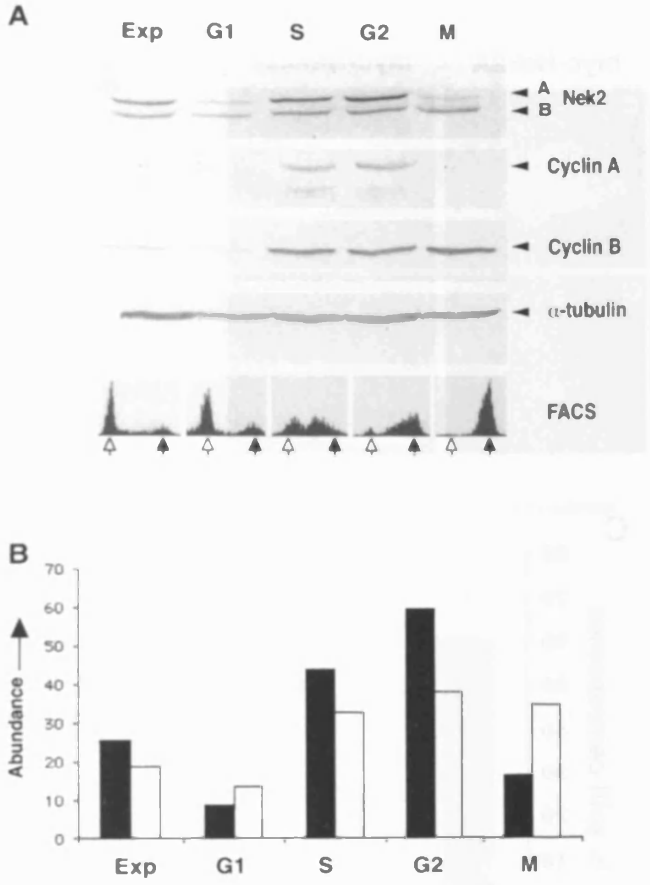

Figure 7 Distinct expression of Nek2A and Nek2B in mitosis

(**A**) Extracts were prepared from U2OS cells synchronized at different stages of the cell cycle, as described in the Experimental section. Samples were processed by SDS/PAGE and Western blotted with antibodies against Nek2, cyclin A, cyclin B or α-tubulin, as indicated. Flow cytometry was carried out on each cell population and cell-cycle profiles are shown below each lane, where the open and closed arrows indicate diploid and tetraploid DNA, respectively. (**B**) Histogram comparing Nek2A and Nek2B abundance at different cell-cycle stages as obtained by quantitative densitometric scanning (arbitrary units) of Western blots shown in (**A**). Black bars, Nek2A; white bars, Nek2B. Exp, cells in the exponential growth phase.

7 implies that Nek2A and Nek2B may be generated through recognition of different polyadenylation signals. The 3′-UTR of the predicted human Nek2B cDNA sequence also contains a cytoplasmic element, UUUUUAU, known to bind factors that regulate mRNA translation in oocytes via a complex cytoplasmic polyadenylation mechanism [49]. *Xenopus* Nek2B protein was reported to increase in abundance during oocyte maturation [30]. Hence, it is possible that vertebrate Nek2 is a general target for this highly specific form of developmentally regulated translational control.

Differential expression of the two Nek2 isoforms during development would imply a biological reason for switching from one isoform with a short C-terminus to another with an extended C-terminus. Importantly, we have found that human Nek2A and Nek2B show distinct patterns of expression during the cell cycle, specifically in mitosis. Whereas expression of both isoforms is low in the G_1 phase and increases in the S/G_2 phases, Nek2A is absent from cells arrested in the prometaphase with nocodazole, whereas Nek2B remains present. We have evidence that human Nek2A is targeted for degradation in prometaphase and that th occurs as a result of motifs present in its distinct C-terminu (R. S. Hames and A. M. Fry, unpublished work). These resul fall in line with the observation that recombinant *Xenopu* Nek2A is also unstable during mitosis of early embryo whereas Nek2B is not [28]. Maintaining a stable version of t Nek2 protein may therefore facilitate the rapid cell cycles th take place during early embryogenesis.

Functions that have been proposed for Nek2 at the centroso include triggering loss of centrosome cohesion and maintenan and/or assembly of the centrosome structure. In mammalia cells, centrosome separation is first detected in the prophase an precedes nuclear-envelope breakdown and spindle formation. model for Nek2 function proposes that phosphorylation in th late G_2 phase of substrates such as C-Nap1 leads directly indirectly to dissolution of a linkage that holds interphas centrosomes together [50]. This would facilitate the establishmen of the bipolar mitotic spindle by MT- and chromosome-base motor proteins. In adult human cells, both Nek2A and Nek2B show cell-cycle-dependent expression, in line with a role late in the cell cycle. The association of Nek2A with active PP1 in the S and early G_2 phases, but with inactive PP1 in the prophase, coul explain how Nek2A achieves a peak of substrate phosphorylatio at the G_2/M transition. Although Nek2B lacks the PP1-bindin motif, heterodimerization of Nek2B with Nek2A could allow phosphorylation by both kinases to be kept in check by PP1 until it is inactivated at the onset of mitosis. However, as Nek2B persists beyond the prometaphase, when Nek2A disappears, this may provide an alternative mechanism for overcoming PP1 inhibition and ensuring that Nek2 function is completed in early mitosis. Importantly, in contrast with Nek2A, overexpression of Nek2B does not stimulate centrosome splitting, implying that the prime function of Nek2B may not relate to centrosome separation. One speculation that is consistent with studies in *Xenopus* embryos is that Nek2B helps to maintain the integrity of spindle poles throughout mitosis. Determining whether the two Nek2 isoforms have separate functions in adult cells will require new approaches to selectively inhibit the function of one or the other protein.

We thank Erich Nigg (Max Planck Institute, Martinsreid, Germany) in whos laboratory the initial chromosome analysis was started, Roger Snowden for help wit flow cytometry, Raj Patel for preparation of peripheral T lymphocytes and Kayo Tanaka (Paterson Institute for Cancer Research, Manchester, U.K.) for the T7-modified pEGFP vector. We also thank the MRC-funded UK HGMP Resource Cent e (Hinxton, Cambridge, U.K.) for the somatic cell hybrid panel, the chromosome 1 gridded filter LL01NC01 and the Nek2-containing cosmid clones ah39-h3, ah419-c2, ah60-d11, ah91-a12 and ah94-g7. Finally, we thank Sue Shackleton for criti al reading of the manuscript and all members of the laboratory for technical help a d useful discussion. This work was supported by grants to A.M.F. from The Wellco e Trust (056335) and the Cancer Research Campaign (SP2486/0101). A.M.F. is a Lister Institute Research Fellow.

REFERENCES

1 Andersen, S. S. L. (1999) Molecular characteristics of the centrosome. Int. Rev. C **187**, 51–109
2 Kellogg, D. R., Moritz, M. and Alberts, B. M. (1994) The centrosome and cellular organization. Annu. Rev. Biochem. **63**, 639–674
3 Zimmerman, W., Sparks, C. A. and Doxsey, S. J. (1999) Amorphous no longer: th centrosome comes into focus. Curr. Opin. Cell Biol. **11**, 122–128
4 Moritz, M., Zheng, Y., Alberts, B. M. and Oegema, K. (1998) Recruitment of the γ-tubulin ring complex to *Drosophila* salt-stripped centrosome scaffolds. J. Cell Bi **142**, 775–786
5 Schnackenberg, B. J., Khodjakov, A., Rieder, C. L. and Palazzo, R. E. (1998) The disassembly and reassembly of functional centrosomes *in vitro*. Proc. Natl. Acad. U.S.A. **95**, 9295–9300

6 Sluder, G. and Hinchcliffe, E. H. (2000) The coordination of centrosome reproduction with nuclear events during the cell cycle. Curr. Top. Dev. Biol. **49**, 267–289
7 Khodjakov, A. and Rieder, C. L. (1999) The sudden recruitment of γ-tubulin to the centrosome at the onset of mitosis and its dynamic exchange throughout the cell cycle do not require microtubules. J. Cell Biol. **146**, 585–596
8 Wittmann, T., Hyman, A. and Desai, A. (2001) The spindle: a dynamic assembly of microtubules and motors. Nat. Cell Biol. **3**, E28–E34
9 Heald, R. (2000) Motor function in the mitotic spindle. Cell **102**, 399–402
10 Bornens, M., Paintrand, M., Berges, J., Marty, M.-C. and Karsenti, E. (1987) Structural and chemical characterization of isolated centrosomes. Cell Motil. Cytoskel. **8**, 238–249
11 Piel, M., Meyer, P., Khodjakov, A., Rieder, C. L. and Bornens, M. (2000) The respective contributions of the mother and daughter centrioles to centrosome activity and behaviour in vertebrate cells. J. Cell Biol. **149**, 317–329
12 Paintrand, M., Moudjou, M., Delacroix, H. and Bornens, M. (1992) Centrosome organization and centriole architecture: their sensitivity to divalent cations. J. Struct. Biol. **108**, 107–128
13 Fry, A. M., Mayor, T. and Nigg, E. A. (2000) Regulating centrosomes by protein phosphorylation. Curr. Top. Dev. Biol. **49**, 291–312
14 Nigg, E. A. (2001) Mitotic kinases as regulators of cell division and its checkpoints. Nat. Rev. Mol. Cell Biol. **2**, 21–32
15 Freed, E., Lacey, K. R., Huie, P., Lyapina, S. A., Deshaies, R. J., Stearns, T. and Jackson, P. K. (1999) Components of the SCF ubiquitin ligase localize to the centrosome and regulate the centrosome duplication cycle. Genes Dev. **13**, 2242–2257
16 Tugendreich, S., Tomkiel, J., Earnshaw, W. and Hieter, P. (1995) CDC27Hs colocalizes with CDC16Hs to the centrosome and mitotic spindle and is essential for the metaphase to anaphase transition. Cell **81**, 261–268
17 Wigley, W. C., Fabunmi, R. P., Lee, C. R., Marino, C. R., Muallem, S., DeMartino, G. N. and Thomas, P. J. (1999) Dynamic association of protosomal machinery with the centrosome. J. Cell Biol. **145**, 481–490
18 Fry, A. M., Meraldi, P. and Nigg, E. A. (1998) A centrosomal function for the human Nek2 protein kinase, a member of the NIMA-family of cell cycle regulators. EMBO J. **17**, 470–481
19 Schultz, S. J., Fry, A. M., Sütterlin, C., Ried, T. and Nigg, E. A. (1994) Cell cycle-dependent expression of Nek2, a novel human protein kinase related to the NIMA mitotic regulator of *Aspergillus nidulans*. Cell Growth Diff. **5**, 625–635
20 Fry, A. M., Schultz, S. J., Bartek, J. and Nigg, E. A. (1995) Substrate specificity and cell cycle regulation of the Nek2 protein kinase, a potential human homolog of the mitotic regulator NIMA of *Aspergillus nidulans*. J. Biol. Chem. **2705**, 12899–12905
21 Helps, N. R., Luo, X., Barker, H. M. and Cohen, P. T. W. (2000) NIMA-related kinase 2 (Nek2), a cell cycle-regulated protein kinase localized to centrosomes, is complexed to protein phosphatase 1. Biochem. J. **349**, 509–518
22 Andreassen, P. R., Lacroix, F. B., Villa-Moruzzi, E. and Margolis, R. L. (1998) Differential subcellular localization of protein phosphatase-1alpha, gamma 1 and delta isoforms during both interphase and mitosis in mammalian cells. J. Cell Biol. **141**, 1207–1215
23 Puntoni, F. and Villa-Moruzzi, E. (1997) Protein phosphatase-1 alpha, gamma 1, and delta: changes in phosphorylation and activity in mitotic HeLa cells and in cells released from the mitotic block. Arch. Biochem. Biophys. **340**, 177–184
24 Fry, A. M., Mayor, T., Meraldi, P., Stierhof, Y.-D., Tanaka, K. and Nigg, E. A. (1998) C-Nap1, a novel centrosomal coiled-coil protein and candidate substrate of the cell cycle-regulated protein kinase Nek2. J. Cell Biol. **141**, 1563–1574
25 Mack, G. J., Rees, J., Sandblom, O., Balczon, R., Fritzler, M. J. and Rattner, J. B. (1998) Autoantibodies to a group of centrosomal proteins in human autoimmune sera reactive with the centrosome. Arthrit. Rheum. **41**, 551–8
26 Mayor, T., Tanaka, K., Stierhof, Y.-D., Fry, A. M. and Nigg, E. A. (2000) The centrosomal protein C-Nap1 displays properties supporting a role in cell cycle-regulated centrosome cohesion. J. Cell Biol. **151**, 837–846

Received 13 July 2001/5 October 2001; accepted 26 October 2001

27 Fry, A. M., Descombes, P., Twomey, C., Bacchieri, R. and Nigg, E. A. (2000) The NIMA-related kinase X-Nek2B is required for efficient assembly of the zygotic centrosome in *Xenopus laevis*. J. Cell Sci. **113**, 1973–1984
28 Uto, K. and Sagata, N. (2000) Nek2B, a novel maternal form of Nek2 kinase, is essential for the assembly or maintenance of centrosomes in early *Xenopus* embryos. EMBO J. **19**, 1816–1826
29 Graf, J.-D. and Kobel, H. R. (1991) Genetics of *Xenopus laevis*. Methods Cell Biol. **36**, 19–34
30 Uto, K., Nakajo, N. and Sagata, N. (1999) Two structural variants of Nek2 kinase, termed Nek2A and Nek2B, are differentially expressed in *Xenopus* tissues and development. Dev. Biol. **208**, 456–464
31 Tanaka, K., Parvinen, M. and Nigg, E. A. (1997) The *in vivo* expression pattern of mouse Nek2, a NIMA-related kinase, indicates a role in both mitosis and meiosis. Exp. Cell Res. **237**, 264–274
32 Rhee, K. and Wolgemuth, D. J. (1997) The NIMA-related kinase 2, Nek2, is expressed in specific stages of the meiotic cell cycle and associates with meiotic chromosomes. Development **124**, 2167–2177
33 Arama, E., Yanai, A., Kilfin, G., Bernstein, A. and Motro, B. (1998) Murine NIMA-related kinases are expressed in patterns suggesting distinct functions in gametogenesis and a role in the nervous system. Oncogene **16**, 1813–1823
34 Kelsell, D., Rooke, L., Warne, D., Bouzyk, M., Cullin, L., Cox, S., West, L., Povey, S. and Spurr, N. (1995) Development of a panel of monochromosomal somatic cell hybrids for rapid gene mapping. Ann. Hum. Genet. **59**, 233–241
35 Churcher, Y. and Moss, S. E. (1993) Modulation of protein tyrosine phosphorylation during G1/S transition in activated human T-lymphoblasts. J. Biol. Chem. **268**, 26144–26149
36 Fry, A. M. and Faragher, A. (2001) Identification of centrosome kinases. Methods Cell Biol. **67**, 305–323
37 Fry, A. M. and Nigg, E. A. (1997) Characterization of mammalian NIMA-related kinases. Methods Enzymol. **283**, 270–282
38 Fry, A. M., Arnaud, L. and Nigg, E. A. (1999) Activity of the human centrosomal kinase, Nek2, depends upon an unusual leucine zipper dimerization motif. J. Biol. Chem. **274**, 16304–16310
39 Lu, K. P. and Hunter, T. (1995) The NIMA kinase: a mitotic regulator in *Aspergillus nidulans* and vertebrate cells. In Progress in Cell Cycle Research, vol. 1 (Meijer, L., Guidet, S. and Tung, H. Y. L., eds.), pp. 187–205, Plenum Press, New York
40 de Saint Phalle, B. and Sullivan, W. (1998) Spindle assembly and mitosis without centrosomes in parthenogenetic *Sciara* embryos. J. Cell Biol. **141**, 1383–1391
41 Calarco-Gillam, P. D., Siebert, M. C., Hubble, R., Mitchison, T. and Kirschner, M. (1983) Centrosome development in early mouse embryos as defined by an autoantibody against pericentriolar material. Cell **35**, 621–629
42 Matthies, H. J., McDonald, H. B., Goldstein, L. S. and Theurkauf, W. E. (1996) Anastral meiotic spindle morphogenesis: role of the non-claret disjunctional kinesin-like protein. J. Cell Biol. **134**, 455–464
43 Megraw, T. L., Kao, L.-R. and Kaufman, T. (2001) Zygotic development without functional mitotic centrosomes. Curr. Biol. **11**, 116–120
44 Heald, R., Tournebize, R., Blank, T., Sandaltzopoulos, R., Becker, P., Hyman, A. and Karsenti, E. (1996) Self-organization of microtubules into bipolar spindle around artificial chromosomes in *Xenopus* egg extracts. Nature (London) **382**, 420–425
45 Khodjakov, A., Cole, R. W., Oakley, B. R. and Rieder, C. L. (2000) Centrosome-independent mitotic spindle formation in vertebrates. Curr. Biol. **10**, 59–67
46 Heald, R., Tournebize, R., Habermann, A., Karsenti, E. and Hyman, A. (1997) Spindle assembly in *Xenopus* egg extracts: respective roles of centrosomes and microtubule self-organization. J. Cell Biol. **138**, 615–628
47 Brinkley, B. R. (2001) Managing the centrosome numbers game: from chaos to stability in cancer cell division. Trends Cell Biol. **11**, 18–21
48 Doxsey, S. (1998) The centrosome – a tiny organelle with big potential. Nat. Genet. **20**, 104–106
49 Richter, J. D. (1999) Cytoplasmic polyadenylation in development and beyond. Microbiol. Mol. Biol. Rev. **63**, 446–456
50 Mayor, T., Meraldi, P., Stierhof, Y.-D., Nigg, E. A. and Fry, A. M. (1999) Protein kinases in control of the centrosome cycle. FEBS Lett. **452**, 92–95